A&A LIBRARY

Norman K. Glendenning

Compact Stars

Nuclear Physics, Particle Physics, and General Relativity

Second Edition

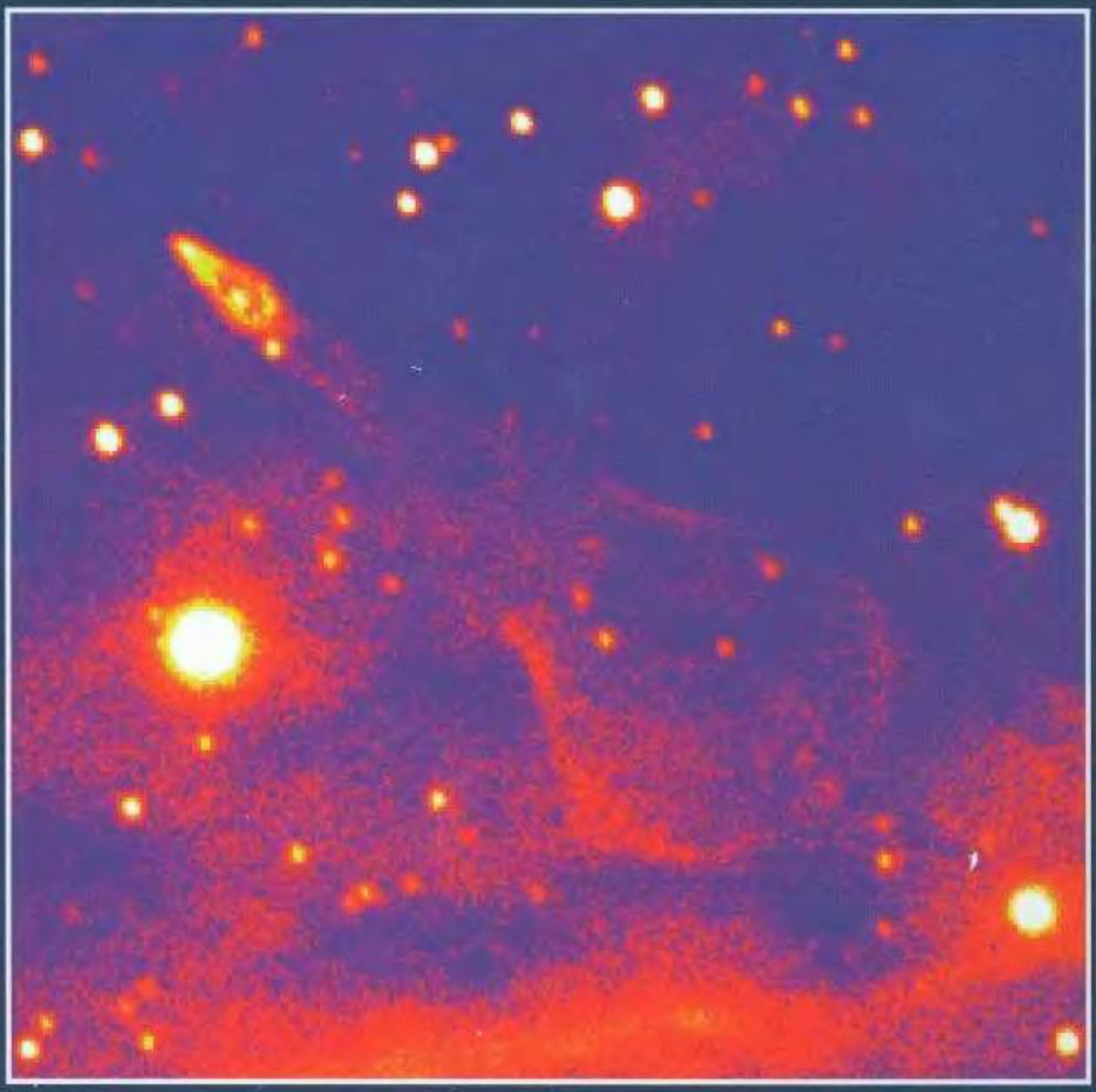

Springer

ASTRONOMY AND ASTROPHYSICS LIBRARY

Series Editors: I. Appenzeller • G. Börner • M. Harwit • R. Kippenhahn
J. Lequeux • P.A. Strittmatter • V. Trimble

Stellar Physics (2 volumes)
Volume 1: Fundamental Concepts and Stellar Equilibrium
Volume 2: Stellar Evolution and Stability
By G.S. Bisnovatyi-Kogan

Theory of Orbits (2 volumes)
Volume 1: Integrable Systems and Non-perturbative Methods
Volume 2: Perturbative and Geometrical Methods
By D. Boccaletti and G. Pucacco

Galaxies and Cosmology
By F. Combes, P. Boissé, A. Mazure, and A. Blanchard

The Solar System 2nd Edition
By T. Encrenaz and J.-P. Bibring

Physics of Planetary Rings
Celestial Mechanics of Continuous Media
By A.M. Fridman and N.N. Gorkavyi

Compact Stars
Nuclear Physics, Particle Physics, and General Relativity
2nd Edition
By N.K. Glendenning

The Physics and Dynamics of Planetary Nebulae
By G.A. Gurzadyan

Stellar Interiors
Physical Principles, Structure, and Evolution
By C.J. Hansen and S.D. Kawaler

Astrophysical Concepts 3rd Edition
By M. Harwit

Physics and Chemistry of Comets
Editor: W.F. Huebner

Stellar Structure and Evolution
By R. Kippenhahn and A. Weigert

Modern Astrometry
By J. Kovalevsky

Astrophysical Formulae 3rd Edition (2 volumes)
Volume 1: Radiation, Gas Processes, and
High Energy Astrophysics
Volume 2: Space, Time, Matter, and Cosmology
By K.R. Lang

Norman K. Glendenning

Compact Stars

Nuclear Physics, Particle Physics, and General Relativity

Second Edition

With 134 Illustrations

Springer

Preface to the Second Edition

I was pleased by the reception of the first edition and have taken the opportunity afforded by publication of a second edition to add two chapters as well as many new sections and figures to the old chapters. I did much rewriting throughout to clarify the text. Problem sets have been added to many of the chapters.

It has been a great pleasure revisiting the book, adding new insights here and there, as well as ideas concerning the possible manifestations of what is happening deep in the heart of neutron stars.

Neutron stars, white dwarfs, and black holes arouse a deep curiosity in us—lay people as well as scientists. Well they might. They form an essential link in the chain of heavenly processes that have created the conditions for life. And as I point out in Section 5.2.11, the existence of neutron stars, and therefore life itself, depends upon a cosmic coincidence!

Like all of science, the field is burgeoning with new discoveries coming almost daily. Fifty percent more pulsars have been discovered since the first edition four years ago. X-ray neutron stars—those that are accreting matter from a companion star—will provide new insights and probably represent the missing link between slowly rotating neutron stars and very fast ones that rotate hundreds of time a second.

Great challenges await those who hear the siren song.

N. K. G.
April 2000

Preface to the First Edition

The heavens are a wonder to us all. When keenly observed they present, not a vast and unchanging panoply, but a cycle of life that embraces our own. Stars are born in primordial clouds of diffuse gases. They lead an active and ever-changing life for millions of years as they synthesize their store of hydrogen into ever-heavier elements. Then they collapse and die. Their last gasp is an enormous explosion—a supernova—which lights the daytime sky for months as it disperses to the heavens the very elements of which the planets, and we ourselves, are made. From the primordial clouds, enriched by the elements of such stellar deaths, new stars are born.

Contemplating these marvels, we arrive at the thought that in the vast reaches of the universe the laws of nature are explored and realized in innumerable imagined—and as yet unimagined forms. In this spirit, compact stars, especially neutron stars, are studied in this book. Neutron stars were a great surprise when first discovered as pulsars, highly magnetized rotating neutron stars that illuminate sensitive radio telescopes at each rotation. They continue to amaze us with their multitude of associated phenomena. These include a high-velocity pulsar that creates a shock front in the interstellar gas, seen as a luminous nebula in the shape of a guitar (see cover picture), and a miniature planetary system consisting of a neutron star and three planets—the first planets discovered outside our own solar system.

Neutron stars—the smallest, densest stars known—are as massive as the Sun, but much smaller than the Earth, yet some of them spin hundreds of times in a second. The very high-mass concentration and very rapid rotation of some pulsars warps the fabric of spacetime. Neutron stars are fully relativistic objects.

There are admirable and comprehensive treatises on General Relativity, those of Misner,Thorne and Wheeler, and of Weinberg. When I began my own study of compact stars a little more than ten years ago, I would have found it useful to have the theory from its origins through to the equations of relativistic stellar structure set down rigorously and directly—along a geodesic path so to speak. With that limited goal, it is accomplished here in a single chapter.

This book differs in several respects from the excellent one by Shapiro and Teukolsky. The range of topics dealt with in this book is narrower, but in general the topics are treated in greater depth. Also, emphasis is placed here on emerging topics—the many forms in which "neutron" stars may be realized in nature—hyperon stars, hybrids stars with intricate crystalline interiors of quark and nuclear matter, and strange quark stars and dwarfs sheathed in nuclear material. These marvelous objects challenge our understanding of dense-matter physics, both nuclear and particle, not to mention our imagination.

There is an immense body of data and lore on the subject of compact stars that can only be ferreted slowly from the literature, learning this here, that there, and then with enough—making the connections. The reader may profit in the time it takes to read these several hundred pages, from what I learned in this respect.

The physics of compact objects attracts the interest of many researchers and students, not only in astrophysics, but also in other fields of the physical sciences such as nuclear and particle physics. The book is self-contained. The author writes in the hope that his book will inform, fire the imagination, and provide a basis for further investigations by newcomers as well as experienced researchers who want to familiarize themselves with a modern view of the topic.

I appreciate the forbearance of Tom von Foerster, Editor-in-Chief of Physics at Springer-Verlag through the six years this book was in preparation. To my great fortune he very wisely assigned an outstanding editor, D. A. Oliver, whom I thank; with his help and prodding the presentation was vastly improved over many revisions. Over the last-half dozen years, F. Weber and I have collaborated on many projects, especially concerning stellar rotation. This book is, in part, a beneficiary of our collaboration. Most of all I thank Laura for who she is.

Norman K. Glendenning
Berkeley, California
October 1996

Contents

Preface to the Second Edition vii

Preface to the First Edition ix

1 Introduction 1
- 1.1 Compact Stars 2
- 1.2 Compact Stars and Relativistic Physics 4
- 1.3 Compact Stars and Dense-Matter Physics 5

2 General Relativity 8
- 2.1 Relativity 10
- 2.2 Lorentz Invariance 12
  - 2.2.1 Lorentz transformations 12
  - 2.2.2 Covariant vectors 15
  - 2.2.3 Energy and momentum 17
  - 2.2.4 Energy-momentum tensor of a perfect fluid 17
  - 2.2.5 Light cone 18
- 2.3 Scalars, Vectors, and Tensors in Curvilinear Coordinates 18
- 2.4 Principle of Equivalence of Inertia and Gravitation 23
  - 2.4.1 Photon in a gravitational field 25
  - 2.4.2 Tidal gravity 26
  - 2.4.3 Curvature of spacetime 26
  - 2.4.4 Energy conservation and curvature 27
- 2.5 Gravity 27
  - 2.5.1 Mathematical definition of local Lorentz frames 30

2.5.2 Geodesics 31
2.5.3 Comparison with Newton's gravity 33
2.6 Covariance 34
2.6.1 Principle of general covariance 34
2.6.2 Covariant differentiation 34
2.6.3 Geodesic equation from covariance principle 35
2.6.4 Covariant divergence and conserved quantities 37
2.7 Riemann Curvature Tensor 39
2.7.1 Second covariant derivative of scalars and vectors . . . 39
2.7.2 Symmetries of the Riemann tensor 40
2.7.3 Test for flatness 41
2.7.4 Second covariant derivative of tensors 41
2.7.5 Bianchi identities 41
2.7.6 Einstein tensor 42
2.8 Einstein's Field Equations 43
2.9 Relativistic Stars 45
2.9.1 Metric in static isotropic spacetime 46
2.9.2 The Schwarzschild solution 47
2.9.3 Riemann tensor outside a Schwarzschild star 48
2.9.4 Energy-momentum tensor of matter 49
2.9.5 The Oppenheimer–Volkoff equations 50
2.9.6 Gravitational collapse and limiting mass 54
2.10 Action Principle in Gravity 55
2.10.1 Derivations 57
2.11 Problems for Chapter 2 60

3 Compact Stars: From Dwarfs to Black Holes 62
3.1 Birth and Death of Stars 62
3.2 Objective 69
3.3 Gravitational Units and Neutron Star Size 70
3.3.1 Units 71
3.3.2 Size and number of baryons in a star 73
3.3.3 Gravitational energy of a neutron star 75
3.4 Partial Decoupling of Matter from Gravity 75
3.5 Equations of Relativistic Stellar Structure 77
3.5.1 Interpretation 77
3.5.2 Boundary conditions and stellar sequences 80
3.6 Electrical Neutrality of Stars 82
3.7 "Constancy" of the Chemical Potential 83
3.8 Gravitational Redshift 84
3.8.1 Integrity of an atom in strong fields 84
3.8.2 Redshift in a general static field 85
3.8.3 Comparison of emitted and received light 89
3.8.4 Measurements of M/R from redshift 89
3.9 White Dwarfs and Neutron Stars 90

3.9.1 Overview 90
3.9.2 Fermi-gas equation of state for nucleons and electrons . 92
3.9.3 High- and low-density limits 98
3.9.4 Polytropes and Newtonian white dwarfs 99
3.9.5 Nonrelativistic electron region 102
3.9.6 Ultrarelativistic electron region: asymptotic white dwarf mass 103
3.9.7 Nature of limiting mass of dwarfs and neutron stars . . 105
3.9.8 Degenerate ideal gas neutron star 107
3.10 Improvements in White Dwarf Models 108
3.10.1 Nature of matter at dwarf and neutron star densities . . 108
3.10.2 Low-density equation of state 111
3.10.3 Carbon and oxygen white dwarfs 112
3.11 Temperature and Neutron Star Surface 115
3.12 Stellar Sequences from White Dwarfs to Neutron Stars 118
3.13 Baryon Number of a Star 119
3.14 Binding Energy of a Neutron Star 121
3.15 Star of Uniform Density 122
3.16 Scaling Solution of the OV Equations 125
3.17 Bound on Maximum Mass of Neutron Stars 126
3.18 Stability 129
3.18.1 Necessary condition for stability 130
3.18.2 Normal modes of vibration: Sufficient condition for stability 132
3.19 Beyond the Maximum-Mass Neutron Star 134
3.20 Black Holes 136
3.20.1 Interior and exterior regions 136
3.20.2 No statics within 139
3.20.3 Black hole densities 141
3.21 Problems for Chapter 3 142

4 Relativistic Nuclear Field Theory 145
4.1 Motivation 145
4.2 Lagrange Formalism 150
4.3 Symmetries and Conservation Laws 152
4.3.1 Internal global symmetries 152
4.3.2 Spacetime symmetries 153
4.4 Boson and Fermion Fields 156
4.4.1 Uncharged and charged scalar fields 156
4.4.2 Uncharged and charged vector fields 157
4.4.3 Dirac fields 159
4.4.4 Neutron and proton 161
4.4.5 Electromagnetic field 162
4.5 Properties of Nuclear Matter 163
4.6 The $\sigma - \omega$ Model 168

4.7 Stationarity of Energy Density 176
4.8 Model with Scalar Self-Interactions 176
4.8.1 Algebraic determination of the coupling constants . . . 178
4.8.2 Symmetric nuclear matter equation of state 181
4.8.3 Negative self-interaction 181
4.9 Introduction of Isospin Force 182
4.10 Inclusion of the Octet of Baryons 188
4.11 High-Density Limit 191
4.12 Effective Versus Renormalized Theory 192
4.13 Bound Versus Unbound Neutron Matter 193
4.13.1 Bound neutron matter 194
4.14 Note on Dimensions 195
4.15 Summary 196
4.16 Problems for Chapter 4 196

5 Neutron Stars **199**
5.1 Discovery 199
5.2 Pulsars: The Observational Basis of Neutron Stars 203
5.2.1 Important pulsar discoveries 203
5.2.2 Pulsar periods 206
5.2.3 Individual pulses and pulse profiles 209
5.2.4 Detection biases 210
5.2.5 Two populations of pulsars 212
5.2.6 Supernova associations with pulsars 215
5.2.7 Why pulsars are neutron stars 216
5.2.8 Mass of the Crab pulsar 221
5.2.9 Pulsar masses: observational 221
5.2.10 Pulsar masses: physical bounds 222
5.2.11 Neutron stars: a cosmic coincidence 225
5.2.12 Pulsar ages 225
5.2.13 Evolution of the braking index 228
5.3 Theory of Neutron Stars 231
5.3.1 Nuclear and neutron star matter: Similarities and differences 232
5.3.2 Chemical equilibrium in a star 233
5.3.3 Hadronic composition of neutron stars 238
5.3.4 Superdense matter 239
5.3.5 Neutron star matter 242
5.3.6 Hints for computation 247
5.3.7 Isospin- and charge-favored baryon species 248
5.3.8 Surface of neutron stars 249
5.3.9 Reprise of white dwarfs to neutron stars 251
5.3.10 Development of neutron star sequences 251
5.3.11 Mass as a function of central density 252
5.3.12 Radius–mass characteristic relationship 254

5.3.13 Limiting mass and the equation of state 255
5.4 Constitution of Neutron Stars 256
5.4.1 Beta equilibrium and symmetry energy 256
5.4.2 Hyperon stars 257
5.4.3 Hyperon coupling constants 258
5.4.4 Hyperon populations and the limiting mass 262
5.4.5 Compression modulus and effective nucleon mass . . . 264
5.4.6 Charge neutrality achieved among baryons 266
5.4.7 Pion and kaon condensation 268
5.4.8 Condensation of Free Pions 270
5.5 Tables of Equations of State 271
5.5.1 Low density 271
5.5.2 High density 271
5.6 Problems for Chapter 5 272

6 Rotating Neutron Stars 277
6.1 Motivation 277
6.2 Dragging of Local Inertial Frames 279
6.3 Interior Solution for the Dragging Frequency 283
6.4 Moment of Inertia of a Rotating Relativistic Star 286
6.5 Kepler Angular Velocity in General Relativity 288
6.6 Effect of Frame Dragging on Kepler Frequency 290
6.7 Approximation to the Kepler Frequency 292
6.8 Hartle–Thorne Perturbative Solution 292
6.8.1 Comparison of Perturbative and Numerical Solutions . 294
6.9 Imprint of Angular Momentum 294
6.10 Rotating Stars with Realistic Equations of State 295
6.11 Effect of Rotation on Stellar Structure 297
6.12 Gravitational-Wave Instabilities 298
6.13 Problems for Chapter 6 306

7 Limiting Rotational Period and Radius of Neutron Stars 307
7.1 Motivation 307
7.2 The Minimal Constraints 309
7.3 Variational Ansatz 310
7.4 Limiting Value of Rotational Period as a Function of Mass . . . 311
7.5 Test of Sensitivity of Results 314
7.6 General Relativistic Limit on Rotation 317
7.7 Lower Limit on Neutron Star Radius 317
7.8 Discussion and Alternatives 319
7.9 Self-Bound Stars 319
7.10 Summary 321

8 Quark Stars 322
8.1 Introduction 322

8.2 Model of Quark Confinement 323
8.3 Quark Matter Equation of State 324
8.3.1 Zero temperature 325
8.3.2 Massless quark approximation 326
8.3.3 First order in α_s 327
8.4 Quark Star Matter 328
8.5 Strange and Charm Stars 329
8.5.1 General considerations 329
8.5.2 Strange quark matter 332
8.5.3 Stability considerations 333
8.6 Problems for Chapter 8 336

9 Hybrid Stars 337
9.1 Introduction 337
9.2 Constant-Pressure Phase Transition 341
9.2.1 Purely neutron star 341
9.2.2 Enforced local charge neutrality 344
9.3 The Confined–Deconfined Phase Transition in Neutron Stars . 345
9.3.1 Conservation laws are global—not local 345
9.3.2 Degrees of freedom in a multicomponent substance . . 346
9.3.3 Nuclear symmetry energy and a coulomb lattice 349
9.3.4 Phase diagram 350
9.3.5 Two energy scales 351
9.4 Large-Scale Structure of a Hybrid Star 352
9.4.1 Energy budget in the reapportionment of charge 354
9.5 Crystalline Structure of the Mixed Phase 355
9.5.1 Crystalline structure as a function of stellar mass . . . 358
9.5.2 Possible implications for glitches 361
9.6 Tables of Equation of State for Hybrid Stars 362
9.7 Problems for Chapter 9 362

10 Bose Condensates in Neutron Stars 366
10.1 Relativistic Mean–Field Model with Kaons 368
10.2 Equation of State with a Kaon Condensate 374
10.2.1 Maxwell versus Gibbs 374
10.2.2 Dependence on parameters 378
10.2.3 Particle populations 378
10.2.4 Comment on coupling schemes 380
10.2.5 Comment on hyperons 382
10.2.6 Mixed-phase properties 382
10.3 Stellar Properties 385
10.3.1 Large-scale features 385
10.3.2 Geometrical structure in the mixed phase 387
10.3.3 Pulsar glitches 390
10.4 Summary 391

10.5 Problems for Chapter 10 391

11 Consequences and Signals of Phase Transitions 392
11.1 Introduction 392
11.2 Mechanism for Formation of Low-Mass Black Holes 393
11.2.1 Hyperonization-induced collapse 394
11.2.2 Deconfinement-induced collapse 396
11.2.3 Density profiles 397
11.2.4 Discussion 397
11.3 A Third Class of Stable Compact Stars 399
11.3.1 Introduction 399
11.3.2 Stability of nonidentical twins 401
11.3.3 Cause of stability of a third class of stars 404
11.3.4 Detection and formation mechanisms 405
11.3.5 Conclusions and prospects 406
11.4 Phase Transition Signal in Pulsar Timing 407
11.4.1 Evolutionary path of neutron stars 407
11.4.2 Calculation 410
11.4.3 Spin-up era 410
11.4.4 X-ray pulsars in low-mass binaries 412
11.5 Caveats 413

12 Strange Stars 414
12.1 The Strange Matter Hypothesis 414
12.2 Compatibility of the Hypothesis with Present Knowledge . . . 416
12.2.1 Energetic considerations 416
12.2.2 The universe and its evolution 417
12.2.3 Stability of nuclei against decay to strange matter . . . 418
12.2.4 Stability of nuclei to conversion by strange nuggets . . 418
12.2.5 Terrestrial searches 419
12.2.6 Summary, prospects, and challenges 421
12.3 Submillisecond Pulsars 421
12.3.1 The fine-tuning problem 422
12.3.2 Limits to neutron star rotation 422
12.3.3 Implausibly high central densities 423
12.3.4 Strange stars as fast rotors 424
12.3.5 Out of the impasse 425
12.3.6 Motivation for searches and prospects for discovery . . 425
12.4 Structure of Strange Stars 426
12.5 Simultaneous Existence of Strange and Neutron Stars 428
12.6 Strange Stars to Strange Dwarfs 428
12.6.1 Strange stars with nuclear crusts 428
12.6.2 Nuclear crust and pulsar glitches 433
12.6.3 Strange dwarfs with nuclear crusts 435
12.6.4 Stability 437

12.6.5 Possible new class of dense white dwarfs 439
12.7 Conclusion 440

Useful Astronomical Data **441**

Books for Further Study **443**

References **445**

Index **459**

1

Introduction

"In the deathless boredom of the sidereal calm we cry with regret for a lost sun . . . ."
Jean de la Ville de Mirmont, L'Horizon Chimérique

Compact stars—broadly grouped as neutron stars and white dwarfs—are the ashes of luminous stars. One or the other is the fate that awaits the cores of most stars after a lifetime of tens to thousands of millions of years. Whichever of these objects is formed at the end of the life of a particular luminous star, the compact object will live in many respects unchanged from the state in which it was formed. Neutron stars themselves can take several forms—hyperon, hybrid, or strange quark star. Likewise white dwarfs take different forms though only in the dominant nuclear species. A black hole is probably the fate of the most massive stars, an inaccessible region of spacetime into which the entire star, ashes and all, falls at the end of the luminous phase.

Neutron stars are the smallest, densest stars known. Like all stars, neutron stars rotate—some as many as a few hundred times a second. A star rotating at such a rate will experience an enormous centrifugal force that must be balanced by gravity or else it will be ripped apart. The balance of the two forces informs us of the lower limit on the stellar density. Neutron stars are 10^{14} times denser than Earth. Some neutron stars are in binary orbit with a companion. Application of orbital mechanics allows an assessment of masses in some cases. The mass of a

neutron star is typically 1.5 solar masses. We can therefore infer their radii: about ten kilometers. Into such a small object, the entire mass of our Sun, and more, is compressed.

We infer the existence of neutron stars from the occurrence of supernova explosions (the release of the gravitational binding of the neutron star) and observe them in the periodic radio emission of pulsars. Just as neutron stars acquire high angular velocities through conservation of angular momentum, they acquire strong magnetic fields through conservation of magnetic flux during the collapse of normal stars. The two attributes, rotation and a strong magnetic dipole field, are the principal means by which neutron stars can be detected—the beamed periodic signal of pulsars.

The extreme characteristics of neutron stars set them apart in the physical principles that are required for their understanding. All other stars can be described in Newtonian gravity with atomic and low-energy nuclear physics under conditions essentially known in the laboratory.[1] Neutron stars in their several forms push matter to such extremes of density that nuclear and particle physics—pushed to their extremes—are essential for their description. Further, the intense concentration of matter in neutron stars can be described only in General Relativity, Einstein's theory of gravity which alone describes the way the weakest force in nature arranges the distribution of the mass and constituents of the densest objects in the universe.

1.1 Compact Stars

Of what are compact stars made? The name "neutron star" is suggestive and at the same time misleading. No doubt neutron stars are made of baryons like nucleons and hyperons, but they also likely contain cores of quark matter in some cases. These physically compelling possibilities will be examined in the various chapters of this book, neutron stars, quark stars, hybrid stars (both those with a core of quark matter or a condensate of bosons), and strange stars.

We use the term "neutron star" in a generic sense to refer to stars as compact as described above. How does a star become so compact and why is there little doubt that such neutron stars are made of baryons or quarks? The notion of a neutron star made from the ashes of a luminous star at the end point of its evolution goes back to 1934 and the study of supernova explosions by Baade and Zwicky [1].

During the luminous life of a star, part of the original hydrogen is converted in fusion reactions to heavier elements by the heat produced by gravitational compression. When sufficient iron—the end point of exothermic fusion—is made, the

[1]Luminous stars evolve through thermonuclear reactions. These are nuclear reactions induced by high temperatures, but involving collision energies that are small on the nuclear scale. In some cases the relevant reaction cross-sections can be measured with nuclear accelerators, and in others, measured cross-sections must be extrapolated to lower energy.

core containing this heaviest ingredient collapses, and an enormous energy is released in the explosion of the star. Baade and Zwicky guessed that the source of such a magnitude that makes these stellar explosions visible in daylight and for weeks thereafter must be gravitational binding energy. This energy is released by the solar mass core as the star collapses to densities high enough to tear all nuclei apart into their constituents.

By a simple calculation one learns that the gravitational energy acquired by the collapsing core is more than enough to power such explosions as Baade and Zwicky were detecting. Their view concerning the compactness of the residual star has since been supported by many detailed calculations, and most spectacularly by the supernova explosion of 1987 in the Large Magellanic Cloud, a nearby minor galaxy visible in the southern hemisphere. The pulse of neutrinos observed in several large detectors carried the evidence for an integrated energy release over 4π steradians of the expected magnitude.

The gravitational binding energy of a neutron star is about 10 percent of its mass. Compare this with the nuclear binding energy of 9 MeV per nucleon in iron which is one percent of the mass. We conclude that the release of gravitational binding energy at the death of a massive star is on the order of ten times greater than the energy released by nuclear fusion reactions during the entire luminous life of the star. The evidence that the source of energy for a supernova is the binding energy of a compact star—a neutron star—is compelling. How else could a tenth of a solar mass of energy be generated and released in such a short period of time?

Neutron stars are more dense than was thought possible by physicists at the turn of the century. At that time astronomers were grappling with the thought of white dwarfs whose densities were inferred to be about a million times denser than the Earth. It was only following the discovery of the quantum theory and Fermi–Dirac statistics that very dense *cold* matter—denser than could be imagined on the basis of atomic sizes—was conceivable.

Prior to the discovery of Fermi–Dirac statistics, the high density inferred for the white dwarf Sirius seemed to present a dilemma. For while the high density was understood to arise from the ionization of the atoms in the hot star, making possible their compaction by gravity, what would become of this dense object when ultimately it had consumed its nuclear fuel? Cold matter was known only in the atomic form it is on Earth with densities of a few grams per cubic centimeter. The great scientist Sir Arthur Eddington surmised for a time that the star had "got itself into an awkward fix"—that it must some how re-expand to matter of familiar densities as it cooled, but it had no remaining source of energy to do so.

The perplexing problem of how a hot dense body without a source of energy could cool persisted until R. H. Fowler "came to the rescue"[2] by showing that Fermi–Dirac degeneracy allowed the star to cool by remaining comfortably in a

[2]Eddington in an address in 1936 at Harvard University.

previously unknown state of dense cold matter, in this case a degenerate[3] electron state. A little later Baade and Zwicky conceived of a similar degenerate state as the final resting place for nucleons after the supernova explosion of a luminous star.

The constituents of neutron stars—leptons, baryons, and quarks—are degenerate. They lie helplessly in the lowest energy states available to them. They must. Fusion reactions in the original star have reached the end point for energy release—the core has collapsed, and the immense gravitational energy converted to neutrinos has been carried away. The star has no remaining source of energy to excite the fermions. Only the Fermi pressure and the short-range repulsion of the nuclear force sustain the neutron star against further gravitational collapse—sometimes. At other times the mass is so concentrated that it falls into a black hole, a dynamical object whose existence and external properties can be understood in the Classical Theory of General Relativity.

1.2 Compact Stars and Relativistic Physics

Classical General Relativity is completely adequate for the description of neutron stars, white dwarfs, and, for the most part, the exterior region of black holes as well as some aspects of the interior.[4] The first chapter is devoted to General Relativity. The goal is to rigorously derive the equations that describe the structure of relativistic stars—the Oppenheimer–Volkoff equations—the form that Einstein's equations take for spherical static stars. Two important facts emerge immediately. No form of matter whatsoever can support a relativistic star above a certain mass called the limiting mass. Its value depends on the nature of matter but the existence of the limit does not. The implied fate of stars more massive than the limit is that either mass is lost in great quantity during the evolution of the star or it collapses to form a black hole.

Black holes—the most mysterious objects of the universe—are treated at the classical level in this book and only briefly. The peculiar difference between time as measured at a distant point and on an object falling into the hole is discussed. And it is shown that in black holes there is no statics. Everything at all times must approach the central singularity. Unlike neutron stars and white dwarfs, the question of their internal constitution does not arise at the classical level. They are enclosed within a horizon from which no information can be received. The ultimate fate of black holes is unknown.

Luminous stars are known to rotate because of the Doppler broadening of spectral lines. Therefore their collapsed cores, spun up by conservation of angular

---

[3]Nucleons and electrons obey the Pauli exclusion principle, according to which each particle must occupy a different quantum state from the others. A degenerate state refers to the complete occupation of the lowest available energy states. In that event, no reaction, and therefore no energy generation, is possible—hence the name: degenerate state.

[4]The density at which quantum gravity would be relevant is 10^{78} higher than found in neutron stars.

momentum, may rotate very rapidly. Consequently, no account of compact stars would be complete without a discussion of rotation, its effects on the structure of the star and spacetime in the vicinity, the limits on rotation imposed by mass loss at the equator and by gravitational radiation, and the nature of compact stars implied by very rapid rotation.

Rotating relativistic stars set local inertial frames into rotation with respect to the distant stars. An object falling from rest at great distance toward a rotating star would fall—not toward its center, but would acquire an ever larger angular velocity as it approached. The effect of rotating stars on the fabric of spacetime acts back upon the structure of the stars and so is essential to our understanding.

1.3 Compact Stars and Dense-Matter Physics

The physics of dense matter is not as simple as the final resting place of stars imagined by Baade and Zwicky. The constitution of matter at the high densities attained in a neutron star—the particle types, abundances, and their interactions—pose challenging problems in nuclear and particle physics. How should matter at supernuclear densities be described? In addition to nucleons, what exotic baryon species constitute it? Does a transition in phase from quarks confined in nucleons to the deconfined phase of quark matter occur in the density range of such stars? And how is the transition to be calculated? What new structure is introduced into the star? Do other phases like pion or kaon condensates play a role in their constitution?

In Fig. 1.1 we show a computation of the possible constitution and interior crystalline structure of a neutron star near the limiting mass of such stars (Chapter 9). Only now are we beginning to appreciate the complex and marvelous structure of these objects. Surely the study of neutron stars and their astronomical realization in pulsars will serve as a guide in the search for a solution to some of the fundamental problems of dense many-body physics both at the level of nuclear physics—the physics of baryons and mesons—and ultimately at the level of their constituents—quarks and gluons. And neutron stars may be the only objects in which a Coulomb lattice structure (Fig. 1.1) formed from two phases of one and the same substance (hadronic matter) exists.

We do not know from experiment what the properties of superdense matter are. However, we can be guided by certain general principles in our investigation of the possible forms that compact stars may take. Some of the possibilities lead to quite striking consequences that may in time be observable (Chapter 11). The rate of discovery of new pulsars, X-ray neutron stars, and other high-energy phenomena associated with neutron stars is astonishing, and was unforeseen only half a dozen years ago.

White dwarfs are the cores of stars whose demise is less spectacular than a supernova—a more quiescent thermal expansion of the envelope of a low-mass star into a planetary nebula. White dwarf constituents are nuclei immersed in an electron gas and therefore arranged in a Coulomb lattice. White dwarfs are

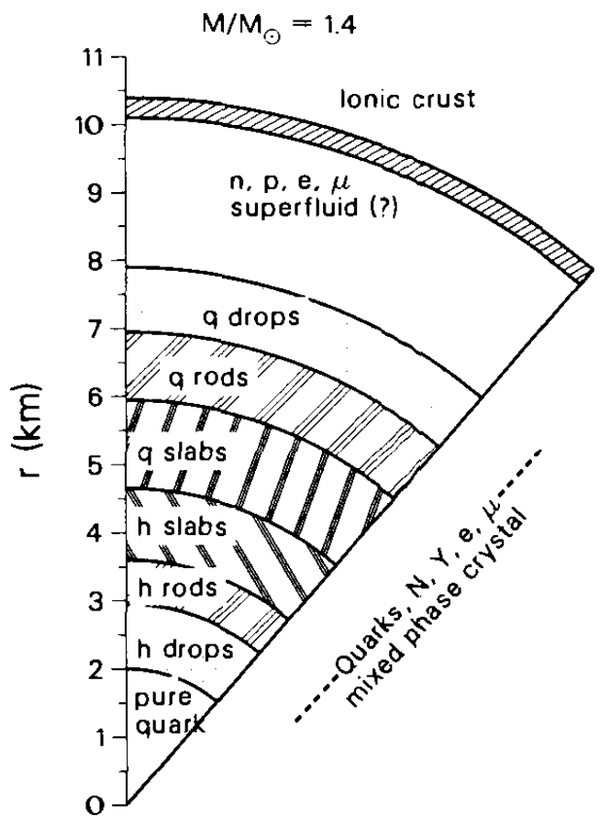

FIGURE 1.1. A section through a neutron star model that contains an inner sphere of pure quark matter surrounded by a crystalline region of mixed hadronic and quark matter. The mixed phase region consists of various geometrical objects of the rare phase immersed in the dominant one labeled by h(adronic) drops immersed in quark matter . . . through to q(uark) drops immersed in hadronic matter. The particle composition of these regions is quarks, nucleons, hyperons, and leptons. A liquid of neutron star matter containing nucleons and leptons surrounds the mixed phase. A thin crust of heavy ions forms the stellar surface.

supported against collapse by Fermi pressure—as are neutron stars—except that the pressure is provided by degenerate electrons. White dwarfs pose less severe and less fundamental problems than neutron stars. The nuclei will comprise varying proportions of helium, carbon, and oxygen, and in some cases heavier elements like magnesium, depending on how far in the chain of exothermic nuclear fusion reactions the precursor star burned before it was disrupted by instabilities leaving behind the dwarf. White dwarfs are barely relativistic.

Of a vastly different nature than neutron stars are *strange stars*. Like neutron stars they are, if they exist, very dense, of the same order as neutron stars. However their very existence hinges on a hypothesis that at first sight seems absurd. According to the hypothesis, sometimes referred to as the *strange-matter hypothesis*, quark matter—consisting of an approximately equal number of up, down, and strange quarks—has an equilibrium energy per nucleon that is lower than the mass of the nucleon or the energy per nucleon of the most bound nucleus, iron. In other words, under the hypothesis, strange quark matter is the *absolute* ground state of the strong interaction.

We customarily find that systems, if not in their ground state, readily decay to it. Of course, this is not always so. Even in well-known objects like nuclei, there are certain excited states whose structure is such that the transition to the ground state is hindered. The first excited state of ^{180}Ta has a half-life of 10^{15} years—five

orders of magnitude longer than the age of the universe! We will discuss why the strange-matter hypothesis is consistent with the present universe—a long-lived excited state—if strange matter is the ground state. The structure of strange stars is fascinating, as are some of their properties. Special attention is placed on what sort of observation on pulsars would count as a virtually irrefutable proof of the strange-matter hypothesis.

2

General Relativity

"Scarcely anyone who fully comprehends this theory can escape its magic."
A. Einstein

"Beauty is truth, truth beauty—that is all
Ye know on earth, and all ye need to know."
J. Keats

General Relativity—Einstein's theory of gravitation and spacetime—is the most beautiful and elegant of physical theories. Not only that; it is the foundation for our understanding of compact stars. Neutron stars and black holes owe their very existence to gravity as formulated by Einstein [2, 3]. Dense objects like neutron stars could also exist in Newton's theory, but they would be very different objects. Chandrasekhar found (in connection with white dwarfs) that all degenerate stars have a maximum possible mass. In Newton's theory such a maximum mass is attained asymptotically when all fermions whose pressure supports the star are ultrarelativistic. Under such conditions stars populated by heavy quarks would exist. Such unphysical stars do not occur in Einstein's theory.[1]

[1] See Section 3.19.

Perhaps the beauty of Einstein's theory can be attributed to the essentially simple but amazing answer it provides to a fundamental question: what meaning is attached to the absolute equality of inertial and gravitational masses? If all bodies move in gravitational fields in precisely the same way, no matter what their constitution or binding forces, then does this not mean that their motion has nothing to do with their nature, but rather with the nature of spacetime? And if spacetime determines the motion of bodies, then according to the notion of action and reaction, does this not imply that spacetime in turn is shaped by bodies whose motion and form it determines?

Beautiful or not, the predictions of theory have to be tested. The first three tests of General Relativity were proposed by Einstein, the gravitational redshift, the deflection of light by massive bodies and the perihelion shift of Mercury. The latter had already been measured. Einstein computed the anomalous part of the precession to be 43 arcseconds per century compared to the measurement of 42.98 ± 0.04. A fourth test was suggested by Shapiro in 1964—the time delay in the radar echo of a signal sent to a planet whose orbit is carrying it toward superior conjunction[2] with the Sun. Eventually agreement to 0.1 percent with the prediction of Einstein's theory was achieved in these difficult and remarkable experiments. It should be remarked that all of the above tests involved weak gravitational fields.

The crowning experimental achievement was the 20-year study by Taylor and his colleagues of the Hulse–Taylor pulsar binary discovered in 1974. Their work yielded a measurement of 4.22663 degrees *per year* for the periastron shift of the orbit of the neutron star binary and a measurement of the decay of the orbital period by $7.60 \pm 0.03 \times 10^{-7}$ seconds per year. This rate of decay agrees to less than one percent with careful calculations of the effect of energy loss through gravitational radiation as predicted by Einstein's theory [4]. A fuller discussion of these experiments and other intricacies involved in the tests of relativity can be found in the book by Will [5].

The goal of this chapter is to provide a rigorous derivation of the Oppenheimer–Volkoff equations that describe the structure of relativistic stars. We start by briefly outlining the Special Theory of Relativity for it is an essential ingredient of General Relativity. Then we formulate the General Theory of Relativity and derive all parts of the theory that are necessary to our goal. A few additional results are derived that will be used in later chapters in dealing with rotating stars and the amazing phenomenon by which the local inertial frames are set into rotation by a rotating star.

---

[2]Superior conjunction refers to the situation when the Earth and the planet are on opposite sides of the Sun.

2.1 Relativity

"The views of space and time which I wish to lay before you have sprung from the soil of experimental physics, and therein lies their strength. They are radical. Henceforth space by itself, and time by itself, are doomed to fade away into mere shadows, and only a kind of union of the two will preserve an independent reality." *H. Minkowski* [6]

The *principle of relativity* in physics goes back to Galileo who asserted that the laws of nature are the same in all *uniformly* moving laboratories. The relativity principle, stated in the narrow terms of reference frames in uniform motion, referred to as inertial frames, implies the existence of an absolute space. The notion of the absoluteness of time goes back to time immemorial. A *Galilean* transformation assumes the absoluteness of space and time:

$$x' = x - a - vt, \quad y' = y, \quad z' = z, \quad t' = t - b. \tag{2.1}$$

Newton's second law $F_x = m\, d^2x/dt^2$ is evidently invariant under this transformation if one assumes that force and mass are independent of the state of motion.

In contrast, Maxwell's equations do not take on the same form if subjected to a Galilean transformation whereas under a *Lorentz transformation* they do.[3] This fact led Einstein to the postulate that the speed of light is the same in all inertial systems and consequently that the principle of relativity should hold with respect to inertial frames connected by *Lorentz* transformations. That is the historical role that light speed played in the discovery of Special Relativity, and the reason for the undoubted influence that the Michelson–Morley experiment [8] had on the early acceptance of the theory.

However, the underlying physics is quite different from how it appears in the historical development of the Special Theory. The speed of light need not have been postulated as an invariant. Minkowski realized soon after Einstein's epochal discovery in 1905 that the spacetime manifold is not Euclidean space in which events unfold in an absolute foliated time[4]. Spacetime is a 'Minkowski' manifold having such a nature that $d\tau^2 \equiv k^2dt^2 - dx^2 - dy^2 - dz^2$ is invariant in the absence of gravity. The constant k is a conversion factor between length and time. Voigt observed in 1887 that $\Box\phi = 0$ preserved its form under a transformation that differed from the Lorentz transformation by only a scale factor [9]. In fact we will see shortly that the d'Alembertian $\Box$ is a Lorentz scalar. Consequently,

$$\left(\frac{1}{k^2}\frac{\partial^2}{\partial t^2} - \nabla^2\right)\phi = 0$$

[3]See, for example, Ref. [7] for the Lorentz invariant form of Maxwell's equations.

[4]Foliated time refers to the time of events as being arranged as pages in a book, one following the other, there never being a question of which preceded another.

informs us that a disturbance described by a wave equation for a massless particle in Minkowski spacetime propagates with velocity k in vacuum as viewed from this and any other reference frame connected to it by a Lorentz transformation. Hence, the constant k of the spacetime manifold is determined empirically by a measurement of the speed of light, c. In this way it is seen that the constancy of the speed of light is a *consequence* of the nature of the spacetime manifold in a gravity-free universe, or in a sufficiently small region of our gravity-filled universe. It is determined by the conversion factor between time and length of the manifold.

That the constancy of the speed of light is a consequence of the local spacetime manifold and not its determiner is most clearly illustrated by a thought experiment proposed by Swiatecki [10]. He shows that the invariance of the differential interval between spacetime events $d\tau^2 = k^2dt^2 - dx^2 - dy^2 - dz^2$ can be verified (at least in principle) *without* resort to propagation of light signals, but with only measuring rods and clocks. And if it were technically feasible to perform the experiment with sufficient accuracy, k would be measured and its value would be found to equal c.

The experiment is conceptually simple. Just to orient our thinking, imagine a few sheets of graph paper lying in random orientations on a desk. If a pin were stuck into the pile at two points, and then the coordinate differences on each sheet recorded as dx_i, dy_i, it would be found that $ds^2 = dx^2 + dy^2$ was the same as determined on each sheet. Space on Earth is Euclidean to great accuracy.

To bring time into the measurement of a spacetime interval, imagine a number of thin boards with identical rectilinear grids and with identical synchronized stopwatches fixed at the grid points of all boards. Let the boards be slid one upon the other in arbitrary directions with arbitrary uniform velocities. Let a blow be delivered to any one of the watches on the top board, and let that blow cause the closest watch on each of the boards beneath to stop. Event '1' thus has been registered as to time and place on each board. Without interrupting the uniform motion of the boards over one another, let a similar event '2' take place. Now form linear combinations of the squares of the distance and time differentials of the events '1' and '2' as registered on each board, $d\tau^2 \equiv dx^2 + dy^2 \pm k^2dt^2$. If the experiment can be carried out with sufficient accuracy, one must find that $d\tau^2$ is the same as measured on each board when the minus sign is used and then only if k is set equal to a number 2.9979×10^{10} cm/sec. The experiment described does not involve any reference to light or Maxwell's equations.

Minkowski's fundamental discovery of the nature of spacetime in the absence of gravity was inspired by Einstein's postulate of the constancy of the speed of light. The constancy of the speed of light is a consequence of the spacetime manifold in which light propagates and its value (as for any massless particle) is equal to the conversion factor between space and time, as we have seen. One might *speculate* on how the nature of spacetime and Special Relativity might have been discovered without the postulate concerning light. Various phenomena, such as the strong nonlinear increase with velocity of both the lifetime of a cosmic ray and the stopping power required to bring it to rest, could have provided the motivation for investigating a different metric for space and time than the Euclidean metric for space. In place of Einstein's postulate on the constancy of light speed, one might

have postulated, based on cosmic ray observations and the relativity principle, that there is a limiting speed, k, such that anything traveling at that speed with respect to one inertial frame must do so with the same speed in any other. One would then have the Minkowski invariant in which k is not a priori the speed of light, but the unknown limiting speed, as yet to be determined. The expression of this hypothesis is $k^2dt^2 = dx^2 + dy^2 + dz^2$.

In either case, it would have been discovered sooner or later that the Minkowski invariant describes the nature of our spacetime (in a suitably limited region) and that the speed of light and that of any other massless particle is equal to the conversion factor k between time and length. In other words, Special Relativity is a consequence of the local spacetime manifold in which we live. The significance of the local restriction will become clear as we follow the development of the General Theory.

2.2 Lorentz Invariance

The Special Theory of Relativity, which holds in the absence of gravity, plays a central role in physics. Even in the strongest gravitational fields the laws of physics must conform to it in a sufficiently small locality of any spacetime event. The Special Theory plays a central role even in the development of the General Theory of Relativity and its applications.

2.2.1 Lorentz transformations

The Lorentz transformation leaves invariant the *proper time* or *differential interval* in Minkowski spacetime

$$d\tau^2 = dt^2 - dx^2 - dy^2 - dz^2 \quad \text{(units } c = 1\text{)} \tag{2.2}$$

as measured by observers in frames moving with constant relative velocity (called inertial frames because they move freely under the action of no forces). The Minkowski manifold also implies an absolute spacetime in which spacetime events that can be connected by a Lorentz transformation lie within the cone defined by $d\tau = 0$. Absolute means unaffected by any physical conditions. This was the same criticism that Einstein made of Newton's space and time, and the one that powered his search for a new theory in which the expression of physical laws does not depend on the frame of reference, but, nevertheless, in which Lorentz invariance would remain a *local* property of spacetime. We will develop the core of the General Theory which extends the relativity principle to arbitrary frames and therefore to a gravity-filled universe, not just unaccelerated frames in relative uniform motion; but here we review briefly the Special Theory.

A *pure* Lorentz transformation is one without spatial rotation, while a general Lorentz transformation is the product of a rotation in space and a pure Lorentz transformation. We recall the pure transformation, sometimes also referred to as a

boost. For convenience, define

$$x^0 = t, \quad x^1 = x, \quad x^2 = y, \quad x^3 = z. \tag{2.3}$$

(In spacetime a point such as that above is sometimes referred to as an *event*.) The linear homogeneous transformation connecting two reference frames can be written

$$x'^{\mu} = \Lambda^{\mu}{}_{\nu} x^{\nu}. \tag{2.4}$$

(We shall use the convenient notation introduced by Einstein whereby repeated indices are summed—Greek over time and space, Roman over space.)

Any set of four quantities A^{μ} ($\mu = 0, 1, 2, 3$) that transforms under a change of reference frame in the same way as the coordinates is a *contravariant* Lorentz four-vector,

$$A'^{\mu} = \Lambda^{\mu}{}_{\nu} A^{\nu}. \tag{2.5}$$

The invariant interval (also variously called the proper time, the line element, or the separation formula) can be written

$$d\tau^2 = \eta_{\mu\nu}\, dx^{\mu}\, dx^{\nu}, \tag{2.6}$$

where $\eta_{\mu\nu}$ is the Minkowski metric which in rectilinear coordinates is

$$\eta_{\mu\nu} \equiv \begin{pmatrix} 1 & 0 & 0 & 0 \\ 0 & -1 & 0 & 0 \\ 0 & 0 & -1 & 0 \\ 0 & 0 & 0 & -1 \end{pmatrix}. \tag{2.7}$$

The condition of the invariance of $d\tau^2$ is

$$\eta_{\alpha\beta}\, dx^{\alpha}\, dx^{\beta} = \eta_{\mu\nu}\, dx'^{\mu}\, dx'^{\nu} = \eta_{\mu\nu} \Lambda^{\mu}{}_{\alpha} \Lambda^{\nu}{}_{\beta}\, dx^{\alpha}\, dx^{\beta}. \tag{2.8}$$

Since this holds for any dx^{α}, dx^{β} we conclude that the $\Lambda^{\mu}{}_{\nu}$ must satisfy the fundamental relationship assuring invariance of the proper time:

$$\eta_{\alpha\beta} = \eta_{\mu\nu} \Lambda^{\mu}{}_{\alpha} \Lambda^{\nu}{}_{\beta}. \tag{2.9}$$

Transformations that leave $d\tau^2$ invariant leave the speed of light the same in all inertial systems, because if $d\tau$ vanishes in one system, it does so in all, and the content of $d\tau = 0$ is that $|\, d\boldsymbol{x}/dt \,| = 1$.

Let us find the transformation matrix $\Lambda^{\mu}{}_{\alpha}$ for the special case of a boost along the x-axis. In this case it is clear that

$$x'^2 = x^2, \quad x'^3 = x^3, \tag{2.10}$$

and, moreover, that x'^0 and x'^1 cannot involve x^2 and x^3. So,

$$\begin{aligned} x'^0 &= \Lambda^0{}_0 x^0 + \Lambda^0{}_1 x^1, \\ x'^1 &= \Lambda^1{}_0 x^0 + \Lambda^1{}_1 x^1, \end{aligned} \tag{2.11}$$

with the remaining Λ elements zero. So the above quadratic form in Λ yields the three equations,

$$\begin{aligned} 1 &= (\Lambda^0{}_0)^2 - (\Lambda^1{}_0)^2 , \\ -1 &= (\Lambda^0{}_1)^2 - (\Lambda^1{}_1)^2 , \\ 0 &= \Lambda^0{}_0\Lambda^0{}_1 - \Lambda^1{}_0\Lambda^1{}_1 . \end{aligned} \tag{2.12}$$

To get a fourth equation, suppose that the origins of the two frames in uniform motion coincide at $t = 0$ and the primed x-axis x'^1 is moving along x^1 with velocity v. That is, $x^1 = vt$ is the equation of the *primed* origin as it moves along the *unprimed* x-axis. The equation for the primed coordinate is

$$0 = x'^1 = \Lambda^1{}_0 x^0 + \Lambda^1{}_1 x^1 = \left(\Lambda^1{}_0 + \Lambda^1{}_1 v\right)t \tag{2.13}$$

or

$$\Lambda^1{}_0 = -\Lambda^1{}_1 v . \tag{2.14}$$

The four equations can now be solved with the result,

$$\begin{aligned} \Lambda^0{}_0 &= \Lambda^1{}_1 = \gamma , \\ \Lambda^1{}_0 &= \Lambda^0{}_1 = -v\gamma , \\ \Lambda^2{}_2 &= \Lambda^3{}_3 = 1 , \end{aligned} \tag{2.15}$$

where

$$\gamma \equiv (1 - v^2)^{-1/2} \equiv \cosh\theta, \qquad v\gamma \equiv \sinh\theta, \qquad v \equiv \tanh\theta . \tag{2.16}$$

So

$$\begin{aligned} x'^0 &= x^0 \cosh\theta - x^1 \sinh\theta , \\ x'^1 &= -x^0 \sinh\theta + x^1 \cosh\theta , \\ x'^2 &= x^2, x'^3 = x^3 . \end{aligned} \tag{2.17}$$

The combination of two boosts in the same direction, say v_1 and v_2, corresponds to $\theta = \theta_1 + \theta_2$. A boost in an arbitrary direction with the *primed* axis having velocity $\boldsymbol{v} = (v^1, v^2, v^3)$ relative to the *unprimed* is

$$\begin{aligned} \Lambda^0{}_0 &= \gamma , \\ \Lambda^0{}_j &= \Lambda^j{}_0 = -v^j\gamma , \\ \Lambda^j{}_k &= \Lambda^k{}_j = \delta^j_k + (\gamma - 1)v^j v^k/\boldsymbol{v}^2 . \end{aligned} \tag{2.18}$$

For a spatial rotation, say in the x-y plane, the transformation for a positive rotation about the common z-axis is

$$\begin{aligned} x'^1 &= x^1 \cos\omega + x^2 \sin\omega , \\ x'^2 &= -x^1 \sin\omega + x^2 \cos\omega , \\ x'^0 &= x^0, \quad x'^3 = x^3 . \end{aligned} \tag{2.19}$$

Transformation of vectors according to either of the above, or a product of them, preserves the invariance of the interval $d\tau^2$. For convenience they can be written in matrix form as

$$\Lambda \equiv \begin{pmatrix} \cosh\theta & -\sinh\theta & 0 & 0 \\ -\sinh\theta & \cosh\theta & 0 & 0 \\ 0 & 0 & 1 & 0 \\ 0 & 0 & 0 & 1 \end{pmatrix}, \tag{2.20}$$

$$R \equiv \begin{pmatrix} 1 & 0 & 0 & 0 \\ 0 & \cos\omega & \sin\omega & 0 \\ 0 & -\sin\omega & \cos\omega & 0 \\ 0 & 0 & 0 & 1 \end{pmatrix}. \tag{2.21}$$

2.2.2 *Covariant vectors*

Two contravariant Lorentz vectors such as

$$A'^{\mu} \equiv (A^0, A^1, A^2, A^3) \tag{2.22}$$

and B'^{μ} may be used to create a *scalar* product (Lorentz scalar)

$$A' \cdot B' \equiv \eta_{\mu\nu} A'^{\mu} B'^{\nu} = \eta_{\mu\nu} \Lambda^{\mu}{}_{\alpha} \Lambda^{\nu}{}_{\beta} A^{\alpha} B^{\beta} = \eta_{\alpha\beta} A^{\alpha} B^{\beta} \equiv A \cdot B\,. \tag{2.23}$$

Because of the minus signs in the Minkowski metric we have

$$A \cdot B = A^0 B^0 - \boldsymbol{A} \cdot \boldsymbol{B}\,, \tag{2.24}$$

and the *covariant* Lorentz vector is defined by

$$A_{\mu} \equiv (A^0, -A^1, -A^2, -A^3)\,. \tag{2.25}$$

A *covariant* Lorentz vector is obtained from its contravariant dual by the process of lowering indices with the metric tensor,

$$A_{\mu} = \eta_{\mu\nu} A^{\nu}\,. \tag{2.26}$$

Conversely, raising of indices is achieved by

$$A'^{\mu} = \eta'^{\mu\nu} A_{\nu}\,. \tag{2.27}$$

It is straightforward to show that

$$\eta^{\mu\alpha} \eta_{\alpha\nu} \equiv \eta^{\mu}_{\nu} = \delta^{\mu}_{\nu}\,, \tag{2.28}$$

where

$$\delta^{\mu}_{\nu} = \begin{cases} 1\,, & \text{if } \mu = \nu\,, \\ 0\,, & \text{otherwise}\,, \end{cases} \tag{2.29}$$

is the Kroneker delta. It follows that

$$\eta_{\mu\nu} = \eta^{\mu\nu}\,. \tag{2.30}$$

The Lorentz transformation for a covariant vector is written in analogy with that of a contravariant vector:

$$A'_\mu = \Lambda_\mu{}^\nu A_\nu \,. \tag{2.31}$$

To obtain the elements of $\Lambda_\mu{}^\nu$ we write the above in two different ways,

$$\eta_{\mu\beta}\Lambda^\beta{}_\alpha A^\alpha = \eta_{\mu\beta}A'^\beta = A'_\mu = \Lambda_\mu{}^\nu A_\nu = \Lambda_\mu{}^\nu \eta_{\nu\alpha}A^\alpha \,. \tag{2.32}$$

This holds for arbitrary A^μ so

$$\Lambda_\mu{}^\nu = \eta_{\mu\alpha}\Lambda^\alpha{}_\beta \eta^{\beta\nu} \,. \tag{2.33}$$

Using (2.28) in the above we get the inverse relationship

$$\Lambda^\mu{}_\nu = \eta^{\mu\alpha}\Lambda_\alpha{}^\beta \eta_{\beta\nu} \,. \tag{2.34}$$

Multiplying (2.33) by $A^\mu{}_\sigma$, summing on μ, and employing the fundamental condition of invariance of the proper time (2.9) we find

$$\Lambda^\mu{}_\sigma \Lambda_\mu{}^\tau = \delta^\tau_\sigma \,. \tag{2.35}$$

We can now invert (2.4) and find that $\Lambda_\mu{}^\nu$ is the inverse Lorentz transformation,

$$x^\mu = \Lambda_\nu{}^\mu x'^\nu \,. \tag{2.36}$$

The elements of the inverse transformation are given in terms of (2.15) or (2.18) by (2.33). We have

$$\begin{aligned} \Lambda_0{}^0 &= \Lambda_1{}^1 = \gamma \,, \\ \Lambda_1{}^0 &= \Lambda_0{}^1 = v\gamma \,, \\ \Lambda_2{}^2 &= \Lambda_3{}^3 = 1 \,. \end{aligned} \tag{2.37}$$

A boost in an arbitrary direction with the primed axis having velocity $\boldsymbol{v} = (v^1, v^2, v^3)$ relative to the unprimed is

$$\begin{aligned} \Lambda_0{}^0 &= \gamma \,, \\ \Lambda_0{}^j &= \Lambda_j{}^0 = v^j\gamma \,, \\ \Lambda_j{}^k &= \Lambda_k{}^j = \delta^j_k + (\gamma - 1)v^j v^k/\boldsymbol{v}^2 \,. \end{aligned} \tag{2.38}$$

The *four-velocity* is a vector of particular interest and defined as

$$u^\mu = \frac{dx^\mu}{d\tau} \,. \tag{2.39}$$

Because $d\tau$ is an invariant scalar and dx^μ is a vector, u^μ is obviously a contravariant vector. From the expression for the invariant interval we have

$$d\tau = \sqrt{1 - \boldsymbol{v}^2}\, dt, \qquad \boldsymbol{v} \equiv \frac{d\boldsymbol{r}}{dt} \,, \tag{2.40}$$

with $\boldsymbol{r} = (x^1, x^2, x^3)$; it therefore follows that

$$u^0 \equiv \frac{dt}{d\tau} = \gamma, \qquad u^i \equiv \frac{dx^i}{d\tau} = \frac{dx^i}{dt}\frac{dt}{d\tau} = v^i\gamma \,, \tag{2.41}$$

or

$$u^\mu = \gamma(1, v^1, v^2, v^3), \qquad u_\mu = \gamma(1, -v^1, -v^2, -v^3), \qquad u^\mu u_\mu = 1\,. \tag{2.42}$$

The transformation of a tensor under a Lorentz transformation follows from (2.5) and (2.31) according to the position of the indices; for example,

$$T'^{\mu\nu} = \Lambda^\mu_{\ \alpha}\Lambda^\nu_{\ \beta}T^{\alpha\beta}\,. \tag{2.43}$$

We note that according to (2.9), the Minkowski metric $\eta^{\mu\nu}$ is a tensor; moreover, it has the same constant form in every Lorentz frame.

2.2.3 *Energy and momentum*

The relativistic analogue of Newton's law $F = ma$ is

$$F^\mu = m\frac{d^2x^\mu}{d\tau} \tag{2.44}$$

and the four-momentum is

$$p^\mu = m\frac{dx^\mu}{d\tau}\,. \tag{2.45}$$

Hence, from (2.39) and (2.40)

$$\begin{aligned} p^0 \equiv E &= m\gamma\,, \\ \boldsymbol{p} &= m\gamma\boldsymbol{v}\,. \end{aligned} \tag{2.46}$$

2.2.4 *Energy-momentum tensor of a perfect fluid*

A perfect fluid is a medium in which the pressure is isotropic in the rest frame of each fluid element, and shear stresses and heat transport are absent. If at a certain point the velocity of the fluid is $\boldsymbol{v}$, an observer with this velocity will observe the fluid in the neighborhood as isotropic with an energy density ϵ and pressure p. In this local frame the energy-momentum tensor is

$$T'^{\mu\nu} \equiv \begin{pmatrix} \epsilon & 0 & 0 & 0 \\ 0 & p & 0 & 0 \\ 0 & 0 & p & 0 \\ 0 & 0 & 0 & p \end{pmatrix}\,. \tag{2.47}$$

As viewed from an arbitrary frame, say the laboratory system, let this fluid element be observed to have velocity $\boldsymbol{v}$. According to (2.36) we obtain the transformation

$$T^{\mu\nu} = \Lambda^\mu_{\ \alpha}\Lambda^\nu_{\ \beta}T'^{\alpha\beta}\,. \tag{2.48}$$

The elements of the transformation are given by (2.37) in the case that the fluid element is moving with velocity v along the laboratory x-axis, or by (2.38) if it has the general velocity $\boldsymbol{v}$. It is easy to check that in the arbitrary frame

$$T^{\mu\nu} = -p\eta^{\mu\nu} + (p+\epsilon)u^\mu u^\nu \tag{2.49}$$

and reduces to the diagonal form above when $v = 0$. We have used the four-velocity defined above by (2.41). Relative to the laboratory frame it is the four-velocity of the fluid element.

2.2.5 *Light cone*

For vanishing proper time intervals, $d\tau = 0$ given by (2.2) defines a double cone in the four-dimensional space x^μ with the time axis as the axis of the cone. Events separated from the vertex event for which the proper time, (or invariant interval) vanishes ($d\tau = 0$), are said to have null separation. They can be connected to the event at the vertex by a light signal. Events separated from the vertex by a real interval $d\tau^2 > 0$ can be connected by a subluminal signal—a material particle can travel from one event to the other. An event for which $d\tau^2 < 0$ refers to an event outside the two cones; a light signal cannot join the vertex event to such an event. Therefore, events in the cone with t greater than that of the vertex of the cone lie in the future of the event at the vertex, while events in the other cone lie in its past. Events lying outside the cone are not causally connected to the vertex event.

2.3 Scalars, Vectors, and Tensors in Curvilinear Coordinates

In the last section we dealt with inertial frames of reference in flat spacetime. We now wish to allow for curvilinear coordinates. Our scalars, vectors, and tensors now refer to a point in spacetime. Their components refer to the reference frame at that point.

A scalar field $S(x)$ is a function of position, but its value does not depend on the coordinate system. An example is the temperature as registered on thermometers located in various rooms in a house. Each registered temperature may be different, and therefore is a function of position, but independent of the coordinates used to specify the locations:

$$S'(x') = S(x). \tag{2.50}$$

A vector is a quantity whose components change under a coordinate transformation. One important vector is the displacement vector between adjacent points. Near the point x^μ we consider another, $x^\mu + dx^\mu$. The four displacements dx^μ are the components of a vector. Choose units so that time and distance are measured in the same units ($c = 1$). In Cartesian coordinates we can write the *invariant interval* $d\tau$ of the Special Theory of Relativity, sometimes called the *proper time*, as

$$d\tau^2 = (dx^0)^2 - (dx^1)^2 - (dx^2)^2 - (dx^3)^2. \tag{2.51}$$

Under a coordinate transformation from these rectilinear coordinates to arbitrary coordinates, $x^\mu \to x'^\mu$, we have (from the rules of partial differentiation)

$$dx'^\mu = \frac{\partial x'^\mu}{\partial x^\nu} dx^\nu . \tag{2.52}$$

As before, repeated indices are summed. We can also write the inverse of the above equation and substitute for the spacetime differentials in the invariant interval to obtain an equation of the form

$$d\tau^2 = g_{\mu\nu} dx^\mu dx^\nu , \tag{2.53}$$

where the $g_{\mu\nu}$ are defined in terms of products of the partial derivatives of the coordinate transformation.

Depending on the nature of the coordinate system, say rectilinear, oblique, or curvilinear, or on the presence of a gravitational field, the invariant interval may involve bilinear products of different dx^μ, and the $g_{\mu\nu}$ will be functions of position and time. The $g_{\mu\nu}$ are field quantities—the components of a tensor called the *metric tensor*. Because the $g_{\mu\nu}$ appear in a quadratic form (2.53), we may take them to be symmetric:

$$g_{\mu\nu} = g_{\nu\mu} . \tag{2.54}$$

In regions of spacetime for which the rectilinear system of the Special Theory of Relativity holds, the metric tensor $g_{\mu\nu}$ is equal to the Minkowski tensor (2.7). In fact, as we shall see, Special Relativity holds *locally* anywhere at any time. We shall refer to reference frames in which the metric is given by the Minkowski tensor as *Lorentz frames*.

The invariant interval or proper time $d\tau$ is real for a timelike interval and imaginary for a spacelike.[5] The notation *proper time* is seen to be appropriate because, when two events occur at the same *space* point, what remains of the invariant interval is dt.

Any four quantities A^μ that transform as dx^μ comprise a *contravariant vector*

$$A'^\mu = \frac{\partial x'^\mu}{\partial x^\nu} A^\nu , \tag{2.55}$$

and

$$g_{\mu\nu} A^\mu A^\nu \equiv A^2 \tag{2.56}$$

is its invariant squared length. It is obviously invariant under the same transformations that leave (2.51) invariant because the four quantities A^μ form a four-vector like dx^μ.

A covariant vector can be obtained through the process of *lowering* indices with the metric tensor:

$$A_\mu = g_{\mu\nu} A^\nu . \tag{2.57}$$

---

[5]The opposite convention $ds^2 = -d\tau^2$ could also be employed. It is often referred to as the line element.

In terms of this vector, the magnitude equation (2.56) can be written as

$$A_\mu A^\mu = A^2 . \tag{2.58}$$

Let A^μ and B^μ be distinct contravariant vectors. Then so is $A^\mu + \lambda B^\mu$ for all finite λ. The quantity

$$g_{\mu\nu}(A^\mu + \lambda B^\mu)(A^\nu + \lambda B^\nu)$$

is the invariant squared length. Because this is true for all λ, the coefficient of each power of λ is also an invariant; for the linear term we find

$$g_{\mu\nu}(A^\mu B^\nu + B^\mu A^\nu) = 2g_{\mu\nu}A^\mu B^\nu , \tag{2.59}$$

where we have used the symmetry of $g_{\mu\nu}$. Thus, we obtain the invariant scalar product of two vectors:

$$g_{\mu\nu}A^\mu B^\nu = A_\nu B^\nu = A \cdot B . \tag{2.60}$$

To derive the transformation law for a covariant vector use the fact, just proven, that $A_\mu B^\mu$ is a scalar. Then using the law of transformation of a contravariant vector (2.55), we have

$$A'_\mu B'^\mu = A_\alpha B^\alpha = A_\alpha \frac{\partial x^\alpha}{\partial x'^\mu} B'^\mu , \tag{2.61}$$

where A'_μ is the same vector as A_μ but referred to the primed reference frame. From the above equation it follows that

$$\left(A'_\mu - \frac{\partial x^\alpha}{\partial x'^\mu} A_\alpha\right) B'^\mu = 0 . \tag{2.62}$$

Because B^μ is any vector, the quantity in brackets must vanish; thus we have the law of transformation of a covariant vector,

$$A'_\mu = \frac{\partial x^\nu}{\partial x'^\mu} A_\nu . \tag{2.63}$$

Compare this transformation law with that of (2.55).

Let the determinant of $g_{\mu\nu}$ be g,

$$g = \det|g_{\mu\nu}| . \tag{2.64}$$

As long as g does not vanish, the equations (2.57) can be inverted. Let the coefficients of the inverse be called $g^{\mu\nu}$. Then find

$$A^\nu = g^{\nu\mu} A_\mu . \tag{2.65}$$

Multiply (2.57) by $g^{\alpha\mu}$ and sum on μ with the result

$$A^\alpha = g^{\alpha\mu} A_\mu = g^{\alpha\mu} g_{\mu\nu} A^\nu , \tag{2.66}$$

or

$$(g^{\alpha\mu} g_{\mu\nu} - \delta^\alpha_\nu) A^\nu = 0 , \tag{2.67}$$

where δ^α_ν is the Kroneker delta. Because this equation holds for any vector, we have

$$g^\alpha_\beta \equiv g^{\alpha\mu} g_{\mu\beta} = \delta^\alpha_\beta \,. \tag{2.68}$$

The two g's, one with subscripts, the other with superscripts, are inverses. In the same way as $g_{\mu\nu}$ can be used to lower an index, $g^{\mu\nu}$ can be used to raise one. Both are symmetric;

$$g_{\mu\nu} = g_{\nu\mu}, \quad g^{\mu\nu} = g^{\nu\mu} \,. \tag{2.69}$$

The derivative of a scalar field $S(x) = S'(x')$ with respect to the components of a contravariant position vector yields a covariant vector field and, vice versa:

$$\frac{\partial S}{\partial x'^\mu} = \frac{\partial x^\nu}{\partial x'^\mu} \frac{\partial S}{\partial x^\nu} \,. \tag{2.70}$$

Accordingly, we shall sometimes use the abbreviations

$$\partial_\mu \equiv \frac{\partial}{\partial x^\mu} \text{ and } \partial^\mu \equiv \frac{\partial}{\partial x_\mu} \,, \tag{2.71}$$

especially in writing Lagrangians of fields. In relativity it is also useful to have an even more compact notation for the coordinate derivative—the "comma subscript":

$$S_{,\mu} \equiv \frac{\partial S}{\partial x^\mu} \,. \tag{2.72}$$

The d'Alembertian,

$$\Box = \partial_\mu \partial^\mu \,, \tag{2.73}$$

is manifestly a scalar.

Tensors are similar to vectors, but with more than one index. A simple tensor is one formed from the product of the components of two vectors, $A^\mu B^\nu$. But this is special because of the relationships between its components. A general tensor of the second rank can be formed by a sum of such products:

$$T^{\mu\nu} = A^\mu B^\nu + C^\mu D^\nu + \cdots \,. \tag{2.74}$$

The superscripts can be lowered as with a vector, either one index, or both,

$$T_\mu{}^\nu = g_{\mu\alpha} T^{\alpha\nu} \,, \quad T^\nu_\mu = T^{\nu\alpha} g_{\alpha\mu} \,, \quad T_{\mu\nu} = g_{\mu\alpha} g_{\nu\beta} T^{\alpha\beta} \,. \tag{2.75}$$

Similarly, we may have tensors of higher rank, either contravariant with respect to all indices, or covariant, or mixed. The position of the indices on the mixed tensor (the lower to the left or right of the upper) refers to the position of the index that was lowered. If $T^{\mu\nu}$ is symmetric, then $T^\mu_\nu = T_\nu{}^\mu$ and it is unimportant to keep track of the position of the index that has been lowered (or raised). But if $T^{\mu\nu}$ is antisymmetric, then the two orderings differ by a sign.

If two of the indices on a tensor, one a superscript the other a subscript, are set equal and summed, the rank is reduced by two. This process is called *contraction*. If it is done on a second-rank mixed tensor, the result is a scalar,

$$S = T^\mu_\mu = T_\mu{}^\mu \,. \tag{2.76}$$

When $T^{\mu\nu}$ is antisymmetric, the contractions $T_{\mu}{}^{\mu}$ and T^{μ}_{μ} are identically zero.

The test of tensor character is whether the object in question transforms under a coordinate transformation in the obvious generalization of a vector. For example,

$$T'^{\mu}_{\ \nu} = \frac{\partial x'^{\mu}}{\partial x^{\alpha}} \frac{\partial x^{\beta}}{\partial x'^{\nu}} T^{\alpha}_{\beta} \tag{2.77}$$

is a tensor.

In general, we deal with curved spacetime in General Relativity. We must therefore deal with curvilinear coordinates. Vectors and tensors at a point in such a spacetime have components referring to the axis at that point. The components will change according to the above laws, depending on the way the axes change at that point. Therefore, the metric tensors $g_{\mu\nu}$, $g^{\mu\nu}$ cannot be constants. They are field quantities which vary from point to point. As we shall see, they can be referred to collectively as the gravitational field. Because the formalism of this section is expressed by local equations, it holds in curved spacetime, for curved spacetime is flat in a sufficiently small locality.

Because the derivative of a scalar field is a vector (2.70), one might have thought that the derivative of a vector field is a tensor. However, by checking the transformation properties one finds that this supposition is not true.

We have referred invariably to the $g_{\mu\nu}$ as tensors. Now we show that this is so. Let A^{μ}, B^{ν} be arbitrary vector fields, and consider two coordinate systems such that the same point P has the coordinates x^{μ} and x'^{μ} when referred to the two systems, respectively. Then we have

$$g'_{\alpha\beta} A'^{\alpha} A'^{\beta} = g_{\mu\nu} A^{\mu} A^{\nu} = g_{\mu\nu} \frac{\partial x^{\mu}}{\partial x'^{\alpha}} \frac{\partial x^{\nu}}{\partial x'^{\beta}} A'^{\alpha} A'^{\beta}. \tag{2.78}$$

Because this holds for arbitrary vectors, we find

$$g'_{\alpha\beta} = g_{\mu\nu} \frac{\partial x^{\mu}}{\partial x'^{\alpha}} \frac{\partial x^{\nu}}{\partial x'^{\beta}}, \tag{2.79}$$

which, by comparison with (2.63), shows that $g_{\mu\nu}$ is a covariant tensor. Similarly $g^{\mu\nu}$ is a contravariant tensor:

$$g'^{\alpha\beta} = g^{\mu\nu} \frac{\partial x'^{\alpha}}{\partial x^{\mu}} \frac{\partial x'^{\beta}}{\partial x^{\nu}}. \tag{2.80}$$

These are called the *fundamental tensors*. Of course, the above tensor character of the metric is precisely what is required to make the square of the interval $d\tau^2$ of (2.53) an invariant, as is trivially verified.

Mixed tensors of arbitrary rank transform, for each index, according to the transformation laws (2.55, 2.63) depending on whether the index is a superscript or a subscript, as can be derived in obvious analogy to the above manipulations.

Tensors and tensor algebra are very powerful techniques for carrying the consequences discovered in one frame to another. That the linear combination of tensors of the same rank and arrangement of upper and lower indices is also a tensor; that the direct product of two tensors of the same or different rank and arrangement of indices, $A^{\mu\cdots}_{\alpha\cdots} B^{\nu\cdots}_{\cdots} = T^{\mu\cdots\nu\cdots}_{\alpha\cdots}$ is also a tensor; and that contraction (defined above)

of a pair of indices, one upper, one lower produces a tensor of rank reduced by two—are all easy theorems that we do not need to prove, but only note in passing. Of particular note, if the difference of two tensors of the same transformation rule vanishes in one frame, then it vanishes in all (i.e., the two tensors are equal in all frames).

2.4 Principle of Equivalence of Inertia and Gravitation

> "The possibility of explaining the numerical equality of inertia and gravitation by the unity of their nature gives to the general theory of relativity, according to my conviction, such a superiority over the conceptions of classical mechanics, that all the difficulties encountered in development must be considered as small in comparison." *A. Einstein* [3]

Eötvös established that all bodies have the same ratio of inertial to gravitational mass with high precision [11]. With an appropriate choice of units, the two masses are equal for all bodies to the accuracy established for the ratio. One might have expected such conceptually different properties, one having to do with inertia to motion (m_I), the other with "charge" (m_G), in an expression of mutual attraction between bodies, to be entirely different. The relation between the force exerted by the gravitational attraction of a body of mass M at a distance R upon the object, and the acceleration imparted to it are expressed by Newton's equation, valid for weak fields and small material velocities:

$$m_I a = G\frac{m_G M}{R^2}\,. \tag{2.81}$$

Einstein reasoned that the near equality of two such different properties must be more than mere coincidence and that inertial and gravitational masses must be exactly equal: $m_I = m_G = m$. The mass drops out! In that case all bodies experience precisely the same acceleration in a gravitational field, as was presaged by Galileo's experiments centuries earlier. For all other forces that we know, the acceleration is inverse to the mass.

The equivalence of inertial and gravitational mass is established to high accuracy for atomic and nuclear binding energies.[6] Moreover, as a result of very careful lunar laser-ranging experiments, the Earth and moon are found to fall with equal acceleration toward the Sun to a precision of almost 1 part in 10^{13}, better than the most accurate Eötvös-type experiments on laboratory bodies. This exceedingly important test involving bodies of different gravitational binding was conceived by Nordtvedt [12]. The essentially null result establishes the so-called *strong* statement of equivalence of inertial and gravitational mass: Free bodies—no matter

[6]Eötvös' experiments on such diverse media as wood, platinum, copper, glass, and other materials involve different molecular, atomic, and nuclear binding energies and different ratios of neutrons and protons.

their nature or constituents, nor how much or little those constituents are bound, nor by what force—all move in the spacetime of an arbitrary gravitational field as if they were identical test particles! *Because their motion has nothing to do with their nature, it evidently has to do with the nature of spacetime.*

Einstein felt certain that a deep meaning was attached to the equivalence; "The experimentally known matter independence of the acceleration of fall is .... a powerful argument for the fact that the relativity postulate has to be extended to coordinate systems which, relative to each other, are in non-uniform motion" [13]. This conviction led him to the formulation of the *equivalence principle*. The equivalence principle provides the link between the physical laws as we discern them in our laboratories and their form under any circumstance in the universe—more precisely, in arbitrarily strong and varying gravitational fields. It also provides a tool for the development of the theory of gravitation itself, as we shall see throughout the sequel.

The universe is populated by massive objects moving relative to one another. The gravitational field may be arbitrarily changing in time and space. However, the presence of gravity cannot be detected in a sufficiently small reference frame falling freely with a particle under no influence other than gravity. The particle will remain at rest in such a frame. It is a *local inertial frame*. A local inertial frame and a *local Lorentz frame* are synonymous. The laws of Special Relativity hold in inertial frames and therefore in the neighborhood of a *freely falling frame*. In this way the relativity principle is extended to arbitrary gravitational fields.

Associated with a given spacetime event there are an infinity of locally inertial frames related by Lorentz transformations. All are equivalent for the description of physical phenomena in a sufficiently small region of spacetime. So we arrive at a statement of the equivalence principle: *At every spacetime point in an arbitrary gravitational field (meaning anytime and anywhere in the universe), a local inertial (Lorentz) frame can be chosen so that the laws of physics take on the form they have in Special Relativity.* This is the meaning of the equality of inertial and gravitational masses that Einstein sought. The restricted validity of inertial frames to small localities of any event suggested the very fruitful analogy with local flatness on a curved surface.

Einstein went further than the above statement of the equivalence principle. He spoke of the laws of nature rather than just the laws of physics. It seems entirely plausible that the extension is true, but we deal here only with physics.

The equivalence principle has great power. It is the instrument by which all the special relativistic laws of physics—valid in a gravity-free universe—can be generalized to a gravity-filled universe. We shall see how Einstein was able to give dynamic meaning to the spacetime continuum as an integral part of the physical world quite unlike the conception of an absolute spacetime in which the rest of physical processes take place.

2.4.1 *Photon in a gravitational field*

Employing the conservation of energy and Newtonian physics, Einstein reasoned that the gravitational field acts on photons. Let a photon be emitted from z_1 vertically to z_2, and only for simplicity, let the field be uniform. A device located at z_2 converts its energy on arrival to a particle of mass m with perfect efficiency. The particle drops to z_1 where its energy is now $m + mgh$, where g is the acceleration due to the uniform field. A device at z_1 converts it into a photon of the same energy as possessed by the particle. The photon again is directed to z_2. If the original (and each succeeding photon) does not lose energy $(h\nu)gh$ in climbing the gravitational field equal to the energy gained by the particle in dropping in the field, we would have a device that creates energy. By the law of conservation of energy Einstein discovered the gravitational redshift, commonly designated by the factor z and equal in this case to gh. The shift in energy of a photon by falling (in this case blue-shifted) in the Earth's gravitational field has been directly confirmed in an experiment performed by Pound and Rebka [14].

In the above discussion the equivalence principle entered when the photon's inertial mass $(h\nu)$ was used also as its gravitational mass in computing the gravitational work. One can also see the role of the equivalence principle by considering a pulse of light emitted over a distance h along the axis of a spaceship in uniform acceleration g in outer space. The time taken for the light to reach the detector is $t = h$ (we use units $G = c = 1$). The difference in velocity of the detector acquired during the light travel time is $v = gt = gh$, the Doppler shift z in the detected light. This experiment, carried out in the gravity-free environment of a spaceship whose rockets produce an acceleration g, must yield the same result for the energy shift of the photon in a uniform gravitational field g according to the equivalence principle. The Pound–Rebka experiment can therefore be regarded as an experimental proof of the equivalence principle.

We may regard a radiating atom as a clock, with each wave crest regarded as a tick of the clock. Imagine two identical atoms situated one at some height above the other in the gravitational field of the Earth. Since, by dropping in the gravitational field, the light is blue-shifted when compared to the radiation of an identical atom (clock) at the bottom, the clock at the top is seen to be running faster than the one at the bottom. Therefore, identical clocks, stationary with respect to the Earth, run at different rates according to their different heights above the Earth. Time flows at different rates in different gravitational fields.

The trajectory of photons is also bent by the gravitational field. Imagine a freely falling elevator in a constant gravitational field. Its walls constitute an inertial frame as guaranteed by the equivalence principle. Therefore, a photon (as for a free particle) directed from one wall to the opposite along a path parallel to the floor will arrive at the other wall at the same height from which it started. But relative to the Earth, the elevator has fallen during the traversal time. Therefore the photon has been deflected toward the Earth and follows a curved path as observed from a frame fixed on the Earth.

2.4.2 *Tidal gravity*

Einstein predicted that a clock near a massive body would run more slowly than an identical distant clock. In doing so he arrived at a hint of the deep connection of the structure of spacetime and gravity. Two parallel straight lines never meet in the gravity-free, flat spacetime of Minkowski. A single inertial frame would suffice to describe all of spacetime. In formulating the equivalence principle (knowing that gravitational fields are not uniform and constant but depend on the motion of gravitating bodies and the position where gravitational effects are experienced), Einstein understood that only in a suitably small locality of spacetime do the laws of Special Relativity hold. Gravitational effects will be observed on a larger scale. *Tidal gravity* refers to the deviation from uniformity of the gravitational field at nearby points.

These considerations led Einstein to the notion of spacetime curvature. Whatever the motion of a free body in an arbitrary gravitational field, it will follow a straight-line trajectory over any small locality as guaranteed by the equivalence principle. And in a gravity-endowed universe, free particles whose trajectories are parallel in a local inertial frame, will not remain parallel over a large region of spacetime. This has a striking analogy with the surface of a sphere on which two straight lines that are parallel over a small region *do* meet and cross. What if in fact the particles are freely falling in curved spacetime? In this way of thinking, the law that free particles move in straight lines remains true in an arbitrary gravitational field, thus obeying the principle of relativity in a larger sense. Any sufficiently small region of curved spacetime is locally flat. The paths in curved spacetime that have the property of being locally straight are called geodesics.

2.4.3 *Curvature of spacetime*

Let us now consider a thought experiment. Two nearby bodies released from rest above the Earth follow parallel trajectories over a small region of their trajectories, as we know from the equivalence principle. But if holes were drilled in the Earth through which the bodies could fall, the bodies would meet and cross at the Earth's center. So there is clearly no single Minkowski spacetime that covers a large region or the whole region containing a massive body.

Einstein's view was that spacetime curvature caused the bodies to cross, bodies that in this curved spacetime were following straight-line paths in every small locality, just as they would have done in the whole of Minkowski (flat) spacetime in the absence of gravitational bodies. The presence of gravitating bodies denies the existence of a global inertial frame. Spacetime can be flat everywhere only if there exists such a global frame. Hence, spacetime is curved by massive bodies. In their presence a test particle follows a geodesic path, one that is always locally straight. The concept of a "gravitational force" has been replaced by the curvature of spacetime, and the natural free motions of particles in it are defined by geodesics.

2.4.4 *Energy conservation and curvature*

Interestingly, the conservation of energy can also be used to inform us that spacetime is curved. Consider a static gravitational field. Let us conjecture that spacetime is flat so that the Minkowski metric holds; we will arrive at a contradiction.

Imagine the following experiment performed by observers and their apparatus at rest with respect to the gravitational field and their chosen Lorentz frame in the supposed flat spacetime of Minkowski. At a height z_1 in the field, let a monochromatic light signal be emitted upward a height h to $z_2 = z_1 + h$. Let the pulse be emitted for a specific time dt_1 during which N wavelengths (or photons) are emitted. Let the time during which they are received at z_2 be measured as dt_2. (Because the spacetime is assumed to be described by the Minkowski metric and the source and receiver are at rest in the chosen frame, the proper times and coordinate times are equal.)

Because the field in the above experiment is static, the path in the z-t plane will have the same shape for both the beginning and ending of the pulse (as for each photon) as they trace their path in the Minkowski space we postulate to hold. The trajectories will not be lines at 45 degrees because of the field, but the curved paths will be congruent; a translation in time will make the paths lie one upon the other. Therefore $d\tau_2 = dt_2 = dt_1 = d\tau_1$ will be measured at the stationary detector if spacetime is Minkowskian. In this case, the frequency (and hence the energy received at z_2) is the same as that sent from z_1. But this cannot be. The photons comprising the signal must lose energy in climbing the gravitational field (see Section 2.4.1).

The conjecture that spacetime in the presence of a gravitational field is Minkowskian must therefore be false. We conclude that the presence of the gravitational field has caused spacetime to be curved. Such a line of reasoning was first conceived by Schild [15, 16, 17].

2.5 Gravity

> "I was sitting in a chair at the patent office at Bern when all of a sudden a thought occurred to me: 'If a person falls freely he will not feel his own weight.' I was startled. This simple thought had a deep impression on me. It impelled me toward a theory of gravitation." *A. Einstein* [18]

Massive bodies generate curvature. Because the galaxies, stars, and other bodies are in motion, the curvature of spacetime is everywhere changing. For this reason there is no "prior geometry". There are no immutable reference frames to which events in spacetime can be referred. Indeed, the changing geometry of spacetime and of the motion and arrangement of mass-energy in spacetime are inseparable parts of the description of physical processes. This is a very different idea of space and time from that of Newton and even of the Special Theory of Relativity. We now take up the unified discussion of gravitating matter and motion.

The power of the equivalence principle in informing us so simply that spacetime must be curved by the presence of massive bodies in the universe suggests a fruitful way of beginning. Following Weinberg [19], or indeed, following the notion expressed by Einstein in the quotation above, we seek the connection between an arbitrary reference frame and a reference frame that is freely falling with a particle that is moving only under the influence of an arbitrary gravitational field. In this freely falling and therefore locally inertial frame, the particle moves in a straight line. Denote the coordinates by ξ^α. The equations of motion are

$$\frac{d^2\xi^\alpha}{d\tau^2} = 0\,, \tag{2.82}$$

and the invariant interval (or proper time) between two neighboring spacetime events expressed in this frame, from (2.6), is

$$d\tau^2 = \eta_{\alpha\beta} d\xi^\alpha d\xi^\beta. \tag{2.83}$$

The freely falling coordinates may be regarded as functions of the coordinates x^μ of any arbitrary reference frame—curvilinear, accelerated, or rotating. We seek the connection between the equations of motion in the freely falling frame and the arbitrary one which, for example, might be the laboratory frame. From the chain rule for differentiation we can rewrite (2.82) as

$$\begin{aligned} 0 &= \frac{d}{d\tau}\left(\frac{\partial\xi^\alpha}{\partial x^\mu}\frac{dx^\mu}{d\tau}\right) \\ &= \frac{\partial\xi^\alpha}{\partial x^\mu}\frac{d^2x^\mu}{d\tau^2} + \frac{\partial^2\xi^\alpha}{\partial x^\mu \partial x^\nu}\frac{dx^\mu}{d\tau}\frac{dx^\nu}{d\tau}\,. \end{aligned}$$

Multiply by $\partial x^\lambda/\partial\xi^\alpha$, and use the chain rule again to obtain

$$\frac{dx^\lambda}{dx^\mu} = \frac{\partial x^\lambda}{\partial\xi^\alpha}\frac{\partial\xi^\alpha}{\partial x^\mu} = \delta^\lambda_\mu\,. \tag{2.84}$$

The equation of motion of the particle in an arbitrary frame when the particle is moving in an arbitrary gravitational field therefore is

$$\frac{d^2x^\lambda}{d\tau^2} + \Gamma^\lambda_{\mu\nu}\frac{dx^\mu}{d\tau}\frac{dx^\nu}{d\tau} = 0\,. \tag{2.85}$$

Here $\Gamma^\lambda_{\mu\nu}$, defined by

$$\Gamma^\lambda_{\mu\nu} \equiv \frac{\partial x^\lambda}{\partial\xi^\alpha}\frac{\partial^2\xi^\alpha}{\partial x^\mu \partial x^\nu}\,, \tag{2.86}$$

is called the *affine connection*. The affine connection is symmetric in its lower indices.

The path defined by equation (2.85) is called a *geodesic*, the extremal path in the spacetime of an arbitrary gravitational field. We do not see here that it is an extremal, but this is hinted at inasmuch as it defines the same path of (2.82), the straight-line path of a free particle as observed from its freely falling frame. In the next section we will see that a geodesic path is locally a straight line.

The invariant interval (2.83) can also be expressed in the arbitrary frame by writing $d\xi^\alpha = (\partial\xi^\alpha/\partial x'^\mu)dx'^\mu$ so that

$$d\tau^2 = g_{\mu\nu}dx'^\mu dx'^\nu \tag{2.87}$$

with

$$g_{\mu\nu} = \frac{\partial\xi^\alpha}{\partial x'^\mu}\frac{\partial\xi^\beta}{\partial x'^\nu}\eta_{\alpha\beta}\,. \tag{2.88}$$

In the new and arbitrary reference frame, the second term of (2.85) causes a deviation from a straight-line motion of the particle in this frame. Therefore, the second term represents the effect of the gravitational field. (To be sure, the connection coefficients also represent any other noninertial effects that may have been introduced by the choice of reference frame, such as rotation.)

The affine connection (2.86) appearing in the geodesic equation clearly plays an important role in gravity, and we study it further. We first show that the affine connection is a nontensor, and then show how it can be expressed in terms of the metric tensor and its derivatives. In this sense the metric behaves as the gravitational potential and the affine connection as the force. Write $\Gamma^\lambda_{\mu\nu}$ expressed in (2.86) in another coordinate system x'^μ and use the chain rule several times to rewrite it:

$$\begin{aligned}
\Gamma'^\lambda_{\mu\nu} &= \frac{\partial x'^\lambda}{\partial x^\rho}\frac{\partial x^\rho}{\partial\xi^\alpha}\frac{\partial}{\partial x'^\mu}\left(\frac{\partial x^\sigma}{\partial x'^\nu}\frac{\partial\xi^\alpha}{\partial x^\sigma}\right)\\
&= \frac{\partial x'^\lambda}{\partial x^\rho}\frac{\partial x^\rho}{\partial\xi^\alpha}\left[\frac{\partial x^\sigma}{\partial x'^\nu}\frac{\partial x^\tau}{\partial x'^\mu}\frac{\partial^2\xi^\alpha}{\partial x^\tau\partial x^\sigma} + \frac{\partial^2 x^\sigma}{\partial x'^\mu\partial x'^\nu}\frac{\partial\xi^\alpha}{\partial x^\sigma}\right]\\
&= \frac{\partial x'^\lambda}{\partial x^\rho}\frac{\partial x^\tau}{\partial x'^\mu}\frac{\partial x^\sigma}{\partial x'^\nu}\Gamma^\rho_{\tau\sigma} + \frac{\partial x'^\lambda}{\partial x^\rho}\frac{\partial^2 x^\rho}{\partial x'^\mu\partial x'^\nu}\,.
\end{aligned} \tag{2.89}$$

According to the transformation laws of tensors developed in Section 2.3, the second term on the right spoils the transformation law of the affine connection. It is therefore a nontensor.

Let us now obtain the expression of the affine connection in terms of the derivatives of the metric tensor. Form the derivative of (2.79):

$$\frac{\partial}{\partial x'^\kappa}g'_{\mu\nu} = \frac{\partial}{\partial x'^\kappa}\left(g_{\rho\sigma}\frac{\partial x^\rho}{\partial x'^\mu}\frac{\partial x^\sigma}{\partial x'^\nu}\right).$$

Take the derivatives and form the following combination and find that it is equal to the above derivative:

$$\begin{aligned}
\frac{\partial g'_{\kappa\nu}}{\partial x'^\mu} + \frac{\partial g'_{\kappa\mu}}{\partial x'^\nu} - \frac{\partial g'_{\mu\nu}}{\partial x'^\kappa} &= \frac{\partial x^\tau}{\partial x'^\kappa}\frac{\partial x^\rho}{\partial x'^\mu}\frac{\partial x^\sigma}{\partial x'^\nu}\left(\frac{\partial g_{\sigma\tau}}{\partial x^\rho} + \frac{\partial g_{\rho\tau}}{\partial x^\sigma} - \frac{\partial g_{\rho\sigma}}{\partial x^\tau}\right)\\
&\quad + 2g_{\rho\sigma}\frac{\partial x^\sigma}{\partial x'^\kappa}\frac{\partial^2 x^\rho}{\partial x'^\mu\partial x'^\nu}\,.
\end{aligned}$$

Multiply this equation by $\frac{1}{2}$ and then multiply the left and right sides by the left and right sides, respectively, of the law of transformation (2.80), namely,

$$g'^{\lambda\kappa} = g^{\alpha\beta}\frac{\partial x'^\lambda}{\partial x^\alpha}\frac{\partial x'^\kappa}{\partial x^\beta}\,.$$

Use the chain rule and rename several dummy indices to obtain

$$\left\{ {\lambda \atop \mu\nu} \right\}' = \frac{\partial x'^{\lambda}}{\partial x^{\rho}} \frac{\partial x^{\tau}}{\partial x'^{\mu}} \frac{\partial x^{\sigma}}{\partial x'^{\nu}} \left\{ {\rho \atop \tau\sigma} \right\} + \frac{\partial x'^{\lambda}}{\partial x^{\rho}} \frac{\partial^2 x^{\rho}}{\partial x'^{\mu} \partial x'^{\nu}} , \tag{2.90}$$

where the prime on {} means that it is evaluated in the x'^{μ} frame and the symbol stands for

$$\left\{ {\lambda \atop \mu\nu} \right\} = \tfrac{1}{2} g^{\lambda\kappa} \left[\frac{\partial g_{\kappa\nu}}{\partial x^{\mu}} + \frac{\partial g_{\kappa\mu}}{\partial x^{\nu}} - \frac{\partial g_{\mu\nu}}{\partial x^{\kappa}} \right] . \tag{2.91}$$

This is called a *Christoffel symbol of the second kind.* It is seen to transform in exactly the same way as the affine connection (2.89). Subtract the two to obtain

$$\left[\Gamma^{\lambda}_{\mu\nu} - \left\{ {\lambda \atop \mu\nu} \right\} \right]' = \frac{\partial x'^{\lambda}}{\partial x^{\rho}} \frac{\partial x^{\tau}}{\partial x'^{\mu}} \frac{\partial x^{\sigma}}{\partial x'^{\nu}} \left[\Gamma^{\rho}_{\tau\sigma} - \left\{ {\rho \atop \tau\sigma} \right\} \right] . \tag{2.92}$$

This shows that the difference is a tensor. According to the equivalence principle, at anyplace and anytime there is a local inertial frame ξ^{α} in which the effects of gravitation are absent, the metric is given by (2.7), and $\Gamma^{\lambda}_{\mu\nu}$ vanishes (compare (2.82) and (2.85)). Because the first derivatives of the metric tensor vanish in such a local inertial system, the Christoffel symbol also vanishes. Because the difference of the affine connection and the Christoffel symbol is a tensor which vanishes in this frame, the difference vanishes in all reference frames. So everywhere we find

$$\Gamma^{\lambda}_{\mu\nu} = \left\{ {\lambda \atop \mu\nu} \right\} = \tfrac{1}{2} g^{\lambda\kappa} \left(g_{\kappa\nu,\mu} + g_{\kappa\mu,\nu} - g_{\mu\nu,\kappa} \right) . \tag{2.93}$$

We use the "comma subscript" notation introduced earlier to denote differentiation (2.72).

Sometimes it is useful to have the superscript lowered on the affine connection

$$\Gamma_{\kappa\mu\nu} = g_{\kappa\lambda} \Gamma^{\lambda}_{\mu\nu} . \tag{2.94}$$

It is equal to the Christoffel symbol of the first kind

$$\Gamma_{\kappa\mu\nu} = \left[{\kappa \atop \mu\nu} \right] = \tfrac{1}{2} \left(g_{\kappa\nu,\mu} + g_{\kappa\mu,\nu} - g_{\mu\nu,\kappa} \right) . \tag{2.95}$$

The above formulas provide a means of computing the affine connection from the derivatives of the metric tensor and will prove very useful. It is trivial from the above to prove that

$$\Gamma_{\kappa\mu\nu} + \Gamma_{\mu\kappa\nu} = g_{\mu\kappa,\nu} . \tag{2.96}$$

2.5.1 *Mathematical definition of local Lorentz frames*

Spacetime is curved globally by the massive bodies in the universe. Therefore, we need to define mathematically the meaning of "local Lorentz frame". In a rectilinear Lorentz frame the metric tensor is $\eta_{\mu\nu}$ (2.7). Therefore, in the local

region around an event P (a point in the four-dimensional spacetime continuum), the metric tensor, its coordinate derivatives, and the affine connection have the following values:

$$g_{\mu\nu}(P) = \eta_{\mu\nu}, \quad g_{\mu\nu,\alpha}(P) = 0, \quad \Gamma^{\lambda}_{\mu\nu}(P) = 0. \tag{2.97}$$

The third of these equations follows from the second and from (2.93). All local effects of gravitation disappear in such a frame. The geodesic equation (2.85) defining the path followed by a free particle in an arbitrary gravitational field becomes locally the equation of a uniform straight line, in accord with the equivalence principle.

Of course, physical measurements are always subject to the precision of the measuring devices. The extent of the local region around P, in which the above equations will hold and in which spacetime is said to be flat, will depend on the accuracy of the devices and therefore their ability to detect deviations from the above conditions as one measures further from P.

2.5.2 *Geodesics*

In the Special Theory of Relativity a free particle remains at rest or moves with constant velocity in a straight line. A straight line is the shortest distance between two points in Euclidean three-dimensional space. In Minkowski spacetime a straight line is the longest interval between two events, as we shall shortly see. Both situations are covered by saying that a straight line is an extremal path between two points. We shall show that in an arbitrary gravitational field, a particle moving under the influence of only gravity, follows a path that is, in the sense that we shall define, the straightest line possible in curved spacetime.

We first show that a straight-line path between two events in Minkowski spacetime maximizes the proper time. This is easily proved. Orient the axis so that the two events marking the ends of the path, A and B, lie on the t-axis with coordinates $(0, 0, 0, 0)$ and $(T, 0, 0, 0)$, and consider an alternate path in the t-x plane that consists of two straight-line segments that pass from A to B through $(T/2, R/2, 0, 0)$. The proper time as measured on the second path is

$$\tau = 2\sqrt{(T/2)^2 - (R/2)^2} = \sqrt{T^2 - R^2}. \tag{2.98}$$

For any finite R, τ is smaller than the proper time along the straight-line path from A to B, namely, T. Therefore, the straight-line path is a maximum in proper time.

We have referred to the equation of motion of a particle moving freely in an arbitrary gravitational field (2.85) as a geodesic equation. In general, a geodesic that is not null (a null geodesic, as is the case for light, has $d\tau = 0$), is the extremal path of

$$\int_A^B d\tau \tag{2.99}$$

where A and B refer to spacetime events on the geodesic. To prove this result, let $x^{\mu}(\tau)$ denote the coordinates along the geodesic path, parameterized by the proper

time, and let $x^\mu(\tau) + \delta x^\mu(\tau)$ denote a neighboring path with the same end points, A to B. From

$$d\tau^2 = g_{\mu\nu} dx^\mu dx^\nu \,, \tag{2.100}$$

we have to first order in the variation,

$$\begin{aligned} 2d\tau\, \delta(d\tau) &= \delta g_{\mu\nu} dx^\mu dx^\nu + 2 g_{\mu\nu} dx^\mu \delta(dx^\nu) \\ &= dx^\mu dx^\nu g_{\mu\nu,\lambda} \delta x^\lambda + 2 g_{\mu\nu} dx^\mu d(\delta x^\nu) \,. \end{aligned} \tag{2.101}$$

Recalling the four-velocity, $u^\mu = dx^\mu/d\tau$, we have

$$\delta(d\tau) = \left(\tfrac{1}{2} u^\mu u^\nu g_{\mu\nu,\lambda} \delta x^\lambda + g_{\mu\lambda} u^\mu \frac{d}{d\tau} \delta x^\lambda\right) d\tau \,. \tag{2.102}$$

Thus

$$\delta \int_A^B d\tau = \int_A^B \left[\tfrac{1}{2} u^\mu u^\nu g_{\mu\nu,\lambda} - \frac{d}{d\tau}\left(g_{\mu\lambda} u^\mu\right)\right] \delta x^\lambda \, d\tau \tag{2.103}$$

where an integration by parts in the second term was performed. Because the variation of the path δx^λ is arbitrary save for its end points being zero, we obtain as the extremal condition,

$$\frac{d}{d\tau}\left(g_{\mu\lambda} u^\mu\right) - \tfrac{1}{2} u^\mu u^\nu g_{\mu\nu,\lambda} = 0 \,. \tag{2.104}$$

The first and second terms can be rewritten:

$$\begin{aligned} \frac{d}{d\tau}\left(g_{\mu\lambda} u^\mu\right) &= g_{\mu\lambda} \frac{du^\mu}{d\tau} + g_{\mu\lambda,\nu} u^\mu u^\nu \,, \\ g_{\mu\lambda,\nu} u^\mu u^\nu &= \tfrac{1}{2}(g_{\mu\lambda,\nu} + g_{\lambda\nu,\mu}) u^\mu u^\nu \,. \end{aligned} \tag{2.105}$$

Now using the relationship (2.95), we find

$$g_{\mu\lambda} \frac{du^\mu}{d\tau} + \Gamma_{\lambda\mu\nu} u^\mu u^\nu = 0 \,. \tag{2.106}$$

Multiplying by $g^{\sigma\lambda}$ and summing on λ, we obtain the geodesic equation (2.85):

$$\frac{du^\sigma}{d\tau} + \Gamma^\sigma_{\mu\nu} u^\mu u^\nu = 0 \,. \tag{2.107}$$

This completes the proof that the path defined by the geodesic equation, the equation of motion of a particle in a purely gravitational field, extremizes the proper time between any two events on the path.

The straight-line path between two events in Minkowski spacetime maximizes the interval between the events. We proved that a geodesic path, in the general case that a gravitational field is present, will be an extremum, but if the spacetime separation of the ends of the path is large, there may be two geodesic paths, one of minimum and one of maximum length. The geodesic path of a particle in spacetime is frequently referred to as its *world line*. A world line is a continuous sequence of points in spacetime; it represent the history of a particle or photon.

In a region of spacetime sufficiently small that the Minkowski metric holds (the existence of which locality is guaranteed by the equivalence principle), we see that the geodesic equation reduces to that for uniform straight-line motion,

$$\frac{du^\mu}{d\tau} = 0\,. \tag{2.108}$$

Therefore, the path of a particle moving under the influence of a general gravitational field will be locally straight. But we know that no global Lorentz frame exists in the presence of gravitating bodies; therefore, geodesic paths will in general be curved. However, in the above sense they will be as straight as possible in curved spacetime.

2.5.3 *Comparison with Newton's gravity*

We confirm the assertion made earlier that the metric tensor $g_{\mu\nu}$ takes the place in General Relativity that the Newtonian potential occupies in Newton's theory. Of course this must be done in a weak field situation for it is only there that Newton's theory applies. For this reason, of the ten independent $g_{\mu\nu}$'s, only one can be involved in the correspondence.

We consider a particle moving slowly in a weak static gravitational field. From the Special Theory of Relativity we have

$$d\tau = \left(dt^2 - d\boldsymbol{r}^2\right)^{1/2} = \left(1 - \boldsymbol{v}^2\right)^{1/2} dt, \qquad \boldsymbol{v} = \frac{d\boldsymbol{r}}{dt}, \tag{2.109}$$

where boldface symbols denote three-vectors. The slowly moving assumption is

$$\frac{d\boldsymbol{r}}{dt} << \frac{dt}{d\tau} \approx 1\,. \tag{2.110}$$

So the geodesic equation (2.85) can be written with the neglect of the velocity terms as

$$\frac{d^2x^\mu}{d\tau^2} + \Gamma^\mu_{00}\left(\frac{dt}{d\tau}\right)^2 = 0\,. \tag{2.111}$$

Because the field is static, the time derivatives of $g_{\mu\nu}$ vanish. Consequently,

$$\Gamma^\mu_{00} = \tfrac{1}{2}g^{\mu\nu}\left(2g_{\nu 0.0} - g_{00.\nu}\right) = -\tfrac{1}{2}g^{\mu\nu}g_{00.\nu}(1 - \delta^\nu_0)\,. \tag{2.112}$$

Because the field is weak we may take

$$g_{00} = (1 + \delta)\eta_{00}\,, \tag{2.113}$$

where $\delta << 1$ and similarly for the other $g_{\mu\nu}$. To first order in the small quantities, we have

$$\Gamma^\mu_{00} = -\tfrac{1}{2}\eta^{\mu\nu}\eta_{00}\frac{d\delta}{dx^\nu}(1 - \delta^\nu_0)\,. \tag{2.114}$$

Thus the geodesic equations become

$$\frac{d^2\boldsymbol{r}}{d\tau^2} = -\tfrac{1}{2}\left(\frac{dt}{d\tau}\right)^2\nabla\delta, \qquad \frac{d^2t}{d\tau^2} = 0\,. \tag{2.115}$$

The second of these tells us that $\tau = at + b$. So we may write the first as

$$\frac{d^2\boldsymbol{r}}{dt^2} = -\tfrac{1}{2}\nabla\delta\,. \tag{2.116}$$

Newton's equation is

$$\frac{d^2\boldsymbol{r}}{dt^2} = -\nabla V\,, \tag{2.117}$$

where V is the gravitational potential. Comparing, we have

$$g_{00} = 1 + 2V\,. \tag{2.118}$$

In particular, if the gravitational field is produced by a body of mass M,

$$V = -\frac{GM}{r} \quad\Longrightarrow\quad g_{00} = 1 - \frac{2GM}{r}\,, \tag{2.119}$$

where G is Newton's constant. Thus we see for weak fields how the metric is related to the Newtonian potential.

2.6 Covariance

2.6.1 *Principle of general covariance*

Physical laws in their form ought to be independent of the frame in which they are expressed and of the location in the universe, that is, independent of the gravitational field. The principle of general covariance states that a law of physics holds in a general gravitational field if it holds in the absence of gravity and its form is invariant to any coordinate transformation. Physical laws frequently involve space-time derivatives of scalars, vectors, or tensors. We have seen that the derivative of a scalar is a vector but that the ordinary derivative of a vector or a tensor is not a tensor (page 22). Therefore, we need a type of derivative—a covariant derivative—that reduces to ordinary differentiation in the absence of gravity and which retains its form under any coordinate transformation, that is, in any gravitational field.

2.6.2 *Covariant differentiation*

Take the derivative of the expression of the covariant vector transformation law (2.63),

$$\frac{dA'_\mu}{dx'^\rho} = \frac{\partial x^\nu}{\partial x'^\mu}\frac{\partial x^\sigma}{\partial x'^\rho}\frac{\partial A_\nu}{\partial x^\sigma} + \frac{\partial^2 x^\nu}{\partial x'^\rho \partial x'^\mu}A_\nu\,.$$

If only the first term were present we would have the correct transformation law for a covariant tensor. Now multiply the left and right sides of (2.89) by the left and right sides of (2.63), respectively, and rearrange to find

$$\Gamma'^\lambda_{\mu\nu}A'_\lambda = \frac{\partial x^\alpha}{\partial x'^\mu}\frac{\partial x^\beta}{\partial x'^\nu}\Gamma^\kappa_{\alpha\beta}A_\kappa + \frac{\partial^2 x^\kappa}{\partial x'^\mu \partial x'^\nu}A_\kappa\,.$$

Subtracting the above two equations after renaming some dummy indices of summation, we get

$$\left(\frac{dA'_\mu}{dx'^\nu} - \Gamma'^\lambda_{\mu\nu} A'_\lambda\right) = \frac{\partial x^\alpha}{\partial x'^\mu}\frac{\partial x^\beta}{\partial x'^\nu}\left(\frac{dA_\alpha}{dx^\beta} - \Gamma^\lambda_{\alpha\beta} A_\lambda\right), \tag{2.120}$$

which proves the tensor character of the quantity in brackets. This we call the *covariant derivative* of a covariant vector. We denote it by

$$A_{\mu;\nu} \equiv \frac{dA_\mu}{dx^\nu} - \Gamma^\lambda_{\mu\nu} A_\lambda\,, \tag{2.121}$$

and the "semicolon subscript" shall denote the covariant derivative, and imply the operations shown on the right. The covariant derivative of a covariant vector is a second-rank covariant tensor which reduces to ordinary differentiation in inertial frames—and therefore locally in any gravitational field.

Through similar manipulations we find the covariant derivative of a contravariant vector,

$$A^\mu_{;\nu} \equiv \frac{dA^\mu}{dx^\nu} + \Gamma^\mu_{\sigma\nu} A^\sigma\,. \tag{2.122}$$

This is a second-rank mixed tensor because its transformation law is

$$\left(\frac{dA'^\mu}{dx'^\nu} + \Gamma'^\mu_{\lambda\nu} A'^\lambda\right) = \frac{\partial x'^\mu}{\partial x^\alpha}\frac{\partial x^\beta}{\partial x'^\nu}\left(\frac{dA^\alpha}{dx^\beta} + \Gamma^\alpha_{\kappa\beta} A^\kappa\right). \tag{2.123}$$

The covariant derivative of a mixed tensor of arbitrary order can be obtained by successive application of the above two rules to each index; there is one ordinary derivative of the tensor and an affine connection for each index with sign as indicated by the above.

In particular, the covariant derivative of the metric tensor is

$$g_{\mu\nu;\lambda} = \frac{\partial g_{\mu\nu}}{\partial x^\lambda} - \Gamma^\rho_{\mu\lambda} g_{\rho\nu} - \Gamma^\rho_{\nu\lambda} g_{\rho\mu}\,. \tag{2.124}$$

In a local inertial frame, where the affine connection and the derivative of the metric tensor vanish, we see that the covariant derivative of the metric tensor vanishes in that frame. But because this itself is a tensor, it must vanish in all frames. Similarly, for the covariant derivative of $g^{\mu\nu}$,

$$g_{\mu\nu;\lambda} = 0 = g^{\mu\nu}{}_{;\lambda}\,. \tag{2.125}$$

2.6.3 *Geodesic equation from covariance principle*

As an important example of the application of the covariant derivative, consider the four-velocity of a free particle in a Lorentz frame in the absence of gravity. We denote the four-velocity by $u^\mu = dx^\mu/d\tau$ and its equation of motion is $du^\mu/d\tau = 0$, or equivalently in differential form,

$$du^\mu = 0\,. \tag{2.126}$$

The covariant derivative (2.123) was introduced to preserve the vector or tensor character so that a law expressed in such form is preserved in form for all coordinate transformations in accord with the principle of relativity. The equation expressing the law is said to be covariant if its form is preserved. Therefore the law of free motion (2.126) in a Lorentz frame in the absence of gravity is generalized to frames in arbitrary gravitational fields by requiring that the covariant differential of the four-velocity vanish:

$$\begin{aligned} 0 = u^{\mu}{}_{;\nu} dx^{\nu} &= \frac{du^{\mu}}{dx^{\nu}} dx^{\nu} + \Gamma^{\mu}_{\sigma\nu} u^{\sigma} dx^{\nu} \\ &= du^{\mu} + \Gamma^{\mu}_{\sigma\nu} u^{\sigma} dx^{\nu} . \end{aligned} \tag{2.127}$$

Dividing the above equation by $d\tau$ yields the expected result—the geodesic equation (2.85)—the equation of motion derived previously for a free particle in an arbitrary gravitational field:

$$\frac{d^2 x^{\lambda}}{d\tau^2} + \Gamma^{\lambda}_{\mu\nu} \frac{dx^{\mu}}{d\tau} \frac{dx^{\nu}}{d\tau} = 0 . \tag{2.128}$$

This is an example of the application of the principle of general covariance and it is seen to rest on the equivalence principle, which assures us that a Lorentz frame can be erected locally. To restate the procedure briefly, *any law that holds in the special theory of relativity and in the absence of gravity can be generalized by replacing the metric* $\eta_{\mu\nu}$ by $g_{\mu\nu}$ *and replacing ordinary derivatives by covariant derivatives.*

We obtain an additional result that we need later, namely, the equations of motion for the covariant components of the four-velocity. The law of motion of a free particle in the special theory, expressed in differential form as in (2.126), implies at once that $du_{\mu} = g_{\mu\nu} du^{\nu} = 0$. The covariant translation of this fact is

$$0 = u_{\mu;\nu} dx^{\nu} = \frac{du_{\mu}}{dx^{\nu}} dx^{\nu} - \Gamma^{\lambda}_{\mu\nu} u_{\lambda} dx^{\nu} \tag{2.129}$$

or

$$\frac{d^2 x_{\mu}}{d\tau^2} - \Gamma^{\lambda}_{\mu\nu} \frac{dx_{\lambda}}{d\tau} \frac{dx^{\nu}}{d\tau} = 0 . \tag{2.130}$$

This is the equation corresponding to (2.128) for the covariant acceleration. We carry the analysis a step further. Examine the second term on the left.

$$\begin{aligned} \Gamma^{\lambda}_{\mu\nu} u_{\lambda} u^{\nu} &= \tfrac{1}{2} g^{\lambda\kappa} \left(g_{\kappa\nu,\mu} + g_{\kappa\mu,\nu} - g_{\mu\nu,\kappa} \right) u_{\lambda} u^{\nu} \\ &= \tfrac{1}{2} \left(g_{\kappa\nu,\mu} + g_{\kappa\mu,\nu} - g_{\mu\nu,\kappa} \right) u^{\kappa} u^{\nu} . \end{aligned} \tag{2.131}$$

Because of the symmetry of the product $u^{\kappa} u^{\nu}$, the last two terms in the bracket cancel. We are left with

$$\frac{du_{\mu}}{d\tau} = \tfrac{1}{2} g_{\kappa\nu,\mu} u^{\kappa} u^{\nu} . \tag{2.132}$$

This proves that if all the $g_{\alpha\beta}$ are independent of some coordinate component, say x^{μ}, then the covariant velocity u_{μ} is a constant along the particle's trajectory. We

will use this result in a much later chapter during a discussion of the phenomenon of dragging of local inertial frames by a rotating star (according to which a body dropped freely from a great distance falls, not toward the star's center, but is dragged ever more strongly in the sense of the star's rotation).

2.6.4 *Covariant divergence and conserved quantities*

The element of four-volume transforms under coordinate change as

$$dx'^0 dx'^1 dx'^2 dx'^3 = J\, dx^0 dx^1 dx^2 dx^3 , \tag{2.133}$$

where J is the Jacobian of the transformation,

$$J = \det \left| \frac{\partial x'^\rho}{\partial x^\mu} \right| . \tag{2.134}$$

For brevity the four-volume element is often written d^4x.

The transformation law for the metric tensor is

$$g_{\mu\nu} = \frac{\partial x'^\alpha}{\partial x^\mu} g'_{\alpha\beta} \frac{\partial x'^\beta}{\partial x^\nu} . \tag{2.135}$$

We may regard this as an element in the product of three matrices. The corresponding determinant equation is

$$g = J g' J = J^2 g' \tag{2.136}$$

where $g = \det|g_{\mu\nu}|$ and is a negative quantity as can be verified by looking at the Minkowski metric. Thus, we may write

$$\sqrt{-g} = J\sqrt{-g'} . \tag{2.137}$$

If $S = S'$ is a scalar field, then

$$\int_{V_4} S\sqrt{-g}\, d^4x = \int_{V_4} S\sqrt{-g'}\, J\, d^4x = \int_{V_4} S'\sqrt{-g'}\, d^4x' \tag{2.138}$$

is an invariant where V_4 is a prescribed four-volume. The quantity

$$\mathcal{S} \equiv S\sqrt{-g} \tag{2.139}$$

is called a *scalar density*, and its integral over a region of spacetime is invariant to a coordinate transformation. Also, and very important to us, $\sqrt{-g}\, d^4x$ is the invariant volume element.

The covariant derivative of a vector A^μ is given by (2.122). If we contract indices, according to (2.76) we have a scalar. This is the *covariant divergence* of A^μ:

$$A^\mu{}_{;\mu} \equiv A^\mu{}_{,\mu} + \Gamma^\mu_{\nu\mu} A^\nu . \tag{2.140}$$

From (2.93) we find

$$\Gamma^\nu_{\mu\nu} = \tfrac{1}{2} g^{\nu\kappa} \left(g_{\kappa\nu,\mu} + g_{\kappa\mu,\nu} - g_{\mu\nu,\kappa} \right) . \tag{2.141}$$

Interchange the names of the dummy summation indices in the second term on the right to see that it cancels the third. Thus

$$\Gamma^{\nu}_{\mu\nu} = \tfrac{1}{2} g^{\nu\kappa} g_{\kappa\nu.\mu} \,. \tag{2.142}$$

We need still another result. Denote the cofactor of the element $g_{\alpha\beta}$ by $C^{\alpha\beta}$. The determinant $g = \det|g_{\alpha\beta}|$ can be expanded in any of the set of minors (i.e., any $\alpha = 0, 1, 2,$ or 3) in the equation

$$g = g_{(\alpha)\beta} C^{(\alpha)\beta} \quad \text{(no sum on } \alpha\text{)}. \tag{2.143}$$

Because the cofactor contains no elements $g_{(\alpha)\beta}$, we find

$$\frac{\partial g}{\partial g_{\alpha\nu}} = \frac{\partial (g_{(\alpha)\beta} C^{(\alpha)\beta})}{\partial g_{\alpha\nu}} = \frac{\partial g_{\alpha\mu}}{\partial g_{\alpha\nu}} C^{\alpha\mu} = \delta^{\nu}_{\mu} C^{\alpha\mu} = C^{\alpha\nu} \,. \tag{2.144}$$

Therefore,

$$g_{.\alpha} = \frac{\partial g}{\partial g_{\mu\nu}} g_{\mu\nu.\alpha} = C^{\mu\nu} g_{\mu\nu.\alpha} \,. \tag{2.145}$$

We need the expression

$$C^{\mu\nu} = g g^{\mu\nu} \,, \tag{2.146}$$

which can be proved by multiplying by $g_{\mu\nu}$ and summing only over ν,

$$g_{(\mu)\nu} C^{(\mu)\nu} = g_{(\mu)\nu} g^{(\mu)\nu} g = g \,. \tag{2.147}$$

This is the determinant expansion in minors (2.143). Thus, we have derived the result

$$g_{.\alpha} = g g^{\mu\nu} g_{\mu\nu.\alpha} \,. \tag{2.148}$$

Hence,

$$\Gamma^{\nu}_{\mu\nu} = \tfrac{1}{2} g^{-1} g_{.\mu} = \tfrac{1}{2} \big(\ln(-g)\big)_{.\mu} = \frac{1}{\sqrt{-g}} \big(\sqrt{-g}\big)_{.\mu} \,. \tag{2.149}$$

We can use this to rewrite the covariant divergence of A^{μ} as

$$A^{\mu}{}_{;\mu} = \frac{1}{\sqrt{-g}} \big(\sqrt{-g} A^{\mu}\big)_{.\mu} \tag{2.150}$$

With (2.149) in (2.140), we obtain the important result for the covariant divergence,

$$\sqrt{-g} A^{\mu}{}_{;\mu} = \big(\sqrt{-g} A^{\mu}\big)_{.\mu} \,. \tag{2.151}$$

The left side is a scalar density. From the invariance of the integral of a scalar density over a prescribed four-volume, we have the invariant

$$\int_{V_4} \sqrt{-g} A^{\mu}{}_{;\mu} \, d^4x = \int_{V_4} \big(\sqrt{-g} A^{\mu}\big)_{.\mu} \, d^4x \,. \tag{2.152}$$

The right side can be converted to a surface integral over a three-volume at a definite time x^0 by Gauss' theorem.

If the covariant divergence vanishes, we get a conservation law as follows:

$$A^{\mu}{}_{;\mu} = 0 \quad \Longrightarrow \quad \left(\sqrt{-g}A^{\mu}\right)_{,\mu} = 0\,. \tag{2.153}$$

As a result, we obtain

$$\left(\sqrt{-g}A^{0}\right)_{,0} = -\left(\sqrt{-g}A^{m}\right)_{,m} \quad \text{(summed over } m = 1, 2, 3)\,. \tag{2.154}$$

Integrate the above expression over a three-volume at definite time x^0 to find

$$\frac{\partial}{\partial x^0}\int_V \sqrt{-g}A^0\, d^3x = -\int_V \left(\sqrt{-g}A^m\right)_{,m} d^3x = -\int_S \sqrt{-g}\boldsymbol{A}\cdot d\boldsymbol{S}\,. \tag{2.155}$$

If there is no three-current $\sqrt{-g}\boldsymbol{A}$ crossing the surface, then the quantity of density $\sqrt{-g}A^0$ contained within V is constant,

$$\int_V \sqrt{-g}A^0\, d^3x = \text{ constant} \tag{2.156}$$

This quantity is frequently referred to as the total charge of whatever A^{μ} represents. We will apply these results in Chapter 3, Section 3.13 and in Chapter 5 to calculate the distribution of various baryon species in neutron stars.

We can apply precisely the same reasoning to the covariant divergence of an antisymmetric tensor:

$$\text{If} \quad A^{\mu\nu} = -A^{\nu\mu}, \quad \text{then} \quad \sqrt{-g}A^{\mu\nu}{}_{;\nu} = \left(\sqrt{-g}A^{\mu\nu}\right)_{,\nu}\,, \tag{2.157}$$

where the quantity on the left is a *vector density* according to the previous section. Similarly we can derive conservation laws for the three-volume integral of the four densities $\sqrt{-g}A^{\mu 0}$ if the covariant divergence vanishes and there is no three-flux through the surface of the volume. However, if the tensor is not antisymmetric, the above theorem does not generally apply in curved spacetime to a tensor of more than one index.

2.7 Riemann Curvature Tensor

The order of ordinary differentiation in flat spacetime does not matter. The order of covariant differentiation does matter in curved spacetime. From an investigation of this fact we arrive at a measure of curvature.

2.7.1 Second covariant derivative of scalars and vectors

If we take the covariant derivative of a scalar twice and then invert the order, the answer is easily verified to be the same:

$$S_{;\mu;\nu} = S_{;\mu,\nu} - \Gamma^{\alpha}_{\mu\nu}S_{;\alpha} = S_{,\mu,\nu} - \Gamma^{\alpha}_{\mu\nu}S_{;\alpha}\,, \tag{2.158}$$

where we use the fact in the second equality that the covariant derivative of a scalar is the ordinary derivative $S_{;\mu} = S_{,\mu}$. The above result is symmetrical in μ, ν.

However for vectors and tensors, a changed order of differentiation in general produces a different result. The operations involved, all defined above, are many but straightforward. The result for the vector A_σ is

$$A_{\sigma;\mu;\nu} - A_{\sigma;\nu;\mu} = A_\rho R^\rho_{\sigma\mu\nu}\,, \tag{2.159}$$

where

$$R^\rho_{\sigma\mu\nu} \equiv \Gamma^\rho_{\sigma\nu,\mu} - \Gamma^\rho_{\sigma\mu,\nu} + \Gamma^\alpha_{\sigma\nu}\Gamma^\rho_{\alpha\mu} - \Gamma^\alpha_{\sigma\mu}\Gamma^\rho_{\alpha\nu} \tag{2.160}$$

is the *Riemann–Christoffel curvature tensor*. We know that it is a tensor because the left side of (2.159) is a tensor and A_ν is any vector. Riemann is the only tensor that can be constructed from the metric tensor and its first and second derivatives (cf. Ref. [19], p. 133).

2.7.2 *Symmetries of the Riemann tensor*

Riemann has a number of symmetry properties that can be easily derived from the above expression:

$$\begin{aligned} R^\mu_{\nu\rho\sigma} &= -R^\mu_{\nu\sigma\rho}\,, \\ R^\alpha_{\nu\rho\sigma} + R^\alpha_{\sigma\nu\rho} + R^\alpha_{\rho\sigma\nu} &= 0\,. \end{aligned} \tag{2.161}$$

Lowering the index on the Riemann tensor, we get

$$R_{\rho\sigma\mu\nu} = g_{\rho\alpha} R^\alpha_{\sigma\mu\nu}\,. \tag{2.162}$$

The additional symmetries follow:

$$\begin{aligned} R_{\mu\nu\rho\sigma} &= -R_{\nu\mu\rho\sigma} = -R_{\mu\nu\sigma\rho}\,, \\ R_{\mu\nu\rho\sigma} &= R_{\rho\sigma\mu\nu} = R_{\sigma\rho\nu\mu}\,. \end{aligned} \tag{2.163}$$

As a consequence of the symmetries only 20 of the $4^4 = 256$ components of Riemann are independent. In two dimensions there are 15 such symmetry relationships. Consequently, there are $2^4 - 15 = 1$ independent components of the Riemann tensor, namely, the Gaussian curvature. (See Ref. [20] p. 60 and appendix B for a discussion of curvature in two dimensions.)

We shall encounter two additional objects that are obtained from the Riemann tensor, the *Ricci tensor*,

$$R_{\mu\nu} = R^\rho_{\mu\nu\rho}\,, \tag{2.164}$$

and the *scalar curvature*,

$$R = g^{\mu\nu} R_{\mu\nu}\,. \tag{2.165}$$

Multiply the left and right side of (2.163) by $g^{\mu\sigma}$ and then rename indices to find

$$R_{\mu\nu} = R_{\nu\mu}\,. \tag{2.166}$$

Because of this symmetry, when we raise an index on the Ricci tensor, it is unnecessary to preserve the location,

$$R^\mu_{\ \nu} = R_\nu^{\ \mu} = R^\mu_\nu\,. \tag{2.167}$$

From the definition of the Ricci tensor in terms of the Riemann tensor, we have the following explicit expression:

$$R_{\mu\nu} = \Gamma^{\alpha}_{\mu\alpha,\nu} - \Gamma^{\alpha}_{\mu\nu,\alpha} - \Gamma^{\alpha}_{\mu\nu}\Gamma^{\beta}_{\alpha\beta} + \Gamma^{\alpha}_{\mu\beta}\Gamma^{\beta}_{\nu\alpha} . \tag{2.168}$$

The first term might appear to contradict the assertion that $R_{\mu\nu}$ is symmetric in μ, ν. However the result (2.149) proves that the Ricci tensor is symmetric.

2.7.3 *Test for flatness*

If spacetime is flat, then we may choose a rectilinear coordinate system in which case the metric tensor is a constant throughout spacetime. Then according to (2.93) the nontensor $\Gamma^{\lambda}_{\mu\nu}$ vanishes in this frame in all spacetime. So also do the derivatives of $\Gamma^{\lambda}_{\mu\nu}$. Therefore the Riemann tensor (2.160) vanishes everywhere at all times in flat spacetime. Because this is a statement about a tensor, it is true in any coordinate system, rectilinear or not. The converse is true but more difficult to prove: If Riemann vanishes, spacetime is flat. We prove this later in Section 2.9.3.

2.7.4 *Second covariant derivative of tensors*

An arbitrary second-rank tensor can be expressed as the sum of products $A_\mu B_\nu$. It is simpler to start by examining the second covariant derivative of such a product:

$$\begin{aligned}(A_\mu B_\nu)_{;\rho;\sigma} &= (A_{\mu;\rho}B_\nu + A_\mu B_{\nu;\rho})_{;\sigma} \\ &= A_{\mu;\rho;\sigma}B_\nu + A_\mu B_{\nu;\rho;\sigma} + A_{\mu;\rho}B_{\nu;\sigma} + A_{\mu;\sigma}B_{\nu;\rho} .\end{aligned}$$

Interchange ρ, σ, and subtract to find

$$\begin{aligned}(A_\mu B_\nu)_{;\rho;\sigma} &= (A_\mu B_\nu)_{;\sigma;\rho} \\ &= A_\mu(B_{\nu;\rho;\sigma} - B_{\nu;\sigma;\rho}) + (A_{\mu;\rho;\sigma} - A_{\mu;\sigma;\rho})B_\nu \\ &= A_\mu B_\alpha R^{\alpha}_{\nu\rho\sigma} + A_\alpha R^{\alpha}_{\mu\rho\sigma} B_\nu .\end{aligned}$$

We can form an arbitrary linear combination of such products of first-rank tensors to obtain the result for a general tensor,

$$T_{\mu\nu;\rho;\sigma} - T_{\mu\nu;\sigma;\rho} = T_{\mu\alpha}R^{\alpha}_{\nu\rho\sigma} + T_{\alpha\nu}R^{\alpha}_{\mu\rho\sigma} . \tag{2.169}$$

2.7.5 *Bianchi identities*

The Bianchi identities are extremely important for the further development of the theory of gravity, allowing us to prove that the Einstein tensor, which we come to next, has vanishing divergence.

Apply the above result to the particular case that the second-rank tensor is the covariant derivative of a vector $T_{\mu\nu} = A_{\mu;\nu}$,

$$A_{\mu;\nu;\rho;\sigma} - A_{\mu;\nu;\sigma;\rho} = A_{\mu;\alpha}R^{\alpha}_{\nu\rho\sigma} + A_{\alpha;\nu}R^{\alpha}_{\mu\rho\sigma} . \tag{2.170}$$

Now write down the additional two equations obtained from this by cyclic permutation of the indices ($\nu\rho\sigma$), and add the three equations. First study the left side of the sum. Use (2.159) to get

$$\begin{aligned}\text{LHS} &= (A_{\mu;\nu;\rho} - A_{\mu;\rho;\nu})_{;\sigma} + (A_{\mu;\sigma;\nu} - A_{\mu;\nu;\sigma})_{;\rho} + (A_{\mu;\rho;\sigma} - A_{\mu;\sigma;\rho})_{;\nu} \\ &= (A_\alpha R^\alpha_{\mu\nu\rho})_{;\sigma} + (A_\alpha R^\alpha_{\mu\sigma\nu})_{;\rho} + (A_\alpha R^\alpha_{\mu\rho\sigma})_{;\nu}\,.\end{aligned}$$

Using (2.161) in the sum of the right-hand sides of the cyclic permutation, we are left with

$$\text{RHS} = A_{\alpha;\nu} R^\alpha_{\mu\rho\sigma} + A_{\alpha;\sigma} R^\alpha_{\mu\nu\rho} + A_{\alpha;\rho} R^\alpha_{\mu\sigma\nu}\,.$$

Equating left and right sides and cancelling common terms, we find

$$A_\alpha(R^\alpha_{\mu\nu\rho;\sigma} + R^\alpha_{\mu\sigma\nu;\rho} + R^\alpha_{\mu\rho\sigma;\nu}) = 0\,. \tag{2.171}$$

Because A_α is any vector,

$$R^\alpha_{\mu\nu\rho;\sigma} + R^\alpha_{\mu\sigma\nu;\rho} + R^\alpha_{\mu\rho\sigma;\nu} = 0\,. \tag{2.172}$$

In addition to the symmetry relationships derived earlier, the Riemann tensor satisfies the differential equations above known as the *Bianchi identities*.

2.7.6 *Einstein tensor*

Let us multiply the differential equations for the Bianchi identities (2.172) by $g^{\mu\nu}$, contract σ with α, and use the fact, already established, that the covariant derivatives of the metric tensor vanish:

$$\begin{aligned}0 &= g^{\mu\nu}(R^\alpha_{\mu\nu\rho;\sigma} + R^\alpha_{\mu\sigma\nu;\rho} + R^\alpha_{\mu\rho\sigma;\nu}) \\ &= (g^{\mu\nu} R^\alpha_{\mu\nu\rho})_{;\alpha} + (g^{\mu\nu} R^\alpha_{\mu\alpha\nu})_{;\rho} + (g^{\mu\nu} R^\alpha_{\mu\rho\alpha})_{;\nu}\,.\end{aligned} \tag{2.173}$$

Examine each term in brackets using the Riemann tensor symmetries. The first term is

$$g^{\mu\nu} R^\alpha_{\mu\nu\rho} = g^{\mu\nu} g^{\alpha\beta} R_{\beta\mu\nu\rho} = g^{\mu\nu} g^{\alpha\beta} R_{\mu\beta\rho\nu} = g^{\alpha\beta} R^\nu_{\beta\rho\nu} = g^{\alpha\beta} R_{\beta\rho} = R^\alpha_\rho\,.$$

The second term is

$$g^{\mu\nu} R^\alpha_{\mu\alpha\nu} = -g^{\mu\nu} R^\alpha_{\mu\nu\alpha} = -g^{\mu\nu} R_{\mu\nu} = -R\,.$$

The third term is

$$g^{\mu\nu} R^\alpha_{\mu\rho\alpha} = g^{\mu\nu} R_{\mu\rho} = R^\nu_\rho\,.$$

Now put these results back into their brackets with the covariant derivatives as indicated in (2.173) to obtain

$$0 = R^\alpha_{\rho;\alpha} - R_{;\rho} + R^\nu_{\rho;\nu} = 2R^\alpha_{\rho;\alpha} - R_{;\rho}\,.$$

Multiply by $g^{\mu\rho}$, and note that

$$\begin{gathered} g^{\mu\rho} R^\alpha_{\rho;\alpha} = (g^{\mu\rho} R^\alpha_\rho)_{;\alpha} = R^{\mu\alpha}{}_{;\alpha} = R^{\mu\nu}{}_{;\nu} \\ g^{\mu\rho} R_{;\rho} = g^{\mu\nu} R_{;\nu} \end{gathered}$$

to arrive immediately at the vanishing divergence

$$(R^{\mu\nu} - \tfrac{1}{2}g^{\mu\nu}R)_{;\nu} = 0\,. \tag{2.174}$$

The object in the brackets is called the *Einstein curvature tensor*,

$$G^{\mu\nu} \equiv R^{\mu\nu} - \tfrac{1}{2}g^{\mu\nu}R\,. \tag{2.175}$$

The Einstein tensor is constructed from the Riemann curvature tensor and has an identically vanishing covariant divergence. It is symmetric and of second rank. Einstein was motivated to seek a tensor that contained no differentials of the $g^{\mu\nu}$ higher than the second—a tensor which was a linear homogeneous combination of terms linear in the second derivative or quadratic in the first (in analogy with Poisson's equation for the gravitational potential in Newton's theory:

$$\nabla^2 V = 4\pi\rho\,, \tag{2.176}$$

where ρ is the mass density generating the field). For the expression of energy and momentum conservation, it is important that the divergence vanish. The energy-momentum tensor of matter accomplishes this and is of second rank.

2.8 Einstein's Field Equations

"The geometry of spacetime is not given; it is determined by matter and its motion."[7] *W. Pauli, 1919*

We know that other bodies will experience gravity in the vicinity of massive bodies. So mass is a source of gravity, and from the Special Theory of Relativity we must say in general that mass and energy are sources. We have just seen that a construction from the Riemann curvature tensor, namely, Einstein's tensor, has vanishing covariant divergence. We have three possibilities,

$$G^{\mu\nu} = 0\,, \tag{2.177}$$

or

$$G^{\mu\nu} = kT^{\mu\nu}\,, \tag{2.178}$$

where $T^{\mu\nu}$ is a symmetric divergenceless tensor constructed from the mass-energy properties of the material medium, or

$$G^{\mu\nu} = kT^{\mu\nu} + \Lambda g^{\mu\nu}\,. \tag{2.179}$$

The constant Λ is the so-called *cosmological constant*. It was not present in the original theory and was added to obtain a static cosmology before it was known that the universe is expanding. Einstein regarded its numerical value as a matter to be settled by experiment—"The curvature constant [Λ] is, however, essentially

[7] Very importantly, the converse is also true.

determinable, and an increase in the precision of data derived from observations will enable us in the future to fix its sign and determine its value" [21].

It is apparent that the cosmological constant corresponds to a constant energy density $\Lambda/(8\pi)$ and a constant pressure of the same numerical value but of opposite sign. The cosmological constant is sometimes referred to as the vacuum energy density. In any case it is small if not zero ($|\Lambda| < 10^{-29}$ g/cm^3), as estimated, for example, as the limiting value that would leave Newtonian celestial mechanics unchanged as concerns its predictions for small clusters of galaxies [22]. Its effect is indeed cosmological; stellar structure is unaffected by it. We need not consider the cosmological term further.

The first set of differential equations (2.177) are those that must be satisfied by the metric in empty space outside material bodies and energy concentrations. An example is the gravitational fields outside a star.

The second set of differential equations (2.178) determine the gravitational fields $g^{\mu\nu}$ inside a spacetime region of mass-energy and in addition determine how the mass-energy is arranged by gravity. With appropriate $T^{\mu\nu}$ it would provide the equations of stellar structure. We have yet to fix the constant k. This can be done by looking to the weak field limit where the General Theory of Relativity should agree with Newton's well-tested, weak-field theory.

There are several remarkable notes we can make at this point. Einstein's field equations tell spacetime how to curve and mass-energy how to configure itself and how to move. Spacetime acts upon matter and in turn is acted upon by matter. This was Einstein's intuition and motivation in seeking a theory that placed spacetime and matter as co-determiners in nature. He was displeased with the Special Theory of Relativity as anything but a local theory, for it gave spacetime an absolute status.

Second, the Einstein field equations are nonlinear in the fields $g^{\mu\nu}$. (This can be verified by tracing back through the objects from which the Einstein tensor is constructed.) Nonlinearity means that the gravitational field interacts with itself. This is because the field carries energy, and mass-energy in any form is a source of gravity. The nonlinearity of the Einstein equations accounts for some of the extraordinary phenomena encountered in strong gravity, including black holes [23] and the reversal of the centrifugal force in their vicinity [24].

We have seen in (2.174) that the Einstein tensor has identically vanishing covariant divergence. Hence (2.178) requires of the matter tensor that

$$T^{\mu\nu}{}_{;\nu} = 0\,. \tag{2.180}$$

The corresponding equation in flat space is

$$T^{\mu\nu}{}_{,\nu} = 0\,. \tag{2.181}$$

The vanishing of the ordinary divergence of the energy-momentum tensor in the Special Theory of Relativity corresponds to the conservation of energy and momentum. However, (2.180) does not assure us of the constancy of any quantity in time. In fact (2.178) ensures that matter and the gravitational fields exchange energy, or in other words do work on each other, for it is the divergence of $G^{\mu\nu} - kT^{\mu\nu}$ that vanishes. So neither matter nor the gravitational field can by itself conserve energy

in any sense. There is no contradiction with laboratory experiments performed on Earth. Over the dimensions of a typical laboratory, spacetime is essentially flat, and nothing that could be done in a laboratory could possibly disturb this flatness in any perceptible way.

This brings us back to the comparison of the weak-field limit between Newton's theory and Einstein's. The inverse-square law of the force between massive objects is not required by the inner structure of Newton's theory. He could have postulated an inverse α law, that force $F \sim Mm/r^{\alpha}$, and then attempted to fit α to the astronomical data of the solar system. Depending on what weight was given to the precession of planets, one would have found a value of α close to two.

Einstein's theory does not possess the flexibility of Newton's in this regard. We saw in (2.119) that Einstein predicts precisely the inverse square law. In this sense, he could claim as his own all the successes of the Newtonian theory in explaining the motion of planets in the solar system. They were computed with the inverse-square law, there being no flexibility in the choice of the power in his theory.

Concerning the precession of planets, an isolated planet in orbit about the Sun under an inverse square law is an ellipse whose orientation is fixed in space. However the total precession of the orbit of Mercury is observed to be about 5600 seconds/century. Most of this is caused by the fact that an earthbound observer is not in an inertial frame far from the Sun. For example, suppose that Mercury did not orbit about the Sun, but instead held a fixed position. Nevertheless, from the Earth it would be appear to move, sometimes to the left of the Sun, sometimes to the right, and alternately passing in front of and in back of the Sun. Taking account of this correction to the apparent motion of Mercury due to the Earth's own motion, the precession of Mercury is about 574 seconds/century. This value is about 43 seconds/century larger than the precession computed by Newtonian physics as due to the perturbation of the orbit by other planets, a small but disturbing discrepancy. An early triumph of Einstein was that he calculated, within the observational errors, the precise value of the excess precession. In Newton's theory only mass contributes to gravity, whereas in Einstein's theory the kinetic energy of the motion of the planets contributes as well.

2.9 Relativistic Stars

Einstein's field equations are completely general and simple in appearance. However, they are exceedingly complicated because of their nonlinear character and because spacetime and matter act upon each other. As already remarked, there is no prior geometry of spacetime. There are a few cases in which solutions can be found in closed form. One of the most important closed-form solutions is the Schwarzschild metric outside a static spherical star. Another is the Kerr metric outside a rotating black hole. Einstein's equations can also be solved numerically

as the coupled differential equations for the interior structure of a spherical static star, which are called the Oppenheimer–Volkoff equations for stellar structure.

In this section we take up the important problem of deriving the equations that govern spacetime and the arrangement of matter in the case of relativistic spherical static stars. They are the basic equations that underlie the development of neutron star models in the rest of the book. They also demonstrate the mathematical existence of Schwarzschild black holes. They can also be used to develop white dwarf models, though Newtonian gravity is a good approximation for these stars.

2.9.1 *Metric in static isotropic spacetime*

We seek solutions to Einstein's field equations in static isotropic regions of spacetime such as would be encountered in the interior and exterior regions of static stars. Under these conditions the $g_{\mu\nu}$ are independent of time ($x^0 \equiv t$) and $g^{0m} = 0$. We choose spatial coordinates $x^1 = r$, $x^2 = \theta$, and $x^3 = \phi$. The most general form of the line element is then

$$d\tau^2 = U(r)\,dt^2 - V(r)\,dr^2 - W(r)r^2(d\theta^2 + \sin^2\theta\,d\phi^2)\,. \qquad (2.182)$$

We may replace r by any function of r without disturbing the spherical symmetry. We do so in such a way that $W(r) \equiv 1$. Then we may write

$$d\tau^2 = e^{2\nu(r)}\,dt^2 - e^{2\lambda(r)}\,dr^2 - r^2\,d\theta^2 - r^2\sin^2\theta\,d\phi^2\,, \qquad (2.183)$$

where λ, ν are functions only of r. Comparing with $d\tau^2 = g_{\mu\nu}\,dx^\mu\,dx^\nu$, we read off [8]

$$g_{00} = e^{2\nu(r)}, \quad g_{11} = -e^{2\lambda(r)}, \quad g_{22} = -r^2, \quad g_{33} = -r^2\sin^2\theta,$$
$$g_{\mu\nu} = g^{\mu\nu} = 0 \quad (\mu \neq \nu)\,. \qquad (2.184)$$

Hence, from $g_{\mu\nu}g^{\nu\rho} = \delta^\rho_\mu$, we have in this special case

$$g_{\mu\mu} = 1/g^{\mu\mu} \quad \text{(not summed)}\,. \qquad (2.185)$$

According to its definition as a contraction of the Riemann tensor, the Ricci tensor can be written

$$R_{\mu\nu} = \Gamma^\alpha_{\mu\alpha,\nu} - \Gamma^\alpha_{\mu\nu,\alpha} - \Gamma^\alpha_{\mu\nu}\Gamma^\beta_{\alpha\beta} + \Gamma^\alpha_{\mu\beta}\Gamma^\beta_{\nu\alpha}\,. \qquad (2.186)$$

We can derive the nonvanishing affine connections (2.93), which are symmetric in their lower indices, from the metric tensor whose general form for static isotropic

[8] Note that in (2.183) some authors use the opposite signs for time and space components, and some use the functions ν, λ but without the factor 2, or use different notation altogether for the metric. Great care has to be exercised in using results from different sources.

regions was derived above:

$$\begin{aligned}
\Gamma^1_{00} &= \nu' e^{2(\nu-\lambda)}\,, & \Gamma^0_{10} &= \nu'\,,\\
\Gamma^1_{11} &= \lambda'\,, & \Gamma^2_{12} &= \Gamma^3_{13} = 1/r\,,\\
\Gamma^1_{22} &= -r e^{-2\lambda}\,, & \Gamma^3_{23} &= \cot\theta\,,\\
\Gamma^1_{33} &= -r\sin^2\theta\, e^{-2\lambda}\,, & \Gamma^2_{33} &= -\sin\theta\cos\theta\,.
\end{aligned} \tag{2.187}$$

The primes denote differentiation with respect to the r-coordinate. Hence, for static isotropic spacetime

$$\begin{aligned}
R_{00} &= \left(-\nu'' + \lambda'\nu' - \nu'^2 - \frac{2\nu'}{r}\right)e^{2(\nu-\lambda)}\,,\\
R_{11} &= \nu'' - \lambda'\nu' + \nu'^2 - \frac{2\lambda'}{r}\,,\\
R_{22} &= (1 + r\nu' - r\lambda')e^{-2\lambda} - 1\,,\\
R_{33} &= R_{22}\sin^2\theta\,.
\end{aligned} \tag{2.188}$$

2.9.2 *The Schwarzschild solution*

In the empty space outside a static star Einstein's equation is $G_{\mu\nu} = 0$, or equivalently

$$R_{\mu\nu} = \tfrac{1}{2} g_{\mu\nu} R\,. \tag{2.189}$$

Multiply by $g^{\alpha\mu}$, and sum on the dummy index to find

$$R^\alpha_\nu = \tfrac{1}{2}\delta^\alpha_\nu R\,. \tag{2.190}$$

Contract by setting $\alpha = \nu$, and sum to get

$$R = 2R \quad\Longrightarrow\quad R = 0\,. \tag{2.191}$$

Hence, the vanishing of Einstein's tensor implies

$$G_{\mu\nu} = 0 \quad\Longrightarrow\quad R = 0,\quad R_{\mu\nu} = 0\,. \tag{2.192}$$

In empty space, Einstein's equation is equivalent to the vanishing of the Ricci tensor or, equivalently, the scalar curvature. Its form for static isotropic spacetime was worked out in the previous section.

From the vanishing of R_{00}, R_{11} we find that

$$\lambda' + \nu' = 0\,. \tag{2.193}$$

(Do not confuse ν and λ when used to denote indices and when used to denote the metric functions as in the above equation.) For large r, space must be unaffected by the star and therefore flat so that λ and ν tend to zero; therefore

$$\lambda + \nu = 0\,. \tag{2.194}$$

Using these results in $R_{22} = 0$, we find that

$$(1 + 2r\nu')e^{2\nu} = 1\,. \tag{2.195}$$

This condition integrates to

$$g_{00} \equiv e^{2\nu} = 1 - \frac{2GM}{r} \quad (r > R)\,, \tag{2.196}$$

where M is the constant of integration, and we introduced Newton's constant. Having studied the Newtonian approximation, one identifies M with the mass of the star. From the foregoing results,

$$g_{11} = -e^{2\lambda} = -e^{-2\nu} = -\Big(1 - \frac{2GM}{r}\Big)^{-1} \quad (r > R). \tag{2.197}$$

This completes the derivation of the *Schwarzschild solution* (1916) of Einstein's equations outside a spherical static star. It was the first exact solution found for Einstein's equations. The proper time is

$$d\tau^2 = \Big(1 - \frac{2GM}{r}\Big)dt^2 - \Big(1 - \frac{2GM}{r}\Big)^{-1} dr^2 - r^2 d\theta^2 - r^2 \sin^2\theta\, d\phi^2$$
$$(r > R)\,, \tag{2.198}$$

where R, in this context, denotes the radius of the star.

Let us summarize the Schwarzschild solution found above:

$$\begin{aligned} g_{00}(r) &= e^{2\nu(r)} = \Big(1 - \frac{2GM}{r}\Big), \quad r > R\,, \\ g_{11}(r) &= -e^{2\lambda(r)} = -\Big(1 - \frac{2GM}{r}\Big)^{-1}, \quad r > R\,, \\ g_{22}(r) &= -r^2, \quad g_{33}(r,\theta) = -r^2 \sin^2\theta\,. \end{aligned} \tag{2.199}$$

Notice that the Schwarzschild metric is singular at the radius $r = r_S \equiv 2GM$. This does not mean that spacetime itself is singular at that radius, but only that this particular metric is. Other nonsingular metrics have been found, in particular, the Kruskal–Szerkeres metric [25, 26]. However, further analysis shows that if r_S lies outside the star where the Schwarzschild solution holds, then it is a black hole—no particle or even light can leave the region $r < r_S$. This radius r_S is called the *Schwarzschild radius* or *singularity* or *horizon*. But because the above metric holds only outside the star, r_S has no special significance if it is smaller than the radius of the star. For then a different metric holds inside the star which does not possess a singularity. We come to this solution shortly.

2.9.3 *Riemann tensor outside a Schwarzschild star*

If spacetime is flat, then the Riemann curvature tensor vanishes (Section 2.7.3). We are now prepared to address the converse (albeit not rigorously): if spacetime is curved, some components of the Riemann tensor are finite (which components, of course, will depend upon how convoluted spacetime is).

The metric tensor and, indeed, the affine connection for the empty space outside a massive body were computed in the preceding section. We have seen in Section 2.4.3 that massive bodies curve spacetime. So we know that the Schwarzschild metric tensor refers to curved spacetime. Referring to the definition of the

Riemann tensor (2.160) and the specific form that the affine connection takes for a static spherical star (2.187), we can compute

$$R^1_{010} = \left(\nu'' + 2\nu'^2 - \nu'\lambda'\right)e^{2(\nu-\lambda)} . \tag{2.200}$$

Thus we exhibit at least one nonvanishing component of the Riemann tensor in the curved spacetime outside a Schwarzschild star. This suggests that Riemann is not identically zero in curved spacetime. An actual proof that if Riemann is finite then spacetime is curved requires the formulation of parallel transport, which we do not take up here. We declare, without rigorous proof, that the Riemann tensor vanishes if and only if spacetime is flat. Notice that, far from an isolated star where spacetime approaches flatness, Riemann approaches zero as it should.

2.9.4 *Energy-momentum tensor of matter*

From the success of Newtonian physics in describing celestial mechanics and other weak gravitational field phenomena, we know that mass is a source of gravity. From the experimental verifications of the Special Theory of Relativity, we know that all forms of energy are equivalent and must contribute equally as sources of gravity. Normally, of course, it is mass that dominates, and the average mass density in the solar system and in the universe is very small; that is why Newtonian physics is so accurate under the typical conditions mentioned above.

An essential aspect of Einstein's curvature tensor is that it automatically has vanishing covariant divergence (2.174). It is also a symmetric second-rank tensor. Accordingly, mass-energy—the source of the gravitational field—must be incorporated into a divergenceless, symmetric, second- rank tensor in flat space. As a tensor, it can be transcribed immediately to its form in an arbitrary spacetime frame by the general covariance principle. Such a tensor is the energy-momentum tensor.

In other parts of this book we shall be interested in specific theories of dense matter from which we will be able to explicitly construct the energy-momentum tensor of the theory. Here we are interested in the general form such a tensor takes. Frequently, matter may be regarded as a perfect fluid. The fluid velocity is assumed to vary continuously from point to point. The perfect fluid energy-momentum tensor in the Special Theory of Relativity can be expressed in terms of the local values of the pressure p and energy density ϵ as in (2.49). The General Relativistic energy-momentum tensor can be written immediately using the Principle of General Covariance spelled out on page 36:

$$T^{\mu\nu} = -pg^{\mu\nu} + (p+\epsilon)u^\mu u^\nu ,$$
$$g_{\mu\nu}u^\mu u^\nu = 1 .$$

In the above equations, u^μ is the local fluid four-velocity

$$u^\mu = \frac{dx^\mu}{d\tau} \tag{2.201}$$

and satisfies (2.201) because of (2.53).

The pressure and total energy density (including mass) are related by the equation of state of matter, frequently written in either form

$$p = p(\epsilon) \quad \text{or} \quad \epsilon = \epsilon(p) \tag{2.202}$$

where p and ϵ are the pressure and energy density (including mass) in the local rest-frame of the fluid. In the next section we shall see how the equations for stellar structure involve these quantities and this relationship.

2.9.5 *The Oppenheimer–Volkoff equations*

We are now prepared to derive the differential equations for the structure of a static, spherically symmetric, relativistic star. For the region outside a star, we found that the vanishing of the Einstein tensor was equivalent to the vanishing of the Ricci tensor or the scalar curvature. This is not the case for the interior of the star. We need both the Ricci tensor and scalar curvature to construct the Einstein tensor. The general form of the metric for a static isotropic spacetime was obtained in (2.184). From Section 2.9.1 we find the scalar curvature,

$$\begin{aligned} R = g^{\mu\nu}R_{\mu\nu} &= e^{-2\nu}R_{00} - e^{-2\lambda}R_{11} - \frac{2}{r^2}R_{22} \\ &= e^{-2\lambda}\left\{-2\nu'' + 2\lambda'\nu' - 2\nu'^2 - \frac{2}{r^2} + 4\frac{\lambda'}{r} - 4\frac{\nu'}{r}\right\} + \frac{2}{r^2}\,. \end{aligned} \tag{2.203}$$

It is more convenient to work with mixed tensors. For example,

$$G_0^{\ 0} = R_0^{\ 0} - \tfrac{1}{2}R \tag{2.204}$$

is obtained with the results of Section 2.9.1 for a static isotropic field, namely,

$$g_0^0 = g_{0\nu}g^{0\nu} = g_{00}g^{00} = 1\,. \tag{2.205}$$

So using results obtained earlier in this section we can find that the components of the Einstein tensor are

$$\begin{aligned} r^2G_0^{\ 0} &\equiv e^{-2\lambda}(1 - 2r\lambda') - 1 = -\frac{d}{dr}[r(1 - e^{-2\lambda})]\,, \\ r^2G_1^{\ 1} &\equiv e^{-2\lambda}(1 + 2r\nu') - 1\,, \\ G_2^{\ 2} &\equiv e^{-2\lambda}\left(\nu'' + \nu'^2 - \lambda'\nu' + \frac{\nu' - \lambda'}{r}\right), \\ G_3^{\ 3} &= G_2^{\ 2}. \end{aligned} \tag{2.206}$$

Because of the assumption that the star is static, the three-velocity of every fluid element is zero, so

$$u^\mu = 0 \quad (\mu \neq 0), \qquad u^0 = 1/\sqrt{g_{00}}\,, \tag{2.207}$$

according to (2.201). For the energy-momentum tensor expressed as a mixed tensor, we have the nonzero components in the present metric,

$$T_0^{\ 0} = \epsilon, \quad T_\mu^{\ \mu} = -p \quad (\mu \neq 0). \tag{2.208}$$

So the (00) component of the Einstein equations gives

$$r^2 G_0{}^0 = -\frac{d}{dr}\{r(1 - e^{-2\lambda(r)})\} = kr^2 T_0{}^0 = kr^2 \epsilon(r) . \tag{2.209}$$

This can be integrated immediately to yield

$$e^{-2\lambda(r)} = 1 + \frac{k}{r}\int_0^r \epsilon(r) r^2 dr . \tag{2.210}$$

Let us define

$$M(r) \equiv 4\pi \int_0^r \epsilon(r) r^2 dr , \tag{2.211}$$

and let R denote the radius of the star, the radial coordinate exterior to which the pressure vanishes. Zero pressure defines the edge of the star because zero pressure can support no material against the gravitational attraction from within. Denote the corresponding value of $M(R)$ by

$$M \equiv M(R) . \tag{2.212}$$

Now comparing (2.119, 2.196, 2.197) we see that, to obtain agreement with the Newtonian limit, we must choose

$$k = -8\pi G \tag{2.213}$$

and interpret M as the *gravitational mass* of the star. Therefore, $M(r)$ is referred to as the *included mass* within the coordinate r. So Einstein's field equations can now be written

$$G^{\mu\nu} = -8\pi G T^{\mu\nu} . \tag{2.214}$$

From the above, we have found so far that

$$g_{11}(r) = -e^{2\lambda(r)} = -\left(1 - \frac{2GM(r)}{r}\right)^{-1} , \tag{2.215}$$

which agrees with (2.197), but now we see that $g_{11}(r)$ has the same form inside and outside the star although it is the included mass $M(r)$, not the total mass, that appears in the interior solution.

Having learned the constant of proportionality in Einstein's equations (2.214), let us now write out the field equations for a spherically symmetric static star, including the one we have already solved. In passing we note that our solution gives a relationship between the included mass $M(r)$ at any radial coordinate and the metric function $g_{11}(r)$ or $\lambda(r)$, but we have yet to learn how to compute one or the other. The differential equations from (2.206) are

$$G_0{}^0 \equiv e^{-2\lambda}\left(\frac{1}{r^2} - \frac{2\lambda'}{r}\right) - \frac{1}{r^2} = -8\pi G \epsilon(r) , \tag{2.216}$$

$$G_1{}^1 \equiv e^{-2\lambda}\left(\frac{1}{r^2} + \frac{2\nu'}{r}\right) - \frac{1}{r^2} = 8\pi G p(r) , \tag{2.217}$$

$$G_2{}^2 \equiv e^{-2\lambda}\left(\nu'' + \nu'^2 - \lambda'\nu' + \frac{\nu' - \lambda'}{r}\right) = 8\pi G p(r) , \tag{2.218}$$

$$G_3^{\ 3} = G_2^{\ 2} = 8\pi G p(r)\,. \tag{2.219}$$

The last equation contains no information additional to that provided by those preceding it.

To simplify notation, choose units so that $G = c = 1$. Solve (2.216) to find

$$-2r\lambda' = (1 - 8\pi r^2\epsilon)e^{2\lambda} - 1 \tag{2.220}$$

and (2.217) to find

$$2r\nu' = (1 + 8\pi r^2 p)e^{2\lambda} - 1\,. \tag{2.221}$$

Take the derivative of (2.221) and then multiply by r:

$$2r\nu' + 2r^2\nu'' = \Big[2r\lambda'(1 + 8\pi r^2 p) + (16\pi r^2 p + 8\pi r^3 p')\Big]e^{2\lambda}\,.$$

Solve for ν'' using (2.221, 2.220):

$$2r^2\nu'' = 1 + (16\pi r^2 p + 8\pi r^3 p')e^{2\lambda} - (1 + 8\pi r^2 p)(1 - 8\pi r^2\epsilon)e^{4\lambda} \tag{2.222}$$

Square (2.221) to obtain the result

$$2r^2\nu'^2 = \tfrac{1}{2}(1 + 8\pi r^2 p)^2 e^{4\lambda} - (1 + 8\pi r^2 p)e^{2\lambda} + \tfrac{1}{2}\,. \tag{2.223}$$

The last four numbered equations provide expressions for λ', ν', ν'', and ν'^2 in terms of p, p', ϵ, and $e^{2\lambda}$ the latter of which, according to (2.215), can be expressed in terms of the included mass. Therefore the metric can be eliminated altogether by substitution of the above results into the remaining field equation (2.218). After a number of cancellations, we emerge with the result

$$\frac{dp}{dr} = -\frac{\big[p(r) + \epsilon(r)\big]\big[M(r) + 4\pi r^3 p(r)\big]}{r\big[r - 2M(r)\big]}\,. \tag{2.224}$$

This and equation (2.211) represent the reduction of Einstein's equations for the interior of a spherical, static, relativistic star. These equations are frequently referred to as the Oppenheimer–Volkoff equations. The stars they describe—static and spherically symmetric—are sometimes referred to as Schwarzschild stars.

Given an equation of state (2.202), the stellar structure equations (2.211) and (2.224) can be solved simultaneously for the radial distribution of pressure, $p(r)$, and hence for the distribution of mass-energy density $\epsilon(r)$. Moreover, in any detailed theory of dense matter, the baryon and lepton populations are obtained as a function of density; hence the distribution of particle populations in a star can be found coincident with a solution of the Oppenheimer–Volkoff equations.

It may seem curious that the expression (2.211) for mass has precisely the same form as one would write in nonrelativistic physics for the mass whose distribution is given by $\epsilon(r)$. How can this be, inasmuch as we know that spacetime is curved by mass and mass in turn is moved and arranged by spacetime in accord with Einstein's equations? The answer is that (2.211) is not a prescription for computing the total mass of an arbitrary distribution $\epsilon(r)$. There are no arbitrary distributions in gravity; rather $\epsilon(r)$ is precisely prescribed by another of Einstein's equations (2.224). As such, M comprises the mass of the star and its gravitational field. Because of

the mutual interaction of mass-energy and spacetime, there is no meaning to the question "What is the mass of the star?" in isolation from the field energy. That is why we refer to M as the gravitational mass or the mass-energy of the star. It is the only type of mass that enters Einstein's theory and is the only stellar mass to which we will refer in this book. Therefore, we shall generally refer to a star's mass as simply the mass without the adjective "gravitational". Sometimes a so-called proper mass is defined. It appears nowhere in Einstein's equations and is an artifact.

It does make sense to inquire about the mass of the totality of nucleons in a star if they were dispersed to infinity. This mass is referred to as the baryon mass. The difference between gravitational mass and baryon mass, if negative, is the gravitational binding of the star. As we shall find, the gravitational binding is of the order of 100 MeV per nucleon in stars near the mass limit as compared to 10 MeV binding by the strong force in nuclei.

Notice that, according to (2.224), the pressure is a monotonic decreasing function from the inside of the star to its edge because all the factors in (2.224) are positive, leaving the explicit negative sign. This makes sense. Any region is weighted down by all that lies above. We have assumed that the denominator in (2.224) is positive. Overall this is true of the Earth, the Sun, and a neutron star. In fact, as we shall see in Section 3.15, $2M/R < 8/9$ for any static stable star. It can also be shown that $2M(r)/r < 1$ for all regions of a stable star [27]; so indeed we are justified in taking the last factor in (2.224) as positive.

In (2.198) we saw a singularity in the Schwarzschild solution if a star lies within $r = 2M$. Such stars are highly relativistic objects called black holes. No light or particle can escape from within their Schwarzschild radius. A luminous star is highly nonrelativistic. A neutron star is relativistic. Newtonian gravity would not produce the same results as General Relativity. This fact is clear, given that $2M$ can be as large as $\frac{8}{9}R$ for a neutron star, which makes the denominator of (2.224) a large correction (as much as 9 instead of 1).

We already have an expression for the radial metric function both inside and outside a star. It is sometimes useful to have the time metric function g_{00}. No general expression for the solution can be obtained, as for g_{11}, (2.215). However using the latter in (2.221) we obtain a differential equation,

$$\frac{d\nu}{dr} = \frac{M(r) + 4\pi r^3 p(r)}{r\big[r - 2M(r)\big]}. \tag{2.225}$$

The solution must match the exterior solution (2.197). This is easily accomplished. If $\nu(r)$ is a solution, we can add any constant to it and still have a solution. We obtain the correct condition at R if we make the change

$$\nu(r) \longrightarrow \nu(r) - \nu(R) + \tfrac{1}{2}\ln\Big(1 - \frac{2M}{R}\Big), \quad r \le R. \tag{2.226}$$

We can start the integration at $r = 0$ with any convenient value of $\nu(0)$, say zero.

Alternately, once the Oppenheimer–Volkoff equations have been solved so that $p(r)$ and hence $\epsilon(r)$ are known, one can find $\nu(r)$ by integration of

$$\frac{d\nu}{dr} = -\frac{1}{p+\epsilon}\frac{dp}{dr}, \tag{2.227}$$

namely,

$$\nu(r) = -\int_0^r \frac{1}{p+\epsilon}\frac{dp}{dr} + \text{constant}, \qquad \nu(\infty) = 0. \tag{2.228}$$

The Oppenheimer–Volkoff equations can be integrated from the origin with the initial conditions $M(0) = 0$ and an arbitrary value for the central energy density $\epsilon(0)$, until the pressure $p(r)$ becomes zero at, say R. Because zero pressure can support no overlying matter against the gravitational attraction, R defines the gravitational radius of the star and $M(R)$ its gravitational mass. For the given equation of state, there is a unique relationship between the mass and central density $\epsilon(0)$. So for each possible equation of state, there is a unique family of stars, parameterized by, say, the central density or the central pressure. Such a family is often referred to as the *single parameter sequence* of stars corresponding to the given equation of state.

2.9.6 *Gravitational collapse and limiting mass*

In Newtonian physics mass alone generates gravity. In the Special Theory of Relativity mass is equivalent to energy, so in the general theory all forms of energy contribute to gravity. It is surprising that pressure also plays a most consequential role in the structure of relativistic stars beyond the role it plays in Newtonian gravity. Pressure supports stars against gravity, but surprisingly, it ultimately assures the gravitational collapse of relativistic stars whose mass lies above a certain limit.

Pressure appears together with energy density in determining the monotonic decrease of pressure (2.224) in a relativistic star. Gravity acts to compress the material of the star. As it does so, the pressure of the material is increased toward the center. But inasmuch as pressure appears on the right side of the equation, this increase serves to further enhance the grasp of gravity on the material. Therefore, for stars of increasing mass, for which the supporting pressure must correspondingly increase, the pressure gradient (which is negative) is increased in magnitude, making the radius of the star smaller because its edge necessarily occurs at $p = 0$. As a consequence, if the mass of a relativistic star exceeds a critical value, there is no escape from gravitational collapse to a black hole [28]. Whatever the equation of state, the one-parameter sequence of stable configurations belonging to that equation of state is terminated by a maximum-mass compact star. The mass of this star is referred to as the *mass limit* or *limiting mass* of the sequence.

2.10 Action Principle in Gravity

We arrived at Einstein's equations by noting the vanishing divergence of the Einstein curvature tensor and equating it to the energy-momentum tensor of matter as the source of the gravitational field. We did not comment on how the energy-momentum tensor might be obtained. In general, this tensor is not given but must be calculated from a theory of matter. In what frame should the theory be solved? Evidently in the general frame of the gravitational field. But this is an entirely different problem than is normally solved in many-body theory.

We are accustomed to solving problems in nuclear and particle theory in flat spacetime (or even flat space) in which the constant Minkowski metric $\eta_{\mu\nu}$ appears, not a general and as yet unspecified field $g_{\mu\nu}(x)$. A tacit assumption is made in passing from the energy-momentum tensor in a Lorentz frame (2.49) to its form (2.201) in a general frame by means of the principle of general covariance, as was done in deriving the Oppenheimer–Volkoff equations of stellar structure. The local region over which Lorentz frames extend is assumed to be sufficiently large that the equations of motion of the matter fields can be solved in a Lorentz frame, that is, in the absence of gravity, and the corresponding energy-momentum tensor constructed from the solution for such a region.

As we shall see in the next chapter, the local inertial frames in the gravitational field of neutron stars (and therefore for the less dense white dwarfs and all other stars) are actually sufficiently extensive that the matter from which they are constituted can be described by theories in flat Minkowski spacetime. We shall refer to such a situation as a partial decoupling of matter from gravity. In other words, the equations of motion for the matter and radiation fields can be solved in Minkowski spacetime. The solutions will provide the means of calculating the energy density and pressure of matter ϵ and p throughout the star. But the general metric functions of gravity $g_{\mu\nu}(x)$ reappear on the right side of Einstein's field equations in the energy-momentum tensor, (2.201), when referred to a general frame in accord with the principle of general covariance. Therefore the gravitational fields $g_{\mu\nu}(x)$ still appear on both sides of Einstein's field equations, and matter in bulk shapes spacetime just as spacetime shapes and moves matter in bulk. However, the local structure of matter is determined only by the equations of motion in Minkowski spacetime.

There are conceivable situations where the partial decoupling just described may not hold. In that case the equations of motion themselves contain, not the Minkowski metric tensor (a diagonal tensor with constant elements), but the general, spacetime-dependent, metric tensor. This is the fully coupled problem and obviously would be enormously difficult to solve. While we do not encounter this situation in this book (see as an example where strong coupling is used, Refs. [29, 30]), nonetheless it is worth seeing in symbolic form what the fully coupled problem looks like. The expectation that the stress-energy tensor should be obtained in general from a theory of matter by solving the field equations of the theory in a general gravitational field will be verified. It is also interesting to see Einstein's equations emerge from a variational principle.

We employ the gravitational action principle. As in all cases, the Lagrangian of gravity ought to be a scalar. We have encountered the Ricci scalar curvature $R = g^{\mu\nu}R_{\mu\nu}$, and from it, as Hilbert did, the Lagrangian density can be formed (with a prefactor that can be known only in hindsight):

$$\mathcal{L}_g = -\frac{1}{16\pi G} R\sqrt{-g}\,. \tag{2.229}$$

Here G is Newton's constant and g is the determinant of the metric $g_{\mu\nu}$, which is negative for our choice of signature for the metric. (Recall, for example, the Minkowski metric, or the Schwarzschild metric.) We also define the Lagrangian density

$$\mathcal{L}_m = L_m\sqrt{-g} \tag{2.230}$$

from the Lagrangian L_m of the matter and radiation fields ϕ_1, $\phi_2, \ldots$, which we denote collectively as ϕ. The total action is

$$I = \int (\mathcal{L}_g + \mathcal{L}_m)\, d^4x\,. \tag{2.231}$$

The coupled field equations for the matter and metric functions emerge as the conditions that yield vanishing variation of the action with respect to all the fields—the gravitational fields described by $g_{\mu\nu}$ and matter fields described by ϕ. The manipulations are quite tedious and are relegated to the next section. The field equations obtained are

$$\frac{\partial L_m}{\partial \phi} - \partial_\mu \frac{\partial L_m}{\partial(\partial_\mu \phi)} = 0\,, \tag{2.232}$$

$$G^{\mu\nu} = -8\pi G T^{\mu\nu}\,, \tag{2.233}$$

where $G^{\mu\nu} \equiv R^{\mu\nu} - \frac{1}{2}g^{\mu\nu}R$ is the Einstein tensor. The first of the field equations reduces to the familiar Euler–Lagrange equations in the limit of weak gravitational fields ($g_{\mu\nu} \to \eta_{\mu\nu}$). We shall encounter the Euler–Lagrange equations in studying theories of dense nuclear matter. The second are Einstein's field equations (2.214).

The matter-radiation energy-momentum tensor that emerges from the variational principle is given by

$$T^{\mu\nu} \equiv -g^{\mu\nu}L_m + 2\frac{\partial L_m}{\partial g_{\mu\nu}}\,. \tag{2.234}$$

The second term is

$$2\frac{\partial L_m}{\partial g_{\mu\nu}} = 2\frac{\partial L_m}{\partial(\partial_\alpha\phi)}\frac{1}{2}\frac{\partial(g_{\alpha\beta}\partial^\beta\phi)}{\partial g_{\mu\nu}} = \frac{\partial L_m}{\partial(\partial_\mu\phi)}\partial^\nu\phi\,.$$

Combining these results yields the canonical form of the energy-momentum tensor in field theory (for example, see (4.27) or Ref. [7]) except that the Minkowski tensor

is replaced by the general metric of gravity. Thus we have

$$T^{\mu\nu} = -g^{\mu\nu}L_m + \sum_{\phi} \frac{\partial L_m}{\partial(\partial_\mu \phi)} g^{\nu\alpha}\partial_\alpha \phi \,, \tag{2.235}$$

where the sum is over the various fields ϕ in L_m. In this way we see how the equations couple all matter and gravitational fields, $\phi(x)$, ..., $g^{\mu\nu}(x)$ in the general case.

2.10.1 Derivations

We write down most of the steps in deriving the Einstein field and matter-radiation equations from the variation of the action. The gravitational and matter fields will be subjected to arbitrary variations except the values and first derivatives will be kept constant on the boundaries. We concentrate on the gravitational part because that is the hardest. First, from (2.68) and (2.96) we readily obtain by differentiation,

$$g^{\alpha\mu}{}_{.\sigma}\, g_{\mu\nu} + g^{\alpha\mu}\left(\Gamma_{\nu\mu\sigma} + \Gamma_{\mu\nu\sigma}\right) = 0$$

Multiply by $g^{\beta\nu}$ and sum on ν to find

$$g^{\alpha\beta}{}_{.\sigma} = -g^{\alpha\mu}\Gamma^{\beta}_{\mu\sigma} - g^{\beta\nu}\Gamma^{\alpha}_{\nu\sigma} \,. \tag{2.236}$$

Next, evaluate

$$\begin{aligned}(g^{\mu\nu}\sqrt{-g})_{,\sigma} &= g^{\mu\nu}{}_{,\sigma}\sqrt{-g} + g^{\mu\nu}(\sqrt{-g})_{,\sigma} \\ &= -g^{\mu\rho}\Gamma^{\nu}_{\rho\sigma}\sqrt{-g} - g^{\nu\rho}\Gamma^{\mu}_{\rho\sigma}\sqrt{-g} + g^{\mu\nu}(\sqrt{-g})_{,\sigma} \,.\end{aligned}$$

Use (2.149) to find

$$(g^{\mu\nu}\sqrt{-g})_{,\sigma} = \left(-g^{\mu\rho}\Gamma^{\nu}_{\rho\sigma} - g^{\nu\rho}\Gamma^{\mu}_{\rho\sigma} + g^{\mu\nu}\Gamma^{\rho}_{\sigma\rho}\right)\sqrt{-g} \,. \tag{2.237}$$

Now set $\sigma = \nu$ and contract. After a cancelation of two terms, find,

$$(g^{\mu\nu}\sqrt{-g})_{,\nu} = -g^{\nu\alpha}\Gamma^{\mu}_{\alpha\nu}\sqrt{-g} \,. \tag{2.238}$$

The above results can now be employed to rewrite the gravitational action (where, as usual, we set $G = c = 1$ whenever convenient);

$$16\pi I_g = \int R\sqrt{-g}\, d^4x \,. \tag{2.239}$$

From (2.168) define

$$\begin{aligned} L &\equiv g^{\mu\nu}\left(\Gamma^{\sigma}_{\mu\nu}\Gamma^{\rho}_{\sigma\rho} - \Gamma^{\rho}_{\mu\sigma}\Gamma^{\sigma}_{\nu\rho}\right) \\ M &\equiv g^{\mu\nu}\left(\Gamma^{\sigma}_{\mu\sigma,\nu} - \Gamma^{\sigma}_{\mu\nu,\sigma}\right) \,. \end{aligned} \tag{2.240}$$

With these definitions the scalar curvature becomes

$$R = M - L \,. \tag{2.241}$$

Use (2.237) and (2.238) to find

$$\begin{aligned} M\sqrt{-g} = {} & (g^{\mu\nu}\Gamma^{\sigma}_{\mu\sigma}\sqrt{-g})_{,\nu} - (g^{\mu\nu}\Gamma^{\sigma}_{\mu\nu}\sqrt{-g})_{,\sigma} \\ & - (g^{\mu\nu}\sqrt{-g})_{,\nu}\Gamma^{\sigma}_{\mu\sigma} + (g^{\mu\nu}\sqrt{-g})_{,\sigma}\Gamma^{\sigma}_{\mu\nu} \,. \end{aligned} \tag{2.242}$$

The first two terms are perfect differentials and so contribute nothing under the integral because of the vanishing of the fields and their derivatives on the boundaries. After some manipulation, the remaining two terms are found to be $2L\sqrt{-g}$. Consequently,

$$\begin{aligned} 16\pi I_g &= \int L\sqrt{-g}\, d^4x \\ &= \int g^{\mu\nu}\left(\Gamma^{\sigma}_{\mu\nu}\Gamma^{\rho}_{\sigma\rho} - \Gamma^{\rho}_{\mu\sigma}\Gamma^{\sigma}_{\nu\rho}\right)\sqrt{-g}\, d^4x\,. \end{aligned} \tag{2.243}$$

Now evaluate the variation, examining separately the two terms in the integrand. Use (2.149) and (2.238) to rewrite the variation of the first term;

$$\begin{aligned} &\delta\left(g^{\mu\nu}\Gamma^{\sigma}_{\mu\nu}\Gamma^{\rho}_{\sigma\rho}\sqrt{-g}\right) = \\ &\Gamma^{\alpha}_{\mu\nu}\delta(g^{\mu\nu}(\sqrt{-g})_{.\alpha}) - \Gamma^{\beta}_{\alpha\beta}\delta(g^{\alpha\nu}\sqrt{-g})_{.\nu} - \Gamma^{\beta}_{\alpha\beta}\Gamma^{\alpha}_{\mu\nu}\delta(g^{\mu\nu}\sqrt{-g})\,. \end{aligned}$$

Use (2.236) to develop the variation of the second term in (2.243) and find

$$\delta(g^{\mu\nu}\Gamma^{\rho}_{\mu\sigma}\Gamma^{\sigma}_{\nu\rho}\sqrt{-g}) = -\Gamma^{\alpha}_{\nu\beta}\delta(g^{\nu\beta}{}_{.\sigma}\sqrt{-g}) - \Gamma^{\beta}_{\mu\alpha}\Gamma^{\alpha}_{\nu\beta}\delta(g^{\mu\nu}\sqrt{-g})\,.$$

Assemble the above two results and introduce the perfect differentials with compensating terms to form the variation of the integrand of (2.243);

$$\begin{aligned} \delta\mathcal{L}_g &= [\Gamma^{\alpha}_{\mu\nu}\delta(g^{\mu\nu}\sqrt{-g})]_{,\alpha} - [\Gamma^{\beta}_{\alpha\beta}\delta(g^{\alpha\nu}\sqrt{-g})]_{,\nu} \\ &\quad + (-\Gamma^{\alpha}_{\mu\nu,\alpha} + \Gamma^{\beta}_{\mu\beta,\nu} + \Gamma^{\beta}_{\mu\alpha}\Gamma^{\alpha}_{\nu\beta} - \Gamma^{\beta}_{\alpha\beta}\Gamma^{\alpha}_{\mu\nu})\delta(g^{\mu\nu}\sqrt{-g})\,. \end{aligned}$$

The first two terms are perfect differentials and yield zero because the variations vanish on the boundary. The remaining bracket is the Ricci tensor (2.168). Therefore, we have for the variation of the gravitational action

$$\delta I_g = \frac{1}{16\pi}\int R_{\mu\nu}\delta(g^{\mu\nu}\sqrt{-g})\, d^4x\,. \tag{2.244}$$

Next, again from (2.68) deduce that

$$\delta g^{\alpha\nu} = -g^{\mu\alpha}g^{\nu\beta}\delta g_{\alpha\beta}\,. \tag{2.245}$$

Also, from (2.148) find

$$2\sqrt{-g}(\sqrt{-g})_{.\alpha} = (\sqrt{-g}\sqrt{-g})_{.\alpha} = g_{.\alpha} = gg^{\mu\nu}g_{\mu\nu,\alpha}\,.$$

Consequently,

$$(\sqrt{-g})_{.\alpha} = \tfrac{1}{2}\sqrt{-g}g^{\mu\nu}g_{\mu\nu.\alpha}\,. \tag{2.246}$$

With this result we now have

$$\delta(g^{\mu\nu}\sqrt{-g}) = -\left(g^{\mu\alpha}g^{\nu\beta} - \tfrac{1}{2}g^{\mu\nu}g^{\alpha\beta}\right)\sqrt{-g}\,\delta g_{\alpha\beta}\,. \tag{2.247}$$

Recalling the definition of Einstein's curvature tensor, we have obtained

$$\delta I_g = -\frac{1}{16\pi}\int G^{\alpha\beta}\sqrt{-g}\,\delta g_{\alpha\beta}\, d^4x\,. \tag{2.248}$$

Thus we derive Einstein's field equation in empty space from the vanishing of the variation of the gravitational action.

If we add the action of matter and radiation fields to the gravitational action, we get the total action. Under arbitrary variations of the gravitational and other fields we insist that the total action vanish. This leads to the Euler–Lagrange equations (2.232) for the matter-radiation fields and to the Einstein equations (2.233) for the gravitational fields. Note, however, that the equations of motion for the matter-radiation fields contain the gravitational fields $g^{\mu\nu}$ and they reduce to the usual form in Minkowski spacetime only when the $g^{\mu\nu}$ can be replaced by the Minkowski tensor.

Return now to the total action (2.231) and vary all fields. Also use the result (2.248) for the variation of $\mathcal{L}_g$

$$\delta I = \int \Big[\Big\{ -\frac{1}{16\pi} G^{\alpha\beta}\sqrt{-g} + \Big(\frac{\partial \mathcal{L}_m}{\partial g_{\alpha\beta}} - \partial_\nu \frac{\partial \mathcal{L}_m}{\partial g_{\alpha\beta,\nu}} \Big) \Big\} \delta g_{\alpha\beta} + \Big\{ \frac{\partial \mathcal{L}_m}{\partial \phi} - \partial_\nu \frac{\partial \mathcal{L}_m}{\partial(\partial_\nu \phi)} \Big\} \delta\phi \Big] d^4x \,. \tag{2.249}$$

The last term in each curly brackets was obtained by an integration by parts, as follows:

$$\frac{\partial \mathcal{L}}{\partial f_\mu} \partial f_{,\mu} = \partial_\mu \left(\frac{\partial \mathcal{L}}{\partial f_{,\mu}} \delta f \right) - \partial_\mu \frac{\partial \mathcal{L}}{\partial f_{,\mu}} \delta f \,,$$

where f stands for either $g_{\mu\nu}$ or ϕ. The integral over the first term on the right vanishes because the f are not varied on the boundary. Because the variations are otherwise arbitrary, the vanishing of the action implies the vanishing of the coefficients of the varied fields. The variation of the matter fields yields (2.232) (where we have removed $\sqrt{-g}$ because it is unaffected by the ϕ variation). The variation of the gravitational fields yields

$$G^{\alpha\beta}\sqrt{-g} = 16\pi \left(\frac{\partial \mathcal{L}_m}{\partial g_{\alpha\beta}} - \partial_\nu \frac{\partial \mathcal{L}_m}{\partial g_{\alpha\beta,\nu}} \right) . \tag{2.250}$$

This equation shows how the gravitational and matter fields are coupled. We use it to derive (2.233) by showing that the right side is the energy-momentum tensor in the form (2.234). The familiar form (2.235) then follows. Evaluate the first term on the right side of 2.250:

$$\frac{\partial \mathcal{L}_m}{\partial g_{\alpha\beta}} = L_m \frac{\partial \sqrt{-g}}{\partial g_{\alpha\beta}} \,. \tag{2.251}$$

Because

$$\frac{\partial g}{\partial g_{\mu\nu}} = g g^{\mu\nu} \,, \tag{2.252}$$

which follows by differentiating the identity $g = g_{\mu\nu} g^{\mu\nu}$, we obtain

$$\frac{\partial \mathcal{L}_m}{\partial g_{\alpha\beta}} = \left(-\tfrac{1}{2} g^{\alpha\beta} L_m + \frac{\partial L_m}{\partial g_{\alpha\beta}} \right) \sqrt{-g} \,. \tag{2.253}$$

The matter Lagrangian will not usually depend on derivatives of the metric, but only on the metric itself. Thus, with the above equation we have derived (2.233) with the energy momentum tensor given by (2.234).

2.11 Problems for Chapter 2

1. Derive and solve the equations (2.12) for the Lorentz transformation (2.15).
2. Derive the transformation for an arbitrary boost, (2.18).
3. Derive the four-velocity components (2.42).
4. Check that the energy–momentum tensor takes the form (2.49).
5. Derive the coordinate expression for $g_{\mu\nu}$ in (2.53). Review the motion of a free particle in an arbitrary gravitational field, and derive the geodesic equation of motion, (2.85).
6. Derive the transformation property of the Christoffel symbol (2.90).
7. Prove the expression of the affine connection (2.93).
8. Prove the expression involving the Christoffel symbols (2.96).
9. Obtain the geodesic equation (2.107) as the extremal of the propertime.
10. Follow all the steps in the derivation of the g_{00} in (2.119).
11. Derive the expression (2.122) for the covariant derivative of a contravariant vector.
12. Two esoteric-looking results that are used in the variational principle for the derivation of Einstein's equations are (2.148) and (2.149). Derive them in detail.
13. Review the details of the derivation of the conservation of total charge (2.156).
14. Derive (2.159) and with it the expression for the Riemann curvature tensor (2.160).
15. Derive the expression for the Ricci tensor (a contraction of the Riemann tensor) given by (2.168). Show that it is symmetric, though not manifestly so.
16. Prove the Bianchi identities (2.172), thus paving the way to the proof that the Einstein curvature tensor has vanishing covariant divergence (2.174). Prove the latter also. Einstein was unaware of the Bianchi identities and this delayed his discovery of General Relativity.
17. From the above, understand the three possibilities of Section 2.8.
18. Derive at least three of the expressions for the affine connections in static spherical isotropic spacetime (2.187).
19. Derive the Schwarzschild solution for relativistic static stars (2.199).
20. Derive the relationship of the components of the Einstein tensor to the metric functions of static spherical spacetime (2.206).
21. Derive all intermediate steps including the identification of k with the Newton constant G (2.213).
22. Derive the explicit Einstein equations for a static spherical star, (2.216) to (2.219).

23. Go through the details of manipulation of the above equations that are outlined in (2.220) to (2.223).

24. Hence, derive the Oppenheimer–Volkoff equation (2.224).

25. Follow the principle steps in the derivation of the coupled matter and gravitational fields as expressed by (2.232) and (2.233) as given in Section 2.10.1.

3

Compact Stars: From Dwarfs to Black Holes

3.1 Birth and Death of Stars

"A star is drawing on some vast reservoir of energy.... This reservoir can scarcely be other than the subatomic energy.... There is sufficient in the Sun to maintain its output of heat for 15 billion years."
A. Eddington, 1920 [31]

Clouds of interstellar gas consisting mostly of molecular hydrogen and a little dust are the incubators of stars. The Horsehead Nebula in Orion is an especially beautiful example. The clouds are diffuse and highly nonuniform, with clumps and filaments interspersed throughout. The gas spans a wide range of temperature. Most of it is cold at 10 K, but some regions are as hot as 2000 K. Interstellar clouds range in size from less than a light year to several hundred light years across and in mass from 10 to $10^7 M_\odot$. A compression of the order 10^{20} is involved in forming a star from this diffuse gas. Stars more massive than a few $M_\odot$ are observed to form in small groups in the densest regions of the clouds. The motion of a given star often suggests the gravitational influence of several nearby stars. About half of all stars are in binaries.

Important factors in stellar formation are gravity, dust, gas pressure, rotation, magnetic fields, winds and radiation from nearby young stars, and radiative shock waves. Our understanding of how these factors conspire to induce collapse of a relatively small region of an otherwise long-lived dynamic, but stable, *molecular cloud* is at a rudimentary level.

The dust in molecular clouds originates on the cool stellar surfaces of *supergiants*, massive stars in a late stage of stellar evolution. Dust shields cloud interiors from ultraviolet starlight, enabling their centers to cool. With lower thermal pressure, gravitational collapse of the denser regions of clouds becomes inevitable.

At some stage a perturbation (such as the passage of a shock wave or of a shell of expanding gas from a supernova remnant) induces an instability in a critical mass of cloud. Sir James Jeans derived the critical mass (now known as the Jeans mass[1]) in the early twentieth century. A clump of gas then begins a fall toward its mass center under the attraction of gravity. Gravitational energy is converted to heat by the compression. The opacity of the gas increases as its density and establishes a temperature and thermal pressure gradient which approximately balances gravity in a state of quasi-hydrostatic equilibrium. Energy loss by radiation at the *protostar's* surface causes further slow contraction and heating until the core temperature rises to the ignition point for fusing hydrogen into helium ($T \approx 10^7$ K). Thereafter fusion becomes the dominant energy source and the thermal and radiation pressure will now nearly balance gravity for millions to billions of years, a time scale depending approximately on the inverse square of the stellar mass (Table 3.1).

The protostar has now joined the *main sequence* of stars, the evolutionary pathway of stars first proposed by H. N. Russell. The star will spend most of its luminous life in this state of suspended collapse as it burns its large store of hydrogen, slowly radiating energy from its surface.

Thermonuclear fusion[2] provides the energy for the "great furnace," in the phrase of Eddington, which drives stars through the various stages of combustion—hydrogen, helium, carbon, neon, oxygen, magnesium, and silicon. Fusion will end when iron, the most bound nuclear species, is reached. Beyond iron, fusion is no longer exothermic. Nuclei in the region of iron are referred to as the iron peak nuclei because of their higher binding than other nuclei; see Fig. 3.1.

After hydrogen is spent in the core, the next phase of burning—helium—will commence. Hydrogen in a surrounding shell will continue to burn. The star is

TABLE 3.1. Evolutionary times of stars

$M/M_\odot$	Years
30	5×10^6
15	1×10^7
10	2×10^7
5	7×10^7
1	1×10^{10}
0.1	3×10^{12}

[1]The Jeans mass depends sensitively on the temperature of the gas cloud.

[2]Thermonuclear fusion refers to nuclear fusion induced by tunneling through the Coulomb barrier between nuclei. Thermal motion provides the energy for tunnelling. Fusion is exothermic up to iron.

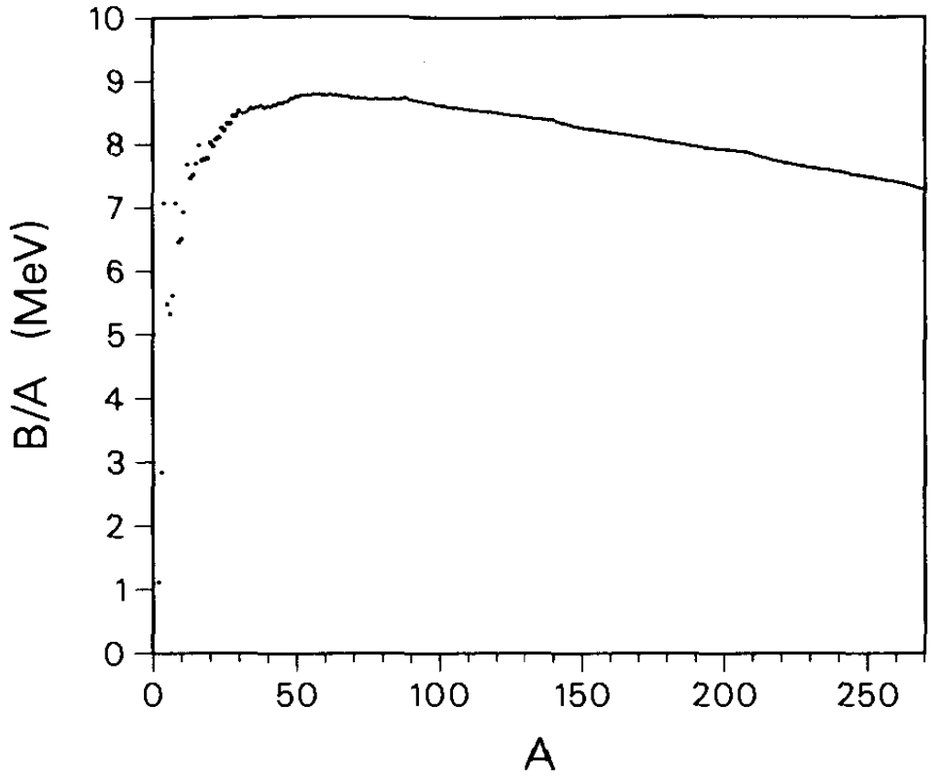

FIGURE 3.1. Binding energy as a function of baryon number showing the peak in binding at iron. (Courtesy of Richard Firestone and the Table of Isotopes Group at Lawrence Berkeley National Laboratory.)

hottest in its center and heat is transported by radiation, conduction, and convection to the surface where it is radiated. Ever higher temperatures are required to drive quantum-mechanical nuclear tunnelling—first explained by George Gamow—through the increasing Coulomb barriers along the reaction chain. Hydrogen and then helium burning in the core sustain the star on the main sequence for most of its life. As helium burns, a carbon core is formed. Concentric burning shells are established as one element after another is synthesized [32]. Carbon burning in the core lasts for only a few thousand years. Copious gamma rays in the core produce electron–positron pairs that annihilate, producing neutrino pairs. Neutrino losses increase as a high power of the temperature. At this stage the loss is so great that succeeding burning stages progress ever more rapidly—oxygen in a year, silicon in a week. At the exhaustion of each elemental fuel, the core contracts further until the ignition temperature for the next step in the chain is reached. In some cases the heat output from combustion in a succeeding step will be so great as to cause a reexpansion of the outer parts of the star.

The cessation of nuclear fusion signals the end of the luminous stage of the star. The duration of the fusion stage (in which a star spends most of its life) as well as its final evolution depends on the stellar mass. Combustion to the iron end point is attained in massive stars[3] which end through a complex terminal stage either as neutron stars or black holes. Combustion is slower and incomplete in light stars. They end as white dwarfs. Whatever the final end point—dwarf, neutron star, or

[3]We shall usually use massive stars to refer to those with mass $M \geq 8M_{\odot}$.

TABLE 3.2. Mass, radius, Schwarzschild radius, and average density of some typical bodies (with all numbers rounded to one significant figure). Nominal neutron star = N.s., white dwarf (Sirius B) = W.d.

Name	$M/M_\odot$	R (km)	r_S (km)	$\overline{\rho}$ (g/cm^3)
N.s.	2	10	6	5×10^{14}
W.d.	1	5400	3	3×10^6
Sun	1	7×10^5	3	1.4
Jupiter	10^{-3}	7×10^4	3×10^{-3}	1.3
Earth	3×10^{-6}	6000	9×10^{-6}	5.5

black hole—it is the gravity of the star's mass that drives stellar evolution and its rate from beginning to end.

For light stars up to a few solar masses, contraction begins again when hydrogen is exhausted in the core. As the temperature increases, hydrogen begins to burn in the outer layers. The envelope expands slowly to become a *red giant* while the core continues to contract and heat. At 10^8 K three helium nuclei fuse to form carbon followed by an additional helium to form oxygen. These reactions sometimes begin explosively. Eventually, pulsations in the envelope become unstable, and most of the star is shaken off to form a *planetary nebula*.

The remaining core of the star is composed mostly of helium, carbon, oxygen, or magnesium (sometimes a mixture) depending on how far the reactions proceeded before the instability removed the compressing weight of the bulk of the star. With the loss of the envelope, its weight and opacity, the combustion temperature can no longer be sustained. The core now contracts under its own gravity to form a white dwarf[4], a star whose high surface temperature makes it appear white[5]. A white dwarf has a radius of a few thousand kilometers and an average density of the order of 10^6 that of the Earth (see Table 3.2). After formation, a white dwarf radiates the residue of its earlier hot existence as photons for 10^{10} years. It cools, crystallizes, and disappears as a *black dwarf*. It is possible that the universe is not yet old enough for the final state of dwarfs to have formed.

Because of the low mass of the progenitor, gravity propels light stars through their evolution at a much slower rate than massive stars. Stars that terminate their life as dwarfs typically attain great age before the dwarf stage. The Sun, presently of age 4.5×10^9 years, is expected to live to 12 billion years before collapsing to the dwarf stage, according to modern theory. Eddington's 1920 estimate is in remarkable agreement.

Stars above eight solar masses evolve more rapidly than the progenitors of dwarfs. Most importantly, the thermonuclear reactions proceed further, the star

[4]Most astronomical objects are named after some descriptive feature. The white dwarf was the smallest star known at the time of its discovery.

[5]White dwarfs have surface temperatures as high as 100,000 K and as low as 4000 K, depending on age and the circumstances of birth.

becoming ever hotter until it expands into a super red giant.[6] In the central region of the star, the reactions burn to the iron end point. The core of the star is now supported against collapse only by the pressure of degenerate nonrelativistic electrons. Nuclear burning continues in surrounding shells of Si, O, ... overlying the now inert, central region of iron. The core has a radius of only several thousand kilometers lying within the red supergiant of radius $> 10^8$ km.

Burning in the outer shells adds to the iron core mass. Gravity crushes the core to such a density that electrons become relativistic. The pressure they provide now increases less rapidly with increasing density than was the case at the earlier stage when the electrons were nonrelativistic.[7] Moreover, the kinetic energies of the relativistic electrons have reached the point that capture on protons—*inverse beta decay*—produces an energetically more favorable state. The supporting electron pressure is thus diminished below the point at which it can support further growth in the mass of the iron core against gravity. The core has attained its maximum possible mass named after S. Chandrasekhar who first discovered the limit for an object supported by the pressure of ultrarelativistic, degenerate electrons.

The core then commences a rapid implosion taking less than a second. It becomes extremely hot, attaining temperatures toward the end of collapse of the order of tens of MeV ($\sim 10^{11}$ K). The core is bloated with energetic neutrinos produced by inverse beta decay in the continued *neutronization* of the core material during collapse. The cross-section for the interaction of energetic neutrinos and nuclei at densities of 10^{12}g/cm^3 is sufficiently large as to trap the neutrinos by collisions in the imploding core. They are swept along with the falling material. Moreover, neutrino pairs are created in great abundance by photoproduction ($\gamma \longrightarrow \nu\bar{\nu}$) as the collapsing core attains temperatures of tens of MeV. As the core matter is crushed to high density, the Fermi energy of the thermalized electrons and neutrinos rises. Their pressure, together perhaps with the short-range repulsion between nucleons, resists further compression.

The infalling core material rebounds from the stiffened core, sending outward a shock wave originating somewhere in the core interior. As the shock travels outward, its energy is dissipated by neutrino losses and by photodisintegration of all nuclei in its path. The shock stalls at a few hundred kilometers from the stellar center.

When the stellar material above the region occupied by the core prior to its implosion is no longer supported by the core, a decompression wave travels outward at the speed of sound in the diffuse stellar material of the red giant, and freefall of this material commences. The signal takes a long time to reach the edge of the star compared to the time from the core implosion to shock rebound and its subsequent stall.

The freefalling material is arrested as it meets the stalled shock front, turning the latter into an accretion shock. The infalling matter heats the region of the accretion

[6]For massive stars the red giant stage is sometimes referred to as supergiant.
[7]Compare (3.90) and (3.93).

shock, and at the same time its momentum and mass exert an inward-directed pressure gradient.

A rarefied bubble region develops between the high-density core and the accreting shock front. Neutrino pairs diffusing from the hot interior, annihilate, heat, and expand the bubble. Through a complex (and not completely understood) interplay of convection and neutrino heating, a fraction (less than one percent) of the immense gravitational binding energy of the neutron star is transported to the accretion front. It is this small fraction that provides the kinetic energy for the ejection of all but the core of the progenitor star in a *supernova* explosion.

An elementary calculation that we shall shortly do reveals that the energy release of the neutron star (foreseen many years ago by Baade and Zwicky (1934) [1] as the engine driving supernovae) is $\sim 10^{53}$ ergs. It has taken some thirty years since the early work of Colgate and White (1966) [33] to arrive at a partial understanding of how a small fraction of this energy release, not much more nor less than 1/100, is so reliably converted to the kinetic energy of ejection (see especially Colgate in [34]).

For those stellar evolutions that end in a supernova explosion, the hot collapsed core or *protoneutron* star, with temperature of tens of MeV, loses its trapped neutrinos over an interval of some seconds and cools to an MeV or less [35]. At that point the collapsed core has reached its equilibrium composition of neutrons, protons, hyperons, leptons, and possibly quarks. Thus is born a *neutron star* of radius about ten kilometers and average density 10^{14} times greater than that of Earth. The star continues to cool for millions of years by the slow diffusion of photons to the surface and their radiation into space.

The bulk of the star blown off in the explosion, the *supernova remnant*, expands outward at great velocity (10,000 km/s) sweeping up interstellar gas. The remnant is visible at all wavelengths between radio and X rays, signifying the richness of the processes taking place in the ejecta and between ejecta and the interstellar medium, including molecular clouds. Only in some cases have associations been made between supernova remnants and *pulsars*, rotating magnetized neutron stars [36]–[39]. The remnants are visible for only about 10^4 to 10^5 years; pulsars are active for $\sim 10^7$ years or more.

For some unknown fraction of massive collapsing stars, the explosion is believed to fail or to fail to eject sufficient infalling material. The progenitor star therefore continues its *prompt* gravitational collapse to a black hole of mass about equal to the presupernova star ($> 8M_\odot$). This is so because there is a maximum mass, called the Oppenheimer–Volkoff mass limit, that can be sustained against gravitational collapse by the pressure of degenerate neutrons and their repulsive interaction. Although not many neutron star masses are known, they appear to be clustered around $1.4M_\odot$ [40], close to the Chandrasekhar limit for a degenerate iron core which undergoes implosion at the end of the luminous stage. If the limit for neutron star masses is not far above this, only a small amount of accretion onto the collapsed core will push it beyond the limit.

There is an additional mechanism for *delayed* collapse after formation of a protoneutron star and ejection in a supernova of most of the star. Some of the

nucleons and high-energy electrons in the protoneutron star can find a lower energy state as the last of the neutrinos are lost. This phenomenon is *hyperonization*, a process analogous to neutronization, in which the pressure of neutrons and protons is diminished by their conversion to hyperons [41]. Hyperonization may bring about the collapse of stars hovering near the limiting mass [42]–[46].

Thus, continued gravitational collapse can occur under several circumstances. Prompt collapse will result if the explosion fails altogether, creating a *black hole* having the approximate mass of the progenitor, more than $8M_\odot$ and perhaps up to $50M_\odot$. Delayed collapse may occur if the protoneutron star is close to the mass limit even if an explosion does eject most of the progenitor star (Section 11.2). In the second case, a low-mass black hole (~ 1.5 to $2M_\odot$) will be created. Black holes of about this mass can also be created in the *accretion-induced collapse* of neutron stars in binary systems.[8] Accretion is a slow process. The surface of the neutron star will be heated by infalling material. When the infall rate is such that the radiation pressure from the hot surface counterbalances the gravitational force acting on the infalling material, a limit is reached. It is known as the Eddington limit.

Another type of black hole deserves mention. It is not the end point in the evolution of a single star, but rather is thought to be formed by the condensation of a dense *star-cluster* [47]. Such supermassive black holes as these are probably the maelstroms of *active galactic nuclei.*

Once formed, isolated neutron stars and white dwarfs will live almost unchanged forever. They will slowly cool, and their magnetic fields will decay. Pulsar rotation will slow and they will eventually become invisible, their emission terminated when the combination of rotation and magnetic field become too feeble. They will join the host of unseen neutron stars accumulated over the life of the universe. However, the internal baryon constitution of neutron stars will be essentially frozen within a few seconds of birth, once the temperature has fallen below a few MeV.[9] White dwarfs will become crystals after cooling for billions of years, when their temperature falls below the lattice energy associated with nuclei embedded in an electron gas. There is no reason other than an encounter with another star that they should not endure forever as dead stars.

Let us briefly consider another perspective. Of all astrophysical phenomena, none are more essential to life as we know it than the evolution of stars and the eventual explosion of some of them in supernovae. Only a few of the lightest elements were produced during the primordial nucleosynthesis in the Big Bang, none heavier then ^{7}Li [48, 49]. Other elements, up to iron, are synthesized by thermonuclear reactions during the 10^7 year evolution of massive stars, the heavier

[8]Compact stars in binary systems can slowly accrete matter from a less dense companion. Accretion onto a neutron star or white dwarf near their respective mass limits can cause collapse to a black hole or white dwarf, respectively.

[9]The notable exceptions are millisecond pulsars, which because of the strong centrifugal force, change internal density and therefore composition, as they slowly spin down.

of these in the last few days of the life of the presupernova star [32]. The heaviest elements are synthesized in supernovae explosions [50].

We ourselves (like the Earth and all life on it) are made in large part from the material of earlier generations of stars. Even now, 10^{10} years after the big bang and a thousand generations of massive stars latter, the abundance of elements is still dominated by hydrogen.[10] Nevertheless, the abundance of elements changes slightly with each succeeding stellar generation. The earliest and oldest stars contain negligible amounts of the elements heavier than helium. Younger stars are richer in heavier elements, referred to as their *metalicity*. The lowest energy state of nucleons and nuclei is ^{56}Fe. This is the ground state toward which the universe is evolving on an unimaginably long timescale. It is interesting to note that since the extinction of the dinosaurs 7×10^7 years ago, seven generations of massive stars have been born and died.

3.2 Objective

In the last chapter we saw that spacetime is curved in our universe, populated as it is by massive objects, galaxies, stars, and so on. This fact, so amazing because of our acquaintance with Euclidean geometry and its apparent accuracy in our vicinity, was arrived at by pursuing the underlying meaning of the equivalence of inertial and gravitational masses. From Schwarzschild's solution to Einstein's equations, we learned the metric of this curved spacetime in the empty space outside a static star.

The interior problem is the central concern of this book, and it is rather more delicate. We are accustomed to thinking of matter in flat spacetime, in terms of the Special Theory of Relativity. Our theories of nuclear matter are worked out in such a frame or even in flat space. By computing properties of matter in flat spacetime (the equation of state, for example), a question of principle must be addressed when the matter resides in strong gravitational fields. Is the local inertial (Lorentz) frame surrounding each spacetime point in the star sufficiently large to justify solving the equations of motion for matter in flat spacetime and, constructing from the solution, the equation of state and the energy-momentum tensor for the relevant densities in the star? If not, we would have to solve the fully coupled problem of gravity simultaneously with the equations of motion containing the general metric functions and the matter and radiation fields (2.232, 2.233).

In this chapter we introduce essential material and concepts for understanding the constitution of compact stars and the various forms in which they may be realized in nature. In the process we answer the question of principle raised in the preceding paragraph. Gravitational units and their relation to the units that are convenient in the nuclear and particle physics of dense matter are introduced. We

[10]The primordial helium abundance is about 23 percent, coming after hydrogen, and is otherwise far more abundant than other elements processed in supernovae.

take the occasion to estimate the mass, baryon number, and radius of neutron stars. Certain general properties of stars and gravity are discussed, including charge neutrality and gravitational redshift.

We introduce elementary models of white dwarfs and neutron stars beginning with the most basic model of dense matter—a free Fermi gas of nucleons. The famous Chandrasekhar asymptotic mass limit of white dwarfs is derived, and then the physical limit imposed by electron capture is discussed. Real white dwarfs are not composed of free nucleons but of nuclei, so carbon and oxygen models are developed.

In the previous chapter we commented on a maximum or limiting mass of compact stars imposed by the nature of gravity. In the present chapter we show that, even if composed of an incompressible medium, a *relativistic* star has a maximum mass.

An upper bound on the limiting mass of neutron stars is obtained from very general considerations and independently of particular theories of dense matter. The limiting mass is important in distinguishing black hole candidates of a few solar masses from neutron stars. Finally, we present a brief section on black holes. Detailed studies of neutron and other compact stars, such as hyperon stars, hybrid stars with an interior region of quark matter surrounded by nuclear matter, and strange stars, await our development of a theory of superdense charge-neutral matter in this and later chapters.

3.3 Gravitational Units and Neutron Star Size

A compact star near the limit of collapse to a black hole has a higher density than any other star. Such a star is referred to as a neutron star. We want to show that the gravitational field (which in General Relativity is the collection of metric functions $g_{\mu\nu}$) changes by an infinitesimal amount over the distance between nucleons in such a star—and hence for all stars. If this is true, and it is as we shall show, it means that we can solve the problem of the matter fields in flat (Minkowski) spacetime as is customary in treating problems having to do with experiments under conditions such as those on the Earth. This is the physical motivation of the section.

This section also has a practical computational motivation—the introduction of convenient units. We deal in this book with three scales—the astronomical or large scale, the macroscopic or intermediate scale of our own experience, and the microscopic or nuclear and subnuclear scale. For example, the center of a neutron star is composed of matter that is a few times the density of nuclear matter while its surface is composed of iron—a difference of 14 orders of magnitude. The size of a neutron star is of the order of ten kilometers—a measure common to our daily experience. Its total mass, the integral of the energy density over its volume, is several solar masses.

3.3.1 Units

Gravitational units $G = c = k = 1$ (where k is the Boltzmann constant) often are useful, not only because they facilitate computation, but because our equations are not burdened with the appearance of c, G, and $\hbar$ in various powers and combinations. We start with gravitational (or geometricised) units:

$$\begin{aligned} 1 &= c = 2.9979 \times 10^{10}\ \mathrm{cm/s}\,, \\ 1 &= G = 6.6720 \times 10^{-8}\ \mathrm{cm^3\ g^{-1}\ s^{-2}}\,, \\ 1 &= k = 1.3807 \times 10^{-16}\ \mathrm{erg/K}\,, \end{aligned} \tag{3.1}$$

where K denotes temperature in degrees Kelvin. These definitions can be treated as equations so that, for example, we have

$$\begin{aligned} 1\ \mathrm{s} &= 2.9979 \times 10^{10}\ \mathrm{cm}\,, \\ 1\ \mathrm{g} &= 7.4237 \times 10^{-29}\ \mathrm{cm}\,, \\ 1\ \mathrm{K} &= 1.3807 \times 10^{-16}\ \mathrm{erg}\,, \\ 1\ \mathrm{s^{-2}} &= 1.4988 \times 10^{7}\ \mathrm{g/cm^3}\,, \\ 1\ \mathrm{erg} &= 1\ \mathrm{g\ cm^2\ s^{-2}} = 8.2601 \times 10^{-50}\ \mathrm{cm}\,, \\ 1\ \mathrm{dyne/cm^2} &= 8.2601 \times 10^{-40}\ \mathrm{km^{-2}}\,, \\ 1\ \mathrm{g/cm^3} &= 7.4237 \times 10^{-19}\ \mathrm{km^{-2}}\,. \end{aligned} \tag{3.2}$$

The last two units are used frequently in astrophysics as units of pressure and energy density, respectively. In particular, note in this last equation that energy density is expressed in inverse squared kilometers. It may seem peculiar that this should be a useful expression. However, if we integrate a quantity with this unit over the volume of a star, it expresses mass in the unit kilometer. As we comment below, the Sun's mass (through the conversion above from grams to centimeters or kilometers) is about 1.5 km. Hence the integral for a neutron star mass will be a number of the order of unity in these units instead of 10^{33} g.

In nuclear and particle physics a convenient unit of energy (or mass, Mc^2) is a million electron volts or MeV. Sometimes the GeV unit is used because it approximates the nucleon mass of $\sim$ 939 MeV. Its value in ergs and other units is given below.

$$\begin{aligned} \mathrm{MeV} &= 1.6022 \times 10^{-6}\ \mathrm{erg} = 1.3234 \times 10^{-55}\ \mathrm{cm}\,, \\ &= 1.7827 \times 10^{-27}\ \mathrm{g} = 1.1604 \times 10^{10}\ \mathrm{K}\,. \end{aligned} \tag{3.3}$$

The range of the nuclear force is $\sim 10^{-13}$ cm which is defined as a fermi and denoted by fm,

$$1\ \mathrm{fm} = 10^{-13}\ \mathrm{cm}\,. \tag{3.4}$$

Two important constants are the Plank constant $h = 2\pi\hbar$ and the elementary electric charge e,

$$\hbar c = 197.33\ \mathrm{MeV\ fm}\,.$$

$$e^2 = 1.4400\ \text{MeV fm} = (1.3805 \times 10^{-34}\ \text{cm})^2 . \tag{3.5}$$

Note the fine-structure constant $e^2/\hbar c$.

From the above value of MeV in grams, we derive energy density as expressed in two popular ways.

$$\begin{aligned} \text{MeV/fm}^3 &= 1.7827 \times 10^{12}\ \text{g/cm}^3 , \\ &= 1.6022 \times 10^{33}\ \text{dyne/cm}^2 \end{aligned} \tag{3.6}$$

The unit on the left is sometimes used in nuclear physics and and the ones on the right in many astrophysics papers.

In nuclear and particle physics, it is useful to use natural units chosen so that $\hbar = c = 1$. Then from the value of $\hbar c$ written above we obtain by dividing by fm^4

$$1/\text{fm}^4 = 197.33\ \text{MeV/fm}^3 . \tag{3.7}$$

These are both units of energy density and pressure, and both are suitable as stellar quantities, especially at nuclear and supernuclear densities. In the astrophysical literature, energy density is frequently expressed in g/cm^3 and pressure in dyne/cm^2 (dyne=erg/cm). It is therefore useful to have on hand the conversion factors

$$\begin{aligned} 1/\text{fm}^4 &= 3.5178 \times 10^{14}\ \text{g/cm}^3 , \\ &= 3.1616 \times 10^{35}\ \text{dyne/cm}^2 . \end{aligned} \tag{3.8}$$

Mixed units, which are useful in stellar calculations, are obtained by combining (3.7) with the value of MeV in cm,

$$\begin{aligned} 1/\text{fm}^4 &= 2.6115 \times 10^{-4}\ /\text{km}^2 , \\ \text{MeV/fm}^3 &= 1.3234 \times 10^{-6}\ /\text{km}^2 . \end{aligned} \tag{3.9}$$

The unit on the right side is appropriate for expressing the pressure and energy density when solving the Oppenheimer–Volkoff equations. As noted earlier, when energy density of a neutron star, expressed in such units is integrated over the radial coordinate, it yields a mass in the unit of kilometers. This can be compared with the solar mass,

$$M_\odot = 1.4766\ \text{km} = 1.989 \times 10^{33}\ \text{g} = 1.116 \times 10^{60}\ \text{MeV} . \tag{3.10}$$

As a curiosity, let us compare the spin of a neutron star expressed in units of $\hbar$. We note first that

$$\hbar = 2.6115 \times 10^{-76}\ \text{km}^2 . \tag{3.11}$$

From the latter we can calculate the spin of a pulsar in units of $\hbar$. In Chapter 5, we find for the moment of inertia of the Crab pulsar, $I \sim 70\ \text{km}^3$. Its period of rotation is $P = 1/30\ \text{s} = (2\pi)/\Omega$. We find it has a spin of

$$J = I\Omega = 1.3 \times 10^4\ \text{km}^3/\text{s} = 1.3 \times 10^4\ \text{km}^2 \cdot \text{km/s} = 5 \times 10^{79}\hbar . \tag{3.12}$$

This has no practical use, but is an interesting contrast with the spins of nuclei that range up to several tens of $\hbar$ for very excited states.

At various places in the book, we shall have occasion to use some of the relations derived above. Dimensional analysis will always aid in converting a computed quantity in gravitational or natural units back to familiar units that express its dimensions. For example, if in a computation it is found that a particle has an acceleration of $a = x/\text{km}$, knowing the dimension of a as length/time^2, we can multiply a by whatever quantities have been set to unity, so as to regain the dimension of a. Thus,

$$a = x/\text{km} = xc^2/\text{km} = (x/\text{km})(3 \times 10^5\ \text{km/s})^2 = 9x10^{10}\ \text{km/s}^2\,. \quad (3.13)$$

Of course sometimes one needs to use several of the quantities that have been set to unity, with various powers. At other times, relations between units derived above can be used. We encounter examples below, where now we return to an estimate of the size and number of baryons contained in a star.

3.3.2 *Size and number of baryons in a star*

We have noted that the Schwarzschild metric becomes singular at $r = r_S \equiv 2M$. For actual stars this radius is interior to the star itself where the Schwarzschild solution does not hold and the singularity therefore does not exist. However, for a neutron star, the Schwarzschild radius is not deep within the star as compared to other heavenly bodies as shown in Table 3.2. But in the special case where the star lies within its "gravitational radius," it must be a black hole.

Next we estimate the mass and radius of a star near the limit of gravitational collapse having $R = 2M$. This will be an estimate of the limiting or maximum mass possible for a neutron star. Assume that gravity packs nucleons up to their repulsive cores, say $r_0 \approx 0.5 \times 10^{-13}$ cm. Then

$$R \approx r_0 A^{1/3}, \quad M \approx Am\,, \quad (3.14)$$

where A is the number of baryons in the star and m is their mass,

$$m \approx 939\ \text{MeV} = 1.7 \times 10^{-24}\ \text{g} = 1.2 \times 10^{-52}\ \text{cm}\,. \quad (3.15)$$

Hence, substituting (3.14) into the equation $R = 2M$, we find

$$A^{2/3} = r_0/(2m) = 1.9 \times 10^{38}\,. \quad (3.16)$$

Putting this result back into the expressions for radius and mass, we have

$$\begin{aligned} A &= 2.6 \times 10^{57}\,, \\ R &= r_0 A^{1/3} = 7\ \text{km}, \\ M &= R/2 = 3.5\ \text{km} = 2.3 M_\odot\,. \end{aligned} \quad (3.17)$$

Here we have an estimate of the baryon number, radius, and mass of a star at the limit. In Figs. 3.2 and 3.3 the baryon number is plotted as a function of stellar mass for a model sequence of neutron stars. Later in this chapter we discuss how this model sequence can be calculated.

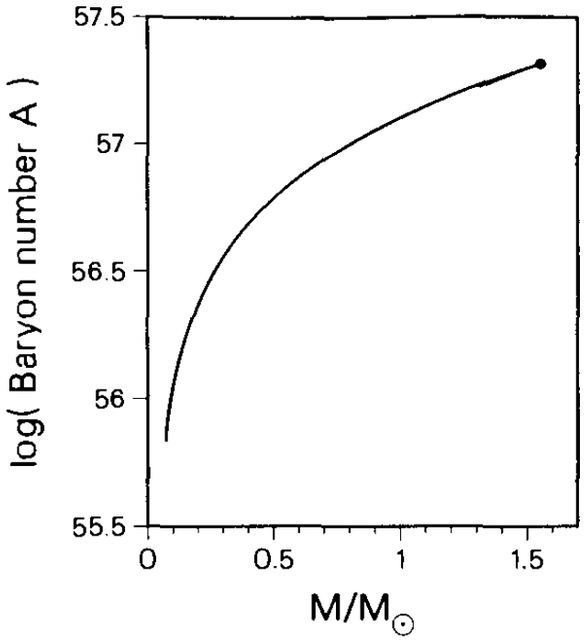

FIGURE 3.2. Total number of baryons vs. mass for neutron stars. See Chapter 5 for details. (K=240 MeV, $m^*_{\rm sat} = 0.78$, $x_\sigma = 0.6$).

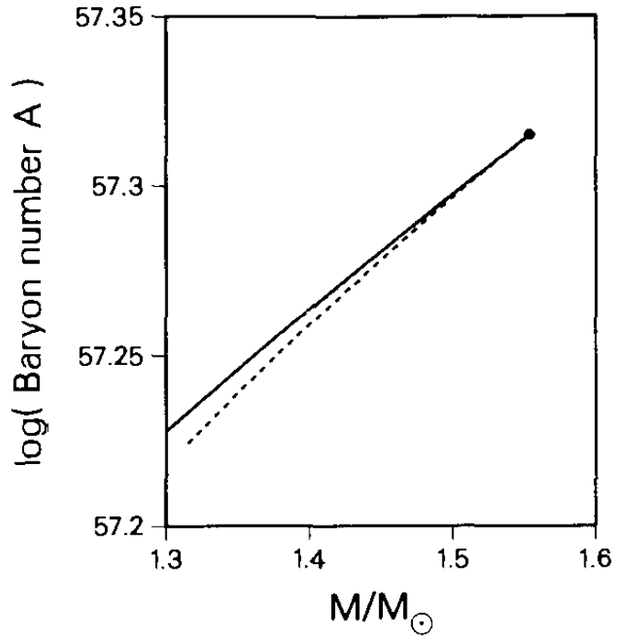

FIGURE 3.3. Enlargement of Fig. 3.2 in the vicinity of the limiting star. Dotted line corresponds to unstable stars above the limiting mass star in density.

Because the matter at the edge of the star will be less compacted than at the center, we expect a somewhat larger radius and smaller mass, say

$$M \approx 2M_\odot, \quad R \approx 10\ \text{km}\,. \tag{3.18}$$

The average density of such an object is

$$\bar{\epsilon} = 10^{15}\ \text{g/cm}^3\,. \tag{3.19}$$

It is interesting to compare this result with the density of normal symmetric nuclear matter. Taking the average of

$$m_n = 939.57\ \text{MeV}, \quad m_p = 938.28\ \text{MeV}\,, \tag{3.20}$$

and using the saturation baryon density and binding per nucleon of nuclear matter obtained from the large A-limit of the droplet model of nuclear masses [51],

$$\rho_0 = 0.153\ \text{baryons/fm}^3, \quad -B/A = 16.3\ \text{MeV}\,, \tag{3.21}$$

we get for the energy density of normal symmetric nuclear matter

$$\epsilon_0 = 141\ \text{MeV/fm}^3 = 2.51 \times 10^{14}\ \text{g/cm}^3\,. \tag{3.22}$$

Compare this with the average density of the Earth which is 5.5 g/cm^3.

The above crude estimate of the gross properties of a compact star near the limit of gravitational collapse suggests that the average density is about four times nuclear matter density. The density of the star near the mass limit is supernuclear. Also a star must be charge neutral because the repulsive Coulomb force for an infinitesimal charge per baryon in the star will expel particles of like charge. Therefore neutrons will be the majority population—hence, the name "neutron" star.

3.3.3 *Gravitational energy of a neutron star*

We can roughly estimate the gravitational energy for a uniform density neutron star with a nominal two solar mass and a 10-km radius such as discussed above. Using (2.211) we find

$$
\begin{aligned}
M(r) &= \frac{4\pi}{3} r^3 \bar{\epsilon}, \quad M = M(R), \\
E_G &\approx \int_0^R \frac{M(r)\,dM(r)}{r} = \int_0^R \frac{M(r)(4\pi r^2 dr\bar{\epsilon})}{r} = \frac{3}{5}\frac{M^2}{R} \\
&= 0.54 \text{ km} = 6.5 \times 10^{53} \text{ erg} = 7.3 \times 10^{32} \text{ g} \\
&= 4.1 \times 10^{59} \text{ MeV}. \qquad (3.23)
\end{aligned}
$$

Thus, the gravitational energy is a significant fraction of the total gravitational mass of the star, namely, 0.54/3 =0.18, or 18% for a two solar mass star ($M_\odot \approx 1.5$ km). To find the gravitational energy per nucleon in the star, refer above to the estimated number of nucleons A to find 157 MeV per nucleon. By contrast, the binding of a nucleon in nuclear matter is about 16 MeV and 8 MeV in a finite nucleus.

The classical estimate of the gravitational energy is not the binding energy of the star; it does not take account of the compression energy resisting the assembly of nucleons in a star arising from the Fermi pressure and the short-range repulsive nuclear force. Nonetheless, the binding energy per nucleon in a limiting mass star is about 100 MeV per nucleon (see page 231). Thus, the weakest force binds nucleons in a neutron star ten times more strongly than the strong force binds them in nuclei. How can this be so? The answer lies in their ranges. The nuclear force acts only on neighbors that lie within its range, typically the several next nearest neighbors, but each particle in the star feels the gravitational force of all others.

From the absolute limit on M/R of a stable star derived in Section 3.15, we can find an upper limit on the gravitational energy of a star relative to its mass. It is $(3/5)(M/R) < 4/15$ or 27%. The import of the large binding of a neutron star is that the energy released during a few seconds in a supernova event is large compared to that produced in thermonuclear fusion reactions during the entire stellar lifetime of a few million years (Table 3.1).

3.4 Partial Decoupling of Matter from Gravity

In nuclear and particle physics, we do not usually think of the matter Lagrangian and matter field equations as depending on the metric because we usually ignore gravity. In this event the metric tensor is the diagonal, constant, Minkowski metric $\eta_{\mu\nu}$ (2.7). For example, the Dirac equation for a nucleon contains the scalar product $\gamma_\mu \partial^\mu$, and the Lagrangian for a scalar meson contains $\partial_\mu \phi \partial^\mu \phi$. But these are merely shorthand notations that avoid the necessity of writing the Minkowski metric explicitly in the scalar product of four-vectors, $\gamma_\mu \partial^\mu = \eta_{\mu\nu}\gamma^\nu \partial^\mu$. They are correct when the metric $g_{\mu\nu}$ can be justifiably replaced by the Minkowski metric

of a Lorentz frame. However, this can be done only in a sufficiently small locality, the smallness of which depends on the curvature of spacetime. It is not possible to erect a global Lorentz frame. The differential equations for the gravitational fields, of which the $g_{\mu\nu}(x^\alpha)$ are the generalizations of the Newtonian gravitational potential, and those of the matter and radiation fields are therefore coupled in general [(2.232) (2.233)].

For applications in strong gravitational fields we need to determine whether it is justified to solve the matter equations of nuclear and particle physics in flat spacetime. For stellar structure, this amounts to ascertaining the relevance of an equation of state for neutron star structure (and hence for all stars), one that is derived in a Lorentz frame. Let us put the mass and radius of a star near the limit of gravitational collapse into the metric for the space outside a star (2.199). We use the fact that, at the origin, $g_{11} = -1$ [see (2.215)] to obtain

$$\frac{g_{11}(R)}{g_{11}(0)} = \left(1 - \frac{2M}{R}\right)^{-1} = \left(1 - \frac{6}{10}\right)^{-1} = \frac{10}{4}. \tag{3.24}$$

The metric changes by a factor 2.5 over the dimension of the star. Therefore the relative change in the metric over the spacing of nucleons in the star is $\sim 2r_0/R = 2A^{-1/3} \approx 10^{-19}$. This is a negligible change over a distance spanning many times the internucleon spacing. The metric would change by a mere 1 part in 10^9 across a shell in the radial direction that is the thickness of, say 10^{10} nucleon spacings. From this it is clear that a volume over which conditions do not change significantly can be defined for every region of the star. The pressure is certainly different in regions that differ in radial location by an appreciable amount. But the conditions for defining the local state of affairs are fully met in all such volumes.

However, such local regions are not inertial regions. The second two of the conditions for local Lorentz frames defined in Section 2.5.1 are satisfied, but not the first. Rather, the gravitational field is finite though uniform in each such region. Therefore we must consider further the question of validity of the notion of an equation of state of matter that describes the role of nuclear, atomic, and molecular physics in the context of the interior of a star. This was done first in the 1965 pioneering work of Wheeler and his collaborators on neutron stars [28]. We follow their reasoning. Imagine an idealized hollow tube extending from the center of the star through one such region as above. Let a small laboratory be propelled upward in the tube at such a velocity that, moving freely, it comes to rest before beginning its descent at just the location of the region in question. From this locally inertial laboratory the volume of the adjacent region and the number of baryons it contains can be measured and therefore also its baryon density. We are interested in stars composed of matter in its lowest energy state and that is charge neutral and at zero temperature.[11] Therefore, all equivalent regions having the same number of baryons and volume also have the same energy, or energy density. The energy density in all small regions of the star is therefore uniquely specified by the baryon

[11] In later chapters, we will discuss such matter, which we call *neutron star matter* or *cold catalyzed matter*, from which all energy that can be extracted has been extracted.

density,

$$\epsilon = \epsilon(\rho)\,, \tag{3.25}$$

where ϵ denotes energy density and ρ baryon density. If we enlarge the tube spoken of above, so that one of the regions can fall freely, it occupies an inertial frame, and the uniqueness in the definition of cold catalyzed matter assures that the properties of matter can be computed in a Lorentz frame to arrive at the equation of state, (3.25).

Thus, each small volume in the star, which, however, is large enough to be uniform in density, can be described by the laws of physics of the Special Theory of Relativity to high accuracy. We make a negligible error for neutron stars by solving the field equations for matter in the absence of gravity (i.e., in flat spacetime). From the solution in Minkowski spacetime, we can construct the energy-momentum tensor that is diagonal in a comoving Lorentz frame (2.47):

$$T^{\mu\nu} = \begin{pmatrix} \epsilon & 0 & 0 & 0 \\ 0 & p & 0 & 0 \\ 0 & 0 & p & 0 \\ 0 & 0 & 0 & p \end{pmatrix}. \tag{3.26}$$

The principle of general covariance (Section 2.9.4) tells us how to construct the energy-momentum tensor in an arbitrary gravitational field from the one derived in Minkowski spacetime. Of course, the general energy-momentum tensor (2.201) contains the metric tensor, which is the gravitational field (but not yet determined). We find how the matter of our theory is arranged under the influence of gravity and how in turn it shapes the gravitational fields $g_{\mu\nu}(x)$ by putting a solution to the matter problem found in Minkowski spacetime into the general energy-momentum tensor on the right side of Einstein's field equations (2.178). The Oppenheimer–Volkoff equations are the result of just such an operation.

3.5 Equations of Relativistic Stellar Structure

3.5.1 Interpretation

In Chapter 2 we saw that for a static isotropic star, Einstein's equations take a special form (2.211, 2.224), derived first by Oppenheimer and Volkoff. By rewriting them we can see the Newtonian part and arrive at the physical interpretation

$$4\pi r^2 dp(r) = -\frac{M(r)dM(r)}{r^2} \left(1 + \frac{p(r)}{\epsilon(r)}\right)\left(1 + \frac{4\pi r^3 p(r)}{M(r)}\right)\left(1 - \frac{2M(r)}{r}\right)^{-1}, \tag{3.27}$$

$$dM(r) = 4\pi r^2 \epsilon(r)\, dr\,. \tag{3.28}$$

The interpretation is very simple. The first of the pair of equations expresses the balance between the force acting on a shell of matter due to material pressure from within and the weight of matter weighing down on it from without. Think of a shell of matter in the star of radius r and thickness dr. The second equation gives the mass–energy in this shell. The pressure of matter at the inner edge of the shell is $p(r)$ and at the outer edge, $p(r)+dp(r)$. The left side of the first equation is the net force acting outward on the surface of the shell by the pressure difference $dp(r)$, and the first factor on the right side is the attractive Newtonian force of gravity acting on the shell by the mass interior to it. The remaining three factors are the exact corrections for General Relativity. So these equations express the balance at each r between the internal pressure as it supports the overlaying material against the gravitational attraction of the mass-energy interior to r. They are the equations of hydrostatic equilibrium in General Relativity.

Why did the equations for stellar structure lead us to the equation for hydrostatic equilibrium? Because they were built in by the condition that each fluid element is at rest in the star (2.207).

The differential equation (3.27) assures that the pressure decreases monotonically in a star. This is clear because the derivative of pressure is negative. It also makes sense because the amount of overlaying material decreases with radial coordinate, meaning that the greatest weight weighs on the center and decreases in the outward direction. The equation of state $p = p(\epsilon)$ is the manner in which the properties of dense matter enter the equations of stellar structure. Otherwise they are completely specified. It is a property of matter that the pressure never decreases as a function of increasing density. The pressure can remain constant during an interval in density as in first-order phase transitions of simple substances, but otherwise increases with density. Therefore we may conclude that the density of matter in a star is also a decreasing function of the radial coordinate.

It is a particularly notable feature of the Oppenheimer–Volkoff equations that the internal pressure of matter appears together with the energy density on the right side of equation (3.27), thus sharpening the pressure gradient in a star, compressing matter, and reducing the stellar radius along the sequence of stars with increasing central density. The radius is ultimately reduced to a value below the Schwarzschild limit (see Fig. 3.4). As a consequence, no matter how large the pressure may be, it ultimately cannot prevent the collapse of stars whose mass exceeds what is referred to as the *limiting mass* (Section 2.9.6).

Closely related to the above discussion is the characteristic relationship between the mass of a degenerate relativistic star and its radius. The smaller the mass, the less the gravitational attraction and the larger the radius. At intermediate mass, the Fermi pressure of electrons in the case of white dwarfs, and of nucleons and their mutual repulsion when in close proximity as in neutron stars, resists gravity, leading to a range of masses for which the radius hardly changes. Finally, as the limiting mass is approached, the radius decreases sharply with mass (Fig. 3.5).

Newtonian stellar structure is obtained as a special case of the Oppenheimer–Volkoff equations by dropping the last three factors in (3.27). In Newtonian stars, ϵ is dominated by the rest mass of the baryons which, however, contribute little

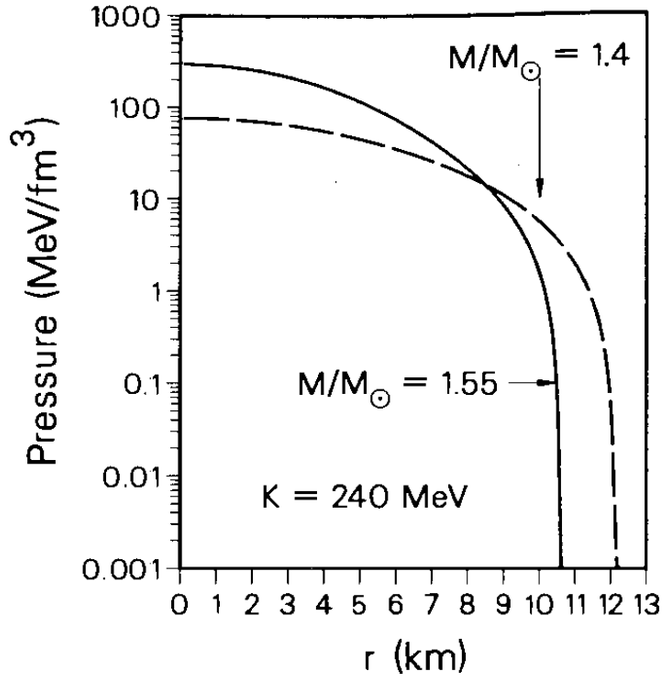

FIGURE 3.4. Illustration of the pressure distribution in two stars of neighboring mass, showing the steeper pressure gradient with increased mass and the corresponding reduction in radius thus, illustrating a mass limit above which the radius will be driven below the Schwarzschild limit. The actual limit for stable stars occurs before the Schwarzschild radius is reached.

to the pressure. Therefore, the first and second terms of the second line of (3.27) are close to unity for the same reason, namely, that $p << \epsilon$. As noted in the first chapter, the last term is always positive for stars. Indeed for stars such as our Sun, $2M/R = 4.3 \times 10^{-6}$, and so the last factor is also unity for Newtonian stars.

The correctness of Einstein's theory, and therefore the equations of stellar structure, is confirmed by the observational tests of General Relativity. The most impressive of these are concerned with the Hulse–Taylor pulsar binary [52], known by its celestial coordinates as 1913+16 and studied with great care since its discovery in 1974 [4, 53, 54]. The orbit's orientation precesses in the strong gravitational field of the neutron stars at a rate of more than 4 degrees per year. This compares with the former classic confirmation of General Relativity—the general relativistic contribution to the precession of Mercury—which is only 43 seconds per century.

Einstein's gravitational radiation prediction, which affects the orbital motion of the binary pulsar pair causing the orbit to decay, is confirmed to less than one percent [4]. All other variants of Einstein's theory of gravitation are ruled out at this level of accuracy. At the measured rate of decay of the orbit due to the radiation of gravity waves, the two members of the binary will collide in about 10^8 years. While this is a long time, it is to be compared with the Galaxy age of 10^{10} years. Collisions of compact stars are therefore likely events in the universe, and are candidates for observation in future generations of gravitational wave detectors. Such collisions are also of possible importance to the question of strange quark nuggets as cosmic radiation, which we discuss in Chapter 12.

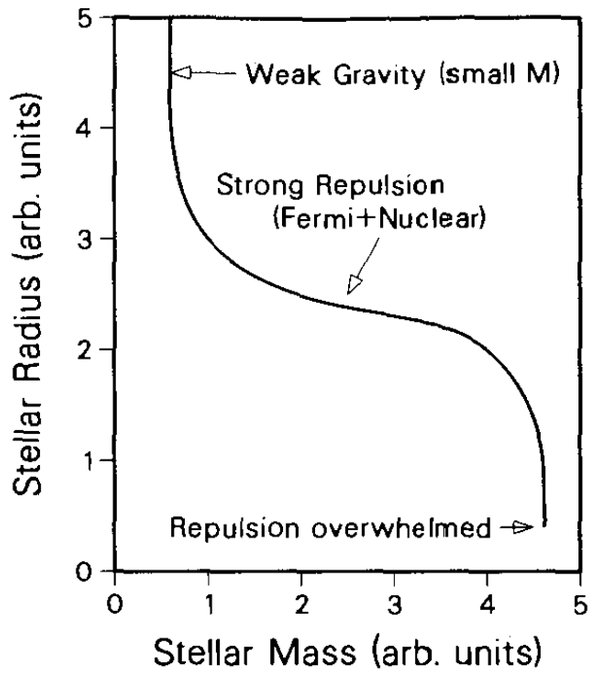

FIGURE 3.5. Mass–radius relationship that is characteristic of degenerate stars—large radius for low mass, smallest radius for star at the mass limit.

3.5.2 *Boundary conditions and stellar sequences*

The two Oppenheimer–Volkoff equations can be integrated from the origin $r = 0$ with the initial conditions $M(0) = 0$ [since near $r = 0$ we may write $M(r) = (4/3)\pi r^3 \epsilon(0)$] and an arbitrary value for the central energy density $\epsilon(0) = \epsilon_c$. The equations are to be integrated until the pressure $p(r)$ becomes zero. Zero pressure can support no overlying material against the gravitational attraction exerted on it from the mass within and so marks the edge of the star. The point R where the pressure vanishes defines the radius of the star and $M(R)$ its gravitational mass.

For a given equation of state, there is a unique relationship between the stellar mass and central density $\epsilon(0)$ because the Oppenheimer–Volkoff equation is of first order. Thus, for each possible equation of state, there is a unique *sequence* of stars parameterized by the central density or, equivalently, the central pressure. For a vast range of densities spanning many orders of magnitude, a sequence of stars from white dwarfs to neutron stars is shown in Fig. 3.6.

The white dwarfs are the lowest density sequence of compact stable stars. Their central densities range from about $\sim 5 \times 10^5$ to 9×10^9 g/cm^3. The more massive ones have densities that are $\sim 10^9$ times greater than the average density of Earth. White dwarfs consist of isotopes from hydrogen to carbon and oxygen with possible admixtures of some heavier ones. All atoms, save at the surface, are ionized by the high compression. As the mass approaches about $M_\odot$, depending on the particular equation of state used to describe the matter of white dwarfs, they become unstable and the sequence of white dwarfs ends.[12]

Stable white dwarfs are supported against gravitational collapse by the pressure of degenerate electrons. Degeneracy refers to a situation for which the temperature

[12]The conditions for stability will be studied in Section 3.18.

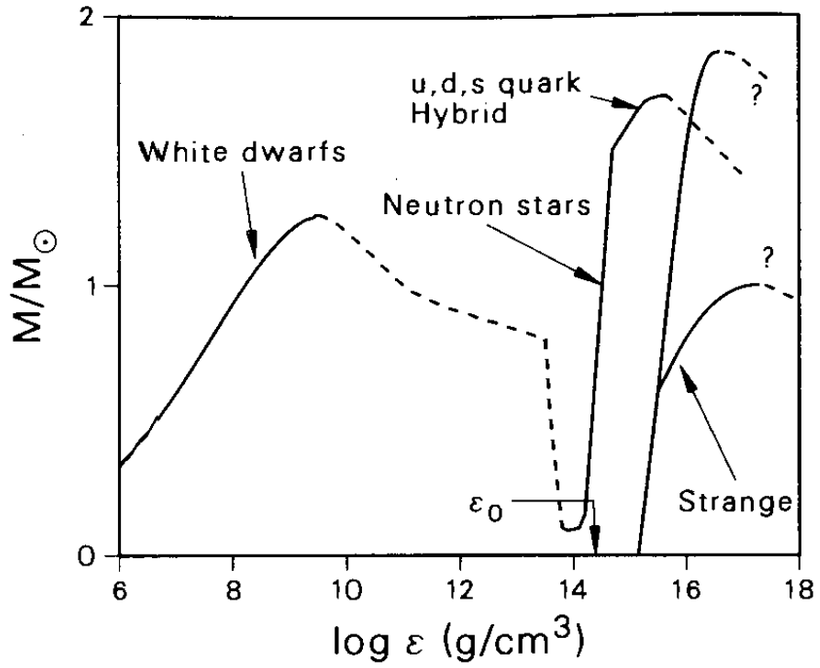

FIGURE 3.6. Schematic illustration of the solution of the O–V equations over a broad range of central densities. Hypothetical strange stars are also shown (see Chapter 12). Solid lines show stable configurations. See discussion of stability in text (Section 3.18).

is much smaller than the Fermi energy of the electrons, so that electrons essentially fill all momentum states allowed by the Pauli principle up to a maximum value, sometimes referred to as the Fermi surface (because momentum is a vector). However, with increasing white dwarf mass (and therefore central density and pressure), the electron Fermi energy rises. A point is reached at which it becomes energetically more favorable for electrons to be captured by protons by inverse beta decay. The supporting pressure of the relativistic electrons is lost, and a region of a few decades in central energy density follows in which no stable stars exist between white dwarfs and neutron stars, as illustrated in Fig. 3.6.

The Fermi pressure of degenerate neutrons reestablishes stability against collapse for the lightest neutron stars. For more massive stars with higher densities, the repulsion of the nuclear force at short range adds additional resistance to compression.

Neutron stars are denser by far than white dwarfs. Neutron stars are five to ten times more dense at their centers than the nuclei of atoms ($\rho_0 \sim 2.5 \times 10^{14}$ g/cm^3). They are about 3×10^{14} more dense than Earth. The density falls from its high central value by some fifteen orders of magnitude to the surface.

It should be clear (but well worth emphasizing) that neutron stars are held together by gravitational attraction, not by the nuclear force. After all, nuclei themselves are stable only for $A \lesssim 250$ and neutron matter not at all. Indeed, except possibly for the very lightest neutron stars, gravity has compacted the neutron matter so severely that the most important part of the nuclear force is the repulsion. If gravity were switched off, a neutron star would explode!

As remarked above, the edge of a star occurs at the point where $p(R) = 0$. Frequently, one assumes that the pressure goes to zero as the energy density. But in cold matter, nucleons that are condensed into nuclei are of lower energy than

a gas of nucleons. Material made of nuclei, like iron or carbon, has zero pressure because it is in equilibrium. So, the edge of an ideal *cold* neutron star or white dwarf occurs at a finite energy density corresponding more or less to the laboratory density of whatever nuclei occur in the edge of the star. As we will discuss later, the prevalent species will depend on the progenitor star in the case of a white dwarf. The dominant species will be iron atoms in a Coulomb lattice (density $\sim$ 7.85 g/cm^3) in the case of a neutron star. We shall discuss the low density range in Section 3.10 in connection with the equation of state of subnuclear matter.

The effects of finite temperature, which in a typical neutron star is far higher than can be achieved in the laboratory, will be discussed with reference to the nature of the surface material in Section 3.11. However, the surface region contributes so little to the large-scale properties of a compact star that the equation of state of cold matter in the ground state is generally employed.

3.6 Electrical Neutrality of Stars

The repulsive Coulomb force acting on any charged particle of the same sign as the net charge on a star will overwhelm the gravitational attraction acting on the additional particle, and it will be expelled unless the net charge on the star lies below a certain minimum value which we wish to calculate. The condition that an additional like charge will not be expelled is given by

$$\frac{(Z_{\text{net}}e)e}{R^2} \leq \frac{GMm}{R^2} < \frac{G(Am)m}{R^2}\,, \tag{3.29}$$

where Z_{net}, R, M, are the net charge on the star, its radius, and mass, respectively, while m and e are the mass of a proton and its charge. The number of baryons in the star is denoted by A, so that we have $M < Am$, that is, the mass of the star, because of its gravitational binding, is less than the mass of the baryons distributed to infinity. Hence (in gravitational units),

$$Z_{\text{net}}/A < (m/e)^2\,. \tag{3.30}$$

A net charge larger than the above value would not allow any additional charged particle of the same sign to be gravitationally bound.

We evaluate $(m/e)^2$ for a proton. In that case using (3.5),

$$\left(\frac{m}{e}\right)^2 \sim \frac{(938\ \text{MeV})^2}{1.44\ \text{MeV fm}} \sim 10^{-36}\,. \tag{3.31}$$

Hence,

$$Z_{\text{net}} < 10^{-36}A\,. \tag{3.32}$$

This is the limit on the net positive charge. If the star had a net negative charge, we could similarly compute its limit considering the balance of Coulomb and gravitational forces on an added electron. The limit would be reduced by the factor m_e/m.

We conclude that the net charge per nucleon (and therefore the average charge per nucleon on any star) must be very small, essentially zero. However, the number of charges of equal and opposite sign is not at all limited. It will be important in another context to note that the above condition on net charge on a star is a global one and not a local one. The above result places no restriction on the value of the charge density as a function of location in the star, so long as it integrates to less than the small value derived above.

3.7 "Constancy" of the Chemical Potential

Let us recall several thermodynamic relationships. The pressure is defined as

$$p = -\frac{\partial E}{\partial V}, \tag{3.33}$$

taken at constant entropy, where E is the energy and V the volume. For the present, we consider stars that are cold on the nuclear scale. The energy density and baryon number density are

$$\begin{aligned} \epsilon &= E/V, \\ \rho &= A/V, \end{aligned} \tag{3.34}$$

where A is the number of conserved baryons in the volume V, which might be a locally inertial region. Suppose the equation of state is known in the form

$$p = p(\rho), \qquad \epsilon = \epsilon(\rho), \tag{3.35}$$

from which ρ can always be eliminated, if desired, to provide $p = p(\epsilon)$. Now we can write

$$p = -\frac{\partial(\epsilon/\rho)}{\partial(1/\rho)} = \rho^2 \frac{\partial}{\partial\rho}\left(\frac{\epsilon}{\rho}\right) = \rho\mu - \epsilon, \tag{3.36}$$

where

$$\mu \equiv \frac{d\epsilon}{d\rho} \tag{3.37}$$

is the baryon chemical potential. From the relationship above between p and μ, we find

$$\frac{dp}{d\rho} = \rho\frac{d\mu}{d\rho}. \tag{3.38}$$

The Oppenheimer–Volkoff equation in the form (2.227) can be written

$$-\int_r^{r'} dv = \int_r^{r'} \frac{dp}{p+\epsilon} = \int_r^{r'} \frac{d\mu}{\mu}, \tag{3.39}$$

where $r < r' < R$, with R the radius of the star. Because r and r' are otherwise arbitrary, we obtain

$$\mu(r)e^{v(r)} = \mu(r')e^{v(r')} = \text{ const} \tag{3.40}$$

This shows that the baryon chemical potential at any depth in a star, corrected by the factor $e^{\nu(r)}$, is a constant. (A theorem for an arbitrary number of chemical potentials of independent components has been proven by Kodama [55].) The correction factor for energy is the inverse of the gravitational time dilation factor we will encounter in the next section.

The pressure p necessarily vanishes at the stellar surface. Let us think what the surface material of a "neutron" star made from the processed material of an evolved star could be. Surely the lowest energy equilibrium state ($p = 0$) of hadronic matter is Fe^{56} which is the end point of fusion reactions in presupernova stars. Solid iron in its equilibrium state has $p = 0$. Iron therefore forms the surface of an idealized *cold* neutron star. From (3.34) and (3.36) we find that

$$\frac{E}{A} = \left(\frac{\epsilon}{\rho}\right)_0 = \mu_{\mathrm{Fe}} \,. \tag{3.41}$$

Hence, we obtain

$$\mu_{\mathrm{Fe}} \approx \frac{1}{56}\, m(\mathrm{Fe}^{56}) = 930.54\ \mathrm{MeV}\,, \tag{3.42}$$

where $m(\mathrm{Fe}^{56})$ is the mass of the iron atom and we have ignored small energies associated with the molecular forces of the solid. Consequently, anywhere in the star it must be true that

$$\mu(r)e^{\nu(r)} = \mu_{\mathrm{Fe}}\left(1 - \frac{2M}{R}\right)^{1/2} . \tag{3.43}$$

This is not a condition that has to be imposed on the solution of the Oppenheimer–Volkoff equation. Rather it is the way that matter is arranged by gravity. From (3.40) we learn that, in the equilibrium configuration of the star, a particle can be brought from infinity to *any* point in the star, with the same gain in gravitational energy. In fact, (3.40) holds not only for the chemical potential, but also for the temperature at various points in a star in equilibrium. Thermal equilibrium does not correspond to $T = \mathrm{const}$ but to $T(r)e^{\nu(r)} = \mathrm{const}$ (cf. [56], p. 263).

3.8 Gravitational Redshift

The dilation in time, measured by observers in relative uniform motion, is familiar from the Special Theory of Relativity. Such an effect of a different origin holds also for stationary observers in a static gravitational field located at positions of different gravitational potential.

3.8.1 Integrity of an atom in strong fields

Consider the question of gravitational effects in the context of comparing spectral lines of atoms located on distant stars with those of atoms located on Earth. In

Chapter 2 we saw that, after a photon is emitted, its frequency will be shifted if it moves from one place to another having different gravitational fields. But is the internal structure of the atom itself unaffected by the gravitational field in which it is located, especially if the field is very strong?

Let us compare the change in the acceleration due to gravity across the diameter of the atom with the acceleration of the electron in the atom by the Coulomb force. The (Newtonian) acceleration due to gravity at the surface of a star is

$$g_\star = \frac{M}{R^2} \leq \frac{1}{2}\frac{1}{R}, \tag{3.44}$$

where we have replaced M/R by $1/2$ to obtain an upper limit. Again, taking $R = 10^6$ cm and $1 = c = 3 \times 10^{10}$ cm/s, we have

$$g_\star < \frac{1}{2}\frac{1}{10^6\,\text{cm}}\left(3 \times 10^{10}\,\text{cm/s}\right)^2 = 4.5 \times 10^{14}\,\text{cm/s}^2. \tag{3.45}$$

(Notice how we have converted back from units with $c = 1$ in which acceleration is expressed in units of inverse length or, equivalently, inverse time to ordinary units of cm/s^2.) The difference of the acceleration across the dimension of the atom is

$$\delta g_\star = \frac{M}{(R-r)^2} - \frac{M}{(R+r)^2} \approx \frac{4r}{R} g_\star. \tag{3.46}$$

We obtain

$$\delta g_\star \approx 2 \times 10^{-14} g_\star = 9\,\text{cm/s}^2. \tag{3.47}$$

By comparison, the acceleration of the electron in a helium atom in a Bohr orbit is

$$a = \frac{1}{m_e}\frac{e^2}{r_{\text{Bohr}}^2} \approx \frac{1.44\,\text{MeV fm}}{0.5\,\text{MeV}(\frac{1}{2}10^{-8}\,\text{cm})^2} \approx 10^{25}\,\text{cm/s}^2. \tag{3.48}$$

So the acceleration experienced by the electron in the hydrogen atom is $\sim 10^{24}$ times larger than the change in the gravitational acceleration across the orbit when the atom is located on the surface of the star. It is also much larger than the gravitational acceleration at the surface of the star. We reach the conclusion that even the strongest gravitational fields on stars cannot affect the workings of an atom (much less a nucleus).

3.8.2 Redshift in a general static field

Now consider an idealized situation in which we have an observer both at a great distance from a static star and from every other body and at rest with respect to the star. The gravitational field is therefore static. Let the mass and radius of the star be M and R, respectively. Let two identical atoms be located, one at the surface of the star and the other with the distant observer whose location we shall denote by ∞. For later simplicity, but by no means essential, let the center of the star, the atom on its surface, and the distant observer lie along the same line. Think of the emission of a photon as corresponding to a wave train. The two ends of a cycle,

or equivalently, successive wave crests emanating from the source, correspond to neighboring spacetime events.

Choose a local inertial frame in which the atom is at rest. Then,

$$d\tau_{\mathrm{a}} = \sqrt{\eta_{00}}\, d\xi_a^0 = d\xi_a^0 \tag{3.49}$$

is the invariant interval of emission from the atom (subscript "a") and is equal to the coordinate time $d\xi_a^0$ between wave crests in this local inertial frame. This relationship holds in the strong field of the star as at the location ∞ of the observer, as proven in the above section. In an arbitrary gravitational field, the spacetime interval dx^μ between crests is governed by

$$d\tau_{\mathrm{a}} = (g_{\mu\nu} dx^\mu dx^\nu)^{1/2}\,. \tag{3.50}$$

In particular, for the atom at rest on the surface of the star,

$$d\tau_{\mathrm{a}} = \sqrt{g_{00}(R)}\, dx^0 \tag{3.51}$$

gives the coordinate time interval dx^0 between crests in the gravitational field at R. But light propagates in the radial direction in the static field according to

$$d\tau^2 = 0 = g_{00}(r)dt^2 - g_{11}(r)dr^2\,. \tag{3.52}$$

Therefore,

$$\Delta t = t_\infty - t_R = \int_R^\infty \left(\frac{g_{11}(r)}{g_{00}(r)}\right)^{1/2} dr \tag{3.53}$$

is the constant transit time for each wave crest to travel from R to ∞. Hence the coordinate interval dx^0 at R governed by (3.51) is also the coordinate interval between wave crests arriving at ∞ from R. Therefore, the stationary observer with his apparatus at the location denoted by ∞ measures the proper time interval between crests arriving from the star,

$$d\tau_{\mathrm{a}'} = \sqrt{g_{00}(\infty)}\, dx^0 \tag{3.54}$$

[say by a process analogous to the inverse of (3.49)].

Denote a spacetime event associated with the distant observer by x'^μ. Similarly to (3.51), we have

$$d\tau_{\mathrm{a}} = \sqrt{g_{00}(\infty)}\, dx'^0\,, \tag{3.55}$$

as the equation that governs the coordinate time dx'^0 for emission from the like atom at rest at the location of the observer, because (3.49) holds equally at both locations. So we can compare the *observed* frequency ω_o of the photon arriving from the surface R of the star, as measured by the observer at ∞ with that of the photon *emitted* by the like atom located with the observer, namely, ω_e. (Of course the atom at the location of the observer can be identified with that on the star by comparing the ratios of a few spectral lines.) Recall that we have proven above that both atoms will emit the same frequency photon as seen by a local observer near the atom. The proper time between crests (multiplied by c) gives the wavelength of the light or the reciprocal of the frequency. Therefore, using (3.54) and (3.55),

respectively, the ratio of the frequency of light coming form the star and *observed* by the distant observer, to the frequency of light *emitted* by his local atom is

$$\frac{\omega_o}{\omega_e} = \frac{d\tau_a}{d\tau_{a'}} = \frac{dx'^0}{dx^0} = \left(\frac{g_{00}(R)}{g_{00}(\infty)}\right)^{1/2}. \tag{3.56}$$

In the last step, we eliminated $d\tau_a$ between (3.51) and (3.55). Thus, as observed at ∞, the photon arriving from the atom located on the surface of the star has a lower frequency

$$\omega_o = e^{\nu(R)}\,\omega_e = \sqrt{1 - 2M/R}\,\omega_e \tag{3.57}$$

than the photon from the identical atom located at ∞. The light is red-shifted. Conversely, if a photon fell from ∞ to the surface of the star and was observed there and compared with a photon from a like atom on the star surface, it would be found that the photon from the distant location had been blue-shifted.

We have introduced the Schwarzschild metric valid for a static spacetime outside a spherical star into the above equations. Otherwise we could keep the expressions in terms of the general metric functions. We can also write (3.57) in terms of energies. Thus, the energy observed at infinity is related to that of an event at r by

$$E = E(r)\sqrt{g_{00}(r)} \tag{3.58}$$

for any r.

The result above can be stated in terms of clocks: time flows more slowly at R than at ∞. For an isolated static spherical star, the gravitational time dilation factor is $e^{-\nu(R)}$.

The conventionally defined gravitational redshift is the fractional change between observed and emitted wavelengths compared to emitted wavelength:

$$z \equiv \frac{\Delta\lambda}{\lambda_e} = \frac{\lambda_o}{\lambda_e} - 1 = \frac{\omega_e}{\omega_o} - 1\,, \tag{3.59}$$

or, in the case of a Schwarzschild star,

$$z = \left(1 - \frac{2M}{R}\right)^{-1/2} - 1\,. \tag{3.60}$$

We can calculate the limit to the redshift from the surface of a neutron star. From the Oppenheimer–Volkoff equations we have noted that $M/R < 1/2$. The equality yields the horizon. But relativistic stars actually observe a more stringent condition, $2M/R < 8/9$, for any star obeying the Oppenheimer–Volkoff equations, as will be shown in Section 3.15. This gives $z < 2$ as the maximum gravitational redshift of a stable star. In Fig. 3.7 we show the gravitational redshift of light emitted at the surface of neutron stars belonging to several model sequences.

The maximum gravitational redshift of light emitted from an atom on the surface of a stable star is enormously different from the redshift of light emitted from just outside the horizon of a black hole. For the star, the redshift is $z < 2$; for a black hole it tends to infinity as the atom approaches the Schwarzschild radius, as can be seen from (3.60).

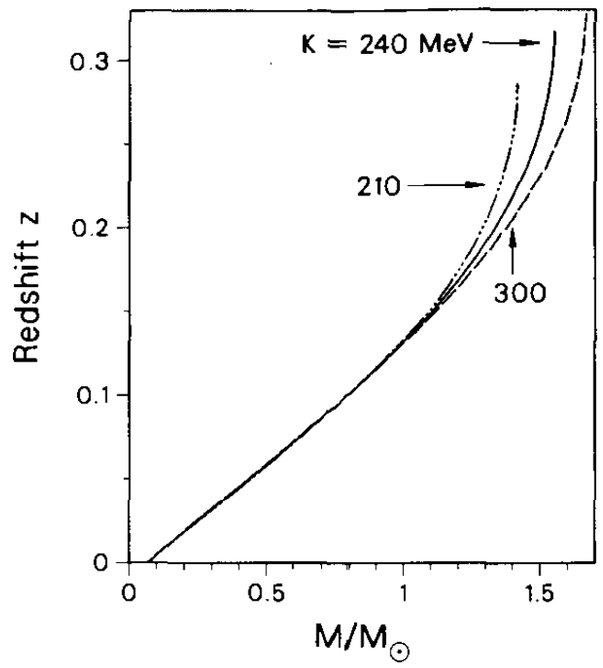

FIGURE 3.7. Surface gravitational redshift of several model neutron star sequences. The resistence of matter to compression is labeled by the value of K—the compression modulus. See Chapter 5 for more details.

We can apply (3.56) to the situation discussed in Section 2.4.1, that of a photon climbing up the constant weak gravitational field of the Earth over a limited height h. The acceleration due to gravity is nearly constant over the limited height. The Newtonian potential is $V(r) = -M/r$ and its relationship to g_{00} was derived in Section 2.5.3:

$$\frac{\omega(R)}{\omega(R+h)} = \left(\frac{g_{00}(R)}{g_{00}(R+h)}\right)^{1/2} \approx 1 - V(R+h) + V(R)$$
$$\approx 1 - \frac{M}{R^2}\, h = 1 - gh\,. \tag{3.61}$$

We see that the frequency of the photon emitted from the atom on the surface of the Earth R compared at $R + h$ with a photon from a like atom at that location is

$$\omega(R) = (1 - gh)\,\omega(R+h)\,, \tag{3.62}$$

in agreement with the earlier weak field result. Einstein discovered the approximate redshift formula (3.61) in 1911 before his discovery of General Relativity. He concluded that the local velocity of light is different according to the gravitational field it travels in. "In this theory the principle of constancy of light velocity does not apply in the same way as in ... the usual relativity theory." [57]

For Earth,

$$M_\oplus = 5.977 \times 10^{27}\ \mathrm{g} = 0.4438\ \mathrm{cm}, \qquad R_\oplus = 6.371 \times 10^{8}\ \mathrm{cm}\,, \tag{3.63}$$

so that

$$g_\oplus = \frac{M}{R^2} = 1.1 \times 10^{-18}\ \mathrm{cm}^{-1}\,. \tag{3.64}$$

We see that the Newtonian approximation to the gravitational field is well justified on Earth.[13]

3.8.3 Comparison of emitted and received light

The derivation above was carried out from the point of view of a hypothetical experiment: comparison of light received from a distant star with light from a laboratory source. Frequently, a simpler derivation of the redshift is given which simply compares (as the theorist can do) the frequencies of light emitted from an atom on the surface of the star and its frequency as received by a distant observer. The proper time corresponding to adjacent wave crests on the star was given by (3.51) which we now refer to with the subscript "e" for emitted,

$$d\tau_e = \sqrt{g_{00}(R)}dx^0 . \tag{3.65}$$

As shown above, the coordinate time taken for each wave crest to propagate from the emission location to the observer's location is a constant in a static field. So the observer measures the proper time

$$d\tau_o = \sqrt{g_{00}(\infty)}\,dx^0 . \tag{3.66}$$

The inverse is proportional to the frequency, so the ratio of the observed to emitted frequencies is

$$\frac{\omega_o}{\omega_e} = \left(\frac{g_{00}(R)}{g_{00}(\infty)}\right)^{1/2} , \tag{3.67}$$

in agreement with the earlier result.

3.8.4 Measurements of M/R from redshift

The potential usefulness of redshift measurements for compact stars is immediately evident from (3.57) in that it permits a determination of M/R. If either M or R is known from other measurements, say the mass from observations on a binary system, then the other quantity is known. So far, an independent measurement of, say M, has not been made for which a redshift measurement has also been made. Of course in comparing the two frequencies, one from the distant star, the other from an earth-bound atom, one cannot à priori be sure one is comparing like atoms. The identification would be more positive if several transition lines were observed and they all had the same ratio when compared to the atom on Earth. There are about 30 known X-ray pulsars for which tentative spectral identifications have been made.

---

[13]Note how helpful the appropriate choice of gravitational units was in the estimate. Mass and radius were both expressed in units of length so that acceleration was expressed in inverse length and when multiplied by height h yielded a dimensionless number as needed in (3.62).

3.9 White Dwarfs and Neutron Stars

"Chandrasekhar . . . has shown that a star of a mass greater than a certain limit remains a perfect gas. . . . The star has to go on radiating and radiating, and contracting and contracting until, I suppose . . . gravity becomes strong enough to hold in the radiation, and the star can at last find peace [as a black hole].

I felt driven to the conclusion that this was almost a *reductio ad absurdum*. . . . I think there should be a law of nature to prevent a star from behaving in this absurd way."
A. Eddington, 1935 [58]

"It is clear from this [above] statement that Eddington fully realized, already in 1935, that given the existence of an upper limit to the mass of degenerate configurations, one must contemplate the possibility of gravitational collapse leading to the formation of what we now call black holes. But he was unwilling to accept a conclusion that he so presciently drew."
S. Chandrasekhar, 1982 [59]

3.9.1 Overview

After sufficient time, a star, either a white dwarf or neutron star, will become cold on the nuclear scale. Ideally, it will be in the lowest energy state, and the neutrinos and photons produced by the reactions in achieving the lowest state, such as

$$\begin{aligned} e^- + p &\to n + \nu\,, \\ n &\to p + e^- + \bar{\nu}\,, \\ \bar{\nu} + \nu &\to 2\gamma\,, \end{aligned} \tag{3.68}$$

will have escaped from the star. After the star has dropped in temperature below an MeV ($= 1.1605 \times 10^{10}$ K), we may say that it is cold for the purpose of computing the energy and pressure, but the temperature is still very high compared to the neutrino masses (presumably very small or zero), so they have velocity sufficient to escape, if not light velocity. Typical white dwarf surface temperatures are a few times 10^4 K with some as high as 10^6 K. Interior temperatures are 10^6 to 10^7 K. Neutron stars are born very hot, of the order of 10^{10} K, but cool rapidly, reaching 10^8 K in a month and 10^6 K in less than a million years. White dwarfs have radii typically of a few thousand kilometers, compared to neutron stars which have radii of around 10 km. White dwarfs are about the smallest faintest stars that are visible in the optical spectrum. Neutron stars make their presence known in the radio spectrum as pulsars, highly magnetized rotating bodies.

Because of their low luminosity (generally several orders of magnitude less than the Sun's) known white dwarfs lie in the immediate neighborhood of the Sun

(100 pc).[14] By comparison, the disk diameter of the Milky Way galaxy is 30,000 pc. White dwarf masses are sharply peaked around $0.6M_\odot$ though Sirius B has an accurately determined mass $M = 1.053 \pm 0.028M_\odot$. The largest known mass is $1.52M_\odot$ (WD 1143+321), and the smallest is $0.33M_\odot$ (WD 0349+27). The latter are deduced from gravitational redshifts [60] and are less certain. Known pulsars are also distributed around the Sun, close to the galactic plane, and some are known at distances of more than 15 kpc. Few mass measurements have been made, and only four have high accuracy. The some 20 presently known masses of radio pulsars have their maximum likelihood values in the range 1.2 to 1.7 $M_\odot$, but the error bars would admit pulsars of masses 0.8 to 2.2 $M_\odot$ [40].

White dwarfs are born under relatively quiescent circumstances, the remnants of a nonexplosive evolution of fairly modest stars of mass up to seven or so solar masses, which comprise most of the stars in the Milky Way galaxy. What remains of the core after the bulk of the star has expanded into a planetary nebula becomes a white dwarf. Dwarf progenitor stars, because of their low mass (unlike the progenitors of neutron stars), have not completed the chain of fusion reactions up to the most bound nucleus, ^{56}Fe. They are therefore composed of matter that is not in its lowest energy state. They are too cold to ignite the nuclear reactions that would bring them there. However, even when cold and crystalline, white dwarfs may evolve on a very long timescale through zero temperature nuclear reactions in which lattice vibrations yield a small but finite probability of Coulomb barrier tunneling. Such a process known as a pycnonuclear reaction, produces some heavier elements [61, 62]. However, the composition is essentially determined at birth.

Because of the circumstances of their birth, white dwarfs are not members of a single sequence corresponding to a unique equation of state. Rather, according to its individual history, each white dwarf is an equilibrium stellar configuration corresponding to an equation of state describing the particular composition attained in the thermonuclear burning of its progenitor (mostly He, C, and O) together with an atmosphere that is the remnant of the vibrations of the envelope that became unstable and formed the planetary nebula.

On the other hand, neutron stars are born in enormous explosions—supernovae—that occur in the last few moments in the evolution of stars more massive than about $8M_\odot$. In their cores, thermonuclear combustion has proceeded through to iron. Neutron stars are therefore composed of matter that has been fully processed to extract all available energy. At each density in their interiors, matter is in its ground state, consistent with charge neutrality. Therefore, neutron stars form a single sequence.

---

[14] A parsec is the distance at which a star is observed with a parallax of 1 sec of arc. 1 parsec (pc) = 3.26 ly (light years) = 3.09 10^{13} km.

3.9.2 *Fermi-gas equation of state for nucleons and electrons*

As a first exercise in the calculation of an equation of state appropriate for the description of compact stars, we consider an idealized composition of dense matter that will illustrate, nonetheless, some of the relationships and contrasts between white dwarfs and neutron stars. We will also learn some of the principles involved in any calculation of the structure of compact stars. In the idealization, both types of stars are members of a single sequence belonging to a particularly simple equation of state. Oppenheimer and Volkoff adopted the equation of state of an ideal gas of neutrons for the first calculation of a neutron star model. However, pure neutron matter is unstable. Neutrons obey the Pauli exclusion principle so that some neutrons in dense matter would have more than enough energy to beta decay to proton, electron and neutrino. The neutrinos diffuse out of the star thus lowering the energy. On the other hand, the low-energy neutrons cannot decay because the proton and electron states are already occupied. We are interested in the equilibrium configuration of matter and of the star after all such processes have occurred and matter has reached its ground state at each relevant baryon density. Therefore neutrinos must be ignored in searching for the ground state of stellar matter.

Our first model for the equation of state of neutron stars and white dwarfs describes a gas of noninteracting neutrons, protons, and electrons in such proportions at each baryon number density that the gas has its lowest possible energy. Such a situation is referred to as beta equilibrium or simply equilibrium. The neutrons will not beta decay; nor will the inverse reaction—electron capture on a proton—occur. In addition, we must demand that the minimum energy be found subject to the constraint of electrical neutrality. Baryon density is usually employed as an independent variable in calculating an equation of state because baryon number is conserved. Baryon species may be transformed from one to another so as to minimize the energy, but the total baryon charge remains unchanged. The example we will consider is a prototype for any more sophisticated model of the equation of state of dense charge-neutral matter.

Because neutrons, protons, and electrons are all fermions (particles of half odd-integer spin), they obey the Pauli exclusion principle—not more than one fermion can occupy a given quantum state. In this section we deal with a *degenerate* ideal Fermi gas. Ideal in this context means that interactions are ignored. Degenerate means that all quantum states up to a given energy, called the Fermi energy, are occupied. Therefore, in summing over the occupied states (which in the absence of interactions are momentum eigenstates), whether over the particle number, over the energies, or whatever, we need to sum or integrate over momentum states. We recall from quantum mechanics, normalization in a box of dimension L (c.f. Ref. [63]), so that

$$\frac{1}{L^3}\sum_{\boldsymbol{k}}\cdots \longrightarrow \int \frac{d^3k}{(2\pi)^3}\cdots = \frac{1}{2\pi^2}\int_0^{k_F} k^2\,dk\cdots . \tag{3.69}$$

For degenerate systems all energy states are filled in order up to some maximum called the Fermi energy, or in the case that momentum eigenstates are used, up to

the Fermi momentum. The subscript "F" is used to denote the Fermi momentum or energy, where needed to avoid ambiguity. The last equality in (3.69) holds provided the integrand depends only on the magnitude of the wave number $k = |\boldsymbol{k}|$, as is usually the case.

Particle momentum p and wave number k are related in the usual way: $p = \hbar k$. But because we set $\hbar = 1 = c$, we refer to k as momentum. Its unit is inverse length.[15] In numerical calculations it is also advantageous to convert mass to inverse length by dividing by $\hbar c = 197.33$ MeV-fm, or alternately, multiplying k by $\hbar c$ and using MeV as the unit.

The assumption of degeneracy is valid for low temperatures—much less than the Fermi energy

$$T << E_F = \sqrt{k_F^2 + m^2} \quad \text{(degeneracy condition)}. \tag{3.70}$$

Consider a white dwarf as an example. Obviously, a lower bound on the Fermi energy can be found by ignoring the momentum. For the electron Fermi energy we have $E_F > m_e = 0.511$ MeV $\sim 6 \times 10^9$ K. This is large compared to the internal temperature of most white dwarfs, $\sim 10^6$ to 10^7 K. Thus, the Fermi energy of electrons (and therefore also nucleons) easily satisfies the degeneracy condition, and we will generally consider cold stars in the above sense.

We wish to calculate the equation of state, which is the pressure and energy density at a common value of the density, or alternately, the value of the pressure at given energy density. The density is obviously obtained by summing over the occupied states in (3.69) and multiplying by the degeneracy of the momentum state. The energy is obtained by performing the same sum over $\sqrt{k^2 + m^2}$. Each Fermion type (n, p, e) contributes to the energy density, pressure, and number density according to

$$\begin{aligned} \epsilon &= \frac{\gamma}{2\pi^2} \int_0^k \sqrt{k^2 + m^2}\, k^2\, dk\,, \\ p &= \frac{1}{3} \frac{\gamma}{2\pi^2} \int_0^k \frac{k^2}{\sqrt{k^2 + m^2}}\, k^2\, dk\,, \\ \rho &= \frac{\gamma}{2\pi^2} \int_0^k k^2 dk\,, \end{aligned} \tag{3.71}$$

To verify that the pressure written above obeys the usual thermodynamic relationship,

$$p = -\frac{\partial E}{\partial V} = \rho^2 \frac{\partial}{\partial \rho} \frac{\epsilon}{\rho} = \rho \frac{\partial \epsilon}{\partial \rho} - \epsilon\,, \tag{3.72}$$

[15]One is accustomed to the combination $p^2c^2 + m^2c^4$ as particle energy squared. In natural units the expression will appear simply as $k^2 + m^2$. In computing a numerical value, k and m will have to be expressed in the same units, for example, as MeV or fm^{-1}.

perform the differentiation using the standard integrals below. Note that the last equality yields

$$\frac{\partial \epsilon}{\partial \rho} = \frac{\epsilon + p}{\rho}. \tag{3.73}$$

In the above equations, γ denotes the degeneracy of each momentum state. The degeneracy is 2 for each Fermion type corresponding to the two spin projections $\pm 1/2$. The upper limit on the integrals stands for the Fermi momentum, sometimes denoted by k_F. For the simplicity of the appearance of formulae to follow, we call it simply k, or k_p when we have to distinguish proton Fermi momentum from others. Clearly, Choosing a value of k is equivalent to choosing the Fermion density.

According to the units just described, ϵ and p can be conveniently computed in units $1/\text{fm}^4$. They can be converted to MeV/fm^3 by multiplying by $\hbar c$ or still other units by using the conversion factors described in Section 3.3.

The integrals can be carried out in closed form using the results of Ref. [64], pp. 86 and 87:

$$\int_0^k \sqrt{k^2+m^2}\, k^2\, dk =$$

$$\frac{1}{4}\Big[k(k^2+m^2)^{3/2} - \frac{1}{2}m^2 k\sqrt{k^2+m^2} - \frac{1}{2}m^4 \ln\Big(\frac{\sqrt{k^2+m^2}+k}{m}\Big)\Big],$$

$$\int_0^k \frac{k^4}{\sqrt{k^2+m^2}}dk =$$

$$\frac{1}{4}\Big[k^3\sqrt{k^2+m^2} - \frac{3}{2}m^2 k\sqrt{k^2+m^2} + \frac{3}{2}m^4 \ln\Big(\frac{\sqrt{k^2+m^2}+k}{m}\Big)\Big],$$

$$\int_0^k \frac{k^2}{\sqrt{k^2+m^2}}dk = \frac{1}{2}\Big[\sqrt{k^2+m^2} - \frac{1}{2}m^2 \ln\Big(\frac{\sqrt{k^2+m^2}+k}{m}\Big)\Big].$$

As the contribution of each fermion type (of degeneracy $\gamma = 2$), we find

$$\begin{aligned}
\epsilon &= \frac{1}{4\pi^2}\Big[\mu k\Big(\mu^2 - \frac{1}{2}m^2\Big) - \frac{1}{2}m^4 \ln\Big(\frac{\mu+k}{m}\Big)\Big],\\
p &= \frac{1}{12\pi^2}\Big[\mu k\Big(\mu^2 - \frac{5}{2}m^2\Big) + \frac{3}{2}m^4 \ln\Big(\frac{\mu+k}{m}\Big)\Big],\\
\rho &= \frac{k^3}{3\pi^2},
\end{aligned} \tag{3.74}$$

where

$$\mu = (m^2 + k^2)^{1/2} \tag{3.75}$$

is the Fermi energy (sometimes referred to as the chemical potential) and k the Fermi momentum. We could eliminate k in favor of ρ in the above equations, yielding $\epsilon(\rho)$ and $p(\rho)$.

Continuing our calculation of the equation of state, we want to minimize the total energy density of neutrons, protons, and electrons $\epsilon(\rho_n, \rho_p, \rho_e) = \epsilon(\rho_n) + \epsilon(\rho_p) + \epsilon(\rho_e)$ at fixed baryon density $\rho = \rho_n + \rho_p$ and subject to the condition of charge neutrality $\rho_p = \rho_e$. This can be done by the method of Lagrange multipliers [65]. Construct a new function from the one we wish to extremize together with the two constraint equations:

$$F(\rho_n, \rho_p, \rho_n) \equiv \epsilon(\rho_n, \rho_p, \rho_n) + \alpha(\rho - \rho_n - \rho_p) + \beta(\rho_e - \rho_p)\,.$$

For arbitrary variations of the three particle densities we require that

$$\frac{\partial F}{\partial \rho_n} = 0, \quad \frac{\partial F}{\partial \rho_p} = 0, \quad \frac{\partial F}{\partial \rho_e} = 0\,.$$

Using the integral expressions for ϵ, we have

$$\frac{\partial \epsilon}{\partial \rho_n} = \frac{\partial \epsilon}{\partial k_n}\frac{\partial k_n}{\partial \rho_n} = \sqrt{k_n^2 + m_n^2}, \qquad \text{etc.} \tag{3.76}$$

Therefore the above conditions on F yield

$$\begin{aligned} \alpha &= \sqrt{k_n^2 + m_n^2} \equiv \mu_n, \\ \alpha + \beta &= \sqrt{k_p^2 + m_p^2} \equiv \mu_p, \\ -\beta &= \sqrt{k_e^2 + m_e^2} \equiv \mu_e\,. \end{aligned} \tag{3.77}$$

Eliminating the Lagrange multipliers, we obtain

$$\mu_e + \mu_p = \mu_n\,. \tag{3.78}$$

Because μ_e is the electron chemical potential, it corresponds to unit negative electric charge while μ_n corresponds to unit baryon charge without electric charge (i.e., neutron).

The expression of chemical equilibrium (3.78) will recur in more general terms many times. It ensures that the particle levels are filled to such a point that no energy can be extracted from the gas by a neutron undergoing a beta decay or a proton an inverse beta decay. Of course, all levels are Fermi-blocked below the Fermi energies.

It is particularly noteworthy that the chemical potentials of three types of particles can all be expressed in terms of the two (Lagrange multipliers) associated with the conservation laws, namely, baryon number and electric charge conservation. The system is said to have three components, of which only two are independent.

As an aside, we remark that the conclusion concerning the possibility of expressing the chemical potentials for m substances in equilibrium in terms of the chemical potentials of the n independent components (or as we shall often say, conserved charges) is not restricted to free particles as in the above example. In general the problem is to find the minimum of, say, the Gibbs free energy Φ, subject to the subsidiary conditions that express the conservation of the independent components (charges). The problem is therefore of the same kind as solved above.

The simple expressions for the chemical potentials (3.75) will not hold. But we will still have $\mu_i = (\partial\Phi/\partial N_i)_{P,T}$, and the derivation will go through as above.

There is an alternate way of deriving the relation of the chemical potentials for the m substances in terms of those for the independent components. It consists of writing down all of the expressions for the possible chemical transformations in the form $\nu_i A_i = 0$, where the ν_i are positive or negative (and not necessarily integers, as in the case of quarks) and the A_i are the chemical symbols. One then replaces the chemical symbols by the chemical potentials. If several chemical transformations are possible, there is an equation for each and the resulting relationships between the chemical potentials allows one to express the chemical potentials of all components in terms of the independent ones alone (see Chapter X of Ref. [66]).

Pursuing our search for the minimum of the total energy at fixed density subject to charge neutrality, we note that the Fermi momenta of nucleons and the baryon density ρ are related by

$$\frac{1}{3\pi^2}(k_n^3 + k_p^3) = \rho\,. \tag{3.79}$$

The condition of charge neutrality can be written

$$k_p = k_e\,. \tag{3.80}$$

These two equations together with (3.78) can be used to determine the k_n, k_p, and k_e such that the energy is minimized subject to the stated conditions. We now analyze how they may be solved.

Suppose $k_p = 0$. Then we obtain

$$k_n^2 = (m_p + m_e)^2 - m_n^2 < 0\,, \tag{3.81}$$

where the values of neutron and proton masses were written earlier and $m_e = 0.511$ MeV. So there is no real solution, and we conclude that k_p is always finite. Next try $k_n = 0$. We find

$$k_p^2 = \left(\frac{m_e^2 + m_n^2 - m_p^2}{2m_n}\right)^2 - m_e^2 = 1.40\ \mathrm{MeV}^2$$
$$= 3.60 \times 10^{-5}\ \mathrm{fm}^{-2}\,. \tag{3.82}$$

This is the smallest value of k_p for which k_n can be finite. Below the density

$$\rho = \frac{k_p^3}{3\pi^2} = 7.29 \times 10^{-9}\ \mathrm{fm}^{-3} \tag{3.83}$$

or below the energy density[16]

$$\epsilon \sim \rho m_p = 3.47 \times 10^{-8}\ \mathrm{fm}^{-4} = 1.22 \times 10^7\ \mathrm{g/cm}^3\,, \tag{3.84}$$

[16]Note that we are making frequent use of the conversion factors derived earlier in the chapter.

a charge-neutral Fermi gas in equilibrium is an equal mixture of protons and electrons with no neutrons. Below this neutron threshold, we have simply

$$k_p = (3\pi^2\rho)^{1/3}, \quad k_e = k_p, \quad k_n = 0, \tag{3.85}$$

and the energy density and pressure can be computed from (3.74) or the low-density approximations derived in the next section.

Above the neutron threshold, we can use the equation for fixed baryon density to write

$$k_n = (3\pi^2\rho - k_p^3)^{1/3} \tag{3.86}$$

together with the condition of charge neutrality to obtain an equation in k_p alone:

$$(k_p^2 + m_e^2)^{1/2} + (k_p^2 + m_p^2)^{1/2} = \left[(3\pi^2\rho - k_p^3)^{2/3} + m_n^2\right]^{1/2}. \tag{3.87}$$

This can be solved numerically for k_p for any ρ, and then the corresponding k_n can be found. The total energy density and pressure can then be calculated.

It is of some interest to look at the above equation in the ultrarelativistic regime where we ignore all masses. Then one obtains

$$\rho_p \to \frac{1}{8}\rho. \tag{3.88}$$

If the existence of all other baryon types and their mutual interactions are ignored, the asymptotic proton density is one-eighth of the baryon density. One can also easily show in the same limit that this fraction is approached from below. For this reason it is sometimes thought that neutron stars are composed mostly of neutrons. Such an assumption is frequently used in calculations of neutron star properties, for example, masses, transport coefficients, or cooling rates.

The Fermi gas model for an equation of state has introduced some of the important principles involved in dealing with dense matter—the equilibrium composition of matter, charge neutrality, and the role of the Pauli principle. The directions in which the model can be improved, include (1) the introduction of additional baryon species such as hyperons, (2) nuclear interactions, (3) an important property of nuclear matter, namely, the energetic preference for an equal number of neutrons and protons, modulo effects of the Coulomb force. This is often referred to as the preference for *isospin symmetry*, about which we shall elaborate in Chapter 4, and finally (4) phase transitions, such as quark deconfinement or kaon condensation. So, within the overriding constraint of charge neutrality, we anticipate that the composition of neutron stars will be very rich in baryon species [67, 68]. We will discuss these important topics in Chapter 5 and later chapters.

While the above formulae for energy density and pressure (3.74) are exact expressions for the equation of state within the limitations of the Fermi gas model, they are a poor basis for numerical computation in the case that a particle momentum is very small compared to its mass. In this case we must derive the nonrelativistic limits of the exact expressions and use them to compute the contributions to the energy density and pressure.

3.9.3 High- and low-density limits

For both the numerical reason mentioned above and for the sake of an interesting partially analytic discussion of white dwarfs as polytropes (which we shortly define), we derive the high- and low-density limits of the exact Fermi gas expressions (3.74) and (3.71), respectively. The high-density limit $k >> m$, which may also be called the relativistic limit if m is not ignored or the ultrarelativistic limit if it can be. The results are

$$\begin{aligned} \epsilon &\approx \frac{1}{4\pi^2}\left[k^4 - \tfrac{1}{2}m^4 \ln\frac{2k}{m}\right], \\ p &\approx \frac{1}{12\pi^2}\left[k^4 + \tfrac{3}{2}m^4 \ln\frac{2k}{m}\right]. \end{aligned} \tag{3.89}$$

The logarithmic terms are small compared to k^4 in the ultrarelativistic limit, so we have

$$\epsilon \to 3p \approx \frac{1}{4\pi^2}(3\pi^2\rho)^{4/3} \quad \text{(high density, } k >> m\text{)}, \tag{3.90}$$

where ρ here is the density of the fermion type considered.

The low-density expansion can easily be found directly from the integral expressions by expanding in k/m:

$$\begin{aligned} \epsilon &\approx \frac{m^4}{\pi^2}\left[\frac{1}{3}\left(\frac{k}{m}\right)^3 + \frac{1}{10}\left(\frac{k}{m}\right)^5 - \frac{1}{56}\left(\frac{k}{m}\right)^7 + \frac{1}{144}\left(\frac{k}{m}\right)^9\right], \\ p &\approx \frac{m^4}{3\pi^2}\left[\frac{1}{5}\left(\frac{k}{m}\right)^5 - \frac{1}{14}\left(\frac{k}{m}\right)^7 + \frac{1}{24}\left(\frac{k}{m}\right)^9\right]. \end{aligned} \tag{3.91}$$

For very low density, the nonrelativistic approximation involves the terms to k^5 only. When written in terms of ρ, they appear as

$$\begin{aligned} \epsilon &\approx \rho m + \frac{(3\pi^2\rho)^{5/3}}{10\pi^2 m}, \\ p &\approx \frac{(3\pi^2\rho)^{5/3}}{15\pi^2 m} \quad \text{(low density, } k << m\text{)}. \end{aligned} \tag{3.92}$$

Notice that the term in ϵ proportional to ρ does not contribute to the pressure. (See (3.72).) These are the contributions of each fermion type to the equation of state.

Of course "low" and "high" density have different meanings for electrons and nucleons. For example, in the domain $m_e < k_e = k_p < m_p$, the electrons are relativistic ($k_e > m_e$), but the protons are nonrelativistic ($k_p < m_p$). This has to be kept in mind in computing an equation of state over a wide range of densities for n, p, and e in equilibrium.

The equation of state of this Fermi gas model is shown in Fig. 3.8. The kink at $\epsilon \approx 10^7$ g/cm^3 marks the neutron threshold. Below this, the gas is an equal mixture of protons and electrons. Above, it rapidly becomes dominated by neutrons. The

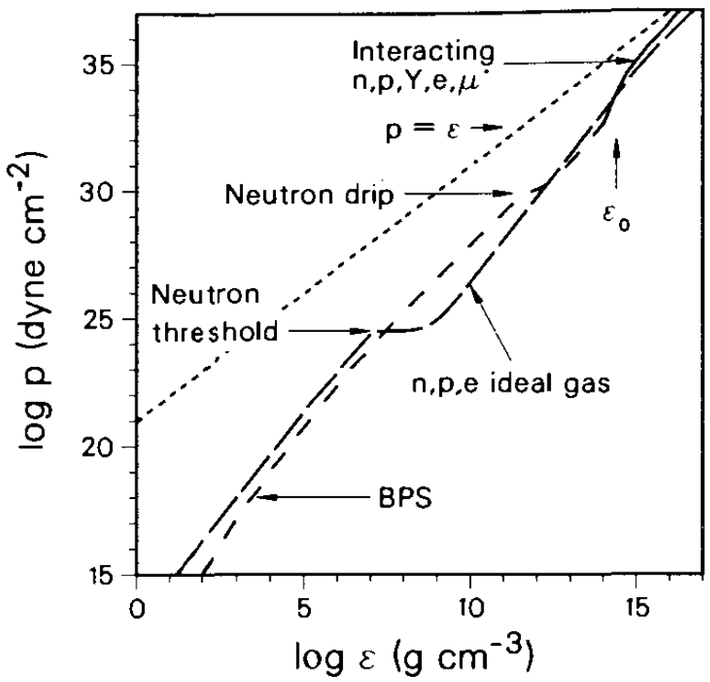

FIGURE 3.8. Charge-neutral Fermi gas equation of state of n, p, and e in beta equilibrium. Flat pressure region corresponds to the neutron threshold. For comparison, the BPS equation of state (see Section 3.10) is also shown, corresponding to the lowest energy state of nuclei located in a lattice with electrons in the interstices. The kink in this equation of state at $\epsilon \approx 4.3 \times 10^{11}$ g/cm^3 is the density at which free neutrons drip from the nuclei. Also shown are a high-density equation of state of hyperonized matter and the limit $p = \epsilon$.

flat region in pressure corresponds simply to the fact that the increase in density in this region is accounted for by low-momentum (threshold) neutrons.

3.9.4 Polytropes and Newtonian white dwarfs

The results above for an ideal gas equation of state could serve to provide a crude model of white dwarf structure. However, what we have derived can be used for an improved description that recognizes the fact that white dwarfs do not consist of a gas of nucleons and electrons, but rather that the nucleons are clumped in nuclei, such as ^{4}He, ^{12}C, and ^{16}O. (Recall page 65.)

For charge neutrality, we require $\rho_p = \rho_e$ or, equivalently, $k_p = k_e$. Let us recall that charge-neutral matter consists only of protons and electrons below a certain nucleon density. The momentum corresponding to the neutron threshold is (3.82)

$$k_e = k_p = 0.00600 \text{ fm}^{-1} \quad \text{(neutron threshold)}. \tag{3.93}$$

This compares with the electron and proton masses of

$$\begin{aligned} m_e &= 0.511 \text{ MeV} = 0.511/197 \text{ fm}^{-1} = 0.00259 \text{ fm}^{-1}, \\ m_p &= 4.76 \text{ fm}^{-1}. \end{aligned} \tag{3.94}$$

Therefore, far below the neutron threshold, electrons are nonrelativistic. From (3.93) we find that the electron pressure is much greater than that of the protons,

$$\frac{p_e}{p_p} = \frac{m_p}{m_e} >> 1 \quad (k_e << m_e). \tag{3.95}$$

Electrons are relativistic at and above the neutron threshold as seen above: $k_e > m_e$. Above the threshold up to the interesting condition that neutron and proton densities are equal (as in nuclei), electrons are relativistic, and nucleons are nonrelativistic, $k_n,\ k_p << m_p$. For relativistic electrons refer to (3.93) and (3.90) to find

$$\frac{p_e}{p_p} = \frac{5}{4}\frac{m_p}{k_e} >> 1 \quad (m_e << k_e << m_p)\,. \tag{3.96}$$

The two equations above show that in the white dwarf domain defined by

$$k_p \text{ and } k_n << m_p \quad \text{(white dwarf domain)}\,, \tag{3.97}$$

electrons—whether relativistic or nonrelativistic—contribute virtually all the pressure, while the nucleons contribute virtually all the energy density. This is a fundamental fact of white dwarf physics. R. H. Fowler was the first to recognize that white dwarfs are supported against gravitational collapse by the pressure of degenerate electrons [69].

We discussed above the white dwarf domain up to the point where neutron and proton densities are about equal. However, because of the short-range attraction between nucleons, a dilute gas of nuclei is a lower energy state than a dilute gas of neutrons, protons, and electrons. Said another way, nucleons are bound in nuclei by about 8 MeV per nucleon so that the average mass of nucleons is less when in nuclei than free. We will return to this subject in a more exacting way.

In the meanwhile it is worth pursuing the present model by modifying the idealized results in a physically motivated ad hoc manner, namely, as a dilute gas of nuclei and electrons. This is straightforward because we have just seen that the nucleons do not contribute appreciably to the pressure. It is only their rest energy that is important. We can therefore consider that the nucleons are bound in nuclei. We express the energy density as a multiple of the nominal mass, m_N, of a nucleon bound in a nucleus times their number. We express the number of nucleons in the nucleus as a multiple

$$\nu = (\rho_p + \rho_n)/\rho_e \tag{3.98}$$

times the electron density ρ_e. Thus, for the energy density we have

$$\epsilon = \rho_e m_N \nu\,. \tag{3.99}$$

In the discussion of the preceding section, ν would have been determined by the equilibrium condition for a neutral Fermi gas of nucleons and electrons. In this section it is a parameter used to represent the nucleon–electron ratio of the dominant nuclear species, in particular, white dwarfs such as He, C, or O. For each of these, $\nu = 2$. We note that, from its definition, we can write

$$\rho_n = \rho_p(\nu - 1)\,. \tag{3.100}$$

Because the neutron threshold occurs at nonzero proton density, it must be so that $\nu \geq 1$.

In the white dwarf domain (3.97), it is easy to confirm that the electron pressure is always less than the electron energy density because of the results that can be deduced from the foregoing;

$$\frac{p_e}{\epsilon_e} \approx \frac{1}{5}\left(\frac{k_e}{m_e}\right)^2 << 1\,, \quad k_e < m_e\,,$$
$$\frac{p_e}{\epsilon_e} \approx \frac{1}{3}\,, \quad k_e > m_e\,. \tag{3.101}$$

The electron energy density itself is small compared to the rest mass density of the nucleons. Consequently, energy density dominates pressure, and we can write

$$p << \epsilon, \quad 4\pi r^3 p << M(r), \quad \frac{2M(r)}{r} << 1\,, \tag{3.102}$$

These inequalities assure that the Newtonian approximation to (3.27) is valid. The last of the inequalities follows from the fact that no region of a star can lie within its Schwarzschild radius [27]. It is also apparent that the pressure would not be monotonic unless the last inequality holds. Considering that the pressure at r supports all material above r, pressure should be increasing monotonically from the edge to the center of the star. The middle inequality follows from the first: rearrange $M(r) \sim (4\pi/3)r^3\bar{\epsilon}$ to read $4\pi r^3 p \sim 3(p/\bar{\epsilon})M(r) << M(r)$.

After the Newtonian approximation has been made, divide what remains of (3.27) by ϵ, differentiate by r, and combine with (3.28) to obtain

$$\frac{d}{dr}\left(\frac{r^2}{\epsilon}\frac{dp}{dr}\right) = -4\pi r^2 \epsilon\,. \tag{3.103}$$

This is the equation that governs the structure of a Newtonian star. As for the Oppenheimer–Volkoff structure equations, the Newtonian equation (9.12) defines a one-parameter family of stars (sometimes referred to as a sequence) for any specified equation of state. The central energy density $\epsilon_c \equiv \epsilon(0)$ is a convenient means of parameterizing the continuum of stars belonging to the sequence.

We now derive a white dwarf sequence. The equation of state can be approximated by the following form in the white dwarf domain (3.97),

$$p = K\epsilon^\gamma\,. \tag{3.104}$$

A star whose equation of state is approximated by such a simple form is known as a *polytrope*. Polytropes are interesting as approximate models of stars because more than the usual amount of work can be done analytically. The power gamma in the polytrope is a constant which has two limiting values depending on whether the electrons are relativistic or nonrelativistic, as we will see in the following two sections.

Boundary conditions for Newtonian stars (3.103) can be found easily. Taking $r \to 0$ shows that, for finite $\epsilon(0)$, we must have $p'(0) = 0$. For a polytrope, $p' = \gamma(\epsilon'/\epsilon)p$ which shows that, for $\epsilon(0) \neq 0$, we must have $\epsilon'(0) = 0$. Summarizing, the boundary conditions on (3.103) are

$$\epsilon(0) = \epsilon_c, \quad \epsilon'(0) = 0\,. \tag{3.105}$$

By transforming variables from r, ϵ to ξ, θ, we get a universal equation for polytropes parameterized by the polytropic index γ. The transformation is

$$r = \left(\frac{K\gamma}{4\pi(\gamma-1)}\right)^{1/2} \epsilon_c^{\frac{\gamma-2}{2}} \xi, \quad \epsilon = \epsilon_c \theta^{\frac{1}{\gamma-1}}, \quad p = K \epsilon_c^{\gamma} \theta^{\frac{\gamma}{\gamma-1}}, \tag{3.106}$$

and the result is the *Lane–Emden* equation of index $(\gamma - 1)^{-1} = n$,

$$\frac{1}{\xi^2}\frac{d}{d\xi}\xi^2\frac{d\theta}{d\xi} + \theta^{\frac{1}{\gamma-1}} = 0. \tag{3.107}$$

The boundary conditions corresponding to (3.105) are

$$\theta(0) = 1, \quad \theta'(0) = 0. \tag{3.108}$$

The Lane–Emden equation can be integrated numerically for various γ. It is easily verified that, for $\gamma > 6/5$, the Lane–Emden function $\theta(\xi)$ is monotonic decreasing with increasing argument (radius), as would be required of the pressure and energy density in a static star. The first zero occurs at a finite argument; call it ξ_1:

$$\theta(\xi_1) = 0. \tag{3.109}$$

Because this is the point where the pressure (3.106) has fallen monotonically to zero, ξ_1 marks the edge of the star. From the equations for the transformation of variables (3.106), the stellar radius is

$$R = \left(\frac{K\gamma}{4\pi(\gamma-1)}\right)^{1/2} \epsilon_c^{\frac{\gamma-2}{2}} \xi_1. \tag{3.110}$$

The mass is given by (3.28) as

$$M = \int_0^R 4\pi^2 \epsilon(r)\, dr = 4\pi \epsilon_c^{(3\gamma-4)/2} \left(\frac{K\gamma}{4\pi(\gamma-1)}\right)^{3/2} \int_0^{\xi_1} \xi^2 \theta^{\frac{1}{\gamma-1}}\, d\xi. \tag{3.111}$$

Using the Lane–Emden equation, the integral is easily evaluated:

$$\int_0^{\xi_1} \xi^2 \theta^{\frac{1}{\gamma-1}}\, d\xi = -\int_0^{\xi_1} \frac{d}{d\xi}\xi^2\frac{d\theta}{d\xi}\, d\xi = -\xi_1^2 \theta'(\xi_1). \tag{3.112}$$

Hence, the mass is found as

$$M = 4\pi \epsilon_c^{(3\gamma-4)/2} \left(\frac{K\gamma}{4\pi(\gamma-1)}\right)^{3/2} \xi_1^2 |\theta'(\xi_1)|. \tag{3.113}$$

Thus, for a specific polytropic sequence, the mass and radius have the relationship

$$R \sim M^{(\gamma-2)/(3\gamma-4)}. \tag{3.114}$$

We return to these results after discussing the stability of stars in Section 3.18.

3.9.5 *Nonrelativistic electron region*

As noted above, the white dwarf region (3.97) itself can be discussed in terms of two regions according to whether k_e is greater or less than the electron mass. In

both cases the energy density is dominated by the rest-mass density of nucleons, whether they be free or bound in nuclei.

The electron pressure dominates over the proton pressure even in the region $k_p = k_e << m_e << m_p$. Neutrons are altogether absent in this region (in the Fermi gas model of the equation of state) because, as shown above, the value of k_e at the neutron threshold is larger than m_e. So it is required that $\nu = 1$. From (3.99), we may write

$$k_e = \left(\frac{3\pi^2\epsilon}{m_N\nu}\right)^{1/3}, \tag{3.115}$$

from which we obtain from (3.93) an expression for the pressure as

$$p = K\epsilon^\gamma, \quad K = \frac{1}{15\pi^2 m_e}\left(\frac{3\pi^2}{m_N\nu}\right)^\gamma, \quad \gamma = 5/3. \tag{3.116}$$

From the solution of (3.107), $\xi_1 = 3.65$ and $-\xi_1^2\theta'(\xi_1) = 2.71$ for $\gamma = 5/3$, we find

$$M = 2.79\,\nu^{-2}\left(\frac{\epsilon_c}{\epsilon_k}\right)^{1/2} M_\odot \quad (\text{for } \gamma = 5/3), \tag{3.117}$$

where $\epsilon_k = \rho_k m_N \nu$ and $\rho_k = m_e^3/3\pi^2$ are the densities corresponding to $k_e = m_e$. We cannot say precisely what the inequality $k_e << m_e$ implies about ϵ_c/ϵ_k, save that it is less than unity. However, we do understand that we are dealing with the lighter white dwarfs. A limit on the density of these stars can be estimated for the regime $k_e < m_e$. It is

$$\epsilon \approx m_p\frac{m_e^3}{3\pi^2} = 9.8 \times 10^5 \text{ g/cm}^3. \tag{3.118}$$

In the $\gamma = 5/3$ range of white dwarfs, the mass is an increasing function of central density, and the radius (3.110) is a decreasing function (for any $\gamma < 2$). A decrease of radius with an increase of mass is quite a general property of degenerate stars, and the physical reason is simple. The gravitational attraction grows as the mass increases, causing a greater compaction of the star.

3.9.6 *Ultrarelativistic electron region: asymptotic white dwarf mass*

Now we study the ultrarelativistic region and the famous Chandrasekhar mass limit for white dwarfs. The electron pressure dominates nucleon or nuclear pressures as noted above. We may say that the ponderous nuclei or nucleons provide mass but little pressure as compared to electrons which are light and fast. From (3.99) we find the electron density in terms of the total energy density, and substituting into (3.90) we find that the pressure is given by the polytropic form

$$p = K\epsilon^\gamma, \quad K = \frac{1}{12\pi^2}\left(\frac{3\pi^2}{m_N\nu}\right)^\gamma, \quad \gamma = 4/3. \tag{3.119}$$

This is the equation of state in the limit of ultrarelativistic electrons throughout the star. In this limit we see that the mass (3.113) is independent of central density and the radius (3.114) tends to zero as $\gamma \to 4/3$.

The value of the unique mass, given in terms of the solution of the Lane–Emden equation $\xi_1 = 6.90$, $-\xi_1^2\theta'(\xi_1) = 2.02$, for $\gamma = 4/3$ is composition-dependent and given by

$$M = 5.87\ \nu^{-2} M_\odot\,, \quad \text{for } \gamma = 4/3\,. \tag{3.120}$$

This is the famous Chandrasekhar mass limit for white dwarfs. To estimate its numerical value, we note that the region

$$m_e << k_e = k_p << m_p \tag{3.121}$$

is well above the neutron threshold. Therefore, we can contemplate approximately equal numbers of neutrons and protons (as in ^{4}He, ^{12}C, and ^{16}O of which real white dwarfs are made). Then from (3.120) we find $M \approx 1.5 M_\odot$. This is a rough estimate of the maximum white dwarf mass [70, 71].

We have thus learned that the sequence of white dwarfs beginning at low through to high density, or correspondingly from $k << m_e$ to $k >> m_e$, has an equation of state in the two limits that are polytropes, and that the polytropic index falls from $\gamma = 5/3$ to $4/3$ along the sequence of increasing density. This corresponds to a softening of the equation of state. Between the limits the equation of state can still be thought of as a polytrope but with γ a function of density ranging between the limits.

It is important to notice that the polytropic index reaches the value $\gamma = 4/3$ only as all electrons in the star become ultrarelativistic. In this limit the radius is zero and the density is infinite. Along the sequence of dwarfs of increasing density, the radius decreases as the mass increases toward the limiting value (3.120). The limit obtained by Chandrasekhar is an asymptotic limit. However, the limit of real white dwarfs is of a different nature, as discussed in the next section. The limiting mass of real white dwarfs is reached at finite density.

Chandrasekhar, while still a student, discovered that completely degenerate configurations have a mass limit when one takes account of special relativity in computing the equation of state. Limits to stellar masses had never been known before. It is not clear that Chandrasekhar fully understood the implication of his limit by enquiring of the ultimate fate of a star with mass above the limit. Eddington did grasp the implication—the collapse to what we now call a black hole—but he dismissed it as absurd [58]. (See the quotations at the beginning of this section.) Eddington was not alone in rejecting the notion of a black hole. Nor was he the first to conceive the notion. Some 150 years before Eddington's inference, the Rev. John Michell had conceived the possible existence of back holes, stars so dense that their light could not escape, and he explained his ideas in a letter to Henry Cavendish dated November 27, 1783. However, the notion languished in the *Philosophical Transactions of the Royal Society (London)* [72] and never stimulated further interest (except possibly in Laplace, 1795).

It was not until the work of Oppenheimer and Snyder (1939) on continued gravitational collapse that the notion of black holes reappeared, and, even at that, it was not until the mid-1960s that intense interest in such objects emerged. Indeed, even John Wheeler, until the end of the 1950s, believed that other processes would intervene to prevent collapse of a star to a black hole. He was partially correct. Not all gravitational collapses result in the formation of black holes. Now we know that the fate of stars more massive than the Chandrasekhar limit is more varied and complicated than envisioned by Eddington. Much mass may be expelled in a planetary nebula or supernova. Even if the collapsing core is more massive than the limit for a white dwarf, the star may still be arrested in its collapse at the stage of a neutron star, and only if the collapsing object exceeds the limiting mass for neutron stars will it collapse forever beyond the Schwarzschild horizon.

Shortly after Chandrasekhar's pioneering work, Landau advanced a general argument for a maximum mass that the Fermi pressure of a degenerate gas of relativistic particles can sustain against gravity [73]. Landau's argument is based on fundamental constants. The maximum possible mass is of the order of a solar mass for either degenerate electrons or neutrons (see Ref. [28] for details). Landau's limit, based on the Fermi pressure of relativistic particles of unnamed type, was therefore a prediction of the limiting mass of white dwarfs and neutron stars.

Landau employed the Newtonian gravitational potential, and for Newtonian gravity there is no limiting mass in the sense of General Relativity. The limit obtained by Chandrasekhar is also Newtonian and, as we have seen, is an asymptotic mass. Nevertheless, real white dwarfs do attain a mass limit along the sequence of equilibrium configurations, but at finite density, as depicted in Fig. 3.9, and it is customarily called the Chandrasekhar limit. We will discuss the nature of the limit in the next section.

Conditions for the validity of the Chandrasekhar limit—that all electrons are ultrarelativistic—can hardly be attained in real stars. After all, the pressure goes to zero at the stellar surface. However, it remains relevant to the iron core mass in stars near the termination of their evolution. In such stars, the weight of the overlaying matter can raise the Fermi energy of all electrons in the core. However, as we discuss next, capture of energetic electrons onto protons and nuclei still limits the Fermi energy in the core.

3.9.7 Nature of limiting mass of dwarfs and neutron stars

We have seen that electrons become relativistic at a much lower density than nucleons and that the pressure of degenerate electrons, both nonrelativistic and relativistic, establishes stable configurations called white dwarfs . These are Newtonian stars; general relativistic corrections are very small [74]. We also learned that the limiting mass of white dwarfs in the models that we have considered till now

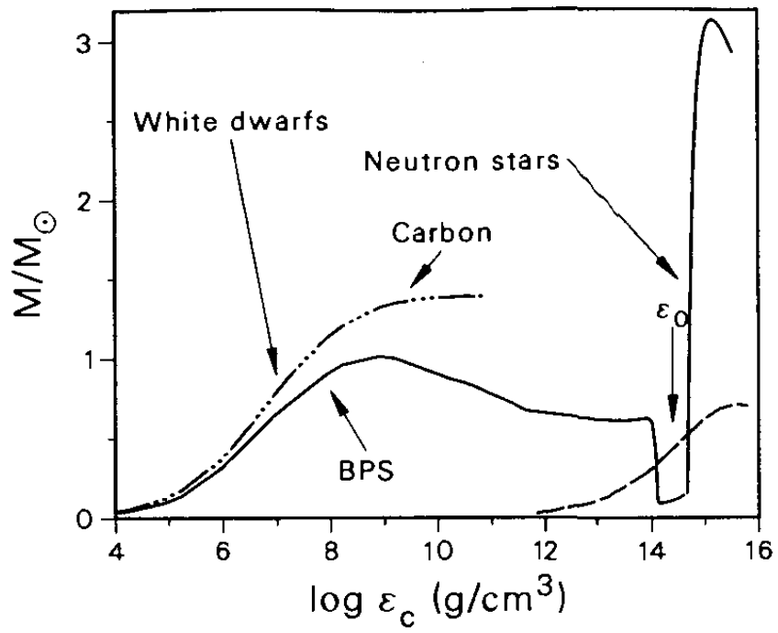

FIGURE 3.9. White dwarf sequences, one corresponding to the equation of state of BPS, the other to a pure carbon white dwarf (see Section 3.10) Two neutron star sequences are also shown: the solid line corresponds to the causal limit equation of state (see Section 3.17), and the dashed to the charge-neutral ideal n, p, e gas in beta equilibrium. Stable stars have positive slope.

is attained only as an asymptotic limit at which the electrons are ultrarelativistic and the density is infinite.[17] This leaves little room for neutron stars.

The dilemma is resolved by noting that, even in the more realistic model considered above in which nucleons reside in nuclei (page 100), the neutron–proton ratio was held fixed. However, an important process is neglected in this approximation. As the electron Fermi energy increases, high-energy electrons are absorbed by protons—either free or in nuclei—in the inverse beta decay,

$$^{A}Z + e^- \longrightarrow {}^{A}(Z-1) + \nu\,. \tag{3.122}$$

The neutrinos diffuse to the edge of the star where, having the escape velocity, they depart. This process is also referred to as *neutronization*. Neutronization depletes the supporting electron pressure as the density increases, bringing the sequence of white dwarfs to an end at central densities of the order of 10^9 g/cm^3. Therefore the mass limit for white dwarfs has to do with their changing internal composition [75, 76]. This limit is unrelated to the limit for relativistic stars, discussed below. What is at issue for white dwarfs is an instability occasioned by electron capture of energetic electrons. Consequently, the white dwarf mass limit is not quite the one envisioned by Chandrasekhar which, as previously noted, is an asymptotic limit attained only at infinite density.

To complete our discussion of the the termination of the white dwarf sequence, we add that, if neutronization did not destabilize white dwarfs, the general relativistic instability discussed next would do so at a somewhat higher density [77].

[17] In the limit $\gamma \longrightarrow 4/3$, we saw that the stellar radius goes to zero (3.114).

White dwarf central densities range over about two orders of magnitude above and below 10^7 g/cm^3. At a much higher density, the Fermi pressure of nucleons (assisted by the short-range repulsion between them) establishes a second sequence of stable configurations, the neutron stars. Neutron star densities can be estimated by finding the neutron number density corresponding to, say the point of transition from nonrelativistic to relativistic neutrons, $k_n = m_n$. In this case $\epsilon \sim \rho_n m_n \sim (1/(3\pi^2))m_n^4 = 6 \times 10^{15}$ g/cm^3.

In contrast to the neutronization instability of white dwarfs, gravitational collapse of a neutron star to a black hole or any relativistic star of sufficiently high mass concentration cannot be evaded by any conceivable form of matter, not even "incompressible" matter, as has been clearly argued by Harrison, Thorne, Wakano, and Wheeler [28]. They refer to the "no escape from collapse" in this connection. Collapse of relativistic stars is intrinsic to the structure of Einstein's theory. It has to do with the fact that pressure, which in Newtonian stars resists collapse, in General Relativity ultimately makes collapse inevitable because it appears together with energy density as a source of gravitational attraction in the Oppenheimer–Volkoff equation (2.224). (Recall Section 2.9.6.) Indeed in Section 3.15 we will see that even in the idealization of incompressible matter, there is a limit to the mass and radius of the star that depends simply on the assumed density of the incompressible medium! In general, compact relativistic stars have a mass limit that occurs at a finite central density. The particular value of the mass limit depends on the equation of state, but its existence does not.

3.9.8 Degenerate ideal gas neutron star

In our study of the Fermi gas equation of state for nucleons and electrons in beta equilibrium, we learned that at high baryon density the proton fraction approaches one-eighth from below. To a first approximation, charge-neutral matter at densities above the white dwarf domain is pure neutron matter.

After the first few minutes of birth, a neutron star is very cold on the nuclear scale so that in the ideal gas model a neutron star is supported solely by the Fermi pressure of the degenerate neutrons, just as white dwarfs are supported by the pressure of degenerate electrons. Oppenheimer and Volkoff [78] were the first to investigate the structure of neutron stars, and they did so by assuming that the star was composed of noninteracting neutrons.

Oppenheimer and Volkoff found that their equations for the structure of relativistic stars yielded a limiting mass of $\approx 0.72 M_\odot$ and a radius of ≈ 9.6 km [78]. This is an interesting result for the following reason. We know that nuclear forces, especially the repulsive components, will become important at densities higher than the equilibrium density of nuclear matter. The nuclear force therefore provides additional resistance to gravitational collapse beyond that provided by the neutron Fermi pressure. So the Oppenheimer and Volkoff result establishes a value of the maximum mass of neutron stars that is close to a lower bound. The ideal gas of nucleons and electrons that we developed earlier in Section 3.9.2 is an even softer equation of state. It allows the pressure of neutrons at the top of their Fermi

sea to be relieved by decay to protons and electrons (always in a charge-neutral equilibrium admixture). The limiting mass in this case is $0.7M_\odot$.

For real neutron stars, the nuclear force is decisive in establishing both the limiting mass and how high it lies above the lower bound just discussed. In Section 3.17 we estimate the maximum amount by which the nuclear force can raise the mass limit above that established by the pressure of a degenerate ideal gas of nucleons and leptons.

The short-range repulsion of the nuclear force stiffens the equation of state compared to that of an ideal gas. Reference to stiff or soft with regard to an equation of state is a relative term. By "stiffer" it is meant that at given energy density the pressure is higher in comparison with a "softer" equation of state. The stiffest equation of state that is compatible with the notion of causality is one for which the speed of sound is the light speed.

However, limiting the sound speed to light speed does not uniquely define the equation of state because the sound speed is given by a derivative $\sqrt{dp/d\epsilon}$. This would allow any normalization of the equation of state. For the purpose of describing neutron stars, the equation of state should obviously match smoothly to a low-density equation of state that describes matter in a regime better known to us. This selects a normalization. We refer to an equation of state at the causal limit at high density and normalized in the above manner near nuclear saturation density as a *causal limit equation of state*. Such an equation of state provides the most resistance to collapse and therefore yields an upper bound on the limiting mass. Ruffini found the maximum possible mass of a nonrotating neutron star to be $\approx 3.2M_\odot$ (see Section 3.17). Figure 3.9 compares neutron star sequences for the two extremes of soft and stiff equations of state. The limiting mass of neutron star models based on realistic equations of state will lie between the two extremes.

3.10 Improvements in White Dwarf Models

3.10.1 Nature of matter at dwarf and neutron star densities

A number of the principles involved in the structure of compact stars have been encountered in the above simple model of a degenerate Fermi gas of free neutrons, protons, and electrons in equilibrium. The major objection that can be raised against it as far as white dwarfs are concerned is that at densities below that of normal nuclei—and white dwarfs lie far below—it is energetically more favorable for nucleons to clump together into nuclei so as to exploit the short-range attractive nuclear force than to be uniformly dispersed at a lower density [28, 79, 80].

A white dwarf spans an enormous range of densities from its center to its surface. For example, Sirius B ($M = 1.053M_\odot$, $R = 5,400$ km) has an average density of

$$\bar{\epsilon} = \frac{M}{(4\pi/3)R^3} = \frac{1.053 \times 1.477 \text{ km}}{(4\pi/3)(5,400)^3 \text{ km}^3} = 2.35 \times 10^{-12} \text{ km}^{-2}$$

$$= 3.17 \times 10^6 \text{ g/cm}^3 = 4.03 \times 10^5 \epsilon_{\text{Fe}} = 1.26 \times 10^{-8} \epsilon_0 . \quad (3.123)$$

(Iron density is denoted by ϵ_{Fe}, and nuclear matter density by ϵ_0.) The central density is even higher than the average. The character of matter varies appreciably in this vast range of densities. For white dwarfs the constitution of matter is also very much influenced by the progenitor star and the extent of nuclear burning that preceded the formation of the white dwarf.

White dwarfs, unlike neutron stars, are not the remnants of progenitors in which nuclear fusion reactions have been driven to the iron end point under the relentless pressure of gravity (recall page 91). Nuclear combustion ceases in stars of a few solar masses at some intermediate element in the low-mass progenitors of dwarfs, so that dwarfs are composed mostly of ^{4}He, ^{12}C, or ^{16}O in some mixture. While such a composition is not the lowest possible energy state, the lowest energy state is not always attainable in a finite time, even astronomical time. Therefore, the most favored state energetically is actually not achieved in white dwarfs. White dwarfs are much more individualistic (depending on the details of the evolution of the particular progenitor) than they would be if nuclear burning had proceeded through to iron, as in the cores of massive stars prior to their collapse to neutron stars or black holes [79, 81].

The pressure is zero at the edge of a star, and the energy density is low. Whatever elements are present at the surface, whether white dwarf or neutron star, are there in their atomic state and are possibly ionized by the high temperature.

Neutron stars are formed from matter that has been fully processed by nuclear combustion, so that all available energy has been extracted at each density. Such hadronic matter in its ground state, is often referred to as "cold catalyzed matter" [28]. At zero pressure, such matter is composed of atoms of the most strongly bound nucleus, ^{56}Fe arranged as in ordinary solid iron. At increasing density, the atoms become progressively more ionized, and the electrons fill the interstices. A Coulomb lattice arrangement of nuclei in the electron gas minimizes the energy. Matter at and near the surface of white dwarfs is similar except that the heaviest element is He, C, O, or Mg, depending on the degree of burning in the progenitor. As we mentioned already, white dwarfs, even of the same mass, are variable in composition, whereas neutron stars of the same mass should be identical.[18]

Whether neutron star or white dwarf, as the density increases from that at the stellar surface, electrons become increasingly relativistic. A lower energy state is achieved through the capture of energetic electrons by nuclei—inverse beta decay. Any neutrinos or photons produced diffuse out of the star, thus lowering its energy. With increasing density, nuclei become increasingly neutron-rich by this neutronization process. Neutronization sets in at a density for which the electron

[18]However, for millisecond pulsars—those that rotate hundreds of times per second—the changing centrifugal effects as the star spins down significantly alter the distribution of density in the star with time. The star's internal constitution will reflect these changes, and the spin-down itself can be effected remarkably by the internal changes, as we will discuss in Chapter 11.

chemical potential, or Fermi energy $\mu_e \equiv \sqrt{m_e^2 + k_e^2}$, equals the threshold for the electron capture reaction (3.122). To find an approximate value of the threshold, let us take the proton–neutron mass difference $Q \sim -1$ MeV for the threshold. The threshold density for neutronization is therefore[19]

$$\epsilon_{\text{neut}} \approx \frac{(Q^2 - m_e^2)^{3/2}}{3\pi^2} \nu m_N \sim 9 \times 10^6 \text{ g/cm}^3 . \tag{3.124}$$

Neutronization ultimately brings the white dwarf sequence to an end at a density of $\approx 10^9$ g/cm^3 by robbing the star of its supporting electron pressure. For neutron stars, neutronization has only a minor effect, altering the preferred nuclear species in the crust from ordinary nuclei to neutron rich nuclei [80].

At higher density,

$$\epsilon_{\text{drip}} \approx 4 \times 10^{11} \text{ g/cm}^3 , \tag{3.125}$$

which is above the highest found in white dwarfs, but still low compared to the central density of neutron stars, another threshold is reached—neutron drip. The most weakly bound neutrons drip out of nuclei, and a gas of neutrons and electrons occupies the interstices in equilibrium with the nuclei [80].

At still much higher density, above the saturation density of nuclear matter (3.22)

$$\epsilon_0 = 2.51 \times 10^{14} \text{ g/cm}^3 , \tag{3.126}$$

nuclei disassemble into a uniform charge-neutral mixture of baryons and leptons. This is the superdense regime, and with reference to neutron stars, is what we refer to as *neutron star matter.* We mean by this phrase that nuclear matter is in its lowest energy state at each density under the constraint of charge neutrality. Superdense matter contains as many baryon species at each density as is required for equilibrium so that no particle transformations by beta decay or otherwise will take place. Hyperons—baryons with one or two strange quarks—form an important part of the population of superdense matter. In later chapters we discuss these developments in our understanding of neutron star interiors, paying special attention to hyperon stars in Chapter 5. Superdense matter, besides being rich in baryon species, may even be composed of the baryon constituents—quarks—at high enough density. Therefore we devote chapters to quark and hybrid stars.

The "low-density" domain, below nuclear density, is not the subject of this book. But neutron stars span a density range from ordinary iron at the surface to superdense matter in the core. The crust region—the outer shell of a kilometer or less—is composed of ever more neutron-rich partially ionized to totally ionized atoms with greater depth in the crust. The ionized atoms are arranged on a Coulomb lattice in a gas of electrons. Above the drip density, neutrons also occupy the interstices between atoms as a diffuse gas. To compute stellar properties, even when dominated by the superdense regime, we must have an equation of state

[19]For the estimate of the neutronization density we have taken the baryon electron ratio ν as 2 and m_N, the typical energy of a nucleon in a nucleus, as 930 MeV.

from the highest density down to the surface density. Therefore we make use of the extensive studies of the "low-density" regime discussed briefly below.

3.10.2 Low-density equation of state

A number of authors have contributed to the calculation of the equation of state for cold catalyzed matter in various density domains below nuclear saturation: Feynman–Metropolis–Teller from 15 to 10^4 g/cm^3, Chandrasekhar upwards to 10^7 g/cm^3, Harrison–Wheeler–Wakano to 10^{12} g/cm^3, Bonche–Negele–Vautherin to 10^{13} g/cm^3. The compendium of results cited above are sometimes referred to as the HW equation of state [28].

Another compendium involving detailed calculation at subnuclear densities can be found in the work by Bethe–Baym–Pethick–Sutherland–Siemens [80, 82, 83], often referred to as the BPS equation of state. Both of these works, as remarked earlier, describe matter in its cold catalyzed state, that is, in the absolute ground state of charge-neutral hadronic matter. For both, the pressure becomes zero at the density of iron, the most bound state of low density matter. The low-density equations of state are tabulated at the end of the chapter.

Both equations of state, the HW or BPS, are suitable for the description of the envelope of neutron stars, which are the product of progenitor stars sufficiently massive as to have sustained nuclear burning to the iron end point. Because zero pressure establishes the edge of a star, the surface of a neutron star is iron. A cold degenerate star has no atmosphere in the sense of the various gases that make up the Earth's atmosphere.

The equation of state corresponding to cold catalyzed matter is not the best description of white dwarf material which is the product of stars whose burning

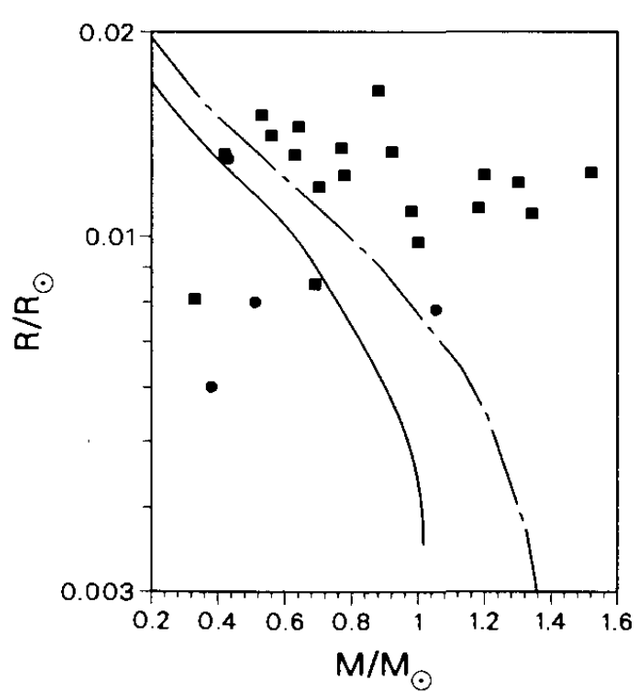

FIGURE 3.10. White dwarf radii and masses compared to the star sequence of the BPS equation of state (solid curve) representing equilibrium matter at each density. Also for carbon white dwarfs (dashed curve). ($R_\odot \approx 7 \times 10^5$ km.)

stops at helium, carbon, or oxygen. As such, dwarfs do not belong to a single sequence of stars having the same equation of state. This is perhaps the inference to be drawn from Fig. 3.10 which shows radii and masses of observed white dwarfs [60] and shows a curve corresponding to the BPS equation of state representing matter in its ground state at each density. Also shown is a sequence of carbon white dwarfs which we discuss in the next section and which was qualitatively described above. The BPS equation of state yields a white dwarf mass limit of $\sim 1M_\odot$ while a C white dwarf (closer to an accurate description of a real dwarf) has a limit $\sim 1.4M_\odot$ (see Fig. 3.9).

Except in certain instances, the mass and radius "measurements" shown in Fig. 3.10 are highly model-dependent. Gravitational redshift measurements establish a relationship between mass and radius for a given star. The radius of a white dwarf is generally inferred from its luminosity and models of the stellar atmosphere, which presumably give a rough estimate but not likely an accurate one. Therefore both mass and radius depend on the atmospheric model.

3.10.3 Carbon and oxygen white dwarfs

White dwarfs constitute the final form into which stars of a few solar masses evolve. Mass loss occurs during their evolution. Because of their low mass, thermonuclear reactions do not burn through to iron, but terminate at lighter nuclei, helium, carbon, or oxygen. An equation of state corresponding to fully catalyzed matter is therefore not quite an accurate description. Here we do a simple calculation of the equation of state of dwarfs that consist of a single nuclear species. More accurate calculations for such white dwarfs were done many years ago by Hamada and Salpeter [79].

Except at the very lowest densities of dwarfs, atoms are compressed to the point that nuclei are fully ionized. Therefore, to lowest approximation, we consider a fully ionized nuclear species immersed in a background of uniform density electrons. The positively charged nuclei will arrange themselves into a lattice with the nuclei at the lattice sites so as to minimize the Coulomb energy. We approximate this situation in the way suggested by Wigner and Seitz, that is, by considering a sphere surrounding each nucleus and touching the neighboring spheres. Each sphere containing a nucleus and its electrons will be neutral. To a good approximation there is no interaction between spheres. We consider one of them.

Most of the mass is contributed by the nuclei, whereas most of the pressure by the electrons (Section 3.9.4). The energy in each sphere consists of the nuclear mass, the electron mass and kinetic energy, the energy of Coulomb repulsion among the electrons, and the attractive Coulomb energy between the electron sea and the nuclei.

The Coulomb energy needed to assemble the electrons into the cell of radius R is a familiar calculation. We need to integrate the interaction between the charge

within the radius r and the charge in a shell at r of thickness dr,

$$E_{\text{self}} = e^2 \int_0^R \frac{1}{r}\left(\frac{4\pi r^3}{3}\rho_e\right) \cdot \left(4\pi r^2\, dr\, \rho_e\right) = \frac{3}{5}\frac{(Ze)^2}{R}\,, \tag{3.127}$$

where the electron number density is given by

$$Z = V\rho_e\,, \qquad V = \frac{4\pi}{3}R^3\,, \tag{3.128}$$

with Z the atomic number of the nucleus and therefore the electron number per cell. The electron gas will have an attractive interaction with the nucleus at the center of the cell,

$$E_{\text{int}} = -\int \frac{1}{r}(Ze)(4\pi r^2\, dr\, e\rho_e) = -\frac{3}{2}\frac{(Ze)^2}{R}\,. \tag{3.129}$$

Adding these we get the lattice energy

$$E_{\text{lat}} = -\frac{9}{10}\frac{(Ze)^2}{R}\,. \tag{3.130}$$

Eliminating R from the expression in favor of V, we have the lattice contribution to the pressure,

$$p_{\text{lat}} = -\frac{\partial E_{\text{lat}}}{\partial V} = -\frac{3}{10}\left(\frac{4\pi}{3}\right)^{1/3} Z^{2/3}\, e^2 \rho_e^{4/3}\,. \tag{3.131}$$

To compute the equation of state in the present approximation for a pure nuclear species, we may choose a baryon density ρ for which case the cell radius R is given by the solution of

$$A = \frac{4}{3}\pi R^3 \rho\,, \tag{3.132}$$

where A is the atomic number of the nuclear species (total nucleon number) and Z its proton number. For such a chosen density ρ, the electron density is $\rho_e = (Z/A)\rho$. We treat the free electrons as a degenerate Fermi gas with maximum wave number

$$k_e = (3\pi^2\rho_e)^{1/3} = \left(3\pi^2\frac{Z}{A}\rho\right)^{1/3}, \tag{3.133}$$

and we denote the corresponding energy density and pressure by $\epsilon_e(k_e)$ and $p_e(k_e)$, respectively. We can compute these from (3.74, 3.90, 3.92) as the numerics dictate. The mass of the nuclei we take from experiment. These masses are measured typically as atomic masses, so we subtract the electron rest masses, but we ignore their atomic bindings. The energy density is $\epsilon = E_{\text{total}}/V$ with the volume $V = A/\rho$. So the energy density and pressure are

$$\begin{aligned} \epsilon(\rho) &= \frac{\rho}{A}\left(M(A,Z) - Zm_e - \frac{9}{10}\frac{(Ze)^2}{R}\right) + \epsilon_e(k_e)\,, \\ p(\rho) &= p_e(k_e) - \frac{3}{10}\left(\frac{4\pi}{3}\right)^{1/3} Z^{2/3} e^2 \rho_e^{4/3}\,. \end{aligned} \tag{3.134}$$

In the above, $M(A, Z)$ denotes the atomic mass. For example,

$$M(^4\text{He}) = 4.00260326U, \quad M(^{12}\text{C}) = 12U,$$
$$M(^{16}\text{O}) = 15.99491502U, \quad U = 931.504\,\text{MeV}. \tag{3.135}$$

where U is called the atomic mass unit, chosen (arbitrarily) so that C^{12} is the standard. This is of no interest except when employing accurate mass tables.

The above equation of state cannot be valid above the density at which high-energy electrons are captured by protons in the nuclei. We have already discussed how the white dwarf sequences are terminated by a decrease of the supporting electron pressure because of inverse beta decay. To account for this process, one should evaluate the difference in energies (3.134) between a medium composed of either the nuclear species (A,Z), (A−1,Z−1),..., (A,Z−1),... to find which is the lower and at what density.

To estimate the lower density range at which the approximation of fully ionized nuclei is valid, we may compare the Bohr radius of the inner orbit of the atomic species we have in mind with the cell radius which depends on the nucleon density, as in the relationship written above between A and the volume of the cell. For simplicity, let $2Z \approx A$, which is exact in the case of He, C, and O stars. The two radii are

$$r_Z = \frac{r_{\text{Bohr}}}{Z} = \frac{\hbar^2}{m_e Z e^2}, \quad R = \left(\frac{3Z}{2\pi\rho}\right)^{1/3}. \tag{3.136}$$

The first is large compared to the second for baryon densities that satisfy

$$\rho > \frac{3Z^4}{2\pi}\frac{1}{r_{\text{Bohr}}^3} \tag{3.137}$$

or energy densities

$$\epsilon > \rho U = 5.4Z^4\ \text{g/cm}^3. \tag{3.138}$$

The computed range for which the fully ionized nuclei occupy Coulomb lattice sites holds for He, C, O, and Mg white dwarfs. Figure 3.10 shows the mass–radius relationship for carbon white dwarfs for an equation of state as computed in the manner described above. We note that the mass limits for the BPS and C equations of state are, respectively $\sim 1M_\odot$ and $\sim 1.4M_\odot$, which illustrates the composition dependence of white dwarfs.

The data on mass and radius of observed white dwarfs lies mostly to the right of the region where the two different types of dwarf sequences lie. Two types of measurements are shown. The circles show measurements from binaries (giving M) combined with redshift measurements (giving M/R) and are rather accurate. The squares are probably much less certain. Again, they involve the redshift measurement, but the other independent determination, this time of radius, is obtained through the less certain chain involving color and flux, distances as measured by parallax, and model atmospheres [60, 84].

There appear to be problems of two kinds in the comparison with theory. To begin, we note that the two curves should rather accurately bracket the theoretical

expectations for cold dwarfs. The BPS curve corresponds to an equation of state consisting of a Coulomb lattice of varying nuclear species, depending on density, embedded in an electron gas. The nuclear species and the arrangement in a lattice represents the lowest energy state of electrically neutral matter matter in the white dwarf domain. Such an equation of state should yield a sequence of dwarfs more compacted than can be realized in nature given the evolution of the progenitors that produce white dwarfs. The carbon equation of state represents a lattice of carbon nuclei with free electrons. It is appropriate to a white dwarf produced before the endpoint of nucleosynthesis is reached in the evolution of its progenitor.

As remarked earlier, essentially the same result for the equation of state is obtained for pure He and O stars as for C. The reason is simply that the result can be thought of as that of a polytrope with an electron to nucleon fraction of 1/2, and with the polytropic index changing continuously from the nonrelativistic value (5/3) to relativistic (4/3) from low to high density. So the equations of state differ only in the small lattice energy, and pressure in going from He to O. The import of this note is that all cold white dwarfs should lie in the band between the two curves of Fig. 3.10. They clearly do not. As discussed, mass measurements for most white dwarfs are not directly made as for binaries, but depend strongly on model-dependent inferences about the radii. Because the equation of state is derived in a physically dependable regime, the inferred mass or radius determinations or both are most likely inaccurate.

3.11 Temperature and Neutron Star Surface

The temperature of neutron stars falls below 1 MeV in 20 seconds so that we may consider them as cold on the nuclear scale [35]. However, close to the surface where the density is low, say below the neutron drip density (3.125) and still closer to the surface than this, temperature becomes important, at least as a matter of principle. In practice, the mass, radius and other such bulk properties can be accurately computed as if the star is cold, and this is the assumption made in the computation of the high-density equation of state (justifiably) and also for low densities as in the work of Baym et al. and of Harrison and Wheeler [76, 80].

On the other hand, for such matters as cooling and phenomena associated with the magnetosphere, the zero temperature assumption for the surface layer becomes questionable. We have already noted that because a neutron star is made from the processed material of a massive star at the endpoint of its evolution, the most bound nucleus Fe^{56} will be the dominant species at its surface. What is the nature of iron on and near the surface? We have noted that neutron stars are born with temperatures of about 10^{11} K and cool quickly to have surface temperatures of 10^8 K in a month and 10^6 K in less than a million years. The melting point of metallic iron at zero pressure is about 1,200 K and the boiling point is about 2,500 K. Certainly ordinary iron atoms cannot exist on the surface.

Let us define the surface region as that extending outward from the point where the density corresponds to the neutron drip density. At that density, the space available to each ion is far smaller than the size of atoms, as we compute shortly. Atoms are completely ionized. We will show that the lattice energy (3.130) is far larger than the thermal energy kT, so the lattice is secure against melting. However, close to the surface, where the density is lower, ionization by pressure becomes less important than thermal ionization. On the surface itself, simple estimates are impossible.

We make some crude estimates of conditions at several densities based on the preceding section by calculating the energy of a Coulomb lattice of iron *nuclei* (not atoms). First we consider matter at a depth within the star where the density is so high that atoms are fully ionized because there is insufficient room for atoms. Earlier we referred to the neutron drip density (page 110). It is a density occurring typically less than a kilometer from the surface, where some of the neutrons drip out of ionized atomic nuclei and join electrons as an interstitial gas. The energy density is given by (3.125). The corresponding baryon number density is

$$\rho_{\text{drip}} \approx 2.4 \times 10^{-4}\ \text{fm}^{-3}\,, \tag{3.139}$$

obtained by dividing the energy density by the nucleon mass in grams. In the previous section we assumed that ionized atoms will form a Coulomb lattice. Here we want to compare the energy of the lattice with the thermal energy. From (3.136) we find the cell size corresponding to a Coulomb lattice of ${}_{26}\text{Fe}^{56}$ (actually approximated as an $A = 2Z$ nucleus for convenience)

$$R = \left(\frac{3 \times 26}{2\pi \times 2.4 \times 10^{-4}}\right)^{1/3} \text{fm} = 37\ \text{fm}\,. \tag{3.140}$$

We now use this to calculate the lattice energy of fully ionized iron.

$$E_{\text{lat}} = \frac{9}{10}\frac{(26)^2 \times 1.44\ \text{MeV fm}}{37\ \text{fm}} = 24\ \text{MeV}\,. \tag{3.141}$$

Because 10^{10} K $\approx$ 1 MeV, the temperature of the star expressed in MeV after a month is 10^{-2} MeV and in a million years 10^{-4} MeV. So the Coulomb lattice at the depth of the drip density is not disturbed by the temperature; neither is it disturbed at greater depth where a Coulomb lattice can exist to the density at which nuclei dissolve into their constituents.

Let us now enquire to what smaller density and lattice energy the temperature can also be ignored. To do this, let us find the density at which each nucleus is allotted a volume corresponding to the lowest Bohr orbit of iron. At that density the atoms must be fully ionized by virtue of the high *density*. Then compare the lattice energy with temperature. The Bohr radius for the lowest electron in iron is

$$r_Z = \frac{\hbar^2}{m_e Z e^2} = \frac{(\hbar c)^2}{m_e c^2 \cdot Z e^2} = 2 \times 10^3\ \text{fm}\,. \tag{3.142}$$

Find the density at which the cell radius R equals r_Z. It is

$$\rho_Z = \frac{3Z}{2\pi r_Z^3} = 2 \times 10^{-9}\ \mathrm{fm}^{-3}\,. \tag{3.143}$$

The corresponding energy density (obtained by multiplying by the nucleon mass) is

$$\epsilon_Z = 3.4 \times 10^6\ \mathrm{g/cm}^3\,. \tag{3.144}$$

The corresponding lattice energy is

$$E_{\mathrm{Lat}} = -\frac{9}{10}\frac{(Ze)^2}{r_Z} = 0.1\ \mathrm{MeV}\,. \tag{3.145}$$

This is large compared to the temperature, either after a month and certainly after a million years. So, fully ionized iron nuclei can exist in a Coulomb lattice at densities in the crust even as low as ρ_Z, which is five orders of magnitude lower than the drip density. Down to this density, and possibly lower, the cold approximation is still good.

Nearer the surface of the star, where atoms are not crushed, we have to consider the ionization energy. The binding of an electron in the lowest Bohr orbit in iron is

$$B = \frac{Ze^2}{2r_Z} = 1 \times 10^{-2}\ \mathrm{MeV}\,. \tag{3.146}$$

The total ionization energy must be less than $Z = 26$ times this or less than 0.3 MeV. This statement, however, is too vague to proceed. We use a well known approximation to the Thomas–Fermi binding energy of electrons in an atom [85, 86]. It is

$$B = 1.4 \times 10^{-5} Z^{2.39} = 3.4 \times 10^{-2}\ \mathrm{MeV}\,. \tag{3.147}$$

This is not small compared to the temperature after a million years so atoms will not be fully ionized by heat at the surface. Will they form a Coulomb lattice as they did at higher densities? Is the lattice energy of partially thermally ionized iron atoms sufficiently large compared to surface temperature to sustain a lattice?

The above questions cannot be answered by the means we have used. Both temperature and density (pressure) will influence the degree of ionization and the solidity or melting of the lattice. The lattice energy will be much smaller than the values computed above for the inner crust because the cell size, R, will be larger and the charge, Z', on the ion smaller than Z. Lattice melting is related to the ratio of lattice to thermal energy $\Gamma \equiv E_{\mathrm{lat}}/T$.[20] However, it is not really known what value of Γ would correspond to the melting point.

Temperature and pressure are so much greater near the surface and into the crust of a compact star than are attainable in the laboratory. So is the degree of ionization for atoms under immense pressure as compared to free atoms. The problem is one

[20] Γ is estimated as $\sim$ 170 MeV in Ref. [87].

of atomic structure under conditions not attainable by laboratory experiment. We do not attempt such an estimate here. Instead we note that in a cold star with mass $1.5M_\odot$ and radius 10 km, the distance from the surface to the radius at which cold matter is fully ionized (3.144) is 76 cm. We conclude that the molten surface of a hot star is very thin and consists of fully ionized atoms.

3.12 Stellar Sequences from White Dwarfs to Neutron Stars

An approximate overall picture of the relative densities of white dwarfs and neutron stars is shown in Fig. 3.9, where the mass as a function of the central density is plotted. The BPS equation of state is used for white dwarfs up to the central density just above normal nuclear density marked as ϵ_0. The equations of state for He, C, or O white dwarfs or any mixture of these elements would each yield a somewhat different sequence with maximum masses as high as $1.4M_\odot$. As explained earlier, white dwarfs do not correspond to a single sequence because of the individuality conferred on them by the particular evolution of their progenitors (page 91).

White dwarfs become unstable above the Chandrasekhar mass because the chemical potential of the increasingly relativistic electrons rises along the sequence of increasing central density to the point where electron capture by protons (inverse beta decay) yields an energetically more favorable composition. Loss of electron pressure terminates the stable sequence of white dwarfs. This occurs at a central density of about 10^9 g/cm^3 in the case of the BPS equation of state and about 6×10^{10} g/cm^3 for C dwarfs.

Stability is not regained along the sequence until, with increasing density, the pressure of degenerate neutrons provides sufficient support against gravity, initiating the stable neutron star sequence. This sequence begins at densities slightly lower than the density of symmetric nuclear matter.

The distributions of mass–energy in two white dwarfs of the BPS sequence are shown in Fig. 3.11, one near the mass limit of the BPS equation of state, the other a very light dwarf. The decrease of radius of the star with increasing mass—characteristic of degenerate gravitationally bound objects—is apparent, as is the very flat energy profile in the stellar interior.

Two extreme neutron star sequences are shown in Fig. 3.9. The sequence with maximum mass $\sim 3.2M_\odot$ corresponds to a choice of equation of state that maximizes the limiting mass subject only to very general constraints on the equation of state —the causal limit equation of state. It will be discussed in connection with an upper bound on neutron star masses (Section 3.17) and is a very stiff equation of state. The other sequence with lower limiting mass corresponds to the soft equation of state developed earlier in this chapter, an ideal gas of neutrons, protons, and electrons that is charge-neutral and in beta equilibrium. Because the Fermi pressure, in this case, is the only agent of resistance to compression, a *lower bound* on the maximum mass limit of neutron stars is $\sim 0.7M_\odot$.

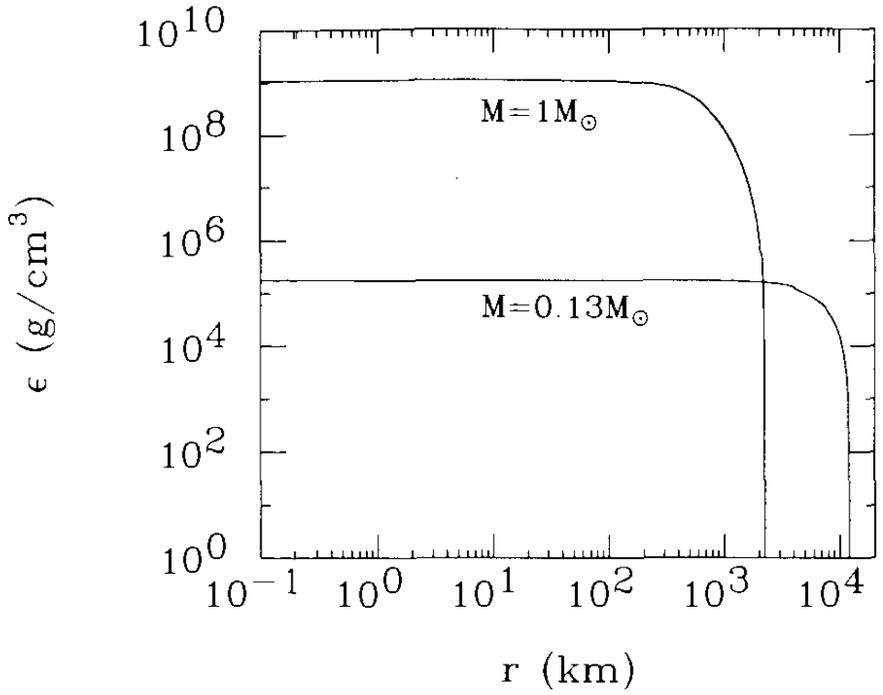

FIGURE 3.11. Mass–energy distribution in two white dwarfs of the BPS equation of state. [88]

Nuclear forces with their short-range repulsion will stiffen the equation of state and increase the limiting mass. Nuclei are bound by the attraction of the nuclear force and have a saturation density that is nearly the same in all nuclei because of the short-range repulsion. In contrast, neutron stars are bound by gravity, and the density is so high that the average nucleon experiences a net repulsion from its interaction with others. Indeed the energy required to compress nucleons to the density found in the cores of neutron stars is 200–300 MeV per nucleon (cf. Fig. 4.3); the nuclear force reduces the binding of neutron stars. In Chapter 5, we will study sequences of neutron stars corresponding to equations of state which respect certain key nuclear properties.

The distribution of mass–energy in the limiting mass neutron stars of these two extreme sequences are shown in Fig. 3.12. The ideal gas stars near the limiting mass have central densities higher by almost a factor of three than those of the stiff equation of state. They also are much more compacted because of their soft equation of state. The profiles of realistic models generally fall between these extremes. In any case, the envelope of the star, comprising densities less than nuclear, is thin—less than 2 km for the star made of matter with limiting softness, and a fraction of a kilometer for the star of limiting stiffness. Lighter stars in each sequence, those with lower central densities, have larger radii and the envelope is thicker (cf. Fig. 5.10).

3.13 Baryon Number of a Star

It is particularly obvious how theorem (2.156) can be applied to a static star to find its baryon number and its binding energy compared to the energy of the dispersed

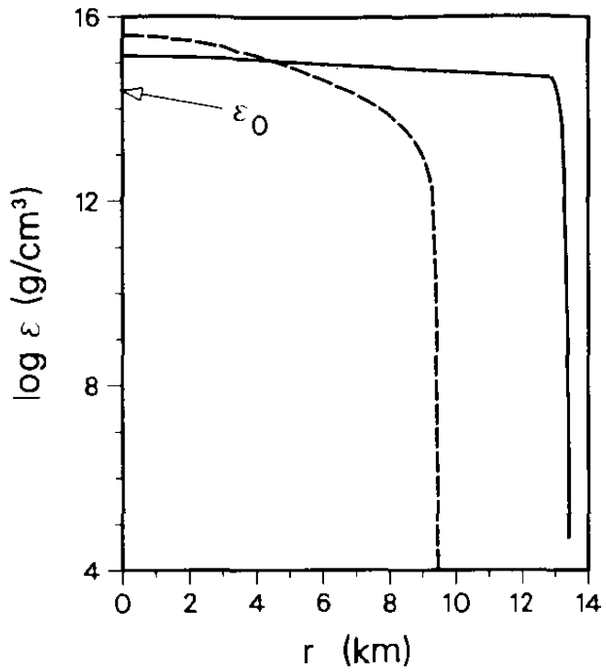

FIGURE 3.12. Mass–energy distribution in the maximum mass neutron stars of the two sequences of Fig. 3.9.

baryons. Let j^μ denote the conserved baryon number current.[21] It is related to the proper baryon number density, ρ in a local inertial frame of a fluid element of the star at r by

$$j^\mu(r) = u^\mu \rho(r) = e^{-\nu(r)}\rho(r)\delta^\mu_0 \tag{3.148}$$

where, as in (2.207), u^μ is the fluid four-velocity. In Section 2.6.4 we learned that $\sqrt{-g}\, d^4x$ is the invariant volume element. For the Schwarzschild metric we have

$$\sqrt{-g} = e^{\nu(r)+\lambda(r)} r^2 \sin\theta\,. \tag{3.149}$$

Using (2.156) we obtain for the total baryon number of the star

$$A = 4\pi \int_0^R e^{\lambda(r)} r^2 \rho(r)\, dr = 4\pi \int_0^R \left(1 - \frac{2M(r)}{r}\right)^{-1/2} r^2 \rho(r)\, dr\,. \tag{3.150}$$

From whatever theory that provided the equation of state, we know $\rho(r)$ for any $p(r)$ or $\epsilon(r)$. We can therefore integrate the above equation concurrent with the Oppenheimer–Volkoff equations. Thus, the total number of baryons in a star can be computed.

Later we shall be interested in a description of neutron stars in which not only the neutron and proton are present, but also higher-mass baryons. This is likely to be the case in the dense interior where the neutron chemical potential may exceed the masses of other baryons, such as the Λ. We will encounter this in Chapter 5. The *proper density*[22] of each species in the stellar model at a point r can be found by reference to the particle composition of the calculated equation of state associated

[21] See Section 4.3 for more on conserved currents.

[22] Proper density is used to denote the density in a local inertial frame at the specified point in the gravitational field.

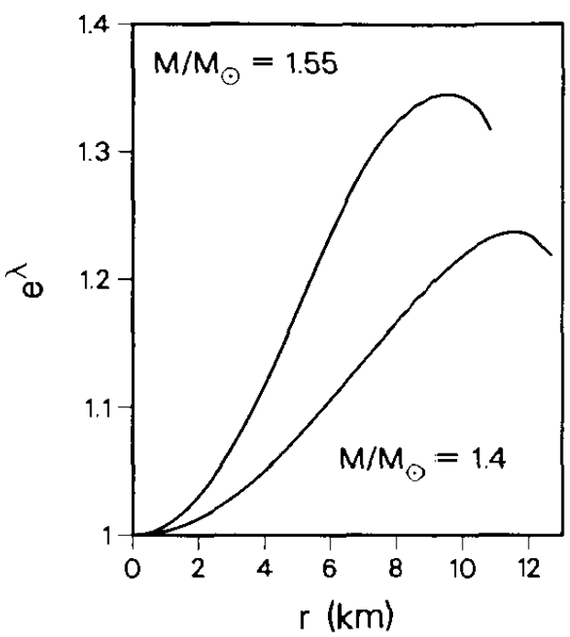

FIGURE 3.13. Metric function interior to neutron stars of two masses. The larger is at the mass limit. See Chapter 5 for details. (K=240 MeV, $m^* = 0.78m$, $x_\sigma = 0.6$).

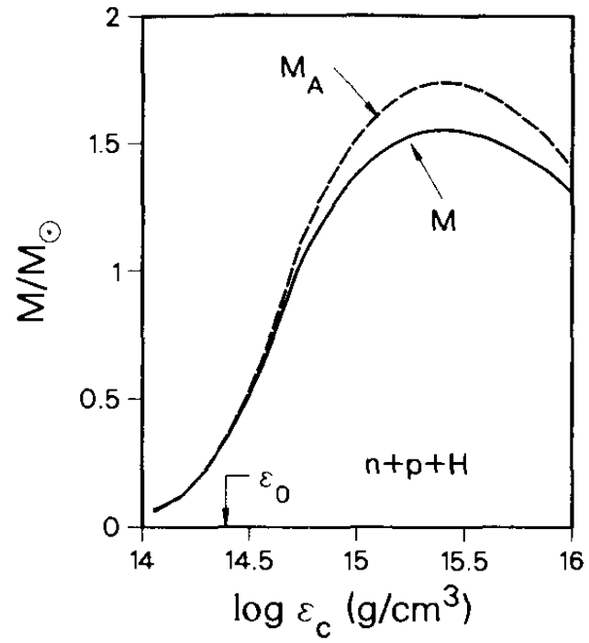

FIGURE 3.14. For the same case as Fig. 3.13, the gravitational mass M is compared with the mass of the corresponding number of neutrons dispersed at rest to infinity M_A.

with the energy density or pressure for that point. The total number in the star of any such baryon type is given by a formula analogous to the one above, with ρ replaced by the number density of the baryon of interest. Fig. 3.13 shows an example of the metric function $e^{\lambda(r)} = \sqrt{-g_{11}(r)}$ that appears in the integral above.

3.14 Binding Energy of a Neutron Star

Because we are able to compute the baryon number, as above, we can compute the mass of the equivalent numbers of neutrons dispersed at rest at infinity,

$$M_A = Am_n \,. \tag{3.151}$$

The mass M_A is sometimes called the *baryon mass* of the star. In Fig. 3.14 we compare the gravitational masses with the baryon masses. By reading the mass difference from the graph at the limiting mass star and its baryon number from Fig. 3.2, one can find that the binding per neutron is about 100 MeV. This compares with our classical estimate of 160 MeV from (3.23), which actually is the classical gravitational energy. The latter refers only to the gravitational attraction and does not include the work required to overcome the Fermi pressure and the resistance to compression of high-density matter. The difference $M - M_A$, which is the binding energy of the neutron star, contains all such effects and is the net energy gained by assembling the A nucleons from infinity to form an equilibrium neutron star.

The binding energy is the energy released when the core of an evolved star of 10 or more solar masses collapses. About one percent actually appears as the kinetic energy of the supernova explosion in which the neutron star is formed. Ninety-nine

percent is carried off by neutrinos in the first few seconds following birth of the neutron star, and a small fraction of one percent appears as light in the supernova remnant.

The baryon mass is usually less than the gravitational mass and always less for configurations near the limiting mass. However, less massive neutron stars have a larger mass than that of all the individual baryons dispersed to infinity. This fact is shown in Fig. 3.15 where the binding energy per nucleon, $B/A = (M_A - M)/A$, is plotted. These stars have even higher gravitational mass as compared to the mass of the equivalent baryon number disassembled in the form of iron nuclei at infinity. Nevertheless, even in the case in which a star is not bound with respect to a simultaneous removal of all constituents to infinity, it is bound with respect to removal of single nucleons (or groups of nucleons, but not all nucleons). The reason for this is the long-range attraction of all the remaining nucleons in the star. From page 84 the energy of a nucleon in the star is $m(1 - 2M/R)^{1/2} =$ const, which is less than m. Thus, Oppenheimer–Volkoff stars will not spontaneously disassemble even if not bound in the sense that $M > M_A$. Such neutron stars are metastable with an essentially infinite barrier for disintegration.

It may be relevant to observe that there may exist no creation mechanism for low-mass neutron stars having small or negative binding, even though they are stable in the sense discussed above. They must evade collapse to a black hole. However, the neutrinos carry almost all the binding energy, and because of their weak interaction with nucleons, transmit very little to the infalling material of the defunct star. Thus a low binding energy may fail to eject the ten or more solar masses of the original star, and there is no chance to do so at all if B/A is negative. A large release of binding energy, only a small part of which can be transmitted to the infalling material because of the weak interaction of neutrinos that carry the energy, is required to eject most of the progenitor star and evade the formation of a black hole. This observation may account for the apparent absence of low-mass neutron stars (say less than $1 M_\odot$). It is also likely that stellar cores do not collapse until a Chandrasekhar mass of degenerate material is evolved.

3.15 Star of Uniform Density

In general the equations of stellar structure have to be integrated numerically for realistic equations of state. However there is one analytic case of particular interest because it provides a limiting value of M/R that coincides with the absolute limit for any static star satisfying the Oppenheimer–Volkoff equations. A rigorous analysis yields the result

$$\frac{2M}{R} < \frac{8}{9}, \tag{3.152}$$

independent of the equation of state. It depends only on the structure of the relativistic equations for hydrostatic equilibrium and was obtained by Buchdahl [89, 19].

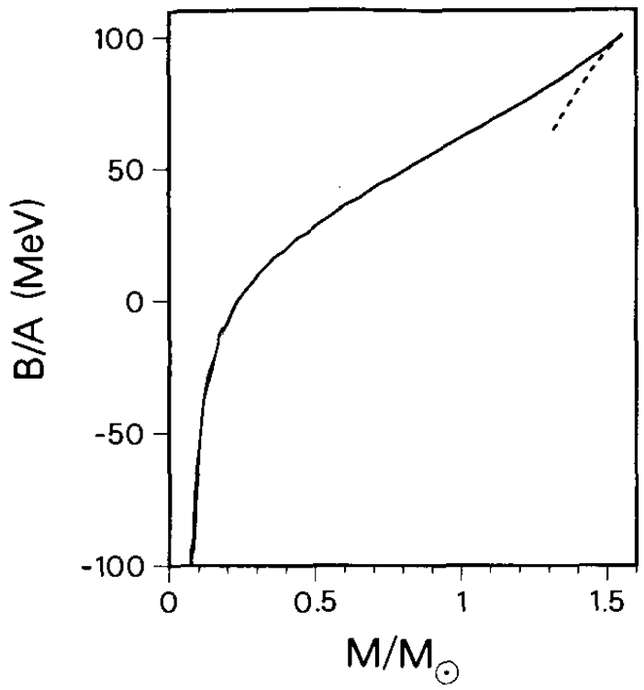

FIGURE 3.15. Binding energy per baryon of a neutron star sequence. The dashed line represents the unstable configurations with central densities higher than that of the limiting mass star. Note the negative binding for stars with $M < 0.2M_\odot$. Calculational details are in Chapter 5. Same case as in Fig. 3.13.

Not surprisingly, the special case that yields the same limit is a star of uniform energy density. The matter of such a star is obviously hypothetical and unphysical because it must be incompressible to maintain a constant density. On the other hand, the idealization is interesting because the energy distribution in neutron stars near their maximum mass limit is rather uniform, though certainly not constant, as we shall see later when treating realistic equations of state. But most importantly, the idealization illustrates that, even in the hypothetical case of incompressible matter, there is a limit on the maximum possible mass of a stable, compact, relativistic configuration. This interesting and instructive idealization was proposed and solved by K. Schwarzschild (see ref. [90]).

For a star of uniform energy density, say ϵ_0, we have from (2.211)

$$M(r) = \frac{4\pi}{3}\epsilon_0 r^3 ,$$
$$M = \frac{4\pi}{3}\epsilon_0 R^3 . \tag{3.153}$$

The equation for hydrostatic equilibrium (2.224) now reads

$$\frac{dp}{dr} = -\frac{4\pi r}{3}\frac{\big(p(r)+\epsilon_0\big)\big(3p(r)+\epsilon_0\big)}{1-8\pi\epsilon_0 r/3} . \tag{3.154}$$

Although the energy density (by the hypothesis of incompressibility) is constant, the pressure varies throughout the star, and the central value is larger, the larger the stellar radius (and therefore the larger the mass of the object). Rearrange the

above equation as

$$-\int_r^R \frac{dp}{(p+\epsilon_0)(3p+\epsilon_0)} = \frac{4\pi}{3}\int_r^R \frac{r\,dr}{1-8\pi\epsilon_0 r^2/3}\,. \tag{3.155}$$

Integrate and remember that the edge of the star is defined by $p(R) = 0$. We easily find

$$\frac{p(r)+\epsilon_0}{3p(r)+\epsilon_0} = \sqrt{\frac{1-2M/R}{1-2Mr^2/R^3}}\,. \tag{3.156}$$

Solve for the pressure,

$$p(r) = \epsilon_0\left[\frac{\sqrt{1-2M/R}-\sqrt{1-2Mr^2/R^3}}{\sqrt{1-2Mr^2/R^3}-3\sqrt{1-2M/R}}\right]. \tag{3.157}$$

The central pressure of the star p_c can be obtained now by setting $r = 0$. Solve the resulting equation (3.156) for $2M/R$:

$$\frac{2M}{R} = 1-\left(\frac{p_c+\epsilon_0}{3p_c+\epsilon_0}\right)^2. \tag{3.158}$$

The larger the radius of a uniform density star, the more massive it is, and the higher the central pressure must be to support this mass. Take the limit of large p_c, but short of infinity. We find

$$\frac{2M}{R} < 1-\left(\frac{1}{3}\right)^2 = \frac{8}{9}\,, \tag{3.159}$$

independent of ϵ_0. As we noted previously, the above relationship gives the absolute limit of M/R for any static star.

We can easily compute the corresponding radius and mass for the uniform density model. From (3.153) we obtain

$$\frac{4\pi}{3}\epsilon_0 = \frac{M}{R^3} = \frac{M}{R}\frac{1}{R^2}\,, \tag{3.160}$$

from which there follows

$$R_{\rm lim} = (3\pi\epsilon_0)^{-1/2}\,,$$
$$M_{\rm lim} = \frac{4}{9}R_{\rm lim}\,. \tag{3.161}$$

The above is the limiting mass for stars made of incompressible matter whose energy density is ϵ_0. Others in the sequence have smaller mass, radius, and lower central pressure. The existence of such a limit is intrinsic to the Reneral Theory of Relativity, as discussed in Section 2.9.6, and is absent from Newtonian theory.

It is also of interest to note a more stringent condition on $2M/R$. If matter is such that $p < \epsilon$ (believed to be the case), then (3.158) yields

$$\frac{2M}{R} < \frac{3}{4}\,. \tag{3.162}$$

The opposite situation $p > \epsilon$ is referred to as ultrabaric matter. Because the energy density of baryonic matter at low pressure is dominated by the rest mass of the baryons, we know that any realistic equation of state must be in the domain $p < \epsilon$ at low pressure (at zero pressure there remains the mass of the baryons). The causality condition that a signal cannot propagate faster that the speed of light requires of the equation of state that $dp/d\epsilon < 1$ [91]. If an equation of state satisfies this condition, it cannot cross into the ultrabaric region. However, whereas the 8/9 limit can be shown to depend only on the structure of the Oppenheimer–Volkoff equations and the finiteness of the pressure, the above limit of 3/4 is derived explicitly for a uniform density star. It is therefore not as secure as the 8/9 limit. However, it lies very close to a limit of 0.78 obtained by Bondi [92] under the reasonable assumptions concerning the equation of state: $\epsilon > 0$, $p > 0$, and $dp/d\epsilon < 1$.

3.16 Scaling Solution of the OV Equations

For certain simple equations of state which are of interest to us in several different contexts, the Oppenheimer–Volkoff equations have scaling solutions [93, 94]. To explain what is meant by this, consider the equation of state

$$p = s(\epsilon - a)\,, \tag{3.163}$$

where s and a are constants. This equation of state obviously describes matter that is bound at the energy density a because the pressure is zero at that point. Now note that the Oppenheimer–Volkoff equations

$$\begin{aligned} \frac{dp}{dr} &= -\frac{\left[p(r)+\epsilon(r)\right]\left[M(r)+4\pi r^3 p(r)\right]}{r\left[r-2M(r)\right]}\,, \\ dM(r) &= 4\pi r^2 \epsilon(r)\,dr\,, \end{aligned} \tag{3.164}$$

have the same form in the scaled variables,

$$\overline{p} = p/a, \quad \overline{\epsilon} = \epsilon/a, \quad \overline{r} = \sqrt{a}\,r, \quad \overline{M} = \sqrt{a}\,M\,. \tag{3.165}$$

Therefore, if the above equations are solved for the sequence of stars corresponding to the equation of state with some particular value of a (and s), then the sequence for any other value of the parameter a can be found (for the same s) simply by scaling:

$$R(a') = \sqrt{\frac{a}{a'}}\,R(a), \quad M(a') = \sqrt{\frac{a}{a'}}\,M(a), \quad \epsilon_c(a') = \frac{a'}{a}\,\epsilon_c(a)\,, \tag{3.166}$$

where, as usual, ϵ_c denotes the central density of the star. Note that if one wants sequences with different $s = dp/d\epsilon$, one must solve the Oppenheimer–Volkoff equations for the desired s, and all other sequences with different a can be found immediately by scaling.

We shall be interested in rotating stars. The Kepler frequency is of interest in this connection. The Kepler frequency expresses the balance of centrifugal and

gravitational forces on a particle on the equatorial plane at the surface of the star. The condition in classical physics is simply

$$\frac{Mm}{R^2} = m\Omega^2 R\,, \tag{3.167}$$

or

$$\Omega_c = \sqrt{\frac{M}{R^3}} \quad \text{(Newton)}\,, \tag{3.168}$$

which is the Newtonian expression for the Kepler angular velocity. This equation need not hold in General Relativity, but as it turns out, it holds to very good accuracy if the right side is multiplied by the factor $\zeta = 0.65$ [95, 96]. From the above scaling law we can also write for the *Kepler* angular velocity

$$\Omega_K(a') = \sqrt{\frac{a'}{a}}\,\Omega_K(a)\,. \tag{3.169}$$

3.17 Bound on Maximum Mass of Neutron Stars

The Rev. John Michell explained to the Royal Society (London) in 1783 that if stars should exist whose light could not reach us (black holes), nonetheless, their presence may be revealed by their gravitational effect on luminous companion stars [72]. This is precisely how one attempts to identify black holes in the few solar mass range. There are a few such candidates [97]–[99]. However, it is necessary to be able to distinguish between a black hole candidate and a neutron star that would also be invisible to us unless its pulsed radiation was directed toward us once each rotation. The invisible member of the Hulse–Taylor neutron star binary is an example of a star whose presence was detected solely because of the doppler shift it produces in the timing of pulses from its pulsar companion. In this case, the mass of the invisible star can be determined very accurately from the orbital motion of the pulsar and it is very nearly the same as the pulsar's mass. But if it were above the limit possible for a neutron star, it would be a black hole candidate. The problem and the direction of its solution were recognized by Zwicky [100] and Ruffini [101]–[105].

In the General Theory of Relativity a maximum mass star with central density a few times nuclear density exists above which mass there are no stable configurations, no matter what the equation of state. We have seen that even if matter were to become incompressible at a certain density, a maximum mass still would exist (Section 3.15). If a compact star, unseen except by its gravitational effects on a luminous companion star, is detected and its mass is inferred to be greater than the limiting mass of neutron stars, then the alternative appears to be that it is a black hole. To place such an identification on the firmest ground, the theoretical limiting neutron star mass must be established in a manner that does not depend sensitively on any details of the equation of state; for we do not know it with confidence above nuclear density.

Rhoades and Ruffini attempted to obtain a limit free of any but very general and accepted assumptions. They were: (1) The equations of stellar structure that follow from General Relativity are valid. (2) Matter is stable against local spontaneous expansion or contraction from equilibrium, (Le Chatelier's principle). The principle can be expressed in terms of the equation of state as $dp/d\epsilon \geq 0$ (the pressure must rise as the density or at least remain constant as in the mixed phase of a first-order phase transition in a single-component substance). (3) Disturbances propagate with speed $\sqrt{dp/d\epsilon} < 1$ (referred to as the causal constraint). (4) The high-density equation of state satisfying the above constraints matches continuously to a low-density equation of state that ultimately describes ordinary matter.

For the maximum mass star, the energy profile, as a function of distance from the center, falls very rapidly to zero at the edge of the star, and very little mass is contained in the thin envelope of low-density matter. So the dependence on a specific choice for the low-density domain is weak.

It is fairly obvious (and will become abundantly clear in our later studies) that the stiffer the equation of state (meaning the more rapidly the pressure rises as a function of density) the greater the limiting mass. A high-density equation of state that is at its causal limit will support a greater limiting mass than softer ones. Any density range of matter $\epsilon_1 < \epsilon < \epsilon_2$ for which $dp/d\epsilon$ vanishes is excluded from a star because the Oppenheimer–Volkoff equations inform us that the pressure is a monotonically decreasing function of the distance from the center. This is a well-known property of the atmosphere of the Earth. The pressure of matter at any radius must support the matter above it against the gravitational attraction of all that lies within. Therefore a constant pressure region in the equation of state contributes nothing to stellar masses. The matter described by such a region, usually a mixed phase, is totally absent from a star. The equation of state at higher density $\epsilon > \epsilon_2$ beyond such a constant pressure region is obviously softer than one that increases with density at ϵ_1. So for the purpose of obtaining an upper bound on the maximum mass, we may consider only equations of state that increase monotonically with density.

Accordingly, let us adopt the BPS equation of state for the low-density domain and match it continuously in density and pressure to an equation of state that is at the causal limit. Let the matching point be denoted by a subscript "f". Then the energy density and pressure given by

$$\begin{aligned} \epsilon(\rho) &= \tfrac{1}{2}\left[\epsilon_f - p_f + (\epsilon_f + p_f)\left(\frac{\rho}{\rho_f}\right)^2\right] \\ p(\rho) &= \epsilon(\rho) - \epsilon_f + p_f, \qquad \rho \geq \rho_f\,, \end{aligned} \tag{3.170}$$

obey the thermodynamic relationship $p = \rho^2 \partial(\epsilon/\rho)/\partial\rho$. This equation of state is obviously at the causal limit $dp/d\epsilon = 1$, and it is equal to $(\epsilon_f,\ p_f)$ at ρ_f.

There remains the choice of matching density below which a specific equation of state is chosen, in this case BPS. There will be some sensitivity to this choice,

and we need to explore it. Let us write the above causal limit equation of state as

$$p = \epsilon - a, \qquad a \equiv \epsilon_f - p_f \,. \tag{3.171}$$

Now recall that the Oppenheimer–Volkoff equations have scaling solutions for such an equation of state (Section 3.16). If the above causal limit equation of state held for all densities, there would be perfect scaling, that is, when the Oppenheimer–Volkoff equations were solved for a particular a and the mass and radius of any star in the sequence, with central density $\epsilon_c(a)$ determined, the corresponding values for any other a would be given by (3.166).

However, because we use the causal limit equation of state only for $\rho > \rho_f$, there is a thin envelope of matter with $\rho < \rho_f$ overlying the major part of the star. This envelope does not obey the scaling rule, but it contributes little in mass or radius, and this statement will be more accurate the smaller ρ_f. On the other hand, the equation of state is certainly not at the causal limit at densities as low as the saturation density of nuclear matter $\rho_0 = 0.153\ \mathrm{fm}^{-3}$ or, equivalently, $\epsilon_0 \approx 2.5\ 10^{14}\mathrm{g/cm}^3$ because the energy per nucleon has a minimum at saturation density in symmetric matter, and even pure neutron matter reflects attraction near saturation density (cf. Fig. 4.3). So the matching density ought to be chosen larger than saturation density ρ_0.

By numerical integration of the Oppenheimer–Volkoff equations using as a matching density one of the grid points in the tabulation of BPS, $\rho_f = 0.2715\ \mathrm{fm}^{-3}$ (which corresponds to $\epsilon_f = 4.636\ 10^{14}\ \mathrm{g/cm}^3 = 3.442\ 10^{-4}\ \mathrm{km}^{-2}$ and $p_f = 6.103\ 10^{33}\ \mathrm{dyne/cm}^2 = 5.041\ 10^{-6}\ \mathrm{km}^{-2}$), we find for the *limiting* mass star

$$M = 3.14 M_\odot, \qquad R = 13.4\ \mathrm{km} \quad \text{(causal limit)}\,. \tag{3.172}$$

From the above numbers it is clear that in the vicinity of saturation density the energy density dominates over the pressure by two orders of magnitude so that to good approximation a is just the energy density at the matching point. More accurately,

$$a = 3.392\ 10^{-4}\ \mathrm{km}^{-2} = 4.569\ 10^{14}\ \mathrm{g/cm}^3\,.$$

So,

$$R(a') = 13.4\sqrt{\frac{4.569\ 10^{14}\ \mathrm{g/cm}^3}{a'}}\ \mathrm{km}\,,$$

$$M(a') = 3.14\sqrt{\frac{4.569\ 10^{14}\ \mathrm{g/cm}^3}{a'}}\ M_\odot\,. \tag{3.173}$$

If we were to choose the saturation density as matching density (as remarked above it would be hard to justify such a small value), we would obtain $4.3 M_\odot$ for the theoretical upper bound of a neutron star mass. It is safe to conclude that neutron stars cannot have masses that exceed this value and probably cannot exceed the first estimate of $3.14 M_\odot$. With the addition of any other constraints in the form of a realistic equation of state, the bound can only become smaller.

We conclude that the Rhoades–Ruffini bound on the maximum possible mass of a neutron star is a good one. Any compact object of mass greater than $\sim 3 M_\odot$

cannot be a neutron star unless it is rotating at or very near its Kepler frequency (the frequency at which the centrifugal force is balanced by the gravitational force at the equator); in that case the mass limit could be increased by 10 to 20% [106, 107].

For the purpose of identifying black hole candidates, it should be emphasized that the estimate of an upper bound on the mass limit must be conservative. On the other hand, we are also interested in neutron stars themselves in which case we should incorporate as much knowledge or physically motivated theoretical consideration as possible. These can only lower the bound. So actual neutron stars are likely to have masses that are less than the bound derived above, perhaps considerably less. We will study this question in the context of realistic constraints on the equation of state in Chapter 5.

One final note to this discussion. The line $p = \epsilon$ is often referred to as the causal limit, particularly in figures showing equations of state in the $p - \epsilon$ plane. This terminology suggests that equations of state below this line are all causal. This is not so. In (3.171) we see an example that lies below $p = \epsilon$ but is itself at the causal limit $dp/d\epsilon = 1$. What is true is that an equation of state that is at any point below $p = \epsilon$ cannot cross into the region above without having slope greater than unity, becoming therefore acausal. For these reasons, the region above $p = \epsilon$ is better referred to as ultrabaric, meaning simply $p > \epsilon$. Because cold, low-density matter, say iron, has mass but no internal pressure under normal conditions, it lies below the ultrabaric line, and, because causal equations of state (in the sense taken here) cannot cross this line, it is likely that $p < \epsilon$ holds in general.

3.18 Stability

Solutions of the Oppenheimer–Volkoff equations correspond to stellar configurations that are in hydrostatic equilibrium. That is clear from the derivation of the equations, as was pointed out in Section 3.5. Equilibrium does not assure stability however. Equilibrium configurations may correspond either to a maximum or to a minimum in the energy with respect to radial compression or dilation. Figure 3.16 illustrates that for a certain range in baryon number of the star, there are at least two equilibrium solutions, one at higher energy and central density than the other. In this section we discuss how to determine whether an *equilibrium* configuration is actually *stable*.

A continuum of equilibrium configurations is shown in Fig. 3.6 which correspond to an equation of state that is smooth and satisfies the condition of *microscopic* stability of matter $dp/d\rho > 0$ (Le Chatelier's principle in its strong form, i.e., without the equality). Two regions along the continuum of compact stars are stable [28]. These are the white dwarf and neutron star regions. There is a broad range extending over many orders of magnitude in central density and in stellar sizes between these two families for which there are no stable stars.

Stars in the unstable region between white dwarfs and neutron stars are subject to vibrational modes that will either cause their disassembly or else their collapse

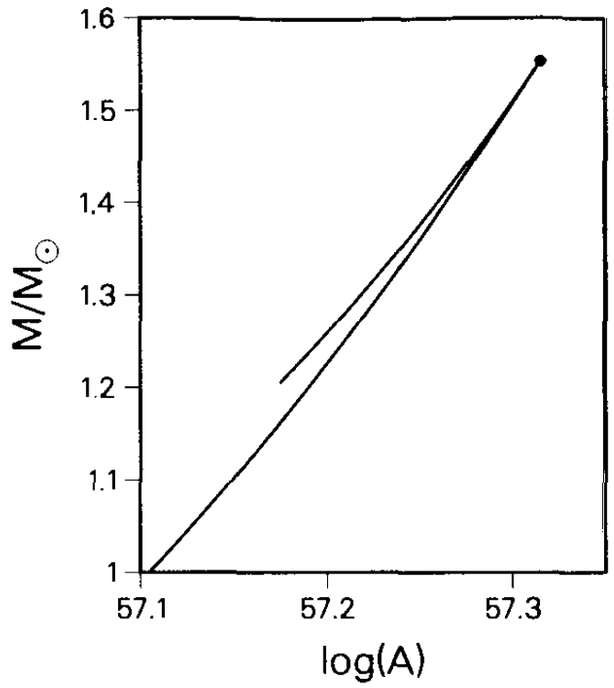

FIGURE 3.16. Mass of neutron stars as a function of baryon number A. Central density increases from low A up to the dot, which is the limiting mass of the stable neutron stars. Central density further increases along the upper curve toward lower values of A. The upper curve corresponds to stars with central densities beyond that of the star at the mass limit. The lower curve represents stable stars.

to neutron stars. Indeed, some neutron stars are believed to have been formed by accretion induced collapse of a white dwarf. At densities below the white dwarf region, there is a long region of instability for cold objects until one reaches other stable bodies, such as brown dwarfs and planets. However, above the stable neutron star sequence, there are no additional regions of stability if the equation of state is of polytropic form, or more generally if it is sufficiently smooth. The physical reasons for this are discussed in Section 3.19. We discuss the necessary and sufficient condition for stability in the next two sections.

3.18.1 Necessary condition for stability

We will prove that along the sequence of equilibrium configurations of the Oppenheimer–Volkoff equations, perfect fluid stars can pass from stability to instability with respect to any radial mode of oscillation only at a value of the central density at which the equilibrium mass is stationary,

$$\frac{\partial M(\epsilon_c)}{\partial \epsilon_c} = 0 . \tag{3.174}$$

This is a key result in the discussion of stability. Moreover, the baryon number of an equilibrium star is stationary at the same central densities as the mass [28]. The proof of the last statement follows from (3.43), which we write as

$$\frac{\partial M}{\partial A} = \mu_{\mathrm{Fe}}\left(1 - \frac{2M}{R}\right)^{1/2} . \tag{3.175}$$

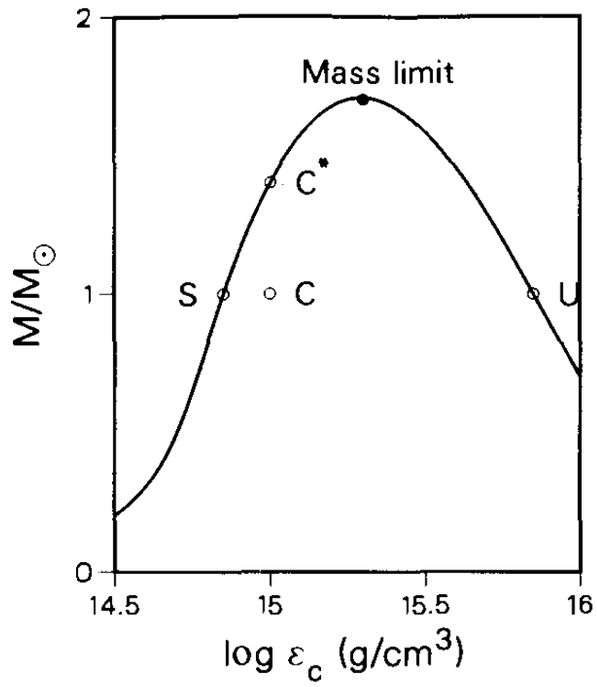

FIGURE 3.17. Schematic of solution of the Oppenheimer–Volkoff equations in a region of increasing and decreasing mass as function of central density. Hydrostatically stable configurations have positive slope so the stable region ends at "Mass limit". See the discussion in the text.

This can be rewritten as

$$\mu_{\rm Fe}\left(1-\frac{2M}{R}\right)^{1/2}\frac{\partial A}{\partial \epsilon_c}=\frac{\partial M}{\partial \epsilon_c}\,, \tag{3.176}$$

which proves the point.

We now give an heuristic proof of (3.174) which at the same time will provide a *necessary* but not sufficient condition for stability of stars along the sequence of equilibrium configurations.

Refer to Fig. 3.17 for a depiction of a sequence of stars in the vicinity of a maximum. Suppose an equilibrium solution S is perturbed so that the central density ϵ_c is increased; the star is displaced to C (compressed). The equilibrium star with this new central density lies in mass at C*. The star at C therefore has a deficit of mass with respect to the equilibrium configuration, a deficit such that gravity underbalances the increased central pressure corresponding to the increased density at C, as compared to the equilibrium configuration of the star of this mass that lies at S. The gravitational force acting on the matter of the star will therefore act to return it toward S. A similar argument shows that, if the star at S undergoes a perturbation that decreases its central density, the force acting on the matter of the star will act to return it to S.

Going through a similar analysis of the star U on the decreasing curve of M vs. ϵ_c, we arrive straightforwardly at the conclusion that, if U is either compressed or decompressed by a radial perturbation, the force acting on the perturbed star will act to drive it further from U, that is to say, equilibrium configurations must satisfy

$$\frac{\partial M(\epsilon_c)}{\partial \epsilon_c} > 0 \quad \text{(necessary condition for stability).} \tag{3.177}$$

This is a necessary but not sufficient condition for stability.

Thus we have proven that the passage from stability to instability along a sequence of equilibrium configurations occur only at the turning points (3.174). Incidentally, Fig. 3.16 shows that the number of baryons in a star, A, reaches its turning point at the maximum mass star, as proven above, and that stars with central density higher than that of the limiting mass star have higher mass than those of the same A on the lower branch. We shall refer to the results proven above—the coincidence of the turning point of both mass and baryon number and the change of stability of a mode of oscillation at each turning point—as the "turning points theorem".

We now apply the necessary condition for stability to polytropes. Recall that the mass given by (3.113) is an increasing function of ϵ_c for $\gamma > 4/3$, is stationary at $\gamma = 4/3$, and is a decreasing function for $\gamma < 4/3$. So a necessary condition for the stability of polytropes is

$$\gamma > 4/3 \quad \text{(necessary condition for stability of polytropes)}. \tag{3.178}$$

The maximum in the mass is known as the mass limit, or limiting mass. White dwarf and neutron star sequences both have a limiting mass, but for different reasons that were discussed in Section 3.9.7.

3.18.2 Normal modes of vibration: Sufficient condition for stability

The only astronomically interesting objects are those that are not only in hydrostatic equilibrium, but are also stable against radial oscillations. Stars can vibrate, or ring, like most objects if perturbed. The vibration may grow or be damped exponentially. To determine which, we solve for the eigenfrequencies of the normal radial modes of vibration. (Any other vibrations can be analyzed in terms of the normal modes.) We refer to the various methods described by Bardeen, Thorne, and Meltzer [108].

For the metric of a spherically symmetric star (2.183), the adiabatic motion of the star is expressed in terms of an amplitude $u_n(r)$ of normal modes of vibration by $\delta r(r,t) = e^{\nu} u_n(r) e^{i\omega_n t}/r^2$ which denotes small perturbations in r. Here n is a mode index with $n = 0$ being the fundamental or nodeless mode. The quantities ω_n are the star's oscillatory eigenfrequencies. We want to find these eigen-frequencies for each central density, that is, for each equilibrium configuration of the stellar sequence under discussion.

The eigenequation for $u_n(r)$ which governs the nth normal mode—first derived by Chandrasekhar [74]—has the Sturm–Liouville form

$$\frac{d}{dr}\left(\Pi \frac{du_n}{dr}\right) + \left(Q + \omega_n^2 W\right) u_n = 0\,, \tag{3.179}$$

where the functions

$$\Pi = e^{(\lambda+3\nu)} r^{-2} \Gamma p \quad ,$$

$$
\begin{aligned}
Q &= -4e^{(\lambda+3\nu)}r^{-3}\frac{dp}{dr} - 8\pi e^{3(\lambda+\nu)}r^{-2}p(\epsilon+p)\,, \\
&\quad +e^{(\lambda+3\nu)}r^{-2}(\epsilon+p)^{-1}\left(\frac{dp}{dr}\right)^2\,, \\
W &= e^{(3\lambda+\nu)}r^{-2}(\epsilon+p)\,, \\
\Gamma &= \frac{d\ln p}{d\ln\rho} = \frac{(\epsilon+p)}{p}\frac{dp}{d\epsilon}
\end{aligned}
\tag{3.180}
$$

are expressed in terms of the equilibrium configuration of the star. [Note that the last equality follows from (3.73)]. The quantities ϵ, p, and dp/dr denote the energy density, the pressure, and pressure gradient as measured by a local observer. They are obtained from the Oppenheimer–Volkoff equations. The symbol Γ denotes the varying adiabatic index at constant entropy. The boundary conditions are $u_n \sim r^3$ at the star's origin and $du_n/dr = 0$ at the star's surface. The second of these assures that the Lagrangian change[23] in the pressure at the surface is zero. Solving the eigenvalue equation leads to the frequency spectrum ω_n^2 ($n = 0, 1, 2, \ldots$) of the normal radial modes.

A characteristic feature the Sturm-Liouville equation is that the squared eigenfrequencies ω_n^2 form an infinite discrete sequence, $\omega_0^2 < \omega_1^2 < \omega_2^2 < \cdots$. If any of these is negative for a particular star, the frequency is purely imaginary and therefore any perturbation of the star will grow exponentially in amplitude of oscillation as $e^{|\omega|t}$. Such stars are unstable.

As a consequence of the ordering of the eigenfrequencies and the fact that one mode of oscillation changes in stability at every stationary point (3.174) we may infer the following. If the fundamental mode ($n = 0$) becomes unstable at the maximum neutron star mass, and it does, then at the next minimum in the sequence, either stability is restored to the fundamental mode or the next ($n = 1$) mode becomes unstable, and so on.

The changes in density that arise because of the radial vibrations may produce changes in the local particle populations. We have seen how the neutron to proton fraction varies with density in the ideal gas model in earlier sections of this chapter. In a more realistic model of dense matter, additional baryon species will be populated, or changes in the phase of matter may occur at specific densities such as quark deconfinement as discussed in Chapters 5 and 9, respectively. Such local changes might be thought to prevent, or at least complicate, the determination of the points in a stellar sequence for which a change between stability and instability occurs. However, this is not so. The period of vibration becomes infinitely long ($2\pi/\omega$) at the points where changes in stability occur ($\omega = 0$). Therefore the location of such points does not depend on the reaction rates.

[23]The Lagrangian perturbation follows moving fluid elements in the perturbed and unperturbed configurations that correspond to one another. In contrast, Eulerian perturbations refer to changes at fixed points in space.

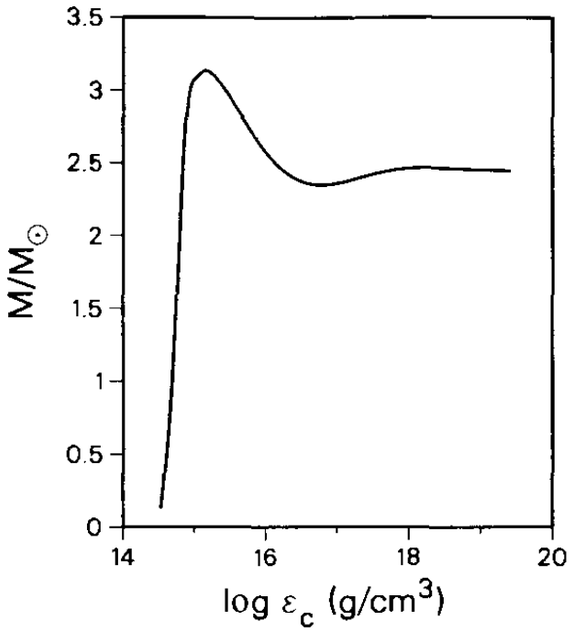

FIGURE 3.18. Stellar sequence corresponding to the causal equation of state of Section 3.17. The first segment with positive slope represent the stable neutron stars. The second is the first in a denumerable infinity of unstable configurations.

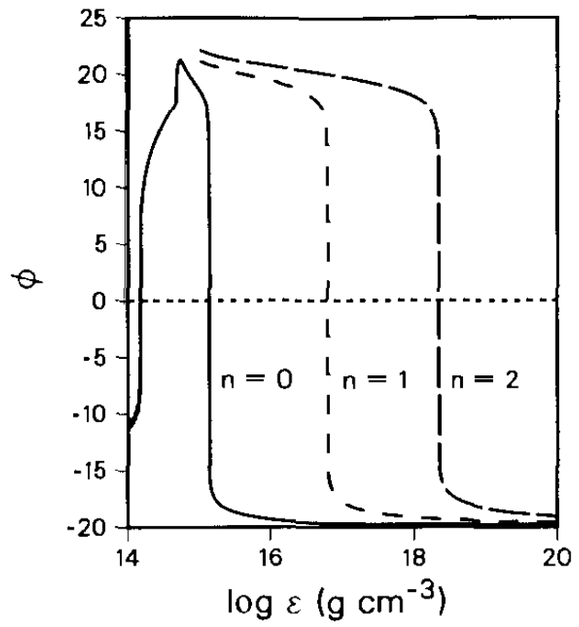

FIGURE 3.19. Stability analysis showing a function ϕ which has the sign of ω^2 as a function of central density along the sequence of stars of the causal-limit equation of state. (I am indebted to Ch. Kettner for this calculation.)

3.19 Beyond the Maximum-Mass Neutron Star

Can superdense stars above the density found in neutron stars exist? The general belief is, or has been, that there are no stable configurations beyond the stable neutron stars [28]. The Oppenheimer–Volkoff equations provide the equilibrium configuration at each central density corresponding to an equation of state of cold matter. There are two density ranges for which these configurations are known to be stable. White dwarfs form a stable sequence. They are stabilized by the pressure of degenerate electrons. Neutron stars form a second stable sequence at higher density. They are stabilized by the nucleon Fermi pressure and by the repulsion between nucleons at short range.

Wheeler and collaborators [28] demonstrated that for a *polytropic* equation of state there are a denumerable infinity of stellar sequences that satisfy the necessary condition for stability $dM/d\epsilon_c > 0$, but that beyond the limiting neutron star in density, all configurations are unstable to vibrational modes. Here we show that even the equation of state corresponding to the causal limit of Section 3.17 satisfies the *conditional* theorem of Wheeler et. al.

Figure 3.18 illustrates two segments of the sequence corresponding to the causal-limit equation of state for which the slope is positive. The first segment represents the stable neutron stars. The second is the first in the infinity of segments that satisfy the necessary condition for stability but nonetheless are unstable. That all configurations above the limiting neutron star in density are unstable is shown in Fig.

3.19.[24] The squared frequency of the fundamental (nodeless $n = 0$) mode becomes negative at about 10^9 g/cm^3 which terminates the stability of white dwarf configurations. The fundamental mode becomes stable again at $\sim 1.5 \times 10^{14}$ g/cm^3, ushering in the stable neutron stars. The same mode becomes unstable at the limiting mass neutron star and remains unstable for all higher central densities. At each succeeding turning point in the mass as a function of central density, whether maximum or minimum, an additional vibrational mode becomes unstable, as illustrated for the $n = 1$ and $n = 2$ modes in Fig. 3.19. This is in accord with the "turning points theorem" stated on page 132.

For those of the sequence shown in Fig. 3.18 with positive slopes that lie higher in central density than the stable neutron star sequence, the energy profile increases so steeply as the center of the star is approached that the star is unstable to radial vibrations. As the amplitude of a radial perturbation grows, the lowest (nodeless) mode may bring the central part of the star within its critical Schwarzschild radius when the amplitude of the vibration is sufficiently high. The core collapses, and then the rest of the star, with nothing to support it, follows. If this does not happen first, then in the outward motion of the vibration, the star may disassemble, or explode. One or the other is the fate of stars more dense than neutron stars if the equation of state is sufficiently smooth, as it might well be.

A comparison is made in Fig. 3.20 between the mass–energy distribution of a stable neutron star at the Oppenheimer–Volkoff limit and that of the unstable star at the next maximum. The remarkably steep energy distribution in the second case is responsible for the instability described above and characterizes the distribution in all stellar configurations above the Oppenheimer–Volkoff limit for neutron stars for most equations of state.

Could there exist in nature additional stable regions of dense stars beyond neutron stars? What else is there to stabilize a higher density sequence than the generic neutron star? If the quark constituents of baryons are deconfined as predicted by the theory of the strong interaction (QCD and its property of asymptotic freedom [109]), then baryon Fermi pressure is simply *replaced* (not supplemented) by the Fermi pressure of quarks. No apparent new agent for stabilization occurs as a consequence of deconfinement. Indeed, deconfinement will soften the equation of state by the loss of the short-range repulsive interaction between nucleons and by the sharing of nucleon Fermi pressure among three low-mass quark Fermi seas. Generally deconfinement is expected to terminate the neutron star sequence when quarks are deconfined from a sufficiently large amount of hadronic matter.

Nevertheless, it is at least theoretically possible that a branch with higher density than normal neutron stars could exist. It may happen that, because of a phase transition, the equation of state is not sufficiently smooth as to obey the conditional theorem of Wheeler et al. referred to above. Then there could exist non–identical twins of the same mass but different internal constitution than the canonical neutron

[24]The function ϕ plotted in Fig. 3.19 has the sign of ω^2 and is defined by $\phi = \mathrm{sgn}(a)\,\log[1 + |a|]$ where $a \equiv (\omega_n/\mathrm{s}^{-1})^2$.

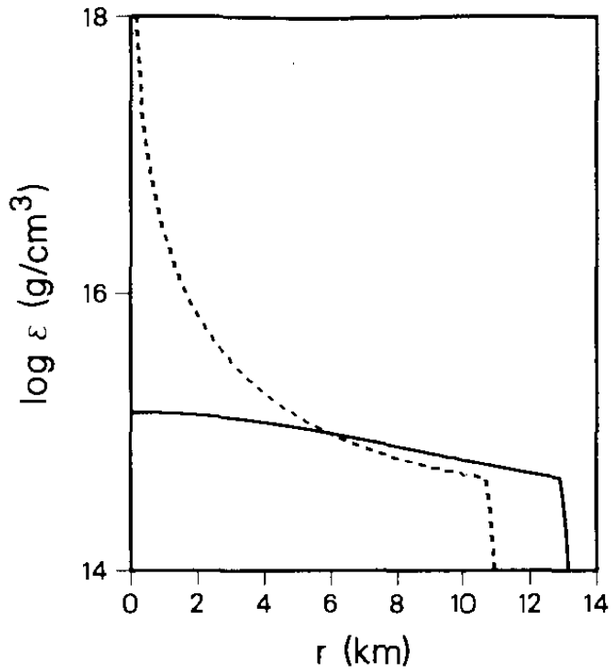

FIGURE 3.20. Mass–energy distribution of the stars at the two maxima of Fig. 3.18. Solid line refers to the first maximum.

stars [110]. We will explore the possible existence, in principle, of a third sequence of stable compact stars in Section 11.3.

3.20 Black Holes

"If there should really exist in nature any bodies, whose ... light could not arrive at us ... we could have no information from sight; yet, if any other luminous bodies should happen to revolve about them we might ... infer the existence of the central ones."
Rev. John Michell in a letter to Henry Cavendish, May 26, 1783 [72]

3.20.1 Interior and exterior regions

So far as is known, the Rev. John Michell, a philosopher and scientist of some repute in his day, was the first person to conceive of a star from which light could not escape. He reasoned that gravity should act on light as it does on mass. According to his understanding, stars might exist for which light would not have the escape velocity. We now know that the velocity of light is a constant; it is the energy (frequency) of light that is diminished in its flight from a star. Indeed, as we analyze the region of spacetime in and around black holes in this section, we will find, as shown in Fig. 3.21, that light cannot even travel in an outward direction, after it is inside a black hole. Nevertheless, Michell's conception was prescient. And as for the condition for confinement of light, consider the condition for the escape of a material body of mass m and velocity v from a star of mass M and

radius R,

$$\tfrac{1}{2}mv^2 > \frac{GmM}{R}\,. \tag{3.181}$$

Letting $v \to c$ and using gravitational units, we find that the critical radius is $R = 2M$, which is the Schwarzschild radius!

Now let us turn again to General Relativity. We have seen that Schwarzschild's solution to Einstein's equations in the region outside a static spherical star becomes singular at

$$r = r_S \equiv 2M\,. \tag{3.182}$$

If the star is enclosed by the Schwarzschild radius, it is a black hole. The spherically symmetric field described by Schwarzschild is that of a nonrotating black hole; it is often referred to as a Schwarzschild black hole. As we shall see in Chapter 7, the field of a rotating star is not described by the Schwarzschild solution.

The collapse of a star to a black hole was first discussed in the General Theory of Relativity by Oppenheimer and Snyder [23]. There are currently two classes of black holes of intense observational activity, objects of a few solar masses, the compact accreting partners of low-mass, X-ray binaries (LMXB) and extremely massive objects of 10^7 to $10^{10}M_\odot$ in active galactic nuclei (AGN). The latter are probably ingesting stars of the surrounding galaxy by first reducing them to an accretion disk. In both cases, the radiation detected is thought to be produced by the accreting matter as it is heated by compression and friction while it spirals toward the hole. In the case of AGNs, radiation has been detected from X rays down to the infrared and probably includes gravitational radiation, though such has never been detected. The lighter black holes in binary systems are doing the same on a smaller scale. We will discuss a third class of low-mass black holes and possible formation mechanisms in Section 11.2.

While not of primary concern to us in this book, it is nonetheless interesting to understand more fully the meaning of the singular point in the Schwarzschild metric. Therefore, we investigate the motion of a particle as it drops radially into a nonrotating black hole. Then two components of its four-velocity vanish, $u^2 = u^3 = 0$. The geodesic equation (2.85) for u^0—the equation of motion for a free particle in a gravitational field—is

$$\frac{du^0}{d\tau} = -\Gamma^0_{\alpha\beta}u^\alpha u^\beta = -2\Gamma^0_{10}u^1u^0 = -2g^{00}\Gamma_{010}u^1u^0\,. \tag{3.183}$$

We used the symmetry of $\Gamma^\lambda_{\mu\nu}$ in its lower indexes (2.86) to arrive at the factor 2. Because $g_{\mu\nu}$ is symmetric, from (2.95) we have $\Gamma_{010} = \frac{1}{2}g_{00,1}$. Hence, we obtain

$$\frac{du^0}{d\tau} = -g^{00}g_{00,1}u^1u^0\,. \tag{3.184}$$

But

$$\frac{dg_{00}}{d\tau} = \frac{dg_{00}}{dr}\frac{dr}{d\tau} = g_{00,1}u^1\,, \tag{3.185}$$

so remembering that for the special case of the Schwarzschild metric, $g^{00} = 1/g_{00}$, as found in (2.185), we arrive at

$$0 = g_{00}\frac{du^0}{d\tau} + u^0\frac{dg_{00}}{d\tau} = \frac{d}{d\tau}(g_{00}u^0) = 0\,. \tag{3.186}$$

Whence

$$g_{00}u^0 = C\,, \tag{3.187}$$

where C is a constant. Let the particle be dropped radially from rest with respect to the hole at $R > 2M$. Then $dr = d\theta = d\phi = 0$ at R and, from the formula for the invariant interval (2.198), we have $u^0(R) \equiv dt/d\tau = 1/\sqrt{g_{00}(R)}$, so that

$$C = \sqrt{g_{00}(R)} = \sqrt{1 - \frac{2M}{R}}\,. \tag{3.188}$$

From (2.53) we find

$$1 = g_{\mu\nu}u^\mu u^\nu = g_{00}(u^0)^2 + g_{11}(u^1)^2\,. \tag{3.189}$$

In the exterior region we have found $g_{00}g_{11} = -1$ from (2.198). Hence we have

$$g_{00} = C^2 - (u^1)^2\,, \tag{3.190}$$

or, using the explicit expression (2.196) for g_{00},

$$u^1 = -\left(C^2 - 1 + \frac{2M}{r}\right)^{1/2}\,, \tag{3.191}$$

where we have chosen the negative square root for the infalling particle. We now have expressions for u^0 and u^1 as functions of r. To get an expression between t and r, we use

$$\frac{dt}{dr} = \frac{dt/d\tau}{dr/d\tau} = \frac{u^0}{u^1} = -C\left(1 - \frac{2M}{r}\right)^{-1}\left(C^2 - 1 + \frac{2M}{r}\right)^{-1/2}\,. \tag{3.192}$$

We are interested in the behavior of t close to r_S. Introduce a new variable ρ defined by

$$r = 2M + \rho\,, \tag{3.193}$$

with $\rho << 2M$, and study the behavior of t for small ρ. Keep only leading terms in ρ:

$$\begin{aligned}\frac{dt}{dr} &= -C\left(1 - \frac{2M}{2M+\rho}\right)^{-1}\left(C^2 - 1 + \frac{2M}{2M+\rho}\right)^{-1/2} \\ &\approx -\frac{2M}{\rho} = -\frac{2M}{r-2M}\,.\end{aligned} \tag{3.194}$$

Integrate to obtain

$$t = -2M\ln\left(\frac{r}{2M} - 1\right) + \text{const}\,. \tag{3.195}$$

From this result we see that, as the particle approaches the Schwarzschild radius $r \to r_S \equiv 2M$, the time $t \to \infty$. An external observer at rest with respect to the star

observes that the particle takes an infinite time to reach the Schwarzschild radius. For any process taking place on the particle (including the emission of light), the time to do so will appear to an exterior stationary observer to approach infinity as the particle approaches r_S. Light emitted from the particle will tend to be infinitely redshifted as seen by an exterior observer!

On the other hand, in a frame falling freely with the particle, we have $d\tau = dt$. So,

$$\frac{dt}{dr} = \frac{d\tau}{dr} = \frac{1}{u^1} = -\left(C^2 - 1 + \frac{2M}{r}\right)^{-1/2}. \tag{3.196}$$

As $r \to r_S$, $dt/dr \to -1/C$. An observer falling with the particle measures a finite time lapse for the particle to reach the Schwarzschild radius. Thus, there is no singularity in spacetime (the singularity being in the metric for which a transformation could be made to new coordinates with a nonsingular metric). If the Schwarzschild radius lies outside a star, it separates space into distinctly different regions. From outside $r = r_S \equiv 2M$, one cannot see a particle drop into the hole. Neither can any particle or light escape from inside the Schwarzschild radius, as we shall see shortly. The Schwarzschild radius is sometimes referred to as the Schwarzschild horizon.

An external observer is unable to obtain any signal of what might happen within the Schwarzschild radius. Only the imprint of the mass is left on the external geometry in the case of a Schwarzschild black hole. In general two other attributes of a black hole leave their imprint on the external geometry: electric charge and angular momentum. The field produced by a rotating or charged star is different from that of Schwarzschild. We discuss rotating stars in Chapter 6.

3.20.2 No statics within

To further analyze the nature of the singularity, let us define a new time coordinate due to Eddington and Finkelstein whose form is suggested by (3.195):

$$t' = t + 2M \ln\left|\frac{r}{2M} - 1\right|. \tag{3.197}$$

Under this transformation, the Schwarzschild metric has no singularity as $r \to r_S$. [The second term cancels the singularity in (3.195)]. There are other coordinate transformations as well that are nonsingular at the horizon. We see that the Schwarzschild singularity is a coordinate singularity.

We now study the behavior of null cones with vertices at different spacetime points both far from, near, and inside r_S. The null cones (or light cones) are the hypercones in four-dimensional spacetime connecting an event at the vertex of a cone to neighboring events between which a light signal can propagate. Light rays travel into the future of the vertex event on those cones opening toward $+t$. Timelike geodesics ($d\tau^2 > 0$)—the paths followed by material particles that pass through the vertex of a cone—lie within the cone. Events in the past of the vertex event lie on or inside the cone opening in the opposite direction.

It will be sufficient to study the behavior of the cones in the t-r plane, taking $d\theta = d\phi = 0$. From the Schwarzschild expression for the proper time (2.198), the equation for the future cone of events at r is

$$\left(1 - \frac{2M}{r}\right)dt^2 = \left(1 - \frac{2M}{r}\right)^{-1} dr^2 . \tag{3.198}$$

Transforming to the new time coordinate, we get

$$0 = \left(1 - \frac{2M}{r}\right)\left(\frac{dt'}{dr}\right)^2 - \frac{4M}{r}\left(1 - \frac{2M}{r}\right)\left|1 - \frac{2M}{r}\right|^{-1}\left(\frac{dt'}{dr}\right) - \left(1 + \frac{2M}{r}\right). \tag{3.199}$$

The solutions are

$$\frac{dt'}{dr} = -1 \quad \text{and} \quad \left(1 + \frac{2M}{r}\right)\Big/\left(1 - \frac{2M}{r}\right). \tag{3.200}$$

So one side of the cone (closest to the star) always has slope -1 and the other has a slope that depends on the position of the event. We can write the equation for the latter as

$$(r_0 - r_S)\,dt' = (r_0 + r_S)\,dr\,, \tag{3.201}$$

where r_0 is used to define the r coordinate at the vertex of the cone.

Far away from the Schwarzschild radius, the side of the cone that is remote from the black hole has slope $+1$. Therefore, the geodesic path of a light ray or particle that is far from the horizon can lead away or toward the black hole. These distant cones have axes parallel to the time axis or, more accurately, as the distance from the star approaches infinity they approach a parallel orientation. At event points closer to r_S, the cones tilt toward the star and have narrower opening angles. The cone with vertex at $r_0 = r_S$ has one side parallel to the t' axis and the other pointing to smaller r, always with slope -1. Therefore a particle located at r_S, or interior to it, can only fall into the hole. Light emitted from the horizon can at best either circle the hole or fall in, but cannot escape.

The future cones of particles or photons already in the hole point only inward. There is no possibility of escape nor even of remaining at a stationary distance from the origin. Within the Schwarzschild radius, there is no possibility of statics or equilibrium! A star that falls through its Schwarzschild radius continues to collapse to a singularity or at least until the Planck scale[25] at which the classical theory may be invalid. (The Planck density is about 10^{78} times the central density of the most massive neutron star.)

To summarize, distant light cones have an opening angle approaching $\pi/2$ as the distance from the black hole increases. The cones tilt toward the hole for events that

[25]Combinations of the Planck constant, the gravitational constant, and the speed of light define a Planck mass, length, and time. The first two define a density of 5×10^{93} g/cm^3. This can be compared to the central density of neutron stars $\sim 10^{15}$ g/cm^3. Therefore, quantum gravity is of no relevance to compact, *stable* stars such as neutron stars and white dwarfs.

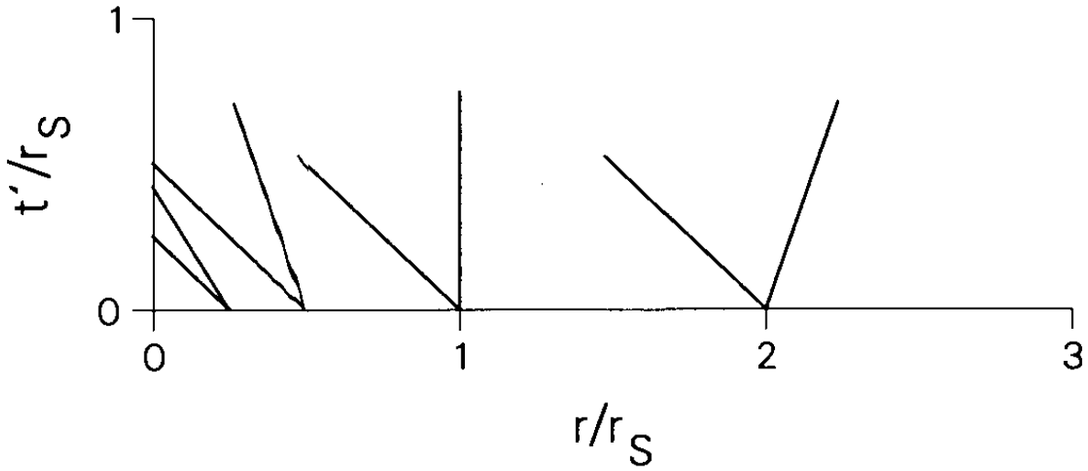

FIGURE 3.21. Future light cones at radial distances both inside and outside a black hole Schwarzschild radius $r_S \equiv 2GM$. Future points in spacetime of a material particle at the vertex of a cone can lie only within the cone; light can propagate on the cone itself.

are closer and their opening angles become smaller. Inside the Schwarzschild radius, both sides of the cone point to a smaller radius: world lines can lead only inward. A few such light cones are illustrated in Fig. 3.21. It should be noted that they are not related to each other, but simply define the future light cone for each vertex point outside the black hole.

3.20.3 Black hole densities

Black holes are usually thought to have enormous densities. This is true of some. Those formed in the collapse of the degenerate cores of evolved stars have very high densities. Indeed, collapse continues to a singularity. We have seen that, within the horizon, all matter and even light can only fall inward. Collapse to the singularity is very rapid for solar mass stars, but slow for the collapse of a black hole having the mass of a galaxy. So it makes sense to enquire about the initial density of black holes of various masses.

Schwarzschild black holes are nonrotating stars whose radius satisfies $R < 2M$. The average density satisfies

$$\rho = \frac{M}{(4\pi/3)R^3} \geq \frac{3}{32\pi M^2}, \tag{3.202}$$

where (3.152) has been employed. Referring to the section on units (3.3), this can be expressed in the more convenient form,

$$\rho \geq \frac{1.8 \times 10^{16}}{(M/M_\odot)^2}\ \mathrm{g/cm^3}. \tag{3.203}$$

The Milky Way galaxy has a mass of about $10^{12} M_\odot$. The density of a black hole formed from its collapse need only be larger than 1.8×10^{-8} g/cm^3. The radius of the horizon is 3×10^{12} km—about a third of a light year.

3.21 Problems for Chapter 3

1. Review how stars are made. Explain in your own words why stars of different mass evolve at different rates; why the final outcome is a white dwarf, neutron star or black hole; and why white dwarfs do not form a single one-parameter family of stars belonging to a unique equation of state. Why do neutron stars form a unique sequence? Write this information in a coherent interesting narrative.
2. Express the nucleon mass in grams, and divide into the Sun's mass to find the approximate number of nucleons contained in the Sun (recall Section 3.3). The Sun's binding energy is too small to be significant in this calculation.
3. On page 66 it was written that as the shock produced in the collapsing core of a star in its terminal stage moves outward, it disintegrates all nuclei in its path. Assuming as a round number that the binding energy per nucleon in a nucleus is 10 MeV, and having learned that there are several times 10^{57} nucleons in a solar mass and that the core mass is approximately the Chandrasekhar mass, show that the energy dissipation is several times 10^{51} ergs. This recall (see page 66) is the same order of magnitude as that of the kinetic energy of the material that will finally be ejected in the supernova. Thus the failure of the *prompt* bounce scenario of supernova.
4. Given the Sun's mass in grams, as in (3.10) calculate its mass expressed in gravitational units, that is, in kilometers. What is the Schwarzschild radius of the Sun?
5. On page 72 the moment of inertia of the Crab pulsar was quoted as 70 km^3. Given a uniform density object of a solar mass and 10 km radius, what is its classical moment of inertia in the above units and in g cm^2.
6. Write computer programs to calculate the equation of state for an ideal gas of neutrons, protons and electrons in a charge neutral admixture (3.80) in the ground state at whatever density (3.78). As remarked at the beginning of Section 3.9.3, the exact equations (3.74) cannot give accurate answers on a computer of finite word length when the momentum is small compared to particle mass (different for nucleon and electron) and vice versa. You will need the formulae (3.74) to compute energy density, pressure and particle number density for all three particle types. But the answers computed will be inaccurate, at different densities, for nucleons and electrons. Therefore, the *exact* algebraic expressions will have to be supplemented by the approximate expressions derived in Section 3.9.3 at high or low density. Be aware that the limits refer to k/m or its inverse so that the approximate expansions will provide more accurate computer results than the exact algebraic expressions at different *baryon* density for nucleons than electrons. Compute the equation of state from below neutron threshold density, (3.83), say, $\rho \equiv \rho_n + \rho_p = 1 \times 10^{-9}$ fm^{-3} to 10 times the density of normal nuclear matter ($\rho_0 \sim 0.15$ fm^{-3}). Compare the *exact* algebraic and the approximate numerical results. You will probably notice that the exact algebraic formula are not even computable over

certain ranges and will have to place conditions in your program to avoid overflows or underflows. Compare your final answer with Fig. 3.8.

7. Verify the expression for the pressure (3.71) by first deriving the explicit expressions (3.75) and then performing the volume derivative of the energy. This type of expression will occur frequently.
8. Make sure to understand the derivation of the equilibrium condition (3.78). Such expressions recur frequently.
9. Derive the Fermi gas expression for k_p in terms of ρ, (3.87). Confirm the limiting proton fraction in this model.
10. Derive (3.90) and (3.90).
11. Derive the low-density approximations (3.92).
12. Verify equation (3.96). Follow the logic that leads to the conclusion that the mass of a white dwarf resides principally in baryons, but it is electron pressure that supports it against collapse.
13. Verify (3.101) from the results preceding the equation and hence confirm the validity of the Newtonian approximation for white dwarfs.
14. Derive the Newtonian equation (3.103).
15. Carry out the Lane–Emden transformation of the Newtonian equation. Verify the expressions for mass and radius and their relationship. For γ precisely 4/3 what is the radius?
16. Verify that the polytrope equation of state written in Section 3.9.6 for the ultrarelativistic electron region. Write a computer program to solve the Lane–Emden equation. Verify that the solution for $\gamma = 4/3$ has a zero at the value of the argument stated in the above section. Confirm the Chandrasekhar mass (3.120).
17. Verify the mass and radius of a purely neutron star that were first obtained by Oppenheimer and Volkoff, as quoted in Section 3.9.8 by writing a computer program to solve the Oppenheimer–Volkoff equations. You will first have to compute the equation of state of pure neutron matter. Derive a table of ϵ, p, and ρ. The equations of stellar structure are of first order and can be solved by a simple difference procedure, starting at the origin, computing dp and dM at the next interval $0 + dr$, and so on. Repeat for a number of values of the central energy density and thus develop a stellar sequence of mass as a function of central density. Express the mass in units of the solar mass. If you have transformed energy density into $1/\text{km}^2$ as in (3.9), then an integration over distance in units of km will produce a mass in units of km. The solar mass is given by (3.10). Test the accuracy of the answers by repeating the calculation for several choices of step size dr.
18. Compute the lattice energy and pressure (3.131). Hence derive the equation of state (3.134) for white dwarf matter consisting of a single nuclear species A, Z plus electrons.
19. Assume the distance dr from a neutron star surface at which the energy density has risen from its surface value to $1 \cdot 10^6$ g/cm^3 is small compared to the radius R of the star. For $R = 10$ km and $M = 1.5 M_\odot$ estimate dr using (2.224) and Table 5.6. Find that $dr \approx 76$ cm.

20. Give details of the proof of (3.188) starting at the geodesic equation for u^0.

21. Prove (3.192) and its approximate form and solution (3.194) and (3.195) to see that an external observer would measure an infinite time for a freely falling particle to approach the Schwarzschild horizon.

22. Prove that in a freely falling frame, $dt/dr \longrightarrow 1/C$ as $r \longrightarrow r_S$—that an object will fall into a black hole with a finite elapse of time as measured in its own frame.

23. Derive the equations defining the slopes of the two sides of the future light cone (3.200).

24. Find the lower limit of black hole density (3.203). Confirm the numbers quoted below the formula for the critical density of the Milky Way and the Schwarzschild radius. Estimate the actual average density of the Galaxy.

4

Relativistic Nuclear Field Theory

4.1 Motivation

Matter and energy warp spacetime and in turn are shaped and moved by the curvature of spacetime. We are guaranteed by the equivalence principle that, at any spacetime point in a star, a local Lorentz frame can be erected. We found that even in a neutron star hovering on the verge of collapse to a black hole, the relative change in the metric over the average distance of baryons is exceedingly small ($\leq 10^{-19}$) (Section 3.4). This is such a small number, that even were the central density tens or hundreds of times larger than the average, the relative change in the metric over a distance spanning an enormous number of nucleons is negligible. Therefore, the extent of a local Lorentz frame[1] in a neutron star is so large on the scale of particle spacings that we may treat the matter at a given density as if it were of infinite extent and neglect the energy associated with boundaries in comparison with the bulk energy. This establishes the frame in which we may work—a Lorentz frame—and the approximation in which we may work—the bulk approximation.

From a wealth of information on nuclei we know that at nuclear density (and for some density above), nuclei and nuclear matter are composed of protons and neutrons that interact through the nuclear force mediated by the exchange of mesons. In equilibrated hadronic matter at densities several times that of normal nuclear matter, the nucleon Fermi energy will be sufficiently large that it is energetically more favorable for some nucleons to transform to heavier baryon species through

[1] Recall the discussion of Section 3.4.

TABLE 4.1. Baryon and meson states. Spin is J, isospin is I, baryon number is b, charge is q, and strangeness is s. The baryon octet comprises the baryons of spin $J = 1/2$.

	m (MeV)	J	I	b	q	s
N	939	1/2	1/2	1	0,1	0
Λ	1115	1/2	0	1	0	−1
Σ	1190	1/2	1	1	−1,0,1	−1
Ξ	1315	1/2	1/2	1	−1,0	−2
Δ	1232	3/2	3/2	1	−1,0,1,2	0
Ω	1673	3/2	0	1	−1	−3
σ	~ 800	0	0	0	0	0
ω	782	1	0	0	0	0
ρ	770	1	1	0	−1,0,1	0
π	139	0	1	0	−1,0,1	0
K^+	494	0	1/2	0	1	1
K^0	494	0	1/2	0	0	1
$\bar{K}^0$	494	0	1/2	0	0	−1
K^-	494	0	1/2	0	−1	−1

the electroweak interaction. In this way the conserved baryon number is shared among a greater number of species of lower Fermi energies.

Some of the baryon and meson species and their quantum numbers are shown in Table 4.1. The most important baryons in neutron stars are the octet baryons which are the lowest mass baryons of spin $\frac{1}{2}$. They comprise the nucleons and some of the hyperons. Hyperons are baryons that carry the strangeness quantum number (one or more of their three quarks are strange). The most important mesons are the scalar σ, the spin one vector ω and the spin and isospin one vector–isovector $\boldsymbol{\omega}$. In the mean field approximation to the relativistic theory that will be used in this chapter, the above mesons mediate the interaction among baryons. The pion and kaon are of possible interest as condensates, but their mean values in the normal ground state vanish in the approximation in which we work because they change parity and strangeness, respectively. As a consequence, the ground state (or any diagonal) matrix element vanishes.

Hadrons—baryons and mesons—are not themselves the fundamental particles they were once thought to be. We now know that they are composed of quarks whose interactions are mediated by the exchange of gluons. So far as we know, the fundamental fields of nature are the quarks, leptons, and gauge bosons (Tables 4.2 and 4.3).

Quarks and leptons are fermions of spin $\frac{1}{2}$. The theory that describes nature at this fundamental level is known as *quantum chromodynamics* (QCD). It is an unusual theory. Unlike quantum electrodynamics (QED), in which the force is mediated by photons that do not interact among themselves, the gluons mediating the strong force do. As a result, QCD is an almost intractable theory.

TABLE 4.2. Quarks and leptons. Mass m in MeV; charge q in units of e.

		Quarks			Leptons		
Family	Flavor	Name	m	q	Name	m	q
I	1	u	~ 0	2/3	ν_e	0	0
	2	d	~ 0	$-1/3$	e	0.511	-1
II	3	c	1500	2/3	ν_μ	0	0
	4	s	150	$-1/3$	μ	106	-1
III	5	t	$\sim 10^5$	2/3	ν_τ	~ 0	0
	6	b	5000	$-1/3$	τ	1784	-1

TABLE 4.3. Gauge bosons. Mass m in GeV; charge q in units of e. The graviton is conjectured.

Force	Carrier	m	Spin	q
Gravity	graviton	0	2	0
EM	γ	0	1	0
Weak	W^+	81	1	1
	W^-	81	1	-1
	Z^0	93	1	0
Strong	8 gluons	0	1	0

The most remarkable aspect of the theory is that quarks, which carry an attribute called *color* charge, can never appear as an observable entity in any combination that has color. There are three colors. An equal number of each color is referred to as a *colorless* state in analogy to light. A quark and antiquark of the same color also form a colorless state. Physical states are colorless. Quarks are *confined* in the sense that they cannot be individually removed from a hadron and isolated. This contrasts with all other hierarchies of composite particles—molecules, atoms, nuclei—which can be separated into their constituents.

There are six *flavors* of quarks, each flavor associated with the mass of the quark. Baryons consist of three (valence) quarks of different color and various flavors. Mesons consist of a quark and antiquark of the same color and different flavor. The light quark flavors are called up, down, and strange. In Chapters 5 and 8 we shall see that these are the only flavors of possible significance in stars. The heavy flavors—charm, beauty, and top—cannot be populated at the densities of stable, compact, stellar configurations (see Section 3.19). Of the leptons, only the electron and muon are of relevance to compact stars. The charge chemical potential or Fermi energy in neutron stars never becomes large enough to exceed the tau lepton mass, so the tau is absent (see Section 5.4.6).

Quantum chromodynamics is noted for the peculiar interaction coupling between quarks: it is strong at low density or momentum transfer, becoming weak at high density or high momentum transfer. The latter is referred to as *asymptotic freedom* [109]. At very high hadronic density or at very high temperature, asymptotic freedom introduces a new phase of matter, one in which the quarks are not

confined in individual hadrons, but are free to explore a larger colorless region. This (locally) *deconfined* phase is called *quark matter*.

Quarks are almost free in the quark matter phase, though confined to a high-density or high-temperature region. Asymptotically, the description of this phase is simple. At the other extreme of low and moderate density (up to a few times nuclear density), a QCD description of matter is difficult to achieve. No useful solution of QCD has been obtained for cold nuclear or neutron star matter, nor is one likely to be forthcoming in the foreseeable future.

As in many problems in physics, it is useful to isolate the degrees of freedom that are relevant at the scale under consideration. Hadrons represent the appropriate degrees of freedom with which to build an effective theory of nuclear matter up to the phase-transition density to quark matter (perhaps 3 to 10 nuclear density). Above the phase-transition density, the appropriate description is in terms of quarks. The quark phase and the phase transition will be discussed in Chapters 8, 9, and 12.

A Lorentz covariant theory of nuclear matter involving hadrons was proposed in its simplest form by Johnson and Teller [111], Duerr [112] in the mid-1950s, and Walecka [113] in the mid-1970s. This theory describes the interaction between nucleons in matter through the two meson fields, the scalar σ and vector ω. We refer to this theory as the $(\sigma - \omega)$ nuclear field theory. It is not a fundamental theory inasmuch as it is not formulated in terms of the fundamental fields mentioned above. In many ways it is not as good a theory as the Schrödinger-based theory of nuclear physics.

Nuclei have been traditionally described by a Schrödinger-based nonrelativistic shell model invented by Mayer and Jensen [114] or various of its extensions [115]–[118]. Shell models consist of a mean field in which nucleons are bound and a residual force through which they interact. One can compute the energy levels and properties of nuclei involving the active participation of at least a few nucleons. Recently, Monte Carlo techniques have been employed to extend the range of applicability of the shell model [119].

Nuclear field theory—particularly its extensions as discussed later in the chapter—is especially suitable for the description of neutron star matter. It does have its successes in describing rather well some single-particle properties of finite nuclei (cf. [120]–[126]). However it is the description of bulk matter that is relevant to neutron star structure, and the theory with the extensions we describe does well in this respect.

For our purpose, relativistic nuclear field theory has several merits. It is automatically causal, whereas the equation of state computed in Schrödinger-based theories is not compelled to be. (It may be up to some density, but causality is not built into the structure of the theory.) Secondly, the coupling constants of relativistic nuclear field theory can be related algebraically to the bulk properties of nuclear matter. Thus, the theory can be anchored firmly to the only information we have on high-density matter—(1) causality; (2) microscopic stability (Le Chatelier's principle, $dp/d\rho \geq 0$); (3) saturation properties of nuclear matter; and (4) at high density the asymptotic freedom of quarks. However, it is clear that these properties

and principles do not uniquely specify the properties of high density matter. Indeed, at his time we do not know a single point on the equation of state, $p = p(\epsilon)$, above nuclear density. However, within this limitation, we can investigate the possible forms that compact stars can take, consistent with the above general principles and the properties of General Relativity, always alert to the means by which various possibilities can be distinguished observationally (See Chapter 11).

Accordingly, our goal is to construct extensions of the above $(\sigma - \omega)$ model that will provide a relativistically covariant theory of dense hadronic matter, such as likely exists in neutron stars [67, 68], [127]–[131]. The first part of this endeavor will be concerned with the important task of making firm contact between the theory and five important properties near normal nuclear matter density. Two of these, the binding energy and saturation density, will normalize the equation of state at one point in the energy–density plane. Two others, the compression modulus and effective nucleon mass, assure that the extrapolation to higher density is correct in the vicinity of saturation. (This being so, we have some expectation that the extrapolation to greater extremes is reasonable, though we cannot say unique.) Finally, the last nuclear matter property, the isospin symmetry energy coefficient, will assure that small extrapolations to isospin asymmetric systems (of which neutron star matter is an extreme) are correct.

As mentioned, we have no present measurements at extremes of density, isospin asymmetry, or temperature, though they are the object of current and planned experimentation in the field of relativistic nuclear collisions. So it is a special advantage of the theory being developed in this chapter that the coupling constants of the theory are related *algebraically* to the properties of matter at saturation and, within the framework of the particular theory, control its extrapolation in density and in isospin density. Thus, the dependence of the properties of neutron stars, arising from the structure of the hadronic matter of which they are made, can be related directly to nuclear matter properties and their uncertainties. In addition, the range of stellar properties associated with uncertainties in the nuclear matter properties can be assessed.

It will become clear that at higher densities nuclear matter will also be populated by higher-mass baryons. Therefore, the second part of the development concerns the inclusion of other members of the baryon octet besides the neutron and proton. It is not possible to control this sector of the theory by the ground-state properties of nuclear matter because only the nucleons populate that state. It will be possible to deduce some constraints on the coupling constants of the hyperons, but we will have to develop considerable additional material before this can be carried out in Section 5.4.3 [132].

The rapid accumulation of data on pulsars and X-ray emitting neutron stars in recent years lends hope that real constraints on the equation of state will be obtained from these manifestations of neutron stars. Eventually, it may be possible to invert the process: that is, from the properties of neutron stars, deduce the equation of state. Indeed the inverse theorem has already been proven—that given a range of M and R measurements of neutron stars, a unique equation of state can be determined [133].

We use relativistic nuclear field theory for the description of the matter of compact stars up to the critical density of the phase transition to quark matter. We do not know empirically where this transition occurs. However, the transition density can be computed for specific choices of theory of the confined and deconfined phases. Quark matter may play an important role in the structure and composition of compact stars and as we will see, may even introduce a crystalline solid of quark matter at lattice sites within a nuclear matter background (Chapter 9).

We have already discussed a simple Fermi gas model of dense matter in Section 3.9.2. Nuclear field theory is an extension which includes interactions of the baryons through the mean fields of certain mesons generated in a self-consistent way. In both cases the ground state is a *degenerate* state consisting of all particle momentum levels filled to the Fermi momentum. We begin by recalling certain pertinent elements of Lagrangian field theory. We introduce the Lagrangian of relativistic nuclear field theory, discuss how to compute solutions of the equations of motion in the mean-field approximation, and introduce the baryons of the octet appropriate to a description of dense matter.

After this summary of the Lagrangians and the equations of motion of fields of various quanta and their associated symmetries and conservation laws, we discuss nuclear matter properties as a prelude to their use as constraints on a field theory of nuclear matter. We construct our field theory in stages so as to be in accord finally with the five important properties of nuclear matter mentioned above. The spinor conventions of Bjorken and Drell [7] are used here. We also recall the operations of raising and lowering indices on contravariant and covariant vectors, derivatives of scalars as vectors, and the Minkowski metric tensor (2.4, 2.7, 2.25, 2.26).

4.2 Lagrange Formalism

The fields representing various particles may each be thought of as satisfying equations analogous to those derived for a continuous system obtained by a limiting process applied to a discrete mechanical system involving m degrees of freedom with m going to infinity [134]. Hamilton's principle states that the equations of motion are those for which the classical action is an extremum,

$$\delta S = 0, \qquad S = \int_{t_1}^{t_2} L[q, \dot{q}]\, dt\,, \tag{4.1}$$

where the Lagrangian depends on generalized coordinates of the system $q \equiv q_1, \cdots q_n$ and the velocities $\dot{q} = dq/dt$. By analogy we consider a Lagrangian *density* in the fields and their four-derivatives,

$$\mathcal{L} \equiv \mathcal{L}[\phi(x), \partial_\mu \phi(x)]\,, \tag{4.2}$$

where,

$$x \equiv x^\mu = (t, x, y, z), \qquad x_\mu = (t, -x, -y, -z)\,. \tag{4.3}$$

Recall the Minkowski metric (2.7) and the notation for a derivative (2.71).

The Lagrangian is the spatial integral

$$L \equiv \int dr\mathcal{L}\big[\phi(x), \partial_\mu\phi(x)\big]. \tag{4.4}$$

As with q, $\phi(x)$ may denote one or many fields. The Lagrangian density is a Lorentz scalar because we shall construct it only from scalar functions of the fields and their derivatives. Relativistic covariance is therefore manifest. The corresponding action is

$$S = \int_{t_1}^{t_2} d^4x\, \mathcal{L}\big[\phi(x), \partial_\mu\phi(x)\big]. \tag{4.5}$$

The variation of the action is given by

$$\begin{aligned}
\delta S &= \int_{t_1}^{t_2} d^4x \left\{\frac{\partial\mathcal{L}}{\partial\phi}\delta\phi + \frac{\partial\mathcal{L}}{\partial(\partial_\mu\phi)}\delta(\partial_\mu\phi)\right\} \\
&= \int_{t_1}^{t_2} d^4x \left\{\left(\frac{\partial\mathcal{L}}{\partial\phi} - \partial_\mu\frac{\partial\mathcal{L}}{\partial(\partial_\mu\phi)}\right)\delta\phi + \partial_\mu\left(\frac{\partial\mathcal{L}}{\partial(\partial_\mu\phi)}\delta\phi\right)\right\} \\
&= \int_{t_1}^{t_2} d^4x \left(\frac{\partial\mathcal{L}}{\partial\phi} - \partial_\mu\frac{\partial\mathcal{L}}{\partial(\partial_\mu\phi)}\right)\delta\phi(x).
\end{aligned} \tag{4.6}$$

The variations of the fields are taken as arbitrary save that they vanish at the end points. Hence, the perfect differential in the above integral yields zero. So the extremal condition is satisfied if

$$\frac{\partial\mathcal{L}}{\partial\phi(x)} - \partial_\mu\frac{\partial\mathcal{L}}{\partial(\partial_\mu\phi)} = 0. \tag{4.7}$$

This is the *Euler–Lagrange* equation for the field $\phi(x)$. We will use this equation frequently in deriving the equations of motion for the fields of our theory on neutron star matter. If $\mathcal{L}$ depends on several fields, there is one such equation for each field.

If the Lagrangian is a Lorentz scalar, then the equations of motion of the theory are Lorentz covariant. So we require that the the Lagrangian be a scalar, $\mathcal{L}'(x') = \mathcal{L}(x)$. By finding certain symmetries in nature (such as the observation that nuclei tend to be most strongly bound when $N = Z$, suggesting that the nuclear force favors isospin symmetric configurations), we can be guided to the construction of a sensible Lagrangian. The symmetry of the action of gravity on all bodies, no matter their composition, was of profound influence on Einstein's discovery of General Relativity as was the logical necessity of the covariance of the laws of nature to changes in the frame of reference or location in the universe. We will be guided here by the conservation laws and symmetries we know of in constructing a sensible nuclear field theory. We first consider symmetries before studying any particular fields and their Lagrangians.

4.3 Symmetries and Conservation Laws

The construction of a scalar Lagrangian from the fields of the quanta we wish to describe, such as the scalars $\phi^2(x)$ or $\partial_\mu\phi(x)\,\partial^\mu\phi(x)$ constructed from a scalar field $\phi'(x') = \phi(x)$, suggests at once that the Lagrangian will be invariant in form to certain types of *manifest*, continuous, symmetry transformations. For example, if $\phi(x)$ is a complex field, the above scalars would be bilinear in the field and its complex conjugate. The two types of terms are obviously each invariant to a global phase transformation, $\phi(x) \to e^{i\epsilon}\phi(x)$. Such an invariance will be seen to correspond to an additive attribute that is conserved, such as charge.

The invariances and associated symmetry transformations are of various types. There are symmetries associated with spacetime, referred to as *external symmetries*, and there are *internal symmetries*, such as phase transformations. Internal symmetries may depend on x, in which case they are referred to as *local*, or may be independent of x and referred to as *global*.

Invariances under local transformations are of central importance to the theory of the fundamental fields mentioned earlier, but they play no role in our work at the level of effective fields for composite particles. Likewise, we shall be interested in manifest symmetries, but not hidden symmetries [135, 136].

4.3.1 Internal global symmetries

We work first on an abstract and general level of internal global symmetries and look later at the specific fields that we shall need in a theory of nuclear matter. Consider a number n of fields $\phi_1(x), \phi_2(x), \ldots, \phi_n(x)$ some of which may refer to different charge or isospin states of particles of particular mass. We do not need to specify whether they are Fermi or Bose fields. Consider an internal, infinitesimal, continuous transformation (finite transformations can be built from a number of infinitesimal ones):

$$\phi_i'(x) = \phi_i(x) + \lambda_j F_i^j\left[\phi_1(x), \ldots, \phi_n(x)\right]. \tag{4.8}$$

F characterizes the transformation and may mix some of the fields. The λ_j are infinitesimal parameters that are spacetime-independent. Suppose a particular $\mathcal{L}$ is found to be invariant to a continuous symmetry transformation defined by a particular set of F_i^j. Its variation with respect to the parameters of the transformation must therefore vanish. To find the consequence, examine the formal expression for the variation,

$$\delta\mathcal{L} = \frac{\partial\mathcal{L}}{\partial\phi_i}\delta\phi_i + \frac{\partial\mathcal{L}}{\partial(\partial_\mu\phi_i)}\delta(\partial_\mu\phi_i). \tag{4.9}$$

Because $\delta\phi_i = \lambda_j F_i^j$ and

$$\delta(\partial_\mu\phi_i) = \partial_\mu(\delta\phi_i) = \lambda_j\partial_\mu F_i^j\,, \tag{4.10}$$

then

$$\delta\mathcal{L} = \Big(\frac{\partial\mathcal{L}}{\partial\phi_i}F_i^j + \frac{\partial\mathcal{L}}{\partial(\partial_\mu\phi_i)}\partial_\mu F_i^j\Big)\lambda_j\,. \tag{4.11}$$

Employing the Euler–Lagrange equations (4.7) for the fields in the first term, we obtain

$$\begin{aligned}\delta\mathcal{L} &= \Big(F_i^j\partial_\mu\frac{\partial\mathcal{L}}{\partial(\partial_\mu\phi_i)} + \frac{\partial\mathcal{L}}{\partial(\partial_\mu\phi_i)}\partial_\mu F_i^j\Big)\lambda_j \\ &= \partial_\mu\Big(\frac{\partial\mathcal{L}}{\partial(\partial_\mu\phi_i)}F_i^j\Big)\lambda_j\,. \end{aligned}\tag{4.12}$$

Hence, if $\mathcal{L}$ is invariant to the transformation, then $\delta\mathcal{L} = 0$. Because the parameters λ_j are arbitrary, the set of n four-vectors

$$J_j^\mu(x) \equiv \frac{\partial\mathcal{L}}{\partial(\partial_\mu\phi_i)}F_i^j \tag{4.13}$$

satisfies

$$\partial_\mu J_j^\mu = 0 \quad (j = 1, 2, \ldots, n)\,. \tag{4.14}$$

Divergenceless four-vectors J^μ following from an invariance of the Lagrangian are referred to as *Noether currents* after Noether's theorem [137]. Because their four-divergences are zero, each current is conserved. Conservation of a divergenceless four-vector is proved quite simply. Write out in full the divergence (where for the moment we suppress the field identifier j):

$$0 = \partial_\mu J^\mu = \partial_0 J^0 + \partial_k J^k = \frac{\partial J^0}{\partial t} + \nabla\cdot\boldsymbol{J}\,. \tag{4.15}$$

This is the *continuity equation*. Integrate it over a 3-volume containing the system and use Gauss's theorem,

$$\frac{\partial}{\partial t}\int_V J^0\,d\boldsymbol{r} = -\int_V \nabla\cdot\boldsymbol{J}\,d\boldsymbol{r} = -\int_S \boldsymbol{J}\cdot d\boldsymbol{S}\,. \tag{4.16}$$

Because the system is contained within V, the current S crossing the boundary is zero. Therefore, the surface integral vanishes. Consequently the time derivative on the left side is zero and we have the conserved charges

$$Q_j = \int_V J_j^0\,d\boldsymbol{r} \tag{4.17}$$

which are constant in time. The invariance of $\mathcal{L}$ to continuous internal symmetries implies the existence of conserved charges. This result will be of use to us in the sequel.

4.3.2 *Spacetime symmetries*

Physical theories in flat spacetime ought to be Lorentz covariant. Our choice for $\mathcal{L}$ must therefore be a Lorentz scalar. As such, the Lagrangian has certain space-

time symmetries or invariances, such as rotation or translation of the spacetime coordinates. We consider the second—an infinitesimal translation,

$$x'^{\mu} = x^{\mu} + \epsilon^{\mu} . \tag{4.18}$$

The corresponding change in $\mathcal{L}$ can be written

$$\begin{aligned} \delta\mathcal{L} &\equiv \mathcal{L}\big[\phi(x^{\nu} + \epsilon^{\nu}),\ \partial_{\mu}\phi(x^{\nu} + \epsilon^{\nu})\big] - \mathcal{L}\big[\phi(x^{\nu}),\ \partial_{\mu}\phi(x^{\nu})\big] \\ &= \epsilon^{\mu}\frac{\partial\mathcal{L}}{\partial x^{\mu}} = \epsilon^{\mu}\partial_{\mu}\mathcal{L} = \epsilon_{\nu}\partial^{\nu}\mathcal{L} . \end{aligned} \tag{4.19}$$

We made a Taylor expansion in the first term on the right and kept terms to first order in ϵ to obtain the second line.

Alternately, because $\mathcal{L}$ depends only on ϕ and $\partial_{\mu}\phi$ and not explicitly on x^{μ}, we also may write the change as

$$\delta\mathcal{L} = \frac{\partial\mathcal{L}}{\partial\phi}\delta\phi + \frac{\partial\mathcal{L}}{\partial(\partial_{\mu}\phi)}\delta(\partial_{\mu}\phi) , \tag{4.20}$$

where, just as for $\delta\mathcal{L}$, we write

$$\begin{aligned} \delta\phi &\equiv \phi(x^{\nu} + \epsilon^{\nu}) - \phi(x^{\nu}) = \epsilon^{\nu}\partial_{\nu}\phi = \epsilon_{\nu}\partial^{\nu}\phi , \\ \delta(\partial_{\mu}\phi) &= \partial_{\mu}\,\delta\phi = \epsilon^{\nu}\partial_{\mu}\partial_{\nu}\phi = \epsilon_{\nu}\partial_{\mu}\partial^{\nu}\phi . \end{aligned} \tag{4.21}$$

The Lagrangian variation then is

$$\delta\mathcal{L} = \Big(\frac{\partial\mathcal{L}}{\partial\phi}\partial^{\nu}\phi + \frac{\partial\mathcal{L}}{\partial(\partial_{\mu}\phi)}\partial_{\mu}\partial^{\nu}\phi\Big)\epsilon_{\nu} . \tag{4.22}$$

Use the Euler–Lagrange equation to replace the first term and find

$$\delta\mathcal{L} = \partial_{\mu}\Big(\frac{\partial\mathcal{L}}{\partial(\partial_{\mu}\phi)}\partial^{\nu}\phi\Big)\epsilon_{\nu} . \tag{4.23}$$

Now we have two expressions for the variation in $\mathcal{L}$ under a translation of coordinates. Equating them yields

$$\partial_{\mu}\Big(\frac{\partial\mathcal{L}}{\partial(\partial_{\mu}\phi)}\partial^{\nu}\phi\Big)\epsilon_{\nu} = \epsilon_{\nu}\partial^{\nu}\mathcal{L} = \epsilon_{\nu}\eta^{\mu\nu}\partial_{\mu}\mathcal{L} \tag{4.24}$$

or

$$\partial_{\mu}\Big(\frac{\partial\mathcal{L}}{\partial(\partial_{\mu}\phi)}\partial^{\nu}\phi - \eta^{\mu\nu}\mathcal{L}\Big)\epsilon_{\nu} = 0 . \tag{4.25}$$

Because this holds for arbitrary translations ϵ_{ν} we have

$$\partial_{\mu}T^{\mu\nu} = 0, \qquad (\nu = 0, 1, 2, 3) , \tag{4.26}$$

where

$$T^{\mu\nu} \equiv \frac{\partial\mathcal{L}}{\partial(\partial_{\mu}\phi_i)}\partial^{\nu}\phi_i - \eta^{\mu\nu}\mathcal{L} \tag{4.27}$$

is the energy-momentum tensor of the theory. Recall that $\mathcal{L}$ may contain many fields, ϕ_i, corresponding to bosons and fermions, and that the sum on i is over all

of them. It is straightforward to demonstrate explicitly that $\mathcal{T}^{\mu\nu}$ transforms as a Lorentz tensor.

Because of the vanishing divergence of the energy-momentum tensor, there are four conserved four-currents and their associated "charges". The vanishing divergence gives the continuity equations

$$\partial_0 \mathcal{T}^{0\nu} + \partial_k \mathcal{T}^{k\nu} = 0 . \tag{4.28}$$

Integrating over a 3-volume containing the fields so that there is no current across the boundary (or assuming the fields vanish at infinity) and using Gauss's theorem, we find four time-constant "charges" which are the integrals over the volume of $\mathcal{T}^{0\nu}$, $\nu = 0, \ldots, 3$.

What are these four currents, and what are the conserved quantities that correspond to the vanishing of their divergence? Recall from classical mechanics the definition of the canonical momentum corresponding to a generalized coordinate, in this case ϕ:

$$\pi(x) = \frac{\partial \mathcal{L}}{\partial(\partial_0 \phi)} . \tag{4.29}$$

The Hamiltonian density is

$$\mathcal{H} = \pi\, \partial^0 \phi - \mathcal{L} = \frac{\partial \mathcal{L}}{\partial(\partial_0 \phi)} \partial^0 \phi - \mathcal{L} . \tag{4.30}$$

This is the (00) component of $\mathcal{T}^{\mu\nu}$. Its integral over three-space is the Hamiltonian

$$H = \int_V d\boldsymbol{r}\, \mathcal{T}^{00} , \tag{4.31}$$

and its value is the energy, E. It is one of the four constants that follows from the vanishing divergence of $\mathcal{T}^{\mu\nu}$.

The corresponding spacelike components,

$$P^k = \int_V d\boldsymbol{r}\, \mathcal{T}^{0k} \quad (k = 1, 2, 3), \tag{4.32}$$

are the remaining conserved quantities. Together with H they form a conserved four-vector, namely, the energy-momentum vector. Therefore, we have the Lorentz scalar (2.23)

$$P_\mu P^\mu = E^2 - \boldsymbol{P}^2 = M^2 = \text{ invariant} , \tag{4.33}$$

with M the invariant length of

$$P^\mu = (E, \boldsymbol{P}) . \tag{4.34}$$

4.4 Boson and Fermion Fields

4.4.1 *Uncharged and charged scalar fields*

The simplest example of a field—one of those that will form a part of nuclear field theory—is the uncharged scalar field which we denote by $\sigma(x)$. Consider the Lagrangian

$$\mathcal{L}_\sigma = \tfrac{1}{2}(\partial_\mu\sigma\,\partial^\mu\sigma - m_\sigma^2\sigma^2)\ , \tag{4.35}$$

where m_σ denotes the meson mass. The Euler–Lagrange equation (4.7) of this Lagrangian is the Klein–Gordon equation for a free spin-zero meson of the indicated mass,

$$(\Box + m_\sigma{}^2)\sigma(x) = 0\,, \tag{4.36}$$

where $\Box = \partial_\mu\partial^\mu$. With the usual operator substitutions for energy and momentum,

$$E \to i\frac{\partial}{\partial t}, \qquad \boldsymbol{P} \to -i\boldsymbol{\nabla}\ , \tag{4.37}$$

the Klein–Gordon equation represents

$$E^2 = P^2 + m_\sigma{}^2\,. \tag{4.38}$$

The Lagrangian written above has the space symmetries of any Lorentz scalar Lagrangian and therefore an energy-momentum tensor of the form derived above; however, it has no internal symmetries.

A scalar Lagrangian that does have an internal symmetry is one representing two scalar mesons of the same mass,

$$\mathcal{L}(\sigma_1,\sigma_2) = \tfrac{1}{2}(\partial_\mu\sigma_1\partial^\mu\sigma_1 - m_\sigma^2\sigma_1^2) + \tfrac{1}{2}(\partial_\mu\sigma_2\partial^\mu\sigma_2 - m_\sigma^2\sigma_2^2)\ . \tag{4.39}$$

The symmetry becomes apparent if we define the complex field

$$\sigma = \big(\sigma_1 + i\sigma_2\big)/\sqrt{2}\,. \tag{4.40}$$

Then the Lagrangian can be rewritten

$$\mathcal{L}(\sigma_1,\sigma_2) = \partial_\mu\sigma^*\partial^\mu\sigma - m_\sigma^2\sigma^*\sigma \tag{4.41}$$

and is clearly invariant to the phase transformation

$$\sigma(x) \to e^{iq\lambda}\sigma(x)\ , \qquad \sigma^*(x) \to e^{-iq\lambda}\sigma^*(x)\,, \tag{4.42}$$

where λ is a continuous variable and we interpret q as the charge of the field, the reason for which will become apparent. The $\sigma(x)$, $\sigma^*(x)$ can be written in terms of the original fields,

$$\begin{aligned}\sigma_1 &\to \sigma_1\cos(q\lambda) - \sigma_2\sin(q\lambda)\,,\\ \sigma_2 &\to \sigma_2\cos(q\lambda) + \sigma_1\sin(q\lambda)\,.\end{aligned} \tag{4.43}$$

The above equations correspond to a rotation around the 3-axis in the orthogonal space $(\sigma_1,\sigma_2,\sigma_3)$. The analogy of rotation will be useful later. For an infinitesimal

λ, we can write the above phase transformation as

$$\delta\sigma = iq\lambda\sigma\,. \tag{4.44}$$

or, in terms of the original fields,

$$\sigma_1 \to \sigma_1 - q\lambda\sigma_2\,, \qquad \sigma_2 \to \sigma_2 + q\lambda\sigma_1\,. \tag{4.45}$$

From the general notation (4.8), we read

$$F_1^2 = -q\sigma_2, \qquad F_2^1 = q\sigma_1, \qquad F_1^1 = F_2^2 = 0\,. \tag{4.46}$$

It is important to note that the invariance of $\mathcal{L}$ involves only one continuous infinitesimal λ so (4.12) defines a single conserved current which is the sum of two terms:

$$\begin{aligned} J^\mu &= q\Big(\frac{\partial\mathcal{L}}{\partial(\partial_\mu\sigma_2)}\sigma_1 - \frac{\partial\mathcal{L}}{\partial(\partial_\mu\sigma_1)}\sigma_2\Big) = q\big(\sigma_1\partial^\mu\sigma_2 - \sigma_2\partial^\mu\sigma_1\big) \\ &= q(\boldsymbol{\sigma}\times\partial^\mu\boldsymbol{\sigma})_3\,, \end{aligned} \tag{4.47}$$

or, in terms of the complex field,

$$J^\mu = -iq\big(\sigma^*\partial^\mu\sigma - \sigma\partial^\mu\sigma^*\big)\,. \tag{4.48}$$

From the general results of Section 4.3.1, this four-vector is divergenceless and corresponds to a conserved current. From the application of Gauss's theorem there follows the conservation of charge within the volume containing the system.[2]

4.4.2 *Uncharged and charged vector fields*

Now consider a Lorentz vector field ω_μ for a meson of mass m_ω. The notation is chosen to correspond with the neutral omega meson of spin and parity 1^-. Define

$$\omega_{\mu\nu} = \partial_\mu\omega_\nu - \partial_\nu\omega_\mu \tag{4.49}$$

as in electromagnetic theory. A scalar that involves second derivatives and a mass term is

$$\mathcal{L}_\omega = -\tfrac{1}{4}\omega_{\mu\nu}\omega^{\mu\nu} + \tfrac{1}{2}m_\omega^2\omega_\mu\omega^\mu\,. \tag{4.50}$$

The Euler–Lagrange equation is

$$\big(\Box + m_\omega^2\big)\omega_\mu - \partial_\mu\partial^\nu\omega_\nu = 0 \tag{4.51}$$

which is the Proca equation. Its divergence is

$$\big(\Box + m_\omega^2\big)\partial^\mu\omega_\mu - \Box\partial^\nu\omega_\nu = 0 \tag{4.52}$$

from which follows

$$m_\omega^2\partial^\mu\omega_\mu = 0\,. \tag{4.53}$$

---

[2]Note that in (4.47), it may at first appear that a factor $\frac{1}{2}$ has been omitted because of the presence of this factor in $\mathcal{L}(\sigma_1, \sigma_2)$. However, note that $\partial_\mu\sigma\partial^\mu\sigma = \eta^{\mu\nu}\partial_\mu\sigma\partial_\nu\sigma$. So the derivative with respect to $\partial_\alpha\sigma$ is $2\partial^\alpha\sigma$.

Because the mass is not zero, the field must be divergenceless. For free omega mesons, each of the four Lorentz components of ω_μ satisfies a Klein–Gordon equation,

$$(\Box + m_\omega^2)\omega_\mu = 0\,. \tag{4.54}$$

Next, we would like to describe the charged triplet of rho mesons ρ^0, $\rho^\pm$ which have the same spin and parity as the omega meson. Therefore, they should be described as Lorentz vector fields. Denote the three isospin components by

$$\boldsymbol{\rho}^\mu \equiv (\rho_1^\mu, \rho_2^\mu, \rho_3^\mu)\,. \tag{4.55}$$

From these we can form one real and two complex fields as for the pair of scalar fields, one the complex conjugate of the other. Therefore, the scalar Lagrangian for free rho mesons,

$$\mathcal{L}_\rho = -\tfrac{1}{4}\boldsymbol{\rho}_{\mu\nu}\cdot\boldsymbol{\rho}^{\mu\nu} + \tfrac{1}{2}m_\rho^2\boldsymbol{\rho}_\mu\cdot\boldsymbol{\rho}^\mu\,, \tag{4.56}$$

has the same phase invariance as for complex scalar fields constructed from two of the fields, say 1 and 2:

$$\rho_\pm^\mu = \frac{1}{\sqrt{2}}(\rho_1^\mu \pm i\rho_2^\mu)\,. \tag{4.57}$$

Analogously, the Lagrangian is invariant to a rotation about the 3-axis in isospin space. There is also an invariance having to do with a general rotation in the space of the three fields. This is an isospin rotation to which $\mathcal{L}_\rho$ is manifestly invariant, consisting as it does of scalar products in the three vectors constructed from $\boldsymbol{\rho}_\mu$. Such a rotation can be written

$$\boldsymbol{\rho}_\mu \to \boldsymbol{\rho}_\mu + \boldsymbol{\Lambda}\times\boldsymbol{\rho}_\mu\,, \tag{4.58}$$

where $\boldsymbol{\Lambda}$ is an infinitesimal vector in isospin space. We can also write the vector product explicitly as

$$\boldsymbol{\rho}_\mu \to \boldsymbol{\rho}_\mu + \epsilon_{ijk}\Lambda_j\rho_{k\mu}\,, \tag{4.59}$$

where ϵ_{ijk} is antisymmetric under interchange of any two indices and symmetric under cyclic permutations,

$$\epsilon_{ijk} = -\epsilon_{ikj} = \epsilon_{kij}\,. \tag{4.60}$$

According to our general notation (4.8), the transformation may be characterized by

$$F_i^j = \epsilon_{ijk}\rho_{k\mu}\,. \tag{4.61}$$

Therefore, according to the general theorem on Noether currents,

$$I_j^\nu = \frac{\partial\mathcal{L}_\rho}{\partial(\partial_\nu\rho_{i\mu})}\rho_{k\mu}\epsilon_{ijk} \tag{4.62}$$

or

$$\boldsymbol{I}^\nu = \boldsymbol{\rho}_\mu\times\frac{\partial\mathcal{L}_\rho}{\partial(\partial_\nu\boldsymbol{\rho}_\mu)} = \boldsymbol{\rho}_\mu\times\boldsymbol{\rho}^{\nu\mu} \tag{4.63}$$

is a Lorentz four-current, the isospin current of the rho field. Each component of this current is a three-vector in isospin space. The charge current is easily obtained as the isospin 3-component multiplied by the charge q,

$$J^{\nu} = q\left(\rho_{\mu} \times \rho^{\nu\mu}\right)_3 \tag{4.64}$$

which follows by taking $\Lambda = (0, 0, \lambda)q$.

Just as for the omega field, we can show that the massive rho field must be divergenceless, by use of the Euler–Lagrange equations. The equations of motion then reduce to

$$\left(\Box + m_{\rho}^2\right)\rho^{\mu} = 0\,. \tag{4.65}$$

4.4.3 *Dirac fields*

The solutions of the Klein–Gordon equations are single-component fields and cannot describe a spin-1/2 particle. Dirac (1928) sought an equation that is linear in all derivatives so as to give equal treatment to space and time and whose energy for a free particle satisfies the relationship [138]

$$H^2\psi(x^{\mu}) = (\boldsymbol{p}^2 + m^2)\psi(x^{\mu})\,. \tag{4.66}$$

Therefore, he wrote

$$H\psi = \left(-i\boldsymbol{\alpha}\cdot\boldsymbol{\nabla} + \beta m\right)\psi = i\frac{\partial\psi}{\partial t}\,, \tag{4.67}$$

where $\boldsymbol{\alpha}$ and β are as yet undetermined. If H is to be Hermitian, then so must $\boldsymbol{\alpha}$, β. Squaring and comparing with the previous equation leads to[3]

$$\begin{aligned} &\alpha_i\alpha_j + \alpha_j\alpha_i = 2\delta_{ij}\,, \\ &\alpha_i\beta + \beta\alpha_i = 0\,, \\ &\alpha_{(i)}^2 = \beta^2 = 1\,. \end{aligned} \tag{4.68}$$

A particular representation is

$$\boldsymbol{\alpha} = \begin{pmatrix} 0 & \boldsymbol{\sigma} \\ \boldsymbol{\sigma} & 0 \end{pmatrix}, \quad \beta = \begin{pmatrix} I & 0 \\ 0 & -I \end{pmatrix}, \quad I = \begin{pmatrix} 1 & 0 \\ 0 & 1 \end{pmatrix}, \tag{4.69}$$

where the σ_i are the Pauli 2×2 matrices

$$\sigma_1 = \begin{pmatrix} 0 & 1 \\ 1 & 0 \end{pmatrix}, \quad \sigma_2 = \begin{pmatrix} 0 & -i \\ i & 0 \end{pmatrix}, \quad \sigma_3 = \begin{pmatrix} 1 & 0 \\ 0 & -1 \end{pmatrix}, \tag{4.70}$$

and I is the identity matrix. Consequently, ψ is a four-component spinor.

In the above and original form, the Dirac equation is not manifestly Lorentz covariant. To make covariance manifest, we define new matrices,

$$\gamma^{\mu} = (\gamma^0, \gamma^1, \gamma^2, \gamma^3), \quad \gamma^0 = \beta, \quad \gamma^i = \beta\alpha_i\,. \tag{4.71}$$

[3]We use brackets around repeated indices that are not summed.

Then the Dirac equation can be written in the compact and manifestly covariant form

$$(i\gamma_\mu \partial^\mu - m)\psi = 0\,. \tag{4.72}$$

A notation of convenience is

$$\not{A} \equiv \gamma_\mu A^\mu = \gamma^\mu A_\mu \tag{4.73}$$

so that the Dirac equation can be written even more compactly as

$$(i\not{\partial} - m)\psi = 0\,. \tag{4.74}$$

The gamma matrices satisfy a number of rules of which some are important to us:

$$\gamma^\mu\gamma^\nu + \gamma^\nu\gamma^\mu = 2\eta^{\mu\nu} = 2\begin{pmatrix} 1 & 0 & 0 & 0 \\ 0 & -1 & 0 & 0 \\ 0 & 0 & -1 & 0 \\ 0 & 0 & 0 & -1 \end{pmatrix}, \tag{4.75}$$

where $\eta^{\mu\nu}$ is the Minkowski metric tensor of flat spacetime. This tells us, for example, that $\gamma_0^2 = 1,\ \ \gamma_{(i)}^2 = -1$.

From the foregoing it follows that

$$\gamma_0 = \gamma_0^\dagger, \quad \gamma^\dagger = (\beta\boldsymbol{\alpha})^\dagger = \boldsymbol{\alpha}\beta = -\beta\boldsymbol{\alpha} = -\boldsymbol{\gamma}\,, \tag{4.76}$$

or more compactly,

$$\gamma_0\gamma_\mu^\dagger\gamma_0 = \gamma_\mu\,. \tag{4.77}$$

The adjoint Dirac equation is,

$$-i\,\partial^\mu\psi^\dagger\gamma_\mu^\dagger - m\psi^\dagger = 0\,. \tag{4.78}$$

Upon defining the *Dirac adjoint* spinor,

$$\overline{\psi} \equiv \psi^\dagger\gamma_0\,, \tag{4.79}$$

we can write the adjoint equation as

$$i\,\partial^\mu\overline{\psi}\gamma_\mu + m\overline{\psi} = 0\,. \tag{4.80}$$

The Lagrangian that yields Dirac's equation is

$$\mathcal{L} = \overline{\psi}(i\not{\partial} - m)\psi \tag{4.81}$$

Because the Euler–Lagrange equation (4.7) yields simply

$$0 = \partial\mathcal{L}/\partial\overline{\psi} = (i\not{\partial} - m)\psi\,. \tag{4.82}$$

The Lagrangian is invariant to a continuous phase transformation,

$$\psi \to e^{-i\lambda}\psi = \psi - i\lambda\psi + O(\lambda^2)\,. \tag{4.83}$$

In terms of our general formulation of transformation of fields (4.8) we have $F = -i\psi$ so that there is a divergenceless four-current,

$$\partial_\mu j^\mu = 0. \tag{4.84}$$

There is therefore a conserved (divergenceless) baryon current,

$$j^{\mu} = \frac{\partial \mathcal{L}}{\partial(\partial_{\mu}\psi)} F = \overline{\psi}\gamma^{\mu}\psi \,. \tag{4.85}$$

The time component is

$$j^{0} = \overline{\psi}\gamma^{0}\psi = \psi^{\dagger}\psi \tag{4.86}$$

which is the baryon density. We shall frequently denote it as ρ. According to the earlier analysis it is a constant in time for any system into or out of which there is no net flow of nucleons. So a particle satisfying the free Dirac equation is conserved. Nucleon decay, if it occurs, has a time-scale on the order of the lifetime of the universe.

4.4.4 *Neutron and proton*

According to the rationale stated in the introduction, we take the neutron and proton to be Dirac particles of the same mass m. The Lagrangian for the pair is

$$\mathcal{L} = \overline{\psi}_{p}(i\,\partial\!\!\!/ - m)\psi_{p} + \overline{\psi}_{n}(i\,\partial\!\!\!/ - m)\psi_{n} \,. \tag{4.87}$$

Combine the four-component spinors into a single eight-component spinor

$$\psi \equiv \begin{pmatrix} \psi_{p} \\ \psi_{n} \end{pmatrix} , \tag{4.88}$$

and write

$$\mathcal{L} = \overline{\psi}(i\,\partial\!\!\!/ - m)\psi \,. \tag{4.89}$$

Let $\boldsymbol{\tau} = (\tau_1, \tau_2, \tau_3)$ denote the 2×2 Pauli isospin matrices, and let $\Lambda = (\Lambda_1, \Lambda_2, \Lambda_3)$ be an arbitrary constant vector in isospin space. The Lagrangian is manifestly invariant to the continuous phase transformation

$$\psi \to e^{-i\boldsymbol{\tau}\cdot\boldsymbol{\Lambda}/2}\psi \,. \tag{4.90}$$

A finite rotation can be built from infinitesimal ones. Taking the $\boldsymbol{\Lambda}$ to have infinitesimal components

$$\delta\psi = -\frac{i}{2}\boldsymbol{\Lambda}\cdot\boldsymbol{\tau}\psi = \boldsymbol{\Lambda}\cdot\boldsymbol{F}, \qquad \boldsymbol{F} = -\frac{i}{2}\boldsymbol{\tau}\psi \,, \tag{4.91}$$

we find

$$\frac{\partial \mathcal{L}}{\partial(\partial_{\mu}\psi)} = \overline{\psi} i\gamma^{\mu} \,. \tag{4.92}$$

By the general method (4.13) given earlier, the conserved *isospin* current of the nucleons results in

$$\boldsymbol{I}^{\mu} = \tfrac{1}{2}\overline{\psi}\gamma^{\mu}\boldsymbol{\tau}\psi \,. \tag{4.93}$$

Because τ_3 has the representation

$$\tau_3 = \begin{pmatrix} 1 & 0 \\ 0 & -1 \end{pmatrix}, \tag{4.94}$$

we find the 3-component as

$$\begin{aligned} I_3^\mu &= \tfrac{1}{2}\overline{\psi}\gamma^\mu\tau_3\psi\,, \\ I_3^0 &= \tfrac{1}{2}\left(\psi_p^\dagger\psi_p - \psi_n^\dagger\psi_n\right) \to \begin{cases} -\dfrac{1}{2}\rho_n & \text{for neutrons} \\ +\dfrac{1}{2}\rho_p & \text{for protons} \end{cases}, \end{aligned} \tag{4.95}$$

with ρ_n and ρ_p the neutron and proton densities.

The Lagrangian is also invariant to the phase transformation

$$\psi \to e^{-i\Lambda q(1+\tau_3)/2}\psi\,. \tag{4.96}$$

Following the familiar construction, we have the conserved current

$$J^\mu = q\overline{\psi}\gamma^\mu\frac{1+\tau_3}{2}\psi\,. \tag{4.97}$$

We find

$$J^\mu = q\overline{\psi}_p\gamma^\mu\psi_p, \qquad J^0 = q\psi_p^\dagger\psi_p\,, \tag{4.98}$$

which have the appearance of a charge current and density.

4.4.5 *Electromagnetic field*

We introduced the nucleon charge current above, but have not so far formally introduced the electromagnetic field. We do so now. The Lagrangian for the free electromagnetic field is

$$\mathcal{L}_{\text{em}} = -\tfrac{1}{4}A_{\mu\nu}A^{\mu\nu}\,, \tag{4.99}$$

where

$$A_{\mu\nu} = \partial_\mu A_\nu - \partial_\nu A_\mu\,. \tag{4.100}$$

A^μ is the Lorentz vector

$$A^\mu = (V, \boldsymbol{A})\,, \tag{4.101}$$

and V and $\boldsymbol{A}$ the scalar and vector potentials of electromagnetic theory. It is not our purpose to review electromagnetic theory here, but only to recall those aspects appropriate to the interpretation of charge on the spinor and complex fields described above. We recall the "minimal" prescription for electromagnetic interactions in quantum mechanics, $p^\mu \to p^\mu - qA^\mu$, or because $p^\mu = i\partial^\mu$ (recall (2.71)),

$$\partial^\mu \to \partial^\mu + iqA^\mu \equiv \mathcal{D}^\mu\,. \tag{4.102}$$

Accordingly, for the spinor field, we introduce the combined Lagrangian

$$\begin{aligned}\mathcal{L} &= \overline{\psi}_p\big(i\gamma_\mu \mathcal{D}_\mu - m\big)\psi_p - \tfrac{1}{4}A_{\mu\nu}A^{\mu\nu} \\ &= \overline{\psi}_p\big(i\,\partial\!\!\!/ - m\big)\psi_p - \tfrac{1}{4}A_{\mu\nu}A^{\mu\nu} - A_\mu J^\mu\,, \end{aligned} \tag{4.103}$$

where J^μ is the same current referred to above as the charge current of the nucleons.

Similarly, say for the complex scalar field (4.39),

$$\begin{aligned}\mathcal{L} &= (\mathcal{D}^\mu\sigma)^\dagger(\mathcal{D}_\mu\sigma) - m^2\sigma^\dagger\sigma - \tfrac{1}{4}A_{\mu\nu}A^{\mu\nu} \\ &= \mathcal{L}(\sigma_1,\sigma_2) - \tfrac{1}{4}A_{\mu\nu}A^{\mu\nu} \\ &\quad + iqA_\mu\big(\sigma\partial^\mu\sigma^* - \sigma^*\partial^\mu\sigma\big) + q^2A^2\sigma^*\sigma\,. \end{aligned} \tag{4.104}$$

This result can also be written

$$\begin{aligned}\mathcal{L} &= \mathcal{L}(\sigma_1,\sigma_2) - \tfrac{1}{4}A_{\mu\nu}A^{\mu\nu} \\ &\quad - \frac{q}{2}A_\mu\big(\sigma_2\partial^\mu\sigma_1 - \sigma_1\partial^\mu\sigma_2\big) + \tfrac{1}{2}q^2A^2(\sigma_1^2+\sigma_2^2)\,. \end{aligned} \tag{4.105}$$

We can now compute the conserved current

$$\begin{aligned}J^\mu &= q\big(\sigma_1\partial^\mu\sigma_2 - \sigma_2\partial^\mu\sigma_1\big) + q^2A^\mu(\sigma_1^2+\sigma_2^2) \\ &= -iq\big[\sigma^*(\mathcal{D}^\mu\sigma) - \sigma(\mathcal{D}^\mu\sigma)^*\big]\,. \end{aligned} \tag{4.106}$$

In contrast to the case of the Dirac field which, in interaction with the electromagnetic field, had the same current as for the free Dirac field, we see here an addition to the free current of the meson fields. It arises because of the additional derivatives. Note that it is quadratic in the charge and that the interaction Lagrangian has also a quadratic charge term. We remark on the quadratic coupling in electromagnetic theory because we shall encounter quadratic coupling in a different context in Section 4.9.

4.5 Properties of Nuclear Matter

We wish to anchor our description of the dense matter of neutron stars to what is known empirically about bulk nuclear matter. In practice this knowledge concerns the properties of symmetric nuclear matter at saturation density, that is, at the density at which the pressure is zero and at which the matter would remain static if not disturbed.

Uniform infinite symmetric matter is an idealization; nevertheless it is an idealization that has very definite properties related to finite nuclei. The history of the notion goes back to Weizsacker and the liquid drop model of the nucleus. All we need to know of the details of the model (much refined in recent years and which now correlates thousands of data on nuclear masses and other bulk properties) is that it seeks to characterize the energy of a nucleus by its atomic and proton numbers A and Z.

The basic property of nuclei or nuclear matter is that they are saturated systems. The reasons for this lie in the short range of the nuclear force, its strong repulsion

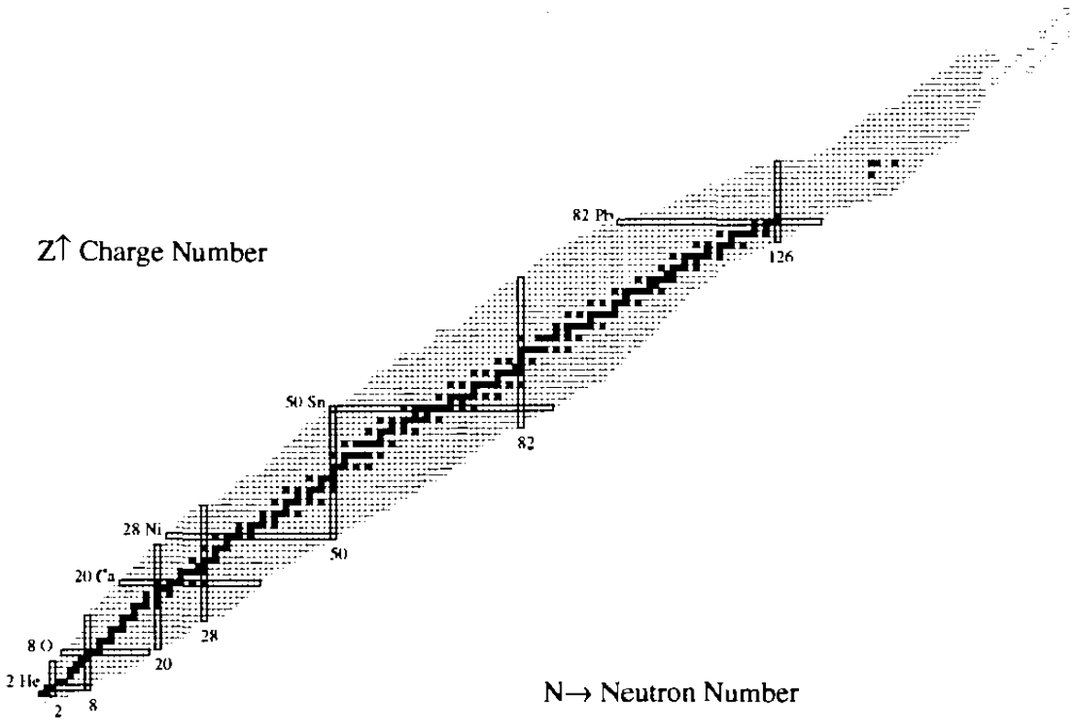

FIGURE 4.1. Most stable isotopes along the valley of beta stability shown by dark shading. (Courtesy of R. Firestone and the Table of Isotopes Project at LBNL [140].)

at a short distance, and the Pauli principle [139], [116, see Ch. 9], [117, see Ch. III]. Saturation means that, as more nucleons are added to nuclei, the density of the central region remains essentially constant. This is why the nuclear radius is given by $R = r_0 A^{1/3}$ where $r_0 =$ constant and A is the atomic number. So the energy density is approximately a constant. Accordingly, we can write the volume energy of a nucleus as the energy density of symmetric matter at normal density ϵ_0 times the volume. This should be modified by the empirical fact that nuclei with neutron number N close to proton number Z are more tightly bound than their neighbors, altered by the increasing importance of the Coulomb repulsion at higher Z. The repulsion shifts the energy minimum of nuclei with increasing A to those with a greater neutron fraction $(A - Z)/Z = N/Z$. The well-known valley of beta stability emphasizes the preference for isospin symmetry of the underlying nuclear force and the nucleon kinetic energy as shown in Fig. 4.1.

In addition to the above volume contributions to the energy, there will be a surface energy, also repulsive. This contribution arises because nucleons at the surface interact with fewer neighbors and so feel less attraction than those in the interior. Surface energy will be proportional to the surface area. There will also be a repulsive Coulomb energy because of the protons. It can be calculated in the same manner as (3.129).

From the above three contributions, we can write the total mass of a nucleus approximately as

$$M(A, Z) = A\left[\frac{4}{3}\pi r_0^3 \epsilon_0 + a_{\text{sym}}\left(\frac{N - Z}{A}\right)^2\right] + 4\pi r_0^2 A^{2/3} \epsilon_{\text{surf}} + \frac{3}{5}\frac{e^2 Z^2}{r_0 A^{1/3}}. \tag{4.107}$$

This formula is sometimes referred to as the semiempirical mass formula or, with its more recent elaborations, the droplet model of nuclear masses. Subtracting $(A-Z)m_n + Zm_p \approx Am$ would give the total binding energy B. In actual practice there are many additional effects with unknown coefficients. These are incorporated in the best fit of the parameters of the more general formula to thousands of data on nuclear masses [141]. We need not dwell on this. The point is that the binding energy per nucleon B/A is a series in various powers of $1/A$ including the zeroth power. Therefore, certain terms become more important with increasing A, and, in the limit, just the volume term (the constant term in B/A) survives. In this way (based on a wealth of information on finite nuclei) one discovers the binding energy per nucleon of infinite, symmetric, nuclear matter and the symmetry energy coefficient:

$$B/A = -16.3\ \text{MeV}, \qquad a_{\text{sym}} = 32.5\ \text{MeV}\,. \tag{4.108}$$

The radius parameter $r_0 = 1.16$ fm in the relationship between the nuclear radius and its atomic number $R = r_0 A^{1/3}$ is obtained by an analysis of electron–nucleus scattering in terms of density distributions [142]. The equilibrium value of the nucleon number density is related to r_0 by

$$\rho_0 = \left[(4\pi/3)r_0^3\right]^{-1} = 0.153\ \text{fm}^{-3}\,. \tag{4.109}$$

A parameter equivalent to the saturation density is the Fermi momentum common to neutrons and protons in symmetric matter at saturation. Density and Fermi momentum are related through (3.71)

$$\rho_0 = 4\int_0^{k_F} \frac{d\boldsymbol{k}}{(2\pi)^3} = \frac{2k_F^3}{3\pi^2}\,, \tag{4.110}$$

where 4 is the spin–isospin degeneracy of the nucleon momentum states. We find

$$k_F = 1.31\ \text{fm}^{-1}\,. \tag{4.111}$$

In terms of an equation of state $\epsilon(\rho)$, the binding energy per nucleon is related to the equilibrium values of the saturation energy density ϵ_0 and baryon number density ρ_0 by

$$\frac{B}{A} = \left(\frac{\epsilon}{\rho}\right)_0 - m\,. \tag{4.112}$$

The subscript "0" denotes evaluation at the saturation density of nuclear matter and $m = 938.93$ MeV $= 4.7582\ \text{fm}^{-1}$ is the average of the neutron and proton masses. Thus, we learn the energy density at saturation:

$$\epsilon_0 = 141\ \text{MeV/fm}^3\,. \tag{4.113}$$

The binding energy per nucleon and nucleon number density at saturation will serve to fix two coupling constants of the theory. Any theory of matter that is intended to describe neutron stars should be anchored to these minimal constraints. Our first example of a nuclear field theory will do just that (and no more).

We note some of the additional important constraints. In Section 3.6 we have shown that stars must be electrically neutral. This means that neutron stars to first approximation are composed of neutrons. They are therefore highly isospin asymmetric. On the other hand, the short-range nuclear force together with the Fermi energies of the isospin-carrying baryons energetically prefer isospin symmetric configurations. So the constraint of charge neutrality exacts the price of a high isospin energy. Consequently, it is important that the theory of matter should correctly reflect the isospin symmetry energy. That is done by extracting the symmetry energy from the semiempirical mass formula above. From (4.107) the symmetry energy coefficient is related to the equation of state $\epsilon(\rho)$ by

$$a_{\text{sym}} = \frac{1}{2}\left(\frac{\partial^2(\epsilon/\rho)}{\partial t^2}\right)_{t=0}, \qquad t \equiv \frac{\rho_n - \rho_p}{\rho}. \tag{4.114}$$

To evaluate these expressions, the energy density and number density must be expressed in terms of the neutron and proton Fermi momenta k_n and k_p. After evaluation of the expression, they are then set equal to the common value k_F of symmetric matter.

The compression modulus K, which defines the curvature of the equation of state $\epsilon(\rho)/\rho$ at ρ_0, is another important contact with empirical knowledge. Its value will obviously be reflected in the high-density behavior of the equation of state though, of course, not uniquely. The larger the value of K, the more steeply the equation of state will increase with density. The high-density behavior is generally referred to as the "stiffness" or "softness" of the equation of state. These are relative terms referring to whether or not $\epsilon(\rho)$ increases rapidly with ρ. The stiffness will directly influence the maximum mass of the neutron star sequence belonging to the equation of state.

The compression modulus at saturation also enters the mass formula, but the dependence is rather weak. The giant monopole excitation in nuclei (an excitation that corresponds to a collective radial or "breathing" mode) ought to be the most direct measure of this important parameter, though its extraction from experiment is not without its ambiguities. The compression modulus likely lies in the range 200 to 300 MeV [143]–[147], although recent evidence from a large body of nuclear data suggests that a value $K = 234$ MeV is preferred [51]. The compression modulus is related to the equation of state through

$$K = \left[k^2 \frac{d^2}{dk^2}\left(\frac{\epsilon}{\rho}\right)\right]_{k_F} = 9\left[\rho^2 \frac{d^2}{d\rho^2}\left(\frac{\epsilon}{\rho}\right)\right]_{\rho=\rho_0}. \tag{4.115}$$

Finally, the nucleon effective mass in matter is also relevant. It plays a role somewhat like the compression modulus as regards the high-density behavior of the equation of state. This is so because the equation of state will contain, among other terms, a sum of $[k^2 + m^{*2}(k_f)]^{1/2}$ over those nucleon momentum states that

lie below the Fermi momentum k_f at the considered density.[4], The quantity $m^*(k_f)$ is the effective nucleon mass in the medium and (perhaps not surprisingly as we shall see explicitly later) it depends on the Fermi momentum, or equivalently, the density of the matter. Therefore, the above mentioned sum will clearly influence the "stiffness" of the equation of state and hence, as with K, will have a direct bearing on the maximum mass that the equation of state can support against gravity. Our theory should make contact with what is known empirically about K and m^*.

The effective mass at saturation density is not known precisely. According to the particular type of data and its analysis, the effective mass is defined in various ways. The value of the isoscalar component of the mean field can be derived from a nonrelativistic analysis of scattering of neutrons from lead nuclei and is found to lie in the range [148, 149, 150]

$$m_S^*/m \approx 0.74 \text{ to } 0.82\,. \tag{4.116}$$

This is not the "Dirac effective mass" which appears in nuclear field theory. It can be identified approximately as the Landau effective mass [146, 150] which in turn is related to the Dirac effective mass of nuclear field theory through

$$m_S^* \approx m_L^* = \left(\frac{k}{\partial\epsilon(k)/\partial k}\right)_{k_F} = (m^{*2} + k_F^2)^{\frac{1}{2}}\,, \tag{4.117}$$

where

$$m^* \equiv m^*(k_F) \tag{4.118}$$

is the nucleon effective mass m^* (Dirac mass) at saturation density and k_F is the corresponding Fermi momentum. Consequently, the range expected for the Dirac effective mass at saturation density is

$$m^*/m \approx 0.7 \text{ to } 0.8\,. \tag{4.119}$$

A remarkable fact about nuclei (in addition to their being saturated systems) is that, to a good approximation, a nucleus behaves as if it were composed of almost independent nucleons moving in a mean field, despite the strong interaction between them in vacuum. Unlike the situation with atoms (where a massive nucleus provides the Coulomb mean field in which the electrons move) the above property of nuclei by no means follows in an obvious way from the nuclear force. It follows, instead, from an intricate interplay between the Pauli exclusion principle, the strong short-range repulsive part of the interaction between nucleons, and the moderate strength of the long-range attractive part of the interaction [139, 151]. For a two-body system, the long-range attractive part is just strong enough to bind the deuteron, but without a bound excited state.

---

[4]Note that we reserve k_F to denote the Fermi energy at the saturation density of symmetric nuclear matter.

4.6 The $\sigma - \omega$ Model

We introduce nuclear field theory by considering the original version of Johnson and Teller [111], Duerr [112], and Walecka [113]. It is based on the fields of four particles: the nucleons, a scalar meson, and the omega vector meson. The Lagrangian must be a Lorentz scalar, but that in and of itself does not uniquely define the form of the interaction between nucleons and the meson fields. It does, however, commend the so-called Yukawa coupling because, in the static limit, one boson exchange of these mesons leads to a Yukawa potential.

We want the Lagrangian to be a Lorentz scalar. Therefore, the scalar meson is coupled to the baryon *scalar* density $\overline{\psi}\psi$ and the vector meson to the baryon four-current $\overline{\psi}\gamma^\mu\psi$ by contraction. The interaction Lagrangian can therefore be written

$$\mathcal{L}_{\text{int}} = g_\sigma\, \sigma(x)\, \overline{\psi}(x)\psi(x) - g_\omega\, \omega_\mu(x)\, \overline{\psi}(x)\gamma^\mu\psi(x)\,, \tag{4.120}$$

where $x \equiv x^\mu \equiv (t, x, y, z)$. The choice of signs of both terms is arbitrary and made in hindsight so that the mean values of the fields are positive numbers. Now, adding the free Lagrangians for nucleons and mesons, we obtain for the total Lagrangian

$$\begin{aligned}\mathcal{L} = \overline{\psi}\Big[i\gamma_\mu(\partial^\mu + ig_\omega\omega^\mu) - (m - g_\sigma\sigma)\Big]\psi \\ + \tfrac{1}{2}(\partial_\mu\sigma\partial^\mu\sigma - m_\sigma^2\sigma^2) - \tfrac{1}{4}\omega_{\mu\nu}\omega^{\mu\nu} + \tfrac{1}{2}m_\omega^2\omega_\mu\omega^\mu\,.\end{aligned} \tag{4.121}$$

We have introduced dimensionless coupling constants g_σ and g_ω, which together with other couplings to be introduced later, can be determined algebraically in terms of bulk properties of matter as in Section 4.8.1. We always use natural units $\hbar = c = 1$ and it is clear that the meson fields σ and ω have the dimension of mass. We draw attention to the section on units at the end of the chapter.

The Euler–Lagrange equations in the presence of the interactions follow as

$$(\Box + m_\sigma{}^2)\sigma(x) = g_\sigma\, \overline{\psi}(x)\psi(x)\,, \tag{4.122}$$

$$\left(\Box + m_\omega^2\right)\omega_\mu(x) - \partial_\mu\partial^\nu\omega_\nu(x) = g_\omega\, \overline{\psi}(x)\gamma_\mu\psi(x)\,. \tag{4.123}$$

Because of nucleon conservation (the divergenceless of the baryon current (4.84)), we have $\partial^\mu\omega_\mu = 0$ for the massive vector field as in 4.52. The Euler–Lagrange equations for the nucleons are

$$\Big[\gamma_\mu\big(i\partial^\mu - g_\omega\omega^\mu(x)\big) - \big(m - g_\sigma\sigma(x)\big)\Big]\psi(x) \;=\; 0. \tag{4.124}$$

The above three-coupled, nonlinear differential equations are clearly complicated.

We now introduce an approximation known as the *relativistic mean-field approximation.* The system we are interested in is static uniform matter in its ground state. We replace the meson fields by their mean values in this state, $\sigma \to \langle\sigma\rangle$, and $\omega_\mu \to \langle\omega_\mu\rangle$. These mean values are to be computed from the above equations with the mean nucleon source currents on the right side evaluated in the ground state of matter. In static uniform matter, the source currents $\overline{\psi}\psi$ and $\overline{\psi}\gamma^\mu\psi$ are independent

of x. So then are the mean meson fields. As a consequence, the Euler–Lagrange equations (4.7) reduce to the simpler form

$$\begin{aligned} m_\sigma^2 \langle \sigma \rangle &= g_\sigma \langle \overline{\psi} \psi \rangle , \\ m_\omega^2 \langle \omega_0 \rangle &= g_\omega \langle \psi^\dagger \psi \rangle , \\ m_\omega^2 \langle \omega_k \rangle &= g_\omega \langle \overline{\psi} \gamma_k \psi \rangle . \end{aligned} \tag{4.125}$$

We shall discuss shortly how the ground-state expectations of the nucleon currents, $\langle \overline{\psi} \psi \rangle$, etc., can be evaluated.

Instead of renaming the mean meson values, we retain their old names, but now without indicating an x dependence. For the nucleons we have

$$\Big[\gamma_\mu (i \partial^\mu - g_\omega \omega^\mu) - (m - g_\sigma \sigma) \Big] \psi(x) = 0 , \tag{4.126}$$

wherein the *mean* meson fields now appear. Because, in the mean-field approximation of uniform static matter, the nucleon fields satisfy an equation with no x-dependent terms, these fields are momentum eigenstates which we write as

$$\psi(x) = \psi(k) e^{-ik \cdot x} \tag{4.127}$$

where

$$k \cdot x \equiv k_\mu x^\mu = k_0 t - \boldsymbol{k} \cdot \boldsymbol{r} . \tag{4.128}$$

Then we obtain

$$\Big[\gamma_\mu (k^\mu - g_\omega \omega^\mu) - (m - g_\sigma \sigma) \Big] \psi(k) = 0 . \tag{4.129}$$

The quantity in the square bracket is a matrix and ψ is an eight-component spinor (4.88). Comparison with the Dirac equation we encountered earlier suggests the definitions,

$$K^\mu = k^\mu - g_\omega \omega^\mu , \tag{4.130}$$

$$m^\star(\sigma) = m - g_\sigma \sigma . \tag{4.131}$$

It is typical of theories with scalar mesons that the Fermion mass is altered in the above way. We call $m^\star$ the effective mass or sometimes the Dirac effective mass especially when we need to distinguish it from effective masses of nonrelativistic theories. Note that the scalar field acts to reduce the effective nucleon mass.

With the above definitions, the Dirac equation can be rewritten

$$\big(\not{K} - m^\star \big) \psi(K) = 0 . \tag{4.132}$$

The Dirac eigenvalues can be found as usual by rationalizing the Dirac operator. Multiply by $\not{K} + m^\star$, and use the properties of the gamma matrices to find

$$\begin{aligned} (\not{K} + m^\star)(\not{K} - m^\star) &= \not{K}\not{K} - m^{\star 2} = \gamma_\mu K^\mu \gamma_\nu K^\nu - m^{\star 2} \\ &= K^\mu K^\nu \frac{\gamma_\mu \gamma_\nu + \gamma_\nu \gamma_\mu}{2} - m^{\star 2} = K_\mu K^\mu - m^{\star 2} . \end{aligned} \tag{4.133}$$

The result is

$$\big(K_\mu K^\mu - m^{\star 2} \big) \psi(K) = 0 . \tag{4.134}$$

Because the operator has now become a number that multiplies $\psi(K)$ to give zero, that number must be zero. We obtain

$$K_0 = \sqrt{\boldsymbol{K}^2 + m^{*2}}\,. \tag{4.135}$$

Let us denote the timelike component of the four-vector $k \equiv (k^0, \boldsymbol{k})$ by

$$e(\boldsymbol{k}) \equiv k_0(\boldsymbol{k}) = K_0 + g_\omega \omega_0\,. \tag{4.136}$$

Hence the nucleon eigenvalues of 3-momentum $\boldsymbol{k}$ for particle and antiparticle are

$$e(\boldsymbol{k}) = E(\boldsymbol{k}) + g_\omega \omega_0\,, \tag{4.137}$$

$$\overline{e}(\boldsymbol{k}) = E(\boldsymbol{k}) - g_\omega \omega_0\,, \tag{4.138}$$

with

$$E(\boldsymbol{k}) \equiv K_0 = \sqrt{(\boldsymbol{k} - g_\omega \boldsymbol{\omega})^2 + (m - g_\sigma \sigma)^2}\,. \tag{4.139}$$

Now we have the form of the Dirac momentum eigenvalues expressed in terms of the mean meson fields σ and ω^μ. But we must still find their values using the equations of motion (4.125, 4.129). This obviously poses a self-consistency problem because the mean meson fields are given in terms of the ground-state expectation values of the baryon currents whose eigenvalues are given in terms of the mean meson fields themselves. To give full expression to the problem, we have to obtain explicit expressions for the baryon currents appearing in (4.125).

An obvious (but not necessarily economical) means of constructing the ground-state expectation values of the nucleon currents is to construct the nucleon spinors first. This can be done because the Dirac equation has the same form as the free equation; only the four-momentum and mass are shifted by the mean meson field values. Then the currents can be constructed with the spinors by matrix multiplication and summation over occupied nucleon states.

However, there is a more economical way of evaluating the ground-state expectation values that avoids the unnecessary construction of the spinors as an intermediate step. This is the method we shall use. A single-nucleon state is characterized in this theory by the momentum $\boldsymbol{k}$ and the spin and isospin projection which we denote together by κ. Of course, each neutron and proton momentum state can have one of two spin projections $\pm 1/2$. Let us denote by a round bracket the expectation value of an operator in a single-particle state, $(\overline{\psi}\Gamma\psi)_{\boldsymbol{k}\kappa}$. The expectation value of an operator in the ground state of the many-nucleon system is obviously

$$\langle \overline{\psi}\Gamma\psi \rangle = \sum_\kappa \int \frac{d\boldsymbol{k}}{(2\pi)^3} (\overline{\psi}\Gamma\psi)_{\boldsymbol{k}\kappa} \Theta[\mu - e(\boldsymbol{k})]\,, \tag{4.140}$$

where the sum on κ is understood to be over the spin-isospin states of the occupied momentum states and $\Theta(x)$ is a step function that is unity for $x \geq 0$ and zero otherwise. We denote the Fermi energy by μ. We also refer to it as the chemical potential. The ground-state expectation values (4.140) are momentum integrals over the filled states of the single-particle expectations in such momentum states;

the integral is from zero up to that value of $\boldsymbol{k}$ for which the eigenvalues $e(\boldsymbol{k})$ lie below the chemical potential μ, i.e., up to some designated energy.

The above formulation in terms of the three-vector $\boldsymbol{k}$ allows for the Fermi surface prescribed by $e(\boldsymbol{k}) = \mu$ to be nonspherical in momentum space; however, our applications will always involve spherical Fermi surfaces. (Nonspherical Fermi surfaces occur in the theory of pion condensation in a many-body system because of the p-wave interaction [152].)

How are the single-particle expectation values appearing in expression (4.140) to be found? The operator, denoted by Γ, appearing in the integral is generally to be found also in the Dirac Hamiltonian. Use the Dirac equation (4.129), and remember that $\gamma_\mu k^\mu = \gamma_0 k_0 - \boldsymbol{\gamma} \cdot \boldsymbol{k}$. Isolate k^0, and find *the Dirac Hamiltonian*:

$$H_D = \gamma_0 \Big[\boldsymbol{\gamma} \cdot \boldsymbol{k} + g_\omega \gamma_\mu \omega^\mu + m^* \Big] . \tag{4.141}$$

Now, take the expectation in a single-nucleon momentum state as defined above:

$$(\psi^\dagger H_D \psi)_{\boldsymbol{k}\kappa} = K_0(\boldsymbol{k}) = E(\boldsymbol{k}) + g_\omega \omega_0 . \tag{4.142}$$

In the present example, note that the right side is independent of the spin–isospin projection label κ, i.e., the momentum states are degenerate with occupation 4. It need not be so in more complicated applications.

Now take a derivative of the left side of (4.142) with respect to any variable ζ in the Hamiltonian,

$$\frac{\partial}{\partial \zeta}(\psi^\dagger H_D \psi)_{\boldsymbol{k}\kappa} = (\psi^\dagger \frac{\partial H_D}{\partial \zeta} \psi)_{\boldsymbol{k}\kappa} + k_0(\boldsymbol{k}) \frac{\partial}{\partial \zeta}(\psi^\dagger \psi)_{\boldsymbol{k}\kappa} . \tag{4.143}$$

Because $\psi(\boldsymbol{k})$ is an eigenfunction, only the first term on the right survives. Use this result from now on in taking derivatives of (4.142). First take a derivative of the above equation (4.142) with respect to ω_0. This yields, immediately, the normalization

$$(\psi^\dagger \psi)_{\boldsymbol{k}\kappa} = 1 . \tag{4.144}$$

Then from (4.140) we have the baryon density,

$$\rho = \langle \psi^\dagger \psi \rangle = 4 \int_0^{\boldsymbol{k}} \frac{d\boldsymbol{k}}{(2\pi)^3} \Theta[\mu - e(\boldsymbol{k})] . \tag{4.145}$$

This is an expected and trivial result, especially when the Fermi surface is a sphere. Then the Θ function is unity for levels below $e(\boldsymbol{k}) \leq \mu$, and the expression for the density becomes the usual expression.

In like manner, we can compute other expectation values that are not so trivial. Take a derivative with respect to k^i:

$$(\overline{\psi} \gamma^i \psi)_{\boldsymbol{k}\kappa} \equiv \frac{\partial}{\partial k^i} E(\boldsymbol{k}) . \tag{4.146}$$

Hence, the nucleon current is

$$\langle \overline{\psi} \gamma^i \psi \rangle = 4 \int \frac{d\boldsymbol{k}}{(2\pi)^3} \left(\frac{\partial}{\partial k^i} E(\boldsymbol{k}) \right) \Theta(\mu - e(\boldsymbol{k}))$$

$$= 4 \int \frac{dk^i\, dk^j\, dk^k}{(2\pi)^3} \left(\frac{\partial}{\partial k^i} E(\boldsymbol{k}) \right) \Theta(\mu - e(\boldsymbol{k}))$$

$$= 4 \int \frac{dk^j\, dk^k}{(2\pi)^3} \int dE(k^j, k^k) = 0 . \tag{4.147}$$

The integral is over the occupied momentum states (meaning over some volume in the momentum space) which is a sphere if $e(\boldsymbol{k})$ depends only on $|\boldsymbol{k}|$, and otherwise is some other closed region. The integral above vanishes because $E(\boldsymbol{k})$ equals the constant $\mu - g_\omega \omega_0$ everywhere on the boundary of the surface of the region of integration. Therefore, the integral over dE is the difference of two equal numbers. As a consequence of the vanishing of the baryon current (a result intuitively expected inasmuch as we are dealing with the ground state of uniform static matter), we see from the equations of motion that the spatial components ω^i vanish. As a further consequence, the region of occupied momentum space is a sphere. The Dirac eigenvalues can then be written more simply as

$$e(k) = g_\omega \omega_0 + E(k), \qquad E(k) = \sqrt{k^2 + (m - g_\sigma \sigma)^2}\,, \tag{4.148}$$

and the density as

$$\rho \equiv \langle \psi^\dagger \psi \rangle = 4 \int_0^{k_f} \frac{dk}{(2\pi)^3} = \frac{2k_f^3}{3\pi^2} . \tag{4.149}$$

This is sometimes referred to as the *vector* density in contrast to the *scalar* density which we take up next. The vector density is the Lorentz time component of the conserved baryon current (4.85) and is simply the baryon density.

We make a special note here. Because of the isotropy of the momentum space for the ground state just proven, the upper limit on momentum integrals (the Fermi momentum at the desired density) will be denoted just by k and the corresponding density for symmetric nuclear matter given by (4.149). The Fermi energy is therefore given by $\mu \equiv e(k)$.

Finally, we need the scalar density $\langle \overline{\psi} \psi \rangle$. Take a derivative of (4.142) with respect to m:

$$(\overline{\psi} \psi)_{\boldsymbol{k}_K} = \frac{\partial E(k)}{\partial m} . \tag{4.150}$$

The result is

$$\rho_s \equiv \langle \overline{\psi} \psi \rangle = \frac{2}{\pi^2} \int_0^{k_f} k^2 dk \frac{m - g_\sigma \sigma}{\sqrt{k^2 + (m - g_\sigma \sigma)^2}} . \tag{4.151}$$

The above technique is quite powerful because it can be used to evaluate the expectation value of any operator that appears in the Dirac Hamiltonian without going through the intermediate step of constructing the Dirac spinors. In some applications the explicit construction is awkward.

Assembling the results just obtained, we find that the equations of motion now have the explicit forms

$$g_\sigma \sigma = \left(\frac{g_\sigma}{m_\sigma}\right)^2 \frac{2}{\pi^2} \int_0^{k_f} k^2 dk \frac{m - g_\sigma \sigma}{\sqrt{k^2 + (m - g_\sigma \sigma)^2}}, \tag{4.152}$$

$$g_\omega \omega_0 = \left(\frac{g_\omega}{m_\omega}\right)^2 \rho, \tag{4.153}$$

$$\omega_k = 0. \tag{4.154}$$

The last two are trivial, but the first expresses a self-consistency condition on the scalar field because it appears in a transcendental equation. It will be noticed that, regarded as equations in $g_\sigma \sigma$ and $g_\omega \omega$, the solutions depend on the coupling constants and meson masses only through the ratios g_σ / m_σ and g_ω / m_ω. This is true in general at the mean-field level for infinite nuclear matter. It is also true for the rho meson which we discuss shortly. Only for finite nuclei do the field equations and nuclear properties become dependent on the individual values of coupling constants and meson masses. These two ratios of coupling constants to meson masses (and others that we encounter later) may be taken as the parameters of the theory. They should be chosen so that the saturation density and binding per nucleon of the theory are in accord with the empirical values discussed in Section 4.5.

The schematic behavior of the solution $g_\sigma \sigma$ of (4.152) is easy to discern. At low nucleon density where k is small, the integral must be small and tend to zero. In fact it is easy to see that the scalar density approaches the nucleon density ρ for small k or ρ. At the other limit, as the density or k increases, the solution for $g_\sigma \sigma$ increases. But if it approaches m, the right side will become small, even for large k. So, at high density, the solution approaches but does not reach m. More precisely,

$$g_\sigma \sigma \to m \left(\frac{g_\sigma k}{m_\sigma \pi}\right)^2 \left[1 + \left(\frac{g_\sigma k}{m_\sigma \pi}\right)^2\right]^{-1}. \tag{4.155}$$

Therefore, the effective mass $m^* = m - g_\sigma \sigma$ has the vacuum value m at small density and it goes to zero in the limit at high density. The fact that the scalar density can be approximated by the density is useful in numerically solving the theory.

In the above expression for the eigenvalue (4.148), we can see the roles played by the scalar and vector mesons. The Lorentz time component of the vector meson shifts the eigenvalue of given k to ever higher energy as the density increases (4.153), whereas the scalar meson tends to reduce it by reducing the effective mass as the nucleon density increases from zero. In consequence (as we shall see), there is a density at which the energy per nucleon becomes a minimum. That density is the equilibrium or *saturation density*, and, from the energy density at that point, we can find the saturation binding per nucleon through (4.112).

To compute the equation of state, we turn to the energy-momentum tensor (4.27) whose expectation value in the rest frame of the matter is diagonal (2.47) and has

as elements the energy density and the pressure [153]. Using the Lagrangian of the present theory (4.121), we find

$$\begin{aligned} \epsilon &= -\langle \mathcal{L} \rangle + \langle \overline{\psi} \gamma_0 k_0 \psi \rangle , \\ p &= \langle \mathcal{L} \rangle + \frac{1}{3} \langle \overline{\psi} \gamma_i k_i \psi \rangle , \end{aligned} \tag{4.156}$$

where we have used $i \partial_\nu \psi = k_\nu \psi$ and the fact that the meson fields are spacetime-independent. (The factor 1/3 appears in the above equation for p because each of the three diagonal spacelike components of the energy-momentum tensor involves the corresponding $\gamma_i k_i$ (i unsummed). By summing these equal diagonal elements, we have to divide by three.) Employing the equations of motion for the Dirac field, the term in that field drops out, and we have simply

$$\langle \mathcal{L} \rangle = -\tfrac{1}{2} m_\sigma^2 \sigma^2 + \tfrac{1}{2} m_\omega^2 \omega_0^2 . \tag{4.157}$$

The second term in ϵ appearing in (4.156) is the contribution of the occupied nucleon momentum states each of whose eigenvalues we derived above. From (4.136, 4.140, 4.148) we have

$$\begin{aligned} \langle \overline{\psi} \gamma_0 k_0 \psi \rangle &= \frac{2}{\pi^2} \int_0^{k_f} k^2 \, dk \, e(k) \\ &= \frac{2}{\pi^2} \int_0^{k_f} k^2 \, dk \Big[g_\omega \omega_0 + \sqrt{k^2 + (m - g_\sigma \sigma)^2} \Big] \\ &= g_\omega \omega_0 \rho + \frac{2}{\pi^2} \int_0^{k_f} k^2 \, dk \sqrt{k^2 + (m - g_\sigma \sigma)^2} \\ &= m_\omega^2 \omega_0^2 + \frac{2}{\pi^2} \int_0^{k_f} k^2 \, dk \sqrt{k^2 + (m - g_\sigma \sigma)^2} . \end{aligned} \tag{4.158}$$

The equation of motion for ω_0 (4.153) and the expression of the baryon density in terms of k were used to rewrite the first term. To evaluate the remaining expectation, we have

$$(\overline{\psi} \gamma \psi)_{\boldsymbol{k}_K} = \frac{\partial E(\boldsymbol{k})}{\partial \boldsymbol{k}} , \tag{4.159}$$

whence

$$\langle \overline{\psi} \gamma \cdot \boldsymbol{k} \psi \rangle = \frac{2}{\pi^2} \int_0^{k_f} \frac{k^4}{\sqrt{k^2 + (m - g_\sigma \sigma)^2}} \, dk . \tag{4.160}$$

Now, assemble the contributions to the energy density and pressure,

$$\epsilon = +\tfrac{1}{2} m_\sigma^2 \sigma^2 + \tfrac{1}{2} m_\omega^2 \omega_0^2 + \frac{2}{\pi^2} \int_0^{k_f} \sqrt{k^2 + (m - g_\sigma \sigma)^2} \, k^2 \, dk . \tag{4.161}$$

The pressure is given by

$$p = -\tfrac{1}{2} m_\sigma^2 \sigma^2 + \tfrac{1}{2} m_\omega^2 \omega_0^2 + \frac{1}{3} \frac{2}{\pi^2} \int_0^{k_f} \frac{k^2}{\sqrt{k^2 + (m - g_\sigma \sigma)^2}} k^2 \, dk . \tag{4.162}$$

In both of these expressions, the first terms are contributions from the meson fields whose mean values are given above, and the integrals are over the occupied nucleon momentum states. The equation of state is here in the form $\epsilon = \epsilon(\rho)$, $p = p(\rho)$ because k, σ, and ω are in that form. If desired, ρ could be eliminated numerically to yield $p = p(\epsilon)$ or its inverse. All of the integrals can be expressed in closed form (Section 3.9.2).

We have seen that $g_\sigma \sigma$ is bounded by the nucleon mass, whereas, according to (4.153), the vector field grows as the baryon density. Because $\rho \sim k^3$, the vector term in both ϵ and p dominate at high density, and $p \to \epsilon$ from below. A disturbance of the medium propagates at speed $(dp/d\epsilon)^{1/2}$ [154], so the theory is causal [155].

The above explicit formula for the pressure was found using the energy-momentum tensor. One might wonder how it accords with the definition, $p = -\partial E/\partial V$. Divide both E and V (volume) by conserved particle number N. Then find

$$p = \rho^2 \frac{\partial(\epsilon/\rho)}{\partial \rho} . \tag{4.163}$$

One can prove algebraically that the above operation yields p in the explicit form written. Clearly, it is more advantageous to have explicit algebraic expressions than to have to take a numerical derivative in computing an equation of state.

The expressions for the equation of state are now at hand. To evaluate ϵ and p as functions of nucleon density ρ, we must solve (4.152) numerically, say for a set of values of k. Because the $(\sigma - \omega)$ theory has two parameters, the saturation density and binding energy per nucleon can be fitted exactly. The other relevant parameters do not agree well with the empirical values noted earlier. In particular, the compression modulus computed for the equation of state at saturation is $K \approx$ 550 MeV, roughly a factor of two times larger than it should be according to the empirical range discussed in Section 4.5. The Dirac effective nucleon mass at saturation is $m^*/m \equiv m - g_\sigma \sigma_0 \approx 0.5$. This is small and in poor agreement with the empirical range (4.119). Both of these properties affect the high-density behavior of the equation of state and in the same direction. The simple $\sigma - \omega$ model has an extremely stiff equation of state.

Moreover, the symmetry energy coefficient is in poor accord with observation. After some calculation, one finds that the symmetry energy coefficient is related to the equation of state (4.114) by

$$a_{\text{sym}} = \frac{k_F^2}{6(k_F^2 + m^{*2})^{1/2}} . \tag{4.164}$$

The derivation follows along the lines of Section 4.9. In our discussion of nuclear matter properties, we saw that the normal nuclear matter density implies $k_F = 1.31$ fm^{-1} and that the effective mass at saturation density falls within a fairly narrow range. In particular we take $m^* = 0.75m = 3.5686$ fm^{-1}. This yields $a_{\text{sym}} = 14.8$ MeV compared to an empirical value of 32.5 MeV.

In consequence of the above deficiencies, the model is not expected to extrapolate well to high density in either symmetric or asymmetric matter of neutron stars. Moreover, it yields a weakly bound state for pure neutron matter for which there is no evidence. (In this connection, see also Section 4.13.)

The main merit of the model from our point of view is that it has provided the opportunity of introducing, in a simple context, the techniques that will be employed in improvements to nuclear field theory. We are now in a position to take them up.

4.7 Stationarity of Energy Density

From results obtained above we can write the energy density as

$$\epsilon = \tfrac{1}{2}m_\sigma^2\sigma^2 - \tfrac{1}{2}m_\omega^2\omega_0^2 + \frac{2}{\pi^2}\int_0^{k_f}\left[g_\omega\omega_0 + \sqrt{k^2 + (m - g_\sigma\,\sigma)^2}\right]k^2\,dk\,. \tag{4.165}$$

Take the derivative with respect to ω_0 for fixed baryon density ρ (or, equivalently, fixed k). We immediately get the field equation for ω_0, namely, (4.153). Similarly for the scalar field. So the field equations are the conditions that the energy density be stationary at fixed baryon density:

$$\left(\partial\epsilon/\partial\omega_0\right)_{k=\text{const}} = \left(\partial\epsilon/\partial\sigma\right)_{k=\text{const}} = 0\,. \tag{4.166}$$

4.8 Model with Scalar Self-Interactions

We have seen that a field theory with only two meson fields, a scalar and vector, can yield the saturation phenomenon characteristic of nuclear matter and nuclei. Because it reduces the effective nucleon mass, the scalar meson contributes a reduction in the energy per nucleon near saturation, and the vector meson contributes repulsion. The repulsion grows with density whereas the attraction saturates so that a balance is reached at which the binding energy is a minimum. This is the equilibrium or saturation point that occurs at the saturation density and binding energy. However, other properties of the model—the compression modulus, the effective nucleon mass and the symmetry energy—were in poor agreement with the empirical values.

Here we study an extension of the theory due to Boguta and Bodmer [156], the main purpose of which is to bring the compression modulus and nucleon effective mass at saturation under control. (For another approach see [157].) Self-interactions of the scalar field are introduced:

$$U(\sigma) = \tfrac{1}{3}bm(g_\sigma\sigma)^3 + \tfrac{1}{4}c(g_\sigma\sigma)^4\,, \tag{4.167}$$

where m is a nominal nucleon mass and is introduced only to make the constants b and c dimensionless; m is taken throughout in this formula to be 938 MeV. Adding

U to the previous Lagrangian we have,

$$\mathcal{L} = \overline{\psi}\Big[i\gamma_\mu(\partial^\mu + ig_\omega\omega^\mu) - (m - g_\sigma\sigma)\Big]\psi + \tfrac{1}{2}(\partial_\mu\sigma\partial^\mu\sigma - m_\sigma^2\sigma^2)$$
$$- \tfrac{1}{4}\omega_{\mu\nu}\omega^{\mu\nu} + \tfrac{1}{2}m_\omega^2\omega_\mu\omega^\mu - \tfrac{1}{3}bm(g_\sigma\sigma)^3 - \tfrac{1}{4}c(g_\sigma\sigma)^4 . \tag{4.168}$$

The Euler–Lagrange equation for the scalar field is now

$$g_\sigma\sigma = \left(\frac{g_\sigma}{m_\sigma}\right)^2\left[\frac{2}{\pi^2}\int_0^{k_f} k^2dk\frac{m - g_\sigma\sigma}{\sqrt{k^2 + (m - g_\sigma\sigma)^2}}\right.$$
$$\left. - \; bm(g_\sigma\,\sigma)^2 - \; c(g_\sigma\,\sigma)^3\right]. \tag{4.169}$$

The other field equations would be unaffected by the addition of $U(\sigma)$ to $\mathcal{L}$. We reproduce them here for completeness:

$$g_\omega\omega_0 = \left(\frac{g_\omega}{m_\omega}\right)^2\rho\,, \tag{4.170}$$

$$m_\omega^2\omega_k = 0\,, \tag{4.171}$$

$$[\gamma_\mu(k^\mu - g_\omega\omega^\mu) - (m - g_\sigma\sigma)]\psi(k) \;=\; 0\,. \tag{4.172}$$

The (Dirac) effective mass, as before, is

$$m^\star(\sigma) = m - g_\sigma\sigma\,, \tag{4.173}$$

with $m^\star \equiv m^\star(\sigma_{\rm sat})$ denoting its value at saturation density. The Dirac momentum eigenvalues are of the same form as before (4.148).

As seen in the earlier result (4.156), the energy density and pressure have contributions $\mp\langle\mathcal{L}\rangle$ so the modifications to the previous results for energy density and pressure are $\pm U(\sigma)$:

$$\epsilon = \tfrac{1}{3}bm(g_\sigma\sigma)^3 + \tfrac{1}{4}c(g_\sigma\sigma)^4 + \tfrac{1}{2}m_\sigma^2\sigma^2 + \tfrac{1}{2}m_\omega^2\omega_0^2$$
$$+ \frac{2}{\pi^2}\int_0^{k_f}\sqrt{k^2 + (m - g_\sigma\sigma)^2}\,k^2\,dk\,, \tag{4.174}$$

$$p = -\tfrac{1}{3}bm(g_\sigma\sigma)^3 - \tfrac{1}{4}c(g_\sigma\sigma)^4 - \tfrac{1}{2}m_\sigma^2\sigma^2 + \tfrac{1}{2}m_\omega^2\omega_0^2$$
$$+ \frac{1}{3}\frac{2}{\pi^2}\int_0^{k_f}\frac{k^4\,dk}{\sqrt{k^2 + (m - g_\sigma\sigma)^2}}\,. \tag{4.175}$$

Note that σ depends on k_f or equivalently on the density at which ϵ is sought through (4.169). (All momentum integrals of the theory can be found in standard tables [64] and as quoted in Section (3.9.2), but for display, the formulae are shorter and more transparent in meaning when left as integrals.)

In deriving the above expression, the field equation of the rho meson was used with the result

$$\tfrac{1}{2}m_\omega{}^2\omega_0^2 = \tfrac{1}{2}\left(\frac{g_\omega}{m_\omega}\right)^2\rho^2\,. \tag{4.176}$$

What is particularly interesting about the above extension of the previous $(\sigma-\omega)$ model is that there are two additional coupling constants. This allows the values of the two additional properties of symmetric nuclear matter, the compression modulus K and the effective nucleon mass m^* at saturation, to be reproduced by the theory. As explained previously, both are important as concerns the high-density behavior of the equation of state.

4.8.1 *Algebraic determination of the coupling constants*

It is perhaps surprising that the four coupling constants g_σ/m_σ, g_ω/m_ω, b, and c, can be found algebraically in terms of the four empirical quantities ρ, B/A, K, and m^* at nuclear saturation. While the algebra is more involved than is worth reproducing here in detail, we indicate the necessary steps and results because the existence of an algebraic solution for the couplings makes the theory especially well defined in terms of the nuclear bulk properties. So far as we are aware, this fact has not been known before.

First, using the expression for the energy density, take a derivative with respect to ρ to find

$$\frac{d\epsilon}{d\rho} = \frac{d\sigma}{d\rho}\left(m_\sigma^2\sigma + \frac{dU}{d\sigma} - g_\sigma\frac{2}{\pi^2}\int_0^k \frac{m-g_\sigma\sigma}{\sqrt{k^2+(m-g_\sigma\sigma)^2}}k^2\,dk\right)$$
$$+ g_\omega\omega_0 + \sqrt{k^2+(m-g_\sigma\sigma)^2}\,. \tag{4.177}$$

The quantity in the parenthesis vanishes identically by virtue of the scalar field equation (4.169). So the derivative $d\epsilon/d\rho$ at saturation is equal to the Fermi energy which we have called μ. We have

$$\mu \equiv g_\omega\omega_0 + \sqrt{k^2+m^{*2}} = \frac{d\epsilon}{d\rho}\,, \tag{4.178}$$

where all quantities, ω_0, ρ, k, $m^*, \ldots$, are evaluated at saturation density. This will be the case throughout the remainder of this derivation. At saturation, the function ϵ/ρ has a minimum as a function of ρ. So we require

$$0 = \frac{d}{d\rho}\frac{\epsilon}{\rho} = \frac{1}{\rho}\left(\frac{d\epsilon}{d\rho} - \frac{\epsilon}{\rho}\right) \quad \text{(at saturation)}\,, \tag{4.179}$$

from which we find

$$\frac{\epsilon}{\rho} = \frac{d\epsilon}{d\rho} = \mu \quad \text{(at saturation)}\,. \tag{4.180}$$

So, from the relations developed,

$$m + \frac{B}{A} \equiv \frac{\epsilon}{\rho} = \left(\frac{g_\omega}{m_\omega}\right)^2\rho + \sqrt{k^2+m^{*2}} \quad \text{(at saturation)}\,. \tag{4.181}$$

The Fermi momentum at saturation k is related to the density in the usual way:

$$\rho = 2k^3/(3\pi^2)\,. \tag{4.182}$$

Next take a second derivative of ϵ/ρ using (4.179), and find at saturation density

$$\frac{d^2}{d\rho^2}\frac{\epsilon}{\rho} = \frac{1}{\rho}\frac{d^2\epsilon}{d\rho^2} = \frac{1}{\rho}\frac{d\mu}{d\rho}\,. \tag{4.183}$$

We have seen in (4.115) an expression for the compression modulus and are now able to write

$$K = 9\rho\frac{d\mu}{d\rho}\,. \tag{4.184}$$

From the expression for μ above, we have

$$\frac{d\mu}{d\rho} = \left(\frac{g_\omega}{m_\omega}\right)^2 + \frac{1}{E(k)}\left(k\frac{dk}{d\rho} - m^\star g_\sigma\frac{d\sigma}{d\rho}\right), \tag{4.185}$$

where

$$E(k) = \sqrt{k^2 + m^{\star 2}}\,, \tag{4.186}$$

as defined before. To evaluate the derivative of σ, use the field equation. Substitute the result in the above equation and that result in the above expression for K at saturation. After some calculation we obtain

$$K = \left(\frac{g_\omega}{m_\omega}\right)^2\frac{6k^3}{\pi^2} + \frac{3k^2}{E(k)} \tag{4.187}$$

$$- \frac{6k^3}{\pi^2}\left[\frac{m^\star}{E(k)}\right]^2\left(\frac{g_\sigma}{m_\sigma}\right)^2\left\{1 + \left(\frac{g_\sigma}{m_\sigma}\right)^2\left[\frac{d^2U}{d(g_\sigma\sigma)^2} + \frac{2}{\pi^2}\int_0^k\frac{k^4\,dk}{E^3(k)}\right]\right\}^{-1}.$$

Note that we know the scalar field strength at saturation, $g_\sigma\,\sigma = m - m^\star$ because $m^\star$ is one of the empirical data whose range is known. So the above equation has only (g_σ/m_σ), b, and c as unknowns. Two additional equations in the same unknowns are the scalar field equation (4.169) and the equation for the energy density (4.174) whose value is known from

$$\epsilon = \rho(m + B/A), \qquad B/A = -16.3\ \text{MeV}\,, \tag{4.188}$$

as in (4.108, 4.109). So we have three equations in the three unknowns just mentioned which are all of the form

$$\alpha_i(m_\sigma/g_\sigma)^2 + \beta_i b + \gamma_i c = \delta_i, \qquad i = 1, 2, 3\,. \tag{4.189}$$

In each case the coefficients α, β, γ, δ are calculable constants given in terms of the saturation properties. We note that all of the momentum integrals appearing in the coefficients can be evaluated in closed form by reference to a table of standard integrals [64] whose expressions are quoted in (3.9.2). Thus all four couplings can be determined *algebraically* from the four nuclear saturation properties after which the equation of state for symmetric nuclear matter can be computed.

We show how to express the solution in one possible way. To yield numbers, all quantities must be expressed in a consistent set of units. In this connection a note on dimensions that are useful in nuclear physics is provided in Section 4.14. Thus

energies and momenta will be expressed in inverse fermis. The vector coupling is obtained simply from (4.181):

$$\left(\frac{g_\omega}{m_\omega}\right)^2 = \frac{m + B/A - \sqrt{k^2 + m^{*2}}}{\rho} . \tag{4.190}$$

All quantities on the right side are provided by the saturation properties of nuclear matter. The coefficients in (4.189) are

$$\begin{aligned}
\alpha_1 &= K - \left(\frac{g_\omega}{m_\omega}\right)^2 \frac{6k^3}{\pi^2} - \frac{3k^2}{\sqrt{k^2 + m^{*2}}} , \\
\beta_1 &= 2(m - m^*)m\alpha_1 , \\
\gamma_1 &= 3(m - m^*)^2\alpha_1 , \\
\delta_1 &= -\alpha_1 I_1 - \frac{6k^3}{\pi^2}\left(\frac{m^*}{\sqrt{k^2 + m^{*2}}}\right)^2 ,
\end{aligned} \tag{4.191}$$

$$\begin{aligned}
\alpha_2 &= \tfrac{1}{2}(m - m^*)^2 , \\
\beta_2 &= \tfrac{1}{3}m(m - m^*)^3 , \\
\gamma_2 &= \tfrac{1}{4}(m - m^*)^4 , \\
\delta_2 &= \rho(m + B/A) - I_2 - \tfrac{1}{2}\left(\frac{g_\omega}{m_\omega}\right)^2 \rho^2 ,
\end{aligned} \tag{4.192}$$

$$\begin{aligned}
\alpha_3 &= m - m^* , \\
\beta_3 &= m(m - m^*)^2 , \\
\gamma_3 &= (m - m^*)^3 , \\
\delta_3 &= I_3 .
\end{aligned} \tag{4.193}$$

For convenience, we have expressed the integrals in algebraic form and defined

$$\begin{aligned}
x &= k/m^* , \\
t &= \sqrt{1 + x^2} , \\
I_1 &= \frac{2}{\pi^2} m^{*2}[\tfrac{1}{2}xt + \frac{x}{t} - \tfrac{3}{2}\ln(x + t)] , \\
I_2 &= \frac{2}{\pi^2} m^{*4}\tfrac{1}{4}[xt^3 - \tfrac{1}{2}xt - \tfrac{1}{2}\ln(x + t)] , \\
I_3 &= \frac{2}{\pi^2} m^{*3}\tfrac{1}{2}[xt - \ln(x + t)] .
\end{aligned} \tag{4.194}$$

The solution can be expressed as

$$c = \frac{(\alpha_3\beta_1 - \alpha_1\beta_3)(\alpha_2\delta_1 - \alpha_1\delta_2) - (\alpha_2\beta_1 - \alpha_1\beta_2)(\alpha_3\delta_1 - \alpha_1\delta_3)}{(\alpha_3\beta_1 - \alpha_1\beta_3)(\alpha_2\gamma_1 - \alpha_1\gamma_2) - (\alpha_2\beta_1 - \alpha_1\beta_2)(\alpha_3\gamma_1 - \alpha_1\gamma_3)} ,$$

$$b = \frac{(\alpha_2\delta_1 - \alpha_1\delta_2) - (\alpha_2\gamma_1 - \alpha_1\gamma_2)c}{\alpha_2\beta_1 - \alpha_1\beta_2} ,$$

$$\left(\frac{g_\sigma}{m_\sigma}\right)^2 = \frac{\alpha_1}{\delta_1 - \gamma_1 c - \beta_1 b}. \tag{4.195}$$

Looking ahead to the section on the isospin force and the symmetry energy, we can write the coupling of the rho meson (4.218) as

$$\left(\frac{g_\rho}{m_\rho}\right)^2 = \frac{8}{\rho}\left[a_{\text{sym}} - \frac{k^2}{6\sqrt{k^2 + m^{*2}}}\right]. \tag{4.196}$$

Notice that the three ratios g/m have the dimension of fermis and b and c are dimensionless.

The five coupling constants of the theory, g_σ/m_σ, g_ω/m_ω, g_ρ/m_ρ, b, and c are defined algebraically in terms of the five saturation properties of symmetric nuclear matter, B/A, ρ_0, a_{sym}, K, and m^*. The field equations of the same Lagrangian with the couplings so obtained can be solved with subsidiary constraints appropriate to charge-neutral, beta-stable matter suitable for neutron star structure as described in Chapter 5. The algebraic connection makes it convenient to explore the effects of uncertainties in the saturation properties on neutron star structure (albeit in the particular theory of this chapter).

4.8.2 *Symmetric nuclear matter equation of state*

In the discussion of nuclear matter properties, it was found that the binding energy and saturation density are well known, but that the compression modulus K and the value of the nucleon effective mass m^* at saturation are known only within a range. It is interesting to see the uncertainty in the equation of state of symmetric nuclear matter that corresponds to the uncertainty in the above two data. This is shown in Fig. 4.2. Considering that it is the binding energy per nucleon that is shown (measured in reference to the nucleon mass (4.112)), the uncertainty does not seem too great, although we shall see that it is reflected in a considerable range in neutron star masses and baryon populations.

As expected, the higher the compression modulus, the steeper (or stiffer) the equation of state at high density. In contrast, the smaller the value of the effective nucleon mass at saturation, the stiffer the equation of state.

4.8.3 *Negative self-interaction*

The coupling constants corresponding to a selection of nuclear matter properties in the range determined by experiment are shown in Table 4.4. The constant c is negative for several entries. From the expression for the energy density, this permits the energy to become unbounded from below for a large enough scalar field. This would certainly be a fatal problem for a quantum field theory. Some authors consider this unacceptable even for an effective theory. We take the view that the theory is an effective theory of composite particles, not of fundamental ones. Further, the field equations provide an equation of state that is well behaved in the density region for which a theory based on composite hadrons is plausible.

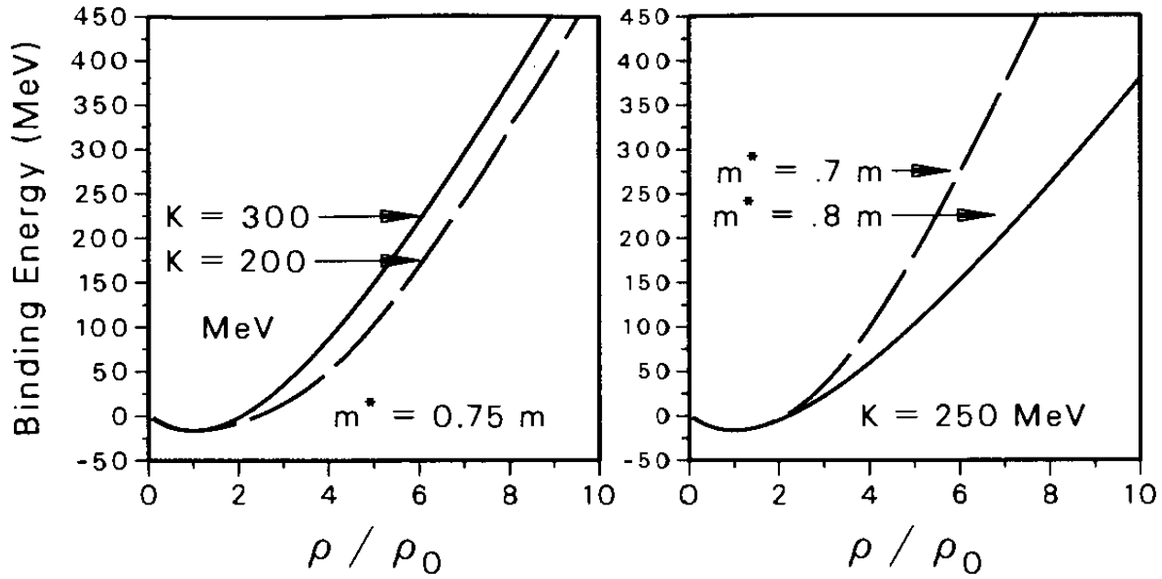

FIGURE 4.2. Equation of state for symmetric nuclear matter for two values of K at fixed m^* and vice versa. The range of both properties is within the experimental bounds.

By choosing the coupling constants so that the saturation properties of nuclear matter are well reproduced by theory, a reasonable behavior of the equation of state is assured in the vicinity of saturation. By continuity, a plausible extrapolation in density and isospin density can also be made when the coupling constants are chosen as above to describe the important properties of nuclear matter at saturation. We shall therefore be interested in the behavior of the theory as a function of density along the trajectory in the field variables that are specified by the Euler–Lagrange equations.

It is evident from Fig. 4.2 that, for the small negative values corresponding to the combinations of matter properties considered realistic, the equation of state is well behaved, even at ten times saturation density. This is certainly at or beyond the range of validity of any theory or model based on (composite) hadrons. However, whenever negative c is encountered, the equation of state should be checked for normal behavior in the interesting region from zero to a few times nuclear density. In the corresponding neutron star models, as we shall see in the following chapters, the central density of even the limiting mass star does not extend as high as ten times the saturation density of nuclei.

4.9 Introduction of Isospin Force

It was seen above how the four properties of nuclear matter at saturation can be accounted for in the theory by adding self-interaction terms for the scalar field. The compression modulus and effective mass are especially relevant to the high-density extrapolation. The binding energy and saturation density serve to normalize the equation of state. Because we wish to have an equation of state for neutron star matter, the theory must be extended to incorporate an isospin restoring interaction, that is, a component in the nuclear interaction that yields an effect such as seen in the empirical mass formula (4.107).

TABLE 4.4. Coupling constants that yield binding $B/A = -16.3$ MeV, saturation density $\rho_0 = 0.153\ \text{fm}^{-3}$, and symmetry energy coefficient, $a_{\text{sym}} = 32.5$ MeV for saturated nuclear matter with the compression K and effective mass m^* listed below.

K MeV	m^*/m	$(g_\sigma/m_\sigma)^2$ fm^2	$(g_\omega/m_\omega)^2$ fm^2	$(g_\rho/m_\rho)^2$ fm^2	b $\times 100$	c $\times 100$
200	0.70	12.684	7.148	4.410	0.5610	−0.6986
200	0.75	11.299	5.696	4.656	0.8784	−1.0098
200	0.80	9.926	4.233	4.876	1.4602	−1.2412
250	0.70	12.230	7.148	4.410	0.4312	−0.4103
250	0.75	10.727	5.696	4.656	0.6275	−0.3409
250	0.80	9.134	4.233	4.876	0.8804	0.6917
300	0.70	11.785	7.148	4.410	0.2948	−0.1071
300	0.75	10.177	5.696	4.656	0.3601	0.3722
300	0.80	8.403	4.233	4.876	0.2480	2.7997

The expression for the energy density (4.174) taken with (4.170) suggests the solution. The vector meson has as its source the (vector) nucleon density, and the energy density is quadratic in this density. We need to introduce a meson that has as its source the 3-component of isospin. As a result we expect a term in the energy density that is quadratic in the deviation from isospin symmetry, or in other words, that is quadratic in the 3-component of the isospin density of the medium.

We have encountered the rho meson in (4.55), a triplet of mesons of the same mass and charges (0, ± 1), which form an isospin triplet with isospin current (4.63). We need to couple this triplet to the isospin of the nucleon given by (4.93) in such a way that a scalar is formed. It also has to be done in such a way as to involve the total conserved isospin current of the Lagrangian.

Recalling the isospin current of nucleon and rho fields (4.93 4.63), we tentatively consider the sum of these two as the isospin current of the combined theory and add an interaction term $\boldsymbol{\rho}_\mu \cdot \boldsymbol{I}^\mu$ to the Lagrangian. However, the contribution of the rho meson to this current contains the derivative of the field, and, from the general expression of the Noether current (4.13), this would itself make a contribution to the current. So the rho meson must contribute an additional piece as a result of its interaction with the isospin current. Let us see what it is.

For this purpose we need only consider the rho meson contribution to the current for which the interaction Lagrangian is

$$\mathcal{L}_{\text{int}} = -g_\rho \boldsymbol{\rho}^\nu \cdot (\boldsymbol{\rho}^\mu \times \boldsymbol{\rho}_{\nu\mu}) = -g_\rho (\boldsymbol{\rho}^\nu \times \boldsymbol{\rho}^\mu) \cdot \boldsymbol{\rho}_{\nu\mu} . \tag{4.197}$$

Now use (4.13) to compute the contribution of this piece of $\mathcal{L}$ to the current, and find $2g_\rho(\boldsymbol{\rho}^\nu \times \boldsymbol{\rho}^\mu) \times \boldsymbol{\rho}_\mu$. So the total conserved isospin current is

$$\boldsymbol{I}^\nu = \tfrac{1}{2}\overline{\psi}\gamma^\nu \boldsymbol{\tau}\psi + \boldsymbol{\rho}_\mu \times \boldsymbol{\rho}^{\nu\mu} + 2g_\rho(\boldsymbol{\rho}^\nu \times \boldsymbol{\rho}^\mu) \times \boldsymbol{\rho}_\mu . \tag{4.198}$$

Correspondingly, the interaction part of the Lagrangian is

$$\mathcal{L}_{\text{int}} = -g_\rho \boldsymbol{\rho}_\nu \cdot \boldsymbol{I}^\nu . \tag{4.199}$$

(The Lagrangian will now involve the square of the coupling constant as in the case of the coupling of a scalar field to the electromagnetic.) The above interaction will modify the Dirac equation and the free equation of the rho meson. The modification of the Dirac equation is the addition of the term

$$\frac{\partial \mathcal{L}_{\text{int}}}{\partial \overline{\psi}} = -\frac{g_\rho}{2}\gamma_\nu \boldsymbol{\rho}^\nu \cdot \boldsymbol{\tau}\psi \,. \tag{4.200}$$

This will alter the eigenvalues in a way analogous to that of the vector-isoscalar (omega) meson.

Now we remark that the presence of any field costs energy. Only those fields that will have nonvanishing mean values in the ground state of matter at a given density must be there. For example, in matter of a given baryon density, the σ and ω_0 fields must have finite mean values because they are solutions to equations with nonvanishing baryon densities as sources (4.169, 4.170). But a vanishing mean field is a possible solution to the free field equation, and thereby the energy is lowered. Otherwise there would be a positive term of the form $(\frac{1}{2})m_\phi^2\phi^2$ present in the energy density. So a nonvanishing baryon density requires the presence of those meson fields which are coupled to the various baryon densities (scalar, vector, isovector . . .), but the condition that the matter be in its ground state at any prescribed baryon density assures that all other meson fields must vanish.

Now apply this reasoning to the rho meson. The ground state is assumed to be a degenerate fermion state with eigenvalues modified by the mean meson fields encountered earlier. These momentum states of neutron and proton are filled pairwise to the Fermi level, so the ground state has definite charge, spin, and parity. Because the first two components of the isospin vector $\boldsymbol{\rho}$ can be written as a combination of the raising and lowering operators for charged rho mesons (4.57), their (diagonal) ground-state expectation values vanish.

The implications of the foregoing remarks are severalfold: (1) Only the isospin 3-component of the $\boldsymbol{\rho}^\mu$ field has finite mean value, i.e., the neutral rho meson ρ_3^μ. (2) The Lorentz three-current part must vanish in the static ground state of matter, just as for the omega meson, leaving only ρ_3^0. (The subscript is for the 3-component of isospin and the superscript is the Lorentz time component.) (3) Although formally the isospin current is (4.198), all that survives as a result of the above conditions is the nucleon contribution. As a result, the equations for the mean values of the rho meson and the Dirac equation are

$$g_\rho \rho_3^0 = \tfrac{1}{2}\left(\frac{g_\rho}{m_\rho}\right)^2 \langle \overline{\psi}\gamma^0\tau_3\psi\rangle = \left(\frac{g_\rho}{m_\rho}\right)^2 \tfrac{1}{2}(\rho_p - \rho_n)\,, \tag{4.201}$$

$$g_\rho \rho_3^k = \tfrac{1}{2}\left(\frac{g_\rho}{m_\rho}\right)^2 \langle \overline{\psi}\gamma^k\tau_3\psi\rangle = 0\,, \tag{4.202}$$

$$\left[\gamma_\mu(k^\mu - g_\omega\omega^\mu - \tfrac{1}{2}g_\rho\tau_3\rho_3^\mu) - (m - g_\sigma\sigma)\right]\psi(k) \;=\; 0\,. \tag{4.203}$$

In the first of these equations, $\frac{1}{2}\rho_p$ and $-\frac{1}{2}\rho_p$ are the isospin densities of the proton and neutron, where $\rho_{p,n}$ are the number densities. In the source for the 3-vector

part of the rho meson field, the operator τ_3 produces a factor of ± 1 and leaves $\langle\overline{\psi}\gamma^k\psi\rangle$ which vanishes as we proved earlier (4.147). So if we intend to solve the problem at the mean field level, we do not need the full isospin current derived above but only the baryon part of it.

The Dirac eigenvalues can be obtained by rationalizing the Dirac operator as before and are

$$\begin{aligned} e_{I_3}(k) &= g_\omega\omega^0 + g_\rho\rho_3^0 I_3 + E(k) \\ E(k) &= \sqrt{k^2 + (m - g_\sigma\sigma)^2}\,, \end{aligned} \tag{4.204}$$

where I_3 is the isospin of the proton (1/2) or neutron (−1/2). In contrast to the earlier models, the rho meson lifts the isospin degeneracy of the baryons and shifts them up or down according to the sign of $\rho_3^0 I_3$ for a given baryon species. We will discuss this effect further in connection with neutron star matter. For the moment, let us note that the sign of ρ_3^0 is determined from the Euler–Lagrange equation (4.201). There we see that the the sign is determined by the dominant species. An added particle having the same sign of I_3 as the dominant species will have its eigenvalue shifted upward, and of opposite sign, downward. In the first case we can say the species is isospin-unfavored; in the other, favored. Clearly, for a neutron star, baryons with the same isospin projection as the neutron are isospin-unfavored.

Because the isospin interaction lifts the degeneracy of the Dirac eigenvalues, the sum on the spin–isospin label κ in the expression for the expectation value of any operator (4.140) will not yield simply the factor 4 but rather a factor 2 (for the two spin projections), and the sum on isospin projection will remain to be done explicitly.

Now the expectation of the Lagrangian has the addition of the field energy of the rho meson as well as the contributions of the scalar self-interactions represented by U,

$$\langle\mathcal{L}\rangle = -\tfrac{1}{2}m_\sigma^2\sigma^2 + \tfrac{1}{2}m_\omega^2\omega_0^2 + \tfrac{1}{2}m_\rho^2\rho_{03}^2 - \tfrac{1}{3}bm(g_\sigma\sigma)^3 - \tfrac{1}{4}c(g_\sigma\sigma)^4\,, \tag{4.205}$$

while the energy density and pressure are given by the general expressions as before,

$$\epsilon = -\langle\mathcal{L}\rangle + \langle\overline{\psi}\gamma_0 k_0\psi\rangle\,, \tag{4.206}$$

$$p = \langle\mathcal{L}\rangle + \frac{1}{3}\langle\overline{\psi}\gamma_i k_i\psi\rangle\,, \tag{4.207}$$

with

$$\begin{aligned} \langle\overline{\psi}\gamma_0 k_0\psi\rangle &= \sum_\kappa \int \frac{d\boldsymbol{k}}{(2\pi)^3}(\overline{\psi}\gamma_0 k_0\psi)_{\boldsymbol{k}\kappa}\Theta[\mu - e_{I_3}(k)] \\ &= \frac{1}{\pi^2}\sum_{I_3}\int_0^{k_f} k^2\,dk\, e_{I_3}(k)\Theta[\mu - e_{I_3}(k)] \\ &= \frac{1}{\pi^2}\int_0^{k_p} k^2\,dk\Big[g_\omega\omega^0 + \tfrac{1}{2}g_\rho\rho_3^0 + \sqrt{k^2 + m^{*2}(\sigma)}\Big] \end{aligned} \tag{4.208}$$

$$+\frac{1}{\pi^2}\int_0^{k_n} k^2\,dk\left[g_\omega\omega^0 - \tfrac{1}{2}g_\rho\rho_3^0 + \sqrt{k^2+m^{*2}(\sigma)}\right],$$

where for brevity we have recalled our definition $m^*(\sigma) = m - g_\sigma\sigma$. Put this result in the expression for ϵ, and find its stationary point with respect to variations in the ρ_{03} field. Thus, obtain the field equation for the rho field. Hence the field equation expresses the stationarity of the energy density at fixed neutron and proton densities. An analogous result was obtained in Section 4.7:

$$\left(\partial\epsilon/\partial\rho_{03}\right)_{k_n,k_p=\text{const}} = 0. \tag{4.209}$$

Because the systems of interest are isospin asymmetric, we have separate Fermi energies for proton and neutron. Their densities are

$$\rho_p = 2\int_0^{k_p}\frac{d\boldsymbol{k}}{(2\pi)^3} = \frac{k_p^3}{3\pi^2} \tag{4.210}$$

and a similar expression for neutrons.

Now use the field equations to get the simpler expression

$$\langle\overline{\psi}\gamma_0 k_0\psi\rangle = m_\omega^2\omega_0^2 + m_\rho{}^2\rho_{03}^2 + \frac{1}{\pi^2}\left[\int_0^{k_p} k^2\,dk\sqrt{k^2+m^{*2}(\sigma)}\right.$$
$$\left.+\int_0^{k_n} k^2\,dk\sqrt{k^2+m^{*2}(\sigma)}\right]. \tag{4.211}$$

Gather together this material to find the energy density and pressure,

$$\epsilon = \tfrac{1}{3}bm(g_\sigma\sigma)^3 + \tfrac{1}{4}c(g_\sigma\sigma)^4 + \tfrac{1}{2}m_\sigma^2\sigma^2 + \tfrac{1}{2}m_\omega^2\omega_0^2 + \tfrac{1}{2}m_\rho{}^2\rho_{03}^2$$
$$+\frac{1}{\pi^2}\left[\int_0^{k_p}\sqrt{k^2+m^{*2}(\sigma)}\,k^2\,dk + \int_0^{k_n}\sqrt{k^2+m^{*2}(\sigma)}\,k^2\,dk\right],$$

$$p = -\tfrac{1}{3}bm(g_\sigma\sigma)^3 - \tfrac{1}{4}c(g_\sigma\sigma)^4 - \tfrac{1}{2}m_\sigma^2\sigma^2 + \tfrac{1}{2}m_\omega^2\omega_0^2 + \tfrac{1}{2}m_\rho{}^2\rho_{03}^2$$
$$+\frac{1}{3}\frac{1}{\pi^2}\left[\int_0^{k_p}\frac{k^4\,dk}{\sqrt{k^2+m^{*2}(\sigma)}} + \int_0^{k_n}\frac{k^4\,dk}{\sqrt{k^2+m^{*2}(\sigma)}}\right]. \tag{4.212}$$

Recall that the earlier models of this chapter had an isospin symmetry energy arising only from a difference in the Fermi energies of neutrons and protons in the event of unequal numbers of these species (4.164). We saw that the Fermi energy contribution could account for only about one-half the observed value of 32.5 MeV for the symmetry energy coefficient. We have now introduced the rho meson for the reason described above; it will introduce an additional restoring energy that favors isospin symmetry as manifested in the valley of beta stability in nuclear physics. This restoring term is the ρ_{03}^2 term in the energy density which, according to the equation for the rho field (4.201), produces a quadratic term in the deviation from isospin symmetry and so favors symmetric systems.

We sketch how to compute the symmetry energy of the theory so as to relate the new coupling constant g_ρ to the empirical value of the symmetry energy. Look at

that part of the energy that depends on the asymmetry between proton and neutron contributions and call it E_s. The symmetry energy per nucleon can be written with the aid of the field equation for the rho meson as

$$\frac{E_s}{A} = \frac{\epsilon_s}{\rho} = \frac{1}{8}\left(\frac{g_\rho}{m_\rho}\right)^2 \rho t^2 + \frac{1}{\rho}\frac{1}{\pi^2}\left[\int_0^{k_p} k^2\, dk \sqrt{k^2 + (m - g_\sigma \sigma)^2}\right.$$
$$\left. + \int_0^{k_n} k^2\, dk \sqrt{k^2 + (m - g_\sigma \sigma)^2}\right], \tag{4.213}$$

where

$$t \equiv (\rho_n - \rho_p)/\rho\,, \qquad \rho = \rho_n + \rho_p\,. \tag{4.214}$$

It is worth commenting that the coupling of the rho meson to the isospin current leads to a contribution in the symmetry energy per nucleon E_s/A proportional to ρ. Such a dependence does not appear in nonrelativistic, Schrödinger-based approaches based on two- and three-body potentials [158]. In the present model, the interaction part of the isospin symmetry term comes exclusively from the coupling between the isospin current and rho meson. We need a coupling constant $(g_\rho/m_\rho)^2$ about twice as large as expected from the rho decay into two pions [120].

The *symmetry energy coefficient* is the coefficient of the quadratic term in t in the energy per nucleon:

$$a_{\text{sym}} = \frac{1}{2}\left[\frac{\partial^2(\epsilon/\rho)}{\partial t^2}\right]_{t=0}. \tag{4.215}$$

To evaluate this expression, write the nucleon Fermi momenta of neutron and proton in terms of t and the Fermi energy at saturation of symmetric matter

$$k_F \equiv \left(\frac{3\pi^2\rho_0}{2}\right)^{1/3}, \tag{4.216}$$

namely,

$$k_n = k_F(1+t)^{1/3}, \qquad k_p = k_F(1-t)^{1/3}\,. \tag{4.217}$$

Now take the indicated derivatives at a constant total baryon number density $\rho = \rho_n + \rho_p$. After some algebra, the result is

$$a_{\text{sym}} = \left(\frac{g_\rho}{m_\rho}\right)^2 \frac{k_F^3}{12\pi^2} + \frac{k_F^2}{6(k_F^2 + m^{*2})^{1/2}} = 32.5\ \text{MeV}\,. \tag{4.218}$$

This expression allows one to evaluate the coupling constant of the ρ meson. There are two parts to the symmetry energy coefficient. The first arises from the explicit coupling between the nucleon isospin and the rho meson; the second from the kinetic energy when there is a relative displacement of the Fermi energies of proton and neutron. The two parts contribute about equally to the empirical value.

4.10 Inclusion of the Octet of Baryons

Our goal is to find a relativistically covariant theory of dense hadronic matter, such as likely exists in neutron stars. In the foregoing we have constrained the theory by what is known empirically about the properties of matter near normal nuclear matter density. Our constraints normalize the equation of state at one point in the energy-density plane, assure that the extrapolation to higher density or isospin asymmetric matter in the vicinity of saturation is correct, and give some expectation that the extrapolation to greater extremes is reasonable. The only certain knowledge above saturation is that the equation of state is causal and obeys Le Chatelier's principle ($dp/d\epsilon \geq 0$).

There remains a further extension of the theory that pertains uniquely to super-dense matter, be it cold, dense matter, or hot matter of any baryon density. Because of the Pauli principle, as the baryon density increases, so will the Fermi momentum and the Fermi energy. Ultimately the Fermi energy will exceed the masses of the heavier baryons. This statement is made in the framework of a free Fermi gas, but it is also valid in an interacting system, provided we simply refer to the eigenenergies of the baryons in the medium. When the Fermi energy of the occupied baryon states rises above the eigenenergies of other species, the energy and pressure of the system will be lowered by conversion of some of those baryons to the other species. The generalization of relativistic, mean-field theory to include higher mass baryons was first implemented by Garpman, Glendenning, and Karant [159]. We need to discuss carefully the method of arriving at an equilibrium balance of baryon species in dense matter.

The theory developed in the foregoing sections is well suited to incorporating additional baryon species. The most important are the remaining members of the lowest baryon octet, the hyperons Λ, Σ, Ξ. Because of the charge neutrality of stars and the interaction with the rho meson, we must distinguish the various isospin and charge states. We do this by affixing a subscript B to Fermi momenta, isospin projections, masses and so on. Therefore, the case of nucleons with different isospin projection is but a special case and readily generalized.

TABLE 4.5. The octet baryons, showing their quantum numbers, spin J, isospin projection I_3, charge q, and strangeness s.

	m (MeV)	J	I_3	q	s
N	939	1/2	1/2	1	0
			−1/2	0	0
Λ	1115		0	0	−1
Σ	1190		1	1	−1
			0	0	−1
			−1	−1	−1
Ξ	1315		1/2	0	−2
			−1/2	−1	−2

A suitable generalization of the Lagrangian is [68, 129, 160]

$$\begin{aligned}\mathcal{L} = \sum_B \overline{\psi}_B(i\gamma_\mu\partial^\mu - m_B + g_{\sigma B}\sigma - g_{\omega B}\gamma_\mu\omega^\mu - \tfrac{1}{2}g_{\rho B}\gamma_\mu\boldsymbol{\tau}\cdot\boldsymbol{\rho}^\mu)\psi_B \\ + \tfrac{1}{2}(\partial_\mu\sigma\partial^\mu\sigma - m_\sigma^2\sigma^2) - \tfrac{1}{4}\omega_{\mu\nu}\omega^{\mu\nu} + \tfrac{1}{2}m_\omega^2\omega_\mu\omega^\mu \\ - \tfrac{1}{4}\boldsymbol{\rho}_{\mu\nu}\cdot\boldsymbol{\rho}^{\mu\nu} + \tfrac{1}{2}m_\rho^2\boldsymbol{\rho}_\mu\cdot\boldsymbol{\rho}^\mu - \tfrac{1}{3}bm_n(g_\sigma\sigma)^3 - \tfrac{1}{4}c(g_\sigma\sigma)^4 . \end{aligned} \tag{4.219}$$

The spinor for the baryon species B, one of those listed in Table 4.5, is denoted by ψ_B. Only nucleons are present in hadronic matter near saturation density, and their coupling constants to the meson fields can be related to nuclear matter properties, as discussed above. However, hyperons, mainly just the Λ, occur only in a few hypernuclei and otherwise hyperons can populate matter only at high density; they do not affect the ground-state properties. Nevertheless, meaningful constraints on their couplings can be obtained [132]. We discuss the constraints in Section 5.4.3 after the necessary groundwork has been laid.

The Euler–Lagrange equations follow from the above Lagrangian. In the mean-field approximation, the Dirac equations in uniform matter for each species B are

$$\left[\gamma_\mu(k^\mu - g_{\omega B}\omega^\mu - \tfrac{1}{2}g_{\rho B}\boldsymbol{\tau}\cdot\boldsymbol{\rho}^\mu) - (m_B - g_{\sigma B}\sigma)\right]\psi_B(k) = 0 , \tag{4.220}$$

where the meson mean fields are the scalar, vector, and isovector σ, ω, ρ . The eigenvalues of particle and antiparticle can be found as

$$\begin{aligned} e_B(k) &= g_{\omega B}\omega_0 + g_{\rho B}\rho_{03}I_{3B} + \sqrt{k^2 + (m_B - g_{\sigma B}\sigma)^2} , \\ \overline{e}_B(k) &= -g_{\omega B}\omega_0 - g_{\rho B}\rho_{03}\overline{I}_{3B} + \sqrt{k^2 + (m_B - g_{\sigma B}\sigma)^2} , \end{aligned} \tag{4.221}$$

where I_{3B} is the isospin 3-component for baryon B. (Recall (4.93.) We have explicitly used the fact (derived in Section 4.9) that only the isospin 3-component of the rho field survives in the mean-field approximation and that the Lorentz three-current part of both the omega and rho fields vanish in the static ground state of matter. The meson field equations in uniform static matter (in which space and time derivatives can be dropped) are

$$\omega_0 = \sum_B \frac{g_{\omega B}}{m_\omega^2}\rho_B , \tag{4.222}$$

$$\rho_{03} = \sum_B \frac{g_{\rho B}}{m_\rho^2} I_{3B}\rho_B , \tag{4.223}$$

$$\begin{aligned} m_\sigma^2\sigma &= -bm_n g_\sigma(g_\sigma\sigma)^2 - cg_\sigma(g_\sigma\sigma)^3 , \\ &\quad + \sum_B \frac{2J_B+1}{2\pi^2} g_{\sigma B}\int_0^{k_B} \frac{m_B - g_{\sigma B}\sigma}{\sqrt{k^2 + (m_B - g_{\sigma B}\sigma)^2}} k^2\,dk . \end{aligned} \tag{4.224}$$

We use the notation $g_\sigma \equiv g_{\sigma N}$, for brevity in denoting the nucleon couplings and denote the other couplings by $g_{\sigma B}$, and similarly for the other coupling constants.

The energy density and pressure can be found in the now familiar manner. They are

$$\epsilon = \tfrac{1}{3}bm_n(g_\sigma\sigma)^3 + \tfrac{1}{4}c(g_\sigma\sigma)^4 + \tfrac{1}{2}m_\sigma^2\sigma^2 + \tfrac{1}{2}m_\omega^2\omega_0^2 + \tfrac{1}{2}m_\rho^2\rho_{03}^2 + \sum_B \frac{2J_B+1}{2\pi^2}\int_0^{k_B}\sqrt{k^2+(m_B-g_{\sigma B}\sigma)^2}\,k^2\,dk \tag{4.225}$$

$$p = -\tfrac{1}{3}bm_n(g_\sigma\sigma)^3 - \tfrac{1}{4}c(g_\sigma\sigma)^4 - \tfrac{1}{2}m_\sigma^2\sigma^2 + \tfrac{1}{2}m_\omega^2\omega_0^2 + \tfrac{1}{2}m_\rho^2\rho_{03}^2 + \frac{1}{3}\sum_B \frac{2J_B+1}{2\pi^2}\int_0^{k_B} k^4\,dk/\sqrt{k^2+(m_B-g_{\sigma B}\sigma)^2}\,. \tag{4.226}$$

These are functions of the baryon density ρ through the dependence on the Fermi momenta. Together they are frequently referred to as the equation of state.

The above equations are not complete when the density is high enough that baryon species beyond the nucleons are populated. It is necessary to supplement the field equations by subsidiary constraints appropriate to the state of matter in which one is interested. Such a state will be characterized by specified values of conserved quantities such as the baryon number, the charge, and strangeness densities,

$$\begin{aligned} \rho_B &= (2J_B+1)b_Bk_B^3/(6\pi^2) \\ Q_B &= (2J_B+1)q_Bk_B^3/(6\pi^2)\,, \\ S_B &= (2J_B+1)s_Bk_B^3/(6\pi^2)\,. \end{aligned} \tag{4.227}$$

The total densities are

$$\rho = \sum_B \rho_B, \quad q = \sum_B Q_B, \quad S = \sum_B S_B\,. \tag{4.228}$$

These conserved charges will have the values determined in the preparation of the system. For example, if we want to describe high-density matter obtained by compressing symmetric nuclear matter on a short time-scale compared to the weak interaction scale (as for a nuclear collision), then we want a solution with $q = \rho/2$, $S = 0$ at all chosen baryon densities ρ. This constraint can be implemented through the use of Lagrange multipliers as in Section 3.9.2.

Let the strangeness chemical potential for positive unit strangeness be μ_K, and let μ_b and μ_q be the chemical potentials for unit positive baryon and electric charge. In general, the chemical potential of particle B with baryon charge b_B, electric charge q_B (in units of e), and strangeness s_B is given by

$$\mu_B = b_B\mu_b + q_B\mu_q + s_B\mu_K\,. \tag{4.229}$$

The Fermi momenta appearing in the expression for the conserved charges (4.228) are related to the chemical potentials (Fermi energies) through

$$\mu_B = e_B(k_B)\,, \tag{4.230}$$

where the eigenvalue $e_B(k)$ was written above. Now we have a system of nonlinear equations in the unknown meson field strengths, the three independent chemical potentials, and Fermi momenta which need to be solved simultaneously.

The above equations hold at zero temperature. Finite temperature results can be obtained in the usual manner by writing the partition function for the system and carrying out the appropriate manipulations [159, 161, 162]. The results may be simply stated. In all the expressions containing a sum over B, the sum is extended over antiparticles as well as particles because the former are thermally excited. The antiparticle quantum numbers—such as baryon number, charge, isospin, and strangeness as well as their chemical potentials—are the negatives of the particles. A thermal factor has to be inserted and the momentum integrals have to be integrated to infinity. The thermal baryon and antibaryon densities are given, respectively, by

$$\rho_B = \frac{2J_B+1}{2\pi^2} b_B \int_0^\infty \Big(\exp[(e_B(k)-\mu_B)/T]+1\Big)^{-1} k^2\, dk \tag{4.231}$$

$$\bar{\rho}_B = \frac{2J_B+1}{2\pi^2} \bar{b}_B \int_0^\infty \Big(\exp[(\bar{e}_B(k)+\mu_B)/T]+1\Big)^{-1} k^2\, dk\,. \tag{4.232}$$

Similar expressions hold for the electric charge and strangeness densities. Note that ρ_B and $\bar{\rho}_B$ are defined as baryon charge densities so that, if there are antibaryons present, $\bar{\rho}_B$ will be negative. The thermal factor is also introduced into all the integrals over momentum in the scalar field equation above and in the expressions for pressure and energy density. At finite temperature, other mesons than those driven by finite baryon currents will be excited thermally. Their contribution to the conserved charge, strangeness, and energy density can be added as in [161, 162].

4.11 High-Density Limit

It is characteristic of any theory having a vector meson interaction that for asymptotically large baryon density, $p \to \epsilon$ [163]. Examine the above expressions for ϵ and p using the field equations in the limit of large k_B. The mass terms in the integrals can be ignored. The σ field is bounded by the order of the baryon masses as can be inferred by an examination of its field equation. Indeed, when only the nucleons are considered, it is bounded by the nucleon mass as we showed explicitly. We find

$$\epsilon \to \tfrac{1}{2}\Big(\sum_B \frac{g_{\omega B}}{m_\omega}\rho_B\Big)^2 + \tfrac{1}{2}\Big(\sum_B \frac{g_{\rho B}}{m_\rho} I_{3B}\rho_B\Big)^2 + \sum_B \frac{2J_B+1}{2\pi^2}\frac{k_B^2}{4} \tag{4.233}$$

$$p \to \tfrac{1}{2}\Big(\sum_B \frac{g_{\omega B}}{m_\omega}\rho_B\Big)^2 + \tfrac{1}{2}\Big(\sum_B \frac{g_{\rho B}}{m_\rho} I_{3B}\rho_B\Big)^2 + \tfrac{1}{3}\sum_B \frac{2J_B+1}{2\pi^2}\frac{k_B^2}{4}\,.$$

The first two terms of both ϵ and p are identical and proportional to k^6, so they dominate the last term at high density. Consequently, p approaches ϵ from below because of the factor $1/3$ in the last term of p. Therefore, the speed of sound $(dp/d\epsilon)^{1/2}$ is always less than the speed of light. The equation of state is causal at all densities.

The low-density limit of this theory is not of interest. At low density (below saturation density), the lowest state of matter is not a uniform gas of nucleons. Rather it is energetically more favorable for nucleons to clump together as nuclei and leave voids between them. We have discussed this limit in Section 3.10.3 and further in Section 5.3.8.

4.12 Effective Versus Renormalized Theory

It is evident that the point of view adopted in the preceding development is that nuclear field theory is to be solved in the mean-field approximation and with coupling constants fitted to nuclear properties. This is a common but not universal point of view. Some authors have insisted on renormalization. The presence of matter alters the vacuum by altering the masses of antiparticles. The filled Fermi sea therefore shifts in energy with the density of fermions. However true this may be of a fundamental theory, we deal in compact stars with baryons. They are composite, not fundamental fields.

The question arises as to what meaning can be attached to renormalized baryon fields when in fact they are composites. Of course, if their substructure is ignored and they are thought of as fundamental, then expressions for the renormalization of the theory derived in the foregoing can be obtained. What we shall show here is that the renormalized theory and the mean-field approximation, derived in detail above, yield the same equation of state to high accuracy if the coupling constants are chosen to reproduce the *five* nuclear matter properties that were emphasized above as important constraints on the theory [164, 129]. This being so, there seems little point in going through the renormalization procedure, at least as concerns the structure of stars.

For the purpose of demonstrating the above correspondence, we recall, without derivation, results that have been obtained elsewhere [165, 120]. With the inclusion of vacuum renormalization energies, the energy density is given by

$$\epsilon_{\mathrm{RHA}} = \epsilon_{\mathrm{MFA}} + V_N + V_\sigma \,. \tag{4.234}$$

The approximation that includes the vacuum renormalization is known as the relativistic Hartree approximation (RHA) [120]. The subscript "MFA" simply denotes the mean-field approximation derived above for any of the versions that include scalar self-interactions. In their absence, the V_σ term should be dropped throughout. The pressure is given in RHA by

$$p_{\mathrm{RHA}} = p_{\mathrm{MFA}} - V_N - V_\sigma \,. \tag{4.235}$$

The last two terms represent the contributions from renormalization of the scalar meson and nucleon, respectively, and are given by

$$V_\sigma = \frac{m_\sigma^4}{(8\pi)^2}\Big[(1+\phi_3)^2\ln(1+\phi_3) - \phi_3 - \frac{3}{2}\phi_3{}^2, \\ - \frac{1}{3}\phi_1{}^2(\phi_1 + 3\phi_2) + \frac{1}{12}\phi_1{}^4\Big] \tag{4.236}$$

$$V_N = -\frac{m_n^4}{4\pi^2}\Big[(1-\chi)^4\ln(1-\chi) + \chi - \frac{7}{2}\chi^2 + \frac{13}{3}\chi^3 - \frac{25}{12}\chi^4\Big], \tag{4.237}$$

where

$$\phi_1 = \frac{2bm_n g_\sigma^3\sigma}{m_\sigma{}^2}, \quad \phi_2 = \frac{3cg_\sigma^4\sigma^2}{m_\sigma{}^2}, \quad \phi_3 = \phi_1 + \phi_2, \quad \chi = \frac{g_\sigma\sigma}{m_n}, \tag{4.238}$$

and m_n and m_σ are the nucleon and σ mass. The Euler–Lagrange equations are the same as before, except that the the equation for the sigma-field is modified by the derivative of the above renormalization terms. The sigma-field equation may be found in the usual way (as the Euler–Lagrange equation) or as a condition that the energy density is a minimum for fixed baryon density:

$$m_\sigma^2\sigma = -bm_n g_\sigma(g_\sigma\sigma)^2 - cg_\sigma(g_\sigma\sigma)^3 - \frac{\partial}{\partial\sigma}[V_N + V_\sigma] \\ + \sum_B \frac{2J_B+1}{2\pi^2} g_{\sigma B}\int_0^{k_B} \frac{m_B - g_{\sigma B}\sigma}{\sqrt{k^2 + (m_B - g_{\sigma B}\sigma)^2}}\, k^2\, dk\,. \tag{4.239}$$

The coupling constants for the two cases, MFA and RHA, that yield the nuclear matter properties listed in the caption are given in Table 4.6. The binding energy per nucleon for symmetric nuclear matter and pure neutron matter are shown in Fig. 4.3. It is evident that, when the two theories are fitted to the same five data, the results are essentially the same [164, 129].

4.13 Bound Versus Unbound Neutron Matter

We emphasize that the simple ($\sigma - \omega$) model of Johnson and Teller [111], Duerr [112], and Walecka [113, 120] was used only as the starting point for the development of a more comprehensive, relativistic, mean-field theory. The original model describes nuclear matter poorly. It is also unsuitable for the description of neutron stars, although it has been employed frequently for this purpose. We discussed one shortcoming earlier and have appropriately extended the simple model in Section 4.10.

However, there is another problem with the simple model; pure neutron matter has a minimum in the binding per nucleon as a function of density that lies at a slightly negative or positive value, depending on the parameters of the theory [120]. In the first case, neutron matter would be bound; in the second there would be a first-order phase transition between neutron matter near saturation density and a very diffuse gas of neutrons.

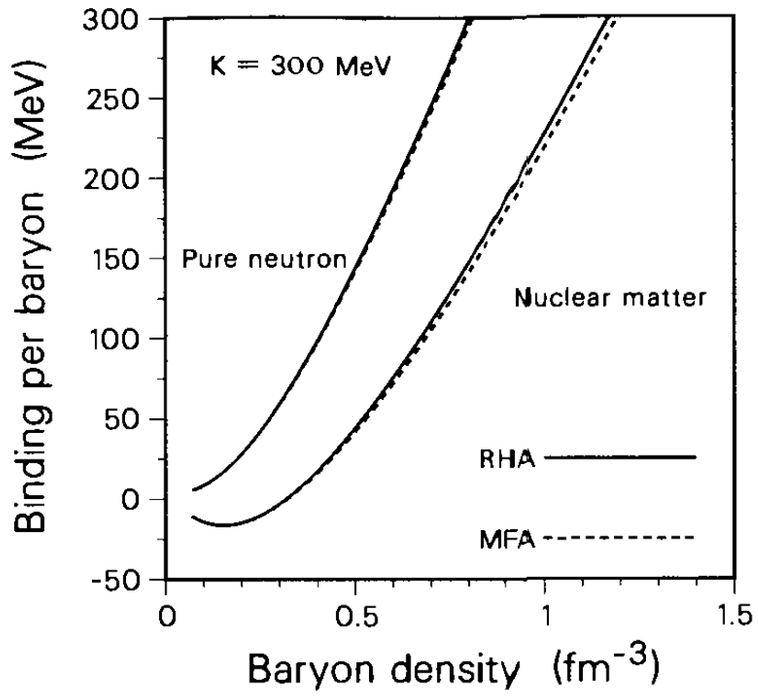

FIGURE 4.3. Binding energy of nuclear and pure neutron matter as a function of density computed with and without vacuum renormalization (denoted RHA and MFA, respectively). The corresponding nuclear matter properties are listed in Table 4.6 (From [129]).

TABLE 4.6. Nucleon–meson coupling constants, corresponding to $K = 300$ MeV, $B/A = -16.3$ MeV, $\rho_0 = 0.153$ fm^{-3}, $a_{\rm sym} = 32.5$ MeV, $m^*_{\rm sat}/m = 0.78$

	$(g_\sigma/m_\sigma)^2$ fm^2	$(g_\omega/m_\omega)^2$ fm^2	$(g_\rho/m_\rho)^2$ fm^2	b	c
MFA	9.031	4.733	4.825	0.003305	0.01529
RHA	9.249	4.732	4.823	0.005723	0.000601

4.13.1 Bound neutron matter

There is no terrestrial evidence that pure neutron matter is bound and stable against beta decay. If it were, bound uncharged nuclei ought to exist, possibly of high baryon number—high enough that surface and shell effects do not render them unstable. Moreover, the behavior of some pulsars suggests that neutron star matter is not bound by the nuclear force[5]. We now take up these issues.

If neutron matter is bound, then $p = 0$ at the equilibrium density; zero pressure can support no overlying layer of matter against the attraction of gravity and so marks the surface of a star. Of course, the density at which neutron matter is bound in the simple model is close to the density at which symmetric matter is bound. Whether the difference is a few percent or even a factor of two or so makes no difference to our argument. The surface of the star in the case of bound neutron

[5]The issue is not whether neutron stars are bound by the nuclear force; they are not. Through most of the star, the nucleons are compressed to a density at which they only exert repulsion on each other. The issue is whether there is a bound state of neutron matter at any density. If so, because an equilibrium state has $p = 0$, the density of the bound state would be that of the star's edge.

matter has a density near the saturation density of nuclear matter (of the order of 10^{14} g/cm^3). The surface would be a nuclear liquid. But this is almost certainly ruled out by the observation of pulsar glitches as we discuss.

In contrast to the above, as we discussed in Section 3.10.1, the region near the surface of a neutron star is thought to form a solid crust of material at subnuclear density, a Coulomb lattice of nuclei immersed in an electron gas. This would occur in the density range from about ($\sim 10^{14}$ g/cm^3) all the way down to near zero pressure at the surface of the star with the corresponding density approximating that of atomic iron. The very surface my be molten, but as the density increases at even a small depth in the star, a Coulomb lattice of partially, and ultimately fully ionized nuclei will be formed. The solid region is important for understanding the glitch phenomenon—irregular small discontinuities in the rotational period—observed in some pulsars. Because a purely liquid or gaseous star has no mechanism by which the moment of inertia of the star can undergo a sudden change, a solid region must be involved.

4.14 Note on Dimensions

In nuclear and particle physics it is convenient to express length in the unit of a fermi (fm= 10^{-13} cm) because it is the order of the dimension of a nucleon, and a nucleus has a radius of a few of these units. It is also convenient to take $\hbar = c = 1$. The unit of $\hbar$ is $\hbar c = 197.33$ MeV-fm. The wave number (which we usually refer to as the momentum) is $k = p/\hbar$ and has the unit of inverse length. This is consistent with our use of it in relating the density and momentum eigenstates

$$\rho = \gamma \int \frac{d\boldsymbol{p}}{(2\pi\hbar)^3} = \gamma \int \frac{d\boldsymbol{k}}{(2\pi)^3} \tag{4.240}$$

with γ the degeneracy of the momentum states and ρ the particle number density in 1/fm^3.

With such a choice of unit for k and because the relativistic energy of a free particle is given by $\sqrt{k^2 + m^2}$, we should use inverse length as the unit of mass and energy also. For example, we have

$$m \approx 939\,\text{MeV} = \frac{939}{197}\,\text{fm}^{-1} = 4.77\,\text{fm}^{-1} \tag{4.241}$$

This means that energy density has the natural unit fm^{-4}, and pressure has the same unit. The conversion to units frequently used in astrophysics is given by (3.8). We call attention to the discussion of units surrounding the quoted equation.

The Lagrangian also has the unit of energy density, or, equivalently, fm^{-4}. Referring to (4.121) (in particular the Lagrangian of the scalar (or vector) meson), the mass term $m_\sigma^2\sigma^2$ informs us that the dimension of the mean scalar and vector fields σ and ω_0 is 1/fm. So the combination $m - g_\sigma\,\sigma$ informs us that the coupling constant is dimensionless, as with g_ω.

Of course, the choice made here to use length as the unit to express dimensions is not unique. Through $\hbar c = 197.33$ MeV-fm, we could as well choose energy, as is frequently done.

4.15 Summary

In this chapter a relativistic nuclear field theory was developed, and a succession of improvements to the early version of the theory were introduced. We placed special emphasis on five important constraints on the theory that are bulk properties of symmetric nuclear matter. The theory was generalized to include the octet baryons, and in fact the generalization could extend over an arbitrary number of baryon types. Algebraic relationships were derived between the bulk properties of nuclear matter and the couplings in the theory. With the addition of the Lagrangians for free leptons (electrons and muons), we will be in a position to develop the equation of state for neutron star matter—matter that is charge-neutral and in generalized beta equilibrium.

4.16 Problems for Chapter 4

1. Work through the steps in (4.6) leading to the Euler–Lagrange equations (4.7).
2. Fill in all steps leading to the divergenceless four-vectors (4.13).
3. Follow the steps in detail that lead to the constant charges (4.17).
4. Prove the tensor character of the energy-momentum tensor (4.27)
5. Derive the conserved current (4.47) of the complex scalar field.
6. Familiarize yourself with the equivalence of the expressions (4.58, 4.59).
7. Derive the Lorentz isospin vector current of the rho meson field (4.63). Obtain the charge current (4.64).
8. Derive the equations of motion (4.65) of the rho meson.
9. Prove the relation for the γ matrices, (4.75).
10. Show that the conserved isospin current is given by (4.93). Obtain the isospin densities (4.95).
11. Derive the charge current of the proton field (4.98).
12. Obtain the charge current and density (4.98).
13. Confirm that J^μ in (4.103) is the is the proton current in (4.98).
14. Derive the conserved current 4.106) for the complex scalar field.
15. Derive the nuclear mass formula (4.107) from the description of each term in the text.
16. Familiarize yourself with the connection between density of a degenerate Fermi system and the Fermi momentum (4.110).
17. Obtain the numerical value of the saturation energy density of symmetric nuclear matter, (4.113).

18. Confirm that the operation on the right of (4.114) will yield the symmetry energy coefficient of (4.107).

19. From the interaction Lagrangian (4.120) confirm the Lagrangian (4.120) of the $(\sigma - \omega)$ model.

20. Derive the Euler–Lagrange equations for the three fields, nucleon, and scalar and vector meson. Write their particular form for static, uniform matter.

21. Noting the x^μ independence of the Euler–Lagrange equation for the nucleon fields in the mean field approximation for the meson fields, confirm the momentum–space equation (4.129).

22. Carry out the operations in (4.133) to obtain (4.135).

23. The ground-state expectations of $\langle \psi^\dagger \psi \rangle$ and $\langle \bar{\psi} \psi \rangle$ were evaluated in the text by a particular method developed there. Instead, construct the nucleon spinors in the traditional way of Dirac theory and evaluate (4.149, 4.151).

24. In the mean field approximation, where the meson fields are constant and the nucleon fields have the dependence (4.127), the expectation values of the diagonal elements of the energy-momentum tensor takes the form

$$\langle \mathcal{T}^{\mu\mu} \rangle = -\langle \mathcal{L} \rangle + \langle \frac{\partial \mathcal{L}}{\partial(\partial_\mu \psi)} \partial^\mu \psi \rangle, \qquad \mu \text{ unsummed}$$

Note that $\partial^\mu \psi = k^\mu \psi(k)$. Verify these results. Then prove (4.156) and (4.157).

25. Derive (4.158) and (4.160) and hence obtain the equation of state (4.161) and (4.162).

26. Verify that the pressure (4.162) satisfies the usual relation (4.163).

27. Verify the symmetry energy coefficient at the present level as given by (4.164), ie. the kinetic energy contribution. Verify the numerical value given in the text.

28. Verify that the Euler–Lagrange equations for the meson fields follow from the stationarity of the energy density with respect to the fields at fixed density (4.166).

29. Confirm the energy density and pressure (4.174, 4.175) in the presence of the scalar self-interactions (4.167).

30. Write a computer program to solve the field equations (4.152, 4.153). Use coupling constants $(g_\sigma/m_\sigma)^2 = 11.74$, $(g_\omega/m_\omega)^2 = 8.586$. Compute the energy per nucleon from (4.112) using (4.161). Plot the resulting curve as a function of baryon density ρ from 0.1 to 1.0. Confirm that the binding energy is about -15.75 MeV at a density of $\rho = 0.193$ (this value used in Ref. [166], $k_f = 1.42\ \text{fm}^{-1}$ is too large). Find that the symmetry energy coefficient is ~ 22.1 MeV and the effective mass is ~ 0.56.

31. Verify that the compression modulus of the model of Section 4.8 is given by (4.187).

32. Verify the algebraic expressions for the coupling constants and of the coefficients b and c of the cubic and quartic scalar terms, given by (4.190) and (4.195).

33. Derive the expression for the isospin symmetry coefficient (4.218).

34. Confirm that the high-density limit of the equation of state is given by (4.234) and confirm that $p \to \epsilon$ from below in the limit. Thus prove causality of the theory.

35. Write a program to verify several entries in Table 4.4.

5

Neutron Stars

"I bow low. I have observed the apparition of a guest star. Its color was an iridescent yellow. . . . The land will know great prosperity."
Yang Wei-T'e, Imperial Astronomer of the Sung Dynasty, 1054.

"With all reserve we advance the view that supernovae represent the transition from ordinary stars into *neutron stars*, which in their final stages consist of closely packed neutrons."
W. Baade and F. Zwicky, 1933 [1].

5.1 Discovery

A year following Chadwick's 1932 discovery of the neutron, Baade and Zwicky conceived the notion of neutron stars in the course of their investigation of supernovae. What source other than the gravitational binding energy[1] of a highly

[1]We estimated the binding energy in Section 3.3.3 to be close to 20% of a neutron star's mass if it is close to the limiting mass. The visible light represents about 1/100 of the energy deposited in the remnant, which in turn is but 1/100 of the total release of binding energy (recall Fig. 3.15). The bulk of the binding energy is carried off by energetic neutrinos that diffuse out of the protoneutron star during the first few seconds of its life.

compact object formed by the collapse of the central core of the presupernova star could render stellar explosions visible in daylight for weeks and hurl the stellar remnant of many solar masses into space at velocities of thousands of kilometers per second?

Compelling though the insight of Baade and Zwicky was or is to us now, no searches for neutron stars were mounted following their paper. Nor were any attempts made to find these fascinating stars until after the serendipitous discovery thirty-five years later. No one knew what to look for. A compact star made of "closely packed neutrons" would have to be degenerate; it could not generate energy after formation, but could only radiate its remaining store of heat over millions of years through the slow process of photon diffusion, just as for white dwarfs. However, because neutron stars are so much smaller than white dwarfs they will seldom be seen in an optical telescope although one exception has been discovered recently.[2] Other types of radiation did not appear likely. Gravitational radiation by a pulsating rotating neutron star would be a fleeting phenomenon because the amplitude of vibrations giving rise to quadrupole or higher multipole mass transport would be rapidly damped.

In 1939, years before the discovery of pulsars, Oppenheimer and Volkoff [78] and Tolman [167] were the first to take seriously the question of the structure of the compact objects of Baade and Zwicky. They estimated their radius and maximum mass to be about ten kilometers and $\frac{3}{4}$ of a solar mass. A year later, Woltjer estimated that the conservation of magnetic flux[3] in a star that contracts from a red giant to a neutron star could produce fields of 10^{12} gauss [168]. Such high fields led Pacini [169] to the prescient notion that energy could be fed from a highly magnetized rotating neutron star, as yet undiscovered, to the Crab nebula—whose luminosity is very high and whose expansion is known to be *accelerating*, now, and presumably since the explosion. Normally one would expect that the expansion of the nebula would slow down as momentum is shared with the interstellar medium, and it does slow down. But not so quickly as momentum conservation would have it.

Meanwhile, Anthony Hewish at Cambridge had designed a radio telescope and auxiliary equipment with a short time response and an extended observing routine for the purpose of studying scintillation[4] of point radio sources such as quasars.[5]

---

[2]Some pulsars can be observed over a wide frequency range, like the Crab, from radio to high-energy gamma rays.

[3]Magnetic fields in stars are detected by measurements of the opposite circular polarization of spectral lines split by the Zeeman effect. Stars have fields ranging from a few to thousands of gauss and in white dwarfs to 10^8 gauss.

[4]Scintillation, or twinkling, as seen in stars, is caused in light or radio waves arriving from a point source that pass along neighboring paths having a fluctuating refractive index, interfering at the point of observation, and thereby causing variation in signal strength.

[5]Quasars are exceedingly luminous objects of small angular size and large redshift, implying distances of 10 billion light years. They were discovered in 1963 and called "quasi-stellar radio sources". The energy source, which produces a luminosity up to a hundred times a normal galaxy, is confined to a volume the size of the solar system. The implication is that the energy source is infall of matter onto an enormous black hole.

It was not the first radio telescope, but it was the first to have the above attributes which proved crucial to the discovery about to be made. Within a month, his student Jocelyn Bell noticed the first indications of a persistent periodic source measured to have a pulse period of 1.337 seconds. Thirty-four years after the suggestion of Baade and Zwicky that the power house driving a supernova must be the gravitational binding of a neutron star, Hewish, Bell, Pilkington, Scott, and Collins published their discovery paper [170]. They had detected a very small source of pulsed radio signal lying outside the solar system, presumably a compact star, either a white dwarf or neutron star. The first *pulsar* had been discovered.

Shortly thereafter, the Crab and Vela pulsars were discovered, and then some 250 others in the large surveys of the 1970s. The total number is now over 1100. The last couple of hundred were discovered only in the last several years in radio surveys of the sky in both hemispheres made by teams using the Jodrell Bank 76 m, Parkes 64 m, and Arecibo 305 m antennas.

Pulsars, so named because they are sources of periodic signals of great timing stability, are the astrophysical objects that are presumed to correspond to neutron stars. They are observed under a variety of circumstances, usually as isolated sources, but sometimes in binary orbit with another star (white dwarf or neutron star), in *X-ray binary* systems, and perhaps *γ-ray bursters* and, as recently realized, soft gamma-ray repeaters [171]. The pulsation of the signal is the manifestation of a cone of radiation of small angular width emitted along the magnetic axis which is fixed in a rotating neutron star and beamed in our direction at each revolution.

Although pulsars are assumed to be neutron stars, we shall not use the names as equivalent. The name "pulsar" is reserved for the astrophysical object having the property that it emits pulsed radiation. For very good reasons, pulsars are believed to be neutron stars. Neutron star is a term reserved for the theoretical object, independent of its observation as a pulsar, or for a very compact star that is not observed by its pulsed radiation but by other means. An example is the partner of the Hulse–Taylor pulsar, which is unobserved as a pulsar. Rather, its presence is made known by its effect on the timing of pulses received from the observed pulsar. The orbital motion of the emitting pulsar about the center of mass produces a Doppler shift in the pulse arrival times. The mass and orbital parameters derived from the observations require the invisible partner to be very compact so that it is almost certain to be a neutron star and not a white dwarf. The companion may also be a pulsar. If so, the Earth is not on the cone swept out by the radio emission along the magnetic dipole as the neutron star rotates.

It is fitting that mention should be made of early work on the theory of neutron stars. It is well known that in 1939 Oppenheimer and Volkoff [78] and Tolman [167] first derived the equations of relativistic stellar structure from Einstein's field equations and discovered the existence of a limit to the mass of stable degenerate relativistic stars. The small book by Harrison, Thorne, Wakano, and Wheeler [28] is broader in scope and of great importance even today, quite aside from the evolutionary development of the field. These authors developed a rigorous framework in which to understand compact stars.

The interpretation of the 1966 discovery of the first pulsar by Hewish and Bell as a highly magnetized neutron star was already available, but unknown to them, in the paper by Pacini published in the same year [169]. Following the discovery, and independently of Pacini, Gold's paper [172] also provided a strong case for identifying the pulsar with a rotating neutron star. Many authors—Canuto and his collaborators [173], Ruderman [174]–[176], Ostriker and Gunn [177]–[179], Pines and Shaham [180]–[182], and Alpar [183]–[185] contributed additional important insights.

The likely existence of hyperons in neutron stars was recognized by Cameron [186] and Ambartsumyan and Saakayan [187] who used a free Fermi gas to describe neutron star matter. Pandharipande [188] and Bethe and Johnson [189] introduced hyperons in a Schroedinger potential approach to interactions among the constituents, as did Moszkowski [190]. Hyperon populations in neutron stars and their effect on a number of pulsar observables including the limiting mass and the possible role they play in supernovae have been emphasized by the author in a number of papers [67, 68, 129, 145, 191, 192, 193]. The vexing problem of connecting hyperon couplings to observables was addressed in Ref. [132]. These works also stressed the importance of constraining the theory by a number of nuclear matter properties [145, 146]. Hybrid stars—neutron stars with mixed phase hadronic and quark matter—were given their modern analysis by the author [194, 195]. In collaboration with Weber, the rotation of neutron star models built on modern equations of state (especially relativistic approaches) were extensively studied [107, 196] as well as rotation of strange stars with nuclear crusts [88], [197]–[199]. Recent research has centered on the very important topic of observable consequences of phase transitions in neutron star interiors [110, 200, 201]. (See Chapter 11.)

These and other researches are referenced in the following sections and chapters dealing with the many facets of neutron stars. Several monographs on pulsars from the observational perspective are the classic "Pulsars" by Manchester and Taylor [202] and the recent "Pulsar Astronomy" by Lyne and Graham–Smith [203]. Important contemporary research can also be found in several conference proceedings [204]–[207].

This chapter is divided into three parts. The first is concerned with the observed objects—pulsars—and the basis for their interpretation as neutron stars. We open the first part by recounting some of the important discoveries involving pulsars. Then we discuss the main observations made on these objects: pulse profiles, the range of observed periods and masses, pulsar ages as estimated from their rate of loss of rotational energy, why we know they are compact objects, supernova associations, and the apparent existence of two evolutionarily different pulsar populations.

We study the theory of neutron stars in the second part. The similarities and differences between nuclear matter and neutron star matter (charge neutral and in general equilibrium) are emphasized. We discuss how strangeness is created in neutron stars in the first few seconds following their birth. Chemical equilibrium in a star is discussed under the circumstance that neutrinos and photons diffuse

out allowing net strangeness to be locked in. This sets the stage for an account in later chapters of the formation of low-mass black holes, of hybrid stars having quark populations, and of strange stars composed entirely of quarks. We return briefly to a discussion of nuclear field theory and the subsidiary conditions needed for a description of *neutron star matter* as compared to symmetric nuclear matter. We are then in a position to compute neutron star models tightly constrained by hadronic interactions consistent with nuclear matter properties. Generic features of neutron stars are emphasized, especially the mass–radius relationship and the limiting mass.

The constitution of neutron stars is the subject of the third part of the chapter. There we discuss the hyperonic composition of stars, their radial distribution in neutron stars, and how hyperons affect the star's limiting mass. We also examine how charge neutrality can be achieved almost exclusively among baryons in the core. (That hyperons and quarks can, under conditions of high density, replace electrons in neutralizing compact stars has ramifications for the core electrical conductivity, for stellar magnetic fields, and for cooling rates.) Possible meson condensates, pion and kaon, are briefly discussed. Kaon condensation is discussed in detail in Chapter 10.

5.2 Pulsars: The Observational Basis of Neutron Stars

5.2.1 Important pulsar discoveries

Pulsars are believed to be highly magnetized rotating neutron stars. An electromagnetic beam is emitted along the magnetic axis with an angular spread typically of ten degrees. If an angular separation between the rotational and magnetic axes exists, the rotating object is analogous to a lighthouse. If, as observers on Earth, we lie on the cone of radiation swept out by the rotating star, we have a chance to observe it as a pulsed source if it is not too distant. The range of the frequencies in the emitted signal in some pulsars, such as the Crab, is enormous, ranging from radio to optical to X rays to γ rays, but most pulsars (including all known millisecond pulsars) have been observed only at radio frequencies.

More than 1100 pulsars have been found since the discovery by Hewish and Bell in 1967 of the pulsed signals of period 1.337 seconds from a source outside the solar system [170]. That source is now known as PSR 1919+21. Two additional pulsars were discovered shortly afterwards, the Crab [208] and the Vela Pulsar [209]. Both are found within supernova remnants, the Crab and Vela nebulae. Both have much shorter periods than the first pulsar discovered. The periods of 33 ms and 89 ms were decisive in identifying the pulsar objects as neutron stars rather than white dwarfs.

Several hundred of the pulsars known today were discovered in large surveys conducted in the 1970s at Arecibo, Jodrell Bank, Molonglo, and Greenbank. All but two of the presently known pulsars lie within our Galaxy. One of the exceptions lies in the nearby Large Magellanic Cloud galaxy (PSR 0540-69) and the other in

the Small Magellanic Cloud (PSR 0042-73). A large number of additional pulsars (about 200) have been discovered in the last several years as the result of a second generation of all-sky searches, from Parkes (Australia) covering the southern sky and from Jodrell Bank (Cambridge) and Arecebo (Puerto Rico) covering the northern sky. Recent observations by the Parkes Multibeam Pulsar Survey team at the Australia Telescope National Facility have found an additional 395 pulsars, so far not published.[6] One optically visible neutron star with a surface temperature of 7×10^5 K has been observed with the Hubble Space Telescope. Other radio telescopes are located at Bologna, Effelsberg, Greenbank, Lovell, Nancay, Sorocco, and Westerbork.

Of course, we expect that other galaxies with populations of massive stars ($M > 8M_\odot$) also have pulsars in them, but they are too distant for detection of the dim signal. Indeed, most observed pulsars lie within a third of the Galaxy radius from the Sun.

A few pulsars are named, such as the Crab, because of the beautiful nebula which is the supernova remnant in which it lies. The supernova event, also named after the suggestive form of the remnant, was recorded by a Chinese court astronomer in 1054. However, most pulsars are designated by "PSR" (for pulsating source of radio) and by their celestial coordinates. Supernova are designated by the year in which they were first detected, together with a letter, a, b, ... aa, ab ..., to distinguish the order of discovery within the year, e.g., SN 1987a.

In addition to the first pulsar discoveries of Hewish and Bell and the Crab and Vela, there are other discoveries of special importance. Hulse and Taylor (1974) discovered the first pulsar (PSR 1913+16) in a binary system in which its partner is also a neutron star [52]. The orbital period of about eight hours is remarkably short and the precession of the orbit remarkably large—4.2 degrees per year, compared to the general relativistic precession of Mercury of 43 seconds per century.

The many careful measurements made on this system by Taylor and collaborators during the intervening years have provided singular tests of General Relativity under strong field circumstances (surface gravity for neutron stars is $M/R \sim 0.2$) [4, 53, 54]. So far, they provide the only evidence of gravitational radiation. Its effect is to damp the orbital motion of the pair of neutron stars. It is estimated that they will collide in $\sim 10^8$ years. This system provides an unusual laboratory for studying General Relativity [210]. A very recent discovery by Wolszczan [211] of a close binary pulsar having a period of 27.9 ms. and with a highly elliptical orbit and short orbital period of 10 hours, PSR 1534+12, promises to be even more rewarding as measurements accumulate over the years [210].

The fastest known pulsar so far is PSR 1937+21 discovered in 1982 by Backer, Kulkarni, Heiles, Davis, and Goss [212]. It has a period of 1.56 ms, and it took great ingenuity to detect such rapid pulses given their dispersion by the interstellar medium (discussed later). It was the first millisecond pulsar to be discovered. Such

---

[6] I am indebted to R. N. Manchester and the Australia Telescope National Facility for permission to add the additional discoveries on Fig. 5.7.

rapid rotation of 650 times a second was quite astonishing. It was the first of a new class of pulsars that had been foreseen by Alpar, Cheng, Ruderman, and Shaham, by Bachus, Taylor, and Damashek and by Radhakrishnan and Srinivasan as the result of spinup of a low-magnetic field neutron star by slow accretion of matter from a Keplerian disk [184, 213, 214]. Support for the interpretation was soon provided by the discovery of a second millisecond pulsar ($P = 6.1$ ms), PSR 1953+29, by Boriakoff, Buccheri, and Fauci in a 120-day orbit with a white dwarf [215]. However, it was not until almost twenty years later that the interpretation was confirmed by Wijnands and van der Klis by the discovery of 2.49 ms X-ray pulsations from a compact X-ray neutron star in a two hour binary orbit with a low-mass companion [216, 217].

The chance that the orbital plane of a pulsar and a companion would lie sufficiently close to the line of sight as to cause the pulsar to be eclipsed is small, but it has been observed for a 1.6 ms pulsar which is in an eight hour orbit with a white dwarf. The pulsar signal is obscured for about one-tenth of the orbital period, as discovered by Fruchter, Steinbring, and Taylor [218].

The importance of *globular clusters* as being rich in fast and binary pulsars has been supposed for some time, but this was confirmed spectacularly in a discovery of ten millisecond pulsars in 47Tucanae by Manchester, Lyne, Robinson, D'Amico, Bailles, and Lim in 1991 [219]. The density of stars in globular clusters is roughly a thousand times greater than in the disk of the Galaxy. Presumably the high density will cause many binary associations and hence the formation of millisecond pulsars through accretion (see Section 5.2.5).

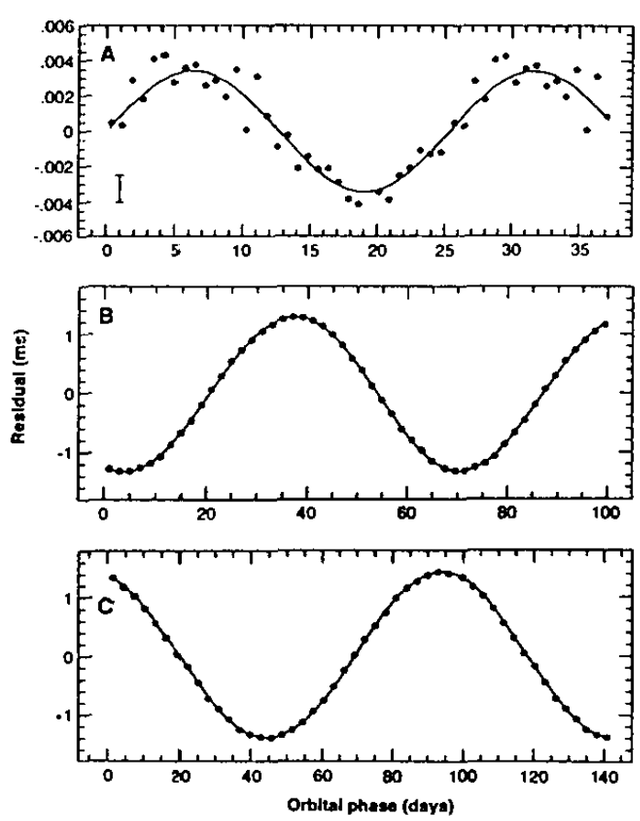

FIGURE 5.1. Timing residuals showing Doppler shift of three planets (the effect the of other two is subtracted in each case) in orbit with a neutron star [220, 221]. Reprinted with permission from *Science*, 264 (1994), 538. ©1994 American Association for the Advancement of Science.

Wolszczan and Frail discovered planets in orbit around a very old ($\sim 10^9$ yr.) millisecond pulsar in 1992 [220]. These were the first planets ever to be discovered that lie outside the solar system. The Doppler shift in the pulsar signal caused by the three planets—two earth-mass bodies and one moon-mass body—are shown in Fig. 5.1. The pulse arrival times of the other planets has been subtracted in each case.

The revolution in technology in the last few years is bringing to light many unusual phenomena. The closest (140 pc) and brightest pulsar called JO437-4715 was discovered by Bell, Bailes, Manchester, Weisberg, and Lyne [222]. It has a period of 5.75 ms and is in a 5.74 day orbit with a low-mass white dwarf companion. A wind from the pulsar creates a bow shock in the interstellar medium as the binary pair passes through it at high velocity (Fig. 5.2).

Another nebula created by a rapidly moving isolated pulsar is illustrated on the cover of this edition and was discovered by Cordes, Romani and Lundgren [223]. It has the shape of a guitar. The pulsar, located at the tip of the neck, is traveling at more than 800 km/s, greater than the escape velocity (500 km/s) from the Galaxy.[7] The length of the guitar represents 300 years of travel time. The shape of the nebula is of course a projection onto a plane of a three-dimensional object. Presumably its peculiar form is caused by a varying density of the interstellar hydrogen in which the shock velocity created by the high-speed pulsar varies. The shock front is made visible by the H alpha spectral line, produced by the de-excitation of shocked hydrogen. The pulsar itself has a long period of about 0.68 s and is quite old,[8] about a million years. It must have had an even higher speed when ejected from the site of the progenitor star's collapsing core. The high "kick" speed is presumed to originate in an aspherical collapse. Unrelated bright spots in the cover photo are background stars. The other nebulosity is believed to be unrelated to the pulsar itself and is possibly created by the passage of a shock wave created in a distant event in time and space.

So far, a binary system consisting of a neutron star and black hole has not been discovered, but such binaries likely exist. Indeed, one of the fascinations of astronomy and astrophysics is that whatever is allowed by the laws of physics does in all likelihood occur somewhere in the universe.

5.2.2 *Pulsar periods*

The periods of the pulsars, so far discovered, range from milliseconds to seconds with the mean period being about 0.7 s. Some of the periods are measured with enormous accuracy, as, for example, PSR 1913+16 (Hulse–Taylor pulsar) where 14 significant figures are known with an error of 1 in the last. The fastest pulsar presently known, PSR 1937+21, discovered as recently as 1982, has a (nominal)

---

[7]The speed is given as a lower limit because the distance to the pulsar is known only as a lower limit.

[8]See (5.16) for how a pulsar's age is estimated.

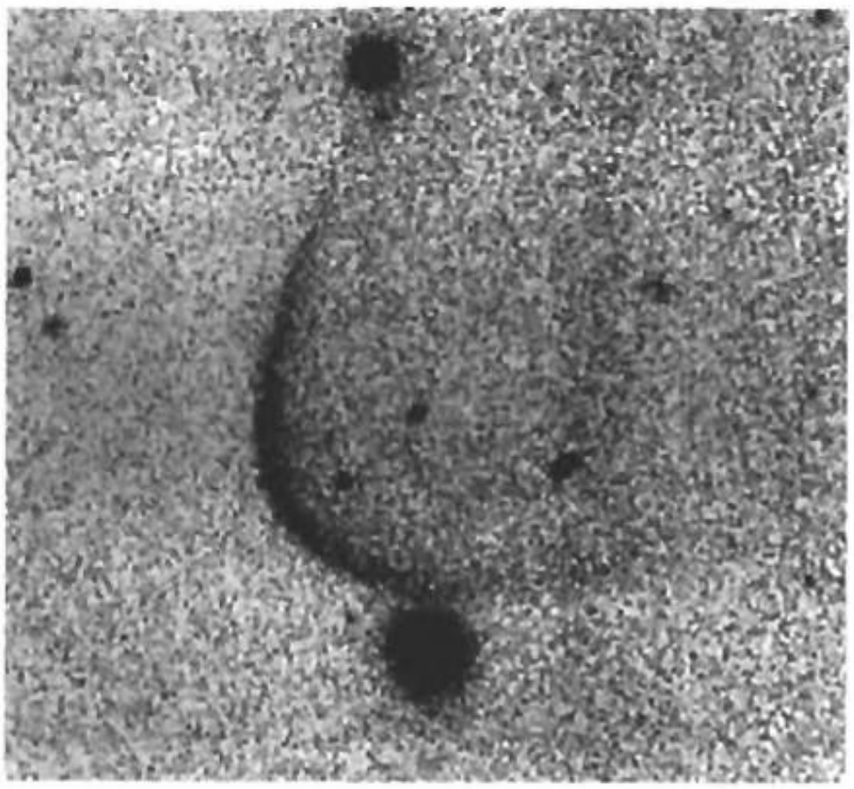

FIGURE 5.2. The bow shock of a fast pulsar and its white dwarf companion (visible just behind the shock front) as it ploughs through the interstellar medium. The H alpha line of hydrogen makes the shock visible. (Other objects are background stars.) Image courtesy of A. Fruchter and Cerro Tololo Inter-American Observatory.

period of 1.56 ms [212]. As we shall discuss, neutron stars carry large magnetic fields. Because the magnetic axis would be coincident with the rotation axis only by accident, the rotation of the star causes a loss of rotational energy because of the torque applied by the magnetic dipole. The rate of rotation therefore decreases with time, albeit very slowly.[9] Consequently, the full accuracy of the measurement of the period can be given only with reference to the time of the measurement! The period of the above pulsar was

$$1.557\,806\,448\,872\,75 \pm 0.000\,000\,000\,000\,03 \text{ ms},$$

as of 29 November 1982 at 1903 UT [224]. The limit on the accuracy of the measurement is actually due to the precision of terrestrial time standards. Such precise timing provides a unique tool for studying certain astrophysical problems [225, 226]. As we shall soon see, the above period is attributable to rotation—more than 600 times per second—of a star having the mass of about our Sun and a radius of about 10 km!

The present discovery rate of *millisecond pulsars* is accelerating with the discovery that globular clusters seem to have a high population of fast pulsars. There are some 150 globular clusters in our Galaxy, distributed approximately spherically outside the central bulge of the Galaxy to distances from the Galaxy center

[9]However, the slow loss of angular momentum does not imply a low rate of energy loss. The Crab pulsar loses energy at the rate of 4×10^{38} ergs/s, but has a rotational energy of 4×10^{49} ergs.

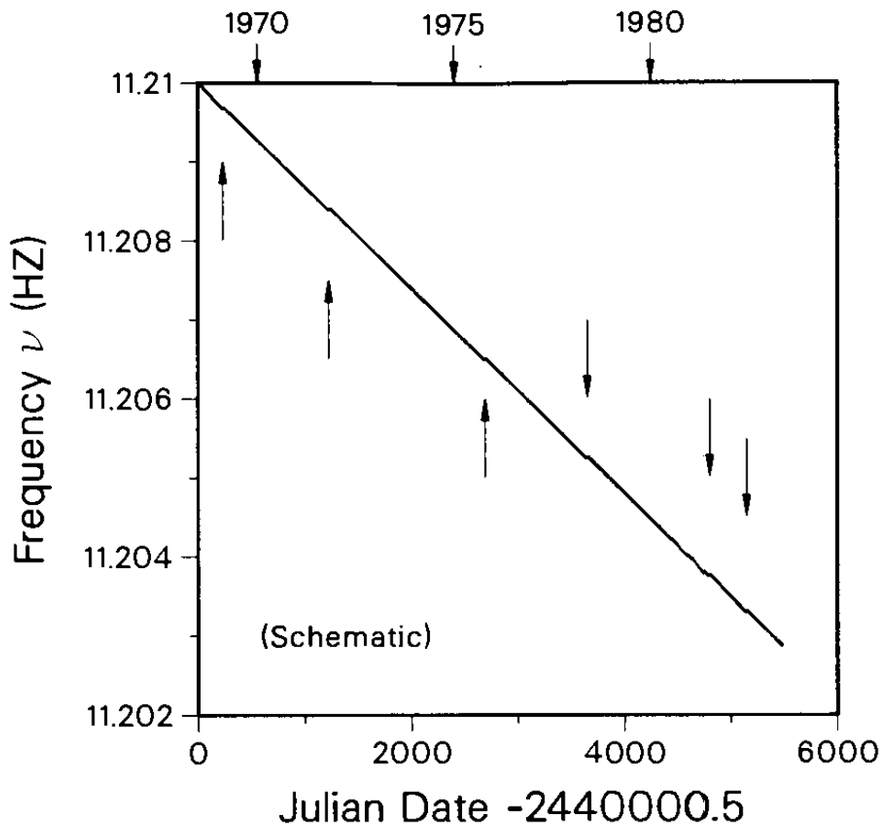

FIGURE 5.3. The slow variation of the rotational frequency of the Vela pulsar, $\dot{P} = 1.2503 \times 10^{-13}$ s/s. Also a number of "glitches" are seen in the time frame, thought to correspond to star quakes.

equal to the radius of the disk. They are self-bound groups of 10^5 to 10^6 stars and the density of stars is about 1000 greater than that part of the Galaxy that our Sun occupies—and presumably any other typical part. These groups of stars are by their nature especially rich in fast pulsars [225], as attested to by the discovery referred to above in the globular cluster 47Tucanae [219]. However, most of the globular clusters are too distant for the detection of the weak pulsar signals. Those that are close enough will prove to be rich in phenomena associated with the fate of old pulsars: rebirth by mass and angular-momentum accretion in binaries and eventual spin-up to millisecond pulsars. Doubtless, many surprises await.

Although the period of pulsars generally change at essentially a constant rate, some pulsars exhibit relatively small, random, and unpredictable changes in periods called *glitches* [227]. The size of glitches varies from pulsar to pulsar, and sometimes in a given pulsar. The relative change in frequency is small and of the order of

$$\Delta\Omega/\Omega = -\Delta I/I = 10^{-8} \text{ to } 10^{-6} \tag{5.1}$$

where Ω denotes angular velocity and I moment of inertia. The time between glitches can vary from months to years with the approximate rate and intensity being rather the same for individual pulsars. The first such glitch phenomenon was observed in the Vela pulsar, and since then glitches have been seen in many others. There is great individuality found in glitch magnitude and recovery of period from pulsar to pulsar [228] and sometimes among glitches observed for the same pulsar

[229]. Both the steady but slow change in period and the glitch phenomena are shown in Fig. 5.3 for the Vela pulsar.

5.2.3 *Individual pulses and pulse profiles*

The radiation emitted by pulsars is not only at radio frequencies, but in some cases covers a frequency range of many orders of magnitude from radio to high-energy gamma rays. The spectrum of the Crab pulsar is very broad as is shown in Fig. 5.4. The power output in the radio band is 10^{-4} or less than the total power radiated. However, most observations and searches are made at radio frequencies by enormously sensitive radio antenae.

What is referred to as the shape of a pulse (or integrated pulse) is actually the shape of individual pulses averaged over a 100 or more. It is the integrated pulse profile in a specified band width that is stable in shape and timing and characteristic of an individual pulsar and which is different from that of other pulsars. Individual pulses, on the other hand, are highly variable in intensity, timing, and in subpulse structure, suggesting small, rapid changes in the conditions of the emission.

The pulse arrival time (at the observing instrument) is often displayed by reducing the time by an integral multiple of the period of the average pulse profile and is sometimes then referred to as the phase or longitude (with 360 degrees corresponding to a full rotation and continuous signal).

For most pulsars the longitude of individual pulses is quite random within the longitude spanned by the integrated pulse profile. However, for some few pulsars there are interesting systematics in individual pulses or subpulses as in Fig. 5.5 [202, 230]. Some show a slow drift in the longitude of a string of individual sub-

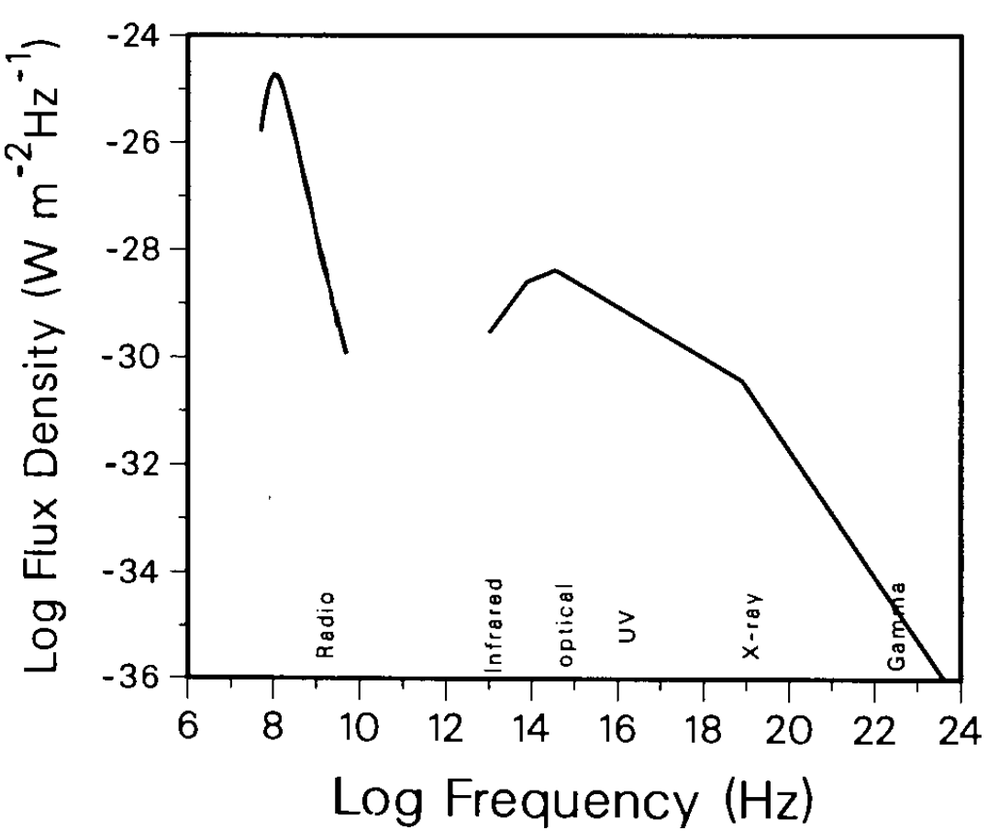

FIGURE 5.4. Spectrum of radiation from the Crab pulsar.

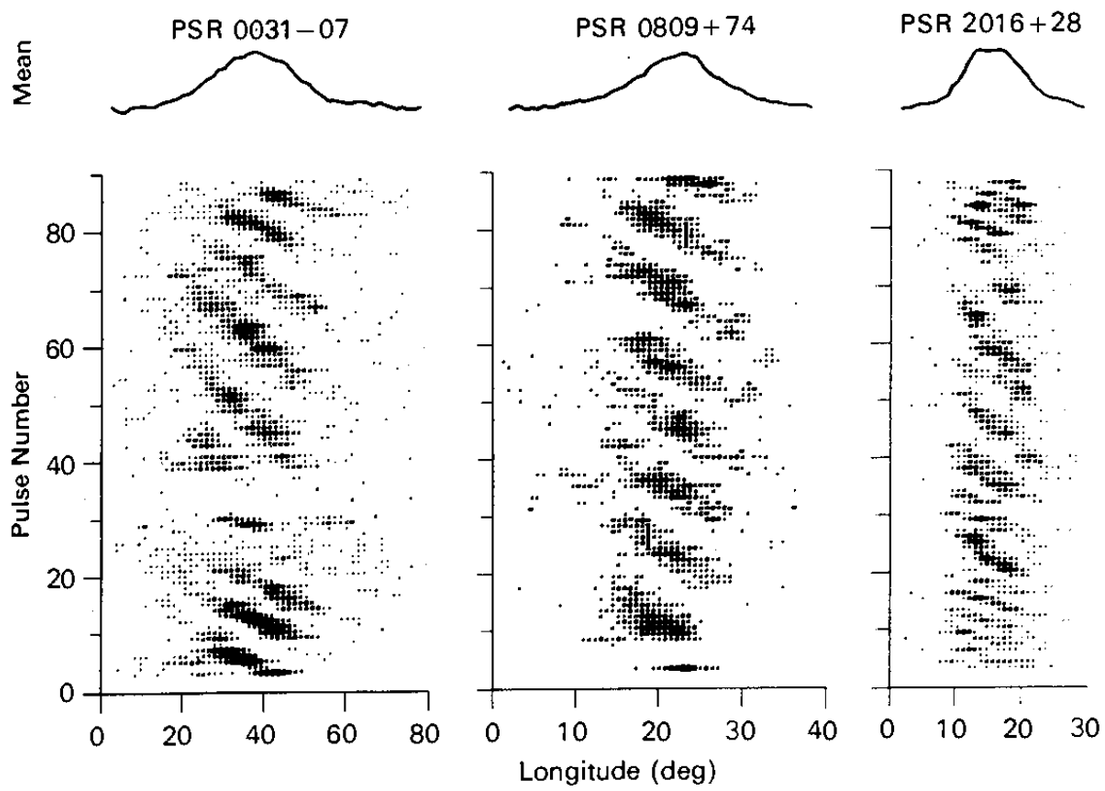

FIGURE 5.5. Longitude of individual pulses are shown which illustrate drifting, and in the case of PSR 0031-07, nulling. Time to the right and upward. Average pulse profiles are shown at the top. Reprinted courtesy of Manchester and Taylor and the *Astrophysical Journal* [202, 230].

pulses across the width of the integrated profile, returning to the original longitude and beginning the drift again. There is a quasi-periodicity associated with such *drifting*, the number of pulses within a string and the longitude of corresponding members of different strings being about the same, but not exactly. Still another class of pulsars exhibits a phenomenon referred to as *mode switching*. A string of individual pulses occurs at or near a given longitude. Then the pulses switch to a neighboring longitude and then back. Approximately the same number of pulses occurs in either string, and they alternate between the two longitudes. A third phenomenon observed in some pulsars is that of *nulling*, a situation in which the signal is so weak or absent that it cannot be seen for some number of periods.

The phenomena of pulse drifting, nulling, and mode switching, characteristic of certain individual pulsars, are possibly associated with complicated electromagnetic phenomena at the surface and in the magnetosphere of the star. Curiously, an isolated freely precessing object with an emission in a direction fixed in the rotating star but offset from the angular momentum axis can exhibit all three phenomena according to the particular parameters—angle between the above axes, direction of observer, and so on [231].

5.2.4 Detection biases

For various reasons, including the beaming effect, the known population of pulsars represents a highly biased sample of the true pulsar population in our Galaxy ($\approx 10^{11}$ stars). Signal intensity is reduced by the inverse-square law. Most known

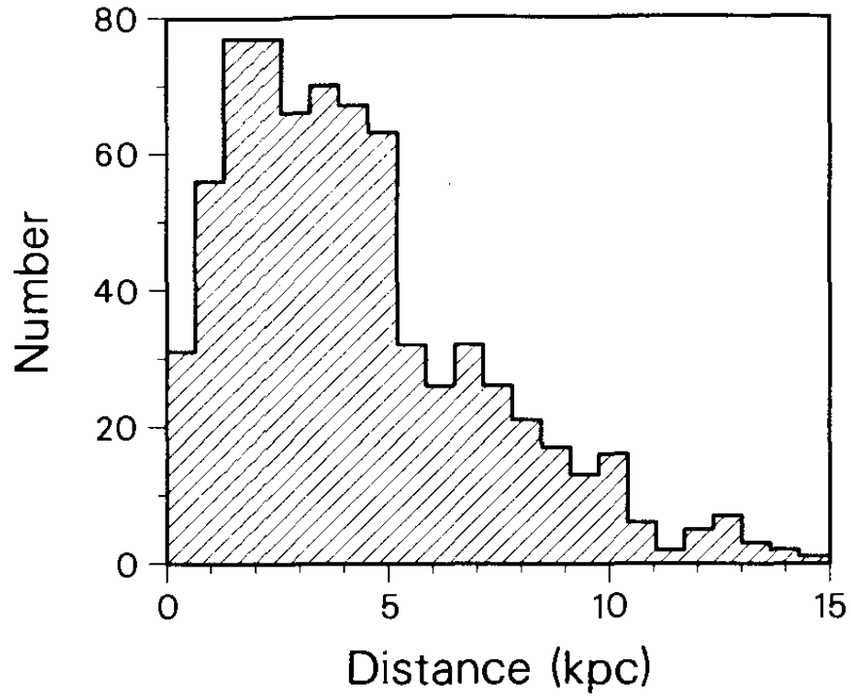

FIGURE 5.6. Distance distribution of pulsars measured in kiloparsecs. (1 kpc $\approx$ 3, 300 ly).

pulsars lie in the vicinity of the Sun. The Sun lies approximately two-thirds of the radius of the Galaxy (R_G = 15 kps $\approx$ 49, 000 ly) from its center and near the galactic plane. The bulk of known pulsars lie within a distance $R_G/3$ of the Sun, though some lie at greater distance. A histogram of pulsar distance distribution up to 15 kpc is shown in Fig. 5.6.

Distances are estimated in a variety of ways, parallax using the Earth's orbital diameter as base line, association with supernova remnants of known distance, absorption or not of spectral lines by known hydrogen clouds which determines whether the pulsar is behind or in front of the cloud, and by the differential dispersion of the various wavelengths in the pulsed radio signal by the interstellar electrons. Because of their interaction with the diffuse ionized interstellar gas, the longer wavelengths suffer a greater time delay in reaching us than the shorter. Having some knowledge of the distribution of electrons in the Galaxy, one can infer the column height of intervening electrons from the dispersion of the various wavelengths in the pulsed signal [232]. When several types of measurements can be applied to the same pulsar, agreement within a factor of two is generally found. The total galactic population is believed to be something like 10^5 active pulsars [233]. Because most pulsars radiate a signal for only 10 million years or so, there must be a much larger population of unseen silent neutron stars.

Because of the dispersion of the radio signal within the chosen frequency band, there are practical limits on the detection of short periods imposed by compromises chosen for the large surveys [234]. For this reason the observed distribution of pulsar periods is not expected to accurately reflect the relative populations of canonical and millisecond pulsars. Even now there is a strong roll-off in sensitivity to periods below about 1 ms [235].

The signals from fast pulsars cannot be seen in the raw data. Each pulse contains a range of radio frequencies, each of which is subject to a different time delay because of dispersion by the interstellar medium. So, although each pulse has a

well-defined beginning and ending at the location of the pulsar as the beam sweeps past our direction, the arrival times of different frequencies are spread out. This problem is most acute for short-period pulsars.

The technique for detecting fast pulsars, i.e., closely spaced pulses, is first to store the radio frequencies occuring in the pulses in bins according to frequency, tagged of course with arrival time. Each bin will contain a finite width of frequencies according to the cost and compromises that have to be made in designing the equipment. The frequencies in each bin will be subject to some as yet unknown average time delay depending on the density of dispersive electrons integrated over the distance the signal has traversed. The integral measuring the electron density between pulsar and observer is known as the dispersion measure (DM). Before the discovery of a pulsar, the dispersion measure to its location is unknown. A dispersion measure is guessed, and the appropriate correction to the arrival times corresponding to each bin of the raw data is made. A fast Fourier transform code is then used to ascertain if any periodicity exists in the reconstructed signal. If not, another DM is tried, and the process repeated. The above procedure is continued until a periodic pulse is detected in the data, or (because one is not sure that there really does exist a pulsar in the direction being searched at a distance that can be observed, and no periodicity has yet been detected) one abandons the process in favor of a new search direction [225]. Clearly, compromises inherent in the detection equipment and in the cost of the analysis of the raw data (there is radio noise in all directions) impose a practical limit to the lowest detectable period of a given search.

The recent discovery of a dozen or more millisecond pulsars in globular clusters was facilitated by the proximity of the pulsars to one another. As soon as one discovery is made, the interstellar dispersion (DM) to that general location is determined. Correction of the data with DMs in the neighborhood much enhances the detection technique. In other words, globular clusters are especially favorable sites in which to discover fast pulsars.

5.2.5 *Two populations of pulsars*

It appears that there are two populations of pulsars. One corresponds to the distribution centered around a period of 0.7 s as in Fig. 5.7 which includes most pulsars presently known. These pulsars are usually isolated stars with strong magnetic fields $\sim 10^{12}$ to 10^{13} gauss. We sometimes refer to them as *canonical pulsars*. The other population consists of the *millisecond pulsars* which are seen in the lower tail of the distribution of Fig. 5.7. More than half of the millisecond pulsars are in binaries and all have weak fields $\sim 10^8$ to 10^9 gauss. Many of them are found in globular clusters. Though fewer millisecond pulsars have been discovered, it is now believed that the field of the Galaxy contains a population of millisecond pulsars that is comparable to the slower ones.

Neutron stars are believed to be born with fairly short periods—spun-up by conservation of angular momentum during formation from the collapse of the white-dwarf-sized iron core of the progenitor star. The young Crab pulsar with

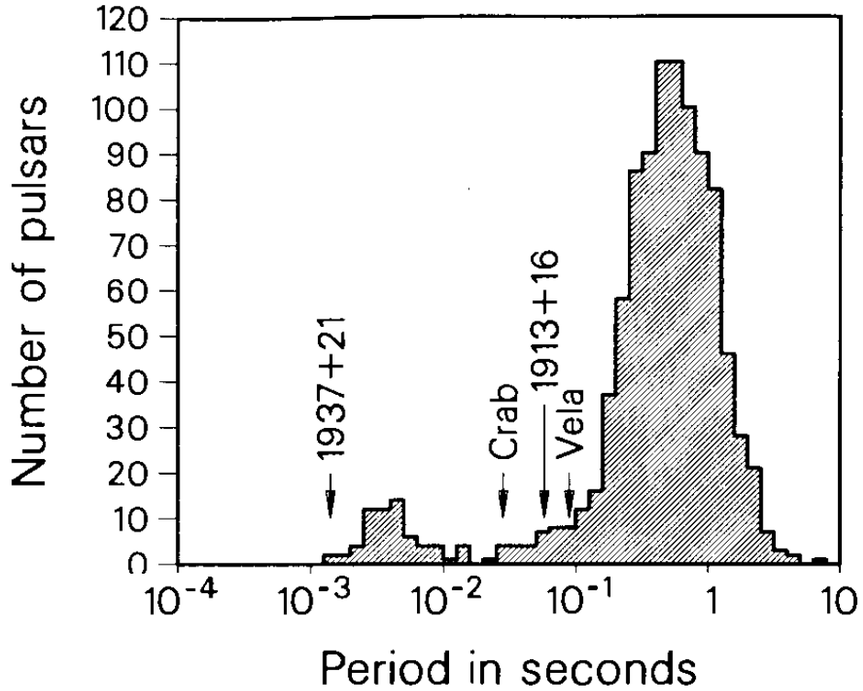

FIGURE 5.7. Distribution of periods for the presently discovered 1139 pulsars, 60 of which have periods between 1.56 and 10 ms and are referred to as *millisecond* or *recycled* pulsars. The main group, referred to as *canonical* pulsars, have an average period of 0.722 s. There is a strong attenuation in sensitivity of radio surveys for periods below about 1 ms, as discussed in Section 5.2.4. (I am indebted to M. Bailes and the University of Swinburne, Australia, for supplying the catalogued data for 744 pulsars as of July 1999. Unpublished data on 395 pulsars as of July 1999 is shown courtesy of the Parkes Multibeam Pulsar Survey team and the Australia Telescope National Facility.)

a period of 1/30 s is possibly typical of newly born neutron stars. Such pulsars then evolve for a few million years through rotational energy loss toward longer periods. During this epoch they are pulsars, though not necessarily visible to us on Earth. That depends on their distance, the strength of their radio emission, and on whether the Earth lies on the cone swept out by the rotating beam.

Depending on a combination of the magnetic field strength and period, the pulsar beam turns off at some critical value of the product of small period and low field strength. Apparently, insufficient energy to power the (little understood) radiation mechanism is fed to the magnetosphere by the rotating field. In any case, when the position of pulsars is plotted on a graph, having the field strength and period as axes, the result is quite striking. Active pulsars all lie to one side of an invisible line called the *death line* (see Fig. 5.8).

Of course, the rotating magnetic dipole radiates less intensely as the pulsar slows down, which it does because of the loss of angular momentum to radiation. Therefore pulsars approach the death line slowly, and Fig. 5.8 shows the accumulation of slow pulsars in the vicinity of the death line.

If the magnetic field is constant or decays very slowly on a timescale of a few million years, the trajectory of pulsars toward the death line will be at approximately constant field strength B. The Crab pulsar will reach the death line in a few million years. A pulsar can no longer be "seen" when its beam turns off. However,

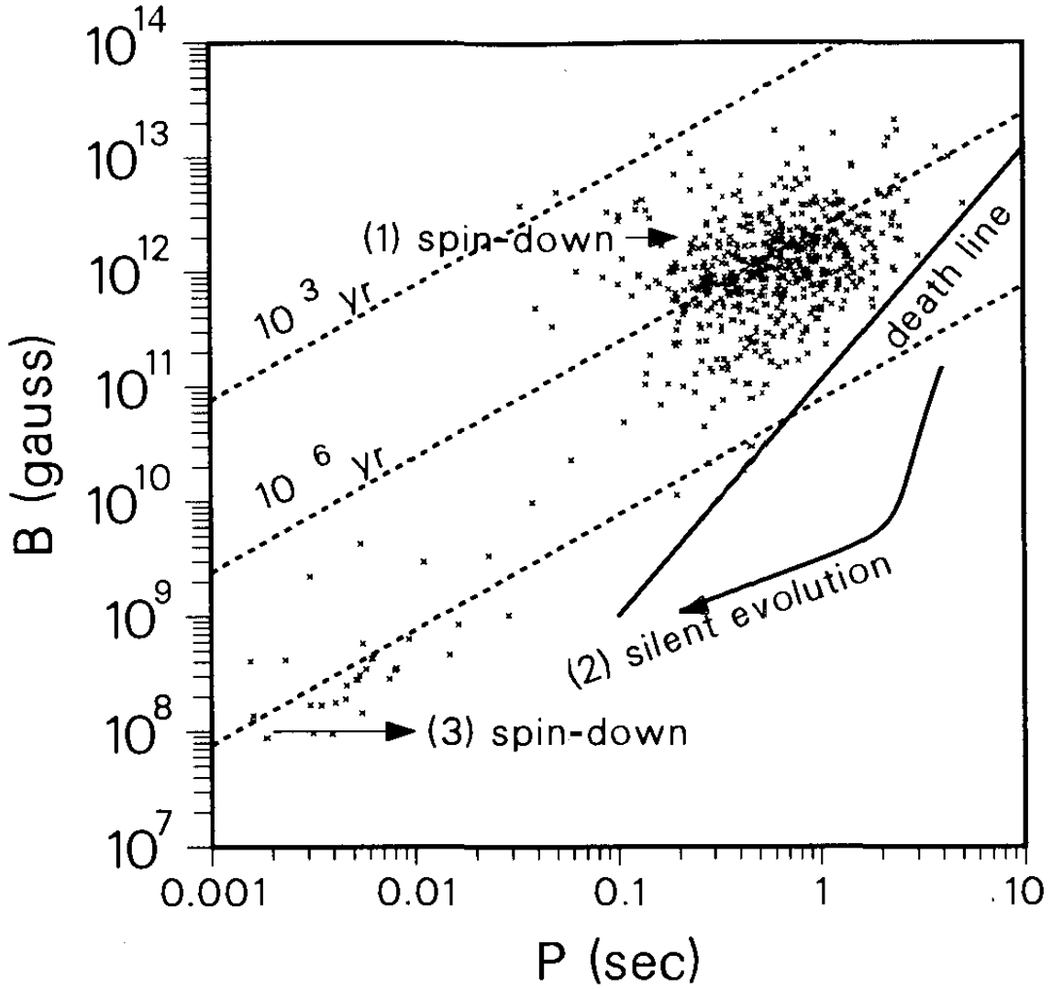

FIGURE 5.8. Magnetic fields of radio pulsars as a function of period. Death line shows a combination of period and field for which no pulsars are observed (see text). Canonical pulsars have large fields—millisecond pulsars smaller ones. Crab is the shortest period canonical pulsar. Three stages are shown: (1) spin-down of canonical pulsars, (2) spin-up by accretion, (3) spin-down of ms pulsars.

the magnetic field of the neutron star presumably continues to decay slowly, so that with time it descends in the above type of plot with the period changing little.

The second population is believed to be more evolved than the first. Pulsars in the second population have passed through the first phase of evolution described above and have reached the death line. They are thought to have possessed a companion star and have been spun up to millisecond periods by the coherent accretion of matter from the less dense binary partner during a late epoch in their lives. Compact X-ray sources are presumably such neutron stars that are accreting matter. The accreted matter forms an accretion disk. X-rays are produced by the energetic impact of this material as it falls on and heats the surface of the star. The magnetic field may also be partially destroyed in this epoch. However, when the critical combination of rotational frequency and magnetic field strength are again attained as a result of the accretion driven spinup, the neutron star turns on again as a pulsar. These conjectures, made in the early 1980s, have been recently confirmed. A millisecond X-ray pulsar has been discovered which evidently represents an example of the missing link between canonical and millisecond pulsars [216]. Other X-ray objects, not yet known to pulse, have been observed which evidently

represent neutron stars in the the intermediate stage of spin-up marked on Fig. 5.8 by (radio) silent evolution.

Millisecond pulsars are sometimes referred to as "recycled" pulsars [225, 236]. For detailed discussion of the whole subject of formation and evolution of binary and millisecond pulsars, see Bhattacharya and van den Heuvel [236]). For further discussion of observations made on compact X-ray sources, neutron stars that are accreting from a low-mass white dwarf companion, see the review by Bildsten and Strohmayer [237].

The extreme age[10] of millisecond pulsars ($\sim 10^9$ years) implied by the above scenario is partially substantiated by the fact that some of their companions are low-mass white dwarfs.[11] A binary pair consisting of a low-mass star and a more massive one will evolve at their respective rates (Table 3.1), producing first a neutron star with a low-mass luminous companion, from which it will accrete and spin up. Eventually the low-mass companion will evolve through the planetary nebula stage leaving a white dwarf companion. The magnetic fields of millisecond pulsars are much smaller than those of the first population by three or four orders of magnitude, perhaps caused by ohmic decay or partial destruction of the field during accretion. The presently known millisecond population is much smaller than the first. However, folding in detection biases, it is possible that the two populations are comparable.

5.2.6 *Supernova associations with pulsars*

Although we believe that neutron stars are born in the supernovae explosions of stars with masses in the range of about $8M_\odot$ or more, there are few cases in which a positive association can be made, for reasons mentioned below. Between 7 and 23 associations seem reasonably secure, depending on how stringent are the conditions used to make the association [36]–[39]. The most obvious problem is that a pulsar and remnant may have the same projection on the sky but lie at much different distances. Convincing associations are especially prominent for young pulsars. The reason is easy to understand. Pulsars are observed to have large velocities with an average value of 450 km/s [238]; one has been discovered with a velocity of 1200 km/s [171]. Consequently, older pulsars have moved a great distance from their birth place. The cause of the large velocities is not known. On the other hand, the supernova ejecta, while having an initial velocity of $\sim 10,000$ km/s, will generally be slowed by its encounter with the interstellar medium. In other words, the pulsar will generally outrun the ejecta on the long term. Moreover, not only have old pulsars, whose ages are millions of years, moved away from their birth site, but old supernova remnants will have faded over a time-scale of the order of 10^4 to 10^5 yrs [239].

---

[10]See Section 5.2.12 for how the age of pulsars can be estimated.

[11]Recall that white dwarfs represent the endpoint of the evolution of a low-mass star whose evolution rate is very slow.

Another contributing factor to an "apparent" discrepancy between pulsars and supernova remnants concerns the strength of the signal. As long as they are visible, supernova remnants are larger and stronger sources and therefore can be seen at greater distances than pulsars. The whole issue is a very subtle one with which observers are just coming to grips [38, 238, 239].

A very interesting association occurs for PSR 1757-24; a high-velocity pulsar with dipole age[12] of about 10^4 years is interacting with the supernova remnant it is overtaking. The pulsar velocity is estimated as $\approx$ 2300 km/s [240]. The velocity of the remnant of the supernova explosion is also high,[13] but is reduced over time by the interstellar gas that the remnant encounters as it moves outward from the explosion site. The bulletlike passage of the pulsar is revealed in Fig. 5.9 by radio emission from the *remnant* stimulated by the passage of the pulsar. The supernova remnant likely had an initial velocity of 10^4 km/s. If it were not for the deceleration of the remnant as it sweeps up interstellar gas, the pulsar would never catch up. The dipole age is therefore an estimate of the time taken to do so.

5.2.7 *Why pulsars are neutron stars*

The pulsation of pulsars is interpreted as the period of their rotation, not their vibration. Why? Pacini [169] and Gold [172] cite a number of reasons which suggest that a rotating magnetized star is the source of such stable periodic signals as are observed. They point to the enormous energy that these stars radiate ($\sim 10^{44}$ MeV/s for Crab) and the spectacular energy ($\sim 10^{55}$ MeV) that can be stored in the rotation of a compact star of solar mass and dimension $\sim$ 10 km. By flux conservation the collapsed star carries a very large magnetic field and so provides the radiating mechanism—a rotating magnetic dipole of enormous strength. To these reasons we can add that over time the amplitude of vibration is diminished by energy loss, but the frequency is not. For rotation, the frequency is damped. This is what is observed, as in the example shown in Fig. 5.3 for the Vela pulsar.

Although the period of pulsars is very stable by most normal standards, and in the case of some millisecond pulsars, rival atomic clocks, the periods do change measurably over time. Depending on the period, the rate of change can be determined by making observations over intervals of days to weeks or months. Known pulsars have period rates of change falling in the range

$$10^{-20} < \dot{P} < 10^{-12}\ \mathrm{s/s}. \tag{5.2}$$

Taking as typical a value of the period derivative, $\dot{P} = 10^{-15}$, the change in period amounts to three seconds in 10^5 years.

---

[12]See (5.16) for definition of dipole age.

[13]Supernova ejecta can have velocities of 10,000 km/s or so. As a rough estimate, equate 1/100 of the gravitational energy of a neutron star (3.23) to the kinetic energy of ejecta of mass $\mathcal{M}$ to find for the velocity (in units of c) $v = \sqrt{(6M^2)/(500R\mathcal{M})}$. Thus we find a velocity of 8000 km/s for a $10M_\odot$ remnant if a $1M_\odot$ neutron star is formed.

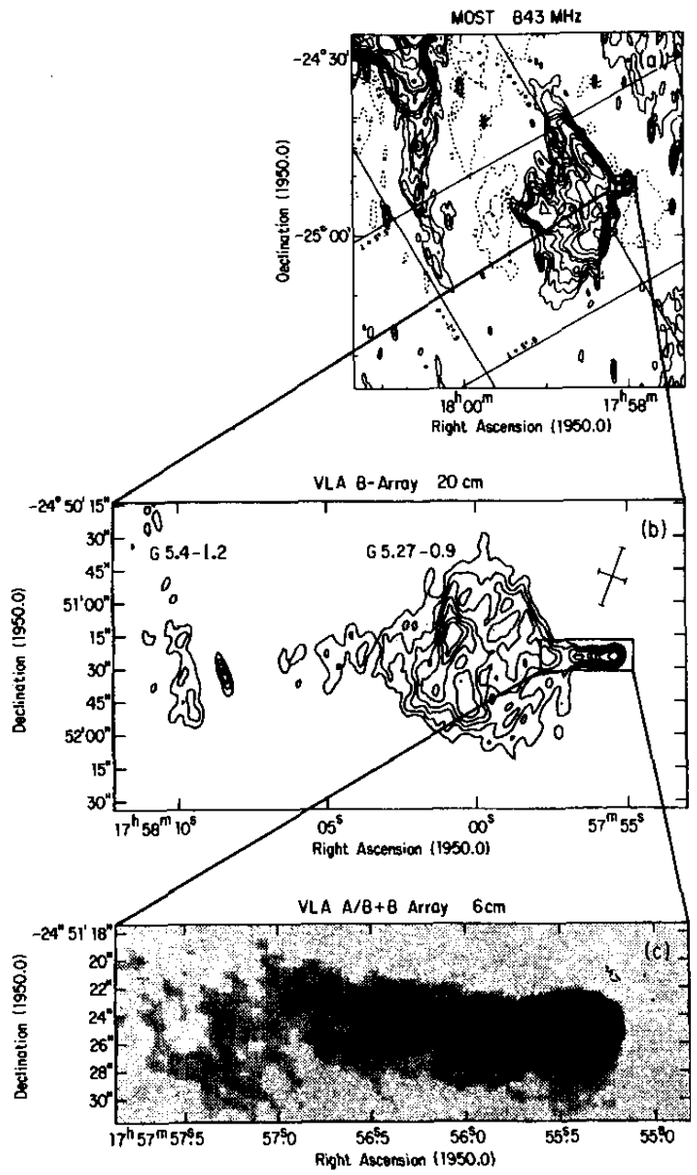

FIGURE 5.9. Radio image of a portion of a supernova remnant excited by the passage of a high-velocity pulsar, PSR 1757-24. Plate courtesy of D. Frail and S. R. Kulkarni [240]. (Reprinted with permission from *Nature*. ©1991 Macmillan Magazines Limited.)

Ordinary stars have magnetic fields ($\sim$ 100 gauss) and rotate. When they collapse from a radius of 10^6 km to 10 km, both the rotational frequency and field are scaled up by the conservation laws of angular momentum and magnetic flux. In the cataclysmic event that created the pulsar, there is no reason to expect that the axis of rotation and the direction of the magnetic field should coincide [169]. The field is typically scaled to 10^{12} gauss. It exerts a strong torque on the rotating star and together with a "wind" of relativistic particles is thought to be responsible for the steady slow decrease in period [241].

The effects on the Crab nebula of the wind and radiation from the rotating dipole of the pulsar have been dramatically observed, most recently, by the Hubble space telescope. Whisps of gas are seen to be accelerated to velocities of $1/2\ c$. Indeed, it has long been known that the remnant of the Crab supernova, some nine hundred years after the explosion, is both accelerating and radiating in radio, optical, X-ray, and gamma-ray bands powered by an energy input from the pulsar of $\sim 4 \times 10^{38}$ ergs/s ([242]; also page 67 of Ref. [202]). For comparison, the Sun's luminosity is $L_\odot \sim 4 \times 10^{33}$ ergs/s. In other words, the power radiated by the pulsar equals that of 100,000 Suns! The luminosity of the 15-ly diameter Crab nebula and its

acceleration were the inspiration for Pacini's postulate that a magnetized rotating neutron star powers the nebula, even before the first pulsar was discovered [169]. Interestingly, before the pulsar discovery, Hewish and Okaye in 1964 observed a radio emission from within the Crab nebula whose scintillation proved the presence of a compact source [243].

We can learn some of the large-scale properties of neutron stars from the power input to the Crab nebula and from the fastest rotating of the known pulsars, PSR 1937+21. Energy balance implies about the same strength for the magnetic field as quoted above from flux conservation. Equate the power input to the nebula to the power loss of the rotating pulsar,

$$4 \times 10^{38}\ \text{ergs/s} = -\frac{dE}{dt} = -\frac{d}{dt}\left(\frac{1}{2}I\Omega^2\right) = \frac{2}{3}R^6 B^2 \Omega^4 \sin^2\alpha\,. \tag{5.3}$$

The last term in the string of equalities is the rate of energy radiation by the rotating magnetic dipole field [244]. Here I is the moment of inertia of the pulsar, Ω its angular velocity, R its radius, B its surface magnetic field strength, and α the angle of inclination of the magnetic axis to the rotational axis. From the power radiated we get an immediate value for the moment of inertia,

$$I = -\frac{\dot{E}}{\Omega\dot{\Omega}}\,. \tag{5.4}$$

From the above relationship, we can also write one between the magnetic field strength and the square root of the product $P\dot{P}$,

$$B = \sqrt{\frac{3I}{8\pi^2 R^6 \sin^2\alpha} P\dot{P}}\,. \tag{5.5}$$

Given the observed period and rate of change of period of the Crab pulsar ($P = 2\pi/\Omega$),

$$P \sim \frac{1}{30}\ \text{s}, \qquad \dot{P} \sim 4 \times 10^{-13}\ \text{s/s}\,, \tag{5.6}$$

and a canonical neutron star radius as estimated in (3.18), we find, taking $\sin\alpha = 1$, and using some of the transformation between units of Section 3.3,

$$\begin{aligned} &I \sim 9 \times 10^{44}\ \text{g cm}^2 \sim 70\ \text{km}^3\,, \\ &B \sim 4 \times 10^{12}\ \text{gauss}\,, \\ &E_{\text{rot}} \sim \frac{1}{2}I\Omega^2 \sim 2 \times 10^{49}\ \text{ergs} \sim 10^{55}\ \text{MeV}\,. \end{aligned} \tag{5.7}$$

The magnetic field was converted to units of gauss by the relation to centimeters

$$3.479 \times 10^{24}\ \text{gauss cm} = 1\,, \tag{5.8}$$

where gravitational units are used. Thus, from the energy imparted by the Crab pulsar to the nebula, we are able to deduce these important properties. We could estimate a size and hence density for the Crab pulsar using the classical expression

for the moment of inertia and its value derived above, by assuming a uniform distribution of matter and making an assumption about the mass.

Alternately, we can use the period of rotation of the fastest known pulsar (1.56 ms) to estimate the radius and the average energy density of a millisecond pulsar. For the star to hold together at its equator under the opposing gravitational and centrifugal forces we must have[14]

$$\zeta^2 \frac{GmM}{R^2} > m\Omega^2 R\,. \tag{5.9}$$

The factor ζ is unity in Newtonian physics and is found empirically to be about 0.65 in General Relativity [95, 96] (see Section 6.7). Hence, for stability against mass loss at the star's equator the radius must satisfy

$$R^3 < \frac{\zeta^2 M}{\Omega^2}\,. \tag{5.10}$$

Taking $M = 2M_\odot$ as estimated in (3.18), we find

$$R < 19\ \mathrm{km}\,, \tag{5.11}$$

in agreement with the estimated radius of Section 3.3.2. Similarly, the *average* density must satisfy

$$\bar{\epsilon} = \frac{M}{(4\pi/3)R^3} > \frac{3\pi}{(\zeta P)^2} = 1.5 \times 10^{14}\ \mathrm{g/cm^3}\,. \tag{5.12}$$

The last two equalities hold for the 1.56 ms pulsar. Because the density of normal nuclear matter is $\epsilon_0 \approx 2.5 \times 10^{14}$ g/cm^3, we learn that the average density of a pulsar has to be about as large as nuclear density. We know from the Oppenheimer–Volkoff equations (3.27, 3.28) that the pressure (and hence the energy density) are monotonically decreasing functions of the distance from the center; so the central density must be greater than the average. Because any net electric charge above an infinitesimal (3.32) would overwhelm the gravitational binding of an additional charged particle of the same sign, a neutron star must be charge-neutral and hence composed largely of neutrons. Therefore, pulsars must be neutron stars, or, more speculatively, another form of dense matter, such as strange quark matter which we discuss in Chapter 12. It is believed, but not understood, that radiation over a broad band of frequencies is beamed within some angular spread typically of 10 degrees along the magnetic axis [245, 246]. Given the rotation, one has a beacon which we may see as pulses as the star rotates. Because of the narrowness of the beam, radio antennae on Earth can detect, in principle, about 1/5 of all pulsars that are in range. Detection efficiency also depends on frequency of the pulsed radiation which was discussed in Section 5.2.4.

The range of densities in neutron stars is enormous. The central density is $\sim 10^{15}$g/cm^3, which is a few times nuclear density. The surface density will be low—a few grams per cubic centimeter. The surface region will consist of products,

[14]Note that we write the gravitational constant G when it aids in recognition of formulae, and then promptly revert to our convention $c = G = 1$.

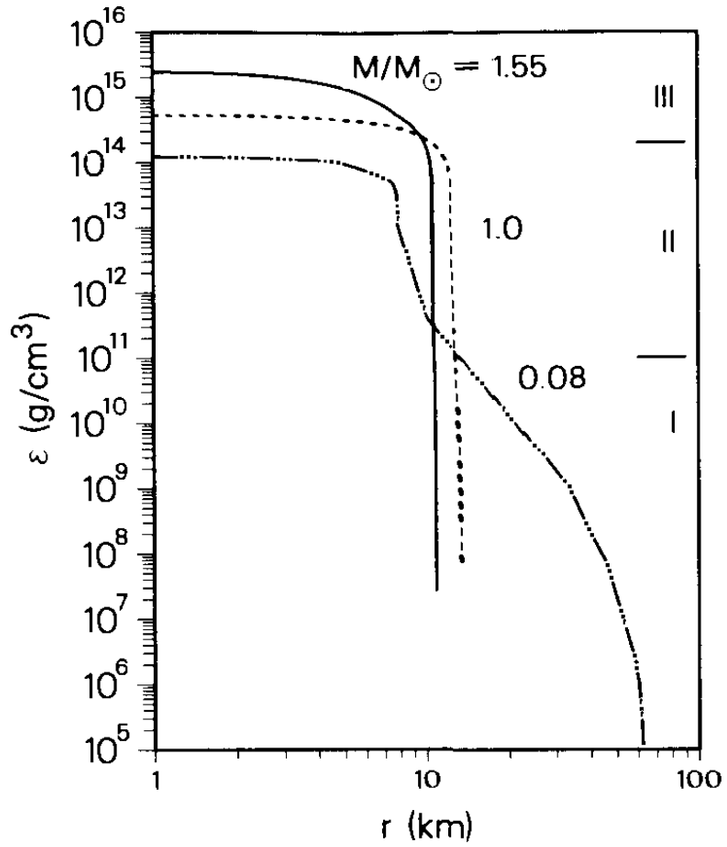

FIGURE 5.10. Mass-energy density profile of several neutron stars. Here, the compression modulus is $K = 240$ MeV and the saturation value of the nucleon effective mass is $m^*/m = 0.8$. The Roman numerals refer to the regions defined in Table 5.1.

to some degree reprocessed, that were produced in the fully evolved core of the progenitor. Iron is the final fully catalyzed material from which all available energy has been extracted by thermonuclear fusion reactions. It is the lowest energy state of hadronic matter. At the edge, where the pressure is zero, iron will exist essentially as it does on Earth in our idealization of a cold star. In reality, the temperature will be high by earthly standards, depending on the time since formation of the neutron star. The temperature will generally lie in the range 10^5 to 10^7 K, which is low on the nuclear scale of an MeV ($\sim 10^{10}$ K). However, the thickness of the molten region is slight because of the rapid increase of pressure toward the interior. Therefore, we can ignore the actual nature of the surface as far as the large-scale properties of the star are concerned, such as mass, radius, moment of inertia and internal composition.

The density profiles of several neutron stars are shown in Fig. 5.10. They range in mass from the limiting mass of the equation of state to one of rather low mass. Notice that in all cases the central region is highly compacted and fairly constant, and the edge is very abrupt except for the lightest stars. The lighter stars are larger than the heavier stars because they are less compacted by gravity. The low-density crust of a light neutron star is thick, of the order of tens of kilometers. However, such low-mass neutron stars are probably not realized in nature as we discuss below in Section 5.2.9.

For a canonical $1.4M_\odot$ star, the crust mass is only 1–2 percent of the total gravitational mass and the thickness—having densities below $\sim$ 1.3 to 1.5 $\times$ 10^{14} g/cm^3—is measured in hundreds of meters—certainly much less than a kilo-

TABLE 5.1. Density regions needed to describe a neutron star: Surface, I and II; Interior, III. Speculative particle populations are in parentheses.

	Density g/cm^3	Nature of matter	Reference
I	$2 \cdot 10^3 < \rho < 10^{11}$	crystalline: light metals	[28], [80]
II	$10^{11} < \rho < 2 \cdot 10^{14}$	crystalline: neutron-rich heavy elements, relativistic electrons	[80], [248]
III	$\rho > 2 \cdot 10^{14}$	relativistic nucleons, leptons hyperons, (pions) (kaons), (quarks)	this work [68] [132] [249]

meter (except in the lightest, and possibly nonexistent, stars of a tenth or so solar mass) [247].[15] The kinks and wiggles that appear in Fig. 5.10 are not numerical inaccuracies, but correspond to features of the equation of state. For example, the neutron drip density at 4×10^{11} g/cm^3 is clearly visible in the profile of the low-mass star. Three density regions, the source for, and the general nature of the equation of state in each, are indicated in Table 5.1.

5.2.8 *Mass of the Crab pulsar*

We deduced above the moment of inertia of the Crab pulsar from its rate of energy loss reflected in the energy input to the nebula, and the observed pulsar frequency and rate of change of frequency using (5.4). The moment of inertia is small in comparison with stellar models illustrated in Fig. 5.11. In fact, it is so small as to agree with all three models illustrated, independent of how stiff the equation of state is, as measured by the compression modulus K of the corresponding symmetric nuclear matter. This suggests that the Crab pulsar has an atypically low mass of ~ 0.8 to $0.9 M_\odot$.

5.2.9 *Pulsar masses: observational*

The white dwarf sequence terminates when the electron Fermi pressure is insufficient to support the star's mass against gravity (Ch. 3). The density at which *neutron* Fermi pressure reestablishes stability marks the beginning of the last family of *known*[16] stable compact stars—neutron stars (recall Fig. 3.9).

[15]Lorenz et al. quote the density at which nuclei dissolve as 0.1 baryons/fm^3. This translates to different energy densities depending on the binding energy of nucleons in a particular mass star.

[16]See, however, Section 11.3.

What do we know of neutron star masses? Of the 744 pulsars that are catalogued, there are mass measurements for about 20. Measurements are possible for binary systems. Those reported in the early work of Joss and Rappaport [250] have been improved in later work of Nagase [251], Kerkwijk et al. [252], and Thorsett et al. [40, 253]. The most accurately measured masses are of the pair of neutron stars in the famous Hulse–Taylor binary (PSR 1913+16). They are close in mass, and the most massive of the pair is $1.4411 \pm 0.0007 M_\odot$ [53, 210].

The most massive observed neutron star is possibly the X-ray pulsar, Vela X-1 (4U0900-40), with $M = 1.77^{+0.27}_{-0.21} M_\odot$ [251, 253]. Most masses are known only within large errors. Figure 5.12 summarizes the present knowledge of *radio* pulsar masses [40]. The error bars would be consistent with an interpretation that presently known neutron stars have masses spanning the range ~ 1 to $1.8 M_\odot$. However, given the large error bars on some measurements, it is consistent with the evolutionary scenario to give weight to the mass that lies closest to the Chandrasekhar mass. So, taking account of the creation mechanism of neutron stars, observed masses may be smaller than the actual maximum possible mass. In any case, with such a small sample of measured masses, we may not have detected the most massive neutron star, nor may we ever.

5.2.10 *Pulsar masses: physical bounds*

The mass of the lightest neutron star is calculated to be of the order of $0.1 M_\odot$. In *theory*, the mass of a neutron star could lie anywhere in the range from this minimum value to the limiting mass of the equation of state of nature, whatever that may be. However, as we saw in Fig. 3.15, the gravitational binding energy of

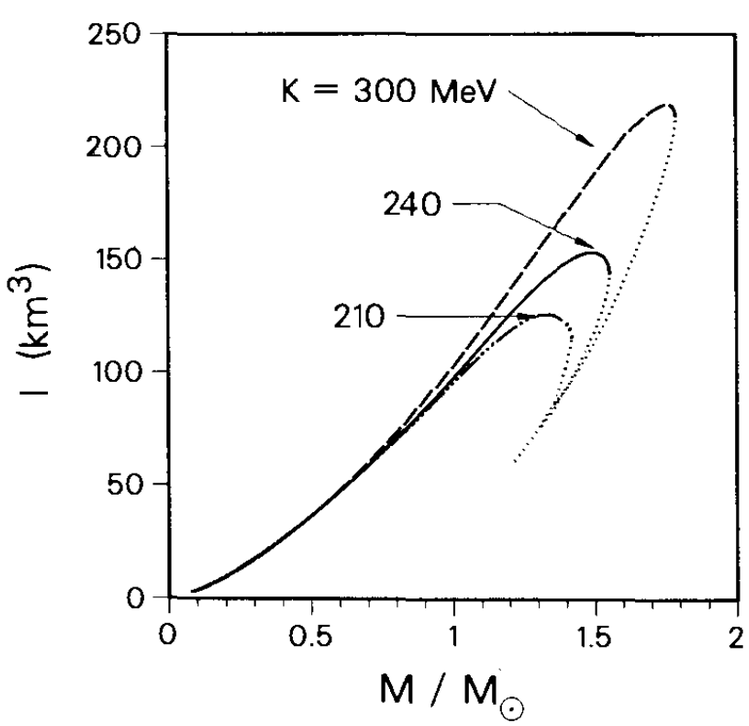

FIGURE 5.11. Moment of inertia for several values of the compression modulus K which measures the resistance to compression of symmetric nuclear matter. Parameters are those of entries 1, 3, 4 of Table 5.5 on page 261. (Dotted lines are unstable configurations that lie above the limiting mass star in central density.)

the lightest neutron stars is of the wrong sign. The mass of the equivalent number of nucleons dispersed at infinity is actually less than the gravitational energy. As we noted, this does not mean that a low-mass star, if somehow formed, would be unstable. In fact it would be stable to removal of single nucleons or groups of nucleons. But formation of the star by compaction would not release energy. Indeed, such low-mass neutron stars have very large radii (see Fig. 5.23). So, unlike the more massive members of the sequence, there would be no release of gravitational binding to power the expulsion of most of the progenitor. Consequently, Fig. 3.15 implies a lower limit on the mass of neutron stars that could be powered by a supernova explosion.

Concerning the maximum possible mass of a neutron star, all we know with reasonable confidence is that it cannot exceed the mass of an equation of state corresponding to the causal limit,[17] augmented by a small amount if the rotational frequency is high. As we showed earlier, the absolute mass limit is about $3M_\odot$ (Sec. 3.17). For theories of matter that incorporate a knowledge of the properties of nuclear matter, the estimated limiting mass is necessarily lower than the causal limit, generally falling in the range of 1.4 to 2.4 $M_\odot$, depending on the equation of state, and in particular on such high-density phenomena as hyperonization and other phase transitions such as quark deconfinement or Bose condensation. We will see later in this chapter that realistic limits lie below $2M_\odot$.

Why do the masses of the most accurately measured stars fall in a very narrow band around $\sim 1.43M_\odot$? Is it significant that all other measurements (which can be made only for stars in binaries) are consistent with this band, within the errors, as can be seen in Fig. 5.12? Perhaps all neutron stars that *are produced in nature* have nearly the same mass.

Indeed, neutron stars are formed in a particular way, namely, in the collapse of the core of a massive star ($M > 8M_\odot$) followed by a supernova explosion. The core collapses because of instabilities that are triggered when the core mass attains approximately the Chandrasekhar mass, 1.4 to 1.5 $M_\odot$ or even more, depending on the mass of the progenitor [255]. The particular value of the Chandrasekhar mass depends on the lepton fraction prevalent in the core (see Section 3.9.6) and can therefore depend weakly on the mass of the presupernova star. The above mass range, augmented by perhaps $0.1M_\odot$ of material accreted during the supernova event, establishes the mass of the neutron star that will be produced at the end of collapse. It also establishes that the equation of state of nature must support stars at least as massive as the Chandrasekhar mass, else no neutron star could possibly exist: Core collapse would lead directly to a black hole.

Thus the creation mechanism is likely to produce neutron stars in a fairly limited range of masses, independent of how large the maximum possible mass allowed

[17] A hypothetical type of star referred to as a Q-star [254] can have a larger mass than that of matter obeying a causal equation of state that is normalized to *normal* nuclear matter. However, the hypothetical Q-stars are exotic solutions of an effective field theory and as such do not constitute a robust class of stars. They have no relationship to any known state of matter, nor to any plausible theory of exotic matter.

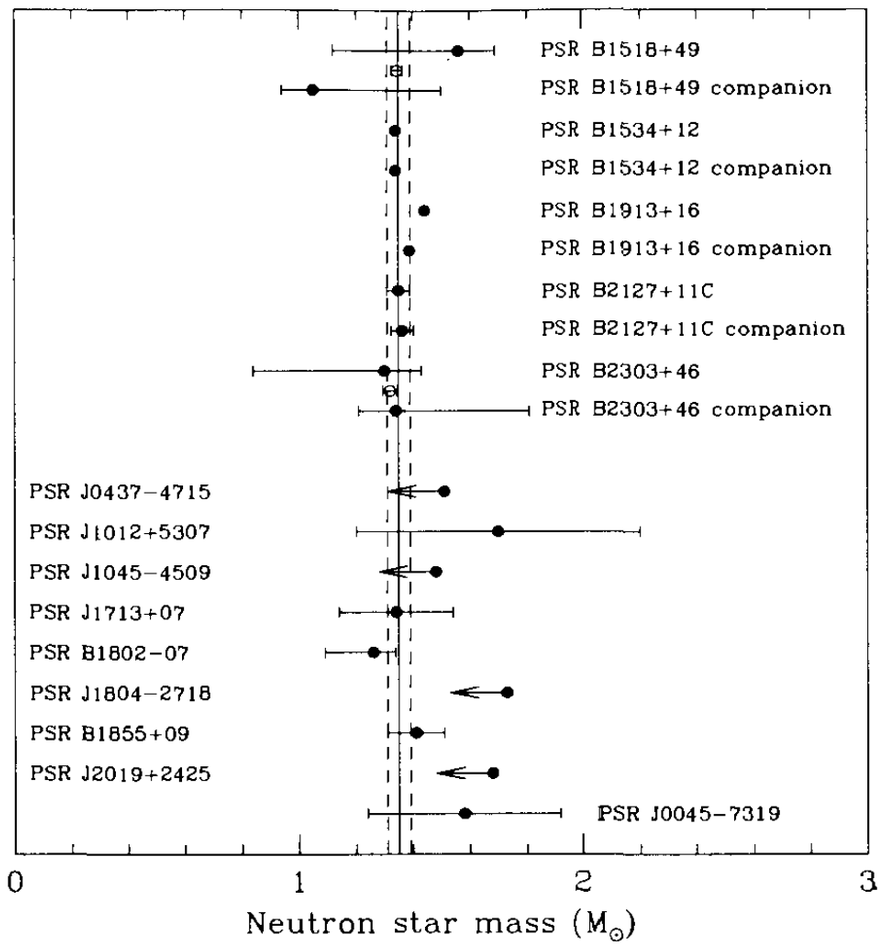

FIGURE 5.12. Compilation of presently known radio pulsar masses, courtesy of S. Thorsett and D. Chakrabarty [40].

by the equation of state of nature may be. There may exist no astrophysical means of producing the most massive neutron star, just as there may exist no means by which the lightest can be made! So a theoretical model must have a limiting mass at least as large as the most massive observed pulsar. And this observed mass may have nothing to do with the limiting mass corresponding to the equation of state of nature.

An additional complication concerning the significance of observed neutron star masses, aside from the fact that they are all members of binaries and so are a select group, concerns the three *close* binary systems. All six of the measured masses are accurately known and are very close to one another. The near equality of masses in a binary implies that the progenitor stars were of nearly identical mass. If this were not so, the progenitors would have evolved at different rates. The neutron star formed by the more massive progenitor would have been the first to exist, and it would have accreted matter from the still luminous low-density and lower-mass companion. In other words, if the progenitors did not have nearly identical masses, neither would the neutron stars of the binary. So, the most accurately measured masses around $1.44 M_\odot$ may in fact be very atypical of neutron stars.

Because the most massive neutron star may never be discovered, theory is only constrained by the requirement that it provide a mass limit that exceeds known masses. Vela X-1 seems to establish for now that theory must be able to account for pulsars of mass at least as large as $1.5 - 1.6 M_\odot$. The more recent discoveries of

millisecond pulsars, about half of which presently have binary companions, leads one to speculate that more mass measurements will be forthcoming in the not too distant future.

5.2.11 *Neutron stars: a cosmic coincidence*

Notwithstanding the above discussion of the creation mechanism of neutron stars, the limiting mass may lie no more than a few tenths of a solar mass above the Chandrasekhar limit, entirely by coincidence. Any high-density phenomenon, such as a phase transition, softens the equation of state and therefore lowers the value that the limiting mass would have in the absence of the phenomenon. Examples are hyperonization, quark deconfinement, and Bose condensation of negative mesons. The latter two phase transitions are the subject of later chapters. In this chapter we discuss hyperonization—the conversion of nucleons to hyperons in superdense matter—and its role in strongly reducing the mass by as much as $\sim 3/4 M_\odot$ as compared to a star imagined to be made solely of nucleons [68, 132, 191].

Theories of dense *purely neutron matter* yield limiting masses typically from 2 to $2.5 M_\odot$ [68, 256]. Such a reduction as cited above caused by any one of several possible phase transitions, places the limiting mass close to the Chandrasekhar mass, but for a different reason than the creation mechanism of neutron stars. Thus, the very existence of neutron stars seems to be a precarious coincidence. They occupy a narrow mass window bounded from below by the Chandrasekhar mass, which is a limit imposed by degenerate electron pressure, and from above by degenerate baryon pressure, short-range nuclear repulsion, and any phenomenon that will soften the hadronic equation of state, such as the hyperonization or the phase transitions mentioned above. Were these limits to be inverted in magnitude, massive stars would collapse to black holes without a supernova explosion powered by the birth of a protoneutron star. Without supernova explosions to disperse the heavier elements that are synthesized in stellar evolution, neither the Earth or life would exist.

5.2.12 *Pulsar ages*

We have seen that pulsars must be very dense. They are therefore likely to be neutron stars, or possibly, as we will later discuss, hybrid stars (Chapter 9) or strange stars (Chapter 12). Neutron stars are born in supernova explosions at the end point of the evolution of massive stars ($M \geq 8 M_\odot$). Initially the angular velocity of the star is determined by conservation of the angular momentum of its core and the conditions accompanying its birth. Because pulsars do emit radiation and a wind of electron–positron pairs, their rotation will be damped by the loss of angular momentum and energy, a small part of which we see in the pulses. The law that governs the decay of the rotation was written in (5.3) for magnetic dipole radiation *and* the customarily *assumed* constant moment of inertia. Other possible

radiation is gravitational. Let us write, in general,

$$\dot{\Omega} = -K\Omega^n \tag{5.13}$$

where $n = 3$ for magnetic dipole electromagnetic radiation and $n = 5$ for quadrupole gravitational radiation. Taking $t = 0$ at birth and Ω_0 as the initial angular velocity, we can integrate the above equation to yield,

$$\begin{aligned} t &= \frac{1}{(n-1)K}\left[\frac{1}{\Omega^{n-1}} - \frac{1}{\Omega_0^{n-1}}\right] \\ &= -\frac{1}{n-1}\frac{\Omega}{\dot{\Omega}}\left[1 - \left(\frac{\Omega}{\Omega_0}\right)^{n-1}\right] \end{aligned} \tag{5.14}$$

This equation does imply that the moment of inertia (absorbed in K) is constant. This is a poor approximation for millisecond pulsars. But for the present, we proceed in the traditional way, valid for ordinary pulsars. After a long time, such that $\Omega << \Omega_0$, the above expression becomes independent of the initial frequency, and we get an estimate of the present age of the pulsar,

$$\tau = -\frac{1}{n-1}\frac{\Omega}{\dot{\Omega}} = \frac{1}{n-1}\frac{P}{\dot{P}}\,. \tag{5.15}$$

The "dipole" age is simply defined as,

$$\tau_{\text{dipole}} = \frac{1}{2}\frac{P}{\dot{P}}\,. \tag{5.16}$$

In Table 5.2 we show a range of pulsar ages as thus determined. That of the Crab is in fair agreement with recorded history.

Equation (5.14) can also be written as

$$P(t) = \left[P_0^{n-1} + (2\pi)^{n-1}(n-1)Kt\right]^{1/(n-1)} \tag{5.17}$$

where the initial period can be found from

$$P_0 = P\left[1 - (n-1)\frac{\dot{P}}{P}\tau\right]^{1/(n-1)} \tag{5.18}$$

in terms of the present values of P, $\dot{P}$, and the present age τ of the pulsar, if known, as in the case of historic supernovae like the Crab. (The value of K can

TABLE 5.2. Pulsars spanning the apparent range of ages

Name	P (s)	dP/dt 10^{-15} s/s	dipole age (yr)
Crab	0.033	422.7	1200
Vela	0.089	125.03	11,000
1913+16	0.059	0.009	10^8
1952+29	0.4266	0.0019	3.6×10^9
1855+09	.0054	1.6×10^{-5}	5×10^9

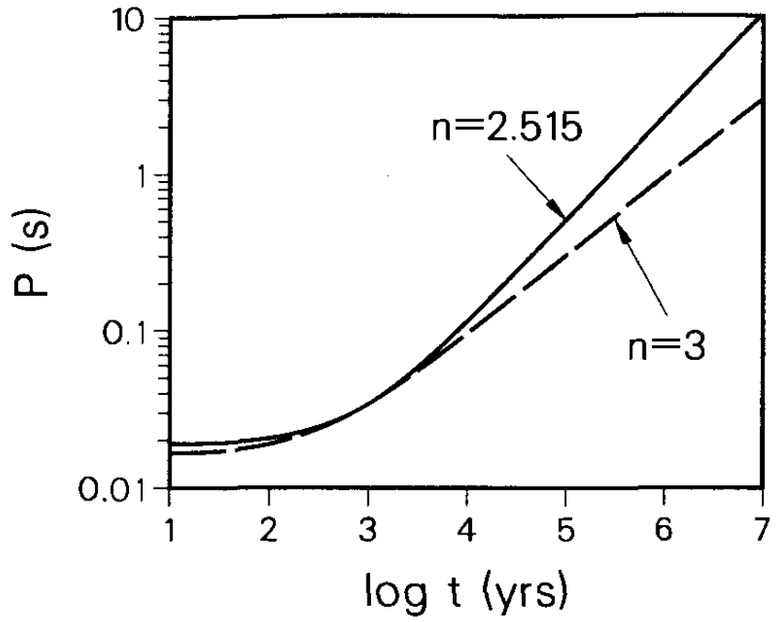

FIGURE 5.13. Evolution of Crab pulsar period as a function of time for the dipole braking index ($n = 3$) and the index measured ($n = 2.5$) in this epoch.

be determined from (5.13)). Thus, from observation using (5.17), we can compute the time variation in a pulsar's period.

The index n is referred to as the braking index and is shown for several pulsars in Table 5.3. According to (5.13) it can be empirically determined if the second time derivative of the frequency has been measured:

$$n = \frac{\Omega\ddot{\Omega}}{\dot{\Omega}^2}. \tag{5.19}$$

For the Crab pulsar as well as several others for which $\ddot{\Omega}$ is measured, the braking index is less than 3, the value expected for magnetic dipole radiation. A component of gravitational radiation in the energy loss would increase the effective braking index. An index less than 3 therefore indicates an incomplete understanding of the rotational energy loss mechanism in pulsars.

Let us use the data of Tables 5.2 and 5.3 for the Crab pulsar and (5.17, 5.18), to see how the period is expected to evolve both for the pure magnetic dipole ($n = 3$) and for the observed braking index. The comparison of the past and future period for the two braking indices is shown in Fig. 5.13. We can infer the initial period of the Crab pulsar to be ~ 0.018 seconds. (We used an historical age $\tau = 930$ yr.) The pulsar will likely have an active life (as a pulsar) for several million years. The behavior of the period with time is characteristically dominated by the first (constant) term in the bracket of (5.17) in the early era during which (short) time the period changes little. There is a transition epoch—the curved part of the graph—followed by a linear relationship between $\log(P)$ and $\log(t)$ with slope $1/(n-1)$. Clearly, a pulsar spends most of its life at a rotational period that is much longer than its initial value.

TABLE 5.3. Pulsar braking indices

Name	n	Ref.
Crab	2.515 ± 0.005	[257, 258]
Vela	1.4 ± 0.2	[259]
1509-58	$2.837 \pm 0.001 \pm 0.2$	[260, 261]
0540-69	2.01 ± 0.02	[262]–[265]

5.2.13 *Evolution of the braking index*

The law for the rate of change of the pulsar period (5.13) is derived from the energy loss equation (5.3) under the assumption that the moment of inertia I is independent of rotational frequency. This is the assumption implicitly made in the literature and leads to the important "dipole" age formula (5.15) for estimating the spin-down time or age of pulsars. The same assumption lies behind the connection between the magnetic field strength B and the period and its time derivative (5.5).

However, the moment of inertia is not constant in time.[18] The shape of the pulsar responds to changes in the centrifugal forces and hence to changes in rotational frequency, more or less according to the softness or stiffness of the equation of state and whether the stellar mass is small or large. We can show that this response reduces the value of the braking index in a frequency-dependent manner, even though the sole energy-loss mechanism is assumed to be pure magnetic dipole. Thus, during any epoch of observation, the measured braking index will be less than 3 for dipole radiation. It will be much less than 3 for millisecond pulsars. However, it is difficult to measure the second time derivative for such pulsars, and no actual measurement has been made.

To investigate for which frequencies the response of the moment of inertia substantially modifies the results (5.13 and 5.19), we rewrite (5.3) in greater generality:

$$\dot{E} = \frac{d}{dt}\left(\frac{1}{2}I\Omega^2\right) = -C\Omega^{n+1} . \tag{5.20}$$

We refer to this equation as the *energy-loss equation*, and it assumes for simplicity of exposition, that there is a single multipole. We refer to n in the above formula as the *intrinsic* (energy-loss) index. For magnetic dipole radiation ($n = 3$), one can read C from (5.3) as

$$C = (2/3)R^6 B^2 \sin^2\alpha . \tag{5.21}$$

We find that (5.13) is replaced by a new *deceleration equation*,

$$\dot{\Omega} = -K\Omega^n\left(1 + \frac{I'\Omega}{2I}\right)^{-1} , \tag{5.22}$$

[18]This section is based in large part on on the work of N. K. Glendenning, S. Pei, and F. Weber in Ref. [200] and also unpublished work.

when the frequency response of the moment of inertia is taken into account. We have used the notation $I' \equiv dI/d\Omega$ and $K = C/I$. Of course, over any observational era, and even over much longer times, $I(\Omega)$ and its *time* derivatives are essentially constant. *However*, what is relevant is that $dI/d\Omega$ is finite and indeed large, especially for millisecond pulsars (Fig. 5.14). This fact changes the braking law from (5.13) to (5.22). Accordingly, for a given strength of radiation process, $\dot{\Omega}$ is reduced for millisecond pulsars by the correction factor in (5.22). The estimate of B from (5.5) based on the assumption of constant I is altered to read,

$$B_{\text{new}} = B_{\text{old}}\left(1 + \frac{I'\Omega}{2I}\right)^{1/2} . \tag{5.23}$$

However, given the uncertainty in the angle α, the correction is insignificant. For the hyperon star illustrated in Fig. 5.14 the correction amounts to 40% at the Kepler frequency, but is negligible for canonical pulsars. Where the effect of changes in moment of inertia really show up strongly is in the measurable braking index $n(\Omega)$.

The index of the energy-loss mechanism is not given by (5.19) except for a rigid body. We can evaluate the *measurable* or apparent braking index, a dimensionless combination of Ω and its first two times derivatives; using (5.22) we find

$$n(\Omega) = \frac{\Omega\ddot{\Omega}}{\dot{\Omega}^2} = n - \frac{3I'\Omega + I''\Omega^2}{2I + I'\Omega} . \tag{5.24}$$

The *measurable* index $n(\Omega)$ reduces to the constant n when changes in I are ignored; otherwise it depends on frequency and therefore time through the appearance of Ω, $I(\Omega)$, and the derivatives of I with respect to Ω. It is less than n because I' and I'' are positive (the moment of inertia increases with Ω and the centrifugal force grows with the equatorial radius). Therefore, the measurable braking index achieves its canonical value n only at low frequencies. It is not the power of the frequency in the energy-loss equation. The measurable index is independent of the strength of the constant C of the energy-loss mechanism (5.20).

It is especially noteworthy that the *magnitude* of the signal—the deviation of $n(\Omega)$ from n—depends on $dI/d\Omega$ which is large, especially for millisecond pulsars, but the *duration* of the signal depends on $d\Omega/dt$ which is small. Therefore, the variation of the braking index over time is very slow, the timescale being astronomical. So what one would observe over any observational era is a constant braking index $n(\Omega)$ that is less than that characteristic of the energy-loss mechanism n (5.20) even if the radiation were a pure multipole.

An expression for the moment of inertia of slowly rotating stars is well known (6.20). It is a constant and therefore inadequate for our purpose because we wish to study the braking index over the history of a star, including frequencies close to the Kepler limit.[19] We derive an expression for the moment of inertia of a relativistic star that accounts for the centrifugal flattening as well as the dragging of local

[19]The Kepler frequency of a star is the frequency at which the centrifugal force would overwhelm gravity at the equator.

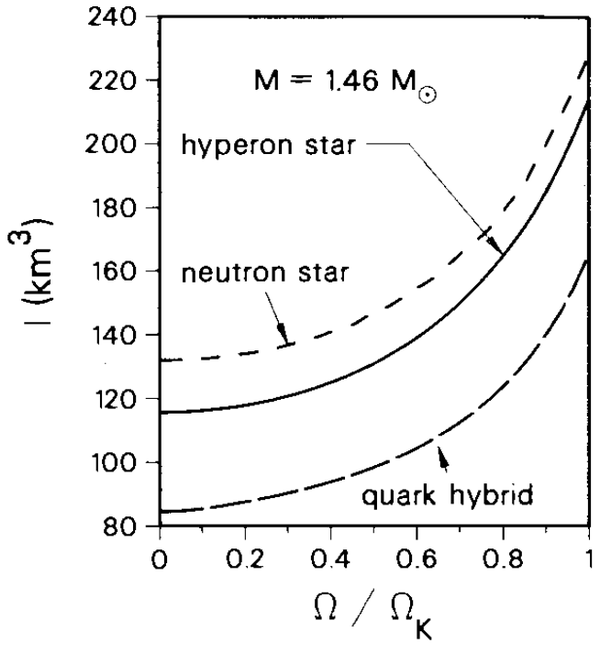

FIGURE 5.14. Moment of inertia for several stellar models as a function of rotational frequency (in units of Kepler). Neutron star denotes a star with only neutrons protons and leptons in equilibrium. See later in this chapter for the meaning of hyperon star, and Chapter 9 for the meaning of hybrid star (quark matter core).

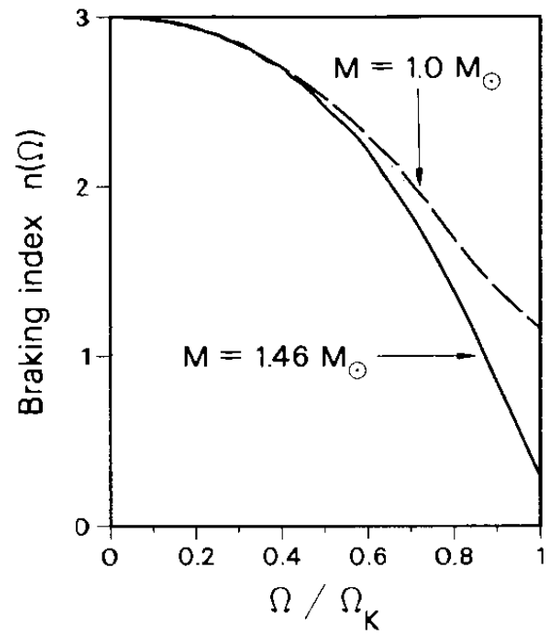

FIGURE 5.15. Apparent braking index for pure dipole ($n = 3$) as a function of rotational frequency for stars of two different masses of the hyperon model. Parameters of the model are entry 3 in Table 5.5. Masses indicated are for slow rotation.

inertial frames in Chapter 6 [197, 266]. We use the referenced expression in our model calculations of the braking index.

For different equations of state describing the matter of a star (that is, for different stellar constitutions), the moment of inertia will respond differently to frequency and to mass of the star. The frequency response is shown for several stellar models in Fig. 5.14. The behavior of the measurable braking index with rotational angular velocity is shown for two pulsars of different mass in Fig. 5.15. For definiteness the illustration is for magnetic dipole loss. Along each sequence the baryon number of the star is constant, as it should be. The braking index for magnetic dipole radiation clearly is not the constant $n = 3$ for high-frequency pulsars. It may be smaller than three over any observational era depending on frequency and on mass of the star.

The behavior of the moment of inertia and the braking index illustrated in Fig. 5.15 are smooth functions; however, the behavior can also be drastic if a phase transition occurs during the course of spin-down. This can happen as a result of an anomalous increase in central density with decreasing centrifugal force as a more compressible phase replaces the relatively incompressible nuclear matter. A very simple and direct signal of a phase transition will be discussed later in the Section 11.4.

The age formula (5.15) that is so universally used in classifying stars for various purposes (glitch activity, two-pulsar populations, etc.) was derived under the assumption that the moment of inertia is constant *throughout* the entire life of the star. Clearly, it will give an incorrect answer for any pulsar that has had a frequency,

during its history, that is a substantial fraction of its Kepler frequency. In general there is no analytic formula for the age, and for a pulsar that was a rapid rotor in any era, the age could only be obtained by integrating the energy-loss equation with a moment of inertia obtained from a model of the star and having an explicit dependence on the frequency.

Measurements of braking indices have been made for four pulsars. All have a rather low frequency of rotation (Table 5.3). As can be seen from Fig. 5.15, the effect of the variation of the moment of inertia with Ω is very small for slow rotation. Therefore, a measured braking index for these slow pulsars should essentially coincide with the intrinsic index of the energy-loss mechanism (5.20). In that case, for whatever reason, the only observed energy-loss indices are less than 3. The reason cannot be attributed to centrifugal effects in the case of canonical pulsars.

5.3 Theory of Neutron Stars

Neutron stars are bound by gravity, not by the nuclear force. This statement may seem obvious to those with an astrophysical orientation rather than to those with a nuclear one. The nuclear force, after all, is the strong force, but it is short-ranged and so acts only on its near neighbors. The gravitational force is long-ranged and acts on all mass–energy. For large and dense enough objects, it is therefore the binding force. One can easily estimate the binding per nucleon due to gravity for a canonical neutron star as was done in Chapter 3 and find a gravitational energy (3.23) of $\sim$ 160 MeV/A compared to the binding energy of nuclear matter at its saturation density of $\sim$ 16 MeV/A. Not only is there a factor of 10 in favor of the gravitational energy, but gravity compresses the matter of neutron stars so that the density lies far above the saturation density of nuclear matter. The nucleons do not feel attraction from their neighbors, but repulsion. In fact the energy required to compress nuclear matter to the density found at the center of the more massive neutron stars is 200–300 MeV per nucleon as we saw in Fig. 4.3. The compression energy reduces the net binding energy (Fig. 3.15) of neutron stars near the mass limit to about 100 MeV per nucleon as compared to the energy of the nucleons dispersed to infinity.[20] So the nuclear force contributes negatively to the binding of neutron stars, but it shapes the equation of state which is uniquely related to the structure and constitution of the star.

[20] Although the center of the star is more highly compressed than elsewhere, we learned in Section 3.7 that, in the equilibrium configuration of a star, no energy is gained or lost by moving a fluid element from one place to another in the star.

5.3.1 *Nuclear and neutron star matter: Similarities and differences*

The idealized matter of the interior of nuclei and the matter of neutron stars have important similarities and differences. The similarities include the fact that they are composed of baryons and the densities are the same within an order of magnitude or less. The differences arise from two facts:

(1) Nuclei are bound by the isospin symmetric nuclear force (see Section 4.9), but neutron stars are bound by gravity. Hence, in nuclei it is true that $N \approx Z$. However, because the repulsive Coulomb force is so much stronger than the gravitational force that binds stars, the net charge in a star must be very small,

$$\frac{(Z_{\text{net}}e)e}{R^2} < \frac{G(Am)m}{R^2} \longrightarrow Z_{\text{net}} \sim |Z_p - Z_e| < 10^{-36}A, \tag{5.25}$$

where Z_p is the proton number and Z_e the electron number. As noted previously, the net charge on a star is essentially zero. Although Z_p need not be zero because the proton charge can be neutralized by leptons or negatively charged hyperons, it is smaller than $A/2$ and generally much smaller. So nuclei tend to be symmetric in isospin whereas neutron stars are very asymmetric.

(2) There is another and profound difference arising from the weak interaction timescale, $\tau_{\text{weak}} \sim 10^{-10}$ seconds. Because of the high density of matter in neutron stars and the fact that baryons obey the Pauli principle, it is energetically favorable for nucleons at the top of the Fermi sea to convert to other baryons, including strange ones (hyperons) so as to lower the Fermi energies. The transformations do not violate strangeness conservation of the strong interactions because strangeness is conserved only on the strong interaction timescale, not on the weak. In the time it took to read the above sentence, strangeness conservation could be violated $\sim 10^{10}$ times. Even the timescale of core collapse in supernova is long compared to that of the weak interaction. Neither is lepton number conserved because of the diffusion of neutrinos out of the star. However, the time-scale is longer, of the order of tens of seconds.

Thus strangeness and lepton number are not conserved in astrophysical objects. Strangeness would not be conserved in stable nuclei either, but it is not energetically favorable to have hyperons in the ground state because their masses exceed the nucleon mass by more than the Fermi energy ($\sim$ 30 MeV) of the nucleons in a nucleus. Nuclear reactions, on the other hand, are so fast ($\sim 10^{-22}$ s) that strangeness is conserved on their timescale. So the matter studied in nuclei or their reactions has zero net strangeness, whereas neutron stars can and almost certainly do contain hyperons and have net strangeness.

In accordance with the above and a subsequent more detailed discussion, we shall mean by the phrase "neutron star matter" cold, charge-neutral, nuclear matter in its lowest energy state (meaning in general beta equilibrium).[21] All baryons

[21] Beta decay refers explicitly to such a process as $n \longrightarrow p + e + \bar{\nu}$ and beta equilibrium refers to equilibrium with respect to this reaction and its inverse. General beta equilibrium

are populated as allowed by baryon conservation and charge neutrality in such proportion as to achieve the ground state of matter at a given baryon number density without regard to the strangeness quantum number.

These are the differences. Of course, the properties of such systems as the hot, symmetric, nonstrange matter produced in relativistic nuclear collisions and the cold, asymmetric, charge-neutral, and strangeness-carrying matter of neutron stars are related in any comprehensive theory of matter. It is through relativistic nuclear field theory that we shall make the connection between them. This theory can be generalized to incorporate nucleons and higher-mass baryon states interacting through the exchange of mesons [159]. Its coupling constants can be fixed by properties of symmetric nuclear matter, as discussed in detail in Section 4.8.1. The theory also describes numerous properties of finite nuclei [267]–[270]. It can be extended to finite temperature [120, 159]. It can be extrapolated to hot, dense matter and its composition (nucleons, deltas, and their excited baryon states) [159], and to dense neutron star matter [67, 68, 128, 129, 160]. One and the same theory with fixed coupling constants describes

1. symmetric nuclear matter and the matter produced in high-energy collisions when the field equations are solved subject to the constraints of *charge symmetry* ($q = \rho/2$) and *strangeness conservation* (in this case zero), and
2. neutron star matter when the field equations, supplemented as we shall discuss, by those of leptons, are solved subject to the constraints of *charge neutrality and generalized beta equilibrium* without conservation of strangeness.

Therefore, we are able to conveniently characterize the neutron star matter equation of state by the compression modulus and other properties of symmetric matter to which the coupling constants are fixed; we shall always do so.

5.3.2 Chemical equilibrium in a star

To understand the nature of chemical equilibrium in a star, it is useful to note that the star evolves and that a cold neutron star in chemical equilibrium is the ultimate ground-state configuration. Many different reactions can occur during the evolution. Reactions between hadrons occur. Certain quantum numbers or particles, such as electric charge and baryon number, are conserved on a long timescale compared to the life of the star. However, any kaons produced in association with hyperons generally will decay on the electro-weak timescale, and their products will end as leptons, photons, and neutrinos.

The neutrinos and photons diffuse to the surface and, having more than the escape velocity, leave the star, lowering its energy and causing a Pauli blocking of the hyperons produced in association with the kaons. This will proceed until the star reaches a degenerate state where further reactions are not possible. Therefore,

---

refers to equilibrium with respect to all reactions that lead to the transmutation of baryons by weak or strong reactions that lead to the lowest energy state that is consistent with the relevent conservation laws; charge neutrality, in the case of stars.

strangeness is not conserved in a star, nor on any macroscopic timescale; a net strangeness carried by hyperons is achieved. At this stage the star is cold on the nuclear scale (1 MeV $\sim 10^{10}$ K), and from the point of view of its hadronic and leptonic composition, it is essentially frozen, aside from centrifugal effects that cause a slow increase in the interior density. The timescale for reaching the frozen state is set by the neutrino diffusion time—about ten seconds.

Although cold, by which we mean 10^5 to 10^9 K, the star is still hot compared to the cosmic microwave background radiation of about 3 K. That is why there is a net radiation of photons and neutrinos. Photon diffusion continues for millions of years. This is a brief statement of the situation [68]. We now discuss it in some detail.

It is generally understood that knowledge of the particular path that a body or substance may follow in reaching its equilibrium state is not needed to find that state. To find it, one needs to identify those components or attributes A_i that are conserved on a timescale longer than the lifetime of the star itself or the epoch during which it is observed and those that have a much shorter timescale [68]. We write the equations of transformation among the components. For example, bring all terms to the left of a reaction equation

$$\nu_i A_i = 0 \tag{5.26}$$

where the ν_i denote the number of independent components of type A_i and may be positive or negative (and are not necessarily integers, as, for example, in relationships involving quarks). The same equations hold for the *chemical potentials* of the components with the "chemical" symbols A_i replaced by the chemical potentials [66]. Thus we may write

$$\nu_i \mu_i = 0 . \tag{5.27}$$

The chemical potentials of any components that are not conserved on the timescale of the star are now set to zero. One then has relationships among the chemical potentials. There are as many *independent* chemical potentials as there are conserved components or attributes, or more generally "charges" that are absolutely conserved, or conserved on a time long compared to the life of the star (or in a more restricted sense, over the epoch of observation). All other nonvanishing chemical potentials can be written in terms of the independent ones. This rule was derived in a special case in Section 3.9.2 by means of Lagrange multipliers.

Any neutrinos and photons produced in reactions during the de-excitation of the star from its hot beginning diffuse out. We are interested in the ground state after such diffusion has occurred and the star has attained its frozen state in which further reactions are forbidden because of Pauli blocking of the reaction products. Because the neutrino population is lost to the star, we must set its chemical potential to zero,

$$\mu_\nu = 0 \quad \text{(all flavors)} . \tag{5.28}$$

As already noted, the timescale of the electroweak interaction is short in comparison to macroscopic scales, so the strangeness quantum number, though conserved

by the strong interaction, is not conserved on the scale of a star. There are therefore only two conserved "charges" with their corresponding chemical potentials—those for baryon and electric charge number. The chemical potentials of all other constituents can be written in terms of these two.

Although, as mentioned above, it is not necessary to trace or enumerate all of the reactions by which the constituents transform, it is necessary to know a sufficient number of them to establish the relationships between the chemical potentials. It is also interesting to discuss a few of them so as to elucidate how a star transforms from its state at birth to its ground state, the state to which it has evolved in all essentials at the time of any observation we may make on it [68]. In general this is the situation in which we are interested—evolved neutron stars. It would be a rare event indeed, and none are yet known, where observations can be made on a newly born neutron star.

Neutron stars evolve from an initially hot *protoneutron star*, bloated with neutrinos and photons, that forms in the collapse of a massive star following the ejection in a *supernova* of most of the progenitor star [35]. The energy carried off by the ejecta is a small fraction, of the order of a percent, of the energy that will be carried off shortly thereafter by neutrinos. The source of the energy is, of course, the gravitational binding energy of the neutron star (up to 100 MeV per nucleon (Fig. 3.15)). This initial protoneutron star is not isothermal and has interior temperatures of several tens of MeV (1 MeV $= 1.1065 \times 10^{10}$ K) and a high density, so that even neutrinos have a long diffusion time compared to the dynamical timescale of the collapse. Indeed, most of the neutrinos escape in about 10 s carrying off almost all of the binding energy, and the temperature falls rapidly to about 10 MeV in the interior and several MeV at the edge in 20 s. Thereafter the star cools by further neutrino emission, by X-ray and later by photon emission, taking a few million years to fall to a surface temperature of 10^5 K [271]–[273]. There is still considerable controversy over what are the most relevant processes by which the cooling occurs [274, 275, 276].

In any case, the temperature has fallen in a short time to less than an MeV. This is cold on the nuclear scale. Before the end of this phase in the evolution of the star, the Fermi momenta of nucleons are high and the fermions are not yet degenerate, so that strong reactions, such as

$$N + N \longrightarrow N + \Lambda + K\,, \tag{5.29}$$

are possible. The associated kaon is free to decay unless it is driven by a phase transition to a condensed state (which we discuss later). Depending on the combination of protons and neutrons that are involved in the above reaction, all three charge states may be formed. Some of their decays are

$$\begin{aligned} &K^0 \longrightarrow 2\gamma\,, \\ &K^- \longrightarrow \mu^- + \bar{\nu}\,, \\ &\mu^- + K^+ \longrightarrow \mu^- + \mu^+ + \nu \longrightarrow 2\gamma + \nu\,. \end{aligned} \tag{5.30}$$

As the temperature falls with neutrino loss, strong reactions such as (5.29) are no longer possible because of the energy required to create the kaon. Nevertheless the growth of strangeness continues through direct weak flavor changing reactions such as

$$n + N + \mu^- \longrightarrow N + \Sigma^- + 2\gamma + \nu \tag{5.31}$$

until equilibrium is reached (see Fig. 5.16).

As remarked, the star's energy is lowered by the leakage of the photons and neutrinos. Consequently, the Λ becomes Pauli-blocked, the reactions (5.29) and (5.31) become irreversible, and net strangeness is evolved [68]. Similar reactions involving other hyperons also may occur. Such processes continue until the star has reached its ground state, the state in which the baryon populations are distributed among the various species so as to account for the least energy for the given number of baryons under the constraint of zero net charge. All photons and neutrinos have escaped. (By all we mean that the temperature has become so low and the degeneracy of the baryon Fermi seas is so complete that further reactions are not possible because of Pauli blocking.)

The role played by the weak interactions is twofold: (1) It allows the direct conversion of nonstrange baryons to hyperons. (2) It allows reactions that cool the star. These reactions cause the strangeness of the kaons to be lost, i.e., to violate the strangeness conservation of the strong interaction. The baryon populations are determined by their masses, charges, isospin projections, and the strong interactions subject only to the constraints imposed by baryon conservation and charge neutrality of the star.

According to the preceding discussion, all particle chemical potentials can be written in terms of those for the conserved charges—baryon and electric—which we denote by μ_n and μ_e. The subscripts stand for neutron and electron. For example, the reaction $n \leftrightarrow p + e^- + \bar{\nu}_e$ tells us

$$\mu_p = \mu_n - \mu_e \tag{5.32}$$

because, as remarked, the neutrino chemical potentials are zero in the evolved star. As the baryon density increases, so does that of protons and electrons (up to a point as discussed later). So, μ_e may attain the value of the muon mass, in

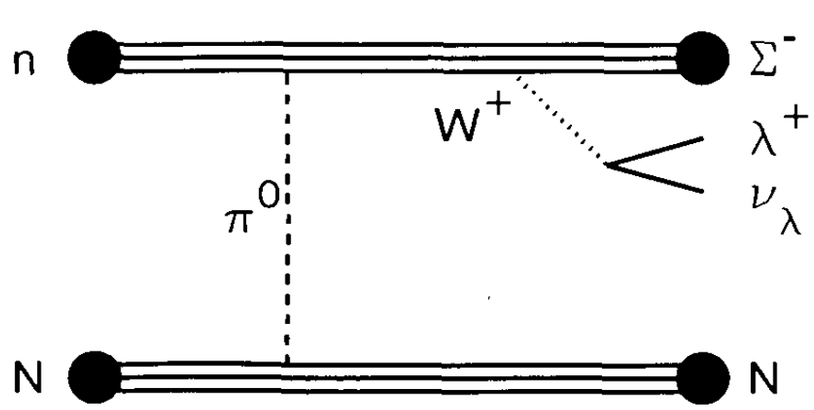

FIGURE 5.16. Illustration of the weak flavor changing reaction (5.31) at the quark level. The three horizontal lines denote the three valence quarks in a baryon. λ denotes lepton, either electron or muon.

which case it also will be populated. The equilibrium with respect to the reaction $e^- \leftrightarrow \mu^- + \nu_e + \overline{\nu}_\mu$ informs us that

$$\mu_\mu = \mu_e \,. \tag{5.33}$$

(The convention adopted is that e^- and μ^- are particles, while the leptons of opposite sign of charge are the antiparticles.)

Given the kaon decay channels (5.30) in which all photons and neutrinos, diffuse out of the star, the kaon chemical potentials are

$$\begin{aligned} \mu_{K^0} &= 0\,, \\ \mu_{K^-} &= \mu_e\,, \\ \mu_{K^+} &= -\mu_e\,. \end{aligned} \tag{5.34}$$

Equilibrium with respect to (5.29) coupled with the decay of the K^0 into gamma rays yields

$$\mu_\Lambda = \mu_n \,. \tag{5.35}$$

The chemical potentials of the other hyperons can be inferred in like manner. For example, a particular form of (5.29) pertaining to the Σ^+ is $n + n \leftrightarrow n + \Sigma^+ + K^-$ from which we learn that

$$\mu_{\Sigma^+} = \mu_n - \mu_e = \mu_p \,. \tag{5.36}$$

We have written only a few of the possible reactions among hadrons and leptons. We need only a sufficient number so as to learn the relationship between the particle chemical potentials and the two independent ones, μ_n and μ_e, for baryon and (negative) electric charge. In general the chemical potential of any particle is a linear combination of these two, weighted by the baryon and electric charge carried by the particle,

$$\mu = b\mu_n - q\mu_e, \tag{5.37}$$

where b is the particle's baryon charge and q is its electric charge (in units of $+e$). The strangeness chemical potential is zero, as discussed previously. From the above expression, the chemical potential for any particle—baryon, meson, lepton, or quark—can be written down immediately.

A particle type is populated only if its chemical potential *exceeds* its lowest energy state in the medium. This would be its vacuum mass, in lowest approximation. However, the masses of particles are effected by their interactions with other particles in a medium. We have encountered one such example in (4.131). The baryon chemical potential must increase with increasing density as assured by the Pauli principle, and the energy of the system will be lowered by sharing the conserved baryon number with other baryon species when their chemical potentials exceeds their masses as modified by interactions. Thus we can expect that superdense matter will be populated by many baryon species—possibly even quarks.

Moreover, there could also exist a condensate of charged negative mesons. This is discussed in Section 5.4.7 and in Chapter 10. In particular, a K^- condensate

has been discussed as a possible high-density phase of nuclear matter [68, 277]. Being a boson, all kaons could occupy the same momentum state, say $k = 0$. The negative kaon could therefore be a neutralizing agent in charge-neutral matter if its effective mass in the medium fell from its value of 494 MeV in vacuum to a value equal to the electron chemical potential μ_e. The point is that the proton density, and therefore the electron density, increases with increasing baryon density. Being Fermions, they must occupy ever higher momentum states as the density increases. If μ_e rises above the medium mass of the K^- it becomes energetically favorable for kaons to condense rather than weak decay. Thus electrons at the top of the Fermi sea are replaced by zero momentum kaons.

However, the electron chemical potential may not increase monotonically as was supposed above and as was discussed in Ref. [68]. We will encounter the reason later in this chapter when we see that charged hyperons tend to neutralize dense matter, thus saturating the electron chemical potential at a value that may be lower than the kaon mass in the medium. The condensation of π^- may seem another possibility, at first sight, even likelier than K^- condensation. However, the π^- interaction with the medium may be repulsive despite a p-wave attractive interaction with nucleons [278]. Nevertheless, Bose condensates are an interesting possibility that we discuss in Chapter 10.

5.3.3 Hadronic composition of neutron stars

Neutron stars, as their name implies, are not pure in neutrons as was first proposed. Charge neutrality is automatically respected by pure neutron matter, but this is not the lowest energy state of dense neutral matter. Some neutrons will beta decay until equilibrium between neutrons, protons, and electrons is reached. This is expressed by the relationship $\mu_p = \mu_n - \mu_e$ among the chemical potentials (see (3.78)).

The chemical potentials grow with increasing density. Therefore, other thresholds are reached, and additional particle species are populated. In a Fermi gas model the thresholds are simply the masses of the particles. For example, the Λ hyperon, whose chemical potential is given by (5.35), will be in equilibrium in the star when the neutron chemical potential attains the value of the lambda mass ($m_\Lambda = 1115$ MeV) and will be one of its constituents when $\mu_n > m_\Lambda$. In general, the particle thresholds depend on the interactions as well, which we include in the sequel.

The isospin symmetry energy arising from the coupling of baryon isospin to the neutral rho meson is very important in this respect (Section 4.9). Obviously it favors conversion of neutrons to baryons of opposite isospin projection to the extent consistent with charge neutrality. For these reasons neutron star matter is very complex in composition and the Lagrangian used in nuclear field theory has to be generalized to include these complications [67, 68], which have been investigated in a number of works [128]–[131], [160], [279]–[281].

The particle populations of a neutron star are shown in Fig. 5.17 when equilibrium is treated in the general manner described. For low density (as compared to saturation density), one sees that charge-neutral uniform matter is almost pure in

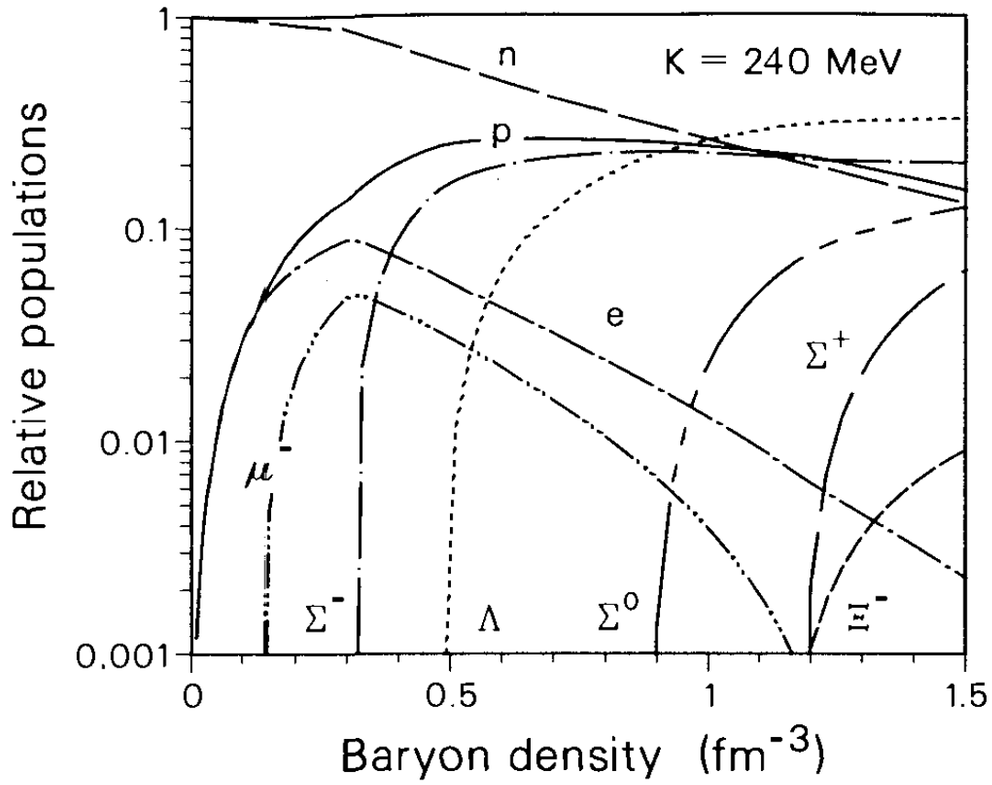

FIGURE 5.17. Populations of various particles in neutron star matter relative to the baryon density as a function of density. The compression modulus of the corresponding symmetric nuclear matter is $K = 240$ MeV. The effective mass at saturation is $m^* = 0.78m$ and hyperon couplings $x_\sigma = 0.6$ (Section 5.4.3). See also Ref. [129].

neutron, but with a small admixture of protons and electrons in equal numbers. With increasing density, the electron Fermi energy increases to the muon mass, and then the muon as well will be populated. As we discuss later, the pion may also condense. Hyperon thresholds are reached at densities beginning at about three times nuclear density, and become important components of neutron star matter with a further increase in density [67, 68, 282].

Neutron stars therefore are not made purely of neutron matter, but rather of hadronic matter in the lowest energy state consistent with charge neutrality. In general, this may be a state that is very rich in baryon species. We call this matter *neutron star matter*. Its baryonic composition changes continuously with increasing baryon density, as is easily understood from the foregoing discussion.

5.3.4 Superdense matter

Essentially nothing is known about superdense matter by direct experiment. Not a single point on the equation of state of symmetric nuclear or neutron matter above the saturation density of nuclei has been measured. Indeed, it is possible that we will never have direct knowledge from the laboratory. We know the properties of symmetric nuclear matter at saturation density (Section 4.5). The compression modulus and the symmetry energy coefficient allow us to extrapolate to moderately higher density and isospin asymmetry, respectively. Beyond that, the extrapolation to higher densities of the magnitude needed for calculating the structure of neu-

tron stars is model dependent. We do not have a tractable fundamental theory of superdense matter.[22]

However, we have a few general principles to guide us. Within such guidelines we can explore various possible high-density phenomena. Some will be more plausible than others, depending on an hierarchy that is established by the physical principles. And we will be alert to possible observations made on pulsars that may reveal something about the properties of superdense matter that we have been unable to learn from laboratory experiments. We list below the general principles and constraints that can be used for an exploration of phenomena that are allowed to occur in neutron stars:

1. Lorentz covariance.
2. General Relativity.
3. Causal equation of state ($v^2 = dp/d\epsilon \leq 1$).
4. Microscopic stability known as Le Chatelier's principle ($dp/d\rho \geq 0$).
5. Baryon and electric charge conservation.
6. Pauli principle.
7. Generalized beta equilibrium (as discussed above).
8. Phase equilibrium (Chapter 9).
9. Asymptotic freedom of quarks (see page 147).
10. Properties of matter at saturation density.

Within these general principles and constraints we will gain considerable insight into the possible constitution of neutron stars and the phase transitions that may take place at various densities. Of course we must choose a specific theory of matter to which the principles are applied. And above all, we must be alert to possible ways in which observation can confirm or deny our models.

All results must necessarily depend for their details on the choice of theory of matter. And nature is neither limited by our imperfect theories, nor is it necessarily similar to our predictions. We discussed a specific theory in Chapter 4—relativistic nuclear field theory solved at the mean field level. We discuss it further in connection with neutron stars.

But first we shall discuss why we prefer relativistic nuclear field theory to many-body theory, or better so say model, in both cases. The aim of the Brueckner–Bethe–Goldstone many-body model is to discover whether properties of nuclear matter can be correctly found from the two-nucleon interaction as it is determined from scattering experiments. One has a natural curiosity in this regard. Such calculations were begun some 30 years or so ago. It was found that not even the saturation or binding energy, which are well-known quantities, could be accounted for without the introduction of additional elements, among them, three-body interactions. Of course, as one considers the interaction of nucleons at ever higher density above the vacuum, the proximity of other nucleons must involve the simultaneous interaction of more than two. However, at that stage one has already lost strict contact with

[22] We do not call into question QCD—only its tractability for cold dense nuclear matter.

the vacuum interaction, believed to arise from meson exchange, and determined more or less well by scattering data.

So it has been that the sensible program set out by Brueckner and Bethe has been elaborated because nuclear properties do not follow, unadorned, from the interaction between a pair of isolated nucleons. With the addition of three-body interactions, boost corrections, and many others, one can now account for binding and saturation of nuclear matter [256]. But these two parameters only normalize the equation of state at one point. The symmetry energy coefficient and compression modulus are important for extrapolating to denser and isospin asymmetric neutron star matter. Generally they are not mentioned in works on the many-body model although the first is quite well known and the second is fairly well known.

Some authors have applied the many-body model to neutron matter with the aim of calculating the limiting mass of neutron stars. In the work cited above, the equation of state becomes acausal before the central density of the limiting mass star is attained. This is quite common in the nonrelativistic approach. Noncausality is not the only problem. Can one reasonably expect that the vacuum two-nucleon interaction mediated by the exchange of mesons will remain unchanged as the density of the environment is changed? It is now well established that meson masses depend on the nuclear environment and are a function of the density. Why not also the two-nucleon interaction in matter?

We know from the electron scattering experiments of Hofstadter that the rms charge radius of the proton and of the magnetic moment of both neutron and proton is 0.8 fm [283]. If nucleons could be packed in a cubic lattice to the point of touching, the density would be $1/(2r)^2 = 0.24\ \mathrm{fm}^{-3}$ or 1.5 times nuclear density. But nucleons as the entities we know in vacuum or in normal nuclei could not be localized in this fashion according to the uncertainty principle. The notion that nucleons retain their usual properties and interactions at such densities seems not to be viable. From all of the above discussion, it appears to us that the many-body model is not suitable for transcribing what is known about the vacuum interaction to the densities found in neutron stars.

There is a related approach to the many-body problem, the Dirac–Brueckner method which is a relativistic extension of the Brueckner theory. This method employs the Dirac equation for single-particle motion in nuclear matter and a one-boson-exchange potential for the interaction [284]–[292]. Nuclear matter properties seem to be better under control. However, the same problems in dealing with dense matter as discussed above exists.

It seems more fruitful to employ a model that is constrained by nuclear matter properties at *saturation density* rather than by scattering data that determines, within errors, the interaction in *vacuum*. We do not regard the relativistic mean-field model as a theory, but rather as a convenient means of incorporating the knowledge we have of nuclear matter at the highest density at which we know it; the model then provides a causal extrapolation to higher density.

Within the model, all sorts of phenomena can be incorporated, such as the conversion of nucleons to hyperons, quark deconfinement, and Bose condensation. Many possibilities can be investigated, such as the prompt collapse of proto-stars

to form a class of low-mass black holes, the possible spontaneous spin-up of a millisecond pulsar over a very long epoch as nuclear matter in its core converts to quark matter, the role of magnetic fields, and even the possible existence of a stable third family of compact star above white dwarfs and neutron stars in density.

5.3.5 *Neutron star matter*

To describe the complex baryonic composition of neutron stars discussed earlier, the Lagrangian of hadronic matter must be sufficiently general as to accommodate not only neutrons and protons, as in nuclear matter, but also higher-mass baryon states. A suitable generalization of the σ, ω, ρ theory, used to describe nuclear matter and finite nuclei, is [67, 68, 160]

$$\begin{aligned}\mathcal{L} = \sum_B \overline{\psi}_B(i\gamma_\mu\partial^\mu - m_B + g_{\sigma B}\sigma - g_{\omega B}\gamma_\mu\omega^\mu - \tfrac{1}{2}g_{\rho B}\gamma_\mu\boldsymbol{\tau}\cdot\boldsymbol{\rho}^\mu)\psi_B \\ + \tfrac{1}{2}(\partial_\mu\sigma\partial^\mu\sigma - m_\sigma^2\sigma^2) - \tfrac{1}{4}\omega_{\mu\nu}\omega^{\mu\nu} + \tfrac{1}{2}m_\omega^2\omega_\mu\omega^\mu \\ - \tfrac{1}{4}\boldsymbol{\rho}_{\mu\nu}\cdot\boldsymbol{\rho}^{\mu\nu} + \tfrac{1}{2}m_\rho^2\boldsymbol{\rho}_\mu\cdot\boldsymbol{\rho}^\mu - \tfrac{1}{3}bm_n(g_\sigma\sigma)^3 - \tfrac{1}{4}c(g_\sigma\sigma)^4 \\ + \sum_\lambda \overline{\psi}_\lambda(i\gamma_\mu\partial^\mu - m_\lambda)\psi_\lambda\,. \end{aligned} \tag{5.38}$$

The baryon spinors are denoted by ψ_B, while $\overline{\psi}_B \equiv \psi_B^\dagger\gamma_0$ denotes the adjoint. (We use the conventions of [7] used also in Chapter 4.) The first line is the sum of baryon Lagrangians and the interactions with the scalar, vector, and vector–isovector mesons (σ, ω, ρ).[23] The baryon species are denoted by B. The sum on B is over all the charge states of the baryon octet, (p, n, Λ, Σ^+, Σ^-, Σ^0, Ξ^-, Ξ^0) as well as the Δ quartet (see Table 4.5). However, in none of our calculations has the Δ been populated up to the highest density that we have found in our neutron star models. Nor have any other baryon states been populated save those of the lowest octet, for reasons given elsewhere [68].

The second line of (5.38) contains the Lagrangians of the scalar and vector mesons, whose interactions with the baryons give rise, respectively, to attraction and short-range repulsion. The third line contains the Lagrangian for the isovector meson which couples to the isospin of baryons and gives rise to the isospin symmetry energy. This line also contains self-interaction terms of the scalar field. The last line contains the Lagrangians for the leptons (electrons and muons) which are important agents in the charge neutrality of neutron star matter.

It is, of course, essential to keep track of the individual baryon charge states so that charge conservation can be enforced (zero in a star and one-half the baryon density in charge symmetric nuclear matter). We describe below how the theory can be solved in the mean-field approximation for the ground state of charge-neutral matter in general beta equilibrium (neutron star matter) [68].

---

[23] Recall Chapter 4.

The Euler–Lagrange equations derived from (5.38) are solved by replacing the meson fields by their mean values in static uniform matter, and the nucleon currents are replaced by the ground-state expectations generated in the presence of the mean meson fields. Such an approximation is the so-called mean-field approximation (MFA). We discussed it in detail in Chapter 4. It is in this approximation that nuclear field theory has been typically solved and applied. Henceforth the meson fields, σ, ω, ρ, denote these mean-field values. They are some of the unknown functions of baryon density that we must solve for.

The fermion field equations for uniform matter in momentum representation (4.127) are

$$(\gamma_\mu k^\mu - m_B + g_{\sigma B}\sigma - g_{\omega B}\gamma_\mu \omega^\mu - \tfrac{1}{2} g_{\rho B}\gamma_\mu \tau_3 \rho_3^\mu)\psi_B(k) = 0 . \tag{5.39}$$

The eigenvalues for particle and antiparticle can be found, as in Section 4.6:

$$\begin{aligned} e_B(k) &= g_{\omega B}\omega_0 + g_{\rho B}\rho_{03} I_{3B} + \sqrt{k^2 + (m_B - g_{\sigma B}\sigma)^2} , \\ \bar{e}_B(k) &= -g_{\omega B}\omega_0 - g_{\rho B}\rho_{03}\overline{I}_{3B} + \sqrt{k^2 + (m_B - g_{\sigma B}\sigma)^2} . \end{aligned} \tag{5.40}$$

We recall that the meson field equations for uniform static matter (in which space and time derivatives can be neglected) are

$$\omega_0 = \sum_B \frac{g_{\omega B}}{m_\omega^2}\rho_B , \tag{5.41}$$

$$\rho_{03} = \sum_B \frac{g_{\rho B}}{m_\rho^2} I_{3B}\rho_B , \tag{5.42}$$

$$m_\sigma^2 \sigma = \sum_B g_{\sigma B}\rho_{s,B} - b m_n g_\sigma (g_\sigma \sigma)^2 - c g_\sigma (g_\sigma \sigma)^3 \tag{5.43}$$

where $m_B^*(\sigma) = m_B - g_{\sigma B}\sigma$ is the effective mass of baryon species B and it depends on σ and therefore on density through the Fermi momenta k_B.

The scalar density ρ_s has been written in its integral form (4.151) for each specise B:

$$\rho_{s,B} = \sum_B \frac{2J_B + 1}{2\pi^2} \int_0^{k_B} \frac{m_B^*(\sigma)}{\sqrt{k^2 + m_B^{*2}(\sigma)}} k^2 \, dk . \tag{5.44}$$

The baryon source currents have been replaced by their ground-state expectation values; the ground state is defined as having the single-particle momentum eigenstates with eigenvalues given by (5.40) filled to the Fermi momentum. We will discuss shortly how the Fermi momenta of the various species B are to be found so that the system is in chemical equilibrium. In the above equations, I_{3B} is the isospin projection of baryon charge state B, and k_B is the Fermi momentum of species B. Only the timelike components of the vector fields and the isospin 3-component of the charged ρ field have nonvanishing values on account of the isotropy of nuclear matter and electric charge conservation, respectively, as found in (4.147).

The baryon number, charge, and strangeness densities of the various particle species read

$$\rho_B = (2J_B + 1)b_B \frac{k_B^3}{(6\pi^2)}, \tag{5.45}$$

$$Q_B = (2J_B + 1)q_B \frac{k_B^3}{(6\pi^2)}, \tag{5.46}$$

$$S_B = (2J_B + 1)s_B \frac{k_B^3}{(6\pi^2)}. \tag{5.47}$$

The total baryon and charge densities, the latter of which must be effectively zero for a star, are

$$\rho = \sum_B \rho_B, \qquad q = \sum_B Q_B = 0. \tag{5.48}$$

The equation of state can be found as follows. Compute the ground-state expectation value of the canonical energy-momentum tensor

$$T^{\mu\nu} = -g^{\mu\nu}\mathcal{L} + \sum_\phi \frac{\partial \mathcal{L}}{\partial(\partial_\mu \phi)} \partial^\nu \phi, \tag{5.49}$$

and compare with (3.26) to read the energy density and pressure. Employ the field equations to rewrite the energy density as

$$\begin{aligned} \epsilon = {} & \tfrac{1}{3} b m_n (g_\sigma \sigma)^3 + \tfrac{1}{4} c (g_\sigma \sigma)^4 + \tfrac{1}{2} m_\sigma^2 \sigma^2 + \tfrac{1}{2} m_\omega^2 \omega_0^2 + \tfrac{1}{2} m_\rho^2 \rho_{03}^2 \\ & + \sum_B \frac{2J_B + 1}{2\pi^2} \int_0^{k_B} \sqrt{k^2 + (m_B - g_{\sigma B}\sigma)^2}\, k^2\, dk \\ & + \sum_\lambda \frac{1}{\pi^2} \int_0^{k_\lambda} \sqrt{k^2 + m_\lambda^2}\, k^2\, dk. \end{aligned} \tag{5.50}$$

The pressure is given by

$$\begin{aligned} p = {} & -\tfrac{1}{3} b m_n (g_\sigma \sigma)^3 - \tfrac{1}{4} c (g_\sigma \sigma)^4 - \tfrac{1}{2} m_\sigma^2 \sigma^2 + \tfrac{1}{2} m_\omega^2 \omega_0^2 + \tfrac{1}{2} m_\rho^2 \rho_{03}^2 \\ & + \frac{1}{3} \sum_B \frac{2J_B + 1}{2\pi^2} \int_0^{k_B} k^4\, dk / \sqrt{k^2 + (m_B - g_{\sigma B}\sigma)^2} \\ & + \frac{1}{3} \sum_\lambda \frac{1}{\pi^2} \int_0^{k_\lambda} k^4\, dk / \sqrt{k^2 + m_\lambda^2}. \end{aligned} \tag{5.51}$$

The energy density and pressure are functions of baryon density ρ through the Fermi momenta k_B of each species. The integrals encountered above can be written out explicitly using the results quoted on page 94.

The first step in the application of the above theory is to fix the five coupling constants g_σ, g_ω, g_ρ, b, and c. This has been discussed in the preceding chapter. They can be fixed by the saturation properties of nuclear matter, in particular, the binding per nucleon, the saturation baryon density, the effective mass of the nucleon

at saturation, the compression modulus, and the symmetry energy coefficient. The coupling constants can even be determined algebraically in terms of these five bulk nuclear properties, as shown there.

Here, we are interested in describing the structure of observable neutron stars, identified as pulsars. At birth, the temperatures of neutron stars are high, falling to 10^{10} to 10^{11} K in a few seconds. Thereafter, their cooling rate is slower, but they cool to insignificant temperatures on the nuclear scale within a minute. The epoch of observation is generally thousands to several millions of years after formation. Still very hot by earthly standards (10^5 to 10^9 K), the star is cold on the nuclear scale of MeV ($= 1.16 \times 10^{10}$ K). We therefore take $T = 0$: the nonrotating star's hadronic degrees of freedom are frozen, at least for slowly rotating or nonrotating stars.

A description of neutron star matter appropriate to a frozen star is obtained by imposing the conditions of charge neutrality and chemical equilibrium as discussed in Section 5.3.2. In general the chemical potential of particle i with baryon charge b_i and electric charge q_i (in units of e) is given by

$$\mu_i = b_i \mu_n + q_i \mu_q, \qquad \mu_S \equiv 0 \tag{5.52}$$

where μ_n and $\mu_q (\equiv -\mu_e)$ are the chemical potentials for unit positive baryon (neutron) number and positive unit electric charge. They correspond to the two conserved quantities in neutron star matter. The strangeness chemical potential is denoted by μ_S: it is zero because strangeness is not conserved on any macroscopic timescale. The above equation is a generalization of (3.78). Chemical equilibrium can now be expressed in terms of the Dirac eigenvalues (5.40) as

$$\mu_B = e_B(k_B), \qquad B = 1, \ldots, N\,. \tag{5.53}$$

These equations relate the Fermi momenta of the baryons to the two independent chemical potentials. For the negative leptons, the corresponding equations are

$$\begin{aligned} (m_{e^-}^2 + k_{e^-}^2)^{1/2} &= \mu_e\,, \\ (m_{\mu^-}^2 + k_{\mu^-}^2)^{1/2} &= \mu_\mu = \mu_e\,, \end{aligned} \tag{5.54}$$

and, for free negative pions should we wish to test the effect of such a population,

$$(m_{\pi^-}^2 + k_{\pi^-}^2)^{1/2} = \mu_{\pi^-} = \mu_e\,. \tag{5.55}$$

The Fermi momenta in all cases are the positive real solutions when they exist and are otherwise zero. We will discuss the important case of Bosons interacting with the medium in Chapter 10 and there study the interesting effects of a Bose condensate.

Neutron star matter is thus obtained as the self-consistent solution to a system of coupled nonlinear equations in $7 + N$ unknowns, as follows:

(1) three field equations for the meson fields (ω_0, ρ_{03}, σ) (5.41, 5.42, 5.43)
(2) one equation for electrical neutrality (μ_q) (5.48)
(3) one equation for baryon density (μ_b) (5.48)
(4) two equations for lepton Fermi momenta, (k_e, k_μ) (5.54)

(5) N equations for the Fermi momenta of N baryon species in chemical equilibrium (k_n, k_p, $k_\Lambda, \ldots, k_{\Xi^-}, \ldots$) (5.53).

Of course, the referenced equations cannot be solved individually because they are coupled. When the system of nonlinear equations is solved, all derived quantities can be calculated, such as the total strangeness, individual particle populations, and the equation of state.

Until recently, most calculations of equations of state for neutron star structure approximate the star as either pure in neutrons, or else as involving beta equilibrium in the restricted sense of equilibrium among only neutrons, protons, and leptons. Approximations that omit the hyperons are not very useful in connection with the mass constraint on the equation of state. Nor do such approximations constitute a meaningful test of the theory by which the equation of state was found. We shall show that an equation of state computed under generalized beta equilibrium derived in this chapter as compared to one for pure neutron matter, or even one that includes beta equilibrium among n, p, e^-, μ^-, yields substantially different results for the neutron star sequence.

Presently, there are few observations available either to test the theory of dense neutron star matter or to guide the formulation of theory. Eventually, connections to observables may be found through high-energy experiments on symmetric nuclear matter involving nuclear collisions [293]. Conversely, neutron star cooling rates depend in principle on particle populations and so might provide information about the nature of dense matter and possibly the effect of the nuclear medium on particle masses [294, 295, 296]. However, to the present, the uncertainties in the cooling processes are so great that meaningful constraints are still not available [274]–[276], [297].

Additionally, it may be possible to discover properties of dense matter from the spin-down behavior of millisecond pulsars such as the the growth of a phase transition in neutron stars (Section 11.4). Certainly, one of the primary goals of research involving relativistic nuclear collisions is the discovery of the deconfined quark matter phase, but evidence for the transition may be more transparent in neutron stars than it is in nuclear collisions [200, 201, 298].

We stress again that the theory employed here is not unique. However, it does have notable merits that any theory of dense matter should share. The present theory is relativistically covariant, and the nucleon–meson coupling constants are related to symmetric nuclear matter properties in a direct (and algebraic) way. Moreover, as we shall see, the coupling to hyperons can be constrained in a meaningful way. Importantly, the equation of state at higher density is connected to that near saturation through continuity and causality.

It is sometimes thought that neutron stars are so dense that nuclear matter properties are irrelevant. This is not so. Although the density at the center of a neutron star may be quite high, the central region contributes little to the mass on account of the volume element. We have found [129, 146] that the mean density is only three or so times nuclear density for the star at the mass limit, and even less otherwise, depending on how stiff or soft the equation of state is. In Fig. 5.18 we

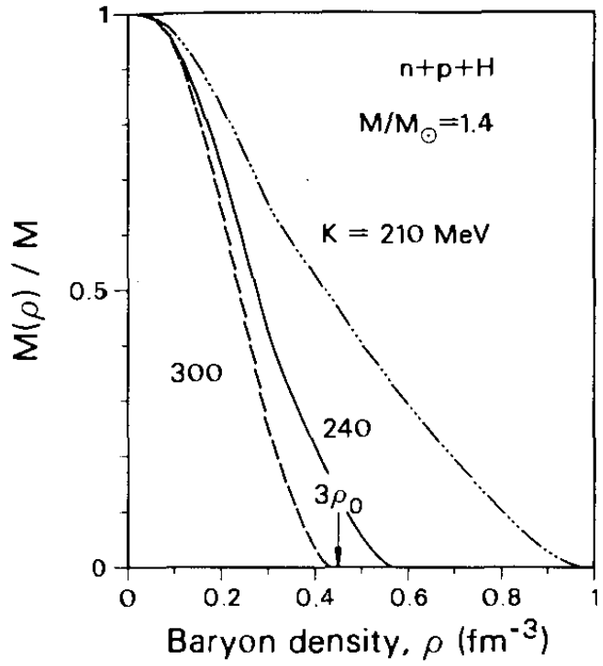

FIGURE 5.18. Fraction of mass of a 1.4-$M_\odot$ neutron star that is resident in matter at densities greater than the value of ρ shown on the x axis.

see that, for the most likely value of the compression modulus $K \sim 240$ MeV, only ten percent of a canonical $1.4M_\odot$ neutron star has density higher than $3\rho_0$. We therefore insist that a meaningful investigation of the possible constitution and properties of neutron stars can be accomplished only through a theory of matter that is causal, obeys Le Chatelier's principle, and that describes correctly (within the experimental uncertainties) the properties of matter at nuclear density.

Any theory of matter described by hadronic degrees of freedom is relevant around nuclear densities and up to some ill-defined upper limit where a description in terms of individual hadrons must break down. For the present, we assume that this density lies above the highest encountered in neutron star interiors. In Chapter 9 we shall consider a possible transition to a quark core in the more massive stars. This is an interesting transition, especially because of the Coulomb lattice structure of the coexistence phase of quark and nuclear matter that has been discovered in recently published work [194, 195].

5.3.6 *Hints for computation*

Numerical solution of the above defined transcendental system of equations comprising the Euler–Lagrange equations and constraint equations expressing charge neutrality and equilibrium is carried out in the following way. At very low density, say 0.1ρ, the scalar density is approximately equal to the baryon density. One sees this by neglecting k compared to $m^\star$ in the field equation for the scalar field. This fact allows one to approximate the scalar field σ defined by (5.43) in terms of the baryon density (ignoring the small cubic and quadratic terms in σ which is justified when σ is small). The ω_0 field is always given through its field equation (5.41) by the baryon density. At the low densities mentioned, neutron star matter is almost purely neutron, so that the ρ_{03} field is also given by the baryon density

through (5.42). One can also approximate the two independent chemical potentials. In summary,

$$g_\sigma \sigma \approx \left(\frac{g_\sigma}{m_\sigma}\right)^2 \rho\,,$$

$$g_\omega \omega = \left(\frac{g_\omega}{m_\omega}\right)^2 \rho\,,$$

$$g_\rho \rho_{03} \approx -\left(\frac{g_\rho}{m_\rho}\right)^2 \frac{\rho}{2}\,,$$

$$\mu_n \approx m - g_\sigma \sigma + g_\omega \omega + g_\rho \rho_{03}\,,$$

$$\mu_e \approx .12m\left(\frac{\rho}{\rho_0}\right)^{2/3}.$$

These five equations can be used to calculate an initial guess in a Levenberg–Marquardt (or similar) type of algorithm for finding the zero of a sum of squares. For this purpose, move all terms of the three field equations and the two conservation equations for the electric charge density (zero) and baryon density to the left of the equations, square, and add. Embed in the algorithm the equations that define the Fermi momenta in terms of the field amplitudes and chemical potentials (5.53, 5.54), and solve for the nonzero Fermi momenta at each desired density. One has a solution for all of the unknowns listed above when the sum of squares of the mentioned equations is zero.

Repeat the above procedure for a neighboring density. After one has obtained solutions at a succession of several low densities, use a spline to extrapolate each of the variables an additional increment in density. Use the extrapolated values as the next guess for the solution and again search for the zero of the sum of squares described above and continue this process. Thus develop all of the unknowns as a function of baryon density up to the highest density likely to occur in a neutron star, which, as we shall see, is typically (6 to 8)ρ_0.

The complete solution of the theory above is characterized by the values of the quantities enumerated above, of which there are $7 + N$. The Fermi momenta can be equally represented by the populations of the particles they represent. These populations were shown in one case in Fig. 5.17. The meson field strengths and the two independent chemical potentials, μ_n and μ_e, are shown for the corresponding case in Fig. 5.19.

5.3.7 Isospin- and charge-favored baryon species

From the expression for the baryon eigenvalue (5.40) and the requirement of charge neutrality, we can understand the terms, additional to the mass, that determine the baryon thresholds as they appear in Fig. 5.17. We introduce here the notion of charge-favored or unfavored and isospin-favored or unfavored species [68].

We can write the threshold equation for a given species by referring to the expression for the baryon eigenvalue (5.40). The condition that the species B can

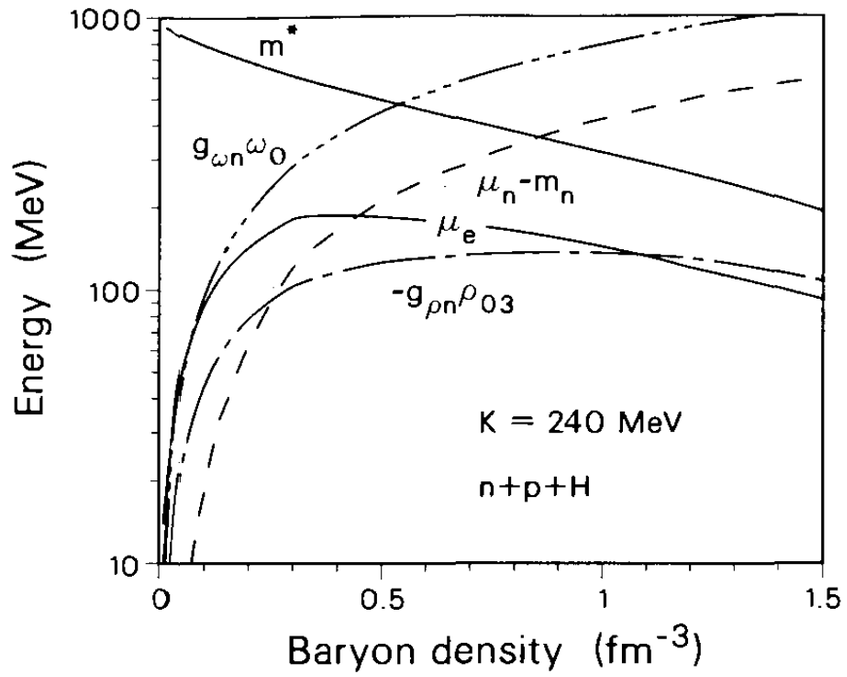

FIGURE 5.19. Solution of the theory for the field strengths and independent chemical potentials with the populations of particles shown in Fig. 5.17. See also Ref. [129].

occupy the eigenstate of zero momentum or higher is

$$\mu_B \equiv \mu_n - q_B\mu_e \geq m_B - g_{\sigma B}\sigma + g_{\rho B}\rho_{03}I_{3B} \,. \tag{5.56}$$

With increasing baryon density above that for which this inequality is first satisfied for the particle species B, that species acquires a finite density.

We refer to a baryon species as *charge-unfavored* if it has the same sign of electric charge as the proton because it must appear together with a particle or particles of opposite sign to maintain charge neutrality. Correspondingly, the left side of (5.56) is reduced by the term $-q_B\mu_e$. From Fig. 5.19 we can learn the values of the various terms in any particular instance.

The isospin term $+g_{\rho B}\rho_{03}I_{3B}$ in the eigenvalue determines whether a species is *isospin-favored or unfavored.* We can deduce what the sign of ρ_{03} will be in neutron star matter from (5.42) and the fact that charge neutrality will assure that the neutron is the dominant baryon species. Therefore, any baryon having the same isospin projection as the neutron is isospin-unfavored. Baryons having opposite sign of the isospin projection are favored because their presence will reduce the absolute value of ρ_{03} given by (5.42) and hence the quadratic isospin symmetry term $(\rho_{03})^2$ in the energy density (5.50).

5.3.8 Surface of neutron stars

The outer shell or crust of a neutron star of typical mass contributes only about one percent to the mass. However, the low-density domain of the stellar crust poses interesting physical problems which we briefly describe. We also need to supplement the equation of state of the higher-density domain that was described in the preceding pages.

Consider the surface of a neutron star where the pressure is zero. The condition is much like that on Earth because one atmosphere of pressure is very little as concerns the structure of matter. Clearly, the nature of low-density neutron star matter is quite different from the uniform dense matter described by the theory of the preceding sections. Therefore, we need to know the equation of state for neutron star matter from zero pressure up to that pressure at which the individuality of nuclei is destroyed. This is the pressure range of white dwarfs, and so, the outer regions of neutron stars will consist of matter somewhat similar to that of white dwarfs described in Section 3.10.

An important distinction exists, however, between white dwarf matter and the matter in the crust of neutron stars. As discussed in Section 3.10, white dwarfs are the end point in the evolution of stars with mass up to $\sim 5M_{\odot}$, which become unstable before nuclear burning to the most stable elements is reached. Neutron stars, on the other hand, are an end point (the other being a black hole) of the evolution of more massive stars which do complete nuclear burning to the most bound nuclei, the so-called iron peak nuclei. As such, the relevant nature of the matter of neutron stars is what is referred to as *cold-catalyzed matter* [28], or, in our terminology, *neutron star matter*. It is the lowest energy state of a neutral system at zero temperature, containing a large number of baryons A, and is the state to which the matter of a neutron star evolves as it cools by neutrino and photon emission.

In our calculations of neutron star structure we will consider the ideal asymptotic state of a cold star. It is true that the surface temperature of stars, even at an age of a few million years, is still very high by earthly standards, so the very surface would be a puddle of molten material. But the pressure rises rapidly with distance from the surface and the resultant high degree of ionization will lead to the formation of a Coulomb lattice, much as described in Section 3.10.3. For the purpose of mass and radius of the star, the precise nature of the very edge is unimportant, and we always make the cold idealization.

The lowest energy state of hadronic matter at zero compression and temperature is solid Fe^{56}. Iron is the most stable element, and therefore has the lowest value for the energy per nucleon. Moreover, it is the principle element in the core of a luminous star in its terminal stage. Therefore, it is present in the material that collapses to form a neutron star and marks the star's edge because the pressure in solid iron is zero.

A little deeper into the star, the pressure will be higher, and the atoms will be compressed so that the nuclear spacings no longer leave room for the normal atomic structure—the atoms will be partially or completely ionized, depending on depth. However, the nuclear forces will hold the nuclei together as individual entities so long as the density is less than the neutron drip density. This state of nuclei embedded in an electron sea is preferred by the short-range nuclear forces to a uniform state of nuclear matter at subnuclear densities. The electrons will form an almost uniform medium in which the positively charged nuclei minimize the total energy by taking up lattice positions, as we studied in Chapter 3. At greater density, the most favored nuclear species will become more neutron rich. Detailed analysis of matter in this density range has been performed by a number

of authors [80, 248], [299]–[302]. Nuclei will dissolve altogether at greater depth where densities are somewhat in excess of the drip density

Whereas we can speak of neutron star matter, as described by the theory of this chapter, as a quantum liquid of various relativistic baryons and leptons, the matter at lower density in the crust of the star is of crystalline form and is qualitatively described in Table 5.1 and in Section 3.10. Two useful tabulations of the equation of state of cold-catalyzed matter at low to moderate density can be found in Refs. [28, 80] and at the end of the chapter .

5.3.9 Reprise of white dwarfs to neutron stars

We recall from Section 3.9.6 that the Fermi pressure of relativistic electrons supports white dwarfs. Due to the changing composition of matter with increasing density in the white dwarf domain shown in Fig. 3.9, this supporting pressure becomes insufficient at a certain density, because of the inverse beta decay in which some of the electrons are absorbed by protons in the *neutronization* process. The white dwarf sequence terminates as a result. Recall that hydrodynamic equilibrium changes between stability and instability when $dM/d\epsilon_c$ changes sign. (see Section 3.18).

Stability is regained for a new family of stars at much higher central density—a density for which the Pauli principle first yields a large enough neutron Fermi pressure to oppose gravitational collapse. This is a qualitative statement of the onset of stability for neutron stars. (More precisely, the matter of which the very lightest stars are composed, in the approximate mass range $0.09 < M/M_\odot < 0.11$, is a Coulomb solid [80]. Therefore, the pressure is less than for free nucleons of the same energy density. Stability is deferred to a somewhat higher density. This is why the two neutron star sequences of Fig. 3.9 differ on the low-density side.) For higher densities found in more massive stars, the Fermi pressure is increasingly eclipsed in its role as the agent resisting collapse by the repulsion between baryons at short distances. The vector mesons cause the repulsion in our theory because they contribute a positive term to the energy density (5.50).

5.3.10 Development of neutron star sequences

Neutron stars are fully relativistic objects. Their structure cannot be derived save in the context of General Relativity. When the solution to the above neutron star matter problem (or any other purporting to describe such matter) is obtained, the equation of state $\epsilon = \epsilon(\rho)$, $p = p(\rho)$ is available. One could eliminate ρ to express $p = p(\epsilon)$ or the inverse. The equations of stellar structure—the Oppenheimer–Volkoff equations— (3.27, 3.28) provide a one-parameter family of stellar models corresponding to a particular equation of state.

Several equations of state corresponding to different degrees of completeness with respect to the baryon types that are included in its derivation are illustrated in Fig. 5.20. The resulting neutron star sequences are shown in Fig. 5.21. (We discuss this figure further in a later section.)

The Oppenheimer–Volkoff equations are easy to solve because they are simple, first-order differential equations each with an initial condition, say, the central density $\epsilon(0) = \epsilon_c$ and $M(0) = 0$ at $r = 0$. The equations have to be integrated until the pressure becomes zero or until the pressure drops so precipitously with increasing r, that, effectively, the edge of the star has been reached. Then the radius R and the mass $M = M(R)$ for the chosen central density are known. Choosing a succession of increasing values for the central density corresponds to developing a *sequence* of stars of increasing mass, until the mass limit is reached. (Of course one can continue to solve the Oppenheimer–Volkoff equations for densities that lie higher than that of the limiting mass star. The part of the sequence with negative $dM/d\epsilon_c$ represents unstable equilibrium configurations.)

From the solution of the Oppenheimer–Volkoff equations for given equation of state and chosen central density, one learns not only the corresponding stellar mass and radius, but, as a result of the numerical integration of the equations, one has the distribution of mass-energy for the particular stellar model. In addition one could, simultaneous with the solution of the structure equations, accumulate the baryon populations (3.150), the radial metric (2.215), and the time metric (2.226 or 2.228) as a function of the radial coordinates. The equation for the moment of inertia (6.20) could be integrated at the same time.

One can learn additional things. The solution of the nuclear matter theory that provided the equation of state also provides many other internal properties of the matter as a function of density, ϵ. For example, the baryon populations are available as a part of the solution, as are the meson fields and chemical potentials. So, having these quantities as a function of ϵ and knowing the distribution of energy density $\epsilon(r)$ as a function of Schwarzschild radius, one can immediately deduce the radial distributions of these other quantities in the star.

5.3.11 Mass as a function of central density

The central density of stable neutron stars lies between about one-half and ten times nuclear energy density ($\epsilon_0 \sim 2.5 \times 10^{14}$ g/cm^3), or up to six to eight times normal baryon density ($\rho_0 = .15$ fm^{-3}).[24] Neutron star sequences are most frequently represented by the relationship between stellar mass and central density. Several sequences are illustrated in this section that correspond to varying degrees of completeness of the underlying theory of the equation of state with respect to general equilibrium among baryon species.

First, we exhibit the effects on the equation of state of extending the description of the matter of neutron stars from pure neutron matter to matter that consists of additional baryon species in equilibrium. Figure 5.20 shows the pressure as a function of energy density. Notice that, with each addition of baryon species, the equation of state is softened for the reason that the Fermi pressure of neutrons and

[24] The energy density of compressed nuclear matter increases more rapidly than the baryon density because of repulsion between nucleons at neutron star densities.

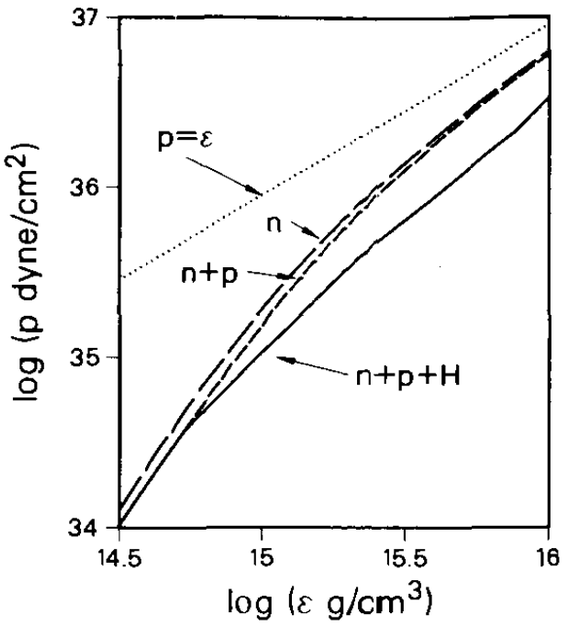

FIGURE 5.20. Compares the equation of state of pure neutron matter (n) and of stable neutron star matter in which neutrons, protons and leptons are in equilibrium (n+p), and lastly one with hyperons in addition (n+p+H). Here $K = 240$ MeV and $m^* = 0.78$. Cf. [129].

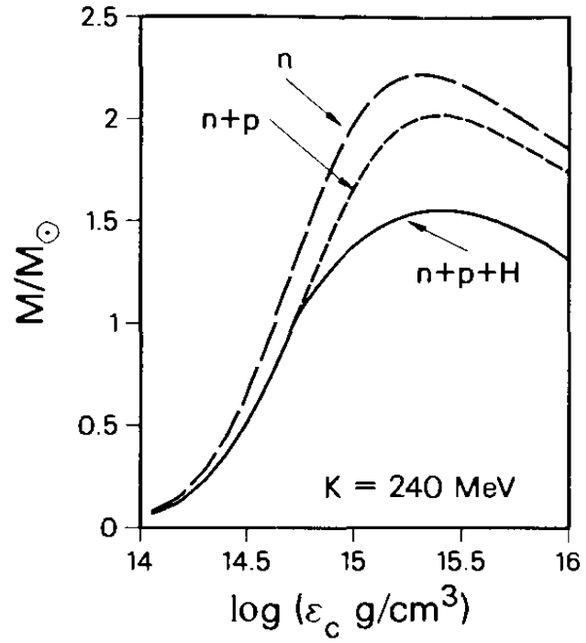

FIGURE 5.21. Neutron star masses for a purely neutron star, one in equilibrium between neutrons, protons and leptons, one with hyperons in addition. The equations of state are those of Fig. 5.20. Cf. [129].

protons near the top of their Fermi seas is relieved by allowing them to hyperonize to unoccupied low-momentum states.

Corresponding to the equations of state shown in Fig. 5.20 we show the neutron star masses in Fig. 5.21. It is clear that gravity effectively exploits the softening of the equation of state due to hyperonization at higher density. This figure also illustrates a generic property of a stable sequence of neutron stars, a minimum and a maximum mass between which $dM/d\epsilon_c > 0$. Recall the discussion of stability in Section 3.18 in this connection. Stability is lost when the slope becomes zero at either end of the sequence.

Below the minimum mass of neutron stars, and for all lower central densities down to the white dwarf maximum mass, the fundamental ($n = 0$) vibrational mode is unstable. We have seen in Fig. 3.15 that low-mass neutron stars are not bound. Presumably, configurations immediately below the onset of positive slope for the neutron star branch are unstable to radial oscillations that destroy them by dispersal.[25]

For more massive neutron stars, and even beyond the maximum mass, we saw in Fig. 3.14 that the configurations, whether stable or unstable to oscillations, are gravitationally bound. If a stable neutron star below the mass limit were to accrete matter adiabatically so as to move it beyond the mass limit, the unstable

[25]Recall that even though the low-mass neutron stars are not absolutely stable in the sense that the mass of the dispersed nucleons is less than the stellar mass, nevertheless they are stable to removal of single or even groups of nucleons.

fundamental vibrational mode would destroy it. The oscillations would grow in amplitude rapidly and would so greatly elevate the density at the center of the star that a central region would fall within its Schwarzschild radius. The star then would begin its collapse to a black hole. Whether or not accretion were adiabatic, there are no stable configurations that correspond to baryon number larger than that of the star at the mass limit. Therefore, one or the other, dispersal or collapse, is the fate of stars lying on the portions of the equilibrium sequence of Oppenheimer–Volkoff stars that have negative slope $dM/d\epsilon < 0$.

As depicted in Fig. 3.2, the baryon number for equilibrium configurations reaches a maximum for the same configuration as has the maximum mass. For stars beyond the limiting mass, the baryon number decreases with increasing density until the next turning point of the curve. Notice also that the stellar mass for a given baryon number is larger on the unstable sequence.

5.3.12 Radius–mass characteristic relationship

The most important representation of a neutron star sequence is its radius–mass relationship. It is uniquely related to the underlying equation of state [133]. While both mass and radius are not known so far for any pulsar, it is, in principle, possible to determine them in some cases. Masses can often be determined for a pulsar that is in binary orbit with a companion. In principle, radius determinations could be made through the measurement of the Doppler shift of known spectral transitions or of the photon produced by the annihilation of electron pairs. The Doppler shift determines M/R from (3.57), which provides the radius if the mass is known. More recently, observations of quasi-periodic oscillations in the X-ray brightness of accreting neutron stars (referred to also as QPO) [303] has been discussed as a possible means of measuring mass and radius [237], [304]–[306].

Neutron stars are degenerate Fermi systems—their matter can be compressed without the generation of heat.[26] Degenerate stars possess a generic relationship between their mass and radius. Rather than being larger, high-mass degenerate stars are smaller than low-mass stars. The reason is simple. For low-mass stars, the gravitational attraction is weak and the corresponding stars large and diffuse. The gravitational attraction is strongest for the limiting-mass star of all those in *stable* hydrostatic equilibrium. Correspondingly, the radius is smallest.[27] With slightly more compaction, the star becomes unstable, collapsing to a black hole. The behavior of the radius vs. mass is illustrated in Fig. 5.22 for three models, one for a purely neutron star, a star with neutrons, protons and leptons in equilibrium,

---

[26]Gravitational compression of pre-main or main-sequence stars, which can be described by an ideal gas equation of state, raises the temperature to the combustion point of ever heavier elements in thermonuclear reactions.

[27]This fact is of importance in connection with rotation. From (5.9) we see that the mass-shedding angular velocity (Kepler) is given by $\Omega_K \approx 0.65(M/R^3)^{1/2}$. Hence, the limiting mass-star in a sequence of degenerate stars can rotate most rapidly because it is the most compact of all.

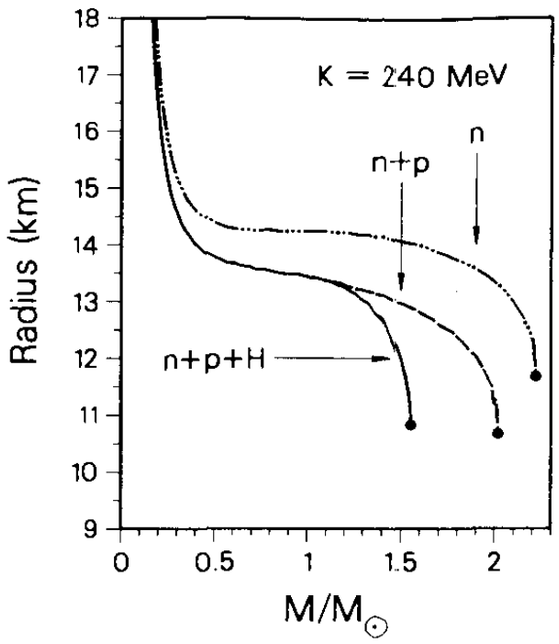

FIGURE 5.22. Radius–Mass relationship characteristic of degenerate stars for three models with particle populations as labeled as in Fig. 5.21.

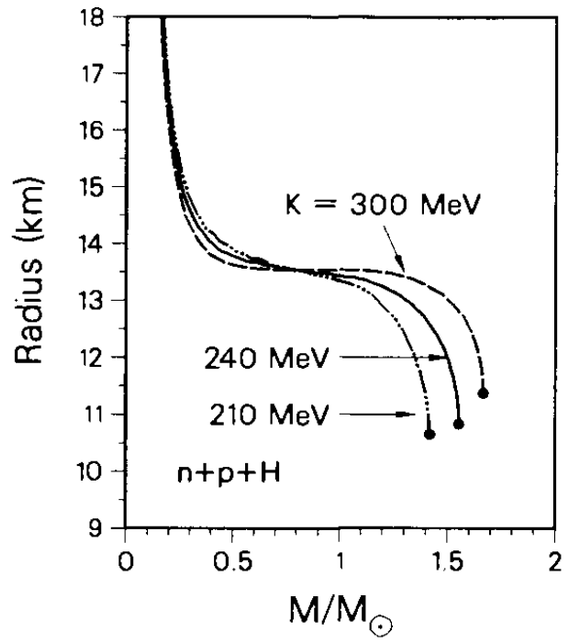

FIGURE 5.23. Radius–Mass relationship for a selection of models having various compression moduli (and $m^* = 0.78m$). In all cases neutron star matter is in equilibrium between neutrons, protons, hyperons, and leptons [307].

and finally one with hyperons in addition. Figure 5.23 shows mass–radius relation for three models distinguished by the compression modulus of the corresponding symmetric nuclear matter. The general form of this radius–mass relationship is *generic* to compact stars that are bound by the gravitational force.

An interesting theorem has been proven by Lindblom [133]. It is the solution of the inverse problem. Given a table of masses and radii of neutron stars, the equation of state that describes the matter of which they are made can be found over a range of densities which is large or small depending on whether the table spans a sufficient radius–mass range. Whether or not the theorem will prove to be useful in that respect depends on whether neutron stars can be produced in astrophysical phenomena with a sufficient spread in mass and radii. At present the masses for those few cases that have been measured to high precision are fairly close in value, and no radius measurements exist.

5.3.13 Limiting mass and the equation of state

We have already learned that there exists a maximum limiting mass that a neutron star can possess. Even in the idealization of *incompressible* matter, the structure of the Oppenheimer–Volkoff equations is such as to impose a limit (Section 3.15). The limiting mass of a model sequence of stars depends on the compressibility of matter. The compressibility is registered in the equation of state. A "soft" equation of state is relatively more easily compressed than a "stiff" one. One equation of state is said to be stiffer than another if the pressure at every energy density (or energy per baryon) is greater for the one than the other. It is easily shown that the

above statement implies and is implied by several other relationships, for example, the energy density and the energy per baryon are both greater at each baryon density for the stiffer equation of state.

The stiffer the equation of state, the larger the mass that can be sustained against collapse. In Figure 3.9, two extreme cases were illustrated, one for which the equation of state was as stiff as allowed by the causal constraint $\partial p/\partial \epsilon \leq 1$. The limiting mass is just over $3M_\odot$. The other case corresponds to a very soft equation of state; it was assumed that dense matter consists merely of a free Fermi gas of neutrons, protons, and leptons in equilibrium. In this case only the Pauli exclusion principle provides the supporting (Fermi) pressure. The limiting mass is $\approx 0.7M_\odot$. We expect any realistic model involving nuclear forces to fall between these extreme cases because the central density corresponding to the maximum mass is so high that the strong, short-range repulsion between baryons dominates the longer-range attraction. It therefore adds to the pressure. Indeed, repulsion dominates attraction in the core for densities not far above nuclear density and not far above the minimum mass star in the sequence.

If we knew precisely the equation of state of nature, then, from the Oppenheimer–Volkoff equations, we could simply compute the sequence of neutron stars. However, we have only imperfect theories of dense matter and for the foreseeable future, QCD will not provide the detail needed. So the inverse strategy is relevant—to attempt, from laboratory experiments and from observations on neutron stars, to infer information about the equation of state and the high-density behavior of matter and the stars made from it.

Having recognized that the limiting mass depends on the stiffness of the equation of state, the questions are then as follows. What makes the equation of state stiff or soft? What physical effects are the most important and must not be neglected in computing a model sequence of stars or in testing a particular theory of matter against what is known about them? We now take up these matters.

5.4 Constitution of Neutron Stars

5.4.1 Beta equilibrium and symmetry energy

Neutron star models have been computed frequently under the simplifying assumption that the star is pure in neutrons. We have already discussed several defects of this assumption. In fact, the constitution of neutron stars may exhibit a fascinating array of high density phenomena [308].

First, although satisfying the constraint of charge neutrality trivially, such a state of matter is an excited state. The neutron Fermi energy exceeds the sum of the eigenenergies in the medium of the proton and the free electron. Indeed, in Section 3.9.2 we found that, for a Fermi gas of neutrons, protons, and electrons, all are present in equilibrated charge-neutral matter except at extremely low density. (Indeed, at very low density, charge-neutral, baryonic matter consists solely of an equal number of protons and electrons.) So at neutron star densities, pure neutron

matter is not in its lowest energy state as expressed by the equations of chemical equilibrium discussed above (Section 5.3.2 and (5.32)).

Second, we know that nuclear forces and Fermi energies favor isospin symmetry. The valley of beta stability of nuclear masses vividly expresses this (Section 4.5). In our theory, this preference is expressed through the rho meson and its repulsive contribution to the energy density, as displayed in (5.50) which (for nucleons only) is $(1/8)(g_\rho/m_\rho)^2(\rho_p - \rho_n)^2$. Isospin symmetry is clearly favored. In addition to the explicit preference of the nuclear force, the kinetic energy contribution (4.218) also favors symmetry.

Charge-neutral matter cannot satisfy the preference for isospin symmetry fully, and we understand that charge neutrality is an overriding constraint. The force that binds stars is the gravitational force. Above a certain small net charge per baryon, additional charged particles would not be bound; they would be blown away by the Coulomb repulsion. But treating the star as if it were purely neutron prevents neutron star matter from reaching its lowest energy state—the one that is charge-neutral *and* in equilibrium. In general, charge-neutral matter always has neutrons as the majority population in the density domain above nuclear density, but populations of protons, leptons, and most likely also hyperons are present. This is even true of a Fermi gas at high density.

If beta equilibrium were neglected, a stiffer equation of state would result than would otherwise be the case. In Fig. 5.21 we can see how large the effect on the mass limit can be. Because a test of theory involves confirming that it can account for measured masses, the test is misleading if either beta equilibrium or the charge symmetry of the nuclear force is neglected. In the next section we study the role of hyperons in greater detail, paying special attention to how their coupling constants might be constrained by observation.

5.4.2 Hyperon stars

Hyperon stars are neutron stars in which some of the baryons have been converted to hyperons [67, 68], [186]–[189] The baryon octet comprises some of the least massive baryons and includes the Λ, Σ and Ξ (Table 4.5). Although hyperons carry strangeness, we understand that conversion of nucleons to hyperons is not hindered on any macroscopic timescale (Section 5.3.2). Hence, with increasing baryon density, the Fermi level of nucleons rises above the mass threshold of other members of the octet, as modified by interactions (cf. (5.53)). The total energy is then reduced by sharing baryon number among several or many baryon species. Conservation of baryon number, violation of strangeness by the weak interaction, and the Pauli principle assure this result. Not only is the energy lowered by sharing baryon number among many species, but also the pressure is lowered [28]; hence the

[28]It may not be obvious that if the energy density is lowered so is the pressure. Recall that $p = \rho^2\partial(\epsilon/\rho)/\partial\rho = \rho\epsilon' - \epsilon$. From this we derive, $\partial p/\partial\epsilon = (\partial p/\partial\rho)/(\partial\epsilon/\partial\rho) = \rho/(\epsilon + p)\cdot(\partial p/\partial\rho)$. But microstability of matter demands that $\partial p/\partial\rho \geq 0$, and the equality

equation of state is softened, and the maximum mass of the neutron star sequence is reduced compared to what it would be if hyperons did not exist.

5.4.3 *Hyperon coupling constants*

Research on the role of hyperons in neutron stars has been performed in the framework of relativistic nuclear field theory [67, 68, 129, 130, 131, 160, 309, 310, 311] the framework in which we work in this book and the same framework in which analysis of hypernuclear levels has been performed also [312]–[315]. The Lagrangian of the theory was derived and discussed in an earlier part of this chapter. The coupling constants appearing in the Lagrangian that involve nucleons can be determined algebraically in terms of the properties of normal symmetric nuclear matter at saturation as we saw in Section 4.8.1. However, hyperons do not exist in normal nuclei or in nuclear matter at saturation density, so the normal state yields no information about their couplings. Consequently, considerable uncertainty surrounds the effect of hyperons on the theoretical maximum mass and on cooling rates of neutron stars.

It is the purpose of this section to show how to find hyperon coupling constants that are constrained by the following:

(1) the binding of the Lambda hyperon in nuclear matter,
(2) hypernuclear levels,
(3) neutron star masses.

By using these constraints we can narrow the uncertainty in the coupling of hyperons and thus arrive at a plausible estimate of the effect of general beta equilibrium on neutron star masses, particularly the limiting mass [132]. We recall that, according to present observations, it appears that the lower bound on the maximum neutron star mass is $\sim 1.5 M_\odot$.

Although hyperons do no exist in normal nuclei, information about their couplings can be gathered from energy levels in hypernuclei. We shall assume that all hyperons in the octet have the same coupling as the Λ. The hyperon couplings are expressed as a ratio to the above mentioned nucleon couplings,

$$x_\sigma = g_{\sigma H}/g_\sigma, \quad x_\omega = g_{\omega H}/g_\omega, \quad x_\rho = g_{\rho H}/g_\rho. \tag{5.57}$$

In most analysis of hypernuclei, the first two ratios are taken equal, and the third is not determined by Λ hypernuclei because the Λ has zero isospin. With the constraint $x_\sigma = x_\omega = x$, it was found that x must be small, in the range 0.21 to 0.4, by various authors [312]–[315]. Under the above constraints, the maximum neutron star masses are too small [129, 309]. For $x = 0.21$ the maximum mass star is $1.02 M_\odot$ and for $x = 0.4$ it is $1.29 M_\odot$ if the nuclear matter value of the compression modulus is taken to be $K = 300$ MeV (which is at the upper end of plausible

---

holds only for first-order phase transitions in simple substances—not in neutron star matter (cf. Chapter 9 and Ref. [195]). Therefore, $\partial p/\partial \epsilon > 0$.

TABLE 5.4. Values of the hyperon to nucleon scalar and vector coupling compatible with the binding of −28 MeV for Λ hyperons in nuclear matter for two values of the nucleon (Dirac) effective mass at saturation density.

x_σ	x_ω	
	$m^* = 0.70$	$m^* = 0.78$
0.2	0.131	0.091
0.3	0.261	0.233
0.4	0.392	0.375
0.5	0.522	0.517
0.6	0.653	0.568
0.7	0.783	0.800
0.8	0.913	0.942
0.9	1.04	1.08
1.0	1.17	1.23

values). Such low masses lie below those of the Hulse–Taylor binary pulsars. This fact rules out small couplings. When the hypernuclear levels are analyzed without the constraint of $x_\sigma = x_\omega$, large correlation errors are found for their values; their determination is highly uncertain, ±100% [314] and ±55% [315].

To resolve the discrepancy between data on hypernuclei and neutron star masses we can employ the accurately extrapolated value of the Λ hyperon binding in saturated nuclear matter [316]. This procedure avoids the idiosyncrasies of individual nuclear levels in favor of bulk nuclear matter, the stuff of which neutron stars are made (in its charge-neutral form, of course).

Now we derive an expression for the Λ binding. Recall the relationships (4.178, 4.180) at saturation between the Fermi energy and the energy per nucleon of a self-bound system $e_F = (\epsilon/\rho)_0$ which is a special case of the Hugenholtz–Van Hove theorem [317]. The Fermi energy of the lowest Λ level is the $k = 0$ value of the Dirac eigenvalue of the theory (5.40),

$$e_\Lambda(k) = g_{\omega\Lambda}\omega_0 + (k^2 + m_\Lambda^{\star\,2})^{1/2}\,. \tag{5.58}$$

Therefore, from the above theorem we obtain $(B/A)_\Lambda = e_\Lambda(0) - m_\Lambda$ for the binding energy of the lowest Λ level, or

$$\left(\frac{B}{A}\right)_\Lambda = x_\omega V + m_\Lambda^\star - m_\Lambda = x_\omega V - x_\sigma S, \tag{5.59}$$

where

$$S = g_\sigma \sigma = m - m^\star{}_{\text{sat.}}\,, \qquad V = g_\omega\,\omega_0 = (g_\omega/m_\omega)^2\rho_0\,, \tag{5.60}$$

are the values of the scalar and vector field strengths for symmetric nuclear matter at saturation. These values can be obtained immediately from the saturation properties of nuclear matter, namely binding energy, saturation density, and effective nucleon mass, B/A, ρ_0, and $m^\star$ (4.181).

Equation (5.59) yields a continuous ambiguity in the pair of values x_σ, x_ω, each pair of which yield the same Λ binding of −28 MeV. Combined with neutron star

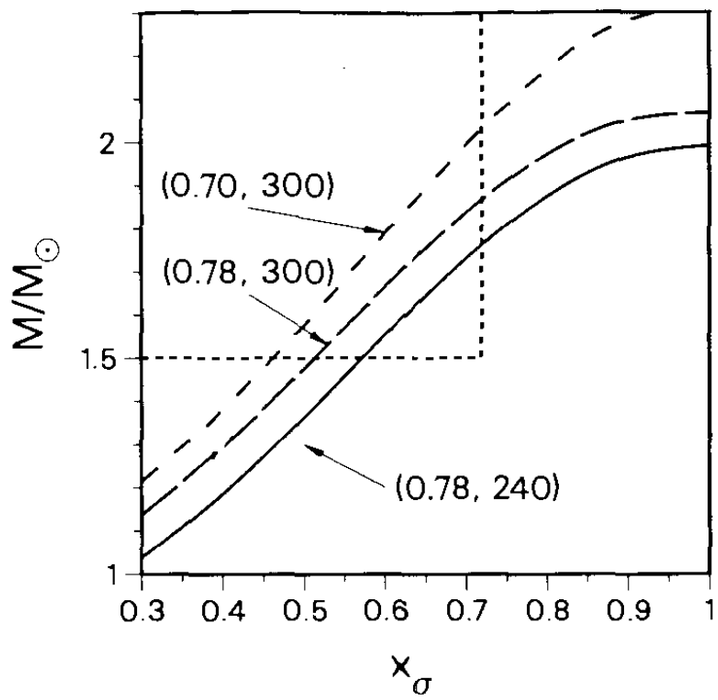

FIGURE 5.24. Maximum neutron star mass as a function of hyperon scalar coupling with vector coupling chosen so as to yield correct Λ binding in nuclear matter. Numbers in parentheses are m^*/m and K in MeV. From Ref. [132].

masses, the ambiguity is bounded from below by $M_{\max} \gtrsim 1.5 M_\odot$. Combined with the reasonable assumption that the hyperon coupling constants are less than those of the nucleon, based both on the observation that the lowest s-state nucleon is bound by approximately twice as much as the Λ hyperon and also on the basis of quark counting [190], the ambiguity is bounded from above; $x_\sigma < 0.9$ (see Table 5.4). It is even more stringently bounded from above from the fit to hypernuclear levels [315]. In the quoted work, it was found that $x_\sigma = 0.46 \pm 0.26$, $x_\omega = 0.48 \pm 0.32$, so that we may take $x_\sigma < 0.72$.

The results of the analysis are shown in Fig. 5.24. Several curves of maximum neutron star mass as a function of x_σ are shown for a range of values of K and m^*. The ambiguity in the empirical values of K lies in the range 240 to 300 MeV [51], [144]–[149], [318]. In view of a recent analysis of nuclear saturation properties [51], the value $K = 240$ may be preferred. The effective (Dirac) nucleon mass at saturation density m^*/m lies in the range 0.7 to 0.78 and corresponds to the empirical, nonrelativistic, effective mass in the range 0.74 to 0.83, which, to a good approximation [150], has been identified as the Landau effective mass [164]. The related coupling constants are listed in Table 5.5.

Recall our discussion in Chapter 4. We regard nuclear field theory as an effective one. When c is negative, the solution of the field equations yields a well-behaved equation of state even though, regarded as a fundamental theory, a negative value would be unsatisfactory, because the energy functional would be unbounded from below. With regard to the variation of the nuclear properties that determine the couplings, the equations of state corresponding to negative c are continuous with those having positive values.

The three curves of Fig. 5.24 span the range of uncertainty in K and m^*. For each value of of x_σ, the value of x_ω is chosen to yield the Λ hyperon binding

TABLE 5.5. Selected coupling constants that yield binding $B/A = -16.3$ MeV, density $\rho = 0.153$ fm^{-3}, and symmetry energy coefficient, $a_{\rm sym} = 32.5$ MeV for saturated nuclear matter with the compression K and effective mass m^* listed below. For hyperons we will choose $x_\sigma = 0.6$ and x_ρ from the previous table.

K MeV	m^*/m	$(g_\sigma/m_\sigma)^2$ fm^2	$(g_\omega/m_\omega)^2$ fm^2	$(g_\rho/m_\rho)^2$ fm^2	100b	100c
300	0.70	11.79	7.148	4.410	0.2948	−0.1071
300	0.78	9.147	4.820	4.791	0.3479	1.3281
240	0.78	9.927	4.820	4.791	0.8661	−0.2421
210	0.78	10.34	4.820	4.791	1.1080	−0.9753

in saturated nuclear matter of −28 MeV. The correspondence is given in Table 5.4. We arbitrarily set $x_\rho = x_\sigma$. The choice is not sensitive; an alternative choice $x_\rho = x_\omega$ yields essentially the same results. The acceptable ranges of M and x_σ, as discussed above, lie in the boxed area in the upper left of the figure. We find a minimum allowable value for the hyperon to nucleon scalar coupling x_σ of ~ 0.5 which is provided by a lower bound on the maximum neutron star mass. Hypernuclear levels yield a somewhat uncertain upper bound of ~ 0.72. The corresponding values of x_ω can be found in Table 5.4. In Fig. 5.25, we show two stellar sequences for the upper bound for x_σ just mentioned. If the upper limit imposed by the somewhat uncertain hypernuclear results were firm, then within uncertainties in nuclear matter properties, K and m^*, the limiting neutron star mass imposed by hyperon populations would be about $2M_\odot$.

In Fig. 5.24 it will be noticed that the weaker the hyperon coupling, the lower the maximum mass star. A shift in baryon populations from nucleons to hyperons occurs only when the shift softens the equation of state. Therefore, the lower stellar mass implies that the hyperons actually participate to a higher degree, the weaker their coupling. In fact, if the couplings of hyperons are reduced to zero (meaning that they are treated as a free Fermi gas), the limiting star mass lies about $\frac{1}{2}M_\odot$ below that corresponding to interacting hyperons [132]. This seemingly paradoxical behavior is easy to understand and has been explained in Refs. [129, 131]. High-density matter is dominated by the repulsion, not the attraction of the nuclear force. Because the coupling of the hyperons to the omega meson is weaker than that of the nucleons, the repulsion contributed by the omega field is weakened by the conversion of nucleons to hyperons.

It is clear and will become clearer in later parts of this chapter, that hyperons play a more or less important role in neutron stars, both as to the limiting mass as well as other properties such as cooling rates. We will also see that hyperon populations play a crucial role in the question of whether a kaon condensate forms in neutron stars.[29] These matters hinge strongly on hyperon coupling constants, which for the Λ we are able to place constraints but not pin down. As for the other hyperon

[29] We take up the meaning of a kaon condensate and the conditions for its formation in Section 5.4.7 and in Chapter 10.

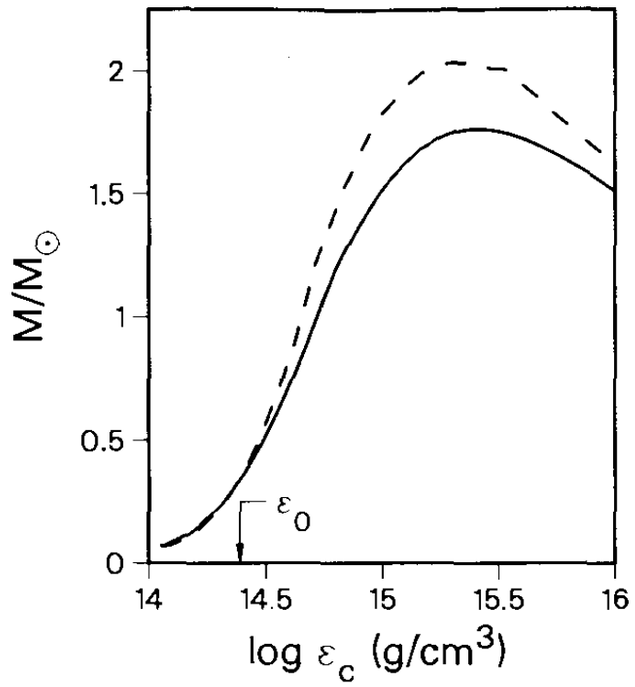

FIGURE 5.25. Two stellar sequences corresponding to the upper limit of x_σ in the boxed part of Fig. 5.24. Dashed and solid lines of the two figures correspond.

couplings, it is reasonable, but unproven, that all hyperons couple with the same strengths as the Λ, as assumed here. Another possible choice can be motivated by SU6 relations [319]. It would be very useful to have more experimental evidence on this question, say as to $\Sigma^{+,0,-}$ hypernuclei. Some theoretical work on hypernuclear levels in selected nuclei is available as a possible guide [320, 321, 322].

5.4.4 Hyperon populations and the limiting mass

Now we illustrate the important role of hyperons in neutron stars—their populations and their effect in softening the equation of state and reducing the limiting mass that would otherwise be computed if hyperons were neglected.

For this purpose, we adopt standard values of the nuclear parameters that are used to fix the coupling constants of the theory. For the standard values of symmetric nuclear matter properties, we choose those discussed in Section 4.5 with special choices for the least well determined properties: $K = 240$ MeV, $m^*/m = 0.78$; we consider these to be good empirical values, as cited in the previous section. The value of K is close to that found in a careful analysis by Myers and Swiatecki [51]. For hyperons we take the coupling $x_\sigma = 0.6$ (and corresponding x_ω) which falls in the middle of the range discussed above. The parameters quoted are used for the figures in this and other chapters unless otherwise noted. Fig. 5.21 shows sequences of stars obtained under three different circumstances:

(1) a purely neutron star,
(2) one in which β equilibrium between neutrons, protons, and leptons is incorporated,
(3) hyperons are included in the above.

Hyperons form a significant population of neutron stars near their limiting mass, and indeed are dominant in the core as can be seen in Fig. 5.26. Integrated[30] over the star, the baryon population is about 65% neutrons. Protons and hyperons appear with near equal populations of about 18% each. In the inner 3 km of the star, hyperons are the dominant species. Thus, while neutrons comprise the largest part of the population, they are by no means dominant, as was originally conceived in the notion of a neutron star. Indeed, even some very recent works neglect the contribution of hyperons whose absence also modifies the proton and lepton populations [256]. We have seen the effect of hyperon populations on the limiting mass—it is a major effect.

Hyperon populations are driven by the Pauli principle in dense matter so as to reduce the energy of the baryon Fermi seas and hence the total energy. The pressure, which resists gravitational collapse, is likewise reduced. Hence we anticipate that hyperons will reduce the limiting neutron star mass in comparison with models in which they are omitted. We can gauge their contribution in this respect by reference to Fig. 5.21. There it is seen that hyperons reduce the limiting mass by about $\frac{1}{2}M_\odot$, depending on the compression modulus and effective nucleon mass [191]. Within the uncertainty of their coupling as limited by the above considerations (boxed region in Fig, 5.24), the hyperons place the limiting mass in the range $M/M_\odot \sim 1.5$ to 2. The more likely value of compression, $K \approx 240$ MeV, sets the range 1.5 to $1.7M_\odot$. The reduction is even greater than it seems at first because the least value of maximum mass that theory provides is that of noninteracting nucleons, i.e., a star supported solely by the Fermi pressure. This value is $\sim 0.7M_\odot$ (Section 3.9.8).

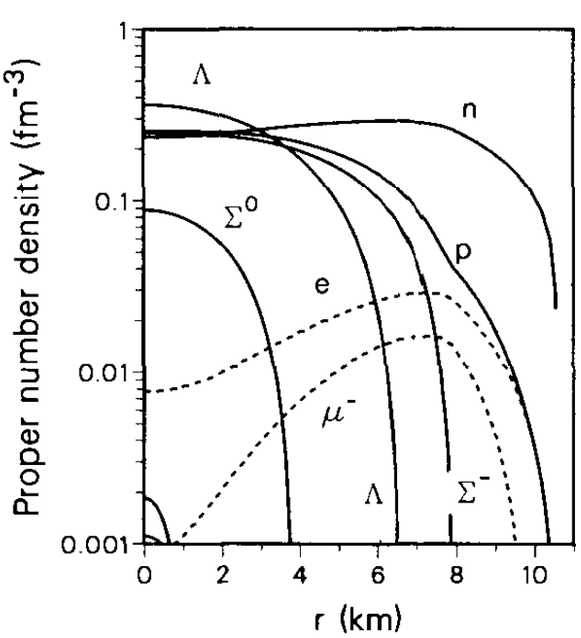

FIGURE 5.26. Composition of the maximum mass star for the case discussed in the text. See also Ref. [132].

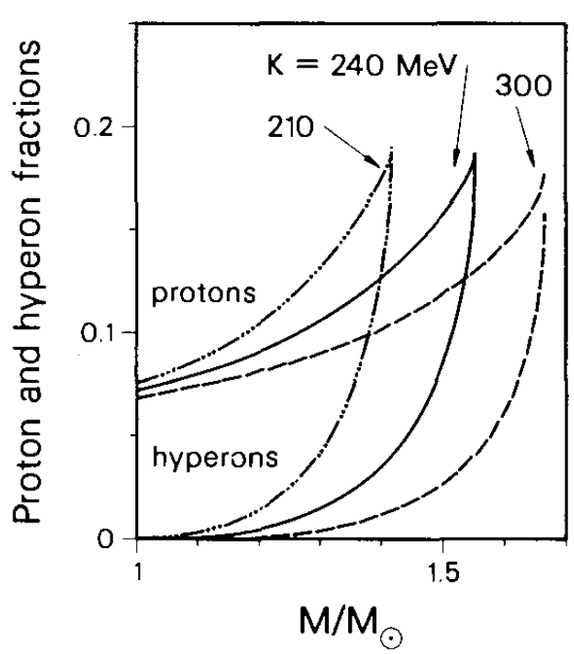

FIGURE 5.27. Proton and hyperon fraction of baryon number density for three values of the compression modulus. After Ref. [132].

[30]Recall (3.150) for the integration.

Hyperon and proton fractions of stars corresponding to three values of compression modulus are shown in Fig. 5.27. These population fractions appear to be independent of the assumed compression modulus for the limiting mass star. What is particularly noticeable is the steep rise in hyperon populations as the limiting mass is approached. The implication is that hyperons will be a strong component, up to 18%, in neutron stars if the true mass limit is $\sim 1.5M_{\odot}$. In fact this may be the case [323]. It is certainly the limit that fits most comfortably with the preferred value of $K = 240$ MeV and the role played by hyperons in softening the equation of state, as we have found.

The strong dependence of hyperon populations on stellar mass can be traced, of course, to the higher central density of stars near the mass limit. Because the cooling rate of neutron stars is influenced by the proton fraction [324] we compare the proton fraction in two stellar models in Fig. 5.28, to see the effect that hyperons have on stars of the *same* mass. We see, for example, that for a $M = 1.5M_{\odot}$ star, the proton fraction is significantly higher in a hyperon star.

The limiting mass is not the only neutron star property that is influenced by hyperons populations. Models of neutron stars that omit the hyperon population are likely to provide an incomplete picture of neutron star cooling [271, 273, 274, 275, 276]. Moreover electrical conductivity and superfluidity will surely be modified by the presence of hyperons [68]. Electrical conductivity cannot be measured directly. However, ohmic resistance influences the decay or persistence of the magnetic field of pulsars and also its location in the star.

The temperature history of neutron stars offers another interesting possibility for studying the interior and surface composition [297]. Present temperatures can be inferred approximately by use of the dipole lifetime or an historical lifetime together with a model for the initial protoneutron star which provides initial conditions for the temperature [325, 326]. Surface temperatures of some neutron stars have been measured, and theoretical models can be compared with these.

5.4.5 Compression modulus and effective nucleon mass

As has been remarked already, the stiffer the equation of state is, the more massive the limiting star of the corresponding one-parameter family of stars. We have also noted that the best-known properties of symmetric matter are the binding energy and saturation density (Chapter 4). The symmetry energy coefficient is quite well known, while the effective nucleon mass at saturation density and the compression modulus are the least well known. At the same time, the latter two strongly influence the high-density behavior of the equation of state of symmetric matter, as we saw in Fig. 4.2. By extension, the effect shows up in neutron-rich, and neutron star matter. Recall that, by the latter phrase, we mean cold, charge-neutral uniform matter in general beta equilibrium. For one choice of nucleon effective mass at saturation, $m^*/m = 0.78$, we show three neutron star sequences corresponding to the indicated values of the compression modulus of the corresponding symmetric nuclear matter in Fig. 5.29.

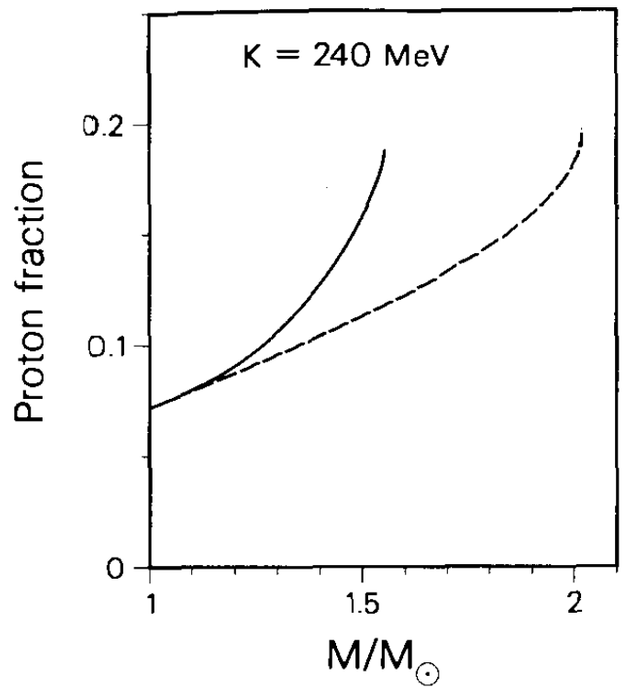

FIGURE 5.28. Proton fraction for two models: hyperon star (solid) and neutron, proton and lepton star (dash).

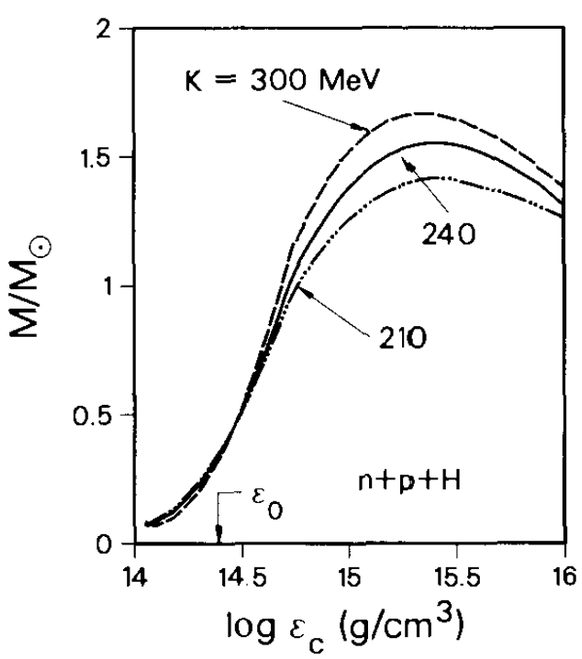

FIGURE 5.29. Neutron star sequences for three values of compression K labeled according to its value in symmetric nuclear matter. Normal nuclear matter density is labeled by ϵ_0. Hyperon couplings as in text [327].

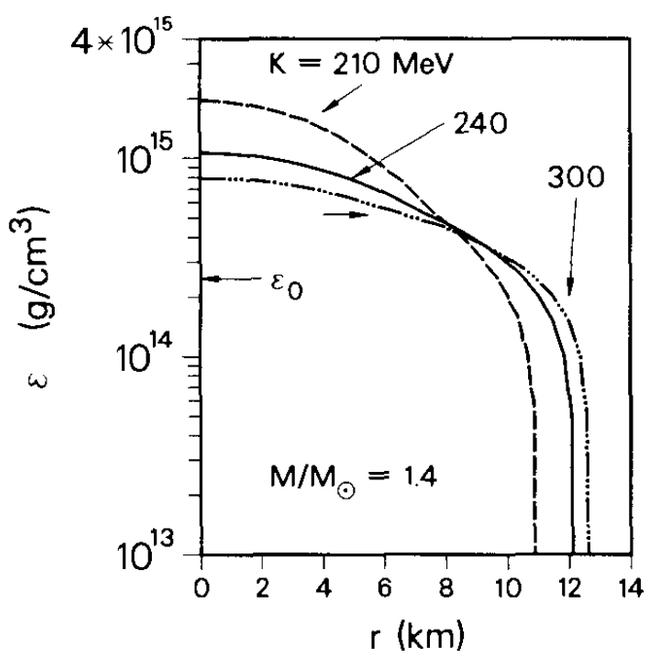

FIGURE 5.30. Mass–energy distributions of three $1.4M_\odot$ mass stars corresponding to the indicated values of K. They belong to the sequences of Fig. 5.29. Hyperon thresholds at a common density are visible by inflections shown by the arrow.

The mass-energy distribution for $1.4M_\odot$ stars for the same three values of K = 210, 240, and 300 MeV are shown in Fig. 5.30. The inflection point in each curve signals the hyperon threshold, evident also in the equation of state of Fig. 5.20. These figures show that the softer the equation of state is, the more compressed the star.

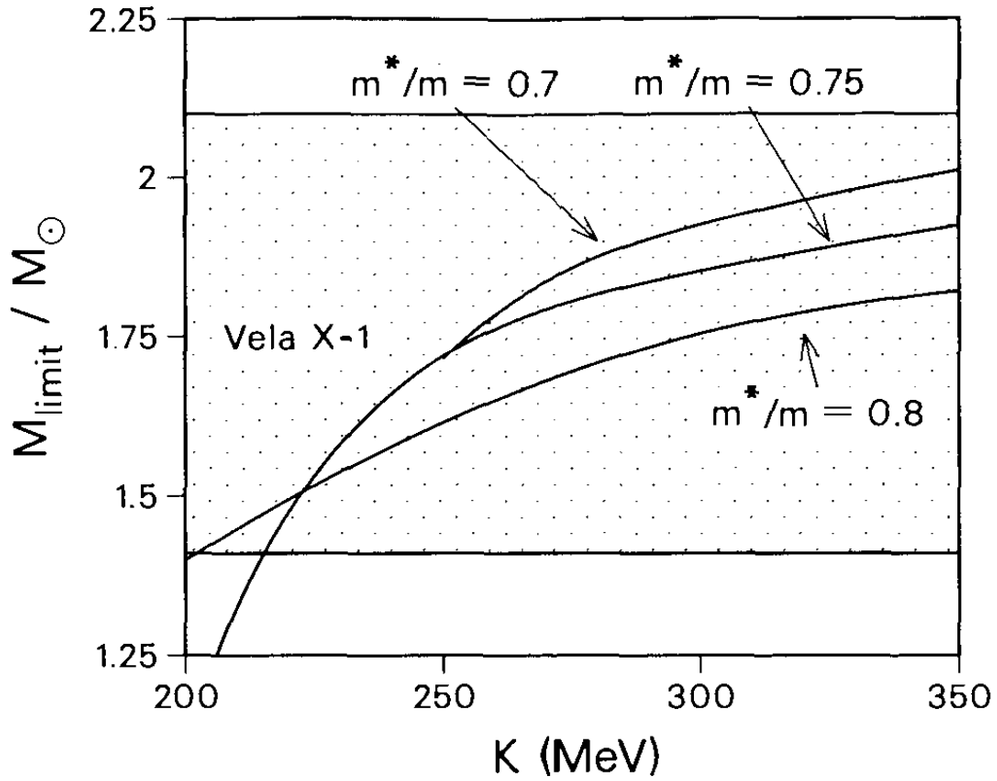

FIGURE 5.31. Limiting mass of various neutron star sequences as a function of the value of the compression modulus of symmetric nuclear matter for several values of the effective nucleon mass. Dotted area denotes uncertainties in Vela X-1 mass. From [146].

Rather than show a similar plot for a range of values of the effective nucleon mass, we summarize the situation with respect to the limiting mass as a function of the compression modulus at several values of the effective nucleon mass in Fig. 5.31. What we learn here is that, when hyperons are included in the equilibrium description of neutron star matter, a compression modulus as low as 210 MeV is only marginally acceptable.

5.4.6 Charge neutrality achieved among baryons

We understand that neutron stars—indeed, any star—must have zero net charge (though this does not imply zero charge density, a fact that has interesting consequences, as we shall see in Chapter 9). The reason is that the star is bound by the long-range gravitational force and any net charge above an infinitesimal (5.25) would unbind additional charge. Let us imagine building up a neutron star, not as nature does in a supernova where the material is approximately symmetric in neutron and proton in the progenitor star, but rather building the star initially using neutrons and adding more and more of them. This is a perfectly legitimate consideration as discovered many years ago in chemical thermodynamics because at this point we are interested in the final ground state and not the path by which it is attained.

What we would find is that even at a modest density compared to nuclear density, the Fermi energy of the neutron at the top of the Fermi sea exceeds the energy of a proton, electron, and neutrino. In that case the neutron would inverse beta decay, and so for all high-lying neutrons. Decay of low-momentum neutrons would be

Pauli blocked by occupied proton states. By such processes a purely neutron star, or any other mixture of nucleons would find the equilibrium number of neutrons, protons, and electrons. Any photons or neutrinos produced in the reactions leading to equilibrium eventually diffuse to the surface and being massless (or nearly so), escape, lowering the energy of the star.

If the only hadrons were neutrons and protons, then the electron chemical potential would increase with density as in Fig. 5.32. However, as the density of neutrons is increased, still higher particle thresholds are reached. Suppose the effective mass of negative pions in dense matter were constant, say equal to their vacuum mass. When the electron chemical potential attained that value, it would be energetically more favorable for π^- to condense because they are bosons and can all occupy the same zero momentum state. The electron chemical potential would then saturate at the pion effective mass as seen in Fig. 5.32, *if* that threshold falls below still a third one, that of the hyperons.

When the eigenvalues of nucleons in the medium exceed those of any or some of the hyperons it becomes energetically favorable for hyperons to replace some of the nucleons. We find that this occurs at two or three times nuclear density. Negatively charged hyperons can replace a proton *and* electron. The electron chemical potential will then saturate as shown in Fig. 5.32 and will actually fall with increasing density. What is happening is that charge neutrality is now being achieved among the one class of particles that must be present by conservation of the number of baryons with which the star was formed [68]. Leptons and mesons such as π^- or K^- are not needed for charge neutrality if it becomes energetically favorable for charge neutrality to be achieved among the conserved baryons. Even though the mesons can occupy zero momentum states, they still have mass.

We can formally state the basis for the phenomenon described above as follows: Lepton number is not conserved in a star (because of neutrino diffusion), nor is meson number conserved. We are assured by the Pauli principle that particles carrying the conserved baryon number will distribute themselves, at high density, among many species so as to lower the Fermi energies and minimize the total energy. Therefore, baryons (or quarks) will tend to neutralize charge among themselves because the cost of their masses and Fermi energies must be paid, but not that of leptons nor mesons. Leptons and charged mesons will in this way be quenched at high density.

The phenomena discussed above can be seen in Fig. 5.17; after reaching a maximum, the lepton populations decrease as the density of neutron star matter increases. This is a noteworthy phenomenon and, possibly, has implications for the cooling of neutron stars as well as their electrical conductivity, hence the decay rate of their magnetic fields and therefore their active lifetimes as pulsars.

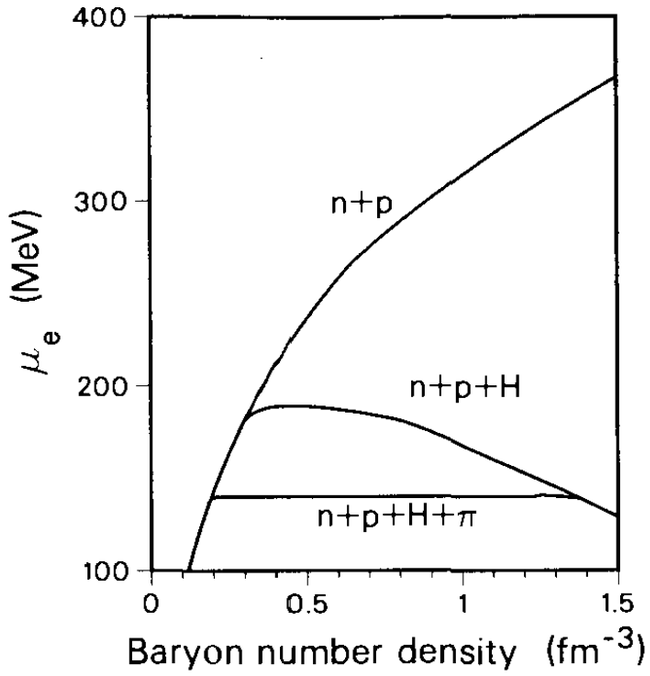

FIGURE 5.32. Electron chemical potential as a function of neutron star baryon number density for three cases as discussed in the text. (Adapted from Ref. [68].)

5.4.7 *Pion and kaon condensation*

In Chapter 4 we saw that the general form of the Euler–Lagrange equation for a meson field ϕ is

$$(\Box + m_\phi^2)\phi(x) = g_\phi \, \overline{\psi}(x)\Gamma_\phi \psi(x) . \tag{5.61}$$

If the source current on the right side is finite in matter, as it is for scalar and vector mesons, and also for the neutral rho meson in isospin asymmetric matter, then $\langle\phi\rangle$ cannot vanish.

However, the quantum numbers of certain mesons are such that the ground-state expectation of the source current on the right-hand side does vanishes identically in the mean-field approximation. This is so for both the pion (spin-parity 0^-) and the kaon (which carries strangeness). For example, only such off-diagonal source currents as $\langle\bar{\Lambda}\gamma_5 N\rangle$ appear on the right side as sources for the kaon. Being off-diagonal, they vanish in the *normal* ground state. If the source current vanishes, the meson field $\langle\phi\rangle$ satisfies the free Klein–Gordan equation and vanishes so as to yield the lowest energy. Otherwise the energy density would contain a positive term like $(1/2)m_\phi^2\langle\phi\rangle^2$ (in the mean field approximation). Nevertheless, a *different* configuration of the fermion state might exist for which the source is *finite*. Such a situation is referred to as a *condensate*. Denote the current by $J = \overline{\psi}(x)\Gamma_\phi\psi(x)$ and the polarization operator by

$$\Pi_\phi = -\lim_{\langle\phi\rangle\to 0} \frac{\langle J\rangle}{\langle\phi\rangle} . \tag{5.62}$$

The brackets denote expectation values with respect to the fermion configuration, typically the ground state. Threshold for condensation is the lowest baryon density at which the ground state has undergone a structural change from the normal state to another that endows $\langle J\rangle$ with a finite value and therefore yields a nonvanishing

$\langle\phi\rangle$. We refer to such a state as a ϕ-condensed state (where ϕ stands for π^- or K^-, for example).

For uniform static matter, we can write the following equation at threshold:

$$[-k_0^2 + \boldsymbol{k}^2 + m_\phi^2 + \Pi_\phi(k_0, \boldsymbol{k})]\langle\phi\rangle = 0\,. \tag{5.63}$$

The condition for nonvanishing $\langle\phi\rangle$ is that the quantity in square brackets should vanish. The threshold for nonvanishing condensate $\langle\phi\rangle$ is the lowest density for which

$$-k_0^2 + \boldsymbol{k}^2 + m_\phi^2 + \Pi_\phi(k_0, \boldsymbol{k}) = 0 \tag{5.64}$$

has a solution for real $\boldsymbol{k}$ and $k_0 = \mu_\phi$. The field ϕ could stand for pion or kaon, and the chemical potential for the negatively charged mesons of these types is the electron chemical potential μ_e (5.34, 5.37). We now discuss the plausibility of condensation of the lowest-mass mesons that have vanishing source currents in the normal ground state of hadronic matter or, more particularly, in neutron star matter, namely, the negative pion and kaon.

Pion condensation was a subject of much investigation a few years ago, especially for symmetric nuclear matter and nuclei. However, pions are more likely to condense in neutron star matter. Condensation occurs in nuclear matter only if the pion energy becomes degenerate with the normal ground state. This might happen if the interaction is attractive and strong enough. Charge neutrality of neutron stars favors pion condensation (or in general a negative meson condensate). This is so because, as a function of increasing density, neutrons at the top of the Fermi sea will decay to proton plus electron. The electrons are fermions and their Fermi level increases with further increase in density. When the electron chemical potential (Fermi energy) becomes equal to the effective pion mass in the medium it will be favorable thereafter for negative pions to play the role that electrons had in preserving charge neutrality. The reason is that pions are bosons and they can all condense in the lowest state. Whereas $\mu_e = \mu_n - \mu_p$ is essentially zero in symmetric matter, it is positive in neutron star matter, thus favoring the π^- because $\mu_{\pi^-} = \mu_e$. On the other hand, the other charge states of the pion are excluded because $\mu_{\pi^+} = -\mu_e$ and $\mu_{\pi^0} = 0$. Similar remarks and relationships hold for the kaon, except that its participation at first sight seems less likely because of its greater mass [68].

However, the electron chemical potential is not likely to grow indefinitely with increasing density. We saw in the previous section that above a certain density it becomes energetically more favorable for charge neutrality to be achieved among baryons than to fill ever-higher electron Fermi levels. In that case, the electron chemical potential will saturate. In the previous section, saturation was seen to occur at several times normal nuclear density, and the electron chemical potential, and therefore the electron population, fell thereafter.

Against such a situation as described, if pions do condense the growth of the electron chemical potential is arrested at a value equal to the effective pion mass as illustrated in Fig. 5.32. The electron population remains constant as the pion

population grows to neutralize any net positive charge on the baryon sector.[31] However, with increasing density and growth of hyperon populations, charge neutrality is achieved mostly among the baryons themselves. The electron chemical potential decreases as a consequence and the pion population will decrease at higher density and the population may actually vanish (Fig. 5.32). So, pion condensation (and similarly with kaon condensation) is most likely an intermediate density phenomenon if it occurs at all.

In the event the electron chemical potential cannot approach the effective mass of the negative kaon, negative kaons cannot condense. Condensation of the other kaon states is even less likely. This is the expectation based on effective masses of pion and kaon not too different from their vacuum values. However, it has also been suggested that kaons may condense at rather low density in nuclear or neutron matter because of attractive interactions that decrease the effective kaon mass with increasing baryon density [277]. This conclusion was made without taking account of the presence of hyperons in dense matter. In several investigations the relevance of hyperons to Bose condensation argued above [68], has been confirmed by detailed calculations [311, 328]. Nevertheless, Bose condensation whether of pions or kaons is an interesting possibility that we revisit in Chapter 10. There we will discover quite unusual phenomena associated with a charged Bose condensate, such as the formation of crystalline structure of the condensate state embedded in a background of the normal state of neutron star matter.

5.4.8 Condensation of Free Pions

For the present, we will test the effect of pion condensation in the simplest possible model, by assuming that pions do not interact and thus will condense at their vacuum mass if the electron chemical attains that value. In that case the electron chemical potential will saturate at the π^- mass (Fig. 5.32). The electron population will remain essentially saturated through a range of density and then decrease as the hyperon populations grow and reduce the electron chemical potential to a value below the pion mass. The pion population at this point will vanish. So, pion condensation, if it occurs (i.e., if the pion effective mass is small enough), is an intermediate density phenomenon in neutron stars, as we reasoned above. This can be seen in Fig. 5.33. Pion condensation does not seem to have a large effect on neutron star structure if the pion effective mass is as large as its vacuum mass. The effect of pion condensation is found to be larger the softer is the equation of state [191].

The role of the pion is probably overestimated by taking the vacuum mass as the effective mass. In neutron star matter, the pion experiences a repulsive s-wave interaction which would increase its effective mass. It also experiences an attractive p-wave interaction which requires the pion to have a finite momentum

[31] However, if the meson condensate interacts with the nuclear medium, its effective mass may decrease with density as in Chapter 10. The discussion in the text remains valid.

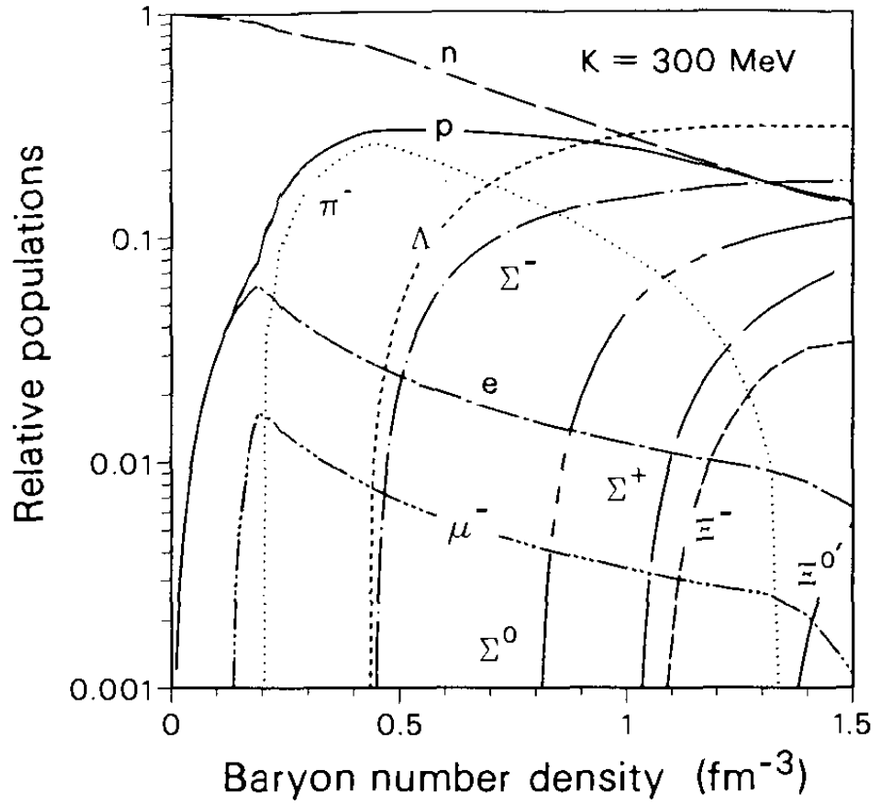

FIGURE 5.33. Particle populations of neutron star matter relative to that of the baryon density in the case that negative pions have an effective mass equal to their vacuum mass. See Ref. [129].

to feel the attraction. Taking such things into account our estimate of the effective mass is $\sim$ 200 MeV [329]. If the effective pion mass is larger than this, then kaon condensation might occur if the interaction with the medium is attractive and strong enough. We discuss kaon condensation in a later chapter.

5.5 Tables of Equations of State

5.5.1 Low density

In this section, tables of the equation of state of neutron star matter at subsaturation densities are due to Harrison and Wheeler and to Baym, Pethick and Sutherland (BPS).

5.5.2 High density

In this section are equations of state for neutron star matter corresponding to nuclear properties identified in Table 5.5. The octet of baryons comprises the composition of the matter which is in generalized beta equilibrium. The ratio of hyperon-to-nucleon coupling to the scalar meson field is denoted by x_σ. The corresponding coupling to the vector fields can be found in Table 5.4. Muons as well as electrons are included.

TABLE 5.6. Equation of stateof Harrison and Wheeler. The first 27 entries are from Ref. [28]. The remainder were computed by Negele and Vautherin as quoted by Pandharipande, Pines, and Smith in *Astrophys. J.* 208 (1976) 550. (A number 3.5 +14 means 3.5×10^{14}.)

ρ (fm^{-3})	ϵ (g/cm^3)	p (dyne/cm^2)	ρ (fm^{-3})	ϵ (g/cm^3)	p (dyne/cm^2)
0.473 −14	7.86 + 0	1.01 + 9	0.602 −9	1.00 + 6	2.80 +22
0.475 −14	7.88 + 0	5.07 + 9	0.145 −8	2.41 + 6	1.21 +23
0.476 −14	7.90 + 0	1.01 +10	0.482 −8	8.00 + 6	8.96 +23
0.485 −14	8.06 + 0	5.07 +10	0.277 −7	4.61 + 7	6.50 +24
0.491 −14	8.15 + 0	1.01 +11	0.455 −7	7.56 + 7	1.21 +25
0.699 −14	1.16 + 1	1.21 +12	0.615 −6	1.02 + 9	3.18 +26
0.990 −14	1.64 + 1	1.40 +13	0.190 −5	3.15 + 9	1.74 +27
0.157 −13	2.60 + 1	4.41 +13	0.139 −4	2.32 +10	2.22 +28
0.272 −13	4.51 + 1	1.69 +14	0.415 −4	6.92 +10	8.50 +28
0.532 −13	8.82 + 1	8.46 +14	1.000 −3	1.00 +11	1.40 +29
0.127 −12	2.11 + 2	5.82 +15	0.200 −2	2.00 +11	3.14 +29
0.425 −12	7.05 + 2	7.23 +16	0.300 −2	4.01 +11	7.16 +29
0.693 −12	1.15 + 3	1.90 +17	0.400 −2	8.02 +11	1.04 +30
0.124 −11	2.06 + 3	5.61 +17	0.500 −2	1.00 +12	1.26 +30
0.300 −11	4.98 + 3	2.85 +18	0.600 −2	2.00 +12	2.12 +30
0.998 −11	1.66 + 4	2.45 +19	0.700 −2	4.01 +12	3.78 +30
0.500 −10	8.30 + 4	4.10 +20	0.800 −2	8.02 +12	8.53 +30
0.200 −9	3.31 + 5	4.46 +21	0.900 −2	1.00 +13	1.16 +31

5.6 Problems for Chapter 5

1. Take as given that the average type II supernova rate (the type that corresponds to the terminal phase of massive stars ($M > 10M_\odot$), is about 1/100 years, estimate the total number of neutron stars in our Galaxy, assuming that each event leaves behind a neutron star.
2. What observations would allow one to infer a supernova rate?
3. Why are so many fewer pulsars observed than the above estimate?
4. Why do we believe that type II supernovae indicate the formation of a neutron star?
5. Practice using gravitational units by verifying the results (5.7).
6. The energy density of symmetric nuclear matter is $\epsilon_0 \approx 2.5 \times 10^{14}$ g/cm^3. Taking account of the binding energy of nuclear matter and other data in Section 4.5, derive the quoted result.
7. Given that pulsars are observed in the disk of the Galaxy, refer to Figure 5.6 and count how many pulsars have been detected to a distance of 5 kps. From the table on page 441, find the radius of the Milky Way and estimate the number of active pulsars in our Galaxy, assuming that, because of the beaming effect, we can detect only one out of five. Because the pulsar density seems to increase toward the center of the Galaxy, out to the detection distance, the estimate is presumably a lower limit.

TABLE 5.7. Equation of state of BPS [80]

ρ (fm^{-3})	ϵ (g/cm^3)	p (dyne/cm^2)	ρ (fm^{-3})	ϵ (g/cm^3)	p (dyne/cm^2)
4.730 −15	7.861 +0	1.010 + 9	9.976 −6	1.659 +10	1.425 +28
4.760 −15	7.900 + 0	1.010 +10	1.256 −5	2.090 +10	1.938 +28
4.910 −15	8.150 + 0	1.010 +11	1.581 −5	2.631 +10	2.503 +28
6.990 −15	1.160 + 1	1.210 +12	1.990 −5	3.313 +10	3.404 +28
9.900 −15	1.640 + 1	1.400 +13	2.506 −5	4.172 +10	4.628 +28
2.720 −14	4.510 + 1	1.700 +14	3.155 −5	5.254 +10	5.949 +28
1.270 −13	2.120 + 2	5.820 +15	3.972 −5	6.617 +10	8.089 +28
6.930 −13	1.150 + 3	1.900 +17	5.000 −5	8.333 +10	1.100 +29
6.295 −12	1.044 + 4	9.744 +18	6.294 −5	1.049 +11	1.495 +29
1.581 −11	2.622 + 4	4.968 +19	7.924 −5	1.322 +11	2.033 +29
3.972 −11	6.587 + 4	2.431 +20	9.976 −5	1.664 +11	2.597 +29
9.976 −11	1.654 + 5	1.151 +21	1.105 −4	1.844 +11	2.892 +29
2.506 −10	4.156 + 5	5.266 +21	1.256 −4	2.096 +11	3.290 +29
6.294 −10	1.044 + 6	2.318 +22	1.581 −4	2.640 +11	4.473 +29
1.581 −9	2.622 + 6	9.755 +22	1.990 −4	3.325 +11	5.816 +29
3.972 −9	6.588 + 6	3.911 +23	2.506 −4	4.188 +11	7.538 +29
5.000 −9	8.294 + 6	5.259 +23	2.572 −4	4.299 +11	7.805 +29
9.976 −9	1.655 + 7	1.435 +24	2.670 −4	4.460 +11	7.890 +29
1.990 −8	3.302 + 7	3.833 +24	3.126 −4	5.228 +11	8.352 +29
3.972 −8	6.590 + 7	1.006 +25	3.951 −4	6.610 +11	9.098 +29
7.924 −8	1.315 + 8	2.604 +25	4.759 −4	7.964 +11	9.831 +29
1.581 −7	2.624 + 8	6.676 +25	5.812 −4	9.728 +11	1.083 +30
1.990 −7	3.304 + 8	8.738 +25	7.143 −4	1.196 +12	1.218 +30
3.155 −7	5.237 + 8	1.629 +26	8.786 −4	1.471 +12	1.399 +30
5.000 −7	8.301 + 8	3.029 +26	1.077 −3	1.805 +12	1.638 +30
6.294 −7	1.045 + 9	4.129 +26	1.314 −3	2.202 +12	1.950 +30
7.924 −7	1.316 + 9	5.036 +26	1.748 −3	2.930 +12	2.592 +30
9.976 −7	1.657 + 9	6.860 +26	2.287 −3	3.833 +12	3.506 +30
1.581 −6	2.626 + 9	1.272 +27	2.942 −3	4.933 +12	4.771 +30
2.506 −6	4.164 + 9	2.356 +27	3.726 −3	6.248 +12	6.481 +30
3.972 −6	6.602 + 9	4.362 +27	4.650 −3	7.801 +12	8.748 +30
5.000 −6	8.313 + 9	5.662 +27	5.728 −3	9.612 +12	1.170 +31
6.294 −6	1.046 +10	7.702 +27	7.424 −3	1.246 +13	1.695 +31
7.924 −6	1.318 +10	1.048 +28	8.907 −3	1.496 +13	2.209 +31

8. Derive a relationship between field strength B and period P of pulsars of fixed dipole age τ (5.15). Thereby show that $B = \text{const} \times P$ and confirm the straight "age" lines drawn in Fig. 5.8.

9. Use Section 3.3 on units to convert the energy density and pressure of two entries in the Harrison and Wheeler equation of state at the end of the chapter, namely, the two for densities $0.474 \cdot 10^{-14}$ fm^{-3} and 0.53210^{-13} fm^{-3} to common units, say fm^{-2}. These two entries differ in energy density by about

TABLE 5.8. Equation of state corresponding to $K = 240$ MeV, $m^*/m = 0.78$, $x_\sigma = 0.6$

ρ (fm^{-3})	ϵ (g/cm^3)	p (dyne/cm^2)	ρ (fm^{-3})	ϵ (g/cm^3)	p (dyne/cm^2)
0.010	1.6758 +13	7.4377 +30	0.660	1.2571 +15	1.5479 +35
0.015	2.5141 +13	8.9843 +30	0.690	1.3224 +15	1.6825 +35
0.020	3.3529 +13	1.2123 +31	0.720	1.3884 +15	1.8239 +35
0.025	4.1911 +13	1.9243 +31	0.750	1.4550 +15	1.9723 +35
0.030	5.0301 +13	3.2767 +31	0.780	1.5224 +15	2.1277 +35
0.060	1.0074 +14	3.6507 +32	0.810	1.5904 +15	2.2903 +35
0.090	1.5151 +14	1.3499 +33	0.840	1.6591 +15	2.4601 +35
0.120	2.0279 +14	3.1938 +33	0.870	1.7284 +15	2.6372 +35
0.150	2.5471 +14	5.9384 +33	0.900	1.7985 +15	2.8187 +35
0.180	3.0735 +14	9.6207 +33	0.930	1.8692 +15	2.9981 +35
0.210	3.6075 +14	1.4377 +34	0.960	1.9406 +15	3.1802 +35
0.240	4.1500 +14	2.0302 +34	0.990	2.0126 +15	3.3665 +35
0.270	4.7019 +14	2.7477 +34	1.020	2.0853 +15	3.5571 +35
0.300	5.2630 +14	3.5979 +34	1.050	2.1586 +15	3.7528 +35
0.330	5.8336 +14	4.3403 +34	1.080	2.2325 +15	3.9536 +35
0.360	6.4112 +14	5.0478 +34	1.110	2.3070 +15	4.1601 +35
0.390	6.9958 +14	5.8246 +34	1.140	2.3822 +15	4.3719 +35
0.420	7.5872 +14	6.6820 +34	1.170	2.4580 +15	4.5894 +35
0.450	8.1859 +14	7.6277 +34	1.200	2.5344 +15	4.8009 +35
0.480	8.7920 +14	8.6647 +34	1.230	2.6114 +15	5.0020 +35
0.510	9.4052 +14	9.6875 +34	1.260	2.6890 +15	5.2021 +35
0.540	1.0025 +15	1.0735 +35	1.290	2.7670 +15	5.4035 +35
0.570	1.0652 +15	1.1831 +35	1.320	2.8456 +15	5.6068 +35
0.600	1.1285 +15	1.2984 +35	1.350	2.9247 +15	5.8129 +35
0.630	1.1925 +15	1.4199 +35	1.380	3.0043 +15	6.0222 +35

a factor 10. Note that energy density dominates pressure at low density. Use the table you have just constructed in the problem below.

10. Use the Oppenheimer–Volkoff equation (2.224) to estimate the distance from the edge of a neutron star where the energy density has increased tenfold over what it is at the edge. The density of iron in absolute vacuum, as in an idealized cold neutron star at its surface is not known. It cannot be much different from its value of 7.86 g/cm^{3}at one atmosphere of pressure. Use the table of energy density and pressure in a common unit that you constructed in the above problem. For the star choose $M = 1.5M_\odot$ and $R = 10$ km. Note that from (2.224) we can write the slope at the surface as

$$\frac{dp}{dr} \approx -\frac{[0+\epsilon(R)]M}{R(R-2M)}\,.$$

Find that the density has increased tenfold at a depth of about 3 mm.

11. Surface temperatures are of the order 10^6 K in a million years from birth. This is much higher than the boiling temperature of solid (atomic) iron (2500 C). Would iron atoms be partially or totally ionized at the surface? If so, would

TABLE 5.9. Equation of state corresponding to $K = 210$ MeV, $m^*/m = 0.78$, $x_\sigma = 0.6$

ρ (fm^{-3})	ϵ (g/cm^3)	p (dyne/cm^2)	ρ (fm^{-3})	ϵ (g/cm^3)	p (dyne/cm^2)
0.010	1.6752 +13	3.9994 +30	0.630	1.1807 +15	1.2170 +35
0.015	2.5131 +13	3.4326 +30	0.660	1.2436 +15	1.3225 +35
0.020	3.3510 +13	5.4699 +30	0.690	1.3071 +15	1.4339 +35
0.025	4.1890 +13	1.2938 +31	0.720	1.3712 +15	1.5515 +35
0.030	5.0273 +13	2.8451 +31	0.750	1.4358 +15	1.6757 +35
0.060	1.0069 +14	3.9881 +32	0.780	1.5009 +15	1.8067 +35
0.090	1.5147 +14	1.4359 +33	0.810	1.5667 +15	1.9446 +35
0.120	2.0278 +14	3.2931 +33	0.840	1.6330 +15	2.0899 +35
0.150	2.5471 +14	5.9640 +33	0.870	1.6999 +15	2.2426 +35
0.180	3.0733 +14	9.4446 +33	0.900	1.7674 +15	2.3941 +35
0.210	3.6068 +14	1.3837 +34	0.930	1.8355 +15	2.5436 +35
0.240	4.1478 +14	1.9208 +34	0.960	1.9042 +15	2.6953 +35
0.270	4.6973 +14	2.5623 +34	0.990	1.9733 +15	2.8502 +35
0.300	5.2552 +14	3.3149 +34	1.020	2.0430 +15	3.0087 +35
0.330	5.8216 +14	3.9817 +34	1.050	2.1131 +15	3.1717 +35
0.360	6.3940 +14	4.5742 +34	1.080	2.1839 +15	3.3396 +35
0.390	6.9723 +14	5.2160 +34	1.110	2.2551 +15	3.5125 +35
0.420	7.5559 +14	5.9208 +34	1.140	2.3269 +15	3.6867 +35
0.450	8.1458 +14	6.6966 +34	1.170	2.3991 +15	3.8357 +35
0.480	8.7414 +14	7.5499 +34	1.200	2.4718 +15	3.9751 +35
0.510	9.3433 +14	8.4437 +34	1.230	2.5448 +15	4.1095 +35
0.540	9.9512 +14	9.3173 +34	1.260	2.6182 +15	4.2384 +35
0.570	1.0564 +15	1.0222 +35	1.290	2.6920 +15	4.3491 +35
0.600	1.1183 +15	1.1171 +35	1.320	2.7659 +15	4.4414 +35

this allow greater compaction? Would the thickness of the skin through which the density increases tenfold be larger or smaller than the above estimate?

12. For a less massive star, say $M = 0.8M_\odot$ of Fig. 5.10 how thick is the skin? How do the above estimates depend on the assumption of the energy density of iron at zero pressure?

13. Derive the field equations (5.41 – 5.43) and the equation of state, (5.50) and (5.51).

14. Use equation (5.56) and the chemical potentials and field quantities plotted in Fig. 5.19 to verify the particle thresholds of Fig. 5.17.

15. Use the hints from Section 5.3.6 and what you have learned about equilibrium and particle populations to construct a computer code for calculating the equation of state of neutron star matter from the relativisitic mean field theory adopted in this book, or some other version of a covariant theory.

TABLE 5.10. Equation of state corresponding to $K = 300$ MeV, $m^*/m = 0.78$, $x_\sigma = 0.6$

ρ (fm^{-3})	ϵ (g/cm^3)	p (dyne/cm^2)	ρ (fm^{-3})	ϵ (g/cm^3)	p (dyne/cm^2)
0.010	1.6770 +13	1.4536 +31	0.660	1.2733 +15	1.7555 +35
0.015	2.5163 +13	2.1180 +31	0.690	1.3405 +15	1.9058 +35
0.020	3.3559 +13	2.7070 +31	0.720	1.4084 +15	2.0630 +35
0.025	4.1957 +13	3.4288 +31	0.750	1.4770 +15	2.2272 +35
0.030	5.0357 +13	4.4907 +31	0.780	1.5463 +15	2.3984 +35
0.060	1.0084 +14	2.9325 +32	0.810	1.6165 +15	2.5766 +35
0.090	1.5159 +14	1.1633 +33	0.840	1.6873 +15	2.7620 +35
0.120	2.0283 +14	2.9844 +33	0.870	1.7589 +15	2.9545 +35
0.150	2.5472 +14	5.8863 +33	0.900	1.8313 +15	3.1506 +35
0.180	3.0737 +14	9.9578 +33	0.930	1.9044 +15	3.3459 +35
0.210	3.6089 +14	1.5355 +34	0.960	1.9782 +15	3.5445 +35
0.240	4.1538 +14	2.2168 +34	0.990	2.0526 +15	3.7474 +35
0.270	4.7093 +14	3.0465 +34	1.020	2.1278 +15	3.9552 +35
0.300	5.2760 +14	4.0295 +34	1.050	2.2037 +15	4.1682 +35
0.330	5.8529 +14	4.8527 +34	1.080	2.2803 +15	4.3864 +35
0.360	6.4383 +14	5.6934 +34	1.110	2.3575 +15	4.6099 +35
0.390	7.0317 +14	6.6156 +34	1.140	2.4354 +15	4.8394 +35
0.420	7.6333 +14	7.6290 +34	1.170	2.5140 +15	5.0744 +35
0.450	8.2436 +14	8.7380 +34	1.200	2.5933 +15	5.3083 +35
0.480	8.8620 +14	9.8832 +34	1.230	2.6732 +15	5.5328 +35
0.510	9.4886 +14	1.1022 +35	1.260	2.7537 +15	5.7570 +35
0.540	1.0122 +15	1.2207 +35	1.290	2.8348 +15	5.9830 +35
0.570	1.0764 +15	1.3448 +35	1.320	2.9165 +15	6.2119 +35
0.600	1.1413 +15	1.4752 +35	1.350	2.9988 +15	6.4440 +35
0.630	1.2070 +15	1.6120 +35	1.380	3.0817 +15	6.6798 +35

6

Rotating Neutron Stars

6.1 Motivation

Galaxies and the individual stars within them rotate, as as is known because of the Doppler broadening of their spectral lines. The Sun rotates rather slowly, with an equatorial speed of 2 km/s, or a period of 2×10^6 s. Some stars rotate with equatorial speeds in excess of 400 km/s, close to the limit at which matter would be torn off by the centrifugal force. When the core of a massive star collapses to produce a neutron star, conservation of angular momentum assures its enhanced rotation. The Crab pulsar, still very young, rotates 30 times a second. It is one of the fastest rotating of the canonical pulsars (Fig. 5.7). The recycled pulsars with millisecond periods are thought to have been spun up by accretion from a companion onto an old canonical pulsar (Section 5.2.5). Therefore, in this chapter we are interested in the effects of rotation on the internal structure and stability of relativistic stars and on spacetime itself.

As inhabitants of a solar system well described by Newtonian gravity, we have no experience of the effect of rotation on the fabric of spacetime. It may be unexpected therefore that an observer in an inertial frame near a rotating star will himself be found to rotate around its center relative to the distant stars. He would require rockets or some other means of propulsion to stop his own rotation. The closer he approaches the star, the more rapidly he rotates. The rotation of local inertial frames has a real effect on the internal structure of rotating stars as is easily imagined. The effect of a rotating star on spacetime is referred to as the dragging of local inertial frames, or sometimes as the Lense–Thirring effect.

Rotation necessarily breaks spherical symmetry—a rotating star is centrifugally deformed and retains only axial symmetry. One might wonder whether the Kerr metric would serve (cf. Ref. [28]). Although it possesses axial symmetry, the Kerr metric is appropriate for spacetime outside a black hole. It is formulated in terms of two *given* parameters, the mass and angular momentum. We are interested in *calculating* the mass, moment of inertia and angular momentum of stars as well as the effect of rotation on their constitution and must necessarily involve ourselves in their interior structure.

The angular velocity associated with dragging of local inertial frames is fundamental to rotation in gravity. We must therefore devote careful attention to its formulation. The frame-dragging frequency is largest at the center of a rotating star and falls to zero at great distances where spacetime becomes flat. Only after having the frame-dragging effect in hand are we prepared to take the next step, a derivation of the expression for the Kepler frequency—the frequency at which a rotating star would shed matter at its equator.[1] We shall find that, rather than being a simple relation expressing the balance of gravitational and centrifugal forces as in Newtonian gravity (5.9), the Kepler frequency depends, in a complicated manner, on the internal structure of the star through the interior metric and the frame-dragging frequency. The Kepler frequency in General Relativity is expressed as a self-consistency condition that must be satisfied by the solution to Einstein's equations rather than a formula for that frequency.

The equilibrium configurations of rotating stars pose a more difficult problem than of nonrotating stars. Hartle and Thorne were the first to address the problem. They employed a perturbative approach [330, 331]. Extensive studies based on the method were reported both by the authors of the method and in later research [107, 196], [332]–[334]. For years the perturbative method was thought to be valid only for slow rotation. We now know that it is valid, within a few percent, up to the Kepler frequency, which can be determined when the Hartle–Thorne method is supplemented by the self-consistency condition spoken of above [107, 196, 333, 334]. Generally, this accuracy is sufficient to answer or probe physically interesting questions.

We employ the perturbative method supplemented by the self-consistency condition because of the greater insight it provides, compared to direct numerical solution. Direct numerical solutions, however, are more accurate [335]. Subsequent to the work of Hartle and Thorne, many authors obtained numerical solutions to Einstein's equations for rotating (but otherwise static) configurations [96, 106, 336, 337].

A useful empirical formula for the Kepler frequency has been proposed by several authors [95, 96]. We show how its simple form can be justified using the general relativistic expression of the Kepler frequency and exhibit thereby another example

[1]The Kepler angular velocity is that possessed by a particle in stable circular orbit at the equator of a star, hence, the limit to rotation of the star itself. For brevity we frequently refer to angular velocity as frequency. The two are related by $\nu = 1/P = \Omega/(2\pi)$.

of how rotation in General Relativity frequently produces nonintuitive results. We shall review properties of rotating stellar models for a wide variety of equations of state derived from both relativistic and nonrelativistic theories of matter and compare them to their nonrotating counterparts. We shall also compare the results of relativistic theories of matter and those based on Schrödinger approaches.

Finally, we briefly discuss the interesting topic of gravitational wave instabilities in rotating stars. Such instabilities may occur—especially in young hot stars—at frequencies below the Kepler frequency. If this happens, the star rapidly loses angular momentum to gravitational radiation until the frequency is reduced sufficiently that the instability can be damped by viscosity. If the gravitational wave instability occurs at a frequency above Kepler, it is irrelevant since the Kepler frequency sets the absolute limit; a stable star cannot attain a frequency higher than that at which it loses mass at the equator. These results are interesting in connection with the two populations of pulsars discussed in Chapter 5. The recycled population consists of old, cold stars for which gravitational instabilities are moved to frequencies higher (sometimes above the Kepler frequency) than those of young, hot stars. In most stellar models, cold neutron stars can rotate more rapidly than hot ones.

6.2 Dragging of Local Inertial Frames

So far we have considered the simplest nontrivial form that Einstein's equations take—the form for static, spherically symmetric stars. In this case, the line element $d\tau^2 = g_{\mu\nu}dx^\mu dx^\nu$ has the general Schwarzschild form (2.183) possessing only diagonal elements,

$$d\tau^2 = e^{2\nu(r)}\,dt^2 - e^{2\lambda(r)}\,dr^2 - r^2\,d\theta^2 - r^2\sin^2\theta\,d\phi^2\,. \tag{6.1}$$

It is evident that the line element for a rotating star must possess some off-diagonal elements. First of all, we expect the rotation to flatten the star more or less depending on the star's angular velocity. Spherical symmetry is thereby broken, but the star maintains axial symmetry. The star is assumed to be static in the sense that, although rotating, it is in uniform rotation and static in the co-rotating frame. Uniform rotation is the configuration that minimizes the total mass–energy at a specified baryon number and angular momentum [338].

The general expression for the line element for a static axial symmetric spacetime has a form dictated by time-translational invariance and axial-rotational invariance:

$$\begin{aligned} d\tau^2 &= e^{2\nu(r,\theta)}\,dt^2 - e^{2\lambda(r,\theta)}\,dr^2 \\ &\quad - e^{2\mu(r,\theta)}\big[r^2 d\theta^2 + r^2\sin^2\theta\big(d\phi - \omega(r,\theta)\,dt\big)^2\big]\,. \end{aligned} \tag{6.2}$$

Time and azimuthal angle enter the last term in the particular way that corresponds to the two invariances mentioned for a static geometry. The polar angle θ makes its appearance in the metric because of the centrifugal flattening of rotating stars and the rotation of inertial frames. We have chosen units $G = c = 1$, so that the terms in (6.2) have the dimension of squared length, or, equivalently, squared time.

The line element goes over to the Schwarzschild metric in case of spherical symmetry ($\omega \equiv 0$, $\mu \equiv 0$). Throughout the chapter, we distinguish the metric functions from those of Schwarzschild by their angular dependence. The metric functions also depend implicitly on the angular velocity of the rotating star which the metric is designed to take into account.

By writing out the square in (6.2), one can identify the various components of the metric tensor. In particular, a new feature appears, a nondiagonal metric,

$$g_{t\phi} = g_{\phi t} = r^2 \sin^2\theta \, e^{2\mu(r,\theta)} \omega(r,\theta) \,. \tag{6.3}$$

The structure of the axisymmetric star and the metric should be the same under a reversal of time as under a reversal of angular velocity. Then ω can depend only on odd powers of the angular velocity Ω of the star, for under one transformation or the other, only one term in the squared expression in (6.2) would otherwise change. Similarly, the other metric functions can have only even powers of Ω.

The function $\omega(r)$ has a most interesting and fundamental significance. It is the angular velocity of local inertial frames. Imagine, for example, that a particle is dropped from rest at a great distance from a star. If the star were not rotating, the particle would fall toward the center of the star. But if the star were rotating, the freely falling path would not be toward the center. The particle would experience an ever increasing drag in the direction of rotation of the star as it approaches (see Fig. 6.1). For this reason, $\omega(r)$ is referred to as the "angular velocity of the local inertial frames." The plural is used because the angular velocity depends on the distance r from the star. As we shall see, it is true that $\omega(r) \sim r^{-3}$ outside the star, so that spacetime is flat at infinity and distant local inertial frames do not rotate about the star.

To prove the above assertion that $\omega(r)$ is the angular velocity of a freely falling particle (and hence that of the local inertial frames), we need to combine an earlier result with some algebra. Equation (2.132) proved that a particle's trajectory conserves the covariant component of the velocity u_ϕ if the metric is independent of ϕ. Consider a particle lying at great distance and momentarily at rest in the equatorial plane of the rotation ($\theta = \pi/2$, $u^\theta = 0$). We write the contravariant

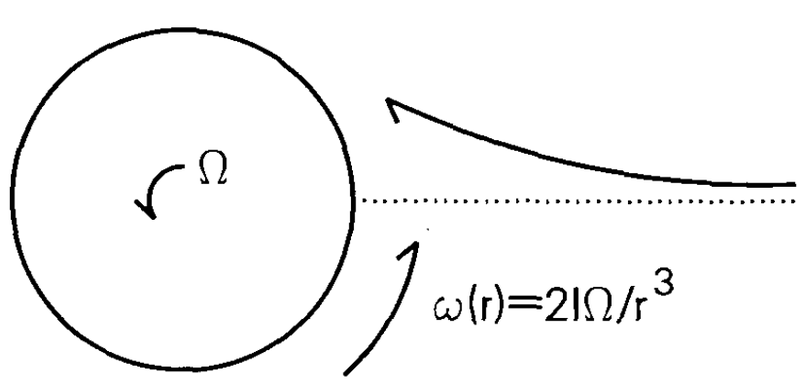

FIGURE 6.1. Schematic of the trajectory of a particle dropped from infinity in the equatorial plane of a rotating star (represented by the circle).

components of the particle's velocity as

$$u^\phi = g^{\phi\mu}u_\mu = g^{\phi\phi}u_\phi + g^{\phi t}u_t\,,$$
$$u^t = g^{tt}u_t + g^{t\phi}u_\phi\,.$$

We imagine dropping a particle from rest at a great distance from the star. Therefore, all three contravariant velocity components of the particle are initially zero. Because u_ϕ is conserved on the particle's trajectory, we have there and for all time on the particle's trajectory, $u_\phi = 0$. Moreover, because $u^t = dt/d\tau$ and $u^\phi = d\phi/d\tau$, we find for the particle,

$$\frac{d\phi}{dt} = \frac{u^\phi}{u^t} = \frac{g^{\phi t}}{g^{tt}}\,. \tag{6.4}$$

We have the metric elements $g_{\mu\nu}$ which can be read off the general form for the line element of an axial symmetric static geometry. We need the inverse elements $g^{\mu\nu}$ because they appear in the above formula. The only off-diagonal elements belong to t and ϕ. We must invert that part of the covariant metric tensor that is not in diagonal form,

$$\begin{pmatrix} g_{tt} & g_{t\phi} \\ g_{\phi t} & g_{\phi\phi} \end{pmatrix}\,. \tag{6.5}$$

The determinant is

$$D = g_{tt}g_{\phi\phi} - (g_{t\phi})^2 \tag{6.6}$$

and the inverse matrix is

$$\begin{pmatrix} g^{tt} & g^{t\phi} \\ g^{\phi t} & g^{\phi\phi} \end{pmatrix} = \frac{1}{D}\begin{pmatrix} g_{\phi\phi} & -g_{t\phi} \\ -g_{\phi t} & g_{tt} \end{pmatrix}\,. \tag{6.7}$$

Hence, we find for $\theta = \pi/2$

$$\frac{d\phi}{dt} = \frac{-g_{\phi t}}{g_{\phi\phi}} = \frac{-r^2 e^{2\mu(r,\theta)}\omega(r)}{-r^2 e^{2\mu(r,\theta)}}\,. \tag{6.8}$$

Accordingly the particle's ϕ coordinate obeys the equation[2]

$$\frac{d\phi}{dt} = \omega(r)\,. \tag{6.9}$$

This is what we sought to prove: though dropped from rest at a great distance from a rotating star, the freely falling particle does not drop toward the star's center, but is deflected. Because it is freely falling in the gravitational field, it defines local inertial frames, frames with rotational angular velocities $\omega(r)$ about the center of the star as measured by an observer at infinity at rest with respect to the star—hence

[2]We have derived the special case for the frame dragging angular velocity in the equatorial plane. However, Hartle proved that ω is independent of θ to first order in Ω [330].

the "dragging of local inertial frames" by a rotating star. This is a remarkable and important effect of rotation that is not present in Newtonian gravity.

We asserted earlier that $\omega(r) \sim r^{-3}$. The constant of proportionality is more difficult to derive. We need to solve for the actual metric functions appearing in (6.2) and use the results in (6.4). The problem divides into two parts: the interior and exterior problem, as in the case of the metric for a static spherical star. The solution of the exterior problem will provide the asymptotic behavior of $\omega(r)$. The solution of the interior problem will provide the form of $\omega(r)$ inside the star together with the normalization of the exterior solution. We take up the internal problem in the next sections.

Dimensional analysis will inform us of the exterior behavior of $\omega(r, \theta)$ modulo the normalization. At great distance from the star, spacetime ought to become asymptotically flat and the dragging frequency ought to vanish, falling off as some power of $1/r$. It should also be proportional to the angular momentum[3] $J = I\Omega \sim MR^2\Omega$ carried by the star, the source of the effect.

We have become accustomed to using gravitational units, but for dimensional analysis must revert to the actual dimensions, because, for example, time and length have the same gravitational units and would be indistinguishable. Because G has units of $\mathrm{cm}^3/(\mathrm{g\ s}^2) = \mathrm{L}^3/(\mathrm{M\ T}^2)$, J has units $\mathrm{M\ L}^2/\mathrm{T}$, and ω has the unit $1/\mathrm{T}$ (where M,L,T stand for mass, length, and time), we can write

$$\omega \sim \frac{GJ^l}{c^m r^n} \sim \mathrm{L}^{3+2l-m-n}\,\mathrm{T}^{-2-l+m}\,\mathrm{M}^{-1+l}\,.$$

The powers are to be found by insuring that the right side has the same dimensions as the left. This gives the equations

$$\begin{aligned} l - 1 &= 0\,, \\ 2 + l - m &= 1\,, \\ 3 + 2l - m - n &= 0\,. \end{aligned}$$

The solution is $l = 1$, $m = 2$, and $n = 3$ which yields $\omega \sim GJ/(c^2 r^3)$ or, reverting to gravitational units,

$$\omega(r) \sim \frac{J}{r^3} = \frac{I}{r^3}\Omega\,, \qquad r \geq R\,. \tag{6.10}$$

As remarked earlier, $\omega(r, \theta)$ has to contain odd powers of Ω, and the above expression is the leading order term. Observe that ω does not depend on θ to leading order.

An expansion in Ω whose magnitude depends on the unit used is nonetheless justified by the remark that (for a uniform sphere) the ratio of rotational to gravitational energy is less than unity, even at the Kepler frequency. The two energies

[3]We are only interested here in dimensions, so we write the classical expression for I.

are

$$E_{\rm rot} \approx \frac{1}{2} I \Omega^2 \approx \frac{1}{5} M R^2 \Omega^2, \qquad E_{\rm grav} \approx \frac{3}{5} \frac{M^2}{R} . \tag{6.11}$$

Denote the rotational frequency at which the centrifugal and gravitational forces balance each other in Newtonian physics by Ω_c; we refer to this as the Kepler frequency in Newtonian gravity (3.168). Therefore, we can write

$$\frac{E_{\rm rot}}{E_{\rm grav}} \approx \frac{1}{3} \left(\frac{\Omega}{\Omega_c} \right)^2 < \frac{1}{3} . \tag{6.12}$$

Thus, rotational perturbations on a star are relatively small. Indeed, using (5.9) as a better estimate of the maximum rotational frequency, we find that in the above expression for the ratio of rotational to gravitational energy, 1/3 can be replaced by 0.14.

Luminous stars are believed to rotate differentially. However, for compact stars, the viscosity is high enough to bring the star into uniform rotation on a short timescale compared to the life of the star [339]. Therefore, we assume that the star rotates uniformly with angular velocity Ω (as measured at infinity).

Recall from Section 3.8 that clocks run at different rates according to the gravitational fields within which they reside. Therefore, neither the angular velocity of the star $\Omega = d\phi/dt$ nor the angular velocities of the local frame $\omega(r)$ at r, as measured by a distant observer who is at rest in the asymptotic Lorentz frame, are the same as those measured by a local observer. Since clocks run more slowly on the surface or within a star than at infinity, an observer in a local inertial frame within the star at r would measure angular velocities larger than those measured by a distant observer by the factor $e^{-\nu(r,\theta)}$, the gravitational time dilation (3.57).

6.3 Interior Solution for the Dragging Frequency

The structure of a rotating star depends in a complicated way on its frequency because of the rotation of the local inertial frames. The centrifugal force acting on a fluid element of the star must depend not on Ω (as would be the case in Newtonian physics), but rather on the difference between the frequency Ω and the frequency $\omega(r)$ of the local inertial frame at the location of the fluid element:

$$\overline{\omega}(r) \equiv \Omega - \omega(r) . \tag{6.13}$$

The relative angular velocity is of prime interest. But it is difficult to obtain the equation that governs its behavior inside the star. Even for a spherically symmetric static star, a great deal of algebra is required to obtain the equations of stellar structure. Hartle [330] has obtained the relevant equation from the Einstein equation

$$G_\phi^{\ t} = 8\pi T_\phi^{\ t} \tag{6.14}$$

and we quote his result:

$$\frac{1}{r^4}\frac{d}{dr}\left(r^4 j\frac{d\overline{\omega}}{dr}\right)+\frac{4}{r}\frac{dj}{dr}\overline{\omega}=0\,. \tag{6.15}$$

Observe that $\overline{\omega}$ depends only on r to lowest order in Ω, as noted previously.

The quantity $j(r)$ used above is defined in terms of the metric for a Schwarzschild star,

$$\begin{aligned} j(r) &\equiv e^{-(\nu+\lambda)}=e^{-\nu}\sqrt{1-2M(r)/r}\,, \qquad r<R\,,\\ j(r) &\equiv 1\,, \qquad r\geq R\,. \end{aligned} \tag{6.16}$$

After some algebra and use of (2.225), we obtain

$$\frac{dj}{dr}=-4\pi r(p+\epsilon)e^{-\nu}/\sqrt{1-2M(r)/r}\,. \tag{6.17}$$

From (6.15) integrated in the interval $(0, R)$, we have

$$\left(r^4\frac{d\overline{\omega}}{dr}\right)_R=\int_0^R 4r^3\frac{dj}{dr}\overline{\omega}\,dr\,. \tag{6.18}$$

Hence, according to (6.10), the angular momentum is

$$J=-\frac{2}{3}\int_0^R dr\,r^3\frac{dj}{dr}\overline{\omega}\,, \tag{6.19}$$

where the proportionality constant has been set to 2/3 (the choice will become immediately clear from a comparison with the classical expression). From the above results we can find

$$J=\frac{8\pi}{3}\int_0^R dr\,r^4\frac{\epsilon(r)+p(r)}{\sqrt{1-2M(r)/r}}[\Omega-\omega(r)]e^{-\nu(r)}\,, \tag{6.20}$$

and from this expression we find the moment of inertia

$$I=J/\Omega \tag{6.21}$$

of a slowly rotating star. The expressions for J and I are referred to as "slowly rotating" approximations because (6.15) was obtained to lowest order in Ω, which means that the structure equations of the star are those of Oppenheimer–Volkoff for a spherically symmetric star. One would be justified in ignoring ω in this approximation. Notice the appearance of the factor $e^{-\nu}$ spoken of above that converts the difference of frequencies $\Omega-\omega(r)$, as it would be measured at infinity, to its value in a local inertial frame at r.

In Newtonian physics (valid if $2M/R << 1$) the dragging frequency does not exist. Because ϵ contains the rest mass of the particles in the star, it will be true that $p << \epsilon$. It can be seen that the above result then reduces to the classical value

$$I_{\text{classical}}=\frac{8\pi}{3}\int_0^R dr\,r^4\epsilon\,. \tag{6.22}$$

At the edge of the star and beyond, the fundamental equation (6.15) for $\overline{\omega}$ becomes simply

$$\frac{d}{dr}\left(r^4\frac{\overline{\omega}}{dr}\right) = 0\,, \qquad r \geq R\,, \tag{6.23}$$

which integrates to

$$\frac{d\overline{\omega}}{dr} = \frac{A}{r^4} \tag{6.24}$$

with A a constant. From the dimensional analysis above, A is proportional to the angular momentum J, namely, $A = 6J$. Next, integrate (6.24) to obtain

$$\Omega - \omega(r) \equiv \overline{\omega} = -\frac{A}{3r^3} + B\,, \qquad r \geq R\,. \tag{6.25}$$

Because ω vanishes far from the star, the constant B has the value $B = \Omega$. We can now write

$$\omega(r) = \frac{2J}{r^3} = \frac{2I}{r^3}\Omega\,, \qquad r \geq R\,. \tag{6.26}$$

The last equation together with the one for $\overline{\omega}(r)$ (6.15) provides a means of calculating the dragging angular velocity everywhere. The differential equation for $\overline{\omega}(r)$ can be integrated from $r = 0$ with an arbitrary choice of the central value $\overline{\omega}(0)$ and with vanishing slope. At the surface, the corresponding Ω and J are found by matching to the exterior solution:

$$J = \frac{1}{6}R^4\left(\frac{d\overline{\omega}}{dr}\right)_R\,, \qquad \Omega = \overline{\omega}(R) + \frac{2J}{R^3}\,. \tag{6.27}$$

It may be noticed from the linearity of the differential equation defining $\overline{\omega}(r)$ and the matching value at the surface of the star that $\overline{\omega}(r)/\Omega$ is a universal function for a given equation of state and value of the central density at the present level of approximation (namely, that a spherical star is set into rotation without any change in its structure). Therefore, we have

$$\omega(r)/\Omega = \omega'(r)/\Omega' \tag{6.28}$$

for a given member of a stellar sequence.

We show an example of the ratio of the frame-dragging frequency to the star frequency in Fig. 6.2. It is always less than unity and decreases monotonically with r. It reaches a value of ~ 0.6 at the star's center and has significant value throughout. Therefore, we can expect appreciable effects on the actual structure of a rotating star as Ω becomes larger, not merely because of the centrifugal flattening, but because it is taking place against the background of a radially dependent frame-dragging frequency. It is therefore of some interest to understand in greater detail the statement that the effects of the centrifugal force depend on the star's frequency relative to those of the local inertial frames. We take this up shortly.

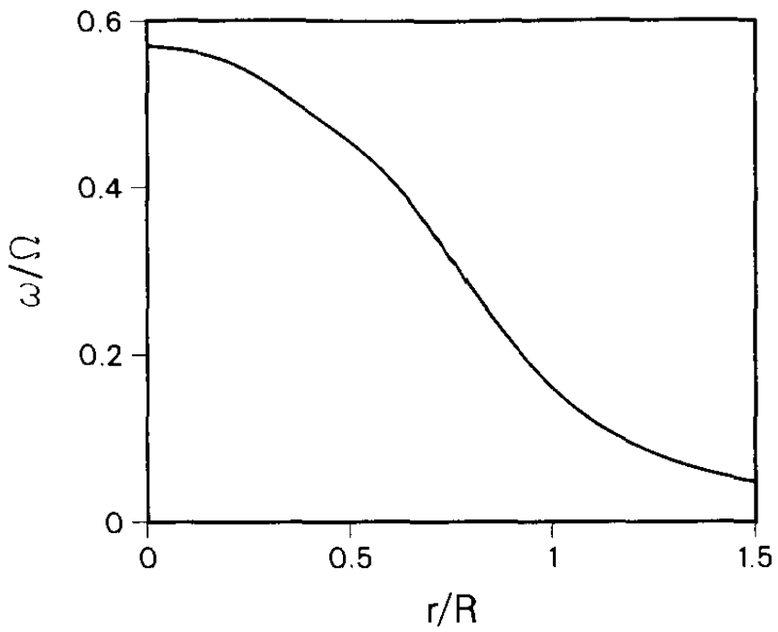

FIGURE 6.2. Ratio of frame-dragging angular velocity to the angular velocity of the star for the limiting-mass star of a typical equation of state (adapted from Ref. [340]).

6.4 Moment of Inertia of a Rotating Relativistic Star

An expression for the moment of inertia that appears frequently in the literature was derived above in (6.20). It is clear from the derivation that the result is for a nonrotating spherical static star, i.e., a Schwarzschild star (cf. (6.16)). However, the equilibrium shape of the star will not be spherical if it is rotating and the metric of spacetime will be altered from the Schwarzschild metric by the rotating mass. Because a pulsar looses angular momentum to radiation, its angular velocity continuously changes and the distribution of matter in the star will respond to changes in the centrifugal forces. Therefore the law that governs the rate of loss of rotational energy of the star (5.20), and the rate of change of the angular velocity (5.22), also depend on the response of the star to the changing centrifugal forces through the moment of inertia. The effect of changes in moment of inertia have been neglected in the literature on neutron stars until recently [197, 200, 266, 341, 342].

More than that, we will see in Section 11.4 that a phase transition in the nature of dense matter may slowly engulf the core of a millisecond pulsar as the central density increases above the critical phase transition density because of the relaxation of the centrifugal forces as the star spins down. The slow growth[4] of a region of new, more compressible phase will cause a concentration of mass in the center, changing the moment of inertia. As a result, a star in the course of the gradual growth of a region of new phase, a growth whose rate is controlled by the slow loss of angular momentum, may actually spin-up even though it is radiating angular momentum [200, 201].

For the above reasons, we are interested in the moment of inertia of a rotating star. If one were to compute numerically the solution of Einstein's equations for a rotating star, one could find the moment of inertia through the relation $I = J/\Omega$.

[4]Recall that the rate of change of pulsar period is very small.

However the equations are extremely complicated because so many components of the Riemann tensor are nonvanishing. The Hartle–Thorne perturbative solution [330, 331] is much easier to compute and is accurate to within a few percent [335]. In this section we will derive an expression for the moment of inertia that is expressed in terms of the metric of a rotating axially symmetric star in rigid rotation [197]. The qualification that the star is in rigid rotation is really not a restriction. It can be shown that uniform rotation is the configuration with least mass at given rotational frequency and baryon number [338, 339]. Our result is therefore general for stars in equilibrium, whether one solves the Einstein equations numerically without other approximation, or solves them in the perturbative approximation, which we discuss later.

The z-component of the moment of inertia (which for a star rotating about its z-axis is the moment of inertia) can be computed from [338].

$$J = I\Omega = \int dr\, d\theta\, d\phi\, \sqrt{-g}\, T_\phi{}^t \tag{6.29}$$

where the required component of the energy-momentum tensor of the stellar material is given by the general expression (2.201) by lowering the ϕ-component

$$T_\phi{}^t = (p + \epsilon) u_\phi u^t \,. \tag{6.30}$$

Recall that u^μ denotes the fluid four-velocity, where $u^t = dt/d\tau$, $u^r = dr/d\tau$, ...

From (6.2) we write out the metric tensor in full,

$$g_{\alpha\beta} = \begin{pmatrix} e^{2\nu} - \omega^2 r^2 \sin^2\theta\, e^{2\theta} & 0 & 0 & \omega r^2 \sin^2\theta\, e^{2\mu} \\ 0 & -e^{2\lambda} & 0 & 0 \\ 0 & 0 & -r^2 e^{2\mu} & 0 \\ \omega r^2 \sin^2\theta\, e^{2\mu} & 0 & 0 & -r^2 \sin^2\theta\, e^{2\mu} \end{pmatrix} . \tag{6.31}$$

The determinant of $g_{\alpha\beta}$ is

$$g = -r^4 \sin^2\theta\, e^{2\nu} e^{2\lambda} e^{4\mu} \,. \tag{6.32}$$

Throughout this section, the metric functions λ, ν, μ are those of an axial symmetric rotating star and depend on r and θ as well as on Ω and $\omega(r)$.

We need the fluid four-velocity to compute the energy-momentum tensor. For rigid rotation, two of the four-velocities of a fluid element vanish $u^r = u^\theta = 0$, and one of the nonzero components is given by

$$u^\phi = \frac{d\phi}{dt}\frac{dt}{d\tau} = \Omega u^t \,, \tag{6.33}$$

where Ω is the rotational angular velocity of the star. The nonvanishing components of the four-velocity are related by the invariant interval (6.2). Inserting (6.33) gives

$$1 = \left[e^{2\nu} - r^2 \sin^2\theta\, (\Omega - \omega)^2 e^{2\mu}\right](u^t)^2 \,, \tag{6.34}$$

which yields

$$u^t = \frac{e^{-\nu}}{\left[1 - e^{2(\mu-\nu)}(\Omega - \omega)^2 r^2 \sin^2\theta\right]^{1/2}} . \tag{6.35}$$

We lower indices to obtain the covariant component of u^ϕ

$$u_\phi = g_{\phi t} u^t + g_{\phi\phi} u^\phi = -(\Omega - \omega) r^2 \sin^2\theta \, e^{2\mu} u^t . \tag{6.36}$$

Thus we obtain,

$$T_\phi{}^t = -\frac{(p+\epsilon)(\Omega - \omega) r^2 \sin^2\theta \, e^{2\mu}}{e^{2\nu} - r^2(\Omega - \omega)^2 e^{2\mu}} . \tag{6.37}$$

For the angular momentum and moment of inertia we find,

$$J = I\Omega = -\int dr \, d\theta \, d\phi \frac{(p+\epsilon)(\Omega - \omega) r^4 \sin^3\theta \, e^{\nu+\lambda+2\mu}}{e^{2(\nu-\mu)} - r^2 \sin^2\theta \, (\Omega - \omega)^2} . \tag{6.38}$$

Taking account of the factor $e^{2\nu}$ in the denominator we see that $(\Omega - \omega)$ is corrected by the time dilation factor $e^{-\nu}$. This expression for the moment of inertia of a rotating star, obtained first in Ref. [197], reduces to that of the nonrotating star in the limit.

6.5 Kepler Angular Velocity in General Relativity

The condition for the balance of centrifugal and gravitational forces can be written in Newtonian gravity as

$$\frac{Mm}{R^2} = m\Omega^2 R . \tag{6.39}$$

The condition that a particle be in a stable circular orbit at the equator of a star (itself rotating or not) is found immediately. The particle has angular velocity

$$\Omega_c = \sqrt{\frac{M}{R^3}} \quad \text{(Newton)} , \tag{6.40}$$

where the subscript c denotes the classical balance of the two forces. Fluid elements at the equator of the star are dislodged at higher angular velocity. The Kepler angular velocity, which we refer to more briefly as the Kepler frequency, is an absolute limit for the rotation of a star.

A star may be subject to other instabilities at lower frequencies that prevent it from reaching rotational frequencies as high as the Kepler frequency. These are the gravitational wave instabilities that we take up later. Only such other instabilities that occur below the Kepler frequency are of physical interest because the instability that occurs at the lowest frequency sets the limit.

The Newtonian expression (6.40) also holds for a body in stable orbit around the equator of a *nonrotating* star in General Relativity. This is not immediately evident, but we show it is true later. What is intuitively evident is that the expression

for the Kepler frequency in the General Theory of Relativity for a rotating star must be more complicated than the above expression. First of all, we expect that a rotating star will become flattened to some degree, and the metric of spacetime is determined by, and in turn determines, the configuration of mass–energy. Accordingly, the metric must in some way be involved. Moreover as we have just seen, the centrifugal force depends on the star's frequency relative to the frequency of the local inertial frames. Hence $\omega(R)$ must enter the expression also.

We now study how the Kepler angular velocity can be found in General Relativity. First, let us repeat that we are interested in stars in uniform rotation and otherwise static. They are therefore describable in a static axisymmetric spacetime for which the metric functions are independent of t and and azimuthal angle, ϕ, as in (6.2). For a particle at the equator of the star $r = R$, $dr = d\theta = 0$, $\theta = \pi/2$. From (6.35), the time component of the four-velocity of a point fixed at the star's equator is given by

$$\frac{dt}{d\tau} = \frac{e^{-\nu}}{\sqrt{1 - V^2}}. \tag{6.41}$$

Here

$$V \equiv e^{\mu-\nu} R \left(\Omega - \omega(R)\right) \tag{6.42}$$

denotes the orbital velocity[5] of a point at the equator relative to an observer with zero angular velocity in the ϕ direction. All functions of position in this section are to be evaluated at the equator. If one wanted to know V, its value can be calculated from this expression if the star is rotating at less than the Kepler frequency. What we want to know however, is how to determine the Kepler frequency.

We can rearrange (6.42) to express the star's rotational angular velocity in terms of V, the metric functions, and the frame-dragging angular velocity. Consider the star at its Kepler angular velocity; we find at the equator

$$\Omega_K = e^{\nu-\mu}\, V/R + \omega(R) \tag{6.43}$$

in which V is as yet unknown because it is needed at $\Omega = \Omega_K$. Consequently in General Relativity, (6.43) does not provide a formula for the Kepler angular velocity. Rather, it is a *self-consistency* condition that must be obeyed by Ω_K. This is so because the metric functions, the frame-dragging angular velocity $\omega(R)$ that appear on the right side of (6.43) and the entire distribution of mass–energy of the star depend themselves on the star's rotational angular velocity Ω. Therefore, we need an expression for V in terms of the metric and frame dragging angular velocity so that it can be eliminated and thus complete the above self-consistency condition on Ω_K.

Think of a particle moving at the Kepler frequency in a circular orbit at the equator of the rotating axisymmetric star. As we have learned, geodesic paths are obtainable as the extremum of the proper time. However, in this case it is simpler

[5]Recall that V is dimensionless because we use units $c = 1$ so that V is velocity relative to c.

to do the variation directly, rather than compute the relevant Christoffel symbols in the geodesic equation. Note that we seek a particle velocity on a circular orbit $r = R$ and $\theta = \pi/2$, so that the line element can be written,

$$d\tau^2 = \left[e^{2\nu(R,\pi/2)} - e^{2\mu(R,\pi/2)}R^2\{\Omega - \omega(R)\}^2\right]dt^2 , \tag{6.44}$$

We seek the extremal of

$$d\tau = \int_{t_1}^{t_2} \sqrt{e^{2\nu} - r^2 e^{2\mu}(\Omega - \omega)^2}\, dt , \tag{6.45}$$

where the variation vanishes at the end points $\delta r(t_1) = \delta r(t_2) = 0$. After some algebra, we obtain

$$\left(\mu' + \frac{1}{R}\right) V^2 - \omega' e^{(\mu-\nu)} R V - \nu' = 0 . \tag{6.46}$$

This equation constitutes a quadratic equation in the equatorial velocity V. The solutions are

$$V_\pm = \frac{R\omega'}{2\,\psi'} e^{(\mu-\nu)} \pm \sqrt{\frac{\nu'}{\psi'} + \left(\frac{R\omega'}{2\,\psi'} e^{(\mu-\nu)}\right)^2} , \tag{6.47}$$

where for convenience we have defined

$$\psi' \equiv \mu' + 1/R . \tag{6.48}$$

The solution V_+ corresponds to co-rotation which is the desired solution in connection with the stability of a star to mass-shedding. The other solution corresponds to a counter-rotating particle at its Kepler frequency. In General Relativity the Kepler frequency of a particle circulating at the equator of a rotating star depends on whether it is co-rotating or counter-rotating.

To obtain the solution of the Einstein equations for a star with given central density and rotating at the Kepler frequency, equation (6.43), with the velocity given by V_+, must be solved simultaneously with the stellar structure equations by means of an iteration procedure [106, 107]. However, the structure equations are different from the simple ones describing a Schwarzschild star. They were first written as a perturbative solution to Einstein's equations by Hartle [330, 331]. The self-consistency condition (6.43) for the Kepler frequency was not noted or used in early applications of the Hartle–Thorne method until the work of Ref. [107]. Until the self-consistency condition was recognized, the Kepler frequency was not known—it was approximated by the Newtonian value.

6.6 Effect of Frame Dragging on Kepler Frequency

We learned above that the effect of rotation on a fluid element of a star depends not on the star's angular velocity Ω but on the angular velocity relative to that of the local inertial frames $\omega(r)$ [330, 331]. The literal implication of this quarter-century-old true statement is that the dragging of the local inertial frames reduces

the effects of the centrifugal force at the observed frequency Ω because $\omega(r)$ is in the same sense as Ω. From our classical understanding, that in turn implies that the frequency at which centrifugal disruption of a star occurs is larger than the Kepler frequency of a particle in a stable circular orbit of the same radius around a nonrotating star of the same mass. We now show the opposite is true [266].

It has been found by comparing actual numerical solutions of Einstein's equations that the Kepler frequency of a rotating relativistic star is less than the classical value (6.40) rather than larger as intuitively expected. The empirical formula is of the form of (6.40), but reduced by a factor of about 0.65, and is accurate to better than 10% [95, 96]. The empirical formula is very useful, for it allows one to deduce an approximate value of the Kepler frequency from the radius and mass of a nonrotating star. The latter are easily obtained from a solution to the Oppenheimer–Volkoff equations, whereas the general relativistic solution for a rotating star is more involved and computationally intensive. For this reason the empirical formula has been employed in a large number of papers as well as in this book (see 5.9).

From the self-consistent condition on the relativistic Kepler frequency, we can obtain a form similar to the empirical one with a reduction factor, thus showing, in part, its origin. We are thus able to demonstrate analytically that centrifugal effects in strong fields are sometimes counter-intuitive and in the process justify the empirical formula [266]. We will make a start on this proof here, where we can get an idea of the results and procedure without the apparatus needed for the full solution of a rotating star.

We obtain our first estimate of the solution of (6.47) by approximating the metric of the rotating star by the Schwarzschild metric. Thus, at the equator, we have

$$\psi' \approx 1/R\,. \tag{6.49}$$

and

$$e^{2\nu(R,\theta)} \approx e^{2\nu(R)} = 1 - \frac{2M}{R}\,. \tag{6.50}$$

Using these approximations and (6.26) in (6.43) and (6.47), we are actually able to solve for the Kepler frequency. As an intermediate step in the algebra, we find

$$\Omega_K^2 + \omega(R)\Omega_K - 2\omega^2(R) = M/R^3\,. \tag{6.51}$$

Hence,

$$\Omega_K \approx \left[1 + \frac{\omega(R)}{\Omega_K} - 2\left(\frac{\omega(R)}{\Omega_K}\right)^2\right]^{-1/2} \sqrt{\frac{M}{R^3}}\,. \tag{6.52}$$

The ratio of frequencies is equal to the constant $\omega(R)/\Omega_K = 2I/R^3$. Thus we have obtained the form of the Newtonian answer with a prefactor that depends on the relative dragging frequency at the equator of the star. It is less than unity if $\omega(R)/\Omega_K < 1/2$. In Fig. 6.2 we saw that this is so. Nevertheless, it is the lowest-order approximation and can be improved upon after development of

more apparatus. Better approximations turn out to strengthen the conclusion—the prefactor is always less than unity [266].

6.7 Approximation to the Kepler Frequency

We have learned that the Kepler frequency of a rotating star in General Relativity cannot be found from a formula as in Newtonian gravity. Rather, it is obtained as a self-consistency condition in the solution of Einsteins' equations for a rotating star. However, a simple approximate formula has been found which involves a prefactor times the Newtonian expression (6.40) for the balance of the centrifugal and gravitational forces at the equator. We saw that just such a form emerged from the analysis in the preceding section. Empirical values of the prefactor have been obtained by several authors by comparison with actual solutions of the Einstein equations for a number of model stars [95, 96]. The results are expressed as

$$\Omega_K \approx \xi' \left(\frac{M/M_\odot}{(R/10\ \mathrm{km})^3} \right)^{1/2}$$

where $\xi' = 0.72 \times 10^4\ \mathrm{s}^{-1}$ as found in the first reference, and 0.72 replaced by 0.77 in the second reference. We adopt an average, and take the power of 10 out of the above expression to arrive at

$$\Omega_K \approx 24 \left(\frac{M/M_\odot}{(R/\mathrm{km})^3} \right)^{1/2} \times 10^4\ \mathrm{s}^{-1}\,. \tag{6.53}$$

We prefer to express this in gravitational units,

$$\Omega_K \approx .65 \left(\frac{M}{R^3} \right)^{1/2}. \tag{6.54}$$

We use this approximation frequently as a general guide.

6.8 Hartle–Thorne Perturbative Solution

The problem of stellar structure for static isotropic stars is solved in the manner of Oppenheimer–Volkoff, a solution we derived in detail. The expression for the proper time was diagonal. We also learned that, for a given equation of state, a one-parameter sequence of solutions exists that are usually characterized by differing central densities.

The situation is different for rotating stars. We shall be interested in static[6] solutions that correspond, however, to a rotating star. In this case there are two off-diagonal metric components, so there is an additional coupled equation. Moreover, an altogether new element has entered—the dragging of the local inertial frames.

[6]Static rotating stars are ones that are static in a co-rotating frame.

Hence, in contrast to the situation for Schwarzschild stars, there is a continuum of solutions for given central densities corresponding to different rotational angular velocities.

The first rotating stellar models were obtained as a perturbative expansion in deviations from a spherical star [330, 331]. However, Hartle and Thorne and succeeding authors who employed their method failed to impose the self-consistency condition discussed above and were not able to determine precisely the all-important Kepler frequency. The method is referred to as the "slow rotation" method. However, the precise meaning of "slow" (the frequency up to which the method is accurate) was not clarified until our recent research [107, 196, 334].

By comparison with direct integration of Einstein's equations for rotating stars, the perturbative method was found to be fairly accurate to periods of about $\frac{1}{2}$ millisecond. This is three times shorter than the presently fastest known pulsar. It is therefore a good approximation when augmented by the self-consistency condition. Highly accurate numerical methods have been developed and can be studied elsewhere. (See Ref. [335, 343] and citations therein.) We pursue the perturbative approach since it will provide a means of improving the analysis of the effect of frame dragging on the Kepler frequency. An elegant formulation of the method can also be found in Ref. [342].

The perturbation expansion of the metric about spherical symmetry has the form

$$e^{2\lambda(r,\theta)} = e^{2\lambda}\left[1 + 2\,\frac{m_0 + m_2 P_2(\cos\theta)}{r - 2M(r)}\right], \tag{6.55}$$

$$e^{2\nu(r,\theta)} = e^{2\nu}\left[1 + 2\big(h_0 + h_2 P_2(\cos\theta)\big)\right], \tag{6.56}$$

$$e^{2\mu(r,\theta)} = 1 + 2(v_2 - h_2)P_2(\cos\theta), \tag{6.57}$$

where m_0, m_2, h_0, h_2, and v_2 are functions of r and Ω and obey the equations derived by Hartle and Thorne [330, 331]. The function $P_2(\cos\theta)$ is a Legendre function. The first term in each case is simply the Schwarzschild metric. The term with a subscript "0" is the monopole correction, and the term with subscript "2" the quadrupole correction (except for $e^{2\mu(r,\theta)}$, where a transformation of the r coordinate that leaves the general form of the line element unaltered has been used to eliminate the monopole correction to this element) [330]. The perturbation functions need to be solved iteratively in connection with the self-consistency conditions (6.43, 6.47) to find the Kepler frequency. For any frequency below Kepler, the self-consistency conditions are, of course, irrelevant.

Although we will not rewrite the basic equations derived by Hartle for the perturbation functions, it is relevant to our purpose here to note the exterior behavior of the monopole correction to the metric. It is given by

$$e^{2\nu}h_0(r) = -\frac{\Delta M}{r} + \frac{J^2}{r^4}, \qquad r > R. \tag{6.58}$$

Here ΔM is the mass–energy increase of the rotating star, and J is its angular momentum, as defined in terms of the Schwarzschild metric (6.20). Equation (6.50)

now assumes the form

$$e^{2\nu(R,\theta)} \approx 1 - \frac{2M}{R} + \frac{2J^2}{R^4} \tag{6.59}$$

while at the monopole level of correction, $\psi(R,\theta)$ is unchanged from the previous approximation (6.49). Using these approximations to the metric in the self-consistency condition for the Kepler angular velocity in General Relativity, we obtain

$$\Omega_K^2 + \omega(R)\Omega_K - \omega^2(R) = M/R^3 , \tag{6.60}$$

the solution of which is

$$\Omega_K \approx \left[1 + \frac{\omega(R)}{\Omega_K} - \left(\frac{\omega(R)}{\Omega_K}\right)^2\right]^{-1/2} \sqrt{\frac{M}{R^3}} , \tag{6.61}$$

where again, $\omega(R)/\Omega_K = 2I/R^3 =$ constant for a given member of the sequence, (6.28). Here M refers to the mass of the rotating star. The prefactor of this equation is always less than unity because $\omega(r) < \Omega$. Corrections through quadrupole confirm this conclusion. It is at the quadrupole level that a weak dependence on the equation of state enters [266]. This would account for the weak dependence of the empirical formula on the stellar model. Other details, including the effect of mass increase due to rotation and centrifugal flattening, can be found in Ref. [107].

6.8.1 *Comparison of Perturbative and Numerical Solutions*

We have mentioned above that two possibilities exist for computing rotating equilibrium stellar models in General Relativity—the method of Hartle and Thorne, which provides an approximate solution of Einstein's equations up to and including quadrupole changes in the stellar configuration, and the numerical solution of Einstein's equations. We compare stellar properties for two equations of state calculated in the two ways in Table 6.1 and find agreement to better than 10%. The central frame-dragging angular velocity is denoted by ω_c and the ratio of rotational energy to gravitational energy by T/W. The equatorial velocity is denoted by $V_{\rm eq}$. The two equations of state used for the comparison and designated by "12" and "14" are specified in more detail in Table 6.2.

6.9 Imprint of Angular Momentum

We will not discuss rotating black holes but can mention that since

$$g_{t\phi} \approx \frac{2J}{r} \sin^2\theta , \tag{6.62}$$

which follows from (6.3) in lowest order (i.e., taking $e^{\mu} = 1$), we see that the imprint of the angular momentum of a black hole will remain in the gravitational

TABLE 6.1. Comparison of the properties of rotating neutron stellar models calculated from Hartle's perturbative solution with those of the numerical solution of Einstein's equations [95, 106]. The description of the equation of state denoted by the number in the first column is explained in Table 6.2.

EOS	Method	$\frac{M_{rot}}{M_\odot}$	ϵ_c[a]	Ω_K	R_{eq} (km)	$\frac{\omega_c}{\Omega_K}$	$\frac{T}{W}$	$\frac{V_{eq}}{c}$	e
	Exact	0.77	0.63	0.542	15.1	0.27	0.10	0.27	0.72
	Hartle	0.77	0.66	0.570	13.7	0.23	0.08	0.26	0.71
12	Exact	1.30	0.92	0.705	14.9	0.43	0.12	0.35	0.77
	Hartle	1.30	0.98	0.780	13.1	0.40	0.09	0.39	0.71
	Exact	0.78	0.51	0.410	18.1	0.25	0.07	0.25	0.71
	Hartle	0.78	0.47	0.406	17.5	0.21	0.07	0.25	0.70
14	Exact	1.29	0.77	0.570	16.9	0.40	0.09	0.38	0.74
	Hartle	1.29	0.75	0.606	15.6	0.34	0.08	0.35	0.70

[a] ϵ_c is measured in 10^{15} g/cm^3, Ω_K in 10^4 s^{-1}. The stellar eccentricity (defined in the text on page 297) is denoted by e while V_{eq} denotes the equatorial velocity.

field outside the horizon. Like its mass, its angular momentum is a property that can be measured from outside. Its electrical charge is also imprinted on the exterior metric, though we do not prove that here. It may be remarked that stars are neutral, in general, for the reason explained elsewhere.

6.10 Rotating Stars with Realistic Equations of State

In this section we review some results for a collection of equations of state, most of which are modern [107]. The references and ingredients of the equations of state are listed in Table 6.2, while the corresponding properties of ordinary symmetric nuclear matter of the various models are provided in Table 6.3. There are two groups—relativistic and nonrelativistic.

Members of the first group are derived from *relativistically* covariant theories and are causal at all densities. The dense matter described in all of these models is in general beta equilibrium, and the composition includes nucleons, hyperons, and leptons, and, in several cases, a phase transition to quark matter at higher density. Some are calculated in the relativistic mean-field theory (also known as the relativistic Hartree approximation) [68, 130] studied in Chapter 5 or in the relativistic Hartree–Fock approximation [130]. Others contain the influence of "dynamical" (Brueckner-type) two-particle correlations that are connected with a two-body meson-exchange potential. These correlations are incorporated in the ladder (Λ) approximation [345] of the scattering T-matrix of two baryons in matter. The Bonn [346] and HEA [347] meson-exchange potentials are used as an input. The latter approximation is similar to the well-known relativistic Brueckner–Hartree–Fock method (see, for example, Refs. [120, 289, 290, 348]). The essential difference between the Λ and the above mentioned Hartree–Fock approximation

TABLE 6.2. Nuclear equations of state used for the construction of models of general relativistic rotating neutron stars [107]

Label	EOS	Description[a]	Reference
	Relativistic field-theoretical equations of state		
1	G_{300}	H, K=300	[129]
2	HV	H, K=285	[68, 130]
3	G^{DCM2}_{B180}	Q, K=265, $B^{1/4}$ = 180	[132, 195]
4	G^{DCM2}_{265}	H, K=265	[193]
5	G^{π}_{300}	H, π, K=300	[129]
6	G^{π}_{200}	H, π, K=200	[145]
7	Λ^{00}_{Bonn} + HV	H, K=186	[196]
8	G^{DCM1}_{225}	H, K=225	[193]
9	G^{DCM1}_{B180}	Q, K=225, $B^{1/4}$ = 180	[132, 195]
10	HFV	H, Δ, K=376	[130]
11	Λ^{00}_{HEA} + HFV	H, Δ, K=115	[196]
	Nonrelativistic potential model equations of state		
12	BJ(I)	H, Δ	[189]
13	WFF(UV_{14}+TNI)	NP, K=261	[158]
14	FP(V_{14}+TNI)	N, K=240	[344]
15	WFF(UV_{14}+UVII)	NP, K=202	[158]
16	WFF(AV_{14}+UVII)	NP, K=209	[158]
17	Pan(C)	H, Δ, K=60	[188]

[a] The following abbreviations are used: N = pure neutron matter, NP = neutrons, protons, and leptons in equilibrium concentrations, π = pion condensation, H = hyperons, neutrons, protons, and leptons, Δ = Δ_{1232} resonance is populated, Q = quark-hadronic hybrid star, K = compression modulus in MeV, $B^{1/4}$ = quark model bag constant in MeV.

consists in the neglect of dynamical correlations in the latter case. More detail can be found in Ref. [107, 349].

The members of the second group are based on *nonrelativistic* theories and become acausal at some density within the limiting-mass star (except one of them). The density at which the equations of state become acausal is shown in the last column of Table 6.3. Several of the latter group are from publications that list no saturation properties of nuclear matter, like that of Bethe and Johnson and of Pandharipande. The latter author gives the compression modulus, and it is extraordinarily small—less than a third of what is believed to be the lower bound on empirically acceptable values (K = 200 – 300 MeV). They are included more for historical interest.

As suggested by the "description" column of Table 6.2, the equations of state are taken from a rather broad selection of theories that incorporate various effects, such as hyperon populations, pion condensation, and quark cores. Illustrations of these equations of state can be found in Ref. [340].

TABLE 6.3. Nuclear matter properties of the equations of state of Table 6.2 [107]

Label	B/A (MeV)	ϱ_0 (fm^{-3})	K (MeV)	m^*/m	a_{sym} (MeV)	ϵ/ϵ_0 [a]
1	−16.3	0.153	300	0.78	32.5	–
2	−15.98	0.145	285	0.77	36.8	–
3	−16.0	0.16	265	0.796	32.5	–
4	−16.0	0.16	265	0.796	32.5	–
5	−16.3	0.153	300	0.78	32.5	–
6	−15.95	0.145	200	0.8	36.8	–
7	−11.9	0.134	186	0.79		–
8	−16.0	0.16	225	0.796	32.5	–
9	−16.0	0.16	225	0.796	32.5	–
10	−15.54	0.159	376	0.62	30	–
11	−8.7	0.132	115	0.82		–
12						23.1
13	−16.6	0.157	261	0.65	30.8	–
14	−16.00	0.159	240	0.64		5.6
15	−11.5	0.175	202	0.79	29.3	6.5
16	−12.4	0.194	209	0.66	27.6	7.2
17			60		35	23.6

[a] Energy density are units of normal nuclear matter density beyond which the velocity of sound in neutron matter becomes larger (superluminal) than the velocity of light. The symbol "–" indicates that causality is not violated.

6.11 Effect of Rotation on Stellar Structure

A number of comparisons have been made in the literature between various properties of the limiting mass stars of nonrotating sequences with those at the limiting mass of rotating sequences (i.e. stars at the Kepler frequency). However, the star at the limit of rotating and nonrotating sequences have different mass and baryon number, and do not in any sense correspond to the same star. While it is interesting to see the increase in limiting mass that rotation is responsible for, for most purposes it is more interesting to compare the properties of a star of fixed baryon number A at different angular velocities. We make the comparison for a star that has $M = 1.4M_\odot$ at zero rotation, and then compare the central density and the moment of inertia of the stars with the same A at various frequencies of rotation. What we find, as shown in Figs. 6.4 and 6.5, is that the change is most pronounced as the star closely approaches its Kepler frequency.

Tables 6.4 and 6.5 can be used to assess the effect of rotation on the masses, radii, and central densities of limiting-mass stars that are rotating at their Kepler frequencies. In particular, masses increase due to rotation typically by 10%, equatorial radii increase typically by 1.5–2 km and central densities decrease by about 20%. Moments of inertia increase by 15–20%. It is noteworthy that, at the Kepler frequency, the velocity at the equator is about $0.5c$. Eccentricities $e = \sqrt{1 - (R_p/R_{eq})^2}$ are

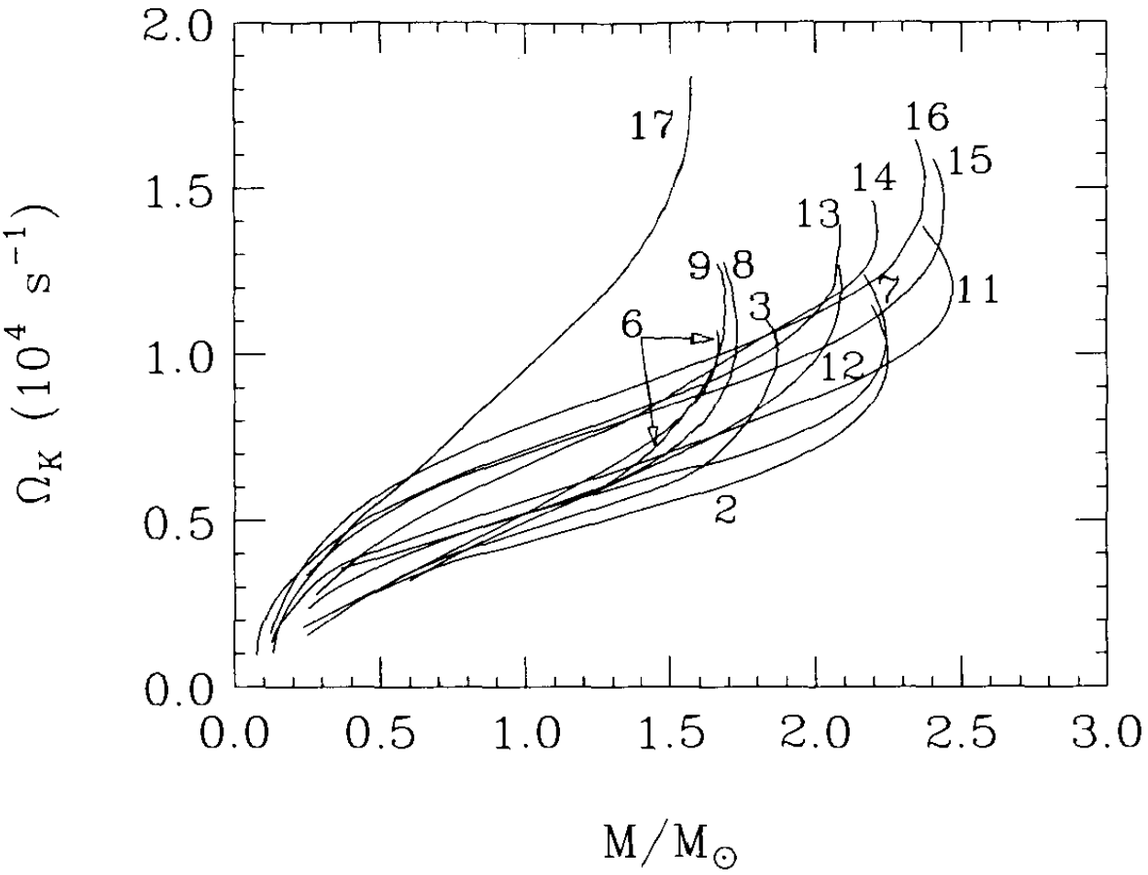

FIGURE 6.3. Kepler angular velocities as a function of the mass of the rotating star are shown for star sequences of a number of the equations of state [107].

rather uniform for all models at about 0.7. The frame-dragging angular velocity ω is an appreciable fraction of the Kepler angular velocity. It is 0.6–0.8 at the center and falls to a value 0.2–0.3 at the star's equator.

The Kepler angular velocities themselves vary appreciably between models; there is about a 50% difference between the slowest and fastest, not counting case 17, for which the compression modulus is unrealistically low. The corresponding range in period is 0.42 to 0.68 ms. For the entire sequence of stars in most of the models studied, the Kepler frequency is shown in Fig. 6.3.

6.12 Gravitational-Wave Instabilities

We have discussed an absolute limit on rotation—the Kepler frequency—the frequency at which the centrifugal force would overcome gravity at a star's equator. There are additional instabilities by which rotation may be limited if they occur at frequencies lower than the Kepler frequency. These instabilities create and are created by gravitational radiation moderated by the viscosity of the stellar material which tends to damp them.

In hot stars certain of these instabilities probably occur below the Kepler frequency in which case they establish the rotation limit. The fact that the viscosity of the star depends on its temperature (being smallest in the hottest, and therefore youngest, newly born stars) suggests that gravitational-wave instabilities probably

TABLE 6.4. Calculated properties of rotating limiting-mass neutron star models [107]

Label	$\Omega_K{}^b$	$\frac{M_{rot}}{M_\odot}$	R_{eq} (km)	$\frac{\epsilon_c}{\epsilon_0{}^a}$	I^c	$\frac{V_{eq}}{c}$	e	$\frac{\omega_c}{\Omega_K{}^b}$	$\frac{\omega_{surf}}{\Omega_K{}^b}$
1	0.93	2.04	13.60	7.16	1.89	0.50	0.70	0.58	0.17
2	0.99	2.25	13.43	7.83	2.15	0.54	0.69	0.67	0.20
3	1.01	1.87	12.42	9.43	1.33	0.51	0.69	0.61	0.16
4	1.01	1.72	12.17	10.3	1.16	0.49	0.69	0.60	0.15
5	1.02	2.06	12.87	8.67	1.81	0.54	0.69	0.64	0.19
6	1.03	1.67	11.91	10.8	1.07	0.48	0.69	0.60	0.15
7	1.04	2.24	12.97	7.96	2.12	0.55	0.69	0.67	0.22
8	1.06	1.73	11.91	10.6	1.16	0.50	0.69	0.61	0.16
9	1.13	1.69	11.31	12.1	1.02	0.51	0.68	0.64	0.17
10	1.16	2.47	12.34	7.12	2.45	0.60	0.69	0.76	0.28
11	1.18	2.47	12.24	7.66	2.44	0.61	0.68	0.76	0.29
12	1.12	2.09	11.59	10.8	1.61	0.57	0.68	0.72	0.22
13	1.29	2.09	10.97	10.0	1.53	0.59	0.69	0.74	0.27
14	1.37	2.21	10.82	10.6	1.73	0.62	0.68	0.77	0.29
15	1.45	2.44	10.70	10.1	2.21	0.66	0.64	0.82	0.35
16	1.51	2.38	10.31	10.5	2.02	0.67	0.65	0.82	0.36
17	1.81	1.58	7.98	20.7	0.64	0.61	0.67	0.76	0.27

[a] The quantity ϵ_0=140 MeV/fm^3 (= $2.5\cdot10^{14}$ g/cm^3) denotes the density of normal nuclear matter, [b] Ω_K is in units of 10^4 s^{-1}, [c] I is in units of 10^{45} g-cm^2.

TABLE 6.5. Calculated properties of nonrotating, limiting-mass, neutron stellar models. The quantity ϵ_0 is defined in Table 6.4 [107]. Moment of inertia I_{45} has a power 10^{45} in the indicated units.

Label	$\frac{M_s}{M_\odot}$	R_s (km)	$\frac{\epsilon_c}{\epsilon_0}$	I_{45} (g cm^2)
1	1.792	11.12	9.37	1.76
2	1.976	11.34	9.29	2.04
3	1.605	10.48	11.36	1.29
4	1.510	10.14	11.99	1.10
5	1.808	10.97	9.57	1.73
6	1.458	10.12	12.10	1.05
7	1.969	10.97	9.29	2.02
8	1.525	9.84	12.79	1.08
9	1.494	9.48	13.93	0.99
10	2.198	10.70	9.64	2.40
11	2.195	10.63	9.64	2.37
12	1.843	9.77	12.50	1.55
13	1.848	9.24	12.79	1.50
14	1.971	9.29	12.16	1.68
15	2.197	9.56	11.54	2.17
16	2.135	9.17	12.50	1.98
17	1.412	6.90	24.07	0.62

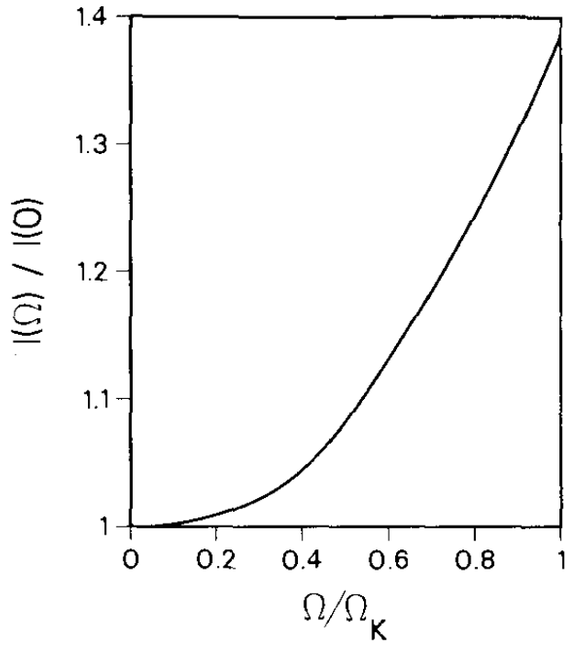

FIGURE 6.4. For fixed baryon number A of the star, the moment of inertia is shown as a function of rotational frequency. (Calculation kindly provided by F. Weber.)

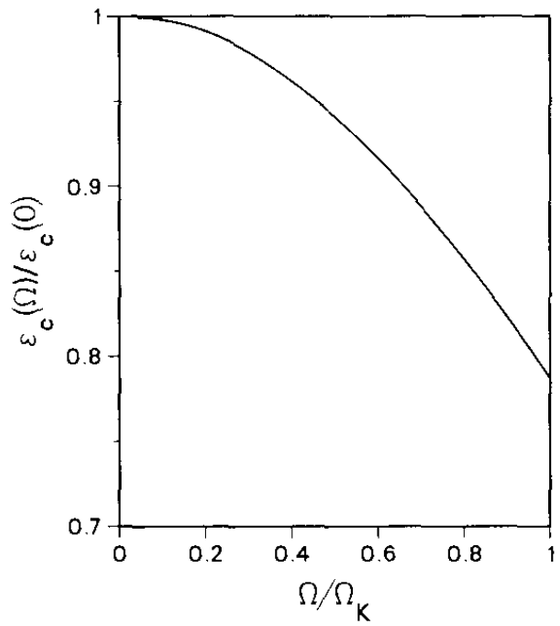

FIGURE 6.5. Comparison of central densities of stars with fixed baryon number A as a function of rotational frequency. (Calculation kindly provided by F. Weber.)

lead to the rapid spin-down of any neutron star born with high frequency near the Kepler frequency.

On the other hand, as we discussed in greater detail elsewhere, it is believed that another population of very fast millisecond pulsars are very old neutron stars that have been spun up by accretion from a companion. Being old, they are cold, say 10^5 K. These old stars are heated by accretion, to perhaps 10^6 K, but not likely anywhere near the temperature of newly born neutron stars of 10^{10} K. From this evolutionary perspective, it is important to have an acquaintance with gravitational-wave, radiation-reaction instabilities as moderated by viscosity.

Like most objects, a neutron star has normal modes of vibration. In realistic nonrotating stars, viscosity damps all vibrations. However, in rotating stars, there are modes that are always unstable in inviscid stars and unstable in viscous stars above certain rotation frequencies.

The cause of instability in viscous stars above a critical frequency is the following. A vibration on a rotating star constitutes an aspherical flow of matter; it produces gravitational radiation. The vibration is unstable if the energy and angular momentum carried off in gravitational waves cause the mode to grow in amplitude. The rotation of the star is thereby damped by gravitational radiation. However, stars do rotate, which tells us the obvious: viscosity damps all rotational instabilities below some frequency of rotation.

We touch only briefly on the subject in this chapter with emphasis on the physical ideas. The topic is too complex to treat in detail here and has a comparatively long history which the interested reader can trace through our more recent references. Some of the pioneering work on the subject can be found in Refs. [350]–[355].

To understand the nature of the gravitational-radiation instability, let a neutron star rotate with angular velocity Ω, and consider a small perturbation with time and angular dependence $e^{i(m\phi-\omega t)}$. Let the perturbation propagate in the direction *opposite* to that in which the star itself rotates. The angular velocity of the *pattern* of constant phase is ω/m. The aspherical transport of matter will disturb the spacetime continuum in the vicinity of the star's surface. The disturbance propagates as gravitational radiation at the speed of light.

First, consider slow rotation of the star. The direction of rotation of the aspherical flow caused by the perturbation will cause the resultant gravitational radiation to carry off angular momentum of sign opposite to that of the star. Because the only source for the sign of this angular momentum is the perturbation itself, the gravitational radiation will damp the perturbation.

However, if the star rotates with sufficiently high angular velocity, the perturbation pattern will be dragged forward in the direction of the star's rotation. In this case the gravitational radiation will have angular momentum of the same sign as that of the star. The amplitude of the perturbation must grow in response because the perturbation is the source of the disturbance of the spacetime continuum and *its* angular momentum has sign opposite to that being carried off by gravity waves.

Therefore any disturbance on the star's surface, in the absence of viscosity, is unstable and will grow if it propagates relative to a co-rotating frame in the opposite sense to the star's rotation but, relative to an inertial frame is rotating in the same sense as the star. Viscosity will tend to counteract the growth of the instability. Therefore there must exist a critical angular velocity above which the perturbation will grow, and below which it will be damped by viscosity. If the angular velocity of the star is above critical, the rate of radiation of angular momentum in gravity waves will rapidly slow the star until it reaches the critical angular velocity in a matter of seconds [353]. Thereafter it can rotate stably.

The above discussion pertains to the damping or initial growth of a small perturbation. It is not our goal to follow the temporal development of the perturbation, but rather to estimate the rotational frequencies Ω_m of stars for which various counter-rotating modes m become unstable. We seek to find the lowest such frequency. It is this frequency that places the upper limit on the angular velocity of the star (or lower limit on its period).

To be more precise, the modes that have turned out to be most important are the so-called $l = m$, f-modes. In the nonrotating limit, these reduce to the $l = m$ spherical harmonic indices, and the f refers to the zero-radial node disturbances. They are initially superficial surface waves with as many waves as the index $l = m$, and they rotate around the equator (see Fig. 6.6).

Here we attempt to outline the theory of gravitational wave instabilities without going into details. We would like to follow the initial evolution of the energy contained in a perturbation about equilibrium, such as discussed above. Schematically we can write the energy contained in the perturbation as

$$E(t) = \tfrac{1}{2}\sum_n \int \eta_n(\delta q_n \cdot \delta q_n^*)d^3r\,, \tag{6.63}$$

where δq_n denotes a displacement from equilibrium associated with shear or bulk stress of the star, or a radial perturbation of density that departs from an axially symmetric flow of matter and therefore couples to some multipole of the gravitational field. The notation is schematic. The label n denotes these various processes. In the case of shear stress, the product will denote a contraction of second-rank tensors.

We assume that all perturbations have a sinusoidal dependence on time and azimuth, $e^{i(m\phi-\omega t)}$, where ω is the frequency of the mode and $m = l$ is an integer index of a spherical harmonic that describes the azimuthal variation of the amplitude of the perturbation. The coefficient η_n denotes the shear or bulk coefficient or is a constant associated with coupling of the vibrations to the gravitational field. Because energy is dissipated by the stresses and added by the gravitational field as described above, the frequency has an imaginary part. Therefore,

$$\frac{dE}{dt} = 2\,\mathrm{Im}(\omega)\,E \equiv -\frac{2E}{\tau}\,. \tag{6.64}$$

Depending on the sign of $\mathrm{Im}(\omega)$, the perturbation is either damped or grows with a timescale τ. A mode m changes from instability to stability as $1/\tau$ passes through zero. If E and its time derivative can be evaluated, then a timescale for each of the processes n can be computed and the sum of their inverses is $1/\tau$. These zeros of $1/\tau$, like the surface waves and gravitational radiation from which they originate, depend on the rate of rotation of the star Ω. They will be different for each $m = l$ mode, so we denote them by Ω_m.

Stars are stable against the $l = m$ mode at rotational frequencies that are less than Ω_m. So the smallest of these critical frequencies sets the limit for the rotation of the star. A star with greater than this limiting frequency will develop an instability that causes a rapid loss of angular momentum through gravitational radiation until its frequency falls below the critical value. The problem then is to evaluate these critical frequencies and determine the smallest of them for a given mass star.

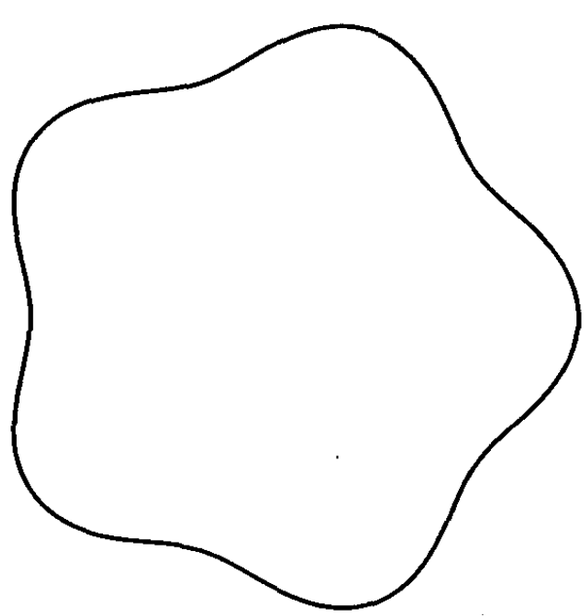

FIGURE 6.6. Illustration of $m = 5$ mode surface wave. Note that for a perturbation $e^{i(m\phi-\omega t)}$ of angular velocity ω, that of the pattern is ω/m.

This is a difficult program—to find the surface vibrations of a rotating star and determine the rotational frequency of the star at which they change from instability to stability. It has never been performed for a rotating star in General Relativity. Newtonian or post-Newtonian physics is sometimes used and frequently the modes of a nonrotating star have been investigated, the idea being that the frequencies of these superficial surface waves, as seen in the rotating frame fixed to the star, will be quite similar to those of a nonrotating star.

Suppose we consider, as an example, shear viscous damping and gravitational radiation-reaction as the relevant processes having to do with the perturbation. The problem is then to find the frequencies Ω_m that satisfy

$$0 = \frac{1}{\tau_{V,m}(\Omega_m)} + \frac{1}{\tau_{G,m}(\Omega_m)} . \tag{6.65}$$

The first term refers to viscosity and the second to gravitational radiation-reaction.

The viscous time-scale was computed for a nonrotating spheroid by Lamb (1881):

$$\tau_{V,m} = \frac{1}{(2m+1)(m-1)} \frac{R^2 \overline{\rho}}{\eta} \tag{6.66}$$

where η is the viscosity coefficient, R is the radius of the spheroid and $\overline{\rho} = M/\left((3/4)\pi R^3\right)$ is the average density. To relate the viscosity to the temperature and average density of a star, we adopt the expression [356, 357]

$$\eta = 347\,\overline{\rho}^{9/4}/T^2 \tag{6.67}$$

where $\overline{\rho}$ is the density in g/cm^3, T is temperature in Kelvin, and η is the shear viscosity in g/(cm s).

Detweiler [358] computed the damping time for gravity waves due to a surface wave of frequency $\omega(0)$ traveling on a nonrotating fluid sphere of radius R and found that

$$\tau_{G,m} = \frac{4m(m-1)^2(2m+1)[(2m-1)!!]^2}{3(m+1)(m+2)\,\omega^{2m+2}(0)\,R^{2m+1}} . \tag{6.68}$$

The eigenfrequencies

$$\omega_m(0) = \sqrt{\frac{M}{R^3}\frac{2m(m-1)}{2m+1}} \tag{6.69}$$

were computed by Thomson (1863) [359] for an inviscid nonrotating star. Comins [360, 361] computed the timescale for damping or growth of a perturbation on Maclaurin spheroids (incompressible, uniform density, hypothetical objects) including both viscosity and gravitational radiation-reaction. His complicated results were put into more tractable form by Lindblom [362] who expressed the solution of (6.65) in the form

$$\Omega_m = -\frac{\omega_m(0)}{m}\left[\alpha_m(\Omega_m) + \gamma_m(\Omega_m)\left(\frac{\tau_{G,m}}{\tau_{V,m}}\right)^{1/(2m+1)}\right] . \tag{6.70}$$

(By the conventions chosen, the counter-rotating surface wave of angular velocity ω/m has a sign opposite to that of the star Ω.)

The functions α_m and γ_m are properties of the particular stellar model under consideration. In other words, they depend on the solution of the equations of stellar structure with a particular equation of state. In practice they have been computed for idealized stellar models, such as Maclaurin spheroids or polytropes. They do not depart far from unity over the entire frequency range Ω and in early work were approximated as such. Indeed, in a study of polytropes, it has been confirmed that Ω_m depends much more strongly on the radius and mass of the neutron star model (through $\tau_{V,m}$ and $\tau_{G,m}$) than on the polytropic index assumed in calculating α_m [363].

We illustrate the results of the above discussion for two temperatures in Fig. 6.7. As a typical example, we show the minimum stable period that a family of neutron stars can have in the face of viscosity-moderated gravitation, radiation-reaction instabilities [193]. The minimum stable period is a very strong function of the mass and radius of the star. For the limiting-mass star, the critical frequency varies typically by about 25% among various models of the equation of state in theories for which the properties of symmetric nuclear matter are fixed within their known range [333].

A neutron star is born hot and cools during its life as an isolated star. If it is born with angular velocity above the limit established by the processes discussed above, the star will rapidly spin down until its frequency falls below that of the minimum stable mode. Thereafter, its frequency falls more slowly (due to the dipole radiation discussed in Chapter 5) on the timescale of the pulsar's active lifetime as a pulsar—an epoch of a few million years. Thus the minimum stable

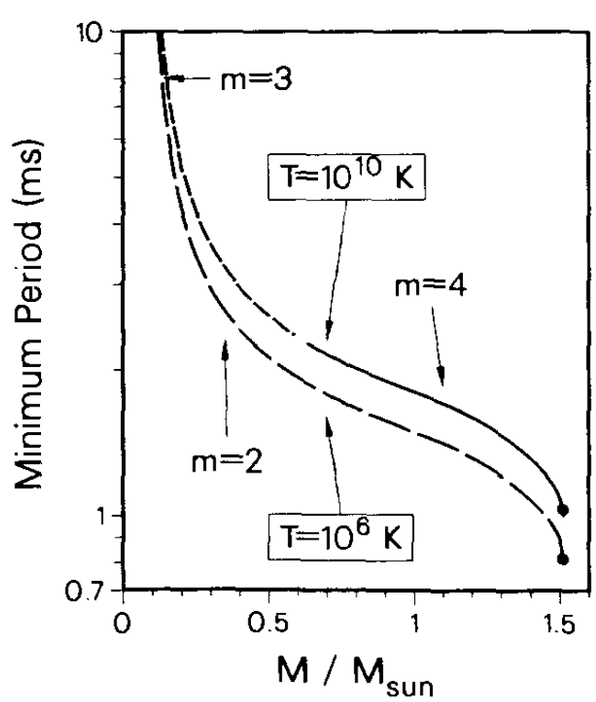

FIGURE 6.7. Minimum period that is stable against gravitational radiation-reaction moderated by viscosity for a hot and cold sequence of stars. The mode that establishes stability is shown by the value of m [193].

period of a hot star, illustrated in Fig. 6.7, establishes the rotational limit of the star during its lifetime as long as it remains isolated.[7]

For the limiting-mass star, the minimum period is about 1 ms as seen in Fig. 6.7. For comparison, the Kepler period of the limiting-mass star of this particular model is $P \sim 0.63$ ms [193]. Therefore, the gravitational wave instabilities set a more stringent limit on stable rotation than the mass-shedding limit for stars whose history has left them isolated from a companion.

On the other hand, the $T = 10^6$ K curve of Fig. 6.7 is relevant to old, cold stars that have acquired a companion and have been spun up and heated by accretion. In this case general relativistic instability is closer to the Kepler mass-shedding instability.

According to what has been said here, the typical limit on rotation of newly born stars is $P \geq P_{\text{limit}} \sim 1$ ms and is set by the gravitational radiation-reaction instability as moderated by viscosity—not by the Kepler period. Typically we have found that the limit placed by gravitational wave instabilities on the rotational period is 30–40% larger than the Kepler period, according to the particular model of the star [196, 333]. However, the result mentioned is not firmly established. There are several reasons. One is that we are able to compute the Kepler period in General Relativity whereas the gravitational viscosity limits can be computed only under what might turn out to be severe limitations—Newtonian or post-Newtonian gravity, and under rough approximations to the actual structure of the star (such as Maclaurin spheroids or polytropes). If the gravitational viscosity limits were compared, instead, with the Newtonian Kepler frequency, the difference would be much smaller. What the difference would be if both were computed in the General Theory of Relativity taking full account of the structure of the star, we simply do not know.

There is a further complication. Ipser and Lindblom [364] have studied Newtonian models in which, in addition to the shear viscosity considered in this section, they have included, as well, estimates of the effect of bulk viscosity. They find that above $T \sim 10^{10}$ K the effects of bulk viscosity dominate and raise the critical frequency above the value it would otherwise have. Cutler, Lindblom, and Splinter have studied more general pulsations induced by the same processes in General Relativity for nonrotating stars and for a range of realistic stellar models rather than the idealized Maclaurin spheroids or polytropes [365]. They conclude that bulk viscosity will dominate over shear in the same high temperature era of the star which lasts for about a day [272].

Because of the absence of general relativistic calculations of possibly unstable modes in rotating stellar models, particularly realistic ones, it is unclear how important the gravitational-viscosity instability is—whether it causes, simply, a small reduction in stable frequency compared to the Kepler frequency or a large reduction as discussed above. From the point of view of fast pulsars and their

[7]Accretion from a low-mass companion may spin up an old cold star to a frequency higher than is possible for the stable rotation of a hot star.

evolutionary history, it appears to us that this is an important and fruitful area of investigation, albeit very complicated.

6.13 Problems for Chapter 6

1. Work thorough the steps to obtain the fact that the term in the line element for a rotating star, $\omega(r, \theta)$, represents the frequency with which local inertial frames at r are dragged around the star.
2. Make sure you understand the analysis leading to the expression for the frame dragging frequency outside the star, (6.10).
3. Use an equality in (5.9) to define an estimate for the GR Kepler angular velocity, $\Omega_K \approx \zeta(M/R^3)^{1/2}$, $\zeta \approx 0.625$. Show that in terms of this,
$$\frac{E_{\text{rot}}}{E_{\text{grav}}} \approx 0.13\left(\frac{\Omega}{\Omega_K}\right)^2.$$
4. Obtain the expression for moment of inertia, (6.19).
5. Fill in the details to obtain the moment of inertia of a nonrotating star (6.20).
6. Integrate (6.22) to obtain the moment of inertia of a uniform sphere of matter. Thus confirm (6.11).
7. Derive the asymptotic expression for the frame-dragging frequency (6.26).
8. Derive the surface connections (6.27).
9. Work through the steps leading to the expression for the moment of inertia of a rotating star, (6.38).
10. Derive the time-component of the four velocity (6.41) of a point on the star that is rotating with angular velocity Ω.
11. Derive the self-consistency condition (6.43) by which the Kepler angular velocity of a rotating star is determined in General Relativity.
12. Find the velocity of a particle in circular stable orbit at the equator of a rotating star. Note that it is different according to whether the particle is co-rotating or counter-rotating (6.47).
13. Derive the approximate expression for the Kepler angular velocity (6.61) that justifies the form of the approximation formula in terms of the mass and radius of a Schwarzschild star.

7

Limiting Rotational Period and Radius of Neutron Stars

7.1 Motivation

Pulsars have been identified with the theoretical objects called neutron stars. The identification is convincing—but not proved. The short rotational periods of millisecond pulsars inform us that the average density (and, therefore, the central density) must be very high—higher than the density of nuclei (5.12). The most obvious inference is that pulsars are the objects conceived of by Baade and Zwicky. However, there is another possibility that has such a fundamental implication that it should not be overlooked. We will find that the conventional interpretation of pulsars as neutron stars—or any any other type of star that is gravitationally bound—can be ruled out if any pulsar is found to rotate at a frequency above a certain limit.

The goal of this chapter is to establish the maximum rate of rotation sustainable by a neutron star [249]. The Kepler frequency[1]—the frequency at which matter at the equator is shed—is the *absolute* limit for rotation. How large can that limit be for any conceivable neutron star model? What would be implied about a pulsar's constitution if it were observed to exceed such a limit?

Several authors have investigated how rapidly neutron stars can rotate based on particular theories of dense matter [95, 336, 337]. The minimum Kepler period

[1]Recall that the Kepler frequency is defined as the frequency of a particle in stable circular orbit at the circumference of a star. It is therefore also the frequency at which disruption of the star would occur.

for several neutron star models is ~ 0.5 ms for $1.44M_\odot$ neutron stars.[2] Given the uncertainty in the equation of state in the high-density domain of matter, no decisive conclusion could be reached if a pulsar with a shorter period were found, save that none of those theories is correct. A decisive rotational limit for gravitationally bound (i.e., neutron) stars can be derived only from a set of constraints that do not exceed our certain knowledge and principles [249, 366].

Our approach is to formulate the least number of constraints that can be imposed with assurance on the equation of state and, within the class satisfying those constraints, find the highest possible rotational frequency of the corresponding neutron star models. The limit on rotation (as a function of stellar mass) is somewhat akin to the mass limit for neutron stars found by Rhoades and Ruffini [101]–[105].

So far we have spoken of neutron stars, but here we broaden the meaning of that name for the purpose of the limit derived in this chapter. A neutron star is bound by gravitational interaction. Above the density of approximately that of Fe^{56} atoms (~ 7.86 g/cm^3) the pressure of cold-catalyzed matter is positive and in the interior of the star, very large. The density is so great that nucleons reside in the range of the repulsive interaction of their neighbors. This repulsion (and the large Fermi energy) would blow the star apart into its constituents if gravity were turned off. As we know, relativistic stars have a limiting mass corresponding to any equation of state for dense matter. We also know the generic form of the mass–radius relationship for degenerate relativistic stars bound by gravity (Section 5.3.12). A star at the mass limit has the smallest radius, as illustrated in Fig. 7.1. It therefore can rotate more rapidly than any other star in the sequence according to the approximate expression for the Kepler frequency discussed in Section 6.7 [95, 96, 107],

$$\Omega_K \approx 0.65(M/R^3)^{1/2}\,. \tag{7.1}$$

Although this result is Newtonian (5.9), reduced by the prefactor, it was justified for General Relativity in the proceeding chapter, and it is accurate to better than 10%. In this chapter, the term "neutron star" is used interchangeably with gravitationally bound star. We make a key distinction between pulsars that are or can be gravitationally bound stars and those that cannot. The limit derived in the sequel is not only valid for neutron stars; it is valid for any conceivable star that is gravitationally bound.

One now glimpses the importance of the rotational limit. If it is violated by observation, then a type of star bound in the absence of gravity must exist—a self-bound star.[3] We discuss the possible existence and constitution of such stars, called strange stars, in Chapter 8 and 12. If such self-bound stars should actually exist, it would signal an astonishing fact about the nature of matter—that the true

[2]However, it should not be concluded from the quoted literature that there are viable descriptions of neutron stars that can rotate at periods as low as 0.5 ms. It turns out that the central density of such models is so high as to invalidate the use of confined baryons in the calculation of the models (Section 12.3.3).

[3]By self-bound star, we mean a star that would be bound even in the absence of gravity.

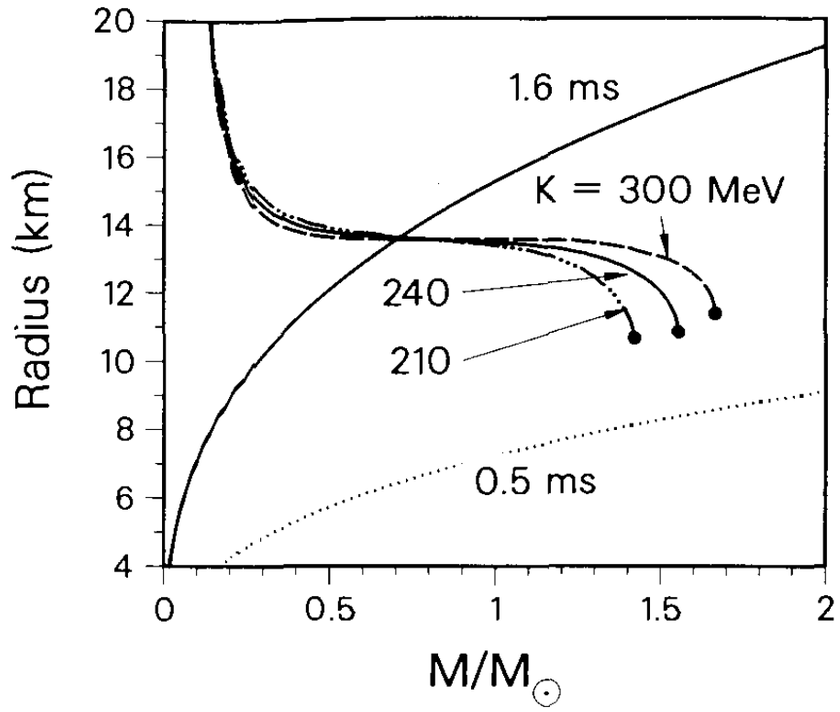

FIGURE 7.1. Generic relationships for neutron stars (or degenerate, relativistic, gravitationally bound stars in general) for several equations of state as labeled according to compression K (with $m^*_{sat}/m = 0.78$). The limits imposed by a 1.6-ms and 0.5-ms pulsar are also shown by solid and dotted curves. Stars below them are stable for still shorter periods (see (7.1)). From [367].

ground state of the strong interaction is not that of the ordinary hadronic matter that we know—nucleons and nuclei—but a new kind of matter—bound strange quark matter.

In the next sections, we enumerate the minimal constraints on the equation of state for finding the minimum rotational period of neutron stars, describe the variational ansatz and present the results that define the region in the mass-period plane inaccessible to neutron stars. We also derive a limit on rotational period for any star that follows from the structure of Einstein's equations alone [249]. Of course, such a limit lies below the limit for neutron stars because fewer constraints are involved. We then discuss the conclusion one would be forced to draw if a pulsar were found in the region forbidden to neutron stars but allowed by General Relativity.

7.2 The Minimal Constraints

We adopt the following as the minimal principles and constraints for finding the minimum rotational period of *gravitationally* bound stars (which means, in practice, neutron stars):

1. Einstein's general relativistic equations for stellar structure hold.
2. The matter of the star satisfies $dp/d\rho \geq 0$ which is a necessary condition that a body is stable, both as a whole and also with respect to the spontaneous

expansion or contraction of elementary regions away from equilibrium (Le Chatelier's principle).

3. The equation of state satisfies the causal constraint for a perfect fluid; a sound signal cannot propagate faster than the speed of light, $v(\epsilon) \equiv \sqrt{dp/d\epsilon} \leq 1$, which is also the appropriate expression for sound signals in General Relativity [155, 368].
4. The high-density equation of state, whatever it is, matches, continuously in energy and pressure, the low-density equation of state of Baym, Pethick, and Sutherland, somtimes designated as BPS [80].

The first two constraints are most secure. The causal constraint, as expressed here, is frequently invoked; most theories of dense matter obey it, at least to densities expected in neutron stars. Some theories, like the (σ, ω, ρ) nuclear field theory of Chapter 4, explicitly obey it at all densities. Strictly speaking, the expression $v(\epsilon) \equiv \sqrt{dp/d\epsilon} \leq 1$, even for a perfect fluid, refers to the signal speed only in a homogeneous body, if v is dependent on ϵ, and, in an inhomogeneous body, only if v is independent of ϵ. Nevertheless, it is a general causal constraint for a perfect fluid. It is not known how to impose a causal constraint on an imperfect fluid. However, the effect, on our results, of lifting the constraint $\sqrt{dp/d\epsilon} \leq 1$ is easily examined. The results of these tests and others are given in Section 7.5. The effect of the fourth constraint is also easily examined.

7.3 Variational Ansatz

In the "low-density" region, up to some fiducial density ρ_0 near nuclear density, we use the equation of state of Baym, Pethick, and Sutherland [80] (referred to as BPS) for charge-neutral nuclear matter. Results from the work of Baym, Bethe, and Pethick [83] and of Siemens [82] were also employed in the above reference. We take the BPS equation of state to be reasonably constrained by the bulk properties of nuclear matter at the saturation density of nuclei. A tabulated entry in the BPS tables that is suitable for the fiducial density occurs at $\rho_0 = 0.1625\ \text{fm}^{-3}$. (We have used a subscript "0" to denote the conditions at normal nuclear matter saturation density in other parts of this book. Because the fiducial density ought to be chosen close to that state, we use the same notation again, but understand that, in the present context, it simply represents the fiducial density close to saturation density.)

Beyond the fiducial density we represent the unknown equation of state by a parameterized form. As an option we allow for the possibility of a first-order phase transition of the type where the pressure is constant and the energy density increases linearly with baryon density over a certain range. This is the most extreme allowable form of an equation of state because it satisfies the equality in Le Chatelier's principle. Above the fiducial density or the phase-transition region as the case may be, we adopt a "gamma law" form. At the density at which the equation of state becomes acausal, we replace it by its causal limit. In summary the equation of state is continuous and defined by the following equations:

(a) low density:

$$\epsilon(\rho) = \epsilon_{BPS}(\rho), \quad p(\rho) = p_{BPS}(\rho), \quad \rho < \rho_0. \tag{7.2}$$

(b) phase-transition region:

$$\begin{aligned} \epsilon(\rho) &= \frac{\rho}{\rho_0}(\epsilon_0 + p_0) - p_0\,, \\ p(\rho) &= p_0 \quad (\text{for } \rho_0 \le \rho \le \rho_1 \equiv \rho_0 + \Delta)\,, \end{aligned} \tag{7.3}$$

where $\epsilon_0 \equiv \epsilon_{BPS}(\rho_0)$, $p_0 \equiv p_{BPS}(\rho_0)$. This satisfies the condition that the baryon chemical potential, $\mu(\rho) \equiv d\,\epsilon/d\,\rho =$ constant in the interval Δ. This segment satisfies Le Chatelier's principle at its limit, namely, the equality in the second constraint.

(c) parameterized region:

$$\begin{aligned} \epsilon(\rho) &= \frac{A}{\gamma - 1}(u^\gamma - u) + u\epsilon_1 + (1 - u)(A - p_0)\,, \\ p(\rho) &= A(u^\gamma - 1) + p_0 \quad (\text{for } \rho_1 < \rho < \rho_s), \end{aligned} \tag{7.4}$$

where $u = \rho/\rho_1$ and $\epsilon_1 \equiv (\rho_1/\rho_0)(\epsilon_0 + p_0) - p_0$ if $\Delta \neq 0$ while $u = \rho/\rho_0$ and $\epsilon_1 = \epsilon_0$ if $\Delta \equiv 0$. The second constraint requires that $A\gamma \ge 0$. If the equation of state (7.4) becomes acausal at ρ_s defined by $(dp/d\epsilon)_{\rho_s} = 1$ (at which density we denote the energy density and pressure by ϵ_s, p_s), we replace it thereafter by

(d) causal limit:

$$\begin{aligned} \epsilon(\rho) &= \epsilon_s - p_s + p(\rho), \\ p(\rho) &= \frac{1}{2}\left\{p_s - \epsilon_s + (p_s + \epsilon_s)\left(\frac{\rho}{\rho_s}\right)^2\right\} \quad (\text{for } \rho \ge \rho_s). \end{aligned} \tag{7.5}$$

In passing, we note that Le Chatelier's principle at its extreme $dp/d\rho = 0$, or, equivalently, $p =$ constant, also corresponds to the mixed phase of a one-component system undergoing a first-order phase transition. This is a special and extreme example of a first-order phase transition. In multi-component systems with a first-order phase transition, in general, the pressure is not a constant in the mixed phase, but rather is an increasing function of density on an isotherm [195]. Nevertheless, we shall refer to the special region, $p =$ constant as a condensate, or phase-transition region. Because compact baryon stars in equilibrium have particles carrying both baryon or electric charge or both, a first-order phase transition region, if it exists, will almost certainly be of the multicomponent type for which $dp/d\rho > 0$. (See Chapter 9.)

7.4 Limiting Value of Rotational Period as a Function of Mass

The maximum-mass star $M_{\max}$ in the sequence of gravitationally bound compact stars belonging to a given equation of state has the minimum Kepler period because

the mass is largest and the radius is smallest (7.1). Therefore, we can incorporate the minimal constraints into a variational search over A, γ, and Δ for the lower limit on the rotational period of a neutron star as a function of maximum mass $M_{\max}$ by minimizing the function $f(M, P) = w_1(M - M_{\max})^2 + w_2 P^2$, where w_1 and w_2 are weights. We use a modified Levenberg–Marquardt method [369] for finding the minimum of a nonlinear function of its arguments. The function has its minimum when $M = M_{\max}$ and P is the least possible Kepler period for that mass. Of course, $M_{\max}$ and P depend nonlinearly on the parameters mentioned above through the solution of Einstein's equations. We used the the approximate expression (6.53) for the absolute limit on the angular velocity Ω or corresponding period of rotation $P = 2\pi/\Omega$, namely,

$$\Omega_K \approx 240\left(\frac{M/M_\odot}{(R/\mathrm{km})^3}\right)^{1/2} \mathrm{ms}^{-1}$$

The results are summarized in Fig. 7.2. We show the minimum Kepler periods for stellar sequences that are subject to the above constraints as a function of the corresponding maximum (limiting) mass star. Neutron stars cannot lie below the solid curve of this figure within the narrow limits discussed in detail below. We also show Kepler periods for the sequence whose maximum mass is $1.8M_\odot$. As an example, a neutron star of canonical mass $1.442M_\odot$ cannot have a rotational period less than 0.33 ms if the equation of state does not have a first-order phase transition. If it does, the period can be further reduced by 0.01 ms, which falls within the uncertainty of (6.53).[4] In Section 7.6 we derive a region forbidden by the structure of General Relativity. It is also shown in the figure.

We compare the two equations of state that yield the minimum period (within the 0.01 ms quoted above) for a $1.442M_\odot$ star in Fig. 7.3 (they are the bottom two curves, one having a constant pressure phase-transition region, the other not). The radii of the corresponding static stars are 6.19 and 6.32 km, respectively, and the central energy densities are 26.1 and 26.0 times normal nuclear saturation density ($\epsilon_0 \approx 2.5 \times 10^{14}$ g/cm^3 = 0.71 fm^{-4} = 140 MeV/fm^3). Such extremely high density required of stellar models (see Fig. 7.4), if they are to withstand ultra-short rotational periods, has been cited as reason enough to suspect that short-period pulsars, if they exist, cannot be neutron stars [370, 371].[5]

The energy density profiles at the edges of two optimally configured spherical stars, the rotating counterparts of which are stable to mass shedding at $P \sim 0.33$ ms, are shown in Fig. 7.5. The notable features of these stellar profiles are the nearly uniform interior density and the rapid drop in density very close to the

---

[4]Koranda, Stergioulas and Friedman have performed an elegant analysis that finds a slightly lower limit by about 6 percent [366]. They find the limit using the BPS equation of state for low density, a constant pressure region, and a causal limit equation of state (thus eliminating the region (c) in our analysis) and an exact numerical solution of Einstein's equations for rotating stars.

[5]The density of nonoverlapping spheres of radius r packed in a cubic lattice is $\rho = 1/(2r)^3$. Such a density as quoted, $26\rho_0$ therefore corresponds to packing of objects of radius 0.03 fm. They can't be nucleons!

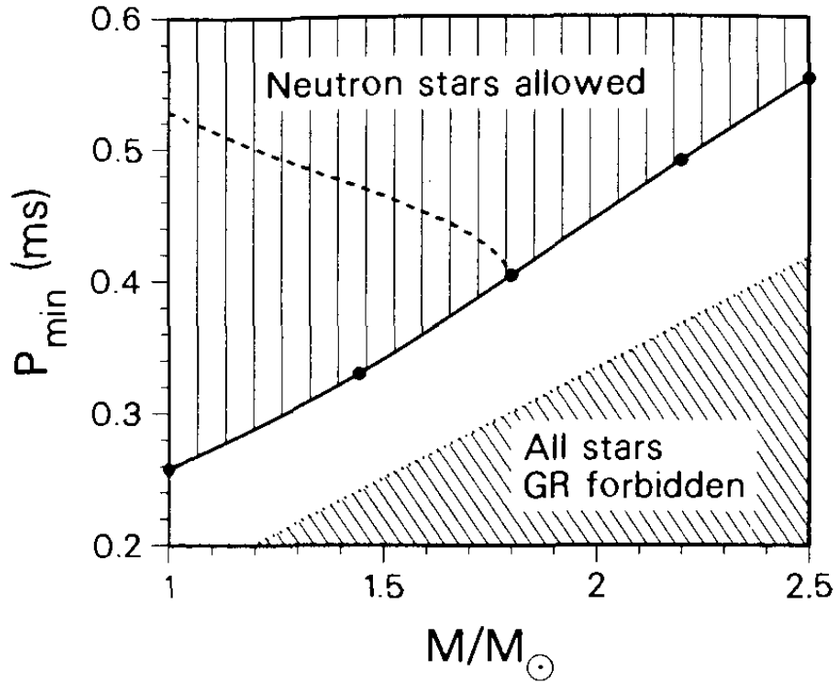

FIGURE 7.2. Minimum rotational period of neutron stars (solid curve). Calculated points are shown by dots. Periods of a sequence of stars whose maximum mass is $1.8M_\odot$ (dashed line). Region forbidden by structure of General Relativity (modulo the approximate formula (6.53)) (diagonal shaded region). [249]

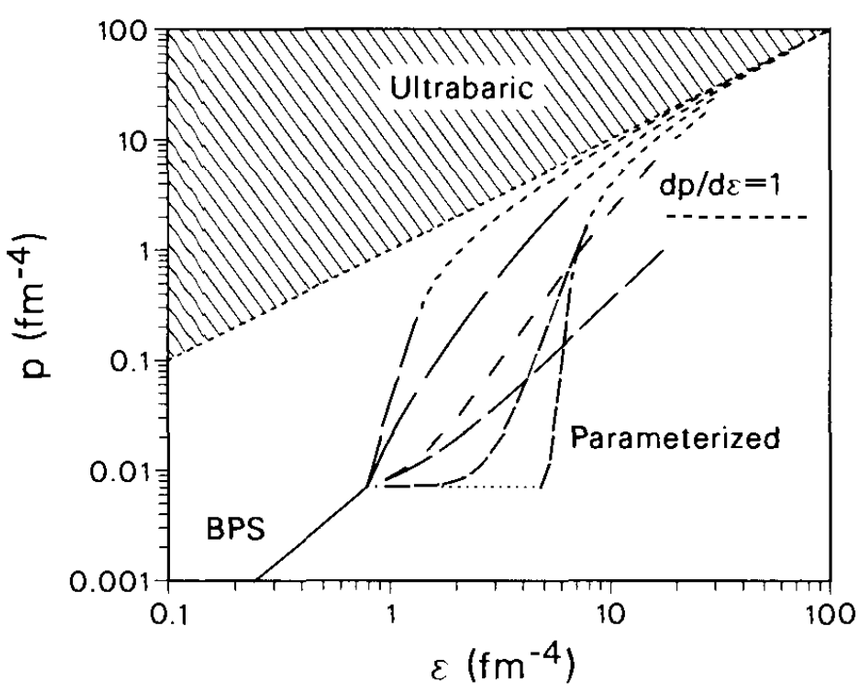

FIGURE 7.3. Bottom two equations of state produce minimum rotational period for a 1.442-$M_\odot$ neutron star, one with condensate ($p =$ constant region) and the other without. Others illustrate the flexibility of the simplest parameterization, (7.3–7.5). The three segments of each are (a) BPS, (b) parameterized region, and (c) causal limit, $dp/d\epsilon = 1$. Ultrabaric region has $p > \epsilon$. Its boundary is $p = \epsilon$. This region is inaccessible from below when $dp/d\epsilon \leq 1$. From [249].

edge. These features are characteristic of an equation of state stiff at high density and very soft at intermediate density, features that promote stability to fast rotation [307, 337].

The fiducial energy density corresponding to the chosen fiducial number density of $\rho_0 = 0.1625$ fm^{-3} is $\epsilon \approx 0.7$ fm^{-4}. The bulge in both profiles in Fig. 7.5 below this density corresponds to neutron star matter below the density of nuclear matter. Low-density matter is represented by the BPS equation of state. We note that the subnuclear crust (magnified in this figure by the suppressed origin) is actually very thin, $\sim$ 0.2 km. (The radii of these stars, as quoted above, lie more than five decades in density below the lowest value of the abscissa in Fig. 7.5.) For comparison we show the profile of a limiting star of the same mass whose Kepler period is 0.5 ms. This is a more conventional neutron star model. It is evident that, to attain the slightly smaller limiting period of 0.33 ms, the structure of the star and the underlying equation of state must be radically different. The central energy density of the spherical star, with the 0.5 ms Kepler period for the rotating counterpart, is $18.6\epsilon_0$.

It may be of some interest that the Oppenheimer–Volkoff limiting-mass star corresponding to an ideal neutron gas has $M = 0.72M_\odot$, $R = 9.6$ km and, for the rotating counterpart, a Kepler period of $P = 0.98$ ms. This star lies far above the scale of Fig. 7.2. The Rhoades–Pietronero–Ruffini maximum mass star has $M = 3.2M_\odot$, $R = 13.7$ km, and the rotating counterpart has Kepler period $P = 0.79$ ms and lies about 0.1 ms above the projection of our limiting curve.

7.5 Test of Sensitivity of Results

We discuss the accuracy with which the limiting curve dividing the period-mass plane into regions accessible and inaccessible to neutron stars is determined. Our tests are performed for a canonical mass of $1.442M_\odot$ because this is likely to be near the mass of most neutron stars produced in supernova. (It is commonly accepted that the favored mass lies in a rather narrow range (around the Chandrasekhar limit) which establishes the mass of the iron core of the progenitor star.)

The sensitivity of the results to the choice of a "low-density" equation of state was tested by setting the pressure to zero at and below the fiducial density. The corresponding period is thereby reduced by a small amount, 0.014 ms. This extreme softening permits the greatest compaction at the surface and therefore the greatest stability to mass shedding. No other low-density equation of state, having the same pressure and energy at saturation, could give a lower value for the limiting period.

We remark here that some early calculations [113] of purely neutron matter which neglect the penalty of the high-isospin asymmetry imposed by the nuclear force actually predict bound neutron matter at a density near normal nuclear density. However, the Fermi energy contributes only about one-half of the value of the symmetry coefficient in the empirical mass formula, the remainder arising from the isospin part of the nuclear force. This part is neglected in the work that finds neutron matter to be bound. If neutron matter were bound, then $p = 0$ at its equilibrium density. This defines the edge of the star which would occur near nuclear density ($\sim 2.5\ 10^{14}$ g/cm^3), as in the above test, instead of at the density of iron

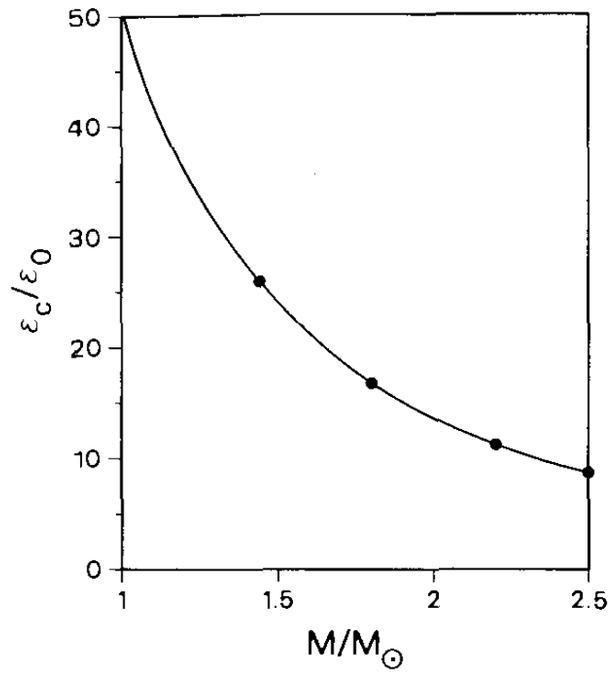

FIGURE 7.4. Least possible central energy density in units of normal nuclear saturation density for the nonrotating neutron stars whose rotating counterparts have the shortest possible Kepler period, namely, those corresponding to Fig. 7.2. From [249].

($\sim$ 7.86 g/cm^3), as for the lowest energy state of cold-catalyzed matter [28]. So our test embraces the extreme case of bound neutron matter. However, there is no reason to expect neutron matter to be bound. Nuclei of Z very different from N become increasingly less bound with increasing $(N - Z)^2$, which gives rise to the well known "valley of stability" (4.107).

We have already stated the result that the shortest period of a $1.442 M_\odot$ star can be reduced by 0.01 ms below 0.33 ms if the equation of state is allowed to have a region of constant pressure as a function of density. Such an equation of state satisfies Le Chatelier's principle at its limit (the equality in the second constraint). This is true whether we take the density of the onset of the constant pressure region lying near nuclear density or above. By the test of the second paragraph in this section, the maximum reduction in period that can be gained by having the onset of the region of constant pressure occur at a lower density than fiducial is < 0.014 ms.

The effect of a specific choice of fiducial density ρ_0 in the range 0.1484–0.1814 fm^{-3} near nuclear saturation amounts to an uncertainty in the minimum period of only ± 0.001 ms for our canonical neutron star.

The parameterization of the equation of state used above and the flexibility to reach the limit allowed by Le Chatelier's principle, through the inclusion of a phase transition with constant pressure, is illustrated by the extremes in Figs. 7.3 and 7.5. The parameterization apparently represents a very flexible family within which we search for a minimum period. To test this conjecture we also expanded the variational ansatz with two additional powers of density to find whether our limit can be significantly lowered. The expanded ansatz is

$$\epsilon(\rho) = \frac{A}{\gamma - 1}(u^\gamma - u) + \frac{B}{\gamma - 2}(u^{\gamma-1} - u) + \frac{C}{\gamma - 3}(u^{\gamma-2} - u)$$

$$+ u\epsilon_0 + (1-u)(A + B + C - p_0),$$

$$p(\rho) = A(u^\gamma - 1) + B(u^{\gamma-1} - 1) + C(u^{\gamma-2} - 1) + p_0, \tag{7.6}$$

where $B > 0$, $C > 0$ are additional parameters that are varied to minimize the period at a given mass. (The restriction to positive values assures that the second constraint is always satisfied when $\gamma > 2$.) The result is that the period could be reduced by only 0.003 ms for a 1.442-$M_\odot$ star, a very small reduction (1%) for an ansatz with two additional parameters.

It is believed that a signal in any medium cannot propagate faster than the speed of light. Nevertheless, the principle of causality (the usual phrase employed to state this belief) does not follow from Lorentz invariance [372]. Although searches for tachyons have so far proved fruitless, the principle is not thereby proved. Moreover, it is not known what condition the equation of state of an imperfect fluid should satisfy so that superluminal signals are not attained. Therefore, we test the effect on the minimum rotational period if the causal constraint is lifted. The result is that the period can be reduced by 0.037 ms. This is the largest of the uncertainties.

All of the above quoted uncertainties are small and lie within the accuracy of the means of estimating the Kepler period (6.53), save the relaxation of the causal constraint, which is slightly larger. We conclude that the solid line of Fig. 7.2 marks the lower boundary for neutron stars rather accurately. Moreover, as pointed out in Section 7.8, gravitational wave instabilities (Section 6.12) are expected to occur at periods longer than the Kepler period. So, the Kepler period is an absolute bound on rotation.

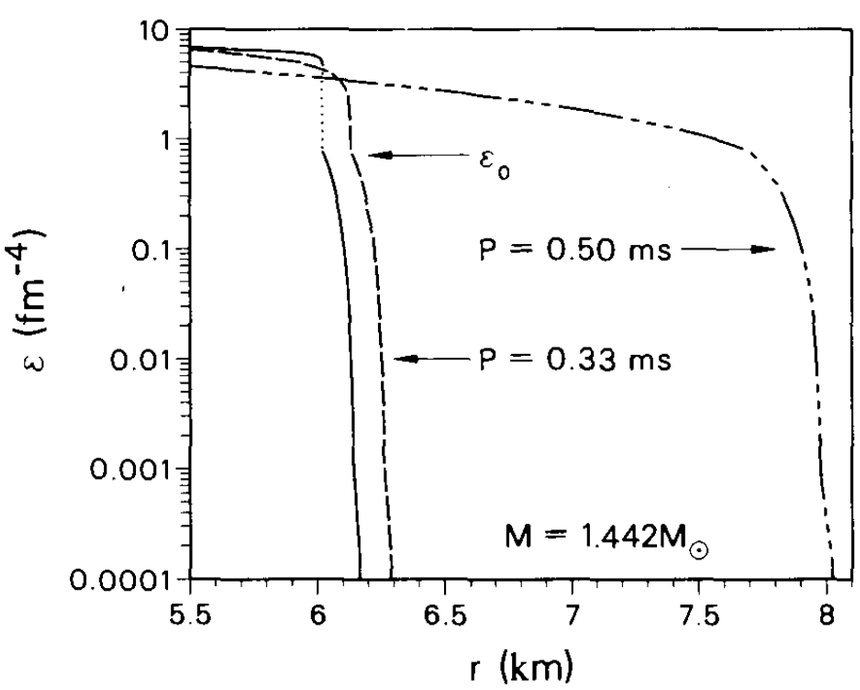

FIGURE 7.5. Density profiles of the edges ($R \sim 6.2$ km) of the two limiting-mass spherical stars corresponding to the bottom two equations of state of Fig. 7.3 each with mass $1.442M_\odot$ and Kepler periods for rotating stars of 0.32 and 0.33 ms for the solid and dashed cases, respectively. The phase-transition region ($p =$ constant) corresponds to the discontinuity in density (dotted). The other profile is ($R \sim 8$ km) for the same limiting mass but Kepler period of 0.5 ms. From [249]

We have not questioned the validity of General Relativity as a theory underlying the structure of compact stars. The value of M/R for the limiting-mass star in various models of the equation of state is generally found to lie in the range of $0.2 - 0.3$. For our minimally constrained models designed to minimize the rotational period, the value of $M/R \approx 0.34$. Solar system phenomena (such as the advance of the perihelion of planets) test General Relativity only in the weak field limit where the surface gravitational field of the Sun is $M/R < 2 \times 10^{-6}$.

Recent experimental results, derived from nearly two decades of accurate timing observations on the binary neutron star system PSR 1913+16 [4, 53], test the theory in much stronger gravitational fields. The conclusion is that correct theories of gravity are tightly constrained. Einstein's theory lies at the center of the constrained region. It appears that there is little ground for questioning the appropriateness of the usual equations for relativistic stellar structure. In any case, we do not know how to assess an error to the first constraint if the correct theory is even a small variant of the usual one.

7.6 General Relativistic Limit on Rotation

Interestingly, a limit on rotation can be derived by assuming only that Einstein's equations of stellar structure hold [249]. Then $M/R < 4/9$ for any static star as we saw in Section 3.15. Using the approximate relationship (6.53), we obtain

$$P \approx 10M\left(\frac{R}{M}\right)^{3/2} > \frac{273}{8}M = 0.167\frac{M}{M_\odot} \text{ ms} \quad \text{(any star)}, \tag{7.7}$$

which, for a star of mass equal to that of PSR1913+16 yields $P > 0.24$ ms. Because the limit on M/R follows from the structure of Einstein's equations, the above limit on period applies both to neutron stars as well as to hypothetical stars made of self-bound matter. The forbidden region is marked in Fig. 7.2.

7.7 Lower Limit on Neutron Star Radius

A model-independent limit on the mass–radius relationship of neutron stars is especially interesting in view of the claim that mass and radius determinations may be possible through the observation of quasi-periodic oscillations (QPOs) in the brightness of compact X-ray stars[6] [304, 305, 306, 373, 374]. It is clear from the foregoing analysis and variational results that having established a lower limit on the rotational period of neutron stars, we have determined a lower limit on the radius as well. For the particular mass of $M = 1.442M_\odot$, we see from Fig. 7.5 that

[6]These compact objects are believed to be neutron stars that are accreting matter from a less dense low-mass companion. The surface of the neutron star is heated by the accreted material so that the star emits abundant X-rays.

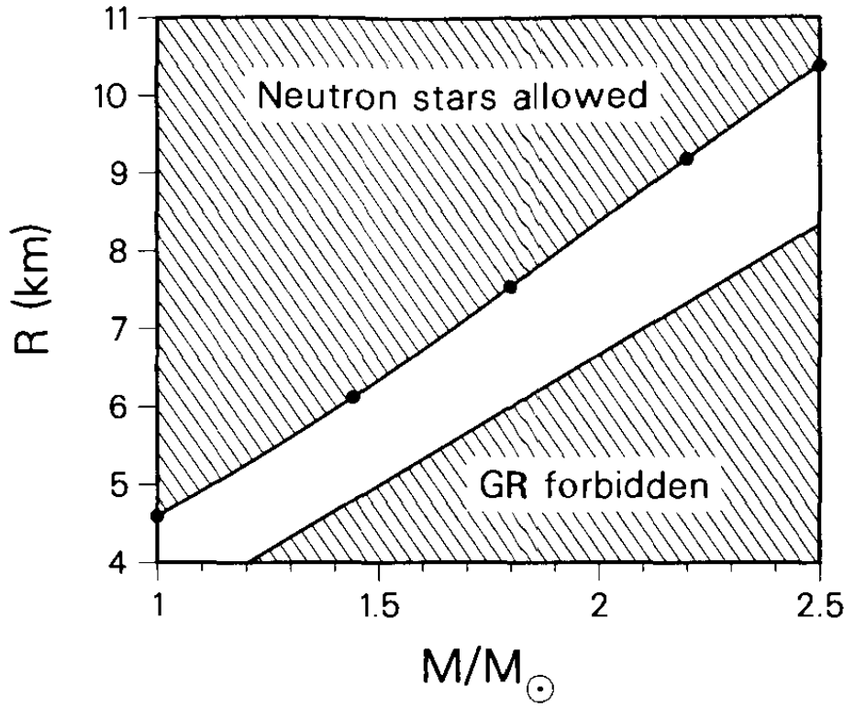

FIGURE 7.6. Allowed region of nonrotating neutron star radii as a function of mass determined independent of specific models of dense matter, but rather by the minimal constraints (causality, etc.) enumerated in the text.

$R > 6.2$ km. Similar limits could be inferred from Fig. 7.2 and the relation between Ω_K, M, and R (6.53). If a radius smaller than the limit for a star of measured mass were found, and the star was known not to be a black hole, it would have to be a star that is made of matter that is self-bound at high equilibrium density, such as we discuss in Chapter 12 on strange stars.

We show the accessible region of neutron star radii as a function of mass in Fig. 7.6. The allowed region is determined, independent of specific models of neutron star matter, but rather by the minimal constraints enumerated earlier. Within an accuracy of about 4 percent, the radii would be consistent with results for the minimum period found by Koranda, Stergioulas and Friedman [366], were they to extract the minimum radius from their results on periods.

The minimum possible radius of a neutron star as a function of mass that is depicted in Fig. 7.6 can be represented approximately by the straight line

$$R = \left(3.856\frac{M}{M_\odot} + 0.7335\right) \text{ km} \quad \left(1 < \frac{M}{M_\odot} < 2.5\right) \tag{7.8}$$

Only radii larger or equal to this limit are allowed to *gravitationally* bound stars. Recall that the limit is obtained using minimal constraints, such as causality, and it may not be possible for a real star to attain the limit. That will depend on the equation of state of the material from which it is made.

We derived a limiting inequality between radius and mass that must be obeyed by any relativisitic star, $M/R < 4/9$, in Section 3.15. This inequality defines a region forbidden to all compact stars. Stars made of matter, if it exists, which is charge-neutral and self-bound at sufficiently high density can lie in the region between the above limiting lines; it is the blank region in Fig. 7.6. We discuss such hypothetical stars further in Section 7.9 and in Chapters 7 and 12.

7.8 Discussion and Alternatives

So far as is known, all stars are bound by gravity including neutron stars and hybrid stars—the form neutron stars take if the pressure in the core is sufficiently high to convert nucleons to quark matter (Chapter 9). Other types of stars have been conceived but not identified [93, 254, 375]. They are made of hypothetical matter that is self-bound and absolutely stable at high density. Such stars would not be subject to the limit on rotation of a gravitationally bound star and could, if self-bound at sufficiently high density, rotate at periods below that limit [371]. We will return to this alternative in Chapter 12.

The purpose of this chapter is to provide a decisive means of distinguishing pulsars that can be (but are not necessarily) gravitationally bound, compact stars, such as neutron or hybrid stars,[7] from those that cannot be bound by gravity alone. The limit that we have obtained for the rotational period as a function of stellar mass is necessarily more severe than would be obeyed by real neutron stars because there is no physical principle that requires the equation of state to minimize the rotation period. Moreover, there are unstable pulsation modes of a rotating star associated with gravitational radiation-reaction [354, 355, 376] which occur at periods larger than the Kepler period [196, 333, 362, 364, 377] (see Chapter 6). If a pulsar has a rotation period smaller than any of the periods for these critical modes, it will spin down by gravitational radiation until its period approaches that of the largest of the unstable modes (Section 6.12). However, the physics that enters the estimate of these instabilities is far less certain than that which determines the Kepler period, so we use this absolute lower bound of a uniformly rotating star. Therefore, if a pulsar with rotation period and mass falling below our limiting curve is found, it actually lies even further below the limit established by nature for neutron stars.

There is a region in the period–mass plane below that allowed to neutron stars and above that forbidden by General Relativity (Fig. 7.2). What could be the general nature of a star that might fall in this intermediate region? The only general category of stars that could have smaller rotation periods than neutron stars is the category of stars that are made of hypothetical matter that is stable and self-bound in bulk at sufficiently high equilibrium energy density [307, 371].

7.9 Self-Bound Stars

The limiting rotational period of a star composed of matter that is self-bound ($p = 0$) at the equilibrium energy density ϵ_b is trivial to establish. Because the density (and pressure) decrease monotonically from the center to the edge of a star, it follows that the energy density (and the average, in particular) satisfies

$$\bar{\epsilon} \geq \epsilon_b \quad (\text{self} - \text{bound star}) . \tag{7.9}$$

[7] Hybrid stars denote neutron stars in which the central part is composed of quark matter or the mixed phase of quark and neutron star matter. They are the subject of Chapter 9.

The equality holds only when gravity is negligible, meaning that the mass is small. The average density also satisfies the identity $M \equiv (4\pi/3)R^3\bar{\epsilon}$. Using this relationship in (6.53), we have $P_K = 1.5(3\pi/\bar{\epsilon})^{1/2} < 1.5(3\pi/\epsilon_b)^{1/2}$. Observing also the limit imposed on M/R by General Relativity (7.7), we write

$$1.1\left(\frac{\epsilon_0}{\epsilon_b}\right)^{1/2} > \frac{P_K}{\text{ms}} > 0.167\,\frac{M}{M_\odot} \quad \text{(self} - \text{bound star)}, \tag{7.10}$$

where $\epsilon_0 \approx 140\,\text{MeV/fm}^3$ is the equilibrium energy density of normal nuclear matter.

From the above equation, it is clear that, if ϵ_b is large enough (a few times nuclear density), the period of a self-bound star can lie in the region prohibited to neutron stars. Such a star's energy profile is unlike those of Fig. 7.5; instead, the star has a sharp edge at which the energy density falls from the high equilibrium value of the bound matter to zero in a strong interaction length (Fig. 8.2). Such a star has a small radius for its mass as compared to a gravitationally bound star (Fig. 12.2). This is what permits it to rotate rapidly without shedding matter at its equator. In passing, we note the limit placed on the equilibrium density of self-bound matter by the general relativistic inequality $M/R < 4/9$ (3.152):

$$\epsilon_b \le \bar{\epsilon} < \left(\frac{4}{9}\right)^3 \frac{3}{4\pi}\frac{1}{M^2} = 52\left(\frac{M_\odot}{M}\right)^2 \epsilon_0\,. \tag{7.11}$$

In the event that self-bound matter exists in bulk, objects from microscopic nuggets to stars could exist, limited in mass only by gravitational collapse [378, 379]. Aside from limiting the maximum mass, gravity prevents self-bound stars from fissioning into smaller bound fragments except by the addition of sufficient energy to compensate for the creation of additional surface area.

The most likely candidates for stars made of matter that is self-bound at high density are strange stars, hypothetical stars composed of almost equal numbers of up, down, and strange quarks. Strange quark matter was hypothesized to be the absolute ground state of the strong interaction by Bodmer [380] and Witten [93, 381] independently. We will study the hypothesis and its consequences in detail in Chapter 12. Several recent accounts can be found in Refs. [371, 382]. As it turns out, the hypothesis is quite plausible on the basis of scale arguments—and very difficult either to prove or disprove (Chapter 12).

Another candidate in the category of self-bound stars is the so-called Q-star [375, 383]. These have been discussed as exotic solutions of effective nuclear field theories. While exotic solutions of fundamental theories, such as the sphaleron [384] of the classical Weinberg–Salam theory of the electroweak interaction, must be taken seriously, the status of an exotic solution of an effective theory is much more tenuous. Moreover, the properties of hypothetical Q-stars, whether dilute, very large and of many solar masses, or dense, small, and of solar mass, are not delimited by any known physics. In contrast, the argument for the possible existence of strange stars depends on simple physics and the QCD energy scale which place the energy per nucleon of strange matter close to the nucleon mass,

the only uncertainty being whether a fraction of a nucleon mass above or below [93, 371].

7.10 Summary

A neutron star cannot have a period for uniform rotation[8] that lies more than a few percent below the solid curve of Fig. 7.2. For a 1.442-$M_\odot$ neutron star, this means that the period must exceed $0.33^{+0.03}_{-0.04}$ ms where the upper error is that of (6.53) and the lower is the largest of the test errors and corresponds to lifting the causal constraint appropriate for a perfect fluid (where 0.037 is rounded to 0.04). This curve refers to the mass-shedding limit (Kepler period). Gravitational-wave instabilities will actually set a more stringent lower bound that lies above our curve. The most conservative bound for the region excluded to neutron stars is the one adopted here.

If a pulsar is found with mass and period, or mass and radius that place it below our critical curves for neutron or more generally a gravitationally bound star, it must be a different kind of object. It appears that the only alternative for breaking the limit on gravitationally bound stars is a state of matter that is self-bound in bulk at an energy density larger than normal nuclear matter by a factor of five to ten. The most plausible candidate to date, in our opinion, is strange quark matter. We introduce quark matter in the next chapter in preparation for a study of hybrid stars in Chapter 9 and strange stars in Chapter 12. Hybrid stars are gravitationally bound objects similar to neutron stars. Strange stars are entirely different objects. They would be bound by the strong interaction even in the absence of gravity.

[8]The rotation that minimizes mass–energy at fixed baryon number is uniform [338].

8

Quark Stars

8.1 Introduction

Quark or hybrid neutron–quark stars are composed, in whole or in part, of quark matter. Such a state of matter was conceived of soon after the realization that quarks, the constituents of nucleons, are asymptotically free. At the extreme of asymptotic momentum transfer, density, or temperature, quarks are free of interaction. Under such circumstances the individuality of nucleons is lost, and the quarks of nuclear matter are free to explore a much larger "colorless" region of space referred to as quark matter.

The deconfined phase of quark matter is of interest in astrophysics for a number of reasons. First, the universe likely passed through this phase in the first few seconds. Second, the conditions in the cores of neutron stars may be such that ordinary hadronic matter in which quarks are confined in individual hadrons is converted by high pressure to quark matter, forming a *hybrid star*—a star with a quark matter central region and a nuclear matter mantle. Third, it is conceivable that the ground state of the strong interaction is actually strange quark matter rather than the ordinary state of nucleons and nuclei that we know so well. In this case pulsars could be strange quark stars instead of neutron stars. In this chapter we introduce material for a discussion of both hybrid stars (Chapter 9) and strange stars (Chapter 12). Because the stellar structure of the latter is simpler than the former, the illustrations of this chapter are of quark stars rather than hybrids.

We do not have a rigorous theory of dense nuclear matter. Quantum chromodynamics (QCD)—although believed to be essentially the fundamental theory at the nuclear and subnuclear scale—is not a theory from which we can derive practical

results for the equation of state. We shall begin, therefore, by discussing a simple model of quark matter, namely the MIT bag model [385], although other models of confined quarks would do as well such as the one used in Ref. [386]. The bag model is a simple model compared to the nuclear field theory with which we attacked the more difficult problem of hadronic matter and neutron stars in Chapters 4 and 5. As a result, our work with quark and hybrid stars will be correspondingly simplified.

8.2 Model of Quark Confinement

The Lagrangian of quantum chromodynamics (QCD) can be solved only numerically on a lattice and then, only under conditions that are not relevant to the cold matter of neutron stars. The solution, even a numerical one, would be useful only if it provided the chemical potentials and quark populations as well as pressure as a function of energy density for charge neutral matter.

However, we can gain many insights using a model of quark confinement, but of course precise predictions, such as the critical density at which quarks begin to become disassociated with individual nucleons, is not possible. We can discuss in general terms, and with some confidence, phenomena that are expected to be associated with the mixed phase of confined and deconfined quark matter. We can even suggest a possible observable signal of the transition in pulsars (Chapter 11).

The MIT bag model was invented to try to account for hadronic masses in terms of their quark constituents [385]. It has been used extensively to discuss quark matter as well. The basic assumption of the bag model concerns confinement and the free motion of quarks in the confined (colorless) region. The "vacuum" of QCD is assumed to have the property that quarks are excluded. Within the hadronic volume, or more generally, within any volume containing quarks, the vacuum must be expelled. This costs energy. The energy per unit volume is called the bag constant and denoted by B. The energy associated with the mere presence of quarks in a volume V is therefore BV. In addition to this, there is energy associated with the kinetic motion of quarks in the volume. For hadrons, it is assumed that quarks move freely in a spherical cavity with boundary conditions so that no current crosses the boundary. For quark matter, energy associated with the surface condition is unimportant compared to the energy content of the interior and we can assume that quarks exist as a Fermi gas. Therefore, the energy density and pressure of quark matter will consist of two parts, the contribution of the confining bag and the kinetic motion of the quarks.

The optimum value of the bag constant B that can account for hadronic masses within such a simple model is $B^{1/4} = 145$ MeV. However, this is not necessarily the appropriate value for quark matter. Nucleons contain only the two light quark flavors, whereas quark matter will contain all three light quarks, up, down, and strange. As we will discuss in Section 8.5, $B^{1/4}$ must exceed a certain minimum value or else the energy per baryon number of three flavor quark matter would be

less than that of the nucleon itself or of the energy per nucleon in the most bound nucleus, ^{56}Fe, depending on the assumed strange quark mass. If this were so, then the ground state of the strong interaction would not be the one containing nucleons and nuclei, but one that is occupied by what is called *strange quark matter*. This is an interesting possibility, because we will see that it is not ruled out by any observable phenomena, including the fact that the universe obviously now is in the confined phase. We will devote Chapter 12 to a discussion and exploration of the "strange matter" hypotheses.

8.3 Quark Matter Equation of State

We derive expressions for the bag model equation of state of quark matter in several approximations. These will be useful to us later in connection with the possible existence of neutron stars with quark matter cores—what we refer to as hybrid stars.

In the simple model of free quarks in a bag, we derive analytical expressions for pressure, energy density, and the other properties from a Fermi gas of quarks in two limits,

$$1)\ T = 0, m \neq 0 \quad \text{and} \quad 2)\ T \neq 0, m = 0\,. \tag{8.1}$$

Expressions for the pressure, energy density, baryon number density, and entropy density for a finite-temperature Fermi gas of quarks of mass m_f and chemical potential μ_f, where f denotes flavor, are

$$\begin{aligned}
p &= \sum_f \frac{1}{3}\frac{\gamma_f}{2\pi^2}\int_0^\infty k\frac{\partial E_f(k)}{\partial k}\Big[n(k,\mu_f)+n(k,-\mu_f)\Big]k^2dk - B\,,\\
\epsilon &= \sum_f \frac{\gamma_f}{2\pi^2}\int_0^\infty E_f(k)\Big[n(k,\mu_f)+n(k,-\mu_f)\Big]k^2dk + B\,,\\
\rho &= \sum_f \frac{1}{3}\frac{\gamma_f}{2\pi^2}\int_0^\infty \Big[n(k,\mu_f)-n(k,-\mu_f)\Big]k^2dk\,,\\
s &= \frac{S}{V} = \left(\frac{\partial p}{\partial T}\right)_{V,\mu_f}\,,
\end{aligned} \tag{8.2}$$

where

$$E_f(k) = \left(m_f^2 + k^2\right)^{1/2} \tag{8.3}$$

is the quark kinetic energy and

$$n(k,\mu_f) = \left(\exp\{[E_f(k)-\mu_f]/T\}+1\right)^{-1} \tag{8.4}$$

is the Fermi distribution function for temperature T. The factor 1/3 occurs in the baryon density because there are three quarks per baryon. The bag pressure is denoted by B. It represents the positive energy shift per unit volume in the

deconfined vacuum relative to the confined vacuum. The quark degeneracy for each flavor is $\gamma_f = 2_{\text{spin}} \times 3_{\text{color}}$.

Other properties of possible interest are, for example, the electric charge density or the strangeness,

$$q = \sum_f \frac{\gamma_f}{2\pi^2} q_f \int_0^\infty \Big(n(k, \mu_f) - n(k, -\mu_f)\Big) k^2 dk\,, \tag{8.5}$$

where q_f is the quark electric charge for flavor f.

8.3.1 Zero temperature

For the first of the two limiting cases above, the distribution functions become step functions at energy μ_f. In that case we can use standard integrals (Ref. [64], p. 87) to express the results. For example,

$$\begin{aligned}
&\int_0^k \frac{k^4}{\sqrt{m^2 + k^2}} dk \\
&= \frac{1}{4}\left[k^3\sqrt{k^2 + m^2} - \frac{3}{2}m^2 k\sqrt{m^2 + k^2} + \frac{3}{2}m^4 \ln\left(\frac{\sqrt{k^2 + m^2} + k}{m}\right)\right].
\end{aligned}$$

We find

$$\begin{aligned}
p &= -B + \sum_f \frac{1}{4\pi^2}\left[\mu_f k_f\left(\mu_f^2 - \frac{5}{2}m_f^2\right) + \frac{3}{2}m_f^4 \ln\left(\frac{\mu_f + k_f}{m_f}\right)\right], \\
\epsilon &= B + \sum_f \frac{3}{4\pi^2}\left[\mu_f k_f\left(\mu_f^2 - \frac{1}{2}m_f^2\right) - \frac{1}{2}m_f^4 \ln\left(\frac{\mu_f + k_f}{m_f}\right)\right], \\
\rho &= \sum_f \frac{k_f^3}{3\pi^2}\,,
\end{aligned} \tag{8.6}$$

where k_f is the Fermi momentum for flavor f defined in terms of the chemical potential,

$$\mu_f = (m_f^2 + k_f^2)^{1/2}\,. \tag{8.7}$$

The above results are suitable for compact star calculations in which the nucleons are believed to be dissolved into quarks by the high pressure in the interior of the star; because temperatures of neutron stars, shortly after birth, have fallen to the KeV region (which is negligible on the nuclear scale), the zero temperature limit is appropriate.

TABLE 8.1. The six known quarks, their masses and quantum numbers, baryon numbers, charges, isospin projections, strangeness, charm, beauty, and truth.

Name	Mass (MeV)	b Number	q	i_3	s	c	b	t
u	5	1/3	2/3	1/2	0	0	0	0
d	7	1/3	−1/3	−1/2	0	0	0	0
s	150	1/3	−1/3	0	−1	0	0	0
c	1500	1/3	2/3	0	0	1	0	0
b	5000	1/3	−1/3	0	0	0	1	0
t	>100000	1/3	2/3	0	0	0	0	1

8.3.2 *Massless quark approximation*

We can also obtain analytic expressions if the quarks are massless, even if the temperature is finite. After some manipulation and using the standard integrals,

$$\int_0^\infty dx \frac{x}{1+e^x} = \frac{\pi^2}{12}, \quad \int_0^\infty dx \frac{x^3}{1+e^x} = \frac{7}{120}\pi^4, \tag{8.8}$$

we obtain the explicit forms

$$\begin{aligned} p &= \sum_f \Big(\frac{7}{60}\pi^2 T^4 + \frac{1}{2}T^2\mu_f^2 + \frac{1}{4\pi^2}\mu_f^4\Big) - B\,, \\ \epsilon &= 3p + 4B\,, \\ \rho &= \sum_f \frac{1}{3}\Big(T^2\mu_f + \frac{\mu_f^3}{\pi^2}\Big)\,, \\ s &= \sum_f \Big(\frac{7}{15}\pi^2 T^3 + T\mu_f^2\Big)\,. \end{aligned} \tag{8.9}$$

For the massless Bose gas of gluons of degeneracy $\gamma_g = 2 \times 8_c$, we similarly obtain the contributions

$$\begin{aligned} p &= \frac{8\pi^2}{45}T^4\,, \\ \epsilon &= 3p\,, \\ s &= \frac{32\pi^2}{45}T^3\,, \end{aligned} \tag{8.10}$$

where we use

$$\int_0^\infty \frac{x^3\,dx}{e^x - 1} = \frac{\pi^4}{15}\,. \tag{8.11}$$

As an example, the pressure for massless quarks and gluons is found from the above results to be

$$p = \frac{8\pi^2}{45}T^4 + \sum_f \Big(\frac{7}{60}\pi^2 T^4 + \frac{1}{2}T^2\mu_f^2 + \frac{1}{4\pi^2}\mu_f^4\Big) - B\,, \tag{8.12}$$

with $\epsilon = 3p + 4B$ and no changes in ρ or s.

The lowest-order gluon interactions have been calculated [387]–[389] and result in the following modification:

$$p = -B + \frac{8\pi^2}{45}T^4\left(1 - \frac{15\alpha_s}{4\pi}\right) + \sum_f\left[\frac{7}{60}\pi^2T^4\left(1 - \frac{50\alpha_s}{21\pi}\right) + \left(\frac{1}{2}T^2\mu_f^2 + \frac{1}{4\pi^2}\mu_f^4\right)\left(1 - \frac{2\alpha_s}{\pi}\right)\right] \quad (8.13)$$

with corresponding changes in ϵ, $s = \partial p/\partial T$, and $\rho = \frac{1}{3}\sum_f \partial p/\partial\mu_f$. The coupling constant is denoted by α_s.

8.3.3 First order in α_s

The thermodynamic potential to first order in the strong interaction coupling constant has been obtained in the literature (see [381] and references therein). Renormalized at the scale σ, the result is

$$\begin{aligned}\Omega_f = -\frac{\gamma_f}{24\pi^2}\Bigg\{&\mu_f\sqrt{\mu_f^2 - m_f^2}\left(\mu_f^2 - \frac{5}{2}m_f^2\right) + \frac{3}{2}m_f^4\ln\left[\frac{\mu_f + \sqrt{\mu_f^2 - m_f^2}}{m_f}\right] \\ &- \frac{2\alpha_s}{\pi}\Bigg[3\left(\mu_f\sqrt{\mu_f^2 - m_f^2} - m_f^2\ln\left[\frac{\mu_f + \sqrt{\mu_f^2 - m_f^2}}{\mu_f}\right]\right)^2 \\ &- 2\left(\mu_f^2 - m_f^2\right)^2 - 3m_f^4\ln^2\left(\frac{m_f}{\mu_f}\right) \\ &+ 6\ln\left(\frac{\sigma}{\mu_f}\right)\left(\mu_f\sqrt{\mu_f^2 - m_f^2}m_f^2 - m_f^4\ln\left[\frac{\mu_f + \sqrt{\mu_f^2 - m_f^2}}{m_f}\right]\right)\Bigg]\Bigg\},\end{aligned} \quad (8.14)$$

where μ_f and m_f denote the chemical potential and mass of the quark flavor f ($f = u, d, s, c$) and $\gamma_f = 2 \times 3_{\text{color}}$ is the degeneracy. (A sign error in the quoted literature has been corrected in the above expression for Ω_f.) The renormalization scale σ should be typical of the chemical potentials of the problem, and we set $\sigma = 300$ MeV. The thermodynamic potentials for the electron (0.511 MeV) and muon (106 MeV) are given also by the above expression with the omission of the α_s terms and the replacement of the degeneracy factor γ_f by that of the leptons, $\gamma_\lambda = 2$. The quark number densities, baryon number density, charge density, energy density, and pressure are given by

$$n_f = -\partial\Omega_f/\partial\mu_f\,, \quad (8.15)$$

$$\rho = \frac{1}{3}\sum_{u,d,s,c} n_f\,, \quad (8.16)$$

$$q = \sum_i n_i q_i\,, \quad (8.17)$$

$$\epsilon = B + \sum_i (\Omega_i + \mu_i n_i)\,, \tag{8.18}$$

$$p = -B - \sum_i \Omega_i\,, \tag{8.19}$$

where the sums over i extend over all four[1] quarks and the two leptons. The difference in the vacuum energy of confined and deconfined phases is denoted by B, and q_i denotes the electric charge on particle type $i = u, d, s, c, e^-, \mu^-$. It is easy to verify that the above results coincide with our earlier $T = 0$ expressions when $\alpha_s = \sigma = 0$.

8.4 Quark Star Matter

As an example, we illustrate hypothetical stars made of quark matter. (We will discuss this topic at a more advanced level in the next two chapters.) We have discussed the fact that stars are charge-neutral and in equilibrium; that is, they are a mixture of species in chemical equilibrium at a given temperature (effectively zero for a mature neutron star) and therefore in the lowest energy state at every density. Because the timescale of a star is effectively infinite compared to the weak interaction timescale, weak interactions violate strangeness conservation. The strangeness quantum number of quarks is therefore not conserved in a star. Any neutrinos or photons produced in the decay of a high-momentum u or d quark, near the top of the Fermi surface, to a low-momentum s quark will leak out of the star. The star's energy is thereby lowered both by loss of the neutrino and photon energy and by lowering of the average energy of the quarks. Chemical equilibrium is therefore found without regard to the conservation of quark strangeness. In other words, the strangeness chemical potential is set identically to zero.

We have derived expressions for the pressure and energy density of quark matter in terms of the quark chemical potentials above. To the energy density and pressure of quark matter, we need to add those of leptons so that charge neutrality can be achieved at the lowest energy. Expressions for these contributions can be found in the last terms of (5.50) and (5.51).

Let us consider how the chemical potentials are to be determined. According to the above discussion of strangeness nonconservation, the relationships between the quark chemical potentials are determined solely by conservation of electric charge and baryon charge. Possible transformations that conserve these charges (and not strangeness) can be inferred from Table 8.1:

$$\mu_u = (\mu_b - 2\mu_e)/3\,, \quad \mu_d = (\mu_b + \mu_e)/3\,, \quad \mu_s = (\mu_b + \mu_e)/3\,, \tag{8.20}$$

where, as usual, μ_e stands for the electron chemical potential (unit negative charge) and μ_b stands for the chemical potential for unit baryon charge (i. e., neutron,

[1] We keep the charm quark only to be able to demonstrate later that it is not a constituent of stable stars.

sometimes also denoted μ_n). From these we have the connections

$$\mu_d = \mu_u + \mu_e\,, \quad \mu_s = \mu_d\,, \quad \mu_c = \mu_u\,. \tag{8.21}$$

We can write the expression for the electric charge density of the quarks analogous to (8.6) and, taking account of leptons, write the condition for charge neutrality as

$$q = \sum_f \left(q_f \frac{k_f^3}{\pi^2}\right) - \frac{k_e^3}{3\pi^2} - \frac{k_\mu^3}{3\pi^2} = 0\,. \tag{8.22}$$

The last two terms are the lepton contributions and

$$k_f = (\mu_f^2 - m_f^2)^{1/2}\,, \quad k_e = (\mu_e^2 - m_e^2)^{1/2} \tag{8.23}$$

are the Fermi momenta of the quark flavors and the electron. Finally, the expression for the baryon number density in (8.6) or (8.15) provides a fifth relationship for the chosen density with which the six chemical potentials μ_u, μ_d, μ_s, μ_c, μ_e, and μ_μ can be determined at specified baryon density.

Knowing the quark chemical potentials, we can now compute the pressure and energy density of the quarks. Because the electron mass is small, it can be neglected or kept in expressions similar to (8.6) or (8.15–8.19) for the electron energy density and pressure contributions. The B should be dropped and electron statistical weight 2 substituted for quark weight 6; that is, multiply p and ϵ by 1/3. The result is then added to the pressure and energy of the quarks to get the total. The procedure is similar for the muon whenever μ_e exceeds the muon mass. This provides a complete description in the approximation of the bag model to the equation of state for quark star matter.

Figure 8.1 shows three sequences of quark stars. We have taken the quarks to be massless. The scaling rules of Section 3.16 apply in this case because of the form of the equation of state, $p = (1/3)(\epsilon - 4B)$.

8.5 Strange and Charm Stars

8.5.1 General considerations

At first sight, the notion of pure quark matter stars may seem unrealistic. The normal expectation is that the phase of quarks confined in nucleons is the ground state of the strong interaction. Quark matter, if present in a neutron star, would exist only in the high-density interior. However, it is possible that three-flavor quark matter consisting of u, d, and s quarks may actually be the ground state of the strong interaction [93, 380]. In such a case, there could exist pure quark matter stars. We shall examine the *strange quark matter hypothesis* carefully in Chapter 12. In the meantime we use the simple equations of state developed above to discuss quark stars as hypothetical objects and contrast several of their features with neutron stars. (As a side issue, our study will be useful in bringing out some general points on stability.)

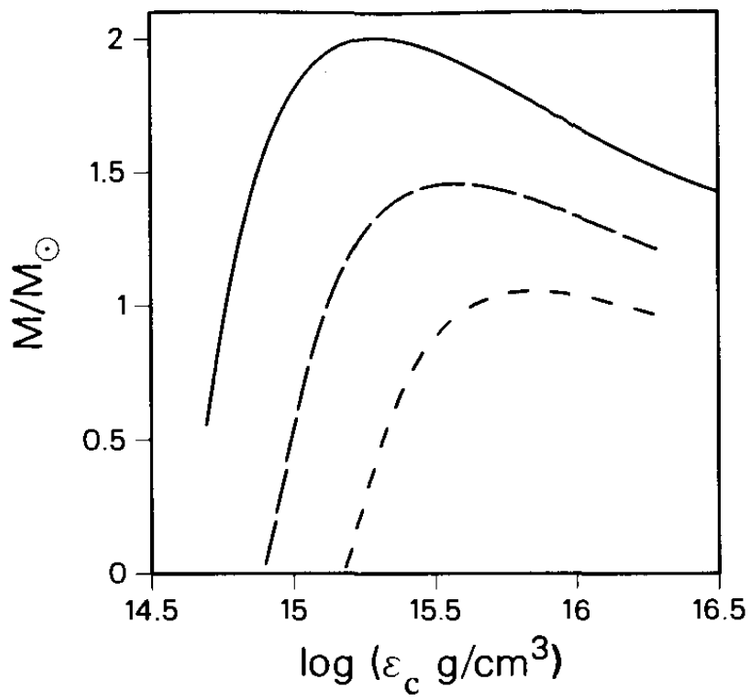

FIGURE 8.1. Three strange quark star sequences (massless quarks). Values of $B^{1/4}$ from top to bottom are 145, 170, and 200 MeV, respectively.

We employ the equation of state described above for cold quark star matter to compute the structure of quark stars. This is done by solving the Oppenheimer–Volkoff equations (3.27, 3.28) with the above equation of state for the pressure and energy density [390]. At low and moderate baryon densities (which we estimate from (8.6), putting $m_f = 0$ for ease), we shall find that the chemical potential for strange quarks (8.21) is larger than the strange quark mass. The strange quark must therefore be included in the description of quark stars having the density range typical of neutron stars.

The charm quark chemical potential (8.21) does not approach the magnitude of the charm quark mass in the same density range. Consequently, the charm quark is not populated except at density far above that found in neutron or analogous strange stars.[2] One is naturally led to ask if there is a sequence of stable charm stars above the neutron or strange star sequences. We address this question later in the chapter.

In the bag model of quark matter, the value of B determines whether strange quark matter has a lower ground state than hadronic matter in the confined phase. We will choose a value that yields a binding per baryon number $E/A \approx 928$ MeV for strange quark matter in equilibrium ($p = 0$). This value is slightly lower than the mass of the nucleon (and also of the energy per nucleon in the Fe^{56} nucleus ($\sim$ 931 MeV)). The value of B that yields $E/A = 928$, making strange matter

[2]We shall call a quark star after the most massive quark flavor with which it is populated. A strange star is composed of the three quark flavors u, d, s; a charm star of four flavors u, d, s, c.

absolutely stable[3] (but just barely), is

$$B^{1/4} = 154.5 \text{ MeV}$$

as in Fig. 1(a) of Ref. [381] for $m_s = 150$ MeV. In this case the star is devoid of nuclear matter. The entire compact star, including its surface region, is (strange) quark matter.

The edge of a star occurs at the radius where the pressure becomes zero. Zero pressure in the equation of state corresponds to equilibrium matter or else to zero density. Under the assumption of a bag constant that makes strange matter the absolute ground state, zero pressure corresponds to the equilibrium energy density of strange quark matter. Therefore the transition in a strange quark star at its edge is from a high interior density to zero on a length scale characterized by the strong interaction range—10^{-13} cm. The density at the inner edge is twice or more that of nuclear density ($\epsilon_0 \sim 2.5 \times 10^{14}$ g/cm^3; see (8.24) below). The strange star has an extremely abrupt edge; it probably has the hardest smoothest surface of any object in the universe.[4]

The edge of a neutron star is not nearly so abrupt as that of a strange star. Because neutron stars are made from material that has been processed in stellar evolution, ordinary iron forms their surface (page 84). The energy density of iron is only a few g/cm^3, or about 14 orders of magnitude less than the central energy density of the star. The density profile of a neutron star in contrast to a strange star therefore falls continuously from nuclear density to the density of iron. At the latter density, there is an abrupt transition to zero density on a length scale of atomic spacing in solid iron.

The density profile of three strange stars of differing mass are illustrated in Fig. 8.2. These results are similar to results of Haensel et al. [378] and of Alcock et al. [379]. Stellar edges all occur at $p = 0$ and therefore at the same (high) energy density corresponding to equilibrium. The stellar interiors are more or less compressed according to mass (weight of the overlying matter). The quark populations of the most massive of them are shown in Fig. 8.3. There we see that electron populations are five orders of magnitude less than quark populations. This is another example in which charge neutrality is achieved more economically among the conserved baryon-carrying particles.

---

[3]For values of $B^{1/4}$ less than 154.5, strange matter becomes more strongly bound (when $m_s = 150$ MeV). Finally, for $B^{1/4} < 145$ MeV, nonstrange quark matter is absolutely stable. Such values are therefore not compatible with observed nuclei, which are describable in terms of nonstrange nucleons.

[4]The skin thickness of a nucleus is also of the same order as that of a strange star, 10^{-13} cm. The cause is the same in each case—the range of the force that binds—the strong force. It is only the small radius of the one and the large radius of the other that makes the skin thickness of the star seem unusually small. Given the short range of the strong interaction, it is of course immaterial to the skin thickness how much matter lies interior to the skin.

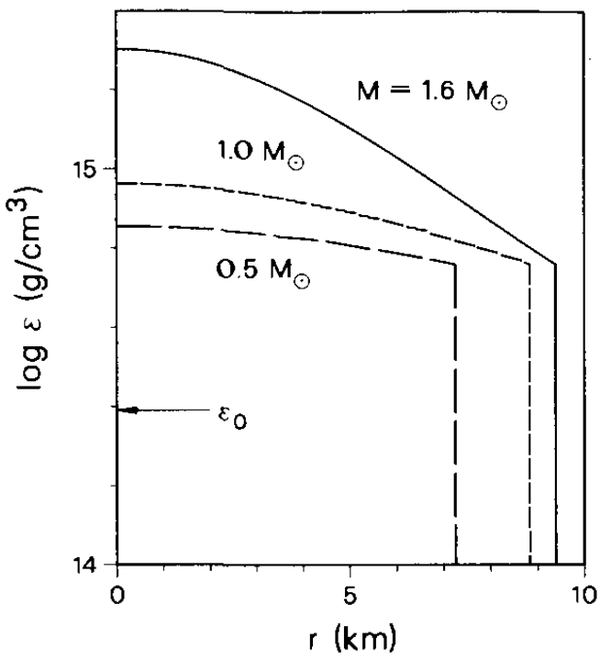

FIGURE 8.2. Density profiles of three strange quark stars of indicated masses. ($B^{1/4}$ = 154.5 MeV and $m_u = m_d = 0$, m_s = 150 MeV).

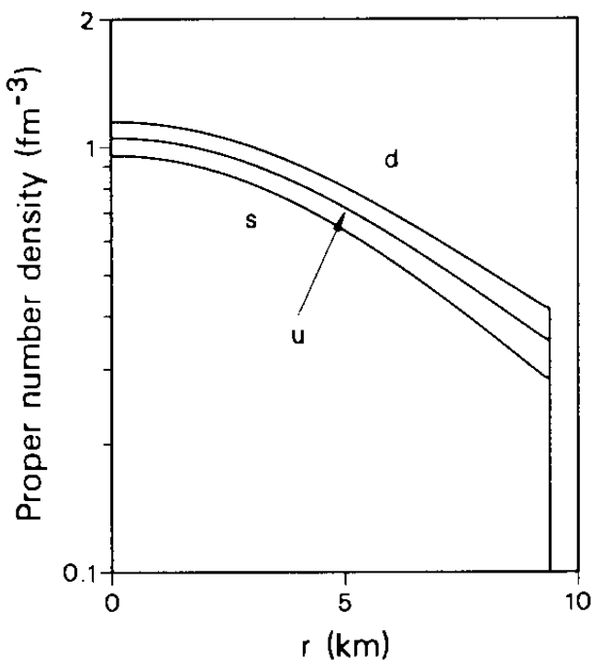

FIGURE 8.3. Quark populations of a $M = 1.6M_\odot$ strange star (close to the limiting mass of $1.64M_\odot$). The electron population lies far below the scale.

8.5.2 *Strange quark matter*

We use the massless quark approximation and zero temperature to discuss some of the results found above. This approximation should give a reasonable description at densities such that the chemical potentials are larger than the masses. From (8.9) we have that $\epsilon = 4B$ at equilibrium ($p = 0$) which occurs at the edge of the star. Translate this to nuclear units using $1 = \hbar c = 197.3$ MeV-fm, and find

$$\epsilon = 4B \sim \frac{4(154\ \text{MeV})^4}{(197\ \text{MeV}\cdot\text{fm})^3} \sim 300\ \text{MeV/fm}^3 \sim 5\times 10^{14}\ \text{g/cm}^3\,. \quad (8.24)$$

This is a little more than twice the energy density of normal nuclear matter (see the section in Chapter 3 on units). It is 14 orders of magnitude greater than the energy density at the edge of a neutron star, namely, the energy of ordinary solid iron (≈ 7.8 g/cm^3). So the density distribution of a strange quark star is quite unusual compared to that of a neutron star or any other star.

Aside from the first few moments of the life of the star, we can take $T = 0$. When we approximate the u, d, and s quark masses as zero, matter made from an equal population of each is identically charge-neutral; therefore $\mu_e \equiv 0$. From the expressions for the density and the pressure (8.6), we then obtain, at the edge of the star ($p = 0$),

$$\mu_u = \mu_d = \mu_s \equiv \mu = \left(4\pi^2 B/3\right)^{1/4} = 1.9B^{1/4}\,. \quad (8.25)$$

We see that the chemical potential is about twice the strange quark mass in this approximation (it would be even larger had a finite strange quark mass been used in the estimate of μ). Consequently, strange quarks will be present, even at the edge of the star, in almost the same number as u and d quarks, not only in its

higher-density interior. In the same approximation, the baryon number density is

$$\rho = \mu^3/\pi^2 = 0.33 \text{ fm}^{-3} \tag{8.26}$$

which is about twice normal nuclear density. The energy per baryon number is

$$\epsilon/\rho = \left(108\pi^2 B\right)^{1/4} = 5.7B^{1/4} = 880 \text{ MeV}. \tag{8.27}$$

This is smaller than the energy per nucleon in Fe required to make strange matter absolutely stable. We call such stable matter, with an approximately equal number of u, d, and s quarks, *strange quark matter*, or simply strange matter.

For a star governed by the simple equation of state $\epsilon = 3p + 4B$, the Oppenheimer–Volkoff equations take on a universal form independent of bag pressure when the following scaling is made [93, 94]:

$$\overline{p} = p/B, \quad \overline{\epsilon} = \epsilon/B, \quad \overline{r} = \sqrt{B}\, r, \quad \overline{M} = \sqrt{B}\, M. \tag{8.28}$$

In terms of the radii and masses of one sequence of stars, the radii and masses for any other choice of B can be found from

$$R(B') = \sqrt{B/B'}\, R(B), \qquad M(B') = \sqrt{B/B'}\, M(B). \tag{8.29}$$

8.5.3 Stability considerations

In Fig. 8.4 the sequence of star masses as a function of central density is shown for the above choice of B. The lower curve is the gravitational mass of the star

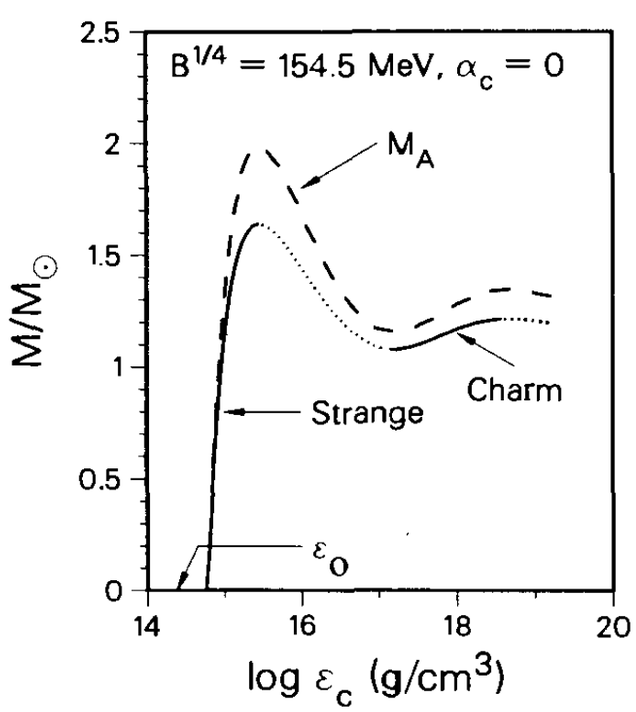

FIGURE 8.4. Gravitational mass of strange and charm stars compared to mass at infinity M_A of the equivalent number of neutrons corresponding to the quark number.

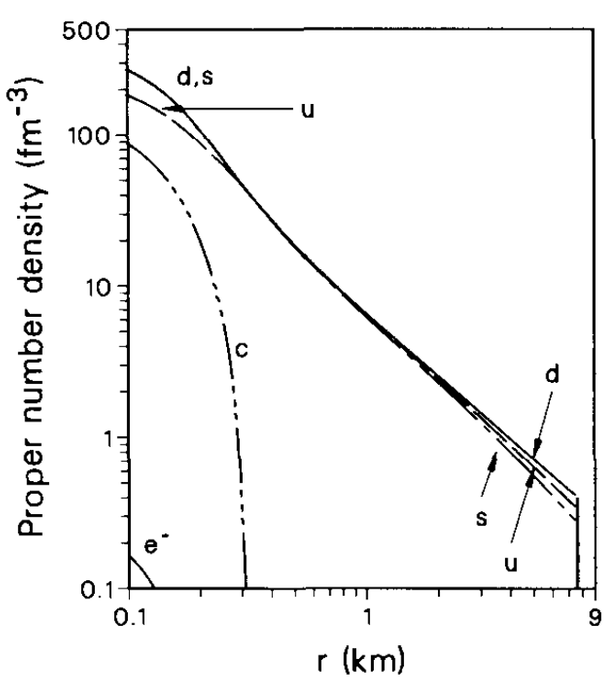

FIGURE 8.5. The distribution of quarks in a charm star near the limiting mass of the family ($m_u = m_d = 0$, $m_s = 150$ MeV and $m_c = 1500$ MeV).

defined in (3.28), that is,

$$M = 4\pi \int_0^R \epsilon(r) r^2 \, dr \, . \tag{8.30}$$

The upper curve is the mass of the equivalent number of baryons if the star were disassembled into neutrons at infinity, and is often referred to as the baryon mass of the star. It is obtained by integrating the baryon number density over proper volume (3.150) and multiplying by the neutron mass m_n:

$$M_A = 4\pi m_n \int_0^R \rho(r) \left[1 - \frac{2M(r)}{r} \right]^{-1/2} r^2 \, dr \, . \tag{8.31}$$

Such stars are stable against disassembly of their equivalent number of neutrons at infinity because the gravitational mass always lies below the baryon mass M_A. This is in contrast to the analogous high-density family of neutron stars studied in the 1960s [391].

On the gravitational mass curve as a function of central density, the regions of positive slope satisfy the necessary condition for stability (Section 3.18). The first sequence of stars with increasing mass as a function of central density can properly be called a strange star sequence, because these stars are an approximately equal mixture of u, d, and s quarks. What of the next sequence having a positive slope which in addition contains the charm quark? An analogous sequence can be found for neutron stars by integrating the Oppenheimer–Volkoff equations to high density. However, stability studies carried out in the early 1960s showed that all configurations with central densities greater than that of the limiting neutron star are unstable to long-wavelength radial vibrations. Such vibrations carry high-density matter in the stellar core across its Schwarzschild radius; collapse to a black hole results [28]. A glance at Fig. 8.5 showing the very steep rise of the particle density (and therefore also mass density), suggests that these stars are indeed of the type of high-density star discussed by Harrison et al. [28] as being unstable to acoustical vibrations. This is also true for charm stars as we now show [198].

The pulsations of stellar configurations can be analyzed in terms of normal modes with time dependence $e^{\pm i\omega_n t}$. Unstable modes are those for which ω_n^2 is negative. (In this case there is an exponentially growing term $e^{Im(\omega_n)t}$. A term with positive exponential time dependence implies unbounded growth of the mode.) As we saw in Section 3.174, the modes are ordered $\omega_n^2 < \omega_{n+1}^2$. A function of ω_n^2 which is negative when the squared frequency is negative is shown in Fig. 8.6. We see that the lowest (nodeless) mode becomes unstable at the limiting mass of strange stars. Successive modes ($n = 1, 2, \ldots$) become unstable at those turning points that occur at increasing central density. Charm stars are therefore unstable, at least in the present model of quark matter. The high masses and the likely smooth behavior of the equation of state at very high density in the quark regime are likely to make the above conclusion quite general.

An interesting study of stability can be found in Ref. [28]. There it is shown that a denumerable infinity of oscillations exists in the mass–density plot of compact stars described by a polytropic equation of state. While the polytrope is an idealization

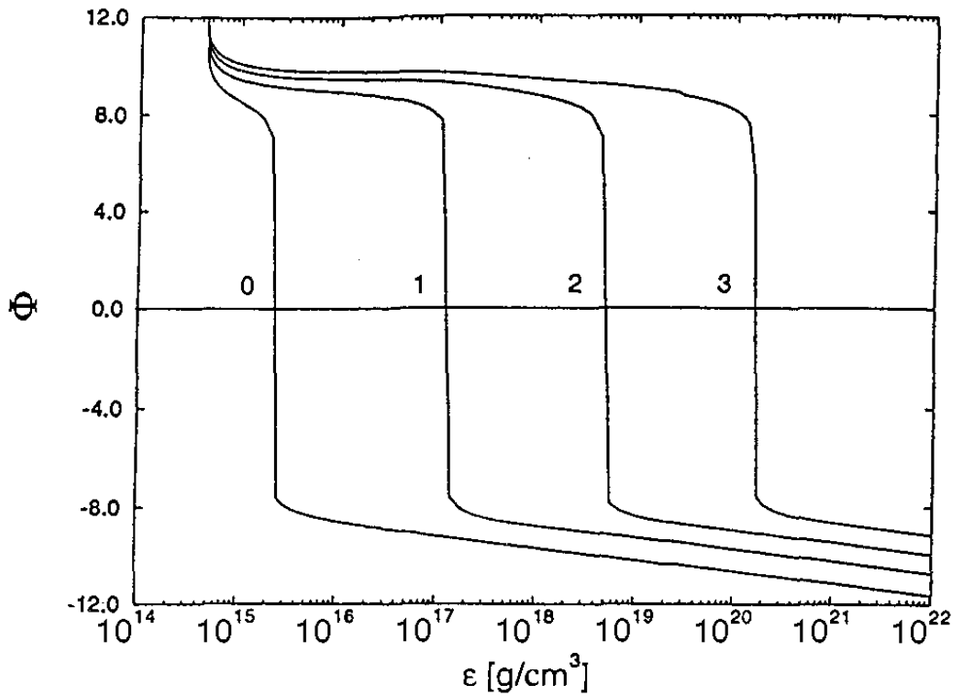

FIGURE 8.6. Pulsation frequencies for the lowest four ($n = 0, 1, 2, 3$) modes of quark stars as a function of central density. For convenience we plot $\Phi(x) \equiv \text{sign}(x)\ \log(1 + |x|)$ where $x \equiv (\omega_n/\text{sec}^{-1})^2$ as the abscissa. For $\Phi < 0$, the squared frequency is negative and the mode unstable. (From [198].)

of the equation of state, it has the common property of many realistic ones—that the the pressure is a rather smooth function of energy density. Presumably the theorem proven for polytropes, for which an analytic treatment of the vibrational modes can be performed, holds for any *sufficiently* smooth equation of state. The lowest (nodeless) mode becomes unstable at the maximum of the stable sequence of neutron stars. An additional higher mode becomes unstable at each higher density where $dM/d\epsilon_c = 0$.

There is no reason to expect a different result for quark stars. The first two maxima for quark stars seen in Fig. 8.4 are the beginning of such an infinite series. All save the first (which are strange stars) are unstable. Here we have shown by numerical means that the theorem holds for quark stars out to the first maximum in the mass that lies beyond the last of the stable stars (Fig. 8.6). However, because the quark matter equation of state, (8.6), takes the form $p = (\epsilon - 4b)/3 \approx \epsilon/3$ for very high density, it is asymptotically a polytrope with $\gamma = 1$. Consequently the theorem proven by Wheeler et. al. holds for certain and ensures that charm and higher flavor quark stars cannot exist.

8.6 Problems for Chapter 8

1. Why does B have the opposite sign in the expression for p and ϵ in (8.2)?
2. Derive the Fermi energy part (absent the thermal factors of energy density and pressure (8.2) by writing the the Lagrangian for free quarks of mass m_f.
3. Derive the results (8.9)–(8.12).
4. Derive the results (8.24)–(8.27.
5. Derive the scaling rule (8.29).

9

Hybrid Stars

"There is no excellent beauty that hath not some strangeness in its proportion."
Sir Francis Bacon

9.1 Introduction

Quark matter no doubt pervaded the universe, just after the Big Bang, sometime in the first few seconds. It may exist naturally today in the cores of neutron stars. The possibility was considered many years ago in the pioneering research of several authors (Itoh [392], Baym and Chin [393], Chapline and Nauenberg [394], and Keister and Kisslinger [395]). The earliest estimates suggested that nuclear matter would not convert to quark matter unless densities of the order $10\rho_0$ were achieved [393]. Such densities are only marginally attainable in stellar models, so for some years the existence of quark matter in neutron stars seemed doubtful.

The very high deconfinement density found in the early work of Baym and Chin can be traced in part to the very stiff hadronic matter equation of state that was employed ($K \approx 550$ MeV). We now believe that quark matter—the deconfined[1] phase of quarks—is quite likely to occupy the inner regions of the more massive

[1]Of course, we mean deconfined in the sense that the density or temperature of matter is so high that individual nucleons have dissolved into uncorrelated quarks that are free to explore the larger region of dense or hot matter. The whole region is colorless, and the liberation of individual quarks is not implied.

neutron stars. We can make a crude estimate of the baryon density at which deconfinement of quarks may occur. The rms charge radius of a proton is 0.8 fm. If nucleons were closely packed as spheres to the point of touching at this radius, the density would be $\rho \sim (1.6\ \text{fm})^{-3} = 0.24\ \text{fm}^{-3}$. It is therefore plausible that quarks lose their correlation with individual nucleons at densities not much higher than nuclear density ($0.15\ \text{fm}^{-3}$).

In earlier chapters we studied nuclear matter and quark matter as separate states of hadronic matter, understanding that under certain conditions of the thermodynamic variables, matter would be in one state or the other. The actual state will depend on the circumstances such as the temperature or density. Generally we consider a neutron star to be cold on the nuclear scale and take $T = 0$. The density, however, varies from a small value at the surface to a large value at the center of a star. In the lower density region, matter will be in its confined phase, which we refer to as nuclear or hadronic matter. At high density, nearer the core of the star, matter may be in its deconfined quark matter phase. However, matter need not be homogeneous. For a certain range of intermediate baryon densities, both phases may be in equilibrium with each other. This condition is familiar in the case of water when the liquid and solid phases are in equilibrium with each other. Such an inhomogeneous state is referred to as the *mixed* or *coexistence* phase.

In studying the phases of matter and the conditions for a change in phase, we often refer to a definite quantity or volume of matter. We recall that even in a dense neutron star, locally inertial regions extend over an enormous number of internucleon spacings (Section 3.4). As a consequence, we can always discuss the state and phases of matter in flat spacetime and for bulk matter. The results are inserted into Einstein's equations in the form of the energy–momentum tensor to find how the matter is arranged by gravity and how in turn matter acts on spacetime.

The most familiar phase transition is the vapor–liquid or liquid–solid transition in water. It is one that takes place at constant pressure and temperature. In early research—and even in quite recent work on phase transitions in neutron stars—a certain simplification in some models and approximations in others rendered phase transitions in neutron stars as the constant pressure type,[2] analogous to phase transitions in H_2O. However, as we discuss below, the constancy of pressure and temperature for all proportions of the two phases in equilibrium, is a special case that is particular to simple substances having a single component, like water. Because pressure varies monotonically in a star, the mixed phase was strictly excluded from a neutron star in all of this research [393]–[402]. Generally the pressure varies as the volume proportion of phases in equilibrium varies [194, 195]. Exclusion of the mixed phase because of the simplification or approximations of the early work on phase transitions had a profound effect on the predicted stellar structure.

[2]This was the case for all phase transitions considered, deconfinement, and pion and kaon condensation.

Quark matter may exist in a neutron star in two forms according to the density range spanned by the star. The core of the star may be composed of the pure quark matter phase surrounded by a shell of mixed phase in which quark and hadronic matter are interspersed spatially and in phase equilibrium with each other. This region is surrounded in turn by a shell of purely hadronic matter such as we discussed in Chapter 5. If this structure should exist in the more massive neutron stars, then for less massive ones the radius of the quark core will be smaller; at some lower mass, the pure quark phase will be absent altogether; the central part will contain the quark phase only as a component of the mixed phase. The lightest stars will contain no quark matter at all; they will be purely neutron stars [194, 195, 403].

We call neutron stars with quark or mixed-phase interiors *hybrid stars* when the quark aspect is emphasized [327]. They are otherwise a variation of the concept of neutron stars, just as hyperon stars are a variation. In both cases the particle populations are a smooth and continuous function of the central density. We show several sequences of hybrid stars displayed in two ways: with mass as a function of central density in Fig. 9.1, and radius as a function of mass, in Fig. 9.2. The inflection in the curves around $M \sim .85 M_\odot$ marks the mass above which a mixed phase occurs in the star. Stars below this mass are neutron (hyperon) stars. Those above are hybrids, containing a neutron matter outer shell surrounding a region of mixed phase, and in some cases, a pure quark matter inner core.

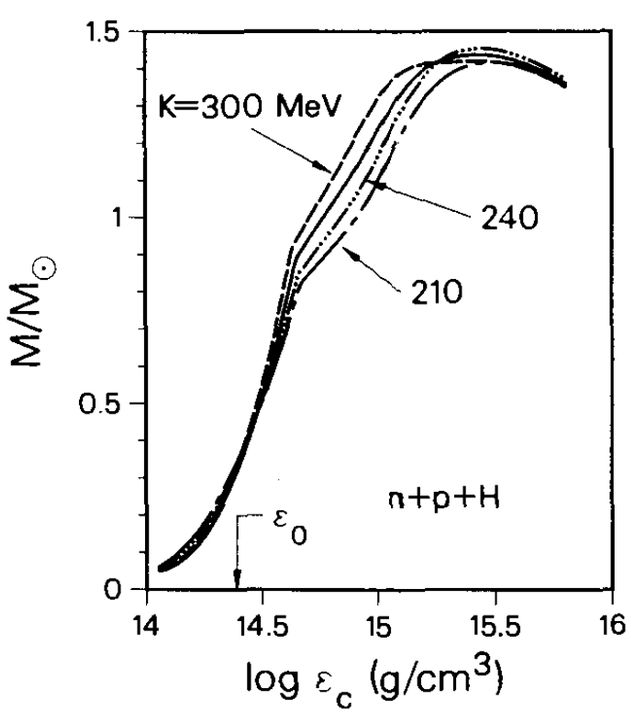

FIGURE 9.1. Four sequences in which the more massive stars above $M \sim .85 M_\odot$ are hybrids. The dashed and solid lines have $m^*/m = 0.7$ and 0.78, respectively. Couplings and parameters are in Table 5.5.

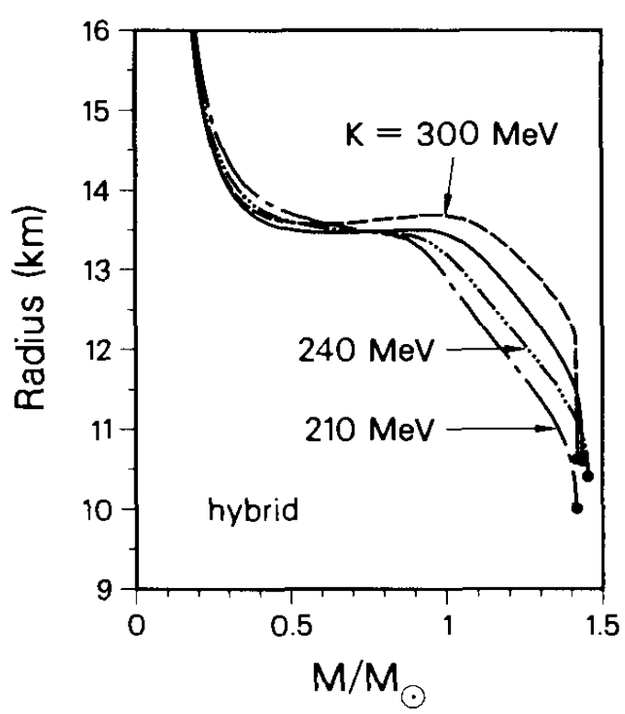

FIGURE 9.2. The same four sequences shown in Fig. 9.1, are diplayed here by the mass–radius relation. The lower-mass stars, as noted in the text, are purely neutron stars; the others contain the mixed phase and in some cases the pure quark phase at highest density.

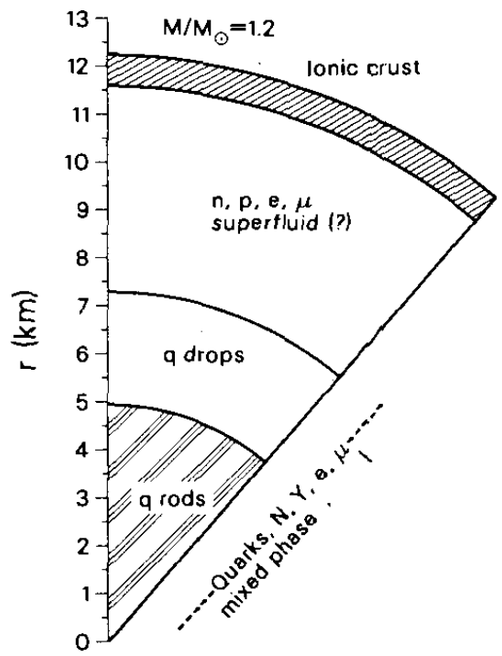

FIGURE 9.3. Section through a star containing geometrical mixed phases of nuclear and quark matter. The geometries are idealized as drops, rods and slabs, Compare with Fig. 1.1.

The mixed phase of confined and deconfined matter is most unusual, as has recently been discovered [194, 195], [404]–[406]. It is expected to form a crystalline lattice. The rarer phase, having various geometric forms, is located at lattice points immersed in the dominant phase. The forms vary in size and spacing according to the density and therefore distance from the center of a star (see Figs. 1.1 and 9.3). The notion of a crystalline lattice that occupies the *crust* of a neutron star is familiar. In the crustal region interior to the edge of the star at densities high enough to ionize atoms, the nuclei are immersed in a background of electrons and assume a crystalline lattice so as to minimize the sum of Coulomb and surface energies. What is unusual about the crystalline mixed phase of confined–deconfined matter is that the two forms of matter are simply different phases of one and the same substance, not different substances like nuclei and an electron gas.

The formation of a lattice in the confined–deconfined mixed phase occurs because the two phases in equilibrium are driven by the isospin symmetry energy of nuclear matter to have opposite charges. This does not violate the condition that a star must be electrically neutral. Charge neutrality of the star will be achieved *globally* [$\int \rho_c(r) d^3r = 0$], not *locally* [$\rho_c(r) \equiv 0$] if that is energetically favored.[3] The distinction was not recognized in earlier work [393]–[402]. Nor was the distinction between first-order phase transitions in single and multicomponent substances recognized.

The crystalline structure of the mixed phase varies in geometry throughout the region that it occupies in neutron stars. There are likely consequences for all transport properties as well as for pulsar glitches. In this chapter we will discuss the general properties of phase transitions in multicomponent substances, of which,

[3]An atom is a familiar example of a system that is neutral, but whose charge density is finite, i.e., globally neutral. A locally neutral atom would be a very highly excited state indeed.

neutron star matter is our special interest. And we will provide the physical reasons and the mathematical demonstration for crystalline structure in neutron stars, including a calculation of the geometrical forms of the lattice, their dimensions and spacings.

Although the discussion of this chapter holds in general, we will illustrate our discussion with reference to the deconfinement phase transition between nuclear and quark matter. In Chapter 10, we will discuss Bose condensation, in particular, kaon condensation. Following that, we devote a chapter to special manifestations or consequences of phase transitions in neutron stars, which include a class of low-mass black holes, a possible new family of compact stars more dense than neutron stars, and a possible signal of the occurrence of a phase transition in a neutron star which would be very easy to observe.

9.2 Constant-Pressure Phase Transition

As stated above and proven below, the confined–deconfined phase transition is not expected to occur at constant pressure. Nonetheless, it is interesting to examine the consequences of the assumption of constant pressure so as to contrast the results with those for a variable pressure phase transition characteristic of multicomponent substances. The first case is familiar, the second not.

In the early literature, first order phase transitions were forced into the constant-pressure mold by one or other of two approximations, neither of which is valid. Some authors treated neutron stars as being purely neutron. Aside from the fact that such a star would be beta unstable, the approximation probably seemed innocuous. Still other authors respected beta equilibrium of neutron stars, at least to the extent of including protons and electrons, but failed to ensure the continuity of the electron chemical potential at the interface of the two phases. Again, the star described in such a way is unstable because of the potential difference between the phases at their interface. Because the pressure in a star is monotonic, the constant pressure region corresponding to the mixed phase was excluded from all such models. We discuss both approximations in turn.

9.2.1 Purely neutron star

A star made purely of neutrons is, of course, a one-component substance. A familiar example of such a substance is the textbook example of the liquid–vapor transition in water, where the single conserved "charge" or independent component is H_2O. First-order phase transitions in simple substances have well-known properties. As the substance is compressed at constant temperature or cooled at constant pressure, it begins condensing the other phase at a certain point. This phase of partial transformation from one pure phase to another, assumed to be in equilibrium, is referred to as the mixed or coexistence phase.

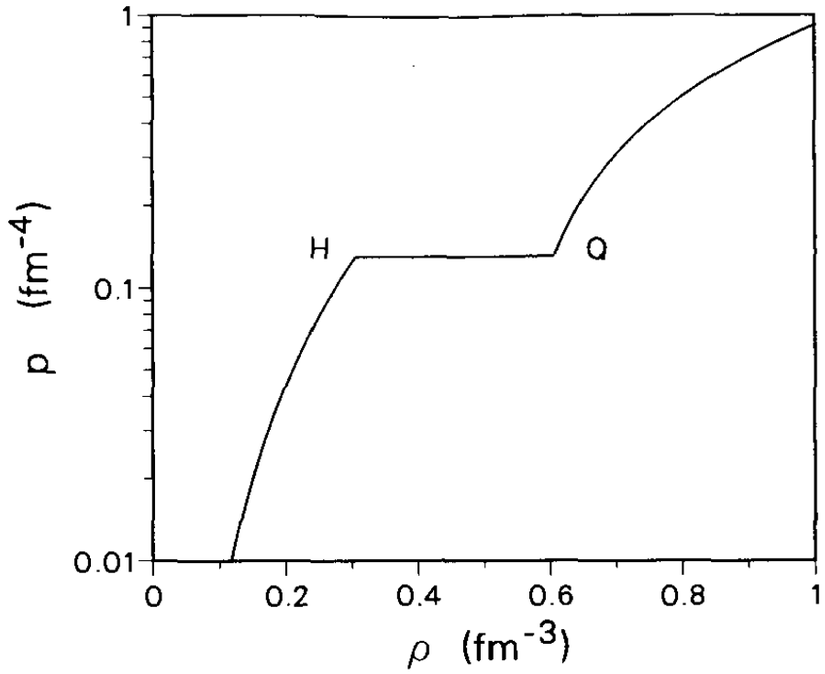

FIGURE 9.4. Behavior of pressure vs. density in the vicinity of a first-order phase transition in a simple substance having one chemical potential corresponding to conserved baryon number. Points labeled H and Q mark the end of the hadronic and beginning of the quark phase, the region between being the mixed phase. See text for further description and also Eq. 9.4

A second notable property of a simple substance is that the mixed phase consists of the two phases in their respective *unchanging* states, no matter what their proportions. The water–vapor transition is a familiar example. In Fig. 9.4 an example is shown of the constancy of the pressure of a first-order phase transition in a simple substance. This particular example is for pure neutron matter in equilibrium with u-d-s quark matter, which is also identically charge-neutral in the limit of massless quarks (as is the case in Fig. 9.4).

In the language of Gibbs, the two phases are in equilibrium when their (baryon) chemical potentials, temperatures, and pressures are equal, corresponding respectively to chemical, thermal, and mechanical equilibrium:

$$\begin{aligned} \mu_H &= \mu_Q = \mu \,, \\ T_H &= T_Q = T \,, \\ p_H(\mu, T) &= p_Q(\mu, T) = p \,. \end{aligned} \tag{9.1}$$

The subscripts H and Q denote the confined (hadronic) and deconfined (quark) phases. At constant temperature the last equation can be solved for the unique value of μ, independent of the proportion of the two phases in equilibrium. The graphical illustration of the solution shown in Fig. 9.4 is one of three ways of implementing the solution often referred to as the Maxwell construction. The other two ways are referred to as the "common tangent" and the "equal area" methods. The common value of the chemical potential which solves (9.1) specifies the constant, but unequal values of the energy density of each phase in equilibrium:

$$\epsilon_H \equiv \epsilon_H(\mu) \neq \epsilon_Q(\mu) \equiv \epsilon_Q \,. \tag{9.2}$$

Notice that because phase equilibrium is specified by a unique value of the single chemical potential μ for a single-component substance, all properties of each phase in equilibrium remain unchanged until the conversion of one phase to the other is complete. This is in accord with our common experience of the liquid–vapor or liquid–solid transition of H_2O.

The volume-weighted energy and baryon number density of the substance in the mixed phase, which we refer to for brevity as averages, are

$$\langle \epsilon \rangle = (1 - \chi)\epsilon_H + \chi \epsilon_Q \,, \tag{9.3}$$

$$\langle \rho \rangle = (1 - \chi)\rho_H + \chi \rho_Q \,. \tag{9.4}$$

Here $(1 - \chi)$ and $\chi \equiv V_Q/(V_Q + V_H)$ are the volume fraction of the hadronic and quark matter phases in coexistence. One can verify that these expressions, linear in χ, imply that the pressure ($p = -\partial E/\partial V$) is constant in the mixed phase of a simple substance, as we already know.

The pressure is shown as a function of the baryon (neutron) chemical potential in Fig. 9.5 for several cases as specified in the caption. If both phases were described in terms of the same theory instead of one theory for the hadronic phase and one for the quark phase, the two solid lines would be joined, as shown schematically by the dashed line. In other words, the pressure as a function of chemical potential turns back and crosses itself at the point of phase equilibrium. At that point, the pressure, temperature (here zero), and chemical potential are equal in the two phases.

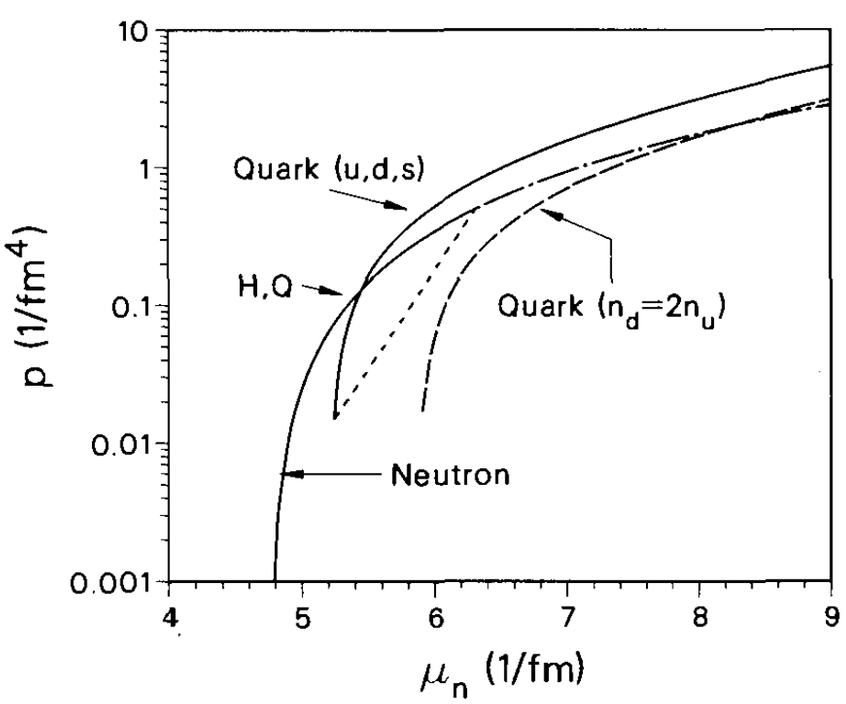

FIGURE 9.5. Pressure vs. baryon chemical potential for pure neutron matter, for u-d-s quark matter, and for quark matter with u-d quarks in the charge-neutral proportion indicated. Note the elevated chemical potential (and therefore baryon density) at which the latter curve crosses the neutron matter curve compared to that of equilibrated u-d-s quark matter. Note that here the points H and Q that denote the density of the beginning and end of the mixed phase in Fig. 9.4 coincide at the chemical potential common throughout the mixed phase in a simple substance [195].

The above properties lead to a particular structure for a star. We know from both the Newtonian and the Oppenheimer–Volkoff equations for stellar structure that the pressure is a monotonic decreasing function of the distance from the center of the gravitating object, just as in our atmosphere. Therefore, the equal pressure points (H and Q at the ends of the mixed phase of a simple substance and all points in between) would be mapped onto the same radial coordinate within the star. At that radial coordinate there would be a discontinuity in the density, $\Delta\epsilon = \epsilon_Q - \epsilon_H$, where the densities are given by (9.2). This is illustrated in Fig. 9.6 where matter interior to the radial point at H,Q would be purely quark matter, and juxtaposed and exterior to it would be purely hadronic matter, each at its respective equilibrium density.

9.2.2 *Enforced local charge neutrality*

If charge neutrality is enforced as a local constraint in the description of a first-order phase transition in a multicomponent substance, as has been frequently done in the literature, the transition is forced into the constant pressure mold. This can be seen as follows. The two conditions that describe the local vanishing of charge density are

$$q_H(\mu_b, \mu_q) = 0\,, \qquad q_Q(\mu_b, \mu_q') = 0\,. \tag{9.5}$$

Note that q_H and q_Q are *different* functions of the chemical potentials because the phases are different physically. Therefore, we can choose one of the chemical potentials to be common, say μ_b, but not both if we want each phase to have vanishing charge density. By insisting on local neutrality, we can solve the above two equations in the form

$$\mu_q = f(\mu_b)\,, \quad \text{and} \quad \mu_q' = g(\mu_b)\,. \tag{9.6}$$

Use these results in the Gibbs requirement for equality of pressure at equilibrium and find

$$p_H(\mu_b, f(\mu_b), T) = p_Q(\mu_b, g(\mu_b), T) = p\,. \tag{9.7}$$

We see that the problem has been reduced to one dimension: the pressure is a function of only one chemical potential. By demanding that each phase in equilibrium be separately charge-neutral—a demand that exceeds the global neutrality required by the physics—the phase transition has been made to resemble that of a simple substance. As in (9.1) the pressure remains constant independent of the proportion of the phases in equilibrium. It can be seen that the above demand of local neutrality is incompatible with Gibbs phase equilibrium, because one of the chemical potentials is forced to be discontinuous, as in (9.6).

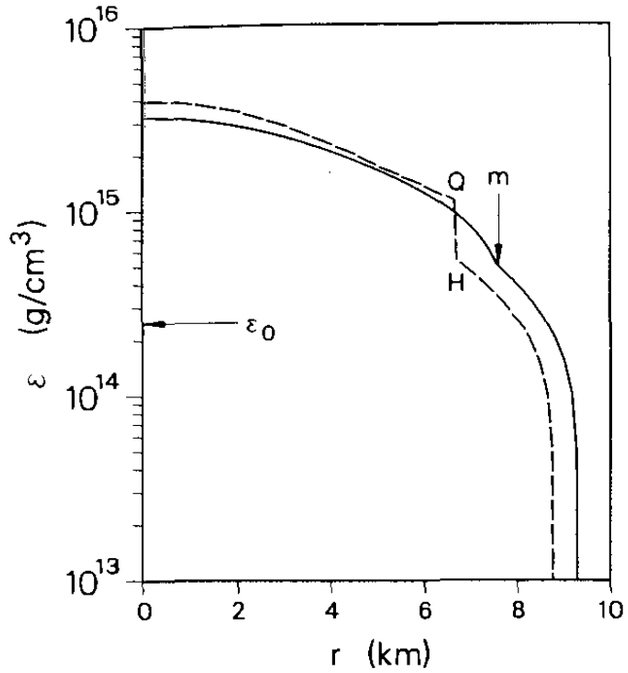

FIGURE 9.6. Density in a star in which the hadronic-quark matter phase transition is modeled as constant pressure simple substance (dashed line). A discontinuity in density, corresponding to the difference between H and Q in Fig. 9.4, occurs at the radial coordinate where the pressure is equal to that of the mixed phase. This contrasts with the continuous density distribution corresponding to the theory developed later in the chapter (solid line). For the particular coupling constants and bag constant B chosen to describe the two phases, the mixed phase extends from the center to the radius marked m [195].

9.3 The Confined–Deconfined Phase Transition in Neutron Stars

9.3.1 Conservation laws are global—not local

Real neutron stars have two conserved charges, electric and baryonic. Beta stability of dense charge neutral demands this. Therefore, neutron star matter is not a "simple" substance but a "complex" one—it has more than one independent component. The characteristics of a first-order phase transition (which we assume the deconfinement transition to be[4]) are quite different in the two cases.

The difference arises because a complex substance possesses degrees of freedom unavailable to a simple substance. These degrees of freedom were frozen out in early research [393]–[402] in one or other of the two ways described above (Sections 9.2.1 and 9.2.2). Recall from (5.25) that stars must be charge-neutral. This statement pertains to the overall net charge on the star. It is a global restriction and not a local one which would correspond to identically vanishing charge density. Nature requires only global neutrality; if it is energetically favorable to have charges separated, it will be so. We have examples of such systems. The neutron is one and

[4]Lattice gauge simulations of QCD are not conclusive on the issue of whether the confined–deconfined phase transition is first- or second-order because they deal generally with hot matter and vanishing baryon chemical potential. There is still great difficulty in dealing with finite quark masses. We shall assume that the transition is first-order.

the atom is another. Both have finite charge distributions; they simply integrate to zero.

9.3.2 *Degrees of freedom in a multicomponent substance*

Consider a substance composed of two conserved "charges" or independent components— Z of one kind,[5] B of the other. In the case of a neutron star, these could denote the net electric charge number (in units of e) and net baryon charge number. Let the substance be closed in a volume V and in a heat bath. Define the concentration of the conserved charges with which the substance was prepared by

$$c = Z/B\,. \tag{9.8}$$

The ratio is fixed and uniform throughout the substance only as long as the substance remains in one pure phase or the other! However, when the substance is in the mixed phase, the concentration in each of the regions of one phase or the other may be different from c such as

$$c_H = Z_H/B_H, \quad c_Q = Z_Q/B_Q\ : \tag{9.9}$$

The concentrations are restricted only by the conservation of the total numbers of each conserved quantity, that is, by

$$Z_H + Z_Q = Z, \quad B_H + B_Q = B\,. \tag{9.10}$$

The subscripts H and Q denote confined hadronic and quark phases, respectively, but could in general refer to any two phases. If the internal forces can lower the energy of the system by rearranging the concentration from the value c with which the substance was prepared, they will do so. The essential point is that conservation laws in chemical thermodynamics are global, not local. Moreover, the concentrations c_H, c_Q will be optimized by the internal forces of the system at each proportion of the phases, so that the properties of the phases *vary* in the mixed phase. This is in contrast with the liquid–vapor transition in water or in any other single-component substance.

The mathematical proof of the above properties is not nearly so illuminating as the physical verbal proof above, but we give it for completeness. The Gibbs condition for phase equilibrium is that the temperature T, the pressure and chemical potentials μ_b and μ_q corresponding to B and Z, are equal in the two phases,

$$p_H(\mu_b, \mu_q, T) = p_Q(\mu_b, \mu_q, T) \tag{9.11}$$

Unlike the case for a single-component substance (9.1) which provides a *unique* solution for the chemical potential, equation (9.11) clearly does not specify a solution by itself. It must be supplemented by one, and only one, additional condition. That condition can be taken as the conservation of electric charge. However, as

[5]If Z denotes the net electric charge, it would be zero for a star, but we retain the symbol for generality.

discussed, the condition of *local* conservation is stronger than required. We are allowed only to apply the weaker condition of *global* conservation in a volume V comprising a bulk quantity of material

$$(1-\chi)q_H(\mu_b,\mu_q,T)+\chi q_Q(\mu_b,\mu_q,T)=Z/V\equiv\langle q\rangle\,, \tag{9.12}$$

$$\chi=V_Q/V\quad(V=V_H+V_Q)\,. \tag{9.13}$$

in which, for a star, $Z\equiv 0$. Now (9.11) and (9.12) can be solved at given T and for any volume proportion of phases in the range $0<\chi<1$. The solution yields the chemical potentials as functions of proportion

$$\mu_b=\mu_b(\chi)\,,\qquad \mu_q=\mu_q(\chi) \tag{9.14}$$

These equations prove that the properties of each phase in equilibrium of a multicomponent substance vary as the proportion of the phases, in particular, the common pressure. As a consequence, the mixed phase corresponding to any phase transition in neutron star matter will occupy the radial extent spanned by the pressure variation defined by (9.11) and (9.14) with $0\le\chi\le 1$.

When the chemical potentials have been found, the average baryon density of the mixed phase as a function of volume[6] proportion of the phases can be computed from

$$\langle\rho\rangle\equiv B/V=(1-\chi)\rho_H(\mu_b,\mu_q,T)+\chi\rho_Q(\mu_b,\mu_q,T)\,, \tag{9.15}$$

We note that the condition of global conservation expressed by (9.12) is compatible, together with (9.11), with the number of unknowns to be determined. It would *not* be possible to satisfy Gibbs conditions if local electric charge conservation were demanded, for that would replace (9.12) by two equations such as $q_H(\mu_b,\mu_q,T)=Z_H/V_H$, $q_Q(\mu_b,\mu_q,T)=Z_Q/V_Q$, and the problem would be overdetermined.

It is important to note that, because of the freedom available to the system to rearrange the concentration(s) of the conserved charges so as to achieve the state of lowest energy, the solution of the equations for Gibbs equilibrium and charge conservation (9.11)–(9.12) is different for each proportion of the phases χ so that all properties, including the common pressure, vary through the mixed phase.

There is another way in which the variation of pressure can be deduced. The energy density is not given by (9.3)—a linear function in χ—but by the highly nonlinear relationship

$$\langle\epsilon\rangle=(1-\chi)\epsilon_H(\chi)+\chi\epsilon_Q(\chi)\,. \tag{9.16}$$

We refer to $\langle\epsilon\rangle$ as the average density as a brief way of denoting the volume-weighted density of each phase. Because the relationship is nonlinear, the pressure varies as χ ($p=-\partial E/\partial V$).

---

[6]The volume V is not that of a star, but of a local inertial frame whose extent in the star, as we have proven in Chapter 3, is large enough by far to validate the bulk approximation or the use of Lorentz frames to solve the equations describing matter.

The discussion above is quite general for substances of more than one independent component, or conserved charge. However, the formulation may be more involved, depending on the model for the two phases. In a comprehensive theory, both phases would be described by a single Lagrangian, as we will encounter for Kaon condensation in Chapter 10. The general problem has been formulated in Ref. [195]. The problem treated in this chapter is particularly simple to solve because each phase is described by a separate theory, and the quark phase properties are given completely by the values of the two independent chemical potentials; this would not be generally true.

Nuclear matter has additional interesting aspects associated with any phase transition. The internal force that can exploit the degree of freedom opened by global charge conservation (neutrality in the case of a star) and which is closed to one in which local conservation is artificially enforced, is the isospin-restoring force experienced by the confined phase of hadronic matter and which is manifested in the valley of beta stability (Fig. 4.1). We saw explicitly in (4.213) how the energy density depends quadratically and repulsively on the neutron–proton density difference, and more generally in (5.42) and (5.50) on the isospin asymmetry. The nuclear regions of the mixed phase can arrange to be more isospin symmetric than in the pure phase by a transfer of charge (and possibly strangeness) between the quark phase in equilibrium with it.[7] Symmetry energy will be lowered thereby at only a small cost in rearranging the quark Fermi surfaces. Thus, the mixed-phase region of the star will have positively charged regions of nuclear matter and negatively charged regions of quark matter. Therefore, the Coulomb force is brought into play in creating a Coulomb lattice of the two phases, as we discuss in detail below.

Whether a phase transition takes place at constant or varying pressure has dramatic effects in the environment of a star or any gravitational field. No region of constant pressure can exist in the hydrostatic equilibrium of a gravitating body. Pressure is a monotonic function according to the Oppenheimer–Volkoff equations. By demanding either identical charge neutrality, as for a star made purely of neutrons, or local charge neutrality, the phase transition was forced to be of this type in the earlier research [393]–[402]. Fig. 9.6 compares the density profiles of neutron stars in which the mixed phase is treated as that of a simple or a complex substance. The properties of the mixed phase in a complex substance are illustrated in Fig. 9.7. Note that all quantities appropriately vary continuously.

Figure 9.8 illustrates a stellar sequence corresponding to the treatment of the phase transition according to Gibbs phase equilibrium as just discussed (solid line), and a sequence for which the phase transition is approximated as a constant

[7]The ground state can be found in chemical thermodynamics without knowledge or specification of the particular reactions involved when a system decays from a state of higher energy to one of lower. To be more specific, however, exchange of a d quark in a neutron with a u quark of the quark phase makes the nuclear phase more positively charged and isospin symmetric. Exchange of a d quark in a neutron and an s quark from quark matter converts a neutron to a Λ and reduces the isospin asymmetry of the confined phase.

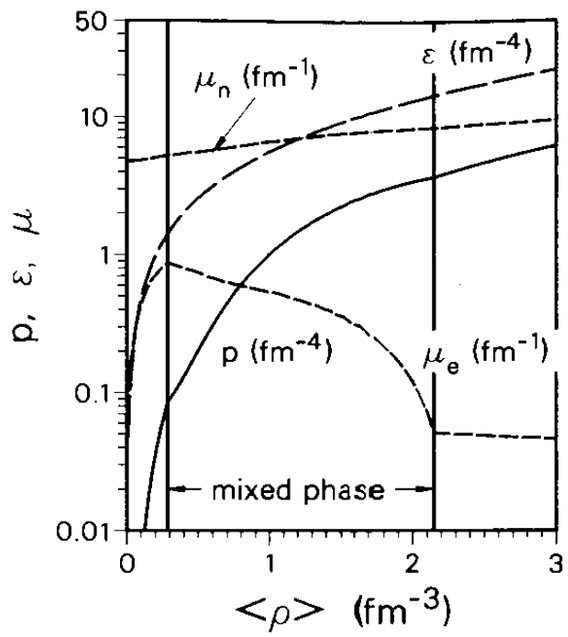

FIGURE 9.7. The pressure, weighted energy density (9.16), and chemical potentials as a function of density for the hadron–quark phase transition in the case that the star is correctly treated as one having two conserved charges, baryon and electric [195].

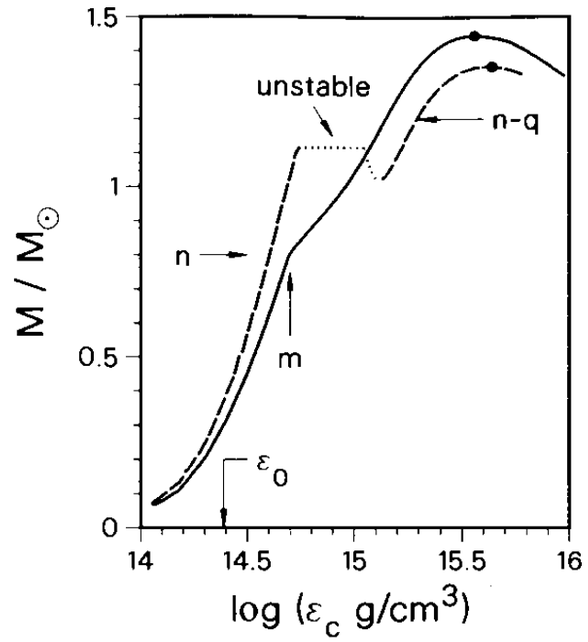

FIGURE 9.8. Dashed line is a stellar sequence with a constant-pressure phase transition. "n" denotes pure neutron stars; "n-q" quark cores with neutron matter mantles. Solid line are stars in beta equilibrium. Stars above "m" have mixed-phase interiors and neutron star matter mantles; stars below 'm' are in the pure neutron star matter phase [195].

pressure one (dashed line). The latter corresponds to a treatment of neutron stars as purely neutron and undergoing a phase transition to quark matter consisting of u, d, s quarks in equal proportion. The stellar configurations with central densities lying in the flat region correspond to densities of the mixed phase and are unstable (because M is not an increasing function of central density). We thus discern a clear difference in the two treatments. When the phase transition is treated as one taking place in a multicomponent substance with due account of Gibbs conditions and conservation laws, there is no region of instability in the sequence between minimum and maximum mass configurations; stable stars with a mixed phase can exist.

It is worth noting in Fig. 9.8 that quark matter appears (in a mixed phase) in stars with mass as low as 0.8 $M_\odot$ (for the parameters used in the illustration). This contrasts with the incorrect treatment of neutron star matter as a simple substance for which quark matter appears first in a star of mass $1.2M_\odot$ and at much higher central density.

9.3.3 Nuclear symmetry energy and a coulomb lattice

We described above how the isospin symmetry energy in neutron rich matter will exploit the degree of freedom of readjusting the charges between hadronic and quark phases in equilibrium so as to reduce the symmetry energy to the extent

consistent with charge conservation. Regions of hadronic matter will have a net positive charge neutralized by a net negative charge on the quark matter regions.[8]

Coulomb repulsion will prevent the regions of like charge from growing too large, and the surface energy will act in the opposite sense in preventing them from becoming too small. We understand, therefore, that the mixed phase will form a particular Coulomb lattice so as to minimize the sum of Coulomb and surface interface energy at each proportion of phases [194, 195]. The proportion of phases will, of course, vary with depth in the star, and the lattice will accordingly vary.

We expect that the outer region of the neutron star will consist of hadronic matter. At a depth where the pressure is higher, some hadronic matter will have been converted to quark matter. The quark matter will consist of a lattice of droplets immersed in hadronic matter. Much deeper in the star, the roles will be reversed in accordance with the associated pressure. In between, other geometric phases may occur corresponding to intermediate pressures. Perhaps the pressure will be high enough in the inner core to convert all the matter to quark matter. The density profile of the star is continuous and, in general, consists of three regions: (1) the outer hadronic region, (2) the intermediate mixed-phase region with the proportion of phases and corresponding crystalline structure varying with depth in the star, and (3) the interior quark matter core. (See Figs. 1.1 and 9.3.) The picture is quite different from that when the second conserved charge is suppressed.

9.3.4 Phase diagram

In the case of a simple substance, the pressure is a function of one chemical potential, and we have seen its general form—the pressure increases with μ up to a point, backtracks below, and then crosses itself. The point of intersection corresponds to the mixed phase. The stable phase is the one with highest pressure (Fig. 9.5). In the case of two chemical potentials, the pressure is a surface, not a line, and the intersection of the surfaces is a line, rather than a point; the mixed phase corresponds to a line in the three-dimensional space of pressure and two chemical potentials. In general, for n independent conserved quantities, the above statements are in a hyperspace of $n + 1$ dimensions [195].

The analogue of Fig. 9.5 for two chemical potentials (corresponding to two conserved charges) is Fig. 9.9. In this example the hadronic phase is represented locally by the surface bounded by X A A′X′. Phase equilibrium occurs on the line A A′ which is the intersection of the hadronic and quark pressure surfaces. However, only a segment of that line pertains to any particular pair of conserved charges. In this schematic plot, the line 0a is the projection of the line defined in

[8]Electrons play a minor role in charge neutrality after densities are reached where neutrality can be achieved in large part among baryons. The conserved baryons must be present in an number equal to that with which the star was born, but electrons must be present *only* to the extent of neutralizing any excess positive charge not already neutralized among particles carrying baryon charge [68, 129].

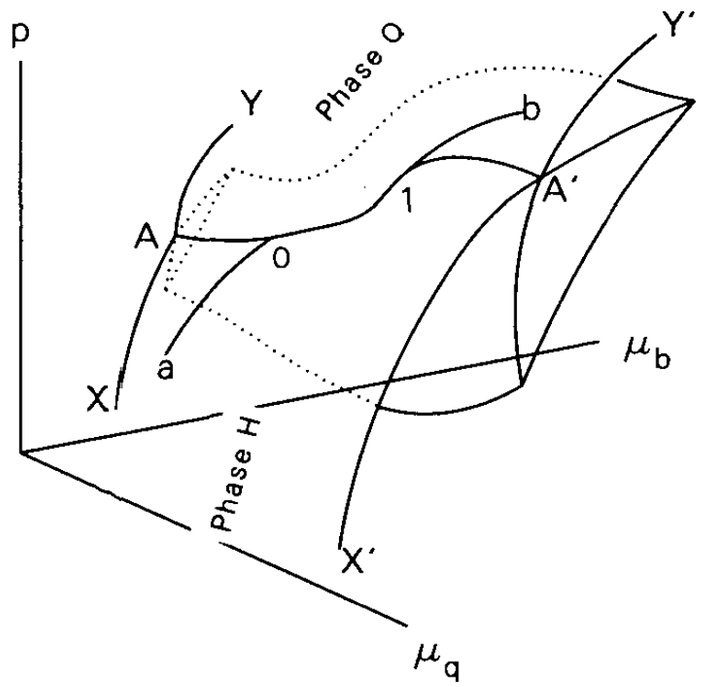

FIGURE 9.9. Schematic of pressure as a function of two chemical potentials. For chosen conserved charges, a0 represents the trajectory that the system will lie on in the pure hadronic phase, 01 in the mixed phase with proportion χ varying from 0 to 1, and 1b the trajectory on which the system will lie when in the pure quark phase [195].

the chemical potential plane by the conservation equations

$$\rho_H(\mu_b, \mu_q) = B/V\,, \qquad q_H(\mu_b, \mu_q) = Z/V \tag{9.17}$$

for the pure hadronic phase. The end of the pure hadronic phase ($\chi = 0$) is denoted 0. Similarly, the line 1b is the projection onto the pressure surface of the line representing the solution of the conservation equations in the quark phase. The line 01 is the mixed phase for which χ, the proportion of quark phase, varies from zero to unity. In other words, for the given amount of conserved charges, the line a01b represents the system in the pure hadronic, mixed, and pure quark phases, respectively; all three phases are charge-neutral; the mixed one, globally, and the pure phases, locally.

9.3.5 Two energy scales

The energy scale of stellar matter in bulk is large, being of the order of GeV per baryon charge. This is because such matter is highly compressed and includes the masses and Fermi energies as well as the compression energy. The energy density of each phase through the mixed phase region is shown in Fig. 9.10. In this chapter we have discussed how a substance possessing a first-order phase transition and having more that one conserved charge of which one is the electric charge, may develop a Coulomb lattice of the rarer phase immersed in the other. The energy scale of this geometrical structure is much smaller than the bulk energy scale because it involves surface and screened Coulomb energies (related by a factor of two as we shall see, and so of the same order). Therefore, we approximate each problem separately:

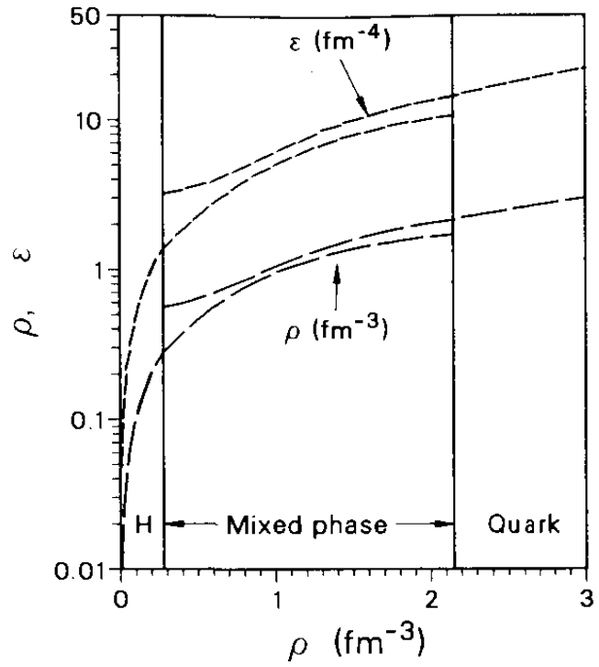

FIGURE 9.10. For the hadronic quark phase transition, the energy density and baryon density in each phase in equilibrium are shown through the mixed phase where the x-axis is the volume-weighted density of the mixed phase [195].

(a) The mass and radius of the star, the pressures, chemical potentials, particle populations, indeed the large-scale structure of the star and the radial location of the mixed phase can be found independently of the crystalline structure of the mixed phase.

(b) The important crystalline properties of the mixed phase can be evaluated quantitatively with input of charge and energy densities of the two phases in equilibrium found in (a). The forms, dimensions, spacings, and location of the crystalline structure can be computed as they evolve with distance from the center of a particular mass star. This is so because all are a function of χ which is a function of pressure and hence of radial location in the star.

9.4 Large-Scale Structure of a Hybrid Star

We use the theories of dense neutron star matter and of cold quark matter developed in earlier chapters to compute the gross properties of stellar models including the phase-transition region. Each theory by itself represents a pure phase—hadronic or quark as the case may be. Each is to be solved subject to charge neutrality (as in (9.17) for the hadronic phase). At each step in density, the pressure of both phases (at equal chemical potentials) can be checked to identify the greater pressure (which identifies the physical phase) and to discover the point at which the pressures first become equal. That point identifies the beginning of the mixed phase.

Throughout the mixed phase, charge neutrality must be enforced only as an overall constraint, as in (9.12), and not separately on each of the phases as explained earlier. In the mixed phase the proportion or fraction χ of volume occupied by the quark phase is a more convenient independent variable than baryon density. The

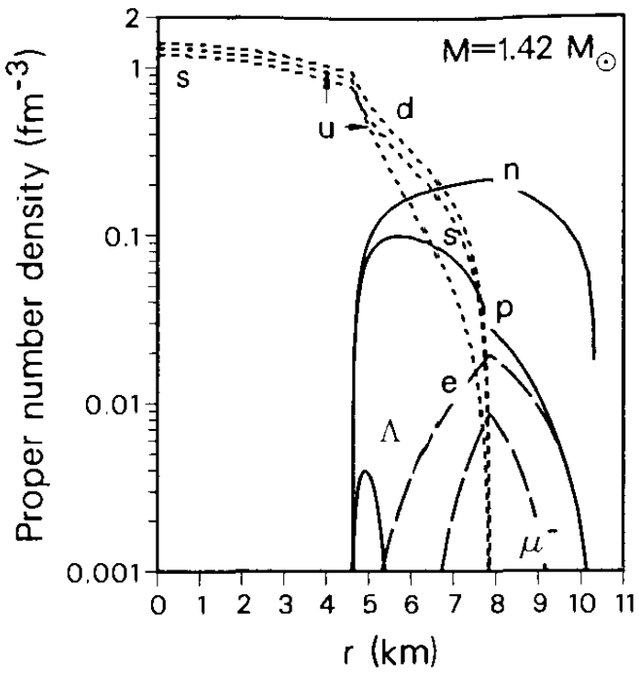

FIGURE 9.11. Population densities per unit volume (9.15) in a hybrid star at the mass limit $1.42M_\odot$ as a function of Schwarzschild radius. The nuclear properties defining the coupling constants in the hadronic phase are $K = 300$ MeV and $m^*/m = 0.7$. Hyperon couplings are chosen as in Section 5.4.3 with $x_\sigma = 0.6$. Calculation is otherwise similar to [195].

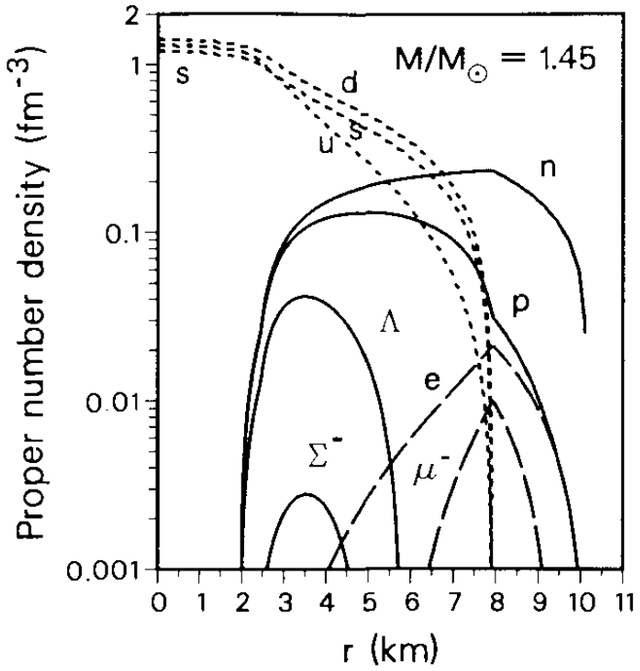

FIGURE 9.12. Population densities in a hybrid star at the mass limit $1.45M_\odot$. Nuclear properties defining the coupling constants in the hadronic phase are $K = 240$ MeV and $m^*/m = 0.78$. Hyperon couplings are chosen as in Section 5.4.3 with $x_\sigma = 0.6$. Calculation is otherwise similar to [195].

pressures of the two phases in equilibrium are equal, but vary with χ. When χ become equal to unity, the matter is in the pure quark phase.

Besides specifying the theories of the two separate phases, we need the relationship between the quark chemical potentials and those for the independent conserved quantities—baryon number $\mu_n(\equiv \mu_b)$ and electron charge $\mu_e(\equiv -\mu_q)$. The relationships are

$$\mu_u = \mu_c = (\mu_n - 2\mu_e)/3, \qquad \mu_d = \mu_s = (\mu_n + \mu_e)/3\,. \tag{9.18}$$

The quark chemical potentials can be obtained from the general rule relating particle chemical potentials to the independent potentials according to the content of the quarks (Table 8.1).

For a bag constant of $B^{1/4} = 180$ MeV and for nuclear matter properties lying in the range of accepted values, we show in Fig. 9.11 the population densities of baryons, quarks, and leptons. For the particular equations of state of hadronic and quark matter, the transition to the pure quark phase is attained because the central density is sufficiently high. The inner 4.6 km of the star forms a quark gas. The region between 4.6 km and 7.8 km is a shell of mixed phase containing, on the microscopic scale, regions of quark and hadronic matter with the rarer phase arranged in a crystalline lattice whose structure we will calculate latter. Exterior to this mixed phase is neutron star matter liquid. At the edge of the star at densities

below nuclear saturation, a thin crust of nuclei is arranged at lattice sites embedded in an electron gas [80].

Lepton populations in the star are quenched at smaller distance from the center as the quark populations rise. This is because charge neutrality of the star is achieved in a more energetically favorable manner among the baryon-carrying particles, and baryon number is conserved. Leptons produced or absorbed in beta decay or its inverse are not conserved in the star because neutrinos diffuse out. The same result was encountered in a purely hadronic star as discussed in Chapter 5. The phenomenon is quite general. However, particular species of baryon-charge-carrying particles are not conserved. Only the total baryon number and the net electric charge (zero) are conserved.

We learned in Chapter 5 that the compression and effective nucleon mass at saturation are not precisely known and the structure of stars is fairly sensitive to the uncertainties. Therefore, particle populations are shown for other values of these parameters in Fig. 9.12. In this case the hyperons play a more important role in the mixed phase. The pure quark matter phase occupies a sphere of only 2-km radius while the crystalline mixed phase forms a shell of 6-km thickness.

9.4.1 Energy budget in the reapportionment of charge

We have emphasized the importance of the degree(s) of freedom corresponding to a reapportionment of conserved quantities among the phases in equilibrium. This degree of freedom is exploited by the internal forces at each proportion of phases in the coexistence phase, so as to minimize the energy. Figure 9.13 vividly illustrates this phenomenon.

Consider the electric charge densities on each phase, quark and hadronic, as a function of the volume proportion χ of quark matter. Matter is purely hadronic at $\chi \equiv 0$. At slightly finite values of χ, hadronic matter is in equilibrium with an infinitesimal amount of quark matter. The high isospin asymmetry of the hadronic matter at that point (and beyond) can be relieved by transferring charge between phases. Near the threshold for the phase transition, there is little quark matter; the relief is slight. The negative charge density carried by quark matter is largest near the threshold because the cost of arranging the u,d,s quark Fermi surfaces to provide positive charge to the regions of the confined hadronic phase is of little importance at the low-threshold proportion of the quark phase. This energy cost is balanced by relief in symmetry energy in the hadronic phase.

However, the cost in Fermi energy in the quark phase required to provide charge to the hadronic phase becomes increasingly important in the energy budget for greater proportions of quark matter. Therefore, as the proportion of quark matter grows, its charge density decreases. The charge density carried on baryons is the inverse of this, rising to its maximum value as the baryon density goes to zero (at $\chi = 1$). The total charge—the sum of the charge densities times the respective volumes of the phases—is zero. Neutrality is global, not local.

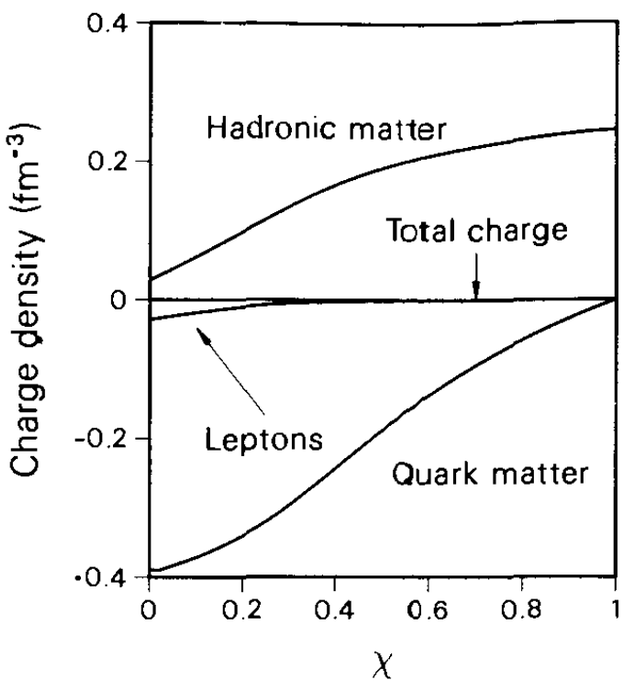

FIGURE 9.13. Charge densities in regions of hadronic and quark matter, respectively, in phase equilibrium as a function of quark matter volume proportion χ. Refer to Fig. 9.11 for other details. See also [406].

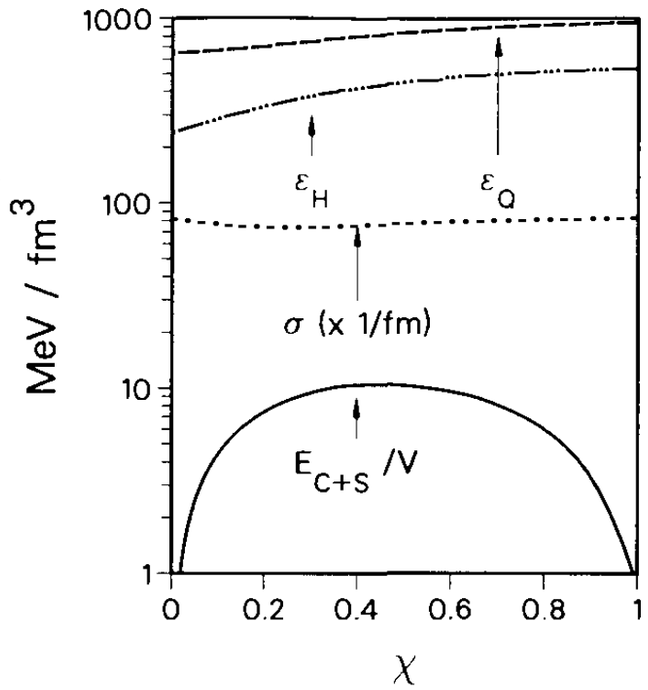

FIGURE 9.14. The energy densities of each phase, the surface interface energy σ (as approximated in the text), and the sum of surface and Coulomb energy densities are shown in the mixed phase of hadronic and quark matter as a function of the volume proportion of quark matter χ. See Fig. 9.11 for other details. See also Ref. [195].

9.5 Crystalline Structure of the Mixed Phase

We have discussed how a crystalline structure in the mixed phase of a complex substance is inevitable if the transition is first-order and the substance has electric charge as one of its conserved charges [195]. The Coulomb interaction will tend to break the regions of like charge into smaller ones, while this process is opposed by the surface interface energy. Their competition will be resolved by forming a lattice of the rare phase immersed in the dominant one whose form, size, and spacing will minimize the sum of surface and Coulomb energies. In other words, a crystalline lattice will be formed. It is not altogether certain that the lattice is rigid, but evidently an ordered phase is energetically favorable.

Consider a Wigner–Seitz cell of radius R containing the rare-phase object of radius r and an amount of the dominant phase that makes the cell charge-neutral. The whole medium can be considered as made of such noninteracting cells. The solution to problems involving a competition between Coulomb and surface interfacial energies is independent of the particular components or system in question.

Let us first see schematically how the varying crystalline structure can be calculated. The Coulomb and surface energies per unit cell volume can be written

$$E_C/V = C(\chi)r^2, \qquad E_S/V = S(\chi)/r\,, \tag{9.19}$$

where χ is the volume proportion of one phase compared to the entire volume. The form of the functions $C(\chi)$ and $S(\chi)$ correspond to a specific geometry, such as spheres, rods, or slabs. Of course, the restriction to three discrete geometries is an idealization, but will serve the purpose of the next section. The r dependence of the above energies can be deduced by dimensional analysis [195].

When there is little of one phase immersed in the other, we expect the rare phase to form spherical droplets to minimize the surface. As an example, let us see what form the function S takes in this case. For a surface energy coefficient σ, we have

$$\frac{E_S}{V} = \frac{4\pi r^2 \sigma}{4\pi R^3/3} = 3\sigma\chi/r\,, \qquad \chi = (r/R)^3\,. \tag{9.20}$$

Now the function $S(\chi)$ can be read for the geometry of spheres. As the quark phase becomes more abundant, the droplets merge to form rods, and, at higher proportion, rods merge to form slabs. As the proportion further increases, a point is reached at which the two phases interchange roles, developing into nuclear droplets of positive charge immersed in a background of negatively charged quark matter at the other extreme of the mixed phase. In all cases the form of Coulomb and surface energies per unit volume have the general form as defined in (9.19). The minimum of their sum occurs when

$$E_S = 2E_C\,. \tag{9.21}$$

The radius of the droplets is then determined by

$$r^3 = \frac{S(\chi)}{2C(\chi)}\,, \tag{9.22}$$

which depends explicitly on the proportion of phases χ. Because $\chi = (r/R)^3$, the distance between droplets is also determined for this value of χ.

The process responsible for creating the conditions for the mixed-phase crystalline structure are quite different from those that create the structure in a mixture of nuclei and electron gas, as is found in the subsaturation matter in the crust of a neutron star. In the latter case atoms are ionized at the densities of the crust, and positively charged nuclei find themselves immersed in an electron gas [301]. A Coulomb structure seems quite natural. The unusual aspect of the situation we describe is that the structure consists of two phases of the same substance—hadronic matter in the confined and deconfined phases which carry opposite charges. The exchange of charge and strangeness is mediated by the weak interaction and driven by the symmetry energy of the confined phase. Nevertheless, the interplay of surface and Coulomb energies in defining the nature, size, and spacing of structure is identical.

Having shown schematically how the problem of structure may be solved, we now turn to the actual formulation. The electrostatics are trivial, but the details are tedious. We quote the results without derivation. The functional form of S and C is distinct for each geometry of the Wigner-Seitz cell and the rare phase contained therein, as is the relation of the dimensions r and R to χ. Recall that χ is defined

as the volume fraction of quark matter.

$$C_d(\chi) = 2\pi \left\{[q_H(\chi) - q_Q(\chi)]e\right\}^2 x f_d(x) \tag{9.23}$$

$$S_d(\chi) = x\sigma d \tag{9.24}$$

where $d = 1, 2, 3$, respectively, for the idealized geometries of slabs, rods and drops of rare phase immersed in the dominant phase, and σ is the surface tension. The second of these equations is easily obtained, as above. The charge densities of hadronic and quark matter (in units of e) at a given proportion χ are denoted by q_H and q_Q.

The ratio of slab, rod or droplet to cell volume of the same geometry, is denoted as

$$x = (r/R)^d, \qquad d = 1, 2, 3. \tag{9.25}$$

For droplets and rods, R and r are the radius of the Wigner-Seitz cell and the object of rare phase within. For slabs, R and r are the half spacing between slabs and the half thickness of the rare-phase slabs. The two quantities, χ and x, are related according to which phase is the dominant (background) phase by

$$\chi = \begin{cases} x, & \text{(background phase is H)} \\ 1 - x, & \text{(background phase is Q)}\ . \end{cases} \tag{9.26}$$

The radius of droplet (or rod, or half-thickness of slab) of the rare phase immersed in the other and the minimum of the sum of Coulomb and surface energies in the case of the three geometries are:

$$r = \left(\frac{\sigma d}{4\pi[q_H(\chi) - q_Q(\chi)]^2 e^2 f_d(x)}\right)^{1/3}, \quad d = 1, 2, 3, \tag{9.27}$$

$$\frac{E_C + E_S}{V} = 6\pi x\left(\frac{\{\sigma d[q_H(\chi) - q_Q(\chi)]e\}^2 f_d(x)}{16\pi^2}\right)^{1/3}. \tag{9.28}$$

For each geometry (drops, rods, or slabs), one can compute $(E_C + E_S)/V$ to find which geometry yields the lowest energy, and then compute the radius of the geometrical object of the rare phase (or half-thickness) r and find the spacing $2R$ between them.

The function $f_d(x)$ is given in all three cases by [301],

$$f_d(x) = \frac{1}{d+2}\left[\frac{1}{(d-2)}(2 - dx^{1-2/d}) + x\right], \tag{9.29}$$

where the singularity at $d = 2$ is well-behaved and has the value

$$\lim_{d\to 2}\left[\frac{(2 - dx^{1-2/d})}{(d-2)}\right] = -(1 + \ln x). \tag{9.30}$$

We have supposed that the electrons are uniformly distributed throughout the mixed phase in both quark and hadronic regions. They therefore do not appear in the above expression. In any case, the electron density is extremely small as we saw above in Fig. 9.13.

The surface tension enters the above determination of the structure as a crucial factor, but it is not known. Fortunately, it is evident from (9.28) that the boundaries of the mixed phase are unaffected by its value because the surface and Coulomb energies vanish at both boundaries; therefore the bulk properties of the medium determine the boundaries. It is interesting, and useful, that the structure size r, cell size R, and the sum of Coulomb and surface energies scale with a power of σ independent of geometry. Also, because of this scaling, the locations in the star where the geometry changes from one form to another is independent of the value of the surface tension. This is obvious because at fixed χ the *ordering* in magnitude of the sum of surface and Coulomb energies is independent of σ.

It is clear that the surface tension should be computed self-consistently with the two models of quark and hadronic matter in equilibrium. Moreover, unlike simple substances, such as water and vapor, the density of each phase changes as its proportion in the mixed phase changes (Fig. 9.14). So, the surface energy is not expected to be a constant.

Referring to Fig. 9.14, note that the varying densities of the two phases, though unequal, tend to track one other. In a simple substance, by contrast, the density of each phase in equilibrium remains constant for all proportions of the phases, and the two phases often have significantly different densities. As a gross approximation, the surface energy is given by the difference in energy densities times a length scale typical of the surface thickness [407]. In the case of mixed quark and hadronic matter, the length scale is of the order of the strong interaction range, $L = 1$ fm. In other words, the surface interfacial energy should depend on the proportion of phases in phase equilibrium just as everything else does:

$$\sigma(\chi) = \text{constant} \times [\epsilon_Q(\chi) - \epsilon_H(\chi)] \times L\,. \tag{9.31}$$

Great care has to exercised in assigning a value to the constant in the above expression. If too large a value is chosen, the structured phase will have an energy higher than the unstructured one. But this would violate the general theorem that when a degree of freedom is opened to a physical system, the energy will not be raised—it can remain unchanged (the degree of freedom remaining unexploited)—or it can and generally will, be lowered. The reason for the *apparent* violation in Ref. [404] of the general theorem is that the division of the energy into volume, surface, and Coulomb energies is an approximation in an infinite series of corrections, the next being the curvature correction [408]. Therefore, a value of σ that would violate the mathematical theorem has been chosen arbitrarily to be too large. In Ref. [404] various arbitrary values of a constant σ were employed. In keeping with the above theorem, we choose a value, as shown in Fig. 9.14, that gives a value not exceeding $10\,\text{MeV/fm}^3$ to the optimized sum of surface and Coulomb energy densities (which is a function of χ).

9.5.1 Crystalline structure as a function of stellar mass

In this section we study the crystalline, mixed-phase region of hybrid stars as a function of stellar mass to see how its geometry, dimensions, and location in the

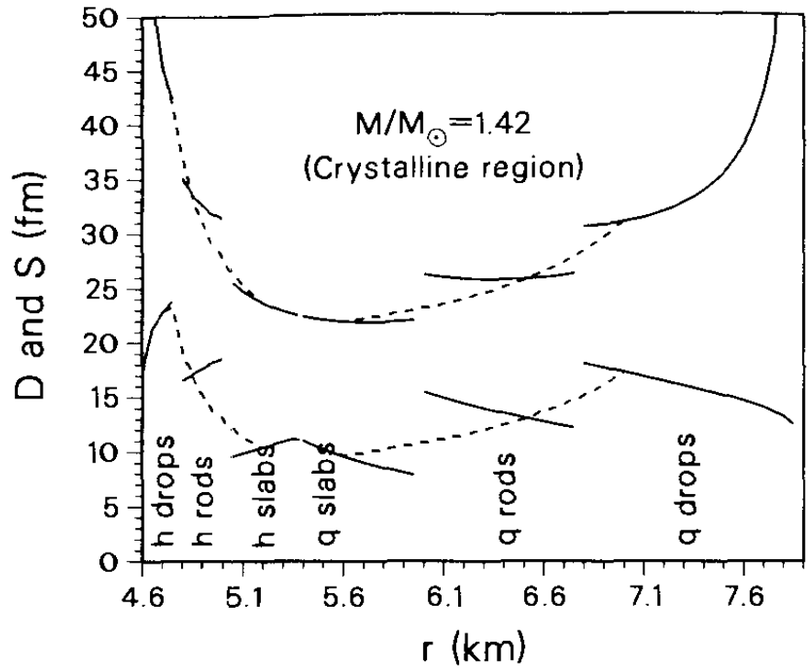

FIGURE 9.15. Crystalline mixed region in a neutron star showing the diameter D (lower curves) and spacing S (upper curves) of indicated geometric structures as a function of radial Schwarzschild coordinate. The region intemal to 4.6 km is pure quark matter. The notation "h drops" denotes hadronic drops immersed in quark matter, and so on. The stellar radius is 10.7 km. The dashed line is continuous dimensionality interpolation. See Fig. 9.11 for particle populations and other details. Taken from [405].

star vary. To demonstrate the extreme dependence of the crystalline structure on stellar mass, we compare two stars differing by only $0.02M_\odot$. In Fig. 9.15 we show the diameter of the geometrical objects, identify their forms, and plot the spacing between centers of the rare-phase objects immersed in the other phase. The mass of the star is at the mass limit $M = 1.42M_\odot$. The pressure at the center and extending to 4.6 km is sufficiently high that this region is occupied by pure quark matter. The region between 4.6 and 7.8 km is in the crystalline, confined–deconfined phase. Because the phase transition is completed before the center of the star is reached, the geometrical structures span the full range of forms. At the outer edges of the mixed phase region, drops of *finite* diameter are spaced in the limit of $\chi = 0$ at *infinite* distance. In all cases the diameters of the geometric forms lie between about 10 and 25 fm. Of course, were it not for the restriction to three discrete geometries, the discontinuities in the diameters and spacings shown in the Figs. 9.15 and 9.16 would be interpolated by intermediate forms. In the formulae (9.27–9.30), d can be treated as a continuous variable in the range (1,3) for this purpose, and the result is shown in the one case.

For lower-mass stars, the central density and pressure may be insufficient to fully convert quark matter to hadronic matter. This is the case for the neighboring mass star $M = 1.40M_\odot$ for which the geometries of the crystalline mixed phase are shown in Fig. 9.16. The crystalline phase extends to the center of the star, and the central geometry consists of rods of hadronic matter immersed in quark matter. For a mere $0.02M_\odot$ change in mass, the situation has changed radically from a star having a 4.6-km quark gas core enclosed by a 3-km thick crystalline shell to a star which is an 8-km crystalline sphere having no quark gas interior.

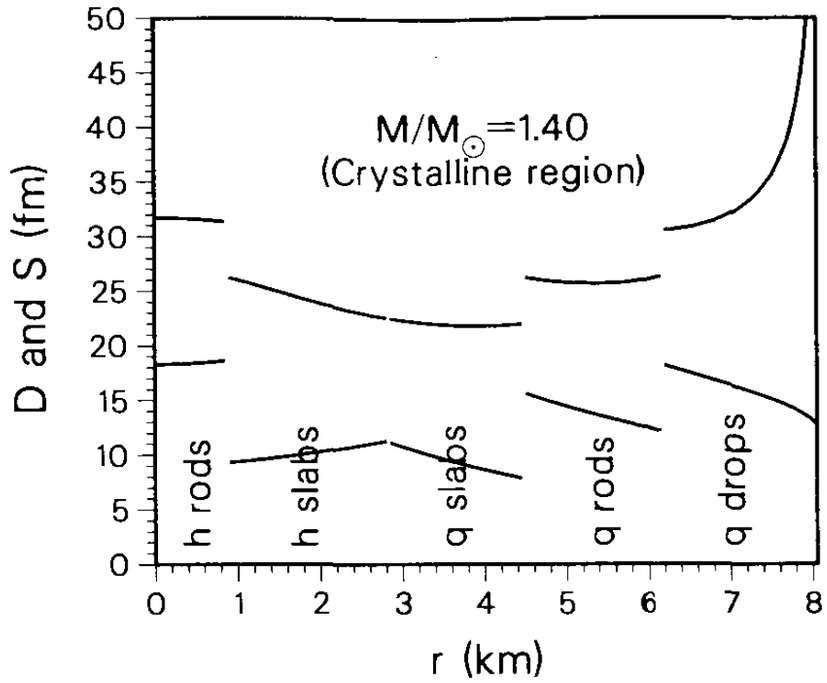

FIGURE 9.16. Similar to the previous figure, but for a slightly less massive star. The pure quark phase is entirely absent and the mixed crystalline phase now extends to the star's center. Taken from Ref. [405]. The stellar radius is 12.3 km.

The extreme sensitivity of the crystalline structure to stellar mass is due to the high compression in neutron stars. Stellar density is a rather flat function of radial coordinates except near the edge of the star. A small change in central density (and therefore mass) has a large effect on where in the star a particular density occurs. Naturally, the details illustrated above are for the particular parameters chosen. The pattern of the results is, however, general.

The results for another parameter set are shown in Figs. 9.17 and 9.18. There the radial coordinates of the boundaries of various regions are shown for various stellar masses up to the limiting mass ($1.454 M_\odot$). It is remarkable, as shown in the detail of Fig. 9.17, that, for only a small range in mass, the core is pure quark matter. For lower-mass stars, the mixed phase extends from the center out to some few kilometers. The stars with mass between 0.84 and $1.07 M_\odot$ contain only quark drops in a hadronic background.

Early research, by inadvertently closing off a degree of freedom, rendered the hadronic–quark transition as one of constant pressure for all proportions in the mixed phase [393]–[402]. In such a case the mixed phase cannot exist in the gravitational field in a star. The pure quark phase was found to occur only at high density or pressure and therefore concentrated near the center. That is true here also. However, the mixed phase extends to a rather low density of only several times nuclear saturation density, as has been found by several authors when the star is allowed to exploit the degree of freedom opened when charge neutrality is imposed globally rather than locally [194, 195, 404, 405, 406, 409].

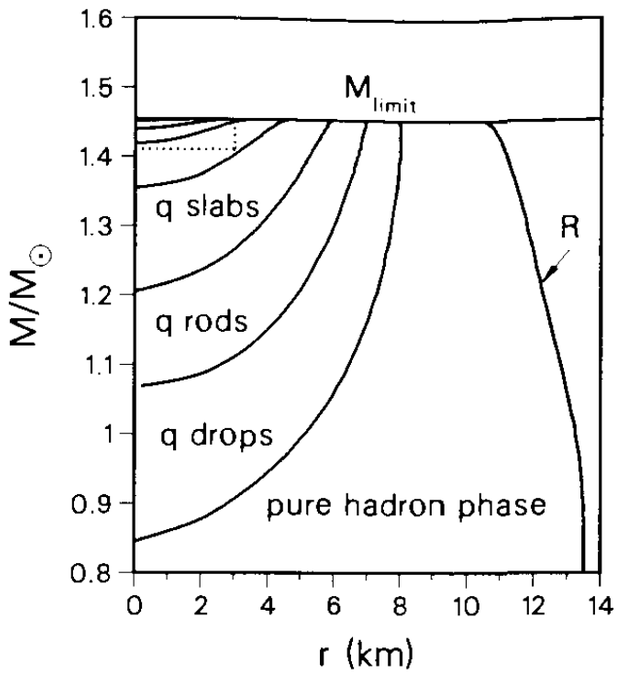

FIGURE 9.17. Showing the radial boundaries of the various geometrical forms for stars above $0.8M_{\odot}$. The stellar radius is shown by R ($K = 240$ MeV, $m^*/m = 0.78$, $x_\sigma = 0.6$, $B^{1/4} = 180$ MeV). [403]

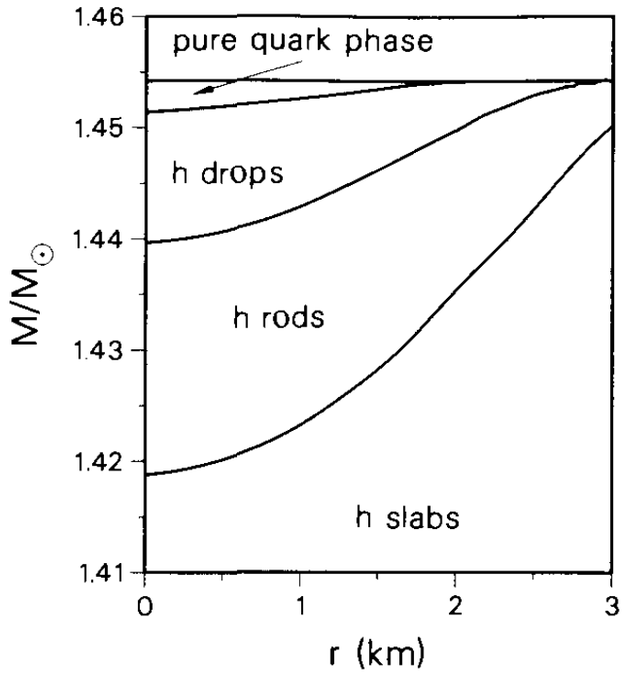

FIGURE 9.18. Showing details of the dotted box in the top left corner of Fig. 9.17. [403]

9.5.2 *Possible implications for glitches*

There is a possible connection between the highly variable crystalline structure of the confined–deconfined mixed phase in neutron stars and the phenomenon of pulsar glitches. Glitches are irregular, unpredictable, and sudden small changes in a pulsar's period. They must therefore be associated with a sudden change in the moment of inertia. A purely liquid or gaseous star is mechanically unable to generate sudden changes in its moment of inertia or angular momentum by any conceivable mechanism. It is certain, therefore, that rigid regions in a pulsar play a role in the period glitch phenomenon.

Glitch behavior is highly individualistic from one pulsar to another [228]. We tentatively suggest that this may be due to the extreme sensitivity on stellar mass of the radial extent of the Coulomb lattice of the mixed phase region and the forms that occupy it as well as the moments of inertia associated with different gaseous (quark), liquid (nuclear), and lattice regions [405]. The interior crystalline region of the mixed phase and the crustal solid, separated by a nuclear liquid, offer interesting possibilities for interaction or stimulated response at the time a glitch originates in one of them and in postglitch recovery. These matters have not been investigated so far.

The crystalline form cannot fit uniformly into the axial symmetry of a rotating star without lattice imperfections. As the star cools we envision that the crystalline structure will develop with relatively few imperfections, but over time and successive glitches their number will grow, creating, eventually, a granular region. Thus, we also expect a long-term change in behavior with pulsar age. In particular, it

is plausible that the glitch behavior will occur in stars that are not so young that crystalline structure cannot form because of the star's high temperature, nor so old that successive glitches will have granulated the formerly solid regions.

9.6 Tables of Equation of State for Hybrid Stars

The following tables provide equations of state for hybrid (neutron-quark) star matter corresponding to nuclear properties identified in Table 5.5. The octet of baryons comprise the composition of the confined phase as described in Chapter 5. The ratio of hyperon to nucleon coupling to the scalar meson field is $x_\sigma = 0.6$. The corresponding coupling to the vector fields can be found in table 5.4. Muons as well as electrons are included. Quark matter is described in Section 8.3.3. The quark masses are taken as $m_u = 0$, $m_d = 0$ and $m_s = 150$ MeV. The bag constants used are $B^{1/4} = 180$ MeV and $\alpha_s = 0$.

9.7 Problems for Chapter 9

1. For a substance of a single independent component, the Maxwell construction for finding phase equilibrium can be done in several ways. Explain the "common tangent" method. Imagine that the energy density ϵ is plotted for both phases as a function of baryon density ρ. Seek the point on each curve that can be connected by a line that is tangent to both curves. The line could be represented by the equation $\epsilon = -a + b\rho$ where a and b are constants. The chemical potential corresponding to ρ is $\mu_b = \partial\epsilon/\partial\rho = b$, so that μ_b is constant on the line. Moreover, the pressure corresponding to the line is given by $p = -\partial E/\partial V$, which, show, is equal to the constant a. So all along the line, including its ends on the equation of state of the two phases, the chemical potential and pressure are constant and common to the two phases. The straight line, therefore, represents mixtures of the two phases that have common pressure and baryon chemical potential, which are both constants. It is the mixed-phase equilibrium equation of state.
2. Given a substance with two independent chemical potentials, could the above Maxwell construction serve to define phase equilibrium? Why not?
3. Confirm that when the energy density is given by (9.3) the pressure is constant, independent of the proportion of the two phases.
4. Prove that the pressure varies as a function of χ when the energy density is given by (9.16).
5. Derive the radius of the droplet and Wigner-Seitz cell radius in the general terms of (9.22).
6. Derive (9.27) and (9.28).
7. Prove the limit (9.30).

TABLE 9.1. Equation of state corresponding to matter with pure confined hadronic phase below a baryon number density 0.26 fm^{-3}, mixed confined-deconfined phase at intermediate densities and pure quark matter at high density above 1.17 fm^{-3}. Nuclear properties correspond to $K = 240$ MeV, $m^*/m = 0.78$. See also Fig. 9.12.

ρ fm^{-3}	ϵ g/cm^3	p $dyne/cm^2$	ρ fm^{-3}	ϵ g/cm^3	p $dyne/cm^2$
0.010	1.6758 +13	7.4377 +30	0.692	1.3047 +15	1.5845 +35
0.015	2.5141 +13	8.9843 +30	0.725	1.3769 +15	1.7514 +35
0.020	3.3529 +13	1.2123 +31	0.759	1.4511 +15	1.9250 +35
0.025	4.1911 +13	1.9243 +31	0.793	1.5258 +15	2.1011 +35
0.030	5.0301 +13	3.2767 +31	0.826	1.5981 +15	2.2725 +35
0.060	1.0074 +14	3.6507 +32	0.856	1.6670 +15	2.4353 +35
0.090	1.5151 +14	1.3499 +33	0.885	1.7318 +15	2.5877 +35
0.120	2.0279 +14	3.1938 +33	0.911	1.7927 +15	2.7291 +35
0.150	2.5471 +14	5.9384 +33	0.936	1.8498 +15	2.8595 +35
0.180	3.0735 +14	9.6207 +33	0.959	1.9035 +15	2.9798 +35
0.210	3.6075 +14	1.4377 +34	0.981	1.9540 +15	3.0905 +35
0.240	4.1500 +14	2.0302 +34	1.001	2.0014 +15	3.1916 +35
0.264	4.5823 +14	2.5825 +34	1.020	2.0465 +15	3.2852 +35
0.286	5.0009 +14	2.7999 +34	1.038	2.0894 +15	3.3718 +35
0.309	5.4220 +14	3.0590 +34	1.055	2.1303 +15	3.4518 +35
0.331	5.8427 +14	3.3598 +34	1.072	2.1697 +15	3.5264 +35
0.354	6.2659 +14	3.7086 +34	1.087	2.2073 +15	3.5951 +35
0.376	6.6933 +14	4.1113 +34	1.103	2.2435 +15	3.6589 +35
0.399	7.1271 +14	4.5758 +34	1.117	2.2787 +15	3.7187 +35
0.422	7.5693 +14	5.1094 +34	1.201	2.4831 +15	4.1354 +35
0.445	8.0224 +14	5.7206 +34	1.231	2.5569 +15	4.3491 +35
0.469	8.4884 +14	6.4181 +34	1.261	2.6313 +15	4.5644 +35
0.494	8.9697 +14	7.2094 +34	1.291	2.7062 +15	4.7813 +35
0.519	9.4685 +14	8.1019 +34	1.321	2.7817 +15	5.0001 +35
0.545	9.9853 +14	9.1000 +34	1.351	2.8578 +15	5.2207 +35
0.571	1.0522 +15	1.0205 +35	1.381	2.9344 +15	5.4430 +35
0.598	1.1077 +15	1.1416 +35	1.411	3.0116 +15	5.6668 +35
0.627	1.1674 +15	1.2753 +35	1.441	3.0892 +15	5.8923 +35
0.659	1.2342 +15	1.4245 +35	1.471	3.1674 +15	6.1193 +35

TABLE 9.2. Equation of state corresponding to $K = 300$ MeV, $m^*/m = 0.70$ See previous table caption for other details. Pure confined hadronic phase lies below baryon number density 0.25 fm^{-3} and pure deconfined quark matter above 0.86 fm^{-3} See also Fig. 9.11.

ρ fm^{-3}	ϵ g/cm^3	p $dyne/cm^2$	ρ fm^{-3}	ϵ g/cm^3	p $dyne/cm^2$
0.010	1.6758 +13	1.1176 +31	0.681	1.2971 +15	1.4839 +35
0.015	2.5151 +13	1.4722 +31	0.695	1.3268 +15	1.5214 +35
0.020	3.3542 +13	1.8839 +31	0.708	1.3558 +15	1.5563 +35
0.025	4.1936 +13	2.5248 +31	0.721	1.3841 +15	1.5889 +35
0.030	5.0326 +13	3.6529 +31	0.734	1.4119 +15	1.6194 +35
0.060	1.0078 +14	3.1818 +32	0.746	1.4391 +15	1.6478 +35
0.090	1.5153 +14	1.2460 +33	0.759	1.4659 +15	1.6745 +35
0.120	2.0278 +14	3.1400 +33	0.771	1.4922 +15	1.6995 +35
0.150	2.5472 +14	6.1711 +33	0.783	1.5181 +15	1.7229 +35
0.180	3.0746 +14	1.0508 +34	0.794	1.5437 +15	1.7449 +35
0.210	3.6114 +14	1.6446 +34	0.806	1.5689 +15	1.7655 +35
0.240	4.1591 +14	2.4246 +34	0.817	1.5938 +15	1.7850 +35
0.246	4.2671 +14	2.5998 +34	0.829	1.6185 +15	1.8033 +35
0.267	4.6611 +14	2.8467 +34	0.840	1.6429 +15	1.8206 +35
0.287	5.0428 +14	3.1158 +34	0.851	1.6671 +15	1.8370 +35
0.308	5.4216 +14	3.4243 +34	0.862	1.6910 +15	1.8524 +35
0.328	5.7994 +14	3.7756 +34	0.891	1.7574 +15	2.0431 +35
0.347	6.1769 +14	4.1721 +34	0.922	1.8246 +15	2.2360 +35
0.367	6.5551 +14	4.6153 +34	0.951	1.8924 +15	2.4311 +35
0.387	6.9343 +14	5.1060 +34	0.982	1.9610 +15	2.6284 +35
0.406	7.3153 +14	5.6422 +34	1.012	2.0302 +15	2.8277 +35
0.426	7.6977 +14	6.2211 +34	1.041	2.1001 +15	3.0291 +35
0.445	8.0811 +14	6.8369 +34	1.071	2.1706 +15	3.2324 +35
0.464	8.4656 +14	7.4841 +34	1.102	2.2417 +15	3.4379 +35
0.484	8.8508 +14	8.1578 +34	1.132	2.3135 +15	3.6450 +35
0.502	9.2318 +14	8.8367 +34	1.161	2.3859 +15	3.8543 +35
0.521	9.6061 +14	9.5082 +34	1.191	2.4589 +15	4.0655 +35
0.539	9.9733 +14	1.0164 +35	1.222	2.5325 +15	4.2783 +35
0.556	1.0332 +15	1.0797 +35	1.252	2.6067 +15	4.4929 +35
0.573	1.0683 +15	1.1404 +35	1.281	2.6814 +15	4.7095 +35
0.589	1.1028 +15	1.1983 +35	1.311	2.7568 +15	4.9277 +35
0.606	1.1371 +15	1.2534 +35	1.342	2.8326 +15	5.1477 +35
0.621	1.1707 +15	1.3057 +35	1.372	2.9091 +15	5.3694 +35
0.637	1.2035 +15	1.3548 +35	1.401	2.9860 +15	5.5926 +35
0.652	1.2356 +15	1.4008 +35	1.431	3.0635 +15	5.8177 +35
0.667	1.2667 +15	1.4438 +35	1.462	3.1416 +15	6.0443 +35

TABLE 9.3. Equation of state corresponding to $K = 300$ MeV, $m^*/m = 0.78$. See previous table caption for other details. Pure confined hadronic phase lies below baryon number density 0.26 fm^{-3} and pure deconfined quark matter above 1.0 fm^{-3}.

ρ fm^{-3}	ϵ g/cm^3	p $dyne/cm^2$	ρ fm^{-3}	ϵ g/cm^3	p $dyne/cm^2$
0.010	1.6770 +13	1.4536 +31	0.741	1.4193 +15	1.8043 +35
0.015	2.5163 +13	2.1180 +31	0.761	1.4639 +15	1.8924 +35
0.020	3.3559 +13	2.7070 +31	0.781	1.5072 +15	1.9765 +35
0.025	4.1957 +13	3.4288 +31	0.800	1.5491 +15	2.0563 +35
0.030	5.0357 +13	4.4907 +31	0.818	1.5896 +15	2.1319 +35
0.060	1.0084 +14	2.9325 +32	0.836	1.6287 +15	2.2032 +35
0.090	1.5159 +14	1.1633 +33	0.853	1.6666 +15	2.2704 +35
0.120	2.0283 +14	2.9844 +33	0.869	1.7033 +15	2.3337 +35
0.150	2.5472 +14	5.8863 +33	0.884	1.7388 +15	2.3932 +35
0.180	3.0737 +14	9.9578 +33	0.900	1.7732 +15	2.4492 +35
0.210	3.6089 +14	1.5355 +34	0.914	1.8066 +15	2.5019 +35
0.240	4.1538 +14	2.2168 +34	0.929	1.8392 +15	2.5514 +35
0.257	4.4599 +14	2.6573 +34	0.942	1.8708 +15	2.5981 +35
0.278	4.8595 +14	2.8840 +34	0.956	1.9017 +15	2.6420 +35
0.300	5.2630 +14	3.1544 +34	0.969	1.9319 +15	2.6835 +35
0.321	5.6665 +14	3.4635 +34	0.982	1.9614 +15	2.7226 +35
0.343	6.0710 +14	3.8151 +34	0.994	1.9903 +15	2.7595 +35
0.364	6.4787 +14	4.2134 +34	1.007	2.0186 +15	2.7944 +35
0.386	6.8903 +14	4.6624 +34	1.036	2.0884 +15	2.9955 +35
0.407	7.3075 +14	5.1657 +34	1.066	2.1588 +15	3.1986 +35
0.429	7.7311 +14	5.7269 +34	1.097	2.2298 +15	3.4035 +35
0.451	8.1620 +14	6.3482 +34	1.127	2.3015 +15	3.6105 +35
0.473	8.6010 +14	7.0314 +34	1.156	2.3738 +15	3.8195 +35
0.496	9.0485 +14	7.7762 +34	1.186	2.4467 +15	4.0301 +35
0.518	9.5044 +14	8.5815 +34	1.217	2.5202 +15	4.2429 +35
0.541	9.9695 +14	9.4465 +34	1.247	2.5943 +15	4.4572 +35
0.564	1.0442 +15	1.0364 +35	1.276	2.6690 +15	4.6735 +35
0.587	1.0916 +15	1.1312 +35	1.306	2.7442 +15	4.8913 +35
0.610	1.1389 +15	1.2281 +35	1.337	2.8200 +15	5.1111 +35
0.632	1.1859 +15	1.3259 +35	1.367	2.8963 +15	5.3323 +35
0.654	1.2325 +15	1.4234 +35	1.396	2.9732 +15	5.5556 +35
0.676	1.2792 +15	1.5206 +35	1.426	3.0506 +15	5.7801 +35
0.698	1.3266 +15	1.6176 +35	1.457	3.1286 +15	6.0064 +35
0.720	1.3734 +15	1.7124 +35	1.487	3.2070 +15	6.2344 +35

10

Bose Condensates in Neutron Stars

Neither pions nor kaons exist as a component of nuclear matter under normal circumstances. The reason for this was discussed in Section 5.4.7. The pion has negative parity and consequently its expectation value in the normal ground state, which is a diagonal matrix element, vanishes. The kaon carries strangeness and its expectation likewise vanishes. However, conditions may arise at higher density that favor a change in the structure of the ground state, yielding finite expectation values and permitting the appearance of a Bose condensate. Pion condensation was much discussed in the 1980s but it was demonstrated ultimately that it could not form in nuclear matter [278]. The negative kaon turns out to be most favored, even though its vacuum mass is high because of its attractive interaction with the nuclear medium. In this chapter we follow closely the development of Refs. [410, 411].

We have seen that the electron chemical potential increases with the density of charge neutral matter to compensate the growing density of protons (Fig. 5.32). The growth of the electron chemical potential can be arrested if hyperons of negative charge become an important component of the baryon population (Section 5.4.7). In any case, the attractive interaction of the negative kaon with the nuclear medium will lower its effective mass, and if it is lowered to the point that it falls to a value equal to the electron chemical potential, negative kaons, being bosons, are able to condense in the lowest momentum ($k = 0$) state. For densities higher than this threshold, the negative kaon will become the neutralizing agent in place of additional electrons and may even quench the electron population.

A crucial question with regard to the occurrence of kaon condensation is how well neutrality can be achieved among baryon carrying species (Section 5.4.6). This is a matter of the hyperon coupling constants. At the present time, only the coupling constant for the Λ can be constrained (Section 5.4.3). For our choice of coupling

constants, the behavior of the electron chemical potential is shown in Fig. 5.32 and kaon condensation would not compete with hyperonization unless the medium modification of the negative kaon energy were a particularly strong function of density. One thing is clear. There is an hierarchy among phase transitions in the order of quark deconfinement, hyperonization, and Bose condensation; earlier ones mentioned can preempt later ones—not the reverse. It is also possible that several of these phase transitions may occur at a sequence of increasing densities. Clearly, quark deconfinement is the ultimate phase transition that needs to be considered in the density and temperature range of neutron stars. With the present uncertainties in hyperon couplings and kaon medium modifications, one cannot say with any certainty whether kaon condensation is likely or not.

But kaon condensation is a possibility that, like deconfinement, has especially interesting consequences in isospin asymmetric nuclear matter, including the formation of spatially ordered regions of the normal and new phase in the range of densities for which both phases are in equilibrium [194, 195, 410]. Moreover, both phases can be described by a single theory, unlike deconfinement, where the nuclear phase is described by our relativistic field theory, and the quark phase by the MIT bag model. Consequently the possibility exists for a self-consistent calculation of the surface interface energy at the boundary between phases.

In early work on pion condensation, the region of phase coexistence was found by use of the Maxwell construction (sometimes with reference to Van der Waal's equation of state; cf. Refs. [412]–[416]). As was discussed in Chapter 9, the Maxwell construction is valid for simple substances—those with *only one* independent component, like water, or pure neutron matter (which nowhere exists). However, this construction can assure that only one chemical potential is common to the two phases, whereas asymmetric nuclear matter, such as neutron star matter, has two independent components (the baryon and electric charge). Consequently, the construction cannot satisfy Gibbs criteria that all chemical potentials as well as pressure and temperature be common to both phases in equilibrium. In short, the states studied were unstable. This is true of the deconfinement transition in early work beginning in the 1970s and also of more recent work on first-order kaon condensation [293, 417, 418, 419].

In this chapter, we study the kaon condensed phase as a *first-order* phase transition in neutron star matter [420]. This will serve as a general example of a Bose condensate. Unlike the previously cited work, compliance with Gibbs criteria for equilibrium is ensured by our treatment. Just as in the case of the deconfinement phase transition, we find that the two phases in equilibrium are oppositely charged, though in sum, neutral, as ought to be so for stellar material. Consequently, the total energy, including Coulomb and surface energies, is minimized by a lattice arrangement of the rare phase immersed in the dominant [194, 195, 410].

The kaon condensed phase differs from the normal nuclear matter state, not merely by the presence of kaons, but by a large difference in the nucleon effective mass [410]. This is necessarily the case because it is, after all, the interaction of the kaons with baryons that alters the kaon mass in the nuclear medium. Even in the mixed phase, where adjacent regions of space are occupied by the normal or con-

densed phases in equilibrium with each other, the nucleons have different masses according to the region they occupy. The high degree of inhomogeniety in the mixed phase—the Coulomb lattice structure, the localization of opposite charge in adjacent regions of different phase and the very different nucleon effective masses in the two regions—has potentially interesting consequences for the transport and superfluid properties of neutron stars which have not so far been investigated.

10.1 Relativistic Mean–Field Model with Kaons

In the approach presented here, we use a relativistic nuclear field theory solved in the mean-field approximation just as in Chapter 5. The interaction between baryons is mediated by the exchange of scalar and vector mesons. This picture is consistently extended to include the kaons. The model is similar to the one used for describing the properties of the H dibaryon in nuclear matter which is known to be thermodynamically consistent [421]. The coupling schemes applied for the kaon are in analogy to the one we used for the H dibaryon [420].

We employ the same Lagrangian for the description of the nucleon sector as before (5.38); however, so as to emphasize features associated with kaon condensation, only nucleons rather than the entire baryon octet are included. The coupling constants in the nucleon sector can be determined algebraically as in Chapter 4 so as to assure a proper normalization of the theory to nuclear matter properties at saturation density. In particular, for normal symmetric matter, the following properties and their values are assured: $E/A = -16.3$ MeV, $\rho_0 = 0.153$ fm^{-3}, $a_{\rm sym} = 32.5$ MeV, $K = 240$ MeV, and $m^*/m = 0.78$. Other parameterizations will not change the overall feature of kaon condensation as discussed here, but may alter the threshold density, limiting neutron star mass and radius.

There are two main schemes for treating the kaon interactions with the nuclear medium. One uses terms derived from chiral perturbation theory [277]—the other couples the kaon to meson fields [46]. We choose to take the latter approach so that nucleon and kaon interactions are treated on the same footing. It is also simpler. However, we couple kaons to the other mesons is a slightly different manner than heretofore. The kaon is coupled to the meson fields using minimal coupling

$$\mathcal{L}_K = \mathcal{D}^*_\mu K^* \mathcal{D}^\mu K - m_K^{*\,2} K^* K \tag{10.1}$$

where the vector fields are coupled by defining

$$\mathcal{D}_\mu = \partial_\mu + i g_{\omega K} \omega_\mu + i g_{\rho K} \boldsymbol{\tau} \cdot \boldsymbol{\rho}_\mu \,. \tag{10.2}$$

Then the vector fields are coupled to a conserved current. The isospin operator $\boldsymbol{\tau}$ is understood to act on the kaon wave function which we denote by K. The form (10.2) results in another coupling term in the Lagrangian (10.1) of the form

$$2 g_{\omega K}^2 \omega_\mu \omega^\mu K^* K \tag{10.3}$$

which gives a nonlinear density dependence of the kaon optical potential. This is in addition to the standard Yukawa coupling term.

The scalar field is coupled to the kaon by analogy to the minimal coupling scheme of the vector fields

$$m_K^* = m_K - g_{\sigma K}\sigma \,. \tag{10.4}$$

In addition to the standard linear Yukawa coupling term, it gives also a quadratic coupling term to the scalar field in the Lagrangian having the form

$$(g_{\sigma K}\sigma)^2 K^* K \,. \tag{10.5}$$

This term is small compared to the linear Yukawa coupling term as it is suppressed by $g_{\sigma K}/(2m_K)$. Nevertheless, it will simplify the equations of motion considerably as we will show in the following.

The equation of motion for the kaon can be written as

$$\left[\mathcal{D}_\mu \mathcal{D}^\mu + m_K^{*\,2}\right] K(x) = 0 \,. \tag{10.6}$$

In uniform infinite matter (which any locally inertial frame in the star approximates), we expand $K(x)$ in momentum eigenfunctions, just as in (4.127). Carrying out the indicated operations, we obtain a long factor times the Kaon momentum eigenstate. Because the eigenstate is not supposed to vanish, the factor must. We thus obtain the dispersion relation for the K^- straightforwardly,

$$-\omega_K^2 + m_K^2 + k^2 + \Pi_K(\omega_K, k, \rho) = 0 \,. \tag{10.7}$$

Here, the time component of the kaon 4-momentum is denoted by ω_K and the magnitude of the 3-momentum by k. Dependence on the baryon density ρ enters through the dependence of the scalar and vector fields, σ, ω_0, and ρ_{03} on the baryon Fermi momentum. The term $\Pi_K(\omega_K, k, \rho)$ is called the K^- self-energy in the medium and is given by

$$\begin{aligned}\Pi_K(\omega_K, k, \rho) = &-2\omega_K\left(g_{\omega K}\omega_0 + g_{\rho K}\rho_{03}\right) - \left(g_{\omega K}\omega_0 + g_{\rho K}\rho_{03}\right)^2 \\ &- 2m_K g_{\sigma K}\sigma + (g_{\sigma K}\sigma)^2\end{aligned} \tag{10.8}$$

and depends on the in-medium kaon energy ω_K. As in our earlier work, ρ_{03} is the timelike Lorentz component and the isospin 3-component. The spacelike components of ρ^μ and ω^μ vanish as we showed in Chapter 5. The preceding two equations can be written

$$[m_K - g_{\sigma K}\sigma]^2 = [\omega_K + \left(g_{\omega K}\omega_0 + g_{\rho K}\rho_{03}\right)]^2 \,. \tag{10.9}$$

We find at once the dispersion relation for s-wave condensation (i.e., for $\boldsymbol{k} = 0$) for the K^-

$$\omega_K = m_K - g_{\sigma K}\sigma - g_{\omega K}\omega_0 - g_{\rho K}\rho_{03} \tag{10.10}$$

which is linear in the meson fields. Thus, the medium-modified kaon energy is reduced from its vacuum value to a smaller, density-dependent value.

There appear additional source terms in the equation of motion for the meson fields if a kaon condensate is present, namely,

$$\begin{aligned} m_\sigma^2\sigma &= g_{\sigma N}\left[\rho_s - b\, m_N(g_{\sigma N}\sigma)^2 - c\,(g_{\sigma N}\sigma)^3\right] + 2g_{\sigma K}m_K^* K^*K \\ m_\omega^2\omega_0 &= g_{\omega N}(\rho_p + \rho_n) - 2g_{\omega K}(\omega_K + g_{\omega K}\omega_0 + g_{\rho K}\rho_{03})K^*K \\ m_\rho^2\rho_{03} &= g_{\rho N}\left(\rho_p - \rho_n\right)/2 - 2g_{\rho K}(\omega_K + g_{\omega K}\omega_0 + g_{\rho K}\rho_{03})K^*K\,. \end{aligned} \tag{10.11}$$

The scalar density is as in (4.152) and ρ_n and ρ_p denote neutron and proton number densities. The vector meson ω_0 is driven by their sum and the isovector ρ_{03} by their difference. Note that the equations of motion for nucleons are unchanged. The conserved current associated with the kaons is derived by using

$$\begin{aligned} J_\mu^K &= i\left(K^*\frac{\partial\mathcal{L}}{\partial^\mu K^*} - \frac{\partial\mathcal{L}}{\partial^\mu K}K\right) \\ &= K^* i\partial_\mu K - (i\partial_\mu K^*)K - 2g_{\omega K}\omega_\mu K^*K - 2g_{\rho K}\boldsymbol{\tau}\cdot\boldsymbol{\rho}_\mu K^*K\,. \end{aligned} \tag{10.12}$$

In the mean-field approximation, the K^- density is given by

$$n_K = -J_0^K = 2\left(\omega_K + g_{\omega K}\omega_0 + g_{\rho K}\rho_{03}\right)K^*K\,. \tag{10.13}$$

For s-wave condensation we can use the dispersion relation in the form (10.10) to get an expression for the scalar density of the kaon,

$$n_K = 2m_K^* K^*K \tag{10.14}$$

which turns out to be identical to the vector density above. This relation holds only for $\vec{k} = 0$ which is the case for cold neutron star matter and s-wave condensation. It is a result of our choice of the scalar coupling scheme (10.4). For the negatively charged kaon the equation of motion are then simplified to

$$\begin{aligned} m_\sigma^2\sigma &= g_{\sigma N}\left[\rho_s - b\, m_N(g_{\sigma N}\sigma)^2 - c\,(g_{\sigma N}\sigma)^3\right] + g_{\sigma K}n_K \\ m_\omega^2\omega_0 &= g_{\omega N}(\rho_p + \rho_n) - g_{\omega K}n_K \\ m_\rho^2\rho_{03} &= g_{\rho N}\left(\rho_p - \rho_n\right)/2 - g_{\rho K}n_K\,. \end{aligned} \tag{10.15}$$

The total charge in the normal and in the kaon condensed phase are respectively

$$\begin{aligned} q_N &= \rho_p - \rho_e - \rho_\mu \\ q_K &= \rho_p - \rho_e - \rho_\mu - n_K\,. \end{aligned} \tag{10.16}$$

When the nuclear medium is in one of the pure phases, the corresponding charge density must vanish identically, and this fact must be placed as a constraint on the solution.

We know from our earlier studies in Chapter 5 how to solve the problem in the pure normal phase, where the kaon density n_K vanishes. With that solution at hand, the energy of a test kaon in the pure normal phase can be computed as a function of the baryon density of the normal phase from (10.10). The kaon energy in the medium, ω_K, will decrease from its vacuum value of m_K with increasing density of the pure normal phase because of the growth of the meson fields appearing in (10.10). At the same time, $\mu_{K^-} = \mu_e$ increases with increasing proton density.

However, at the density for which the equality

$$\omega_K = \mu_e \tag{10.17}$$

is first achieved, kaons will occupy a small fraction of the total volume of the medium—the kaon condensed phase. The kaon density n_K has acquired a finite value and appears as a contribution in the meson field equations (10.15). We can now combine (10.10) and (10.17)

$$\omega_K = m_K - g_{\sigma K}\sigma - g_{\omega K}\omega_0 - g_{\rho K}\rho_{03} = \mu_e \,. \tag{10.18}$$

We recall that $\mu_p = \mu_n - \mu_e$ where the latter two chemical potentials are the independent ones. We also recall that the Fermi momentum for nucleons or leptons is given in terms of chemical potentials by a relation such as $k_F = \sqrt{\mu^2 - m^2}$ for each fermion type. So all densities and other necessary integrals are defined. Thus, three field equations (10.15), the relation (10.18), the second of the charge equations (10.16) with q_K set to zero, and the condition that all baryons add up to yield the total baryon density

$$\rho_p(\mu_n - \mu_e) + \rho_n(\mu_n) = \rho_{\text{total}} \tag{10.19}$$

provide six equations in the unknowns σ, ω_0, ρ_{03}, μ_n, μ_e and n_K. In this manner we see that the pure kaon condensed phase has been completely specified by our equations for any chosen baryon density.

We turn now to the mixed phase. Here, Gibbs conditions for equilibrium (we assume common T of zero so do not mention it) and the conservation laws can be satisfied simultaneously for substances of more than one conserved charge by applying the conservation law(s) only in a *global* rather than a *local* sense [194, 195]. We discussed this thoroughly in connection with hybrid stars. Thus, for neutron star matter that has two conserved charges, the Gibbs conditions and conservation of electric charge read

$$p_N(\mu_n, \mu_e) = p_K(\mu_n, \mu_e) \tag{10.20}$$

$$q_{\text{total}} = (1 - \chi)q_N(\mu_n, \mu_e) + \chi q_K(\mu_n, \mu_e) = 0 \,. \tag{10.21}$$

where p_N, q_N and p_K, q_K denote the pressure and charge densities of the *normal* and *kaon condensed* phases respectively. For any volume proportion of kaon phase χ in the interval (0,1), the six equations (10.15), (10.18)–(10.20), and (10.21) determine the same six unknowns quoted above. Note that we have changed independent variable in the mixed phase from baryon density to kaon volume fraction χ. The total baryon density in the mixed phase is given as a function of χ by

$$\rho_{\text{total}} = (1 - \chi)\rho_N(\mu_n, \mu_e) + \chi\rho_K(\mu_n, \mu_e) \,, \tag{10.22}$$

where $\rho_N = \rho_p + \rho_n$ and ρ_K denote *baryon* number density in the two phases, respectively. A similar equation holds for the energy density.

Therefore, the chemical potentials and all field quantities are functions of the volume proportion χ of kaon condensed phase, and so are all other properties of the two phases in equilibrium, including the common pressure. This is a mathematical proof that, in general, properties will vary as the proportion. *Why* and how they

vary depends on how the internal driving forces can exploit the degrees of freedom (one less than the number of independent chemical potentials) so as to minimize the total energy [195].

It will be noted that the pressure equality (10.20) cannot be solved simultaneously with conditions of *local* charge neutrality, $q_N(\mu_n, \mu_e) = 0$, $q_K(\mu_n, \mu_e) = 0$, because then seven equations would have to be satisfied with the same six variables mentioned.

The total energy density is given by

$$\epsilon = \begin{cases} \epsilon_N , & \text{if normal phase ;} \\ \epsilon_N + \epsilon_K \equiv \epsilon_C , & \text{if condensed phase .} \end{cases} \tag{10.23}$$

The nucleon part consists of the standard terms (cf. Chapter 5)

$$\epsilon_N = \frac{1}{2}m_\sigma^2\sigma^2 + \frac{b}{3}m_N(g_{\sigma N}\sigma)^3 + \frac{c}{4}(g_{\sigma N}\sigma)^4 + \frac{1}{2}m_\omega^2\omega_0^2 + \frac{1}{2}m_\rho^2\rho_{03}^2 + \sum_{i=N,l}\frac{\nu_i}{2\pi^2}\int_0^{k_F^i} dk\, k^2\sqrt{k^2 + m_i^{*2}} . \tag{10.24}$$

The sum is over nucleons and leptons. In principle, it could extend over baryons of the octet, but we neglect the higher members in the present study. Note that though the expression for the energy contribution in the nucleon sector, ϵ_N, has the same appearance whether or not kaons have condensed, it is nonetheless composed of fields that either have or have not a contribution from the condensed kaons through the last term in each of the field equations (10.15). The specific kaon contribution to the energy density reads

$$\epsilon_K = 2m_K^{*\,2}K^*K = m_K^* n_K . \tag{10.25}$$

The kaon does not contribute directly to the pressure as it is a (s-wave) Bose condensate so that the total pressure

$$p = -\frac{1}{2}m_\sigma^2\sigma^2 - \frac{b}{3}m_N(g_{\sigma N}\sigma)^3 - \frac{c}{4}(g_{\sigma N}\sigma)^4 + \frac{1}{2}m_\omega^2\omega_0^2 + \frac{1}{2}m_\rho^2\rho_{03}^2 + \frac{1}{3}\sum_{i=N,l}\frac{\nu_i}{2\pi^2}\int_0^{k_F^i} dk\,\frac{k^4}{\sqrt{k^2 + m_i^{*2}}} \tag{10.26}$$

is just the familiar expression known from relativistic mean field theory for nucleons and leptons only (Chapter 4). The factor ν_i is the spin degeneracy, 2 for (spin 1/2) nucleons and leptons. Kaons, if present (in the zero momentum state), do not contribute to the pressure. But the pressure is modified in the condensed phase indirectly through the change of the meson fields by the additional kaon source terms that enter into the equations of motion (10.15). Thus, in the Gibbs condition for equality of pressures in the two phases, although the mathematical expressions for the pressures are the same, we differentiate the two by the subscripts N and K because they are indeed to be calculated with different values of the field quantities.

Because all kaons can condense in the lowest energy state, they become energetically more favorable than electrons as the neutralizing agent of positive charge.

With further increase of density and decrease in kaon energy ω_K, the electron chemical potential will decrease, and the electron population will decrease. It is evident from from (10.18) that as the fields grow with density, ω_K will decrease from its vacuum value and turn the electron chemical potential into a decreasing function of density. (We see this in Fig. 10.3 that we discuss again later.)

The condition for condensation of the isospin partner of the K^-, namely, the neutral kaon K^0, is $\omega(K^0) = 0$. Hence, if there were no isovector potential for the kaons, the K^0 could appear only after charged kaons have appeared, and provided that the electron chemical potential falls to zero. This seems quite unlikely and, to our knowledge, was therefore completely ignored in previous works. Nevertheless, the isospin potential of the nucleons shifts the energy of the K^0 below that of the K^- in neutron-rich matter so that

$$\omega(K^0) = \omega(K^-) + 2g_{\rho K}\rho_{03} = \omega(K^-) - 2\frac{g_{\rho K}^2}{m_\rho^2}\left(\rho_n - \rho_p\right) . \tag{10.27}$$

So, indeed, the possibility exists for neutral kaon condensation induced by K^- condensation. For the sake of simplicity we ignore the K^0 in the following, but note that it is clear from our discussion that K^0 condensation should be taken into account in a more realistic calculation.

The Lagrangian for the kaons (10.1) describes the kaon–nucleon interaction as well as the kaon–kaon interaction. The K^- in a nuclear medium is certainly a coupled channel problem due to the opening of the $\Sigma\pi$, $\Lambda\pi$ channels and can not be treated on the mean-field level. Coupled channel calculations at finite density, first done by Koch [422], yield an attractive potential for the K^- at normal nuclear density of about $U_{K^-}(\rho_0) = -100$ MeV. Waas and Weise find a value of $U_{K^-}(\rho_0) = -120$ MeV [423]. Kaonic data support the conclusion that there is a highly attractive kaon optical potential in dense nuclear matter [424]. Because the kaon is a boson it does not add directly to the pressure; it forms a Bose condensate in the s-wave with zero momentum [277]. This is contrary to pion condensation which condenses in a p-wave with a finite momentum. A self-consistent treatment of the in-medium self-energy of the pion prevents pion condensation [278]. A coupled channel calculation including the modified self-energy of the kaon has been studied in [425] and it was found that the kaon still sees an attractive potential at high density.

On the mean-field level considered here, the three kaon coupling constants, $g_{\sigma K}$, $g_{\omega K}$, and $g_{\rho K}$ can be fixed to kaon–nucleon scattering lengths. The in-medium potentials for the K^- are given by G-parity, that is by switching the sign of the vector potential. This gives similar results for the K^- optical potential compared to the coupled channel calculations [426]. We choose to couple the vector fields according to the simple quark and isospin counting rule

$$g_{\omega K} = \frac{1}{3}g_{\omega N} \quad \text{and} \quad g_{\rho K} = g_{\rho N} . \tag{10.28}$$

The scalar coupling constant is fixed to the optical potential of the K^- at ρ_0:

$$U_K(\rho_0) = -g_{\sigma K}\sigma(\rho_0) - g_{\omega K}\omega_0(\rho_0)\,. \tag{10.29}$$

The kaon potential is fixed, as quoted above, at normal nuclear density and varies as a function of the density ρ.

10.2 Equation of State with a Kaon Condensate

In this section we discuss the equation of state including kaons emphasizing the difference between the hitherto applied Maxwell construction and the thermodynamic consistent Gibbs condition. Then the dependence of the presence of the condensate state on the parameters of the theory, in particular, the kaon optical potential in matter. After this, we study properties of the mixed phase consisting of normal neutron star matter and the kaon condensed state in equilibrium one with the other.

10.2.1 Maxwell versus Gibbs

The standard thermodynamic rule for two phases in thermodynamical equilibrium is given by the Gibbs condition

$$p^{\rm I} = p^{\rm II}\,, \quad \mu_i^{\rm I} = \mu_i^{\rm II}\,, \quad T^I = T^{II}\,, \tag{10.30}$$

which simply states that the two phases are in mechanical, chemical, and thermal equilibrium. For the special case of only *one* chemical potential, the resulting equation $p^{\rm I}(\mu, T) = p^{\rm II}(\mu, T)$ has a unique solution for μ. It is often found by use of a Maxwell construction in one form or another. For example, the common tangent method, is based on the fact that $\mu = d\epsilon/d\rho = dE/dN$. Write the equation of state in the form $\epsilon = \epsilon(\rho)$. The segment of the common tangent, $\epsilon = -p_0 + \mu_0\rho$ touching the equation of state once in each phase describes the mixed phase with common and constant values of p_0 and μ_0, independent of the proportion of the two phases. Clearly, the Maxwell construction can assure that only a single chemical potential is common to both phases.

However, neutron star matter has two chemical potentials, μ_n and μ_e, each of which must be equal in the two phases to assure equilibrium. Hence, a Maxwell construction *cannot* be used as it will produce a discontinuity in one of the chemical potentials and will describe an unstable state—one for which there is a potential difference at the boundary between phases. This general fact concerning phase transitions with more than one conserved charge inside neutron stars was realized only a few years ago [194, 195]. It was shown (i) how to assure equilibrium in substances of an arbitrary number of conserved charges, (ii) that conservation laws cannot be locally imposed, but only globally over the entire region of mixed phase, (iii) how internal forces redistribute conserved charges between equilibrium phases so as to minimize the energy, (iv) and how, in the case that the electric charge is among the conserved charges, a Coulomb lattice will be formed.

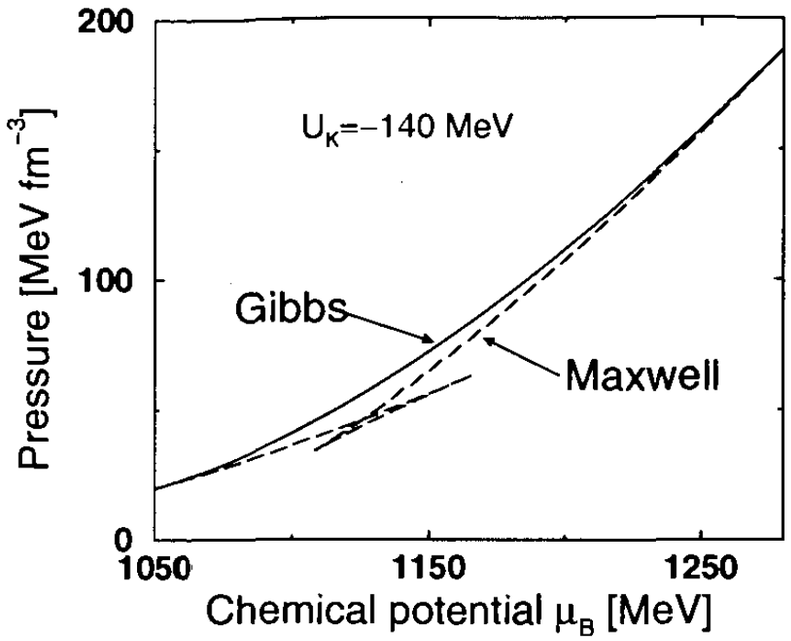

FIGURE 10.1. The pressure versus the baryon chemical potential for a Maxwell construction (dashed line) compared to the Gibbs condition (solid line). The Gibbs condition is thermodynamically more stable.

For kaon condensation, we contrast the Maxwell and Gibbs construction of phase equilibrium in a multi–component system, the latter having been formulated in Ref. [195]. A Maxwell construction is often implemented by looking at the thermodynamical potential of interest, here the pressure, as a function of the chemical potential as depicted in Fig. 10.1. The first portion of the curve corresponds to the normal phase and is physical up to the crossing point; from that point, the curve represents the kaon condensed phase. The crossing of the curve is the point of equal pressure and baryon chemical potential in the two phases. The temperature, being constant along the curve ($T = 0$), the crossing *point* represents phase equilibrium in this construction, *if* there is only one chemical potential; that is, the substance has only one independent component.

By contrast, Gibbs conditions implemented as described above (10.21) with global conservation of charge yields the smooth monotonic curve. It is the thermodynamically favored state because its pressure is higher than the pressure of the Maxwell construction. And by construction described above, the pressure and both chemical potentials of this two component substance are common to the two phases along the curve. The mixed phase is not a point, as in the case of Maxwell, but the *line* and the mixed phase begins and ends where it touches the curves of the two pure phases (dashed line).

The pressure difference between the two cases depicted in Fig. 10.1 depends on the equation of state and the optical potential of the kaon. In addition, it is also sensitive to surface interface and Coulomb corrections. Here, we discuss only bulk matter. Coulomb and surface energy will reduce the pressure in the mixed phase. However the Gibbs construction, even with such corrections, cannot fall below the Maxwell curve as discussed on page 358. The actual energy difference between the Maxwell and Gibbs curves depends on the surface tension, which is unknown for a kaon condensed phase immersed in dense nuclear matter and will shift the

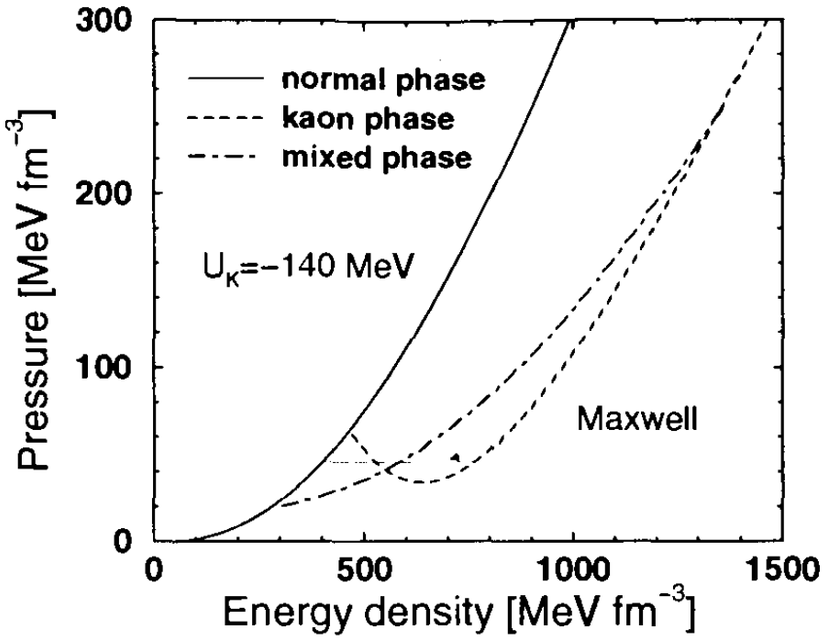

FIGURE 10.2. The equation of state for a pure nuclear matter (solid line), pure kaon matter (dotted line) for $U_K(\rho_0) = -140$ MeV. The Maxwell construction is shown by the horizontal line, the Gibbs solution by the dashed-dotted line.

curve for the Gibbs condition case to slightly lower values. But because the sum of Coulomb energy and surface energy vanishes at the boundaries of the mixed phase (see (9.26) and (9.28)) the boundaries are unaffected. We will discuss the geometric features of the mixed phase in more detail later.

The differences between the two descriptions, Maxwell and Gibbs, are most striking for the relevant ingredient for neutron star calculations, namely, the equation of state as plotted in Fig. 10.2. The solid line shows the equation of state for the normal hadronic phase of neutron star matter, the dotted line the one for pure kaon condensed matter. The Maxwell construction results in a region of constant pressure (solid horizontal line) connecting the two different equation of states. Applying the Gibbs condition with conservation of two (or more) conserved charges causes two major differences compared to the Maxwell construction. First, the pressure increases monotonically through the mixed phase rather than being constant as for a one-component substance. Second, the density range of the mixed phase is much broader; it starts at a lower density and ends at a much higher density. Hence, the mixed phase can well be the dominant portion of a neutron star.

There is another striking feature apparent in Fig. 10.2; The Gibbs phase transition for a substance having more than one independent component resembles a second-order phase transition in form. Nevertheless, it is a first-order transition because there is a region of density for which two distinct phases of the substance are simultaneously present and in equilibrium.

Figure 10.3 shows the behavior of the chemical potentials using Gibbs and Maxwell construction for comparison. The region of the mixed-phase of neutron star matter is indicated by the vertical dotted lines. The electron chemical potential increases in the pure hadronic phase as the density of neutrons and protons increase. However, at the critical density for kaon condensation the electron chemical potential decreases with further increase of density as kaons replace electrons

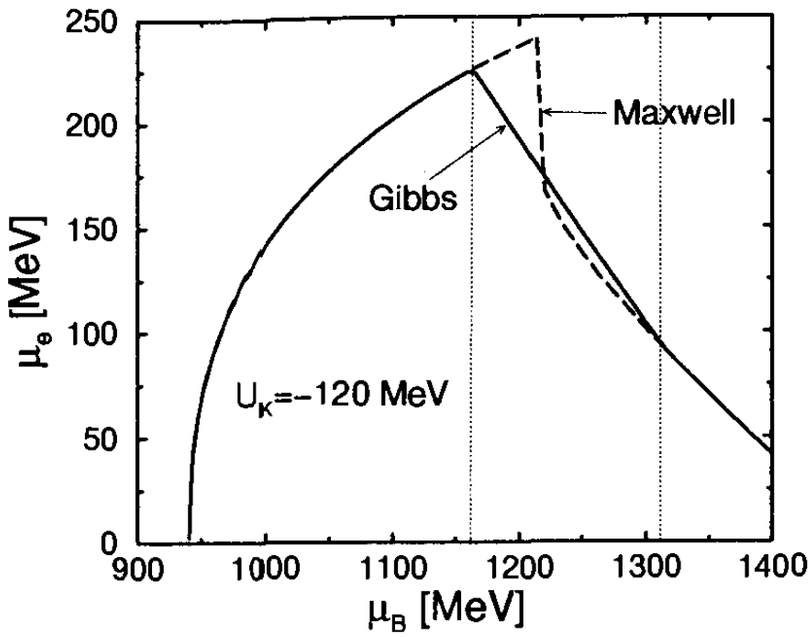

FIGURE 10.3. The electron chemical potential and the baryon chemical potential (denoted by μ_n in the text) for the case $U_K(\rho_0) = -120$ MeV using the Gibbs condition (solid line) and a Maxwell construction (dashed line). The large electric potential difference that occurs for the Maxwell construction gives rise to an instability.

in their role of neutralizing the charge on protons. We note that when the conservation of electric charge is imposed as a global constraint, as described above and in Chapter 9, the electron chemical potential is continuous. In contrast, if the transition were (incorrectly) treated by use of the Maxwell construction, the electron chemical potential has a discontinuity—a potential difference between the two phases [195]. Such a construction cannot describe an equilibrium situation. In the Maxwell construction, the electron chemical potential drops from $\mu_e = 240$ MeV to $\mu_e = 167$ MeV at the phase boundary resulting in a huge difference in the Fermi energy of the leptons between the two phases.

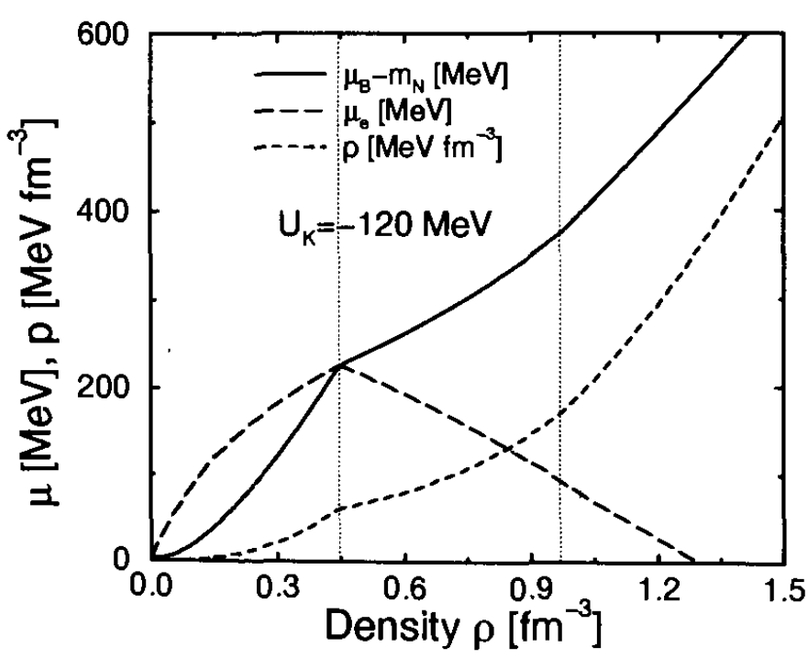

FIGURE 10.4. The pressure, the electron chemical potential, and the baryon chemical potential are plotted over the mixed-phase region using the Gibbs condition.

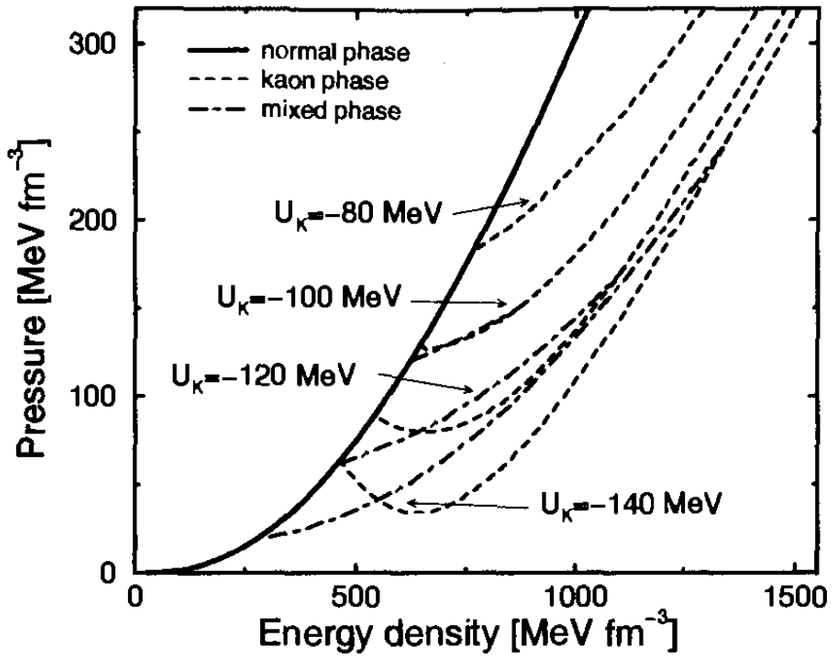

FIGURE 10.5. The equation of state for various choices of the optical potential of the kaon.

The behavior of the thermodynamic potential, the pressure, and the two chemical potentials over the mixed-phase region using the Gibbs condition is summarized in Fig. 10.4. The baryon chemical potential as well as the pressure increase monotonically with density. The electron chemical potential increases to the mixed-phase threshold; then it is decreases continuously with density. There is now no discontinuity in any of these variables and none stays constant over the mixed-phase region.

10.2.2 Dependence on parameters

The form of the equation of state depends sensitively on the chosen optical potential of the kaon, which reflects its interaction with the nuclear medium. Figure 10.5 shows the equations of state for kaon optical potentials whose values at normal nuclear matter density vary between -80 and -140 MeV. For $U_K(\rho_0) = -80$ MeV, the mixed phase is absent and the phase transition is of second order. For a deeper optical potential, a mixed phase appears as plotted in dashed-dotted lines. The deeper the optical potential of the kaon, the *lower* is the threshold density of the mixed phase and the *wider* is the density range of the mixed phase. The equation of state is considerably softened by the presence of the kaon condensate. The critical density for the onset of the kaon condensed phase is summarized for various kaon optical potentials in Table 10.1. For the cases $U_K(\rho_0) = -80$ MeV and -90 MeV the phase transition is of second order. (To see the dependence of the critical density on the underlying nuclear properties, see Ref. [411].)

10.2.3 Particle populations

The populations of the nucleons, leptons, and kaons for the case $U_K(\rho_0) = -120$ MeV are shown in Fig. 10.6. As it is more favorable to produce kaons in association

TABLE 10.1. The critical density for the appearance of the kaon condensed phase for different kaon optical potentials and parameter sets (TM1 is taken from [427], GL70 with $m^*/m = 0.70$ from [132]). GL78 refers to the parameters otherwise used in this chapter. The phase transition is of second order for the smallest two potentials.

$U_K(\rho_0)$ (MeV)	−80	−90	−100	−110	−120	−130	−140	−150
GL78: ρ_c/ρ_0	4.5	4.2	3.8	3.4	2.9	2.4	1.8	1.2
GL70: ρ_c/ρ_0	3.9	3.7	3.5	3.2	3.0	2.8	2.6	2.3
TM1: ρ_c/ρ_0	5.2	4.8	4.3	4.0	3.6	3.4	3.1	2.9

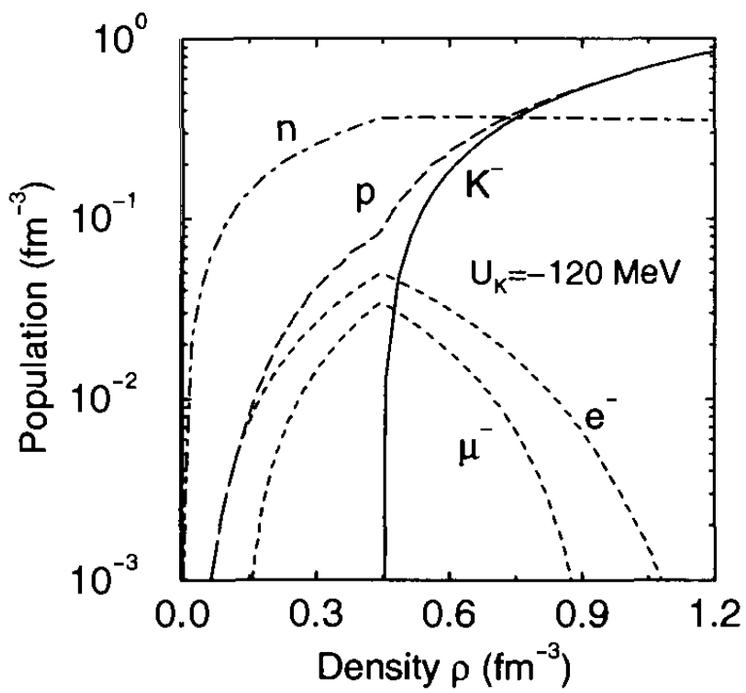

FIGURE 10.6. The population densities computed as the volume-weighted average in the two phases as functions of the nucleon density. The neutron density stays nearly constants when kaon condensation appears.

with protons, the neutron density remains (nearly) constant over the whole density range starting with the critical density. This has been found also in other work [419, 428, 429]. Because lepton populations are not conserved in a star because of the escape of neutrinos, the leptons decrease as the K^- becomes the new neutralizing agent for protons.

Figure 10.7 shows the population in the mixed phase for the two phases separately as a function of volume proportion χ of condensed phase. The normal phase population is denoted as I, the kaon phase population as II. For $\chi = 0$ the proton population in the normal phase is small and neutrality is achieved by a balance with the sum of the lepton populations. This corresponds to local neutrality in the pure phase. However, with a growing fraction of condensed phase, charge neutrality is achieved more economically between the two phases in equilibrium as a global constraint—the proton population increases to near equality with neutrons as the proportion of condensed phase increases, while the lepton populations decrease to the vanishing point. Isospin symmetry is thus closely achieved in the normal phase. This behavior is expected and explained in Chapter 9 and Ref. [195] as a

general feature of the action of the isospin driving force toward symmetry in phase transitions of asymmetric nuclear matter.

The population behaviors in the condensed phase are different. We can understand this as follows: compare the energy of neutron and of a proton-K^- pair, whose chemical potentials are the same. They are, respectively,

$$\mu_n = E_n = \sqrt{m^{*2} + k_{F,n}^2} + g_{\omega N}\omega_0 - g_{\rho N}\rho_{03} \tag{10.31}$$

$$\begin{aligned}\mu_n = \omega_{K^-} + E_p &= m_K - g_{\sigma K}\sigma - \frac{1}{3}g_{\omega N}\omega_0 - g_{\rho N}\rho_{03} \\ &\quad + \sqrt{m^{*2} + k_{F,p}^2} + g_{\omega N}\omega_0 + g_{\rho N}\rho_{03} \\ &= m_K - g_{\sigma K}\sigma + \sqrt{m^{*2} + k_{F,p}^2} + \frac{2}{3}g_{\omega N}\omega_0 \,. \end{aligned} \tag{10.32}$$

From these two expressions of μ_n we have,

$$\sqrt{m^{*2} + k_{F,p}^2} = \sqrt{m^{*2} + k_{F,n}^2} + \frac{1}{3}g_{\omega N}\omega_0 - g_{\rho N}\rho_{03} \,, \tag{10.33}$$

from which it is clear that $k_{F,p} > k_{F,n}$ when the sum of the last two terms is positive. Because ω_0 is proportional to the density, whereas ρ_{03} is proportional to the difference in isospin densities of proton and neutron, the sum will generally be positive, and is in the present case. That is, p-K^- pairs are preferred to neutrons. However, the symmetry restoring term in the energy will prevent an uninhibited growth of protons compared to neutrons.

We have neglected K^0 condensation (as has everyone else). It is clear that eventually there will be a competition between p-K^- pairs and n-K^0 pairs. It appears that with increasing density, the condensed phase will tend toward symmetry in neutrons and protons and similar densities of K^- and K^0.

Finally, we return again to the charge densities of the two phases in equilibrium. The overall charge vanishes as shown in Fig. 10.8, but the charges on each phase separately are finite except that the normal phase charge density goes to zero when it is the sole phase present ($\chi = 0$) while the condensed phase density vanishes when it becomes the sole phase ($\chi = 1$). The variation of the charge density for intermediate proportions of the two phases is such as to minimize the energy. The finite charge densities are responsible for the formation of a Coulomb lattice, which we discuss in Section 10.3.2.

10.2.4 Comment on coupling schemes

We comment here on the coupling schemes that have been employed in studies of the kaon condensate. As previously noted, we couple the kaon directly to the meson fields. In particular, the scalar meson is coupled in a minimal scheme as in (10.4). Coupling of kaon to meson fields was also employed in Refs. [310, 328]. However the scalar coupling was implemented there through $m_K^{*\,2} = m_K^2 - g_{\sigma K}\sigma$. In contrast to our scheme, the kaon effective mass is reduced from its vacuum value through the scalar field by only half as much (in leading order). As a consequence,

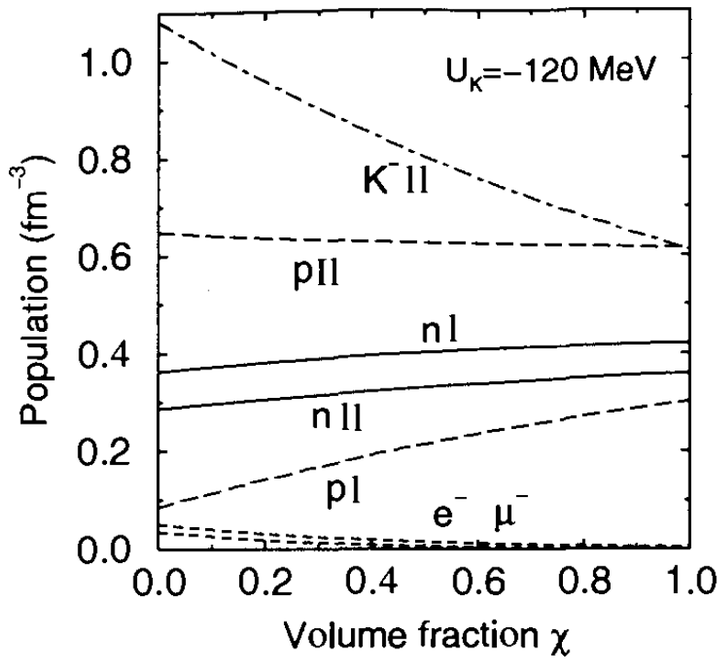

FIGURE 10.7. The population density in each phase shown separately as a function of volume fraction of kaon condensed phase. Normal phase is denoted by I and condensed phase by II.

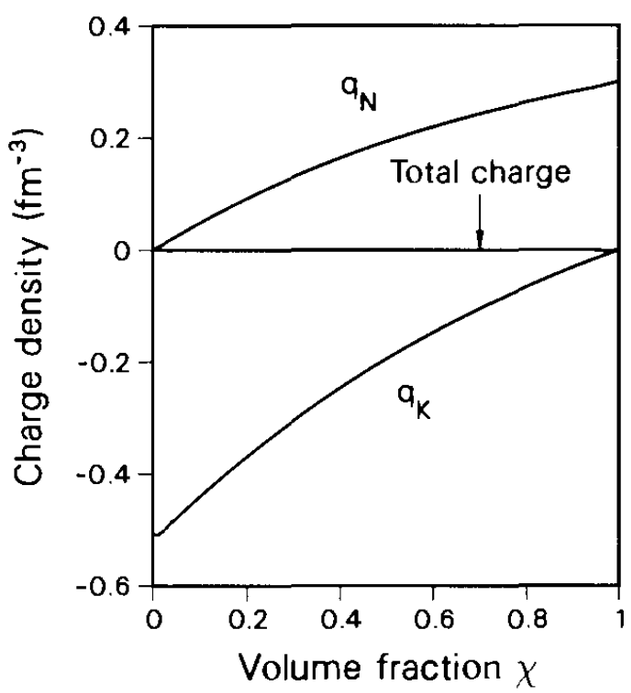

FIGURE 10.8. Charge densities of the normal and condensed phase as a function of proportion χ of the condensed phase.

even though much stronger optical potentials result from the coupling constants used in Refs. [310, 328], namely $U(\rho_0) \sim 180$ MeV, as compared with those favored by Koch [422] and Waas and Weise [423] of $U(\rho_0) = 100 - 120$ MeV, which we also favor, the phase transition found was weak and of second order. The order of the phase transition and the critical densities corresponding to several parameterizations of nuclear matter can be found in Table 10.1.

10.2.5 Comment on hyperons

The Pauli principle practically assures that hyperons will be present in dense charge-neutral matter. Their effect will be to quench the growth of the electron chemical potential and therefore either to raise the threshold density at which kaon condensation occurs, or to preempt condensation altogether [68]. Whether kaon condensation can actually occur therefore depends upon whether negative or neutral hyperons form a large part of the baryon population of charge-neutral matter at several times nuclear matter density. This in turn depends on two factors, neither of which is under strong control.

One is the strength of the coupling constants of hyperons to the scalar, vector and isovector mesons as compared to the nucleon couplings to these mesons. Only the coupling constants for the Λ can be constrained from hyperonic data and the extrapolated value of the Λ binding in nuclear matter [132, 430].

The other factor that effects to some degree the hyperon fraction are the assumed compression modulus and effective nucleon mass at saturation density of symmetric nuclear matter [191]. At the same time, as we see in Table 10.1, the phase transition order and the threshold density of kaon condensation also are rendered uncertain by the imprecision with which the properties of ordinary nuclear matter are known. So as to emphasize the interesting role that kaons *may* play in neutron stars, we have omitted hyperons completely. At the present time, we are unable to say with any degree of confidence whether kaon condensation will occur before it is preempted by the ultimate phase transition in the density and temperature domain of neutron stars—deconfinement. These effects should be studied in more detail in future work.

10.2.6 Mixed-phase properties

We will show in the following that the two phases in equilibrium have completely different properties from each other. We will focus on the case $U_K = -120$ MeV in this section.

Why should the nucleons not be the same in the two phases, and why can they not move freely between normal and kaon condensed phases? The answer is that when the nucleons are treated as dynamical particles they are quite different in the two phases; they have different masses. Their interaction with the kaon field is what causes the decrease of the kaon effective mass with increasing density. The decrease in kaon mass ultimately leads to the condensation of kaons. Conversely, the interaction also changes the nature of a nucleon. Figure 10.9 illustrates the dynamical nature of the nucleon: its effective mass is shown as a function of baryon density. Up to $\rho = 0.45\ \mathrm{fm}^{-3} = 2.94\rho_0$ there exists only one solution—the pure nucleon phase. The effective mass m_N^* decreases with density from its vacuum value at low density, to ~ 670 MeV at the density of normal nuclear matter, and further down to ~ 510 MeV at the end of the pure normal phase ($\sim 3\rho_0$).

A second solution appears for those regions of the medium that are occupied by the condensed phase in equilibrium with the normal phase. In contrast with the first

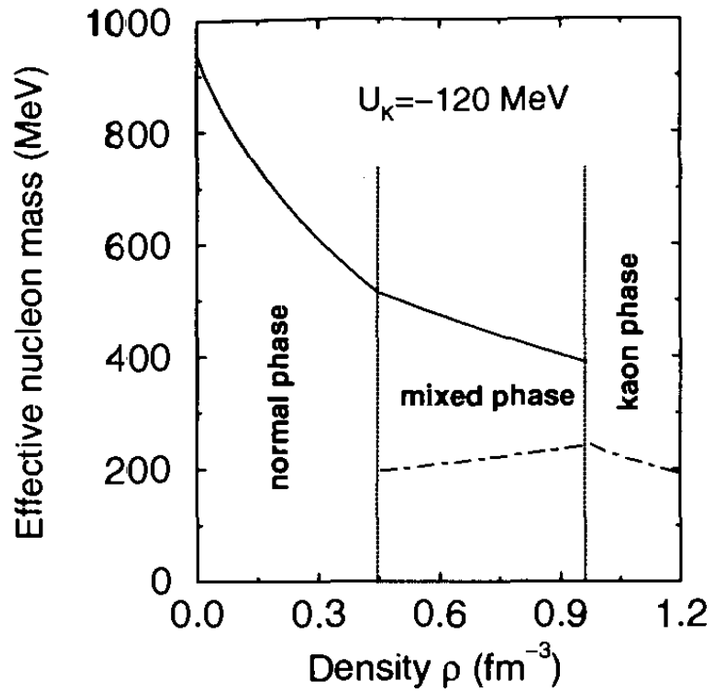

FIGURE 10.9. The effective nucleon mass as a function of the nucleon density. Shown by vertical lines is the onset and offset of the mixed phase.

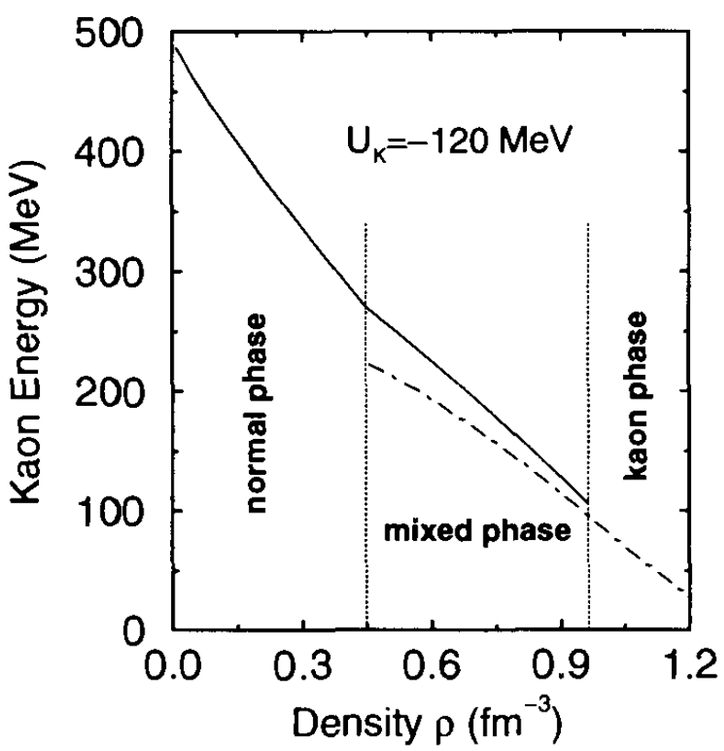

FIGURE 10.10. The K^- energy, ω_K, as a test particle in the normal phase (solid) and as a condensed kaon in the abnormal phase as functions of the nucleon density.

solution, the effective mass in the condensed phase is much smaller, $m_N^* \sim 196$ MeV. The mixed phase ends at $\rho = 0.97$ fm$^{-3} = 6.34\rho_0$ and only the second solution remains. The nucleons have different effective masses in the two phases due to the different mean-fields in the two phases. Hence, the nucleons cannot move freely between one phase and the other; a phase boundary develops. In Ref. [418] the nucleons in the two phases were treated only implicitly through a phenomenological equation of state. They did not appear as dynamical degrees of freedom, so the two solutions could not be found.

Figure 10.10 depicts the analogue to Fig. 10.9 for the energy ω_K of the K^- in the medium. Note that the kaon is only a test particle in the normal phase. The kaon appears physically only in the condensed phase, whether that phase be in equilibrium with the normal phase, or whether the medium is fully occupied by the condensed phase. The kaon energy decreases with density due to the attractive vector interaction with nucleons, but kaons do not appear in the medium until the threshold condition discussed above is satisfied. The energy of a test kaon in the medium is shown in Fig. 10.10 as dashed-dotted line. Its energy as a test particle is also shown in the regions of the mixed phase that are occupied by the normal phase. When the kaon energy sinks to a value satisfying the threshold condition, kaons begin to appear. But because the phase transition is first order they appear discontinuously with finite density (Fig. 10.7) in a small fraction of the total volume which is the kaon condensed phase in equilibrium with the normal phase. The energy of these medium modified kaons is less than that of a test kaon in the normal phase by about 50 MeV at the condensation threshold. The two energies are shown in the Fig. 10.10.

The most pronounced differences between the two phases is in the energy density and the charge density. As can be read from Fig. 10.11, the energy density of the nucleon phase at the onset of the mixed phase is $\epsilon = 460$ MeV fm^{-3} while it amounts to $\epsilon = 1140$ MeV fm^{-3} for the kaon condensed phase. The volume weighted sum of the energy densities of the two phases in equilibrium is

$$\epsilon = (1 - \chi)\epsilon_N(\chi) + \chi\epsilon_C(\chi) \tag{10.34}$$

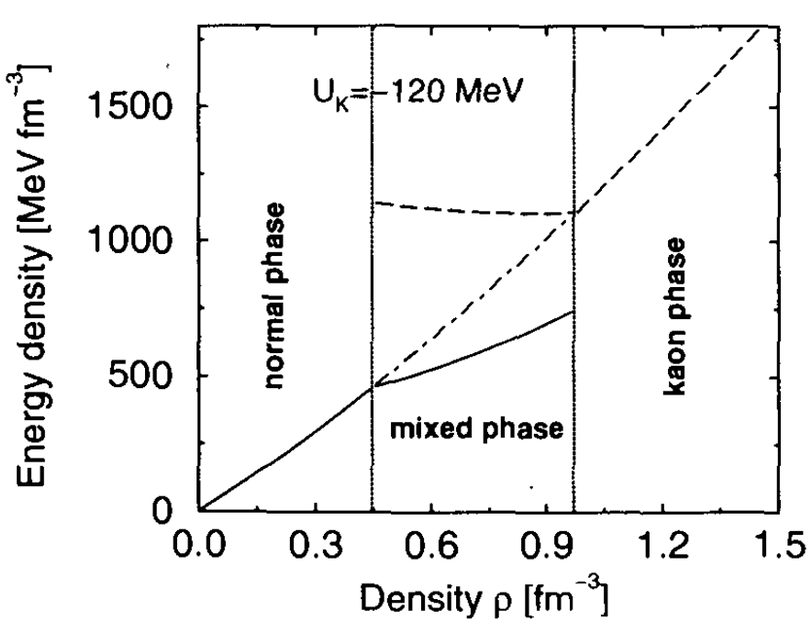

FIGURE 10.11. The energy density of normal phase (solid) and kaon condensed phase (dashed). The total energy in the mixed phase is the volume-weighted sum (dash-dotted).

and grows monotonically with density, but *not* linearly, as is the case in the Maxwell construction.[1] The nonconstant pressure is of course associated with the nonlinearity of the energy.

10.3 Stellar Properties

10.3.1 Large-scale features

We have already stressed how differently the computed equation of state and matter properties are, depending on whether the Maxwell construction is used to determine (incorrectly) the mixed phase of normal and condensed phase, or whether Gibbs criteria for equilibrium are fully respected. We start our discussion of the large-scale properties of stars by illustrating the difference in the mass-energy distribution in a star depending on which method is used. Figure 10.12 shows the distribution in the two cases.

For the Maxwell construction the energy density is discontinuous at the particular radius at which the pressure has the constant value of the Maxwell construction. The discontinuity is analogous to the separation of the phases in a gravitational field that is characteristic of a substance having a single component (like the steam above water). As we discussed earlier, neutron star matter in beta equilibrium does not behave like that: it has two independent components and all properties are continuous from one phase to another. The distribution of mass–energy for such a star is the continuous curve with a discontinuity only in *slope* but not in *value* at the boundary between mixed and pure normal phase. The central core of mixed phase is surrounded by normal dense nuclear matter. For the particular value of $U(\rho_0) = -120$ MeV, the mixed phase extends all the way to the center of the star and the pure condensed phase does not appear.

Depending on the kaon potential $U_K(\rho_0)$, the pure kaon condensed phase may not appear in the star, even for the star at the mass limit. Such is the case in the above Fig. 10.12. However, for a potential $U_K(\rho_0) = -140$ MeV, the pure kaon condensed phase would form the core of stars with a mass above about $1.25 M_\odot$, and for the limiting mass star, the condensed phase would extend to about 4.5 km. Likewise, for $U_K(\rho_0) = -130$ MeV, the central part of the more massive stars are occupied by a pure condensed phase.

The distribution of particles in the limiting mass star is dominated by the neutron in the normal phase outside 3 km as can be seen from Fig. 10.13. The K^- and proton are the dominant species in the mixed phase core. Lepton populations fall rapidly, as expected, as the K^- becomes dominant. However, overall, the proton population is far less than the neutron, and there appears little justification in referring to a star with a kaon condensate as a *nucleon* star.

---

[1] $\epsilon_C(\chi)$ denotes the total energy density of the kaon phase, both nuclear (as modified by the kaons) and the kaon contributions as defined in (10.23).

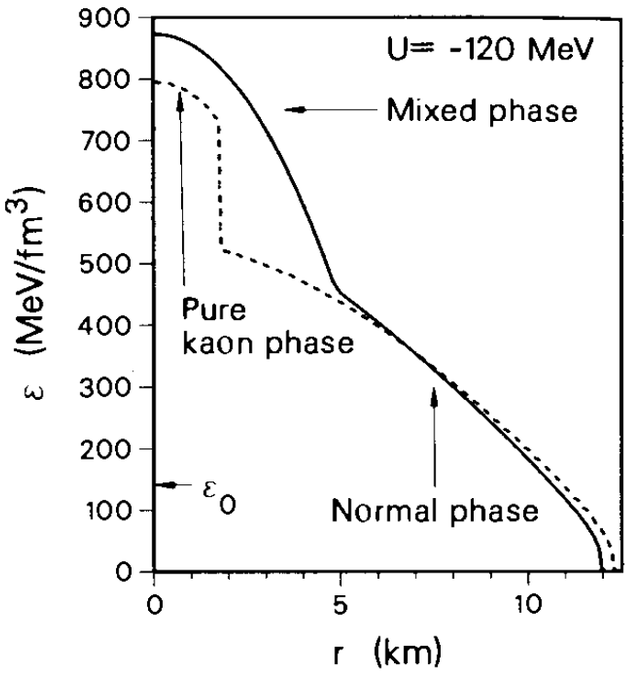

FIGURE 10.12. Mass–energy distribution according to whether the mixed phase is treated by the Maxwell construction (dashed line), or so as to respect the continuity of both chemical potentials (solid line) [411].

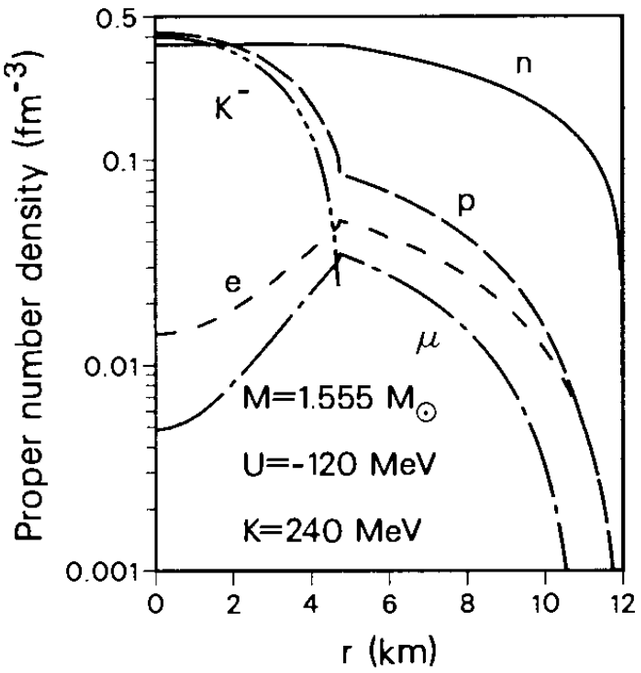

FIGURE 10.13. The composition of the maximum mass neutron star with a mass of $M = 1.555\,M_\odot$. Note that while protons are the dominant species at the center of the star, overall, they are a minority population [411].

Stellar sequences for several choices of the kaon potential $U_K(\rho_0)$ are shown in Fig. 10.14. Naturally the limiting mass decreases with increasing potential (for which the condensate density threshold is lower). Potentials with values only a little below $U_K(\rho_0) = -120$ MeV would not be compatible with the mass of the Hulse-Taylor pulsar, for the underlying theory of matter used here. There is a mechanical instability for the Maxwell case that is initiated by the central densities for which the pressure remains constant. In this case the *necessary* condition for stability, $dM/d\epsilon_c > 0$ is not satisfied. (The section of the dashed curve in Fig. 10.15 for which R is an decreasing function of M is the corresponding unstable region.) Such an unstable region is absent when the phase transition is treated using Gibbs's conditions.

The mass–radius relation for several sequences is shown in Fig. 10.15. Comparison is made with the case corresponding to the Maxwell construction for the phase transition. It is clear that the radius especially and the limiting mass are sensitive functions of $U_K(\rho_0)$. For the preferred value of $U_K(\rho_0) = -120$ MeV, radii are similar to neutron stars without the condensate. There appears to be a sharp break in behavior of M vs. R for $U_K(\rho_0) < -120$ MeV. However the behavior is actually continuous, but depends sensitively on $U_K(\rho_0)$: a pure kaon condensed core develops with decreasing values of the optical potential below ~ -120 MeV and this causes the change of the radius from $R \approx 12.5$ km to $R \approx 8$ km for $U_K(\rho_0) = -140$ MeV.

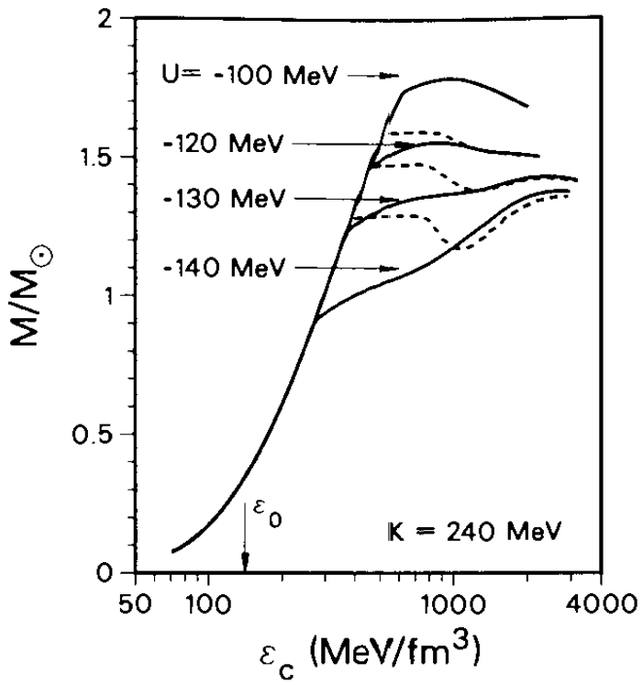

FIGURE 10.14. The mass sequence for kaon condensed neutron stars treated by the Maxwell construction (dashed line), or so as to respect the continuity of both chemical potentials (solid line) [411].

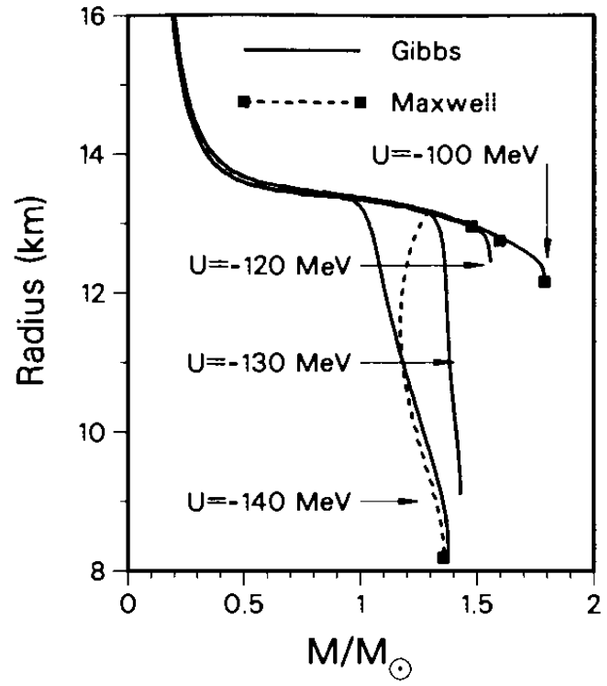

FIGURE 10.15. The mass–radius relation for kaon condensed neutron stars using a Maxwell construction (dashed line) or Gibbs condition (solid line) [411].

10.3.2 Geometrical structure in the mixed phase

Neutron star matter in the normal phase is necessarily highly isospin asymmetric because charge neutrality is imposed by the weakness of the gravitational field compared to the Coulomb force. However, because kaons are bosons, they can all occupy the zero momentum state. Consequently, when the two phases, normal and kaon condensed, are in phase equilibrium, the normal phase can come closer to isospin symmetry as can be seen in Fig. 10.7. This is achieved by charge exchange as driven by the isospin restoring force arising in part from the Fermi energies and in part from the coupling of the ρ meson to the nucleon isospin.

Naturally, the possibility of achieving isospin symmetry varies as the proportion of the kaon phase. Regions of normal matter will be positively charged while regions of the kaon condensed phase will be negatively charged. In this way, the overall energy is reduced by exploitation of the possibility of achieving charge neutrality globally rather than locally (recall Section 9.3). As was discussed in Chapter 9 and in Ref. [195], regions of like charge will tend to be broken up into small regions while the surface interface energy will resist. The competition is resolved by formation of a Coulomb lattice much as nuclei embedded in an electron gas. The difference here is that it is two phases of nuclear matter that are involved. The rarer phase will occupy lattice sites embedded in the dominant phase. As the proportion of phases changes, the total energy consisting of volume, surface and Coulomb energies will be minimized by a sequence of geometrical forms at the lattice sites, which we idealize as drops, rods and slabs, just as for nuclear matter embedded in a background of free electrons and neutrons [431].

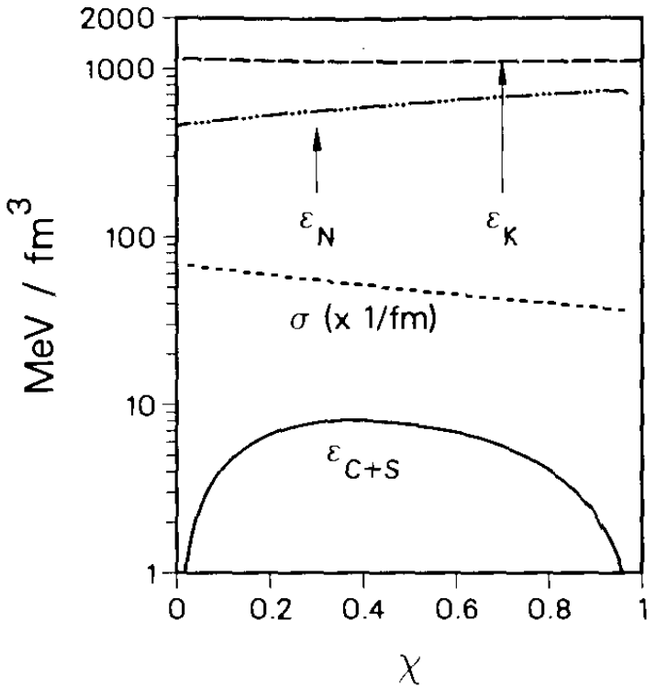

FIGURE 10.16. Bulk energy densities of normal and kaon phases as a function of the volume fraction of the kaon phase, the surface tension σ which is assumed to be proportional to their difference, and the sum of Coulomb and surface energy density [110].

Relevant details of the structure calculation can be found in Chapter 9 and in Refs. [405, 406]. In the present situation, the physical quantities that determine the geometrical structure are shown in Figs. 10.8 and 10.16.[2]

Of course a calculation of the geometric structure, which results from a competition between Coulomb and surface energies, requires a knowledge of the surface tension σ at the interface between the phases. This is not known although a calculation is in progress [432]. What we do know is that: (1) The sizes, spacings and the sum of Coulomb and surface energies scale as $\sigma^{1/3}$. (2) To first approximation, the locations of the transition from one geometric phase to another does not depend on σ. (3) The threshold density of the mixed phase and the density at which it ends is not disturbed by our uncertainty in σ because the sum of Coulomb and surface energies vanishes at the end points (Fig. 10.16; see Eq. (2) in Ref. [405]). (4) The structured phase lies lower in energy than the unstructured (see near end of the Introduction of Ref. [433].) This is because the structured phase results from a degree (or degrees) of freedom—that of rearranging the concentration(s) of conserved quantities between the two phases in equilibrium—which were closed in treatments of the phase transition in which conservation of charge was imposed as a local constraint,[3] $\rho_q(x) \equiv 0$, instead of as a global constraint $\int \rho_q(x) d^3x = 0$, which is all that is required. For the above reasons the dimensions shown in Fig. 10.18—the size of the geometrical structures and their spacing—provide a guide, but the locations of phases should be quite accurate.

[2]We illustrate features of the geometrical structure for the case $U(\rho_0) = -120$ MeV from this point on.

[3]The energy of a constrained physical system can never lie below that of an unconstrained one.

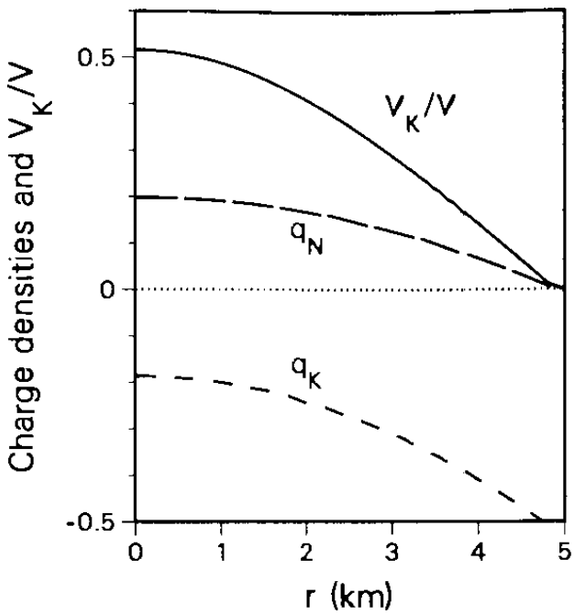

FIGURE 10.17. Charge densities in the normal and kaon condensed fractions of the mixed phase in the limiting mass star of the case $U(\rho_0) = -120$ MeV. Volume fraction of kaon phase is also plotted [411].

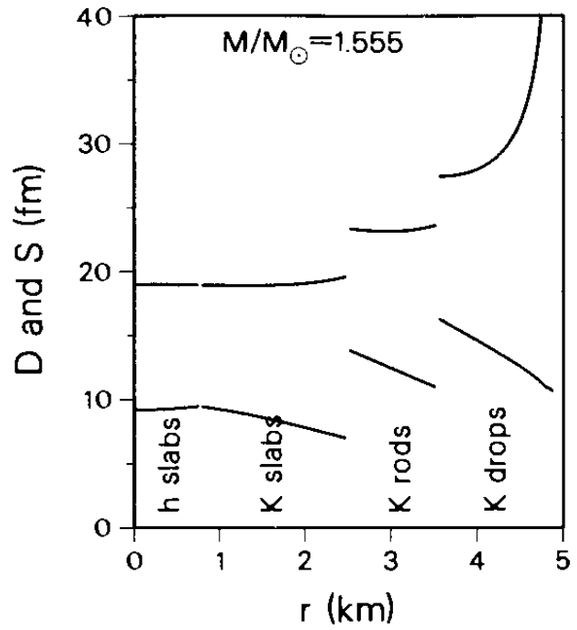

FIGURE 10.18. Diameter D (lower curve) of objects (drops, rods, slabs) of the rarer phase immersed in the dominant phase, located at lattice sites spaced S apart (upper curve) [411].

The charge densities carried by the two phases and the volume fraction of the kaon phase is shown in Fig. 10.17 as a function of radial coordinate in a star. Of course, the net charge vanishes in the global sense just described. Outside of 5 km, matter is in the pure nuclear phase and it is identically chargeless, the proton population being balanced by electrons. In the idealized geometry of shapes, the kaon phase will first form at the threshold density of condensation as spheres spaced far apart. As the fraction of kaon phase increases, the spacing will decrease and eventually the spheres will merge to form rods and then slabs. As the volume fraction of the kaon phase comes to dominate, slabs of normal phase will be present in a background of kaon phase, and the role of the two phases is interchanged. The diameter and spacing of the geometrical forms of the crystal lattice is shown in Fig. 10.18 for the limiting mass star. Notice that the mixed phase extends in this case from the center of the star to about 4.8 km. The kaon condensed phase disappears at larger radius or lower density as the spacing of the droplets of condensed phase tends to infinity. The location of the boundaries of the various phases can be seen in Fig. 10.19 for stars of various mass.

These are rather remarkable properties of the mixed phase, which in the limiting mass star occupy the inner 5 km. It is filled with geometrical forms of varying shapes and spacings, according to depth in the star. The charge density within the geometrical objects and the background phase is opposite in sign and varying in magnitude with depth. Finally, the effective mass of the nucleons is radically different in the two phases as can be seen in Fig. 10.20. All of these features must have their effect on transport properties and possibly on Glitch phenomena.

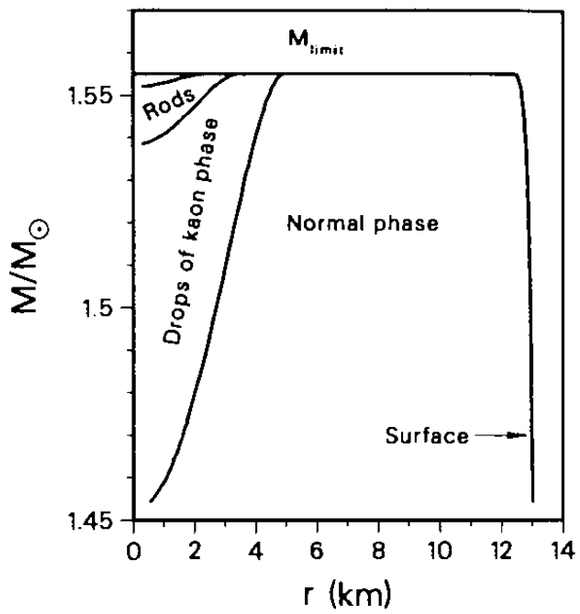

FIGURE 10.19. Radial boundaries between phases are shown for a range of stellar masses [411].

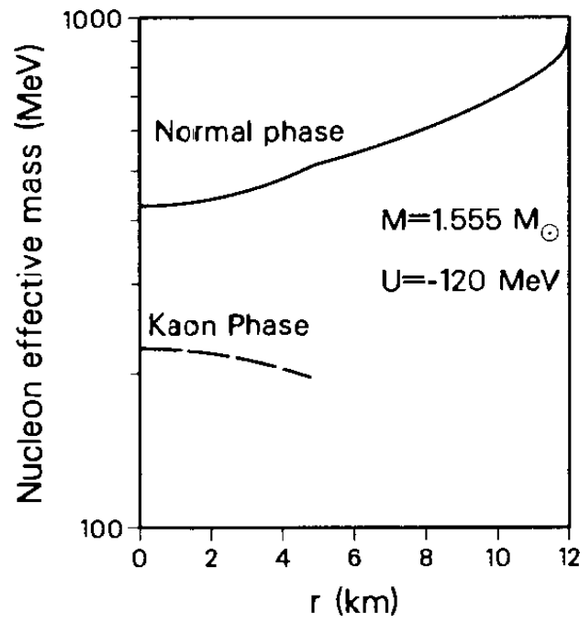

FIGURE 10.20. Nucleon effective mass in the normal and kaon condensed phase as a function of radial location in the limiting mass star [411].

10.3.3 Pulsar glitches

Glitches are thought to correspond to changes induced in the moment of inertia of the star either as a crack in the crustal region or as a massive number of superfluid vortex lines undergo shifts in the location of the sites in the solid regions to which they are pinned [185]. The relocation of vortex lines or crustquake, whichever is the case, occurs unpredictably as the instantaneous configuration carrying the angular momentum comes out of equilibrium with decreasing spin of the star and creates stresses that are relieved by massive unpinning or cracking of the crust. The thin crust is a location at which the vortex lines can be pinned. But in the present model, the vortex lines do not thread through the entire star, pinned at each end on the crust, but are pinned at one end on the interior crystalline mixed phase. The extent of this region varies sensitively as the mass of the star, perhaps accounting for the wide variety in glitch phenomena observed in different pulsars.

Alternately, if the glitch is caused by a crustquake, it may trigger changes in the interior crystalline region. In either case, the thickness of the inner crystalline region, whether it occupies a central spherical region or a shell of some kilometers of thickness, depends very sensitively on the mass of the star (See Fig. 10.19). These are speculative thoughts on a possible effect of an interior solid region, which could nonetheless lie behind the large degree of individuality with which pulsars glitch [228]. They certainly need, and possibly deserve, detailed investigation.

10.4 Summary

We have discussed the properties associated with kaon condensation in neutron star matter. This phase transition is particularly interesting when the interaction of kaons and the medium is sufficiently strong as to render it a first-order transition. In this event, there is a mixed phase in which normal and kaon condensed nuclear matter are in phase equilibrium. As is general for any phase transition in a substance having more than a single conserved charge, the mixed phase does occupy a finite extent in the star, and in that region is quite rich in phenomena. First, a Coulomb lattice of rare phase immersed in the dominant one will will form, having various geometries at the lattice sites, according to the pressure. This feature is common to nuclear systems having a mixed phase (independent of the phase transition) so long as the temperature is low on the nuclear scale. Second, nucleons have different mass depending on whether they are in the objects at the lattice sites, or in the background medium. Third, the objects at the lattice sites have opposite charge compared to the background. Thus, the mixed phase region, which we calculate to occupy a region of a few kilometers in extent, is highly heterogeneous. We believe this will be an important factor in determining the transport properties of this region. Moreover, the solid region, if present, is likely to play a role in the pulsar glitch phenomenon and its extent in the core, being very sensitive to stellar mass, may account for the variety of glitch phenomena observed in different pulsars.

10.5 Problems for Chapter 10

1. Derive the dispersion relation for Bose condensation (10.7) and (10.8).
2. Find the s-wave dispersion relation for kaons, (10.10).
3. Derive the kaon density (10.13).
4. Derive the Euler-Lagrange equations for static uniform matter that can be found in (10.15).

11

Consequences and Signals of Phase Transitions

11.1 Introduction

The phase transitions that have been discussed in previous chapters occur, if they do, deep within the interior of neutron stars, and preferentially in the more massive stars for the evident reason that the density reaches a higher value. But the large-scale properties of a star do not depend radically on whether its core contains a different phase of matter than what exists in the outer regions. One could not readily identify the presence of the interior phase, let alone its nature. For example, the masses and radii of stars shown in Fig. 9.17 are not substantially different from a model in which, say, by a change of the parameters defining the high-density phase, a phase transition did not occur at all.

If there are consequences of phase transitions such as hyperonization, deconfinement, or kaon condensation, what are they? It is true that within a given model there are consequences. For example, we have seen that all three phase transitions will lower the limiting neutron star mass compared to the same model in which the phase transition has been foreclosed. But we are able to examine such consequences only in our calculations, and even at that, could not readily distinguish between the above phase transitions in their effect on the limiting mass or radius. How then are we to learn eventually, whether abnormal phases really do exist in the cores of neutron stars? We explore that question in this chapter.

11.2 Mechanism for Formation of Low-Mass Black Holes

Any one of the three phase transitions that we have studied, hyperonization of dense matter, quark deconfinement, or Bose condensation may play a crucial role in the formation of *low-mass* black holes in the range $M \sim 1.5$ to $2M_\odot$. In this section we study how collapse may be triggered in a *protoneutron star* whose mass falls within a certain range near the mass limit.

Evolved stars with masses $M > 8M_\odot$ are believed to collapse either directly into black holes of mass *equal* to that of the progenitor star, and unaccompanied by a supernova and neutrino signal, or to a metastable protoneutron stars with the remainder of the star ejected in a supernova to seed the universe with elements heavier than those produced in the big bang. (Recall Section 3.1.) In the latter case, protoneutron stars near the mass limit may shortly subside into a black hole.

A protoneutron star is hot and lepton-rich. Neutrinos produced during the collapse of the core by the inverse beta decay of protons are trapped by scattering from nuclei at densities $\sim 10^{12}\text{g/cm}^3$ [434]. They are thermalized with all flavors of neutrinos and antineutrinos. As the core temperature rises upon continued contraction, the binding of the protoneutron star further increases and more neutrinos with high-energy are produced in the hot dense medium. They will ultimately carry off most of the binding energy of the neutron star (about a 100 MeV per nucleon for a neutron star near the mass limit according to Fig. 3.15). The high energy neutrinos and convection in the hot core are thought to be equal partners in driving the explosion [435].

The neutrinos are trapped for a duration of about ten seconds by the hot, dense material of the compact star [35]. The protostar core will otherwise contain a charge-neutral admixture of neutrons, protons, electrons, and muons in close to equilibrium proportions. If the baryon number is not too great, the protoneutron star will deleptonize, cool, and evolve quickly to a stable neutron star.

Alternatively, if the mass of the protoneutron star falls in a certain window *above* the limiting mass of the fully evolved neutron star that it will become upon deleptonization, it will suffer a *delayed* collapse to a low-mass black hole somewhat in excess of the neutron star limiting mass. Such a black hole is formed following escape of the initially trapped neutrinos on a timescale not longer than the diffusion time (~ 10 s) and after the processed stellar material of the progenitor star has been ejected in a supernova explosion [42]–[46].

In Chapter 5 we saw that the mass limit of a neutron star, computed as if it were made of matter involving only beta equilibrium among neutrons and protons and leptons can be considerably reduced by other processes. Hyperonization of nucleons was discussed in detail in Chapters 9 as causing a reduction in limiting mass by $\sim 1/2$ to $3/4M_\odot$ [132]. This reduction is an approximation of the window spoken of above.

The observation of the neutrino signal from the 1987 supernova in the nearby Large Magellanic Cloud (SN1987A), but the absence of a pulsed signal or evidence

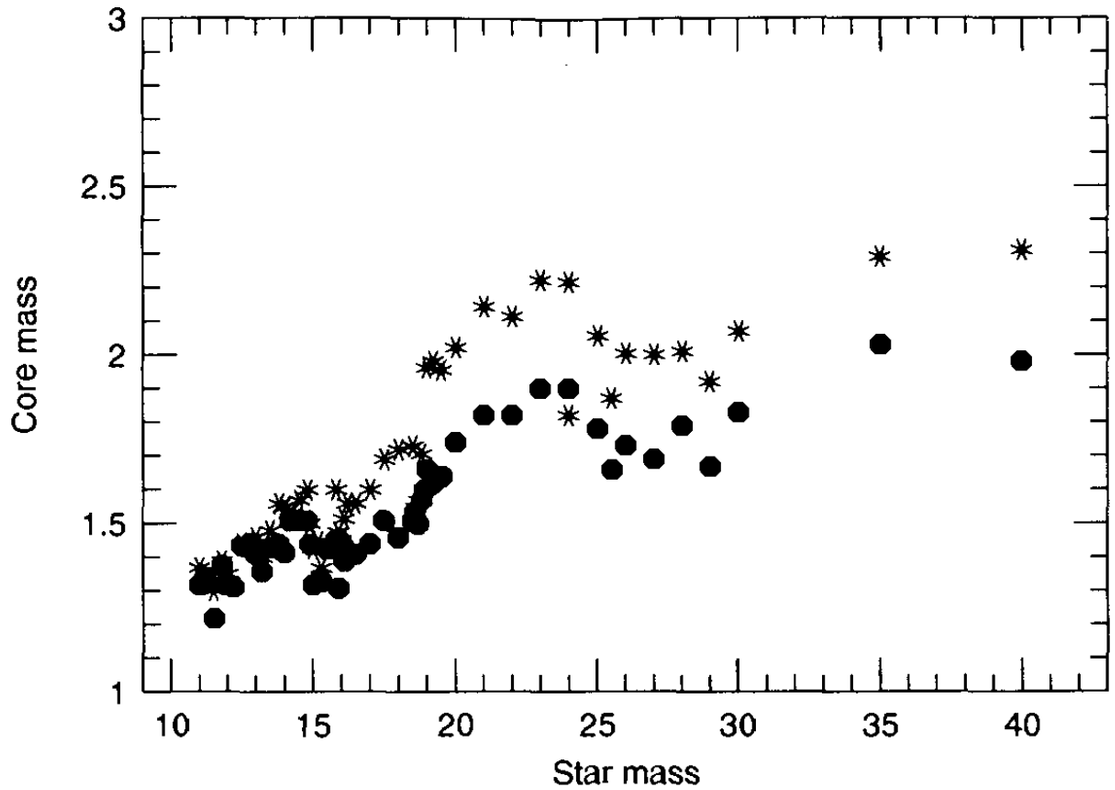

FIGURE 11.1. The mass of the core formed in a star prior to collapse of the core as a function of mass of the whole star showing general trend toward higher core mass with increasing stellar mass. (Courtesy of Timmes, Woosley and Weaver [255]. See also Ref. [436].)

of a neutron star in the light curve of the supernova remnant, suggests that a supercritical protoneutron star may have been formed which collapsed to form a black hole subsequent to neutrino emission. In any case, the processes described here are possibly responsible for the formation of black holes after the supernova explosion and neutrino signal. They may be relevant to any disparity in neutron star birthrates and type II supernova rates in the Galaxy.

Brown and Bethe [437] have suggested that many stars in the mass range 18–30 $M_\odot$ produce black holes instead of neutron stars. They proposed kaon condensation as a possible destabilizing influence on protoneutron stars in a window of about $0.2M_\odot$ [418] augmented by about 0.04 to $0.1M_\odot$ by thermal and lepton pressure in the protoneutron star prior to deleptonization [438]. However, for reasons discussed in Chapter 5, it is not clear that kaon condensation occurs in neutron stars. That will depend on hyperon couplings that are not well known as well as the underlying description of dense matter. The hyperons, recall, tend to saturate the electron chemical potential, perhaps to a value too small, considering the kaon mass and its density dependence in the nuclear medium (recall Fig. 5.32). So hyperonization is likely to take precedence over kaon condensation, and deconfinement over both. We consider the latter two effects in an approximate scheme.

11.2.1 Hyperonization-induced collapse

Neutrinos and gammas produced in the hyperonization reactions (5.29)–(5.30) will diffuse out of the star, lowering its energy and making the conversion of nucleons

to hyperons irreversible. However, this final ground state is not accessible to a newly formed neutron star until after the trapped neutrinos have escaped and the protostar has cooled and shrunk to its final density.

It takes only a few seconds for neutrinos to diffuse from the star thus cooling it. Prior to neutrino diffusion, it is possible that the collapsing core forms a more massive quasi-stable protoneutron star than ultimately can be supported by the softer equation of state of the fully equilibrated matter containing hyperons (or bosons, or a deconfined quark phase). In this case a low-mass black hole will be formed. However, the window or mass range of such black holes must be narrow, because the core mass that is formed before collapses increases roughly as the mass of the presupernova star (see Fig. 11.1). When the core mass plus any fallback of material exceeds the mass that can be supported, even quasi-statically by a hot, neutrino-rich protoneutron star, the *entire* star will collapse. Therefore, we expect a narrow window of low-mass black holes, perhaps 1.5 to $2M_\odot$, separated from the more massive black holes of 10 to $50M_\odot$ that are formed when the entire star collapses [42]–[46].

A sequence of stellar masses as functions of baryon number A is shown in Fig. 11.2. One sequence represents, in a crude way, protoneutron stars with a prehyperonized composition of (n, p, e, μ) matter. The other sequence corresponds to fully equilibrated neutron stars having a composition of (n+p+e+μ+H), and represents the ground state.

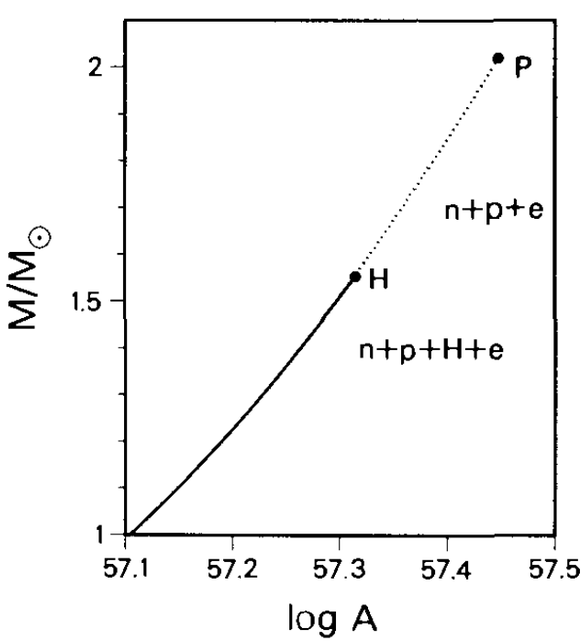

FIGURE 11.2. Masses of protoneutron stars represented by (n+p+e+μ) and hyperonized neutron stars (n+p+e+μ+H) are shown as a function of baryon number A. The region between the two mass limits (marked by H and P) is the range of protoneutron stars having A for which there is no stable configuration after deleptonization. Parameters of the theory are set three of Table 5.5.

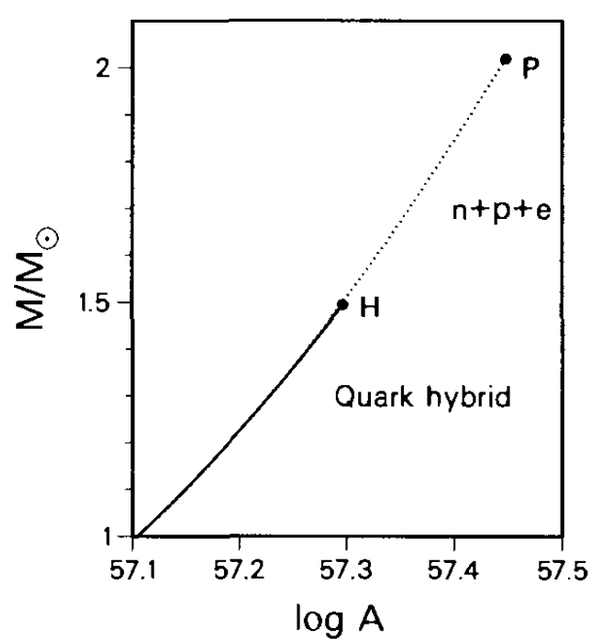

FIGURE 11.3. Similar to Fig. 11.2, but in which hadronic matter undergoes a transition to a mixed phase and a pure quark phase comprising the sequence labeled "hybrid" at greater depth in the star. The bag constant is $B^{1/4} = 185$ MeV and $\alpha_s = 0$. Parameters in the hadronic sector are those of Table 5.5, set three. (From Ref. [43].)

The nonoverlapping segment of the dotted lines H–P in Fig. 11.2 represents protoneutron stars whose baryon number exceeds that of any stable configuration of hyperonized stars. Therefore, when hyperonization commences during diffusion of neutrinos out of a protoneutron star, these initially stable configurations will begin to collapse. We see that the mass range of protoneutron stars that would suffer such a fate is about $\frac{1}{2}M_{\odot}$. Certainly, the lower part of the window for collapse, and perhaps all of it, is compatible with estimates of the masses involved in core collapse [436] and ejecta fallback [439].

One can say something qualitative about the lifetime of the protoneutron stars that have baryon number falling above the point H in Fig. 11.2. As explained above, protoneutron stars with baryon numbers that place them between the points H and P have no stable configuration after *complete* deleptonization. Those that lie closer to H will be stabilized for a longer time since intermediate stages of hyperonization will still support them.

In other words, there is a continuum of sequences of partially hyperonized stars between H and P with complete hyperonization corresponding to H and no hyperonization to P. Therefore, a star at P (or of greater A than corresponds to H) has no temporarily stable, partially hyperonized configuration, whereas one closer to H has a continuum of configurations differing in degree of hyperonization that can still support its baryon number against collapse (for some short time) before total deleptonization and hyperonization to the ground state. This process takes of the order of ten seconds and is the lifetime expected for a protoneutron star whose baryon number (or mass) just exceeds the limit at H, while a shorter life is expected for those nearer P.

As is clear from the discussion, those configurations lying below H are absolutely stable upon hyperonization, and form neutron stars while those above P suffer immediate collapse of the entire presupernova star to form massive black holes. Those configurations whose baryon number places them between H and P will suffer delayed collapse to low-mass black holes ($\sim$ 1.5 to $2M_{\odot}$).

11.2.2 Deconfinement-induced collapse

An alternative possibility is that upon deleptonization, cooling, and shrinkage, the hadronic matter in the core of the protoneutron star converts to the quark matter phase containing u, d, and s quarks [43, 44]. This also happens only because deleptonization softens the equation of state, as described above. In both cases we find a substantial window of roughly $0.5M_{\odot}$ into which a protoneutron star may fall and be temporarily stabilized prior to deleptonization and ultimate subsidence into a black hole. The mechanism is evidently robust. In Fig. 11.3 we compare the stable hybrid star sequence (solid line) with the sequence that is temporarily stabilized by the trapped neutrinos, similar to Fig. 11.2. Again there is an extensive range of baryon numbers above H for which the temporarily stabilized stars (n+p+e+μ) have no stable configuration when the matter undergoes the transition to the lower energy state. Protoneutron stars with masses above about $1.5M_{\odot}$ therefore collapse.

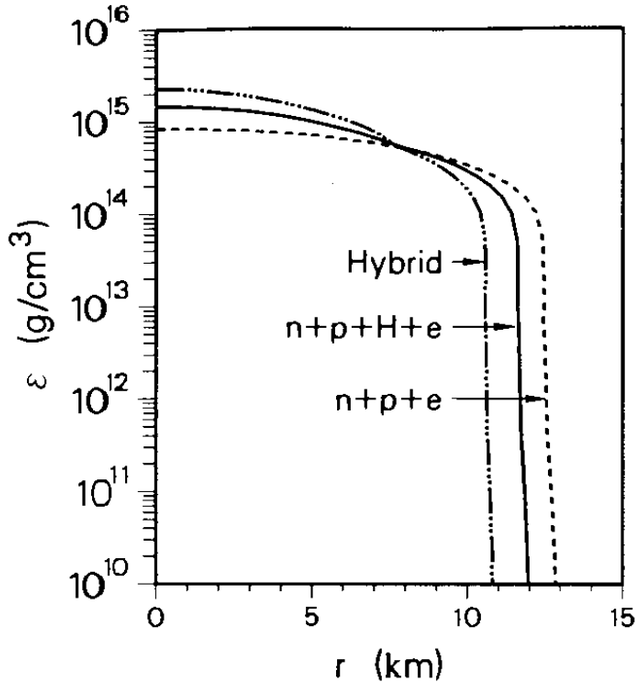

FIGURE 11.4. Mass–energy profile of protoneutron star (dashed) and hyperonized neutron star and hybrid star having the same A and mass $1.49M_\odot$ for the same cases as the previous figure. Note the more compact configuration of the ground state, whether it be a hyperonized neutron star or a hybrid.

11.2.3 Density profiles

It is of some interest to see the change in the stellar configuration for those protoneutron stars that *do* have a stable final state of hyperonized matter or of quark matter, that is, those that have a baryon number that falls in the range of the solid line below H in Figs. 11.2 and 11.3. The three configurations—the protoneutron star stage, and the two possible final ground states, hyperonized stars or hybrid stars—are compared in Fig. 11.4 for the same baryon number. (The temperature here is taken as zero. The temperature of the protoneutron star would be mainly reflected in the lower density tail of the star, giving it a larger radius. Thermal pressure is insignificant in comparison with compression and Fermi energy.) The comparison is made for stars of fixed $A = 1.974 \times 10^{57}$ and mass $\sim 1.49M_\odot$ (slightly larger for the (n, p, e, μ) configuration).

It can be seen that the protoneutron star composed of the (n, p, e, μ) charge-neutral matter subsides into a denser and more compact configuration as the matter in the interior hyperonizes or converts to quark matter. There will be a modest spin-up in angular velocity as this happens. The moments of inertia of protoneutron star, hyperonized, and hybrid stars are 119.5, 103.7, and 89.64 in units of $M_\odot$-km^2, so that the hyperonized and quark stars are spun up by factors of 1.15 and 1.33, respectively, over the angular velocity of protoneutron stars.

11.2.4 Discussion

It is believed that the core of a massive evolved star collapses either directly into a black hole or forms a hot, lepton-rich protoneutron star which deleptonizes to form a stable neutron star. A third possibility considered here is that the protoneutron

star has a supercritical baryon number larger than that of stable evolved neutron stars and less than that which would lead to immediate collapse of the entire pre-supernova star. The supercritical protoneutron star is therefore accompanied by a supernova explosion and subsides into a low-mass black hole after deleptonization. The latter two eventualities would both eject heavy elements into the universe in a supernova event signaled by a neutrino pulse of a few seconds duration. They differ in the final fate of the core and in the duration of the neutrino signal. The width of the window for delayed subsidence and the frequency with which it is populated is relevant to the outcome of particular events (for example, SN1987A) as well as for understanding the statistics on supernova–pulsar associations.

Because subsidence of a protoneutron star to a black hole or to a stable hyperonized or hybrid star is triggered by deleptonization, it takes place during that era on its timescale—of the order of ten seconds. The process is regulated by neutrino loss since the other two timescales—hydrodynamic ($\tau_{\text{hydro}} \approx 10^{-3}$ s) and weak interaction ($\tau_{\text{weak}} \approx 10^{-10}$ s), which governs transformation of nucleons to hyperons—are small by comparison.

Neutrinos trapped in a core that undergoes direct collapse to a black hole (i.e., the baryon number lies above the point P) will be carried within the horizon by the collapsing core. In contrast, most or all of the neutrinos (depending on where between H and P the baryon number of the protoneutron star lies) will escape during the deleptonization that causes the delayed subsidence of the core into a black hole. However, if the mass is toward the upper end of the window for only temporary stability, the signal will be shortened and in any case the tail will be infinitely red-shifted as the star sinks toward the horizon (page 139). Whether the protoneutron star is subcritical and collapses to a stable hyperonized or hybrid star, or is supercritical and collapses by one of the delayed mechanisms to a black hole, the neutrinos produced by hyperonization or formation of quark matter will form the tail of the neutrino signal in either case.

Neutron stars near the upper mass or baryon limit of stability may still suffer collapse to black holes on a much longer timescale of hours to months or years if they are hovering at the limit of evolved neutron stars and there is sufficient mass fallback ($\sim 0.1 M_{\odot}$) or mass accretion from a less dense companion. The process is complex. Because of the longer timescale, we do not include it as a broadening of the window for prompt subsidence. Moreover, the window for accretion-induced collapse in binary systems is small compared to the two mechanisms we include.

In the cases for which a neutron star is the final ground state, the contracting protoneutron star (Fig. 11.4) may execute damped oscillations about the final configuration, producing a surplus of hyperons (or quark matter) compared to the final equilibrium state of the star and then a deficit, as the density oscillates. Because the diffusion timescale for neutrinos and gammas, produced as decay products of associated kaons, is very long compared to the hydrodynamic timescale, no signature of the density oscillations would be observable in these signals.

If the oscillations were not purely radial pulsations, they would produce gravitational radiation because all stars rotate. Indeed, the density dependence of the

shear viscosity in a rotating star would possibly cause deviations from purely radial pulsations. However, we will not explore this possibility here.

The neutrino signal from SN1987A informs us that a protoneutron star was formed [440], but, according to the processes discussed here, it does not inform us that an evolved neutron star was ultimately formed. No pulsed radiation has been observed, and the present evidence from the light curve of the supernova remnant is compatible with the presence of a low-mass black hole, but not of a neutron star [441].

If continuing observation of the remnant and search for pulsed radiation from the site of SN1987A reveals no pulsar, one of the mechanisms discussed here may be responsible for turning high-mass protoneutron stars into low-mass black holes *after* the processed stellar material has been ejected in a supernova and the neutrino signal of the event has been emitted.

It has been estimated that about one-half of the supernovae in our Galaxy leave no promptly observable star [442]. The mechanisms discussed here, which have the immediate signature of neutron star formation—supernova and neutrino signal—but which are followed by the unannounced subsidence to a low-mass black hole ($M \sim 1.5$ to $2M_{\odot}$), may contribute to or be responsible for the apparent discrepancy.

11.3 A Third Class of Stable Compact Stars

11.3.1 Introduction

The work of J. A. Wheeler and collaborators in the mid 1960s showed that for *smooth* equations of state no stable stellar configurations with central densities above that corresponding to the limiting mass of "neutron stars" (in the generic sense) were stable against acoustical vibrational modes [28]. A perturbation would cause any such star to collapse to a black hole or explode. Accordingly, there has been no reason to expect that a stable degenerate family of stars with higher density than the known white dwarfs and neutron stars might exist. We have found[1] a class of *certain* equations of state that describe a first-order phase transition and are insufficiently smooth to obey the general expectation. We identify the attributes that give rise to a third family of stable dense stars. We discuss how such a higher-density family of stars could be formed in nature, and how the promising new exploration of oscillations in the X-ray brightness of accreting neutron stars might provide a means of identifying them.

There are two known classes of compact stars, white dwarfs—which were discovered in 1910, and neutron stars, discovered in 1967. Distinct classes (or families) of compact degenerate stars originate in properties of gravity; the distinction is made rigorous by the "turning points" theorem that we discussed in

[1] Unpublished work of N. K. Glendenning and Ch. Kettner, LBNL report - 42080, 1998; Astron. & Astrophys. **353** (2000) L9-12.

Section 3.18.1 [28]. The theorem concerns solutions of the stellar structure equations, whether Newtonian or relativistic. It states that there is a change in stability of one radial mode of normal vibration when and only when the mass reaches a maximum or minimum as a function of central density. For example, the fundamental nodeless mode becomes unstable at the white dwarf maximum mass and terminates this type of star, but the same mode regains stability at the minimum mass between white dwarfs and neutron stars. Therefore, it must lose stability again at the neutron star maximum mass. Stability for a third family of compact stars has not been regained for any stellar model tested heretofore. Even for an equation of state that is stiff as can be because it is at the causal limit, all sequences above neutron stars are unstable (Fig. 3.19).

Indeed, Wheeler et al. showed analytically for polytropic equations of state that for general relativistic stars there is a denumerable infinity of turning points of the mass as a function of central density and therefore an infinity of sequences for which the mass has positive slope. However, all configurations with densities greater than the first mass limit for neutron stars are unstable to acoustical radial vibrations, and end either by exploding or imploding to a black hole. Other nonanalytic models have been tested for stability. These include the "Harrison–Wheeler" equation of state [28], and more recently new families associated with higher quark flavors were thought to exist [198, 443]. However, in each case, families above the neutron stars were found to be unstable. (Note that connotations like hyperon star or hybrid star simply refer to the fact that particle populations vary continuously with density within a given family, and the adjective simply refers to an important population. These connotations do not refer to the rigorously defined classes of degenerate stars based on the turning point theorem.)

On the basis of the pioneering work of Wheeler and his collaborators, a conditional theorem can be inferred: For any *sufficiently smooth* equation of state, neutron stars are the last stable class of compact stars. Configurations of higher density oscillate in mass as a function of density and by the turning point theorem, acquire an additional unstable mode of vibration at each maximum and minimum. Moreover, and this is important, the demonstration of instability of polytropes above the neutron star family proves that positive slope of stellar mass with respect to central density, $dM/d\rho_c > 0$, is not a sufficient condition for stability.

Is there a physical basis for anticipating the possible existence of a third distinct stable family? Not from the physics underlying the stable and unstable points of the two known families. It is understood that white dwarfs are stabilized by degenerate electron pressure which fails at such density that electron capture reduces their effectiveness (Section 3.9.7). Stability is reestablished at densities about five orders of magnitude higher when the baryon Fermi pressure (and ultimately the short-range nuclear repulsive interaction) supports neutron stars. When neutron stars loose stability at their maximum mass, there is no evident mechanism for stabilizing a denser family. At higher density the Fermi pressure of nucleons and hyperons is replaced—not supplemented—by the pressure of their quark constituents. Indeed a phase transition will generally reduce the pressure at a given energy density, and ultimately bring about the termination of stability. Moreover, at ever higher

density, the Fermi pressure of quarks must be shared among a greater number of flavors according to the Pauli principle. A mechanism for stabilizing a third family is therefore not apparent from the point of view of Fermi pressure.

11.3.2 Stability of nonidentical twins

In this section, contrary to the expectation and experience recalled above, we demonstrate that the equations of stellar structure do admit stable solutions above neutron stars in density, and for equations of state that are physically admissible, that is to say, that (i) are causal, (ii) microscopically stable, (iii) obey Le Chatelier's principle in the strong sense ($dp/d\rho > 0$) as is required of matter having two (or more) conserved charges [195], and (iv) describe the saturation properties of symmetric nuclear matter within the range they are known.

The equations of state for which a third family of compact stars exists are certain of those that describe the deconfinement phase transition. Only certain combinations of parameters defining the equations of state of nuclear and quark matter yield a sequence of high-density stellar configurations above the neutron stars. Presumably any phase transition would also yield a third family if the corresponding equation of state possessed the appropriate attributes. Two of many examples of a stable denser family above the white dwarfs and neutron stars in density are shown in Fig. 11.5. The physical reason for the appearance of a third stable family given a particular structure of the equation of state are discussed in the next section. There is no reason to associate a third family specifically with the deconfinement phase transition, though this may be the most plausible one.

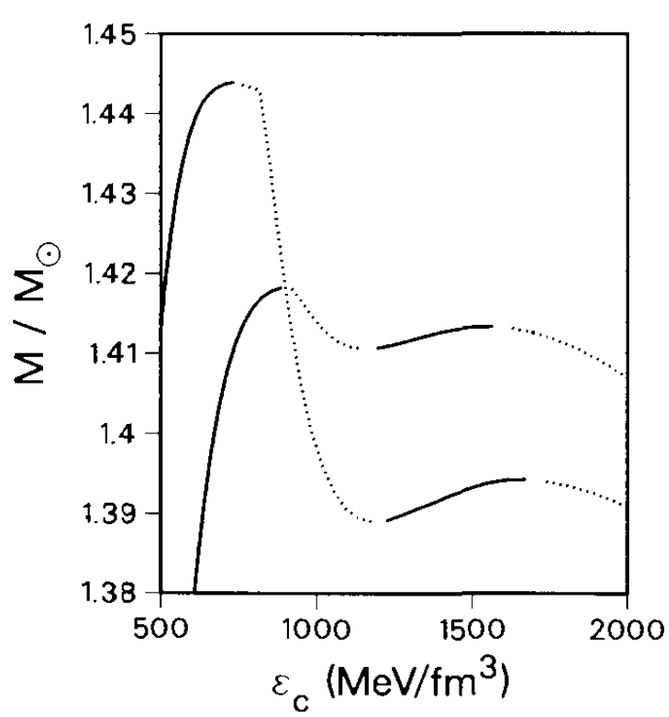

FIGURE 11.5. Two out of many examples of stellar sequences for which neutron stars and a higher-density stable family of "nonidentical twins" exist. In some, the denser family has a larger limiting mass than the neutron star family. Stability is proven in connection with the discussion of Fig. 11.8.

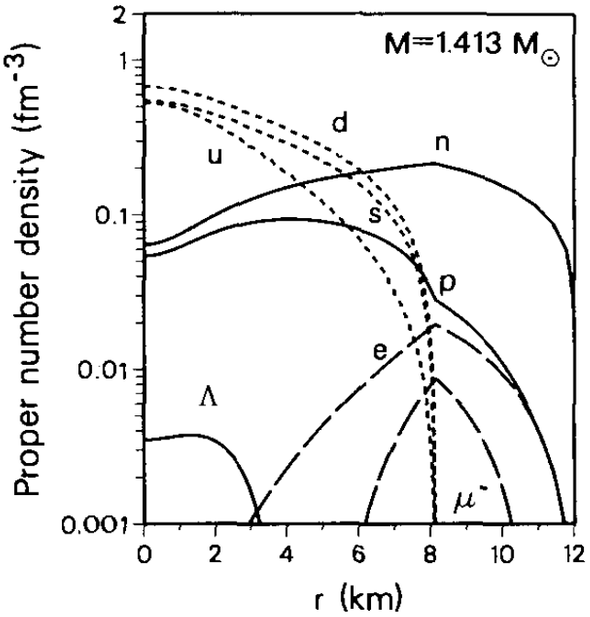

FIGURE 11.6. Particle populations in the lower-density star of mass $1.413M_\odot$. Note that the coexistence of the two phases, confined and deconfined, persists from the center to 8 km.

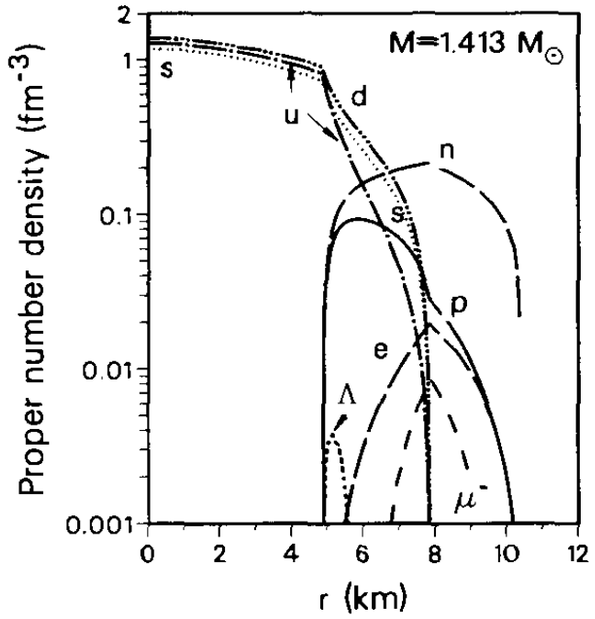

FIGURE 11.7. The high-density twin with the same mass of the star in Fig. 11.6 has all three phases of matter. The pure deconfined quark phase extends to 5 km.

We refer to stars of the denser sequence in Fig. 11.5 as nonidentical twins of neutron stars because for both families it is the Fermi pressure of particles carrying baryon number that supports the star against gravity in addition to repulsion at short distance between any nucleons that may be present. In the present examples, both families contain deconfined quark matter, but in the first, only in the mixed phases. As we will stress below, however, it is not the particular content of the star that creates the additional family, but rather a particular way in which the adiabatic index changes with density.

The particle populations of twin stars of the same mass but belonging one to the "neutron star" family, the other to the higher-density family, are shown in Figs. 11.6 and 11.7.[2] Both stars are hybrids in the sense used in Chapter 9; they have regions occupied by quark matter or quark matter in equilibrium with confined hadronic matter, surrounded by pure hadronic matter—the matter usually associated with the notion of a neutron star. The lower-mass members of the "neutron star" family of course have no quark matter whatever, namely those with central densities that lie below the critical deconfinement density (roughly about twice nuclear density in our models).

Details of the models of hadronic and quark matter can be found in Chapters 5 and 8. The nuclear matter properties that are used to determine the hadronic equation of state (beside the well established saturation density, binding, and symmetry energy coefficient) are the compression modulus and effective nucleon mass at saturation, $K = 290$ MeV and $m^*/m = 0.57$ and 0.66, respectively for the two

[2]The common mass of the twins shown in the figures is $1.413M_\odot$, which clearly identifies which curve of Fig. 11.5 we are talking about.

cases of Fig. 11.5. (The effective mass $m^*/m = 0.66$ corresponds to the case where the maximum neutron star mass is $\sim 1.42 M_\odot$.) The bag constant for the quark equation of state is $B^{1/4} = 180$ MeV and the quark model equation of state is given in Section 8.3.3 with $\alpha_s = 0$ [381].

We now demonstrate the stability to radial vibrations of the higher-density sequence of one of the examples shown in Fig. 11.5. Recall that positive slope $dM/d\rho_c > 0$ is a necessary but *not a sufficient* condition for stability. Usually, and in all cases tested heretofore, the sequence more dense than neutron stars, and all higher-density sequences were found to be unstable to radial vibrations [28, 198, 443]. Stability can be deduced from the behavior of the mass–radius relation, but a more transparent test involves an analysis of the radial modes of oscillation, as was discussed in Section 3.18.2 [74]. The squared frequency ω^2 of the fundamental vibrational mode is plotted in Fig. 11.8. Positive values indicate stability and correspond to the segments with positive slope in Fig. 11.5. Negative values of ω^2 mean that a perturbation is exponentially divergent, $\exp(|\omega|t)$. The analysis shows that the fundamental (nodeless $n = 0$) oscillation becomes unstable at the first maximum, as is usual, but unusually, stability of this mode is regained at the following minimum, to be lost again at the next maximum. The usual pattern is that the fundamental mode becomes unstable at the maximum in the neutron star family and a higher mode in order $n = 1, 2, 3 \ldots$ becomes unstable at *each* higher minimum and maximum.

We used the equilibrium equation of state shown in Fig. 11.10 for the calculation of the oscillation modes. Pressure oscillations bring particle populations instantaneously out of equilibrium. We do not know the timescale for equilibration of the transition between quark matter and nuclear matter and how it compares with *typical* periods of oscillations. This does not matter. The turning points in the stellar

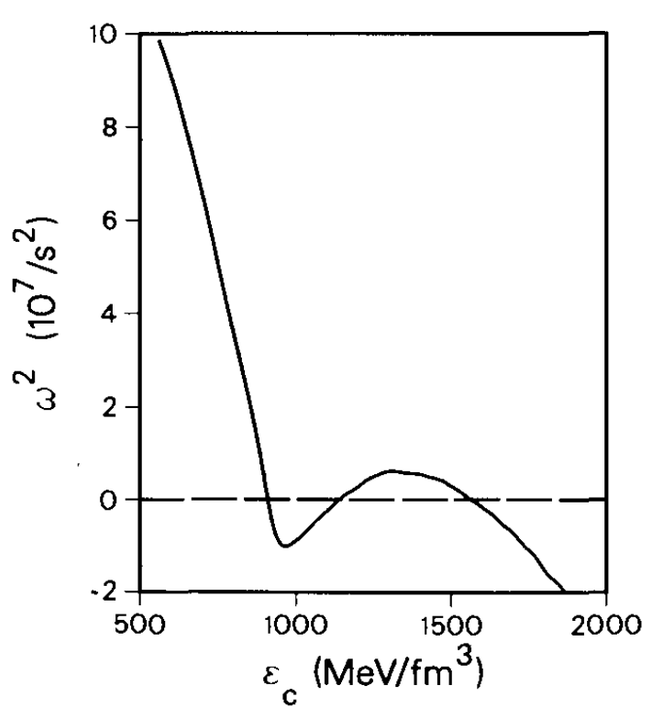

FIGURE 11.8. The square of the frequency of the fundamental ($n = 0$) radial vibration as a function of central density. Perturbations behave as $\exp(i\omega t)$ so they are unstable with diverging amplitude $\exp(|\omega|t)$ when $\omega^2 < 0$.

sequence between stability and instability occur only at the zeros of ω^2, and because the stellar oscillations are infinitely slow at the turning points their location can be determined exactly. Thus, independent of the timescales, the stability for all members of the stellar sequence can be determined.

11.3.3 Cause of stability of a third class of stars

The features of the stellar sequence shown in Fig. 11.5 can be identified with features in the equation of state shown in Fig. 11.10, which is a general form for first-order phase transitions of whatever origin in degenerate stellar matter [195]. The limiting mass star at $\approx 1.418 M_\odot$ has a central density (≈ 900 MeV/fm^3) falling very near the upper end of the mixed phase where all quarks become deconfined. One can see from the equation of state near the end of the mixed phase that $dp/d\epsilon$ becomes small and therefore also the local adiabatic index (3.180),

$$\Gamma = \frac{d \ln p}{d \ln \rho} = \frac{p+\epsilon}{p} \cdot \frac{dp}{d\epsilon}$$

(where p, ϵ, and ρ denote pressure, energy density, and baryon density, respectively). In this upper region of the mixed phase, the pressure is too weak a function of energy density to sustain stability. However, the adiabatic index is discontinuous at the density boundary between the mixed and pure phases, being smaller in the mixed than in the pure phases. This is a characteristic of phase equilibrium. The larger adiabatic index in the pure quark phase restores stability over a short range of central densities between ~ 1150 MeV/fm^3 and ~ 1550 MeV/fm^3, above which the mass becomes too large to be supported by the Fermi pressure of quark matter and the second sequence of stable stars terminates.

While the behavior of the adiabatic index described above is a quite general attribute for phase transitions in multicomponent substances, a stable third family is not. Stability is an integral property that depends on the entire configuration of the star and therefore on the equation of state over the entire density range spanned by the star. Consequently, the behavior of the adiabatic index described above is likely to be a necessary condition for stability of a family at densities above neutron stars, but it is insufficient to ensure that there will be a denser stable family.

From the above proof of stability we have demonstrated that General Relativity can have at least three stable families of stable degenerate stars, white dwarfs and neutron stars being the lowest in central density. While in principle a third family of stable degenerate stars could exist, actual existence depends on the equation of state of dense matter and on an astrophysical mechanism for producing them. The third family could span masses that match a range in normal neutron stars. Each star on the high-density branch has a nonidentical twin on the low-density branch, having the same mass, but different composition and radius.

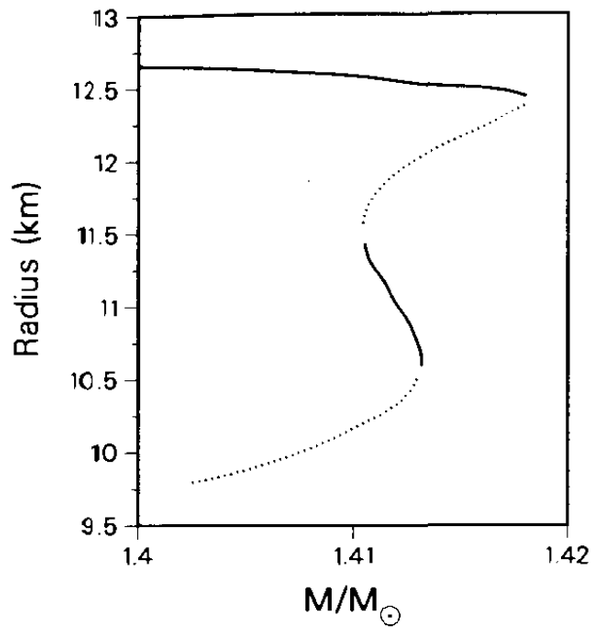

FIGURE 11.9. Radius–mass relationship for neutron star twins. Solid segments are stable configurations. Identification of as few as three stars, one on one branch, two on the other would establish the distinct brances and a third family of compact stars.

11.3.4 Detection and formation mechanisms

Can such twins be distinguished? One possible avenue is through observations on the so-called quasi-periodic oscillations[2] in the X-ray brightness of accreting neutron stars. According to theory, mass, and radius determinations may be possible [304, 305, 306, 373, 374]. If twins exist, then the mass–radius curve will exhibit two segments of stable stars instead of one as in Fig. 11.9; observed stars will fall on one or the other of the two distinct segments. The discovery of only about two stars on each branch with a radius resolution of a kilometer in our example would suffice to establish the existence of twin branches.

How could a high-density twin be made in nature? The likely path to the high-density twins is through the initial core collapse of a star, in which the core implodes through the normal star to the high-density twin. Since no two supernova are likely to be identical, there being many variables that affect the outcome, such as mass, rotation, symmetry, chemical composition of the progenitor, and the chaotic process of convection, it seems plausible that either twin could be produced.

A second possible formation mechanism of the high density twin is through accretion onto a member of the low-density sequence of Fig. 11.5. This is perhaps the most interesting route, though not necessarily the most likely. Accretion onto a normal neutron star near the mass limit of the low-density sequence could conceivably lead to collapse to a member of the high-density sequence, with the excess mass being blown off in a minor nova by the release of gravitational binding energy, much as it is thought that some white dwarfs may collapse by accretion to a neutron star.

[2]Also known as QPO.

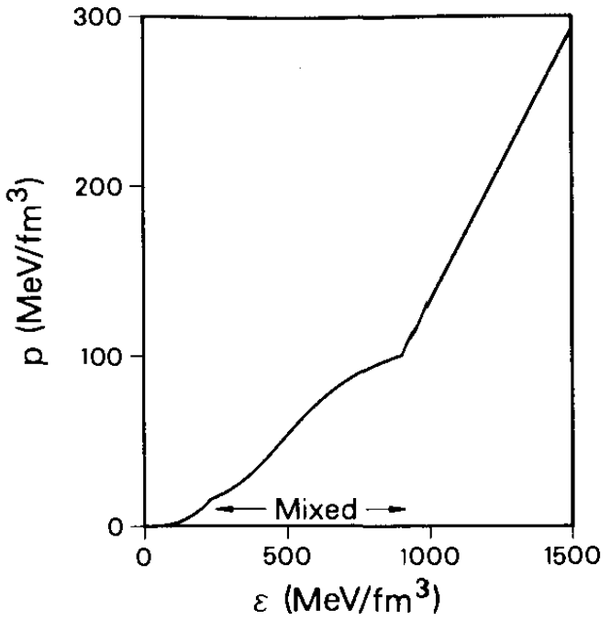

FIGURE 11.10. Equation of state from the low-density normal nuclear matter through the mixed phase and into the pure quark-matter phase at high density The phase transition is first-order and the pressure varies in the mixed phase because neutron star matter has two independent components, baryon and electric charge [195]. (The normal density of nuclear matter is 140 MeV/fm^3.)

11.3.5 Conclusions and prospects

Are there even higher-density families of relativistic compact stars? It is not ruled out by virtue of the proof given here that a third family is allowed by reason of structure in the adiabatic index introduced into the equation of state by a phase transition. There could be a series of phase transitions such as we have discussed, following one another at a succession of densities. But the quark deconfinement phase transition may be the ultimate attainable in compact stars that are stable to collapse to black holes. At such high densities that matter is in the pure quark phase, asymptotic freedom [444] is likely to assure that the equation of state is smooth like a polytrope. Indeed, asymptotically, that is precisely the case for the MIT bag equation of state. From the density where a smooth asymptotic behavior is reached, we are assured of the denumerable infinity of turning points in the stellar sequence having an increasing number of unstable normal modes such as was found by Wheeler et al. [28].

The existence of a third stable class of degenerate stars makes special demands on the equation of state—demands that cannot be met if dense matter simply evolves in a continuous way with density. Our particular model is limited in both its description of nuclear and quark matter so that the examples we have found are presumably limited in the range of masses and densities for which a third class can exist. We have no knowledge from experiment of a single point on the equation of state above nuclear density. But we do have expectations of phase transitions; asymptotic freedom of quarks would appear to elevate one of them to a law of nature. A phase transition can produce the requisite structure discussed above into the equation of state so as to restore stability for a finite density range after stability has been lost by the canonical neutron stars. The possible existence of a

third family of compact stars hinges on such details that we may never determine in laboratory experiments. Therefore, the actual discovery of members of the third family would reveal, however imperfectly, a nonsmooth behavior of the equation of state possibly caused by a change in phase of dense matter—that we may never know by laboratory experimentation. If some of them were X-ray sources, QPO observations may permit the use of Linblom's inverse theorem [133] to gain rather particular knowledge of the equation of state.

11.4 Phase Transition Signal in Pulsar Timing

Neutron stars have a high enough interior density as to make phase transitions in the nature of nuclear matter a distinct possibility. We have discussed three examples, hyperonization, negative Bose condensation (such as π^- and K^-), and quark deconfinement. According to the QCD property of asymptotic freedom, the most plausible is the quark deconfinement transition. From lattice QCD simulations, this phase transition is expected to occur in very hot ($T \sim 200$ MeV) or cold but dense matter. It turns out that a millisecond pulsar, as it spins down, may produce a very distinct signal of a phase transition [200]. In this section we will use the deconfinement transition as an example, but in principle, any transition that is accompanied by a sufficient softening of the equation of state and occurs at or near the limiting mass star, can produce a similar signal.[3]

We discuss first the physical reason why a rapidly rotating pulsar, as it slows down over millions of years because of angular momentum loss through the weak electromagnetic process of magnetic dipole radiation, will change in density due to weakening centrifugal forces and possibly encounter, first at its center, and then in a slowly expanding region, the conditions for a phase transition. Conversely, an accreting star will be spun up from low to high frequency by accretion from a low-mass companion. This too will have a very long timescale because accretion is regulated by the radiation pressure of the star's surface, heated by infalling matter.[4]

The manifestations of a phase transition can be quite dramatic both in the braking index as shown in Fig. 11.11, and in the actual spin-up of a pulsar during the spin up epoch [200], though less dramatic manifestations may occur instead [342].

11.4.1 Evolutionary path of neutron stars

Neutron stars are born with only moderate rotational angular frequencies (30 Hz for the Crab pulsar) so they are also born with the highest central density that they will have in the initial spin-down phase of their lifetime. They are very little deformed by centrifugal forces. They will possess cores of the high-density phase

[3]Most of the calculations in this section were carried out in collaboration with F. Weber.

[4]The effect on the spin evolution of a phase change in the interior of an accreting neutron star is under investigation by F. Weber and the author.

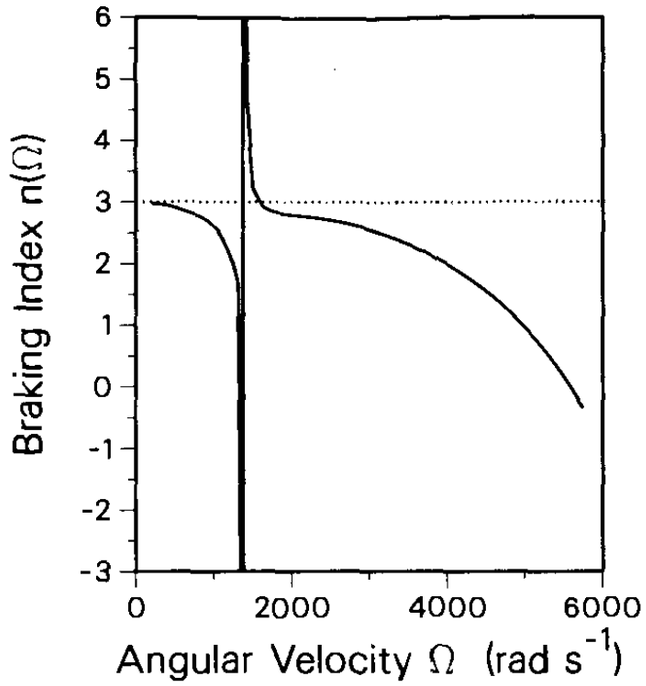

FIGURE 11.11. Braking index as a function of angular velocity. The singularities are a consequence of a phase transition. Otherwise the trend of the curve is characteristic of neutron stars over a broad range of angular velocity. The canonical value of the braking index is 3, valid for a rigid object.

essentially from birth if the critical density falls in the range of neutron stars. However the global properties, such as mass or size, of a slowly rotating neutron star are little affected by whether or not it has a more compressible phase in the core. In principle, cooling rates should depend on interior composition, but cooling calculations are beset by many uncertainties, and competing assumptions about composition can yield similar cooling rates depending on other assumptions about superconductivity and the cooling processes. Moreover, for those stars for which a rate has been measured, not a single mass is known. It is unlikely that these measurements will yield conclusive evidence in the present state of uncertainty [275, 445].

Nevertheless, it may be possible to observe the phase transition in millisecond pulsars by the easiest of measurements—the sign of $\dot{\Omega}$. Normally the sign should be negative corresponding to loss of angular momentum by radiation. However a phase transition that occurs near or at the limiting mass star, can cause spin-up during a substantial era compared to the spin-down time of millisecond pulsars [200, 201, 298, 308]. The transition may be of either first- or second-order provided that it is to an appreciable more compressible phase. We sketch the conventional evolutionary history [236] of pulsars with the addition of the supposition that the critical density for quark deconfinement falls in the density range spanned by neutron stars.

As already remarked, with the supposition above, the star has a quark core from birth, but its properties are so little affected that this fact cannot be discerned in members of the canonical pulsar population. It is born with moderate rotation period, acquired by the conservation of angular momentum during core collapse and with high magnetic field by flux conservation. The evolutionary track of pulsars

are from high magnetic field and moderate rotation period to long period in about 10^7 to 10^8 years, to accreting X-ray neutron stars (marked silent), to millisecond pulsars with low magnetic fields is shown in Fig. 5.8. A pulsar is born near the line marked 10^3 years (since birth) and with $B \sim 10^{13}$ gauss. It evolves quickly at constant B toward a longer period for $\sim 10^6$ to 10^8 years. There it lingers with the bulk of the pulsar population at long periods (because $\dot{P} \sim 1/P$) before the combination of field strength and rotation period are insufficient to accelerate charged particles that produce the radiation. At that time the star has entered the radio-silent epoch.

Some pulsars will have had a less dense companion or will acquire one from which they accrete matter and angular momentum. Some will be seen as X-ray emitters during the radio-silent epoch. During spin-up to frequencies much higher than those with which pulsars are born, the neutron star becomes increasingly centrifugally deformed and its interior density falls. Consequently, the radius at which the critical phase transition density occurs moves toward the center of the star—quarks that were deconfined at the birth of the star recombine to form hadrons. (This era may also be detectable as discussed in Section 11.4.4.) When accretion ceases, and if the neutron star has been spun up to a state in which the combination of reduced field strength (perhaps to ohmic decay) and increased frequency turn the dipole radiation on again, the pulsar recommences spin-down as a radio visible millisecond pulsar.

During spin-down as a millisecond pulsar, the central density increases with decreasing centrifugal force. First at the center of the star, and then in an expanding region, the highly compressible quark matter will replace the less compressible

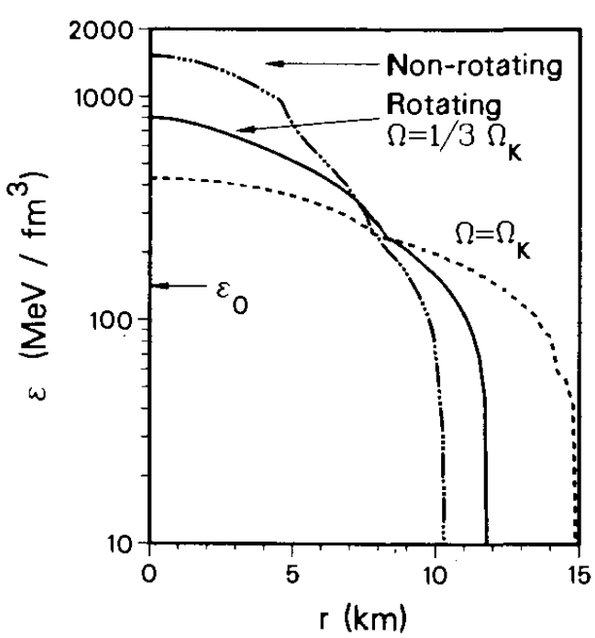

FIGURE 11.12. Energy-density profiles of a star at three rotation rates [201]. Notice the 5-km radius quark matter core when the star is not rotating (or only slowly as a canonical pulsar). Mixed phase extends to 8 km.

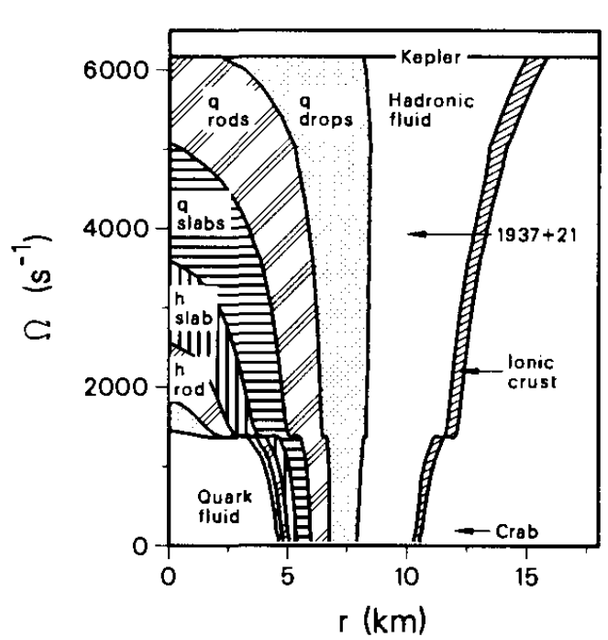

FIGURE 11.13. Radial boundaries between different phases for stars of mass indicated on the y axis. Composition consists of quarks, the baryon octet, and leptons. The geometric phases were discussed in Section 9.5 [308].

nuclear matter. The quark core, weighed down by the overlaying layers of nuclear matter is compressed to high density, and the increased central concentration of mass acts on the overlaying nuclear matter, compressing it further (see Figs. 11.12 and 11.13). The resulting decrease in the moment of inertia causes the star to spin up to conserve angular momentum not carried off by radiation [200, 201, 298, 308, 341].

The above phenomenon is analogous to that of "backbending" predicted for rotating nuclei by Mottelson and Valatin [446] and discovered in the 1970s [447, 448] (see Fig. 11.14). In nuclei, it was established that the change in phase is from a particle spin-aligned state at high nuclear angular momentum to a superfluid state at low angular momentum. The phenomenon is also analogous to an ice skater who commences a spin with arms outstretched. Initially spin decreases because of friction and air resistance, but a period of spin-up is achieved by pulling the arms in. Friction then reestablishes spin-down. In all three examples, spin-up is a consequence of a decrease in moment of inertia beyond what would occur in response to decreasing angular velocity.

11.4.2 Calculation

In our calculation, nuclear matter was described in a relativistically covariant theory [68, 132, 159] and quark matter in the MIT bag model [385]. The phase transition occurs in a substance of two conserved quantities, electric charge and baryon number, and must be found in the way described in Ref. [449] and in Section 9.3. The moment of inertia must incorporate all effects described above—changes in composition of matter, centrifugal stretching—and frame dragging, all within the framework of General Relativity. The expression derived by Hartle is inadequate because it neglects these effects [330, 338]. Rather, we must use the expression derived in Section 6.4 [197, 266].

For fixed baryon number we solve General Relativity for a star rotating at a sequence of angular velocities corresponding to an equation of state that describes the deconfinement phase transition from charge-neutral nuclear matter to quark matter. The equation of state is shown in Fig. 11.15. The moment of inertia as a function of angular velocity does not decrease monotonically, as it would for a gravitating fluid of constant composition. Rather, as described above, the epoch over which an enlarging central region of the star enters the more compressible phase may be marked by spin-up (Fig. 11.16). We remark that the glitch phenomenon is microscopic on the scale shown in the figure, being smaller than the line width in the figure (see equation (5.1)). Does the spin-up epoch endure long enough to provide a reasonable chance of observing it in some members of the pulsar population? This question we turn to now.

11.4.3 Spin-up era

To estimate the duration of the spin-up, we solve the deceleration equation for the star with moment of inertia having the behavior shown in Fig. 11.16. From the

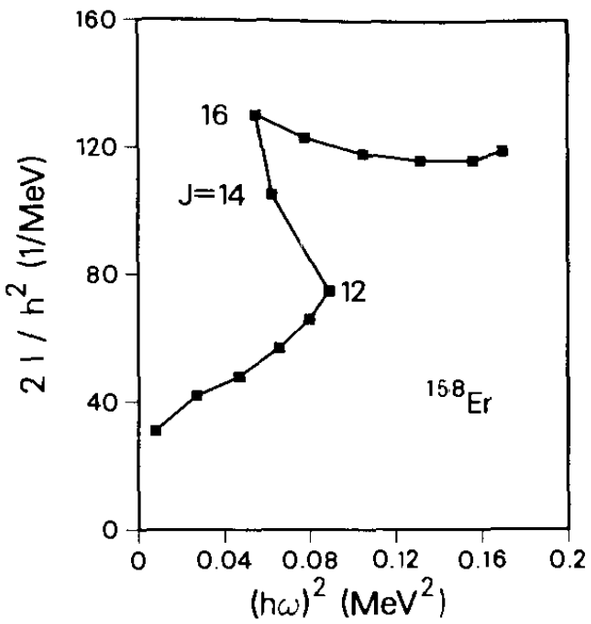

FIGURE 11.14. Nuclear moment of inertia as a function of squared frequency for ^{158}Er, showing backbending in the nuclear case.

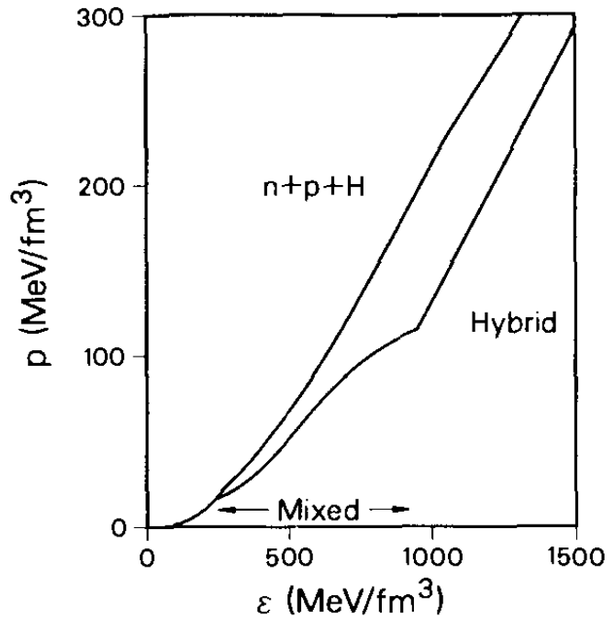

FIGURE 11.15. Equation of state for the first-order deconfinement phase transition described in the text.

energy loss equation

$$\frac{dE}{dt} = \frac{d}{dt}\left(\frac{1}{2}I\Omega^2\right) = -C\Omega^4 \tag{11.1}$$

for magnetic dipole radiation, we find [200]

$$\dot{\Omega} = -\frac{C}{I(\Omega)}\left[1 + \frac{I'(\Omega)\,\Omega}{2I(\Omega)}\right]^{-1}\Omega^3 . \tag{11.2}$$

This expression reduces to the usual braking equation when the moment of inertia is held fixed. The braking index is a dimensionless combination of three quantities that are observable in principle, namely, the angular velocity and its first two time derivatives. It is generally thought to have a constant value of 3, for magnetic dipole radiation. However, constancy would follow only if the star rotated rigidly. Instead it varies with angular velocity and therefore time according to

$$n(\Omega) \equiv \frac{\Omega\ddot{\Omega}}{\dot{\Omega}^2} = 3 - \frac{3I'\Omega + I''\Omega^2}{2I + I'\Omega} \tag{11.3}$$

where $I' \equiv dI/d\Omega$ and $I'' \equiv dI^2/d\Omega^2$. This holds in general even for a star whose internal composition does not change with angular velocity (inconceivable). In particular one can see that for very high frequency, the derivatives will be largest and the braking index for any millisecond pulsar near the Kepler frequency will be less than the dipole value of $n = 3$.

To find the time evolution of the braking index we can use the moment of inertia as a function of Ω shown in Fig. 11.16 and solve the deceleration equation (11.2). The braking index can then be obtained as a function of time [201, 298]. It is shown in Fig. 11.17. An anomalous value, far removed from the canonical value of three, endures for 10^8 years corresponding to the slow spin-down of the pulsar and the

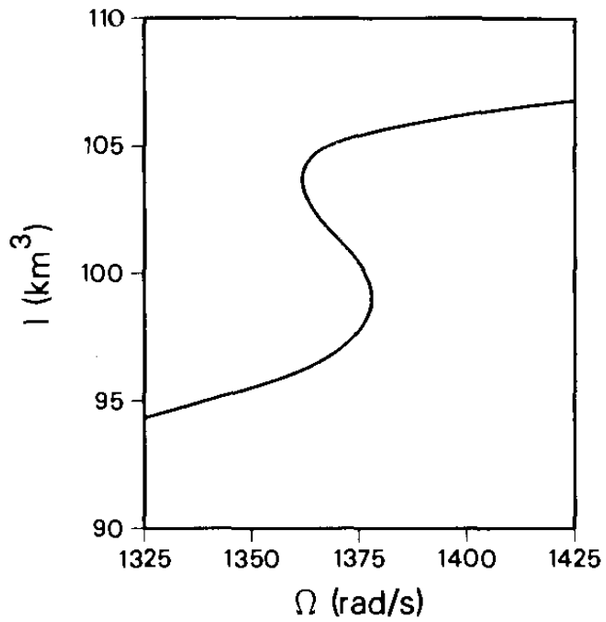

FIGURE 11.16. Evolution of moment of inertia corresponding to a change of phase [200]. Time flows from large to small I.

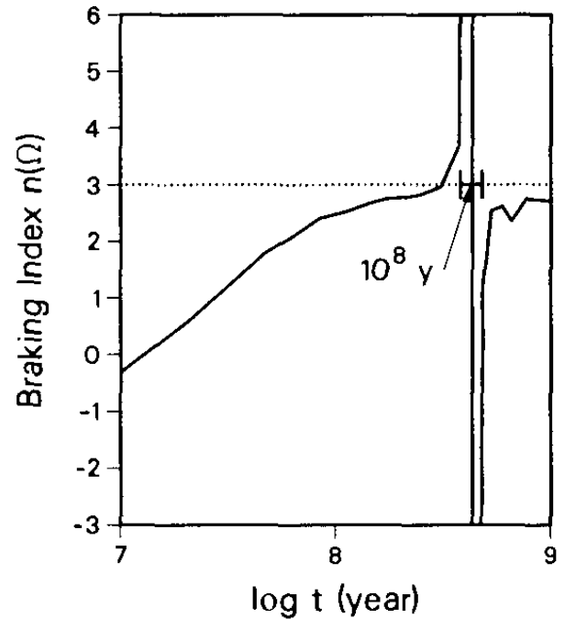

FIGURE 11.17. The time evolution of the braking index plotted over two decades that include the epoch of the phase transition [308, 298].

corresponding slow envelopment of a growing central region by the new phase. The two points that go to infinity correspond to the infinite derivatives of I at which according to (11.2), the deceleration vanishes. They mark the boundaries of the spin-up era. The actual spin-up lasts for 2×10^7 years or 1/50 of the spin-down time for this pulsar. This could be easily observed in a solitary pulsar and would likely signal a phase transition.

11.4.4 X-ray pulsars in low-mass binaries

As has been discussed in the recent literature [304, 305, 306, 373, 374], neutron stars that are accreting mass that is channeled to their surface from a low-mass companion have been observed to rotate in the millisecond range. One of the goals in those studies is to observe phenomena associated with the last stable orbit. Mass, radius, pulsar frequency, and the frame-dragging frequency can be determined according to a theory of the quasi periodic oscillations (QPO) observed in accreting X-ray neutron stars. If the theory is correct, the moment of inertia can be obtained from (6.26) as

$$I = \frac{1}{2}\frac{\omega}{\Omega}R^3 \quad \text{(gravitational units)} \tag{11.4}$$

where the frame dragging angular velocity $\omega(R)$ corresponds to R, and Ω is the rotational angular velocity of the pulsar. A few such sets of data corresponding to stars of the same mass would represent points on a plot of moment of inertia vs. angular velocity, as in Fig. 11.16. If indeed quark matter cores exist in slower pulsars, then the possibility exists that some of the X-ray emitters will lie on the upper branch and others on the lower branch. Even if one did not have observations that

lay on the backbend, observations that established the existence of two asymptotes would be quite convincing evidence of a different phase on the two branches.

11.5 Caveats

The physics of spontaneous spin-up of pulsars as a consequence of conversion of matter from one phase to another in the core of the star is easy to understand, is analogous to the "backbending" phenomena discovered in rotational nuclei, and is witnessed in the performance of ice skaters. However, it is not a necessary consequence of a phase transition. In Fig. 5.11 we saw a case where spin-up did not occur, even though the moment of inertia itself was remarkably affected by the internal constitution. There are also intermediate situations, where spin-up does not occur, but the braking index, nonetheless, is quite anomalous [341, 342]. Consequently, the failure to observe spontaneous spin-up does not necessarily imply that a phase transition is actually occurring in the core of a millisecond pulsar.

12

Strange Stars

12.1 The Strange Matter Hypothesis

It is usually assumed without further consideration that the *ground state* of hadronic matter is the state in which quarks are confined in individual hadrons. This phase of matter occupies the observable universe. Even though we look to the farthest reaches of the cosmos, we recognize spectral lines—whether Doppler, gravitationally or cosmologically shifted—identifiable with transitions of atoms and nuclei known on Earth. Most of the mass of every object we can study experimentally resides in its nuclear constituents. Indeed, our experience so firmly affirms the confined phase as the normal phase of matter that we usually do not question it. However, there is presently no evidence to show that the ground state of matter must be that of quarks confined in hadrons. The confined state may simply be a very long-lived state, but not an absolutely stable one. Indeed, it is not possible to prove otherwise save by the discovery of a lower energy state.

In this chapter a very different possibility is considered—*the strange matter hypothesis*—due independently to Bodmer [380] and Witten [93]. According to the hypothesis, the true and absolute ground state of the strong interactions is the deconfined state of quark matter consisting of an approximately equal proportion of up, down, and strange quarks. Matter in such a state is called strange matter.

The strange matter hypothesis may seem manifestly incorrect because all that we know is the confined state. Nevertheless, as we study the hypothesis more deeply we shall see that it is compatible with all known facts including the present

appearance of the universe.[1] We will find that the universe would have evolved along the path that it is presumed to have followed and would appear essentially as it is today even if the hypothesis is true [307, 371, 451, 452]. Only on a very long timescale—that of stellar evolution—is it possible for small amounts of the confined state of individual hadrons to transform into strange matter.

One way in which the confined phase could slowly evolve into strange matter is through the formation of neutron stars. Neutron stars possess dense cores in which the phase transition to quark matter is likely to occur. In this process the weak interaction would convert about a third of the quarks to the strange flavor because at high density such a state has a lower energy than two-flavor quark matter (because the baryon number is shared among three Fermi seas instead of two). If strange matter were the true ground state, then no barrier would exist for the conversion of the *entire* star, once the core has converted. In this way neutron stars would be converted to strange stars.

How could one tell a strange star from a neutron star? In Chapter 8 it was found that neutron and strange stars have about the same mass and radius. However, in Chapter 7 we established a lower bound on the rotational period of *gravitationally* bound stars (such as neutron stars). We shall see that stars made of matter that is saturated and self-bound,[2] at sufficiently high-energy density, can rotate faster than gravitationally bound stars (like neutron stars). Consequently, *if a pulsar with a period falling below the limit of gravitationally bound stars were discovered, the conclusion that the confined hadronic phase of nucleons and nuclei is only metastable would be virtually inescapable.*[3]

Just as a limit on rotation of a gravitationally bound star exists, so also a model independent lower limit on radius exists. This follows immediately from Chapter 7. Recall that the limiting (Kepler) rotational angular momentum is given approximately by $\Omega_K \approx 0.65(M/R^3)^{1/2}$. So, for a given mass a lower limit on R follows from the upper limit we found on Ω_K. For a mass $M \sim 1.44 M_\odot$ it is $R > 6.2$ km, as follows from Fig. 7.2 and 7.5. If a star were found to have the above mass and a smaller radius, it would have to be a strange star, or some other self-bound star, if not a black hole.

We shall study the strange matter hypothesis because strange matter is the most likely candidate for the substance of any pulsar found to rotate faster than is possible for a neutron star. First, we examine the compatibility of the hypothesis with our present knowledge of matter, the present nature of the universe, and its evolution in

---

[1] Alpar [450] has argued that strange stars could not glitch, as is seen sometimes in pulsars. We will address this question later.

[2] By saturated we mean that a bound system's density does not increase with particle number; instead its size increases (as with nuclei). By "self-bound" we mean matter that is bound in bulk by the strong interaction and does not require gravity for the stability of stellar objects made from it. In contrast, nuclei are unstable above about $A = 250$. By "self-bound" we also imply saturated matter. The pressure of self-bound matter is zero in the equilibrium (normal) state.

[3] Metastable refers to a state of a system that is not its ground configuration but is possibly very long-lived.

the confined hadronic phase. We will find that there is no scientific basis on which the hypothesis can presently be confirmed or refuted. We derive a condition on strange matter that would allow a star made of it to rotate rapidly—more rapidly than a neutron star. If the hypothesis were true, a host of rare but exotic phenomena could exist, some of which we explore in later parts of this chapter. The discovery of any phenomenon that would confirm the hypothesis would be a fundamental discovery.

12.2 Compatibility of the Hypothesis with Present Knowledge

12.2.1 Energetic considerations

From many aspects of nuclear physics, we know that nuclei are composed of nucleons containing up and down quarks—not quark matter. Therefore, two-flavor (nonstrange) quark matter lies above the energy per nucleon of nuclear matter. However, what if the equilibrium (normal) state of three-flavor quark matter is at a density sufficiently high that the quark chemical potential is large compared to the strange quark mass? In that case the baryon number can be shared among three Fermi seas, thus lowering the energy per baryon number.

To compare the energy per nucleon number of two- and three-flavor quark matter we make the following considerations. The available energy scale for comparison is that of QCD, say 100 MeV, established by lattice simulations. From this we might expect that two-flavor quark matter lies about 100 MeV per nucleon above that of the energy per nucleon in nuclei (930 MeV in Fe), or roughly 1100 MeV. We want to estimate how much lower than this, three-flavor quark matter would be. As an order of magnitude estimate, treat the quarks as a Fermi gas. The energy density scales as $\epsilon \sim \gamma\mu^4$ and the baryon density as $\rho \sim \gamma\mu^3$, where $\gamma = 2, 3$ is the degeneracy for two and three flavor quark matter. (Use the zero temperature approximation to Section 8.3.2 and neglect B.) Compare the two types of quark matter at the same baryon density: because $\mu \sim \gamma^{-1/3}$, three-flavor quark matter has an energy per baryon ϵ/ρ of approximately $(2/3)^{1/3} \sim 0.9$ times that of two-flavor, or about 110 MeV lower. In other words, three-flavor quark matter lies below two-flavor quark matter by *about* the same amount as two-flavor quark matter lies above the nucleon mass, or the mass per baryon in a nucleus. This places the energy per nucleon of strange quark matter in the vicinity of that of nuclear matter. Whether it lies above the nucleon mass or below the energy per nucleon in iron ($\sim$ 930 MeV) may be a matter of only one percent.

Two things are clear from the above. First, the strange matter hypothesis cannot be rejected out of hand. Second, under the circumstance that the phases of hadronic and strange quark matter lie so close in energy per baryon, models of

confinement such as the bag model or even lattice QCD[4] cannot provide any convincing argument as to which phase is lower. While it is certainly interesting to explore the predictions of models, they are not sufficiently precise to portray either the *limitations or possibilities* for strange stars.

12.2.2 The universe and its evolution

The strange matter hypothesis could be true even though the universe evolved along a path that brought it to its present phase—a metastable one if the hypothesis is true. The fact that most of the mass in every object that we know—from our own bodies to all the visible galaxies—resides in nucleons and nuclei tells us for certain only that this is one possible state of matter and that it is very long-lived—not necessarily that it is the lowest energy state. How misleading the present composition of the universe is in revealing the nature of the ground state is immediately exposed by noting that the lowest energy state of the confined phase is Fe^{56}—and there is little of that in the universe. We understand perfectly well why this is so. Only a few of the lightest elements were produced in the primordial nucleosynthesis. Heavier elements are fused very slowly in massive stars on the timescale of their evolution ($\geq 10^7$ years).

Witten [93] hypothesized that strange quark matter is absolutely stable as a possible solution to the so-called missing mass or dark matter problem. It is believed by most astronomers, based both on a cosmological argument (observed flatness of the universe) and on the observations that the visible matter of the universe is subject to greater gravitational forces than the visible matter itself would exert, and that there is much more matter in the universe, indeed within our own Galaxy, than can be seen. Such matter is referred to as dark matter, and has been the subject of much speculation. It is believed to amount to 90% of the total mass of the universe.

In the early high-temperature era, the universe almost certainly passed through the deconfined quark matter phase, of which three-flavor quark matter is lower in energy than two-flavor as explained above. Witten reasoned that, if strange matter were the ground state, much matter would have remained in this phase. If it is truly the ground state, then objects from microscopic to starlike would be stable. Such matter in microscopic and macroscopic lumps, called strange nuggets, would be nonluminous and therefore invisible as objects in space. Hence the suggestion that strange matter formed the dark matter of the universe.

However, it was soon shown that, even if strange matter is the ground state, all (or almost all) strange matter would have evaporated in the high-temperature era into ordinary hadrons. There would be little or no relic strange matter [453, 454]. Strange matter as a candidate for dark matter did not turn out to be a viable suggestion. Nevertheless, it may still be true (in view of the energetic reasons

[4] Solutions of QCD, the confined theory of hadronic matter, are simulated on a spacetime lattice on computers. Even so, attention has been focused only on a very restricted class of problems.

given above) that it is the ground state. Because of the evaporation of hot primordial strange matter into hadrons, we understand why the subsequent evolution of the universe is undisturbed by the question as to which is the absolute ground state of cold matter—the confined or deconfined strange matter state. And we understand why there can be little strange matter present now: it can be recreated only in the interiors of neutron stars and therefore on the timescale of stellar evolution.

12.2.3 Stability of nuclei against decay to strange matter

We know from the arguments presented above that strange quark matter likely has an energy per nucleon that places it close to that of Fe^{56} ($\sim$ 930 MeV per nucleon). Theory is not accurate enough to decree whether it is above or below, making it unstable or absolutely stable. Even if strange matter is lower in energy per baryon number, ordinary nuclei can decay into the strange quark phase only on a timescale that is long in comparison with the age of the universe.

The decay is inhibited by the need for A *simultaneous* strangeness-changing weak interactions, where A is the atomic number of the nucleus [381]. It is energetically unfavorable for the transition to take place one quark at a time because this would initially produce only hypernuclei—which are higher in energy than the original ordinary nuclei. It is important in the above argument to realize that surface and shell effects place a lower but uncertain bound ($A = 10 - 1000$) on the baryon number for which small nuggets of strange matter are bound even if strange matter in bulk is absolutely stable as is suggested by Fig. 12.1 [381, 455, 456]. Thus, low-mass nuclei are stable even though only a few simultaneous weak interactions are required to convert them to strange nuclear nuggets. The lower energy of the nucleon compared to the lambda is an extreme example. It should also be said that stable nuggets with A as small as ten occur only under the most favorable choice of Bag constant $B^{1/4} = 145$ MeV (which leaves charge-neutral ud quark matter unstable, as is empirically the case; nuclei are made of nucleons, not u and d quarks.)

12.2.4 Stability of nuclei to conversion by strange nuggets

Although the mass of the strange quark is larger than that of the up and down quarks, the quark chemical potential exceeds the mass difference at any density above several times nuclear (8.25). All three quarks are therefore almost equally populous (Chapter 8, Section 8.5.2). Because of the mass difference, a slight deficit of strange quarks exists which provides a nugget with a positive charge, but with low Z/A.

The positive charge of strange matter insures that a nugget will repel nuclei. As a result, nuggets will be inert except in a neutron-rich environment such as neutron stars, in massive stars in the late stage of collapse when the density exceeds the neutron drip density, or in very high-temperature matter where the kinetic energy of charged particles may overcome the Coulomb barrier. Any strange nuggets present on Earth will not grow to become conspicuous. Moreover, because of their

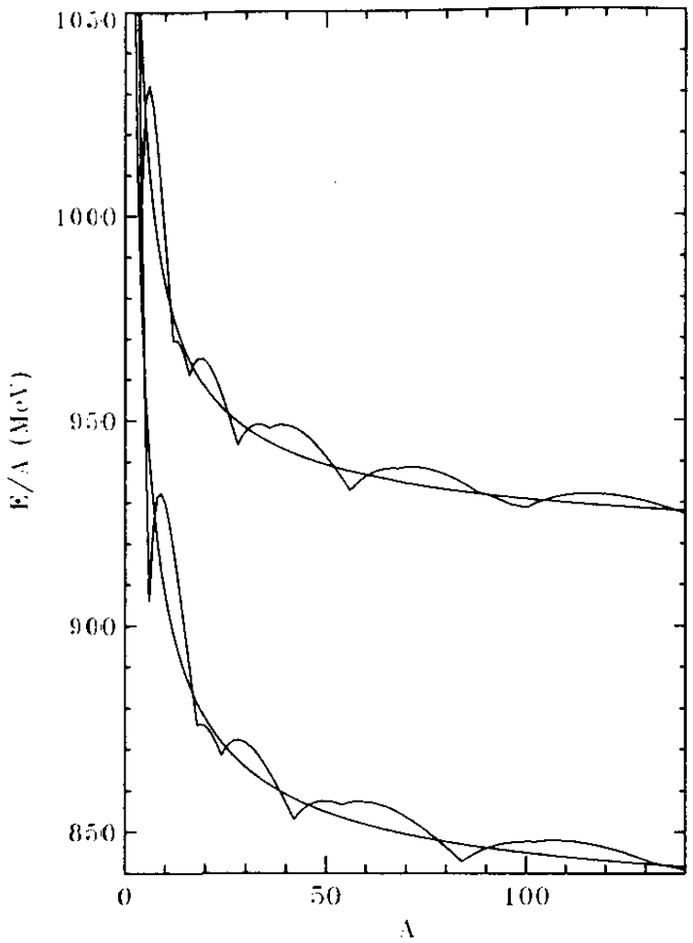

FIGURE 12.1. Energy per baryon number A for strange matter nuggets as a function of A. Smooth curves are liquid drop estimates. Others show shell effects. Top pair for ud quark matter and bottom for uds in equal proportions and all quarks massless. Bag constant is $B^{1/4} = 145$ MeV, the minimum possible value that would leave charge neutral ud quark matter unstable. (Courtesy of J. Madsen. See also Ref. [456].)

high density (a few times nuclear density), the surface gravitational force acting on nuggets with $A > 10^{17}$ would exceed the electrostatic forces holding solid material together so that such nuggets would sink toward the center of the Earth [381]. The anomalously low charge-to-mass ratio Z/A provides a signature for their identification if they occur on Earth with sufficient concentration to be found. However, as we shall see in the next section, the concentration expected on Earth is small.

12.2.5 Terrestrial searches

If strange stars exist, there will be some abundance of strange nuggets present on Earth, accumulated as cosmic rays over the Earth's lifetime. We now estimate an upper limit to see if strange matter as the ground state is ruled out by present experimental limits. For 20 years of observations on the Hulse–Taylor binary pair of compact stars (one of which is the pulsar with celestial coordinates 1913+16), the observed decay of the binary orbit has confirmed Einstein's gravitational radiation to an accuracy of less than one percent [4, 53]. Eventually, the decay of this orbit will cause the compact stars to collide, and some fraction of their material will be injected into the Galaxy. The decay time, estimated to be about 10^8 years, is short

compared to the galactic age. So many such collisions will have occurred in the past.

In our estimate of the abundance of such material that has accumulated on Earth, we employ accepted cosmological figures for those items that are available and overestimates of others, so as to get an upper bound on the concentration of strange nuggets. For this purpose we need the age of the Galaxy (10^{10} years), the frequency of galactic type II supernovae[5] ($\sim 1/(100$ yr)) [457], the fraction of pulsars that occur in binary compacts ($< 1/100$), and the fraction of mass ejected from a collision ($1/10$) [458]. We find a mass of debris of $10^5 M_\odot$ spread over the Galaxy from compact star collisions. We can translate this into baryon number by noting that $M_\odot \approx 10^{57} m$ where m is the nucleon mass.

For the Galaxy volume we take its luminous radius of 15 kpc and approximate the thickness uniformly as 2 kpc. This yields $V_G = 4 \times 10^{67}\text{cm}^3$. We find, for the mass density of debris, $\rho < \frac{1}{2} 10^{-29}\ \text{g/cm}^3$ or a baryon number density $n < \frac{1}{4} 10^{-5}/\ \text{cm}^3$. As an extreme overestimate, assume that all such compacts were strange and that all mass is ejected in minimum mass fragments ($A \approx 1000$). We find a number density of strange nuggets of $N_G < \frac{1}{4} 10^{-8}/\text{cm}^3$. Assuming a typical galactic velocity of 10^7 cm/s, there would be an influx of $< 10^{15}/\text{cm}^2$ over the age of the Earth (5×10^9 yr). (However, the velocity assumed corresponds to the measured typical velocity of pulsars transverse to the galactic plane [459]. If the isotropic component is less, then our flux is an overestimate.)

The Earth's crust is not tranquil. Mountains are cast up, then eroded; continents drift; tectonic plates collide and slide over one another. Material that can be recognized as once having been at the Earth's surface resurfaces in the lava of volcanic eruptions, having been subducted to the molten core below the mantle. We estimate a geologic mixing depth of the order of ten kilometers (a conservative estimate). Even if all cosmic nuggets were stopped at the Earth's surface, they would be diluted to a concentration of $10^9/\text{cm}^3$ or less over geologic times, or $< 10^{-15}$ nuggets per nucleon given an Earth density of 5 g/cm^3. This extreme overestimate is to be compared with the upper limit of 10^{-14} established by experiment [460].

We conclude the strange matter hypothesis cannot be ruled out by present experimental limits on the abundance of strange nuggets in the Earth's crust! There are probably no favorable samples on Earth for strange nugget searches, in view of the high degree of dilution. Meteorites have their surfaces burned off in traversing the atmosphere if they are not completely destroyed, and are also not favorable. However, the moon's surface has been exposed to the hypothetical strange cosmic rays without geologic mixing. In addition, only minor meteoritic activity has disturbed the lunar surface since early times. Moon rock might prove to be a favorable sample for mass spectroscopy (because of the anomalously small Z/A of strange matter) or for a Coulomb back scattering experiment such as that of Ref. [460].

---

[5]Type II supernovae are the fates of massive stars. The core produces a neutron star or black hole.

12.2.6 Summary, prospects, and challenges

Since shortly after Witten's paper, it has been understood that, even if strange matter is the lowest energy state when cold and that the early universe passed through this phase, it was so hot at the time that strange matter would have evaporated into hadrons [453, 454]. Little if any primordial material is expected to have survived [461]. For these reasons and those developed in the preceding paragraphs, we understand that the universe would have evolved along essentially the same path, and, aside from very subtle signals, would appear the same now, no matter which is the ground state. Only at the death of massive stars (when dense matter that is cold on the nuclear scale is produced in the resulting neutron stars) may conditions for the creation of *cold* strange matter occur for the first time. Whether such conditions have ever been achieved depends on the unknown phase-transition density and whether it has been reached in the core of any neutron star. In Chapter 9 we have estimated that it does.

We are only just now entering an era in which advances in technology may allow the detection of the necessarily subtle signals that might be present if the universe exists in a metastable (albeit long-lived) phase instead of the ground state. There being little or no relic strange matter, strange matter can be recreated now, only in the cores of dense neutron stars and only slowly on the scale of evolution of massive stars—about 10^7 years or more.

From the discussion in the introduction to this chapter, we understand that the discovery of a very rapidly rotating pulsar with period smaller than could plausibly be attributed to a neutron star would signal that the universe is in a metastable phase of matter [367, 370]. Detection of the proposed signal is feasible. We expand upon this theme in the next section.

Alternately, we have seen in Chapter 7 that there is a limit as to how small a neutron star can be (see especially Fig. 7.6). If a mass and radius determination were made on a star that was known not to be a black hole, and that radius was smaller than the model independent limit for the given mass, one would also have to conclude that the object was a self-bound star, possibly a strange star. Only recently do observed quasi-periodic oscillations (QPO) in the X-ray brightness of accreting neutron stars lend an interpretation that mass and radius measurements may be possible [237, 304, 305, 306, 373, 374].

12.3 Submillisecond Pulsars

No submillisecond pulsar has yet been discovered; this is not surprising in view of the detection biases that have been imposed on large-scale searches (Section 5.2.4). As commented on before, the limits on search sensitivity are not easily overcome, but they are not insurmountable. In this section we discuss the difficulties that would be encountered in a conventional interpretation if a submillisecond pulsar were discovered. We then show how its interpretation as a strange star would be

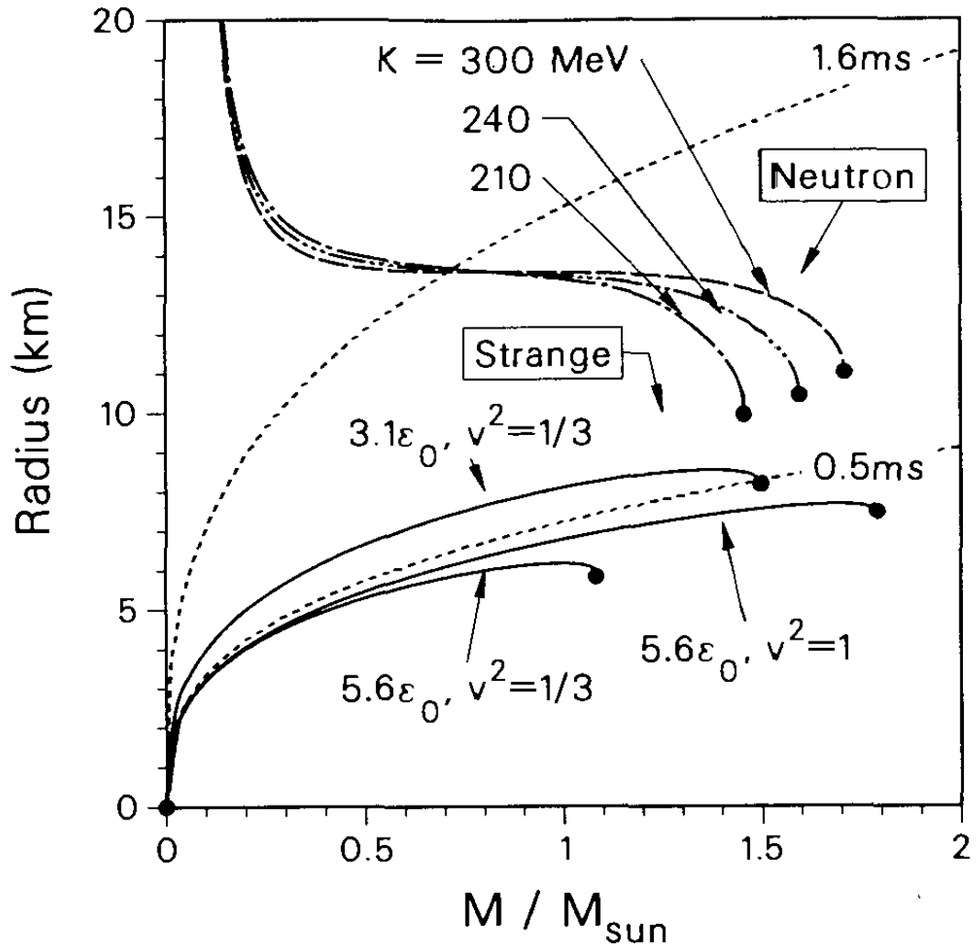

FIGURE 12.2. Generic relationships for compact stars bound only by gravity (neutron stars) and stars made of self-bound matter (strange). Stars below solid lines can rotate at or faster than the indicated period. These curves are representations of (7.1). The equation of state for self-bound matter is parameterized as $\epsilon = p/v^2 + \epsilon_b$, and star families are labeled by the value of ϵ_b and v^2. (From Ref. [371].)

natural and, under a certain circumstance, inevitable. A discovery of this sort would be fundamental, so we carefully lay out the arguments in the following sections.

12.3.1 The fine-tuning problem

The mass–radius relationship has a characteristic form shown in Fig. 12.2 for compact stars that are bound only by gravity (like neutron stars). For low masses where the gravitational attraction is weak, the star is large. For higher masses (near the limit for collapse to a black hole), the radius decreases rapidly with increasing mass. For such stars, only those very close to the mass limit can rotate rapidly because their radius is smallest and mass greatest (see (5.9) and (5.12)). In other words, to rotate rapidly a neutron (or hybrid) star must be finely tuned in mass or, equivalently, baryon number. In contrast, the entire sequence of self-bound stars can rotate rapidly, as the figure shows. We discuss the reason for this shortly.

12.3.2 Limits to neutron star rotation

Concerning the question of what is the minimum rotational period of a neutron or hybrid star, we refer to Chapter 7. There we derived the lower limit on the period

as a function of stellar mass using only well-established principles and minimal constraints on the equation of state. We found, for example, that a canonical neutron star of mass $1.44M_\odot$ cannot have a period of less than ~ 0.3 ms. This is a very conservative and absolute limit, because there is no physical principle requiring that the structure of stars be optimized so as to minimize their rotational period. Stars with periods below this limit must be made of material that is self-bound at a high equilibrium density. The most plausible candidate is strange matter. Because the absolute limit derived in Chapter 7 is extremely conservative, it is worth exploring a less stringent constraint that would still constitute a strong case that a pulsar violating the constraint could not be a neutron star. We did this in Chapter 6, page 305 and found a realistic limit based on numerous models of neutron stars imposed by gravitational-wave instabilities [333]. We concluded that the discovery of a pulsar with period less than ~ 1 ms would constitute strong evidence that the star is not a neutron star or any star bound only by gravity.

12.3.3 Implausibly high central densities

It is true that some neutron star models have been found to possess Kepler periods around 0.5 ms [95]. However, the central densities for such models are so high that their description as neutron stars is implausible. In other words, the basis of the calculation on which such stars are founded is contradicted by the outcome. To underline the situation, in Fig. 12.3 we show the *minimum* possible value of the central density of gravitationally bound stars of canonical mass $1.44M_\odot$ as a function of Kepler period [371]. We see that a 0.5 ms pulsar must have an anomalously large density if its matter is in the form of baryons.

It is not known either from experiment or from lattice simulations of QCD at what density the confined hadronic phase would dissolve into the unconfined phase of quark matter. We have found fairly low transition densities in Chapter 9, but those findings are not definitive. We could enquire concerning the density of hadronic matter if compressed to such a degree that all nucleons, treated as spheres of radius equal to the experimental charge radius of the proton (0.8 fm), were in contact in a cubic lattice. That density is $1/(2r)^3$, which is less than 1.5 times normal nuclear density. But nucleons as the entities we know in vacuum or in normal nuclei could not be localized in this fashion according to the uncertainty principle. It is quite possible that confinement persists to a somewhat higher densities. However, it seems hard to reconcile densities of ten or more with confinement of quarks in individual hadrons.

We conclude that such high central densities, as are required for stable rotation at a period of 0.5 ms, are unreasonably high for the confined phase but quite natural for the deconfined phase. At first sight the conclusion reached would seem compatible with hybrid stars. But because hybrids are gravitationally bound, they are subject to the rotational constraints discussed for such stars in Chapter 7; moreover, gravitational-wave instabilities moderated by viscosity set the limit, as it appears, of $P \geq 1$ ms (Section 6.12). A strange (self-bound) star is not likely to be subject to the same constraint because the viscosity of quark matter is computed to

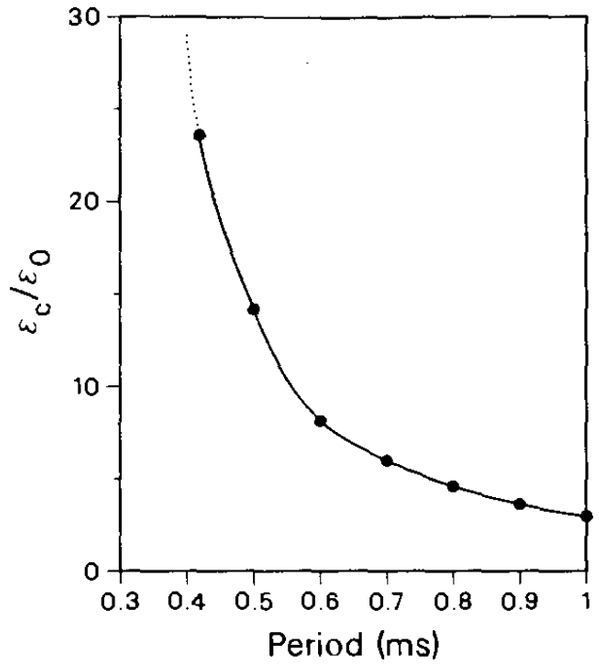

FIGURE 12.3. The least possible central density of 1.44-$M_\odot$ stars required for stable rotation as a function of rotational period. (From Ref. [371].)

be high [462, 463, 464]. The surface modes that give rise to gravitational radiation are expected to be damped and the instability deferred to much higher rotational frequency (Section 6.12).

12.3.4 Strange stars as fast rotors

If strange quark matter is self-bound and absolutely stable, as has been suggested [93, 380], the structure of a compact star composed of such matter would be entirely different from that of a neutron star because of QCD confinement [93, 378, 379]. Such a star is called a strange star, or a strange quark star. While gravity binds all known stars, it merely prevents strange stars from fissioning into smaller bodies, compresses them, and of course, imposes a mass limit that cannot be evaded by relativistic stars (Section 2.9.6). Strange stars are otherwise bound by the strong interaction. They form an entirely distinct and disconnected branch of compact stars and are not part of the continuum of equilibrium configurations that include white dwarfs and neutron or hybrid stars (Fig. 3.6).

Gravitational binding diminishes with lower mass, so that the radius of gravitationally bound stars, like neutron stars, increases as the mass decreases. Below a critical mass ($M \lesssim \frac{1}{10} M_\odot$), neutron stars are unstable. The mass–radius relation is shown in Fig. 12.2. This relation is in sharp contrast to that of hypothetical self-bound stars, such as strange stars. We see this formally as follows. Denote the equilibrium, or normal energy density of self-bound matter (the density at which the internal pressure vanishes) by ϵ_b. A small nugget therefore has mass

$$M = \frac{4}{3}\pi R^3 \epsilon_b \quad \text{(no gravity)} \tag{12.1}$$

so that, unlike neutron stars (or more generally stars bound only by gravity), the mass radius relationship for small mass is

$$R \propto M^{1/3}, \tag{12.2}$$

except near the mass limit where gravity terminates the sequence, as in Fig. 12.2.

The above dependence of the radius on mass has a generically different form from that of gravitationally bound stars as shown in Fig. 12.2. Because of the relationship between M and R, the entire family of strange stars can rotate rapidly, as can be seen from (7.1), not just those near the limit of collapse to a black hole [370]. This is so because, for such a radius–mass relationship as depicted in the figure, the expression for the Kepler frequency (7.1) is a constant for low-mass strange stars (use (12.1)) and only increases for those near the mass limit because gravity compresses the star to a smaller radius. From (6.54) we can derive a condition on the normal density of self-bound stable matter that will allow all such stars to rotate with period P [307, 371]:

$$\epsilon_b \geq \frac{3}{4\pi G}\left(\frac{\Omega}{\zeta}\right)^2 = 1.3\epsilon_0\left(\frac{\mathrm{ms}}{\mathrm{P}}\right)^2. \tag{12.3}$$

(The empirical factor $\zeta \approx 0.65$ for General Relativity was discussed in connection with (5.9) and in Section 6.7.) For example, all strange stars can rotate with $P = \frac{1}{2}$ ms if $\epsilon_b > 5.2\epsilon_0$ (where $\epsilon_0 = 2.5 \times 10^{14}$ g/cm^3 is normal nuclear density).

Gravitational radiation-reaction instabilities are unimportant for quark stars because of the expected high viscosity [462, 463, 464]. Therefore the Kepler frequency sets the limit.

12.3.5 Out of the impasse

Fast rotation poses problems for understanding a pulsar as a neutron star. On the other hand, four difficulties would be solved by the interpretation of the discovery of a submillisecond pulsar as a strange star.

(1) Very short periods are possible for strange stars provided only the normal density satisfies the above relationship.
(2) Rotation of strange stars is not likely to be limited by gravitational radiation-reaction instabilities because of the expected high viscosity of quark matter.
(3) High central densities, as required by fast rotation (see (5.12) or Fig. 12.3), are natural for quark matter, but implausible for confined hadronic matter.
(4) A strange star does not have to be finely tuned in mass (as does a neutron star) to be stable at very fast rotation as illustrated in Fig. 12.2. The whole sequence can rotate rapidly subject to (12.3).

12.3.6 Motivation for searches and prospects for discovery

The factors that presently limit the sensitivity of searches for short-period radio pulsars were discussed in Section 5.2.4. The dispersion of the radio signal by the

interstellar medium forces compromises to be made in the search techniques.[6] These compromises cause a sharp roll-off in sensitivity to pulsars with periods below about a millisecond [234, 235]. The limit is not absolute and will be lowered in time, as the search technology is further improved.

Because of the observational bias, the cutoff in short periods that appears in Fig. 5.7 is possibly an artifact. It would indeed be a coincidence if the present technical cutoff in sensitivity coincided with the true lower range of pulsar periods. Therefore, the growing number of pulsar discoveries[7] with periods very close to the search cutoff suggests the tantalizing possibility that pulsars with still shorter periods really do exist.

A special opportunity and challenge exists for radio astronomy. The discovery of additional millisecond pulsars is exciting, both because of their novelty and for what they may reveal of the evolutionary processes involved in their creation and the environment of galactic globular clusters. (Globular clusters are now understood to provide an environment that is especially favorable for the incubation of fast pulsars [225].) But the discovery of a single submillisecond pulsar, especially below $\frac{1}{3}$ ms [249] or even below 1 ms (with less decisiveness), would be an experimental result of fundamental importance. A successful search would inform us that the true ground state of the strong interaction is not that of quarks confined in hadrons, but of matter that is selfbound at high density such as deconfined strange quark matter. It would also tell us that the universe is in a very long-lived but excited state. This possibility cannot be ruled out at the present time. Aside from a few subtle signals, such as the possible existence of submillisecond pulsars *or* of extremely compact stars, more compact than the limit established for gravitationally bound stars (Fig. 7.6), the universe would have evolved in the manner it did, no matter the ground state (Section 12.2).

12.4 Structure of Strange Stars

We can use the results of Chapter 8 to compute the structure of strange stars and to gain further insight into why self-bound stars can rotate rapidly, provided the equilibrium energy density of the matter from which they are made is high enough. The pressure is zero at equilibrium. That is what equilibrium requires and implies. As we have learned, zero pressure marks the edge of a star. It occurs very abruptly—the mass–energy density falls from $\sim 10^{15}$ g/cm^3 to zero in a distance characteristic of the range of the force that binds it—the strong interaction length (10^{-13} cm).

The mass–energy profiles of a self-bound star and a neutron star are compared in Fig. 12.4 for stars of the same mass. Because a self-bound star is clearly much more compact, it is more stable to centrifugal disruption. (The edges of neutron

[6]So far, all millisecond pulsars are observed only at radio frequencies.

[7]The number of known millisecond pulsars tripled between 1992 and 1996.

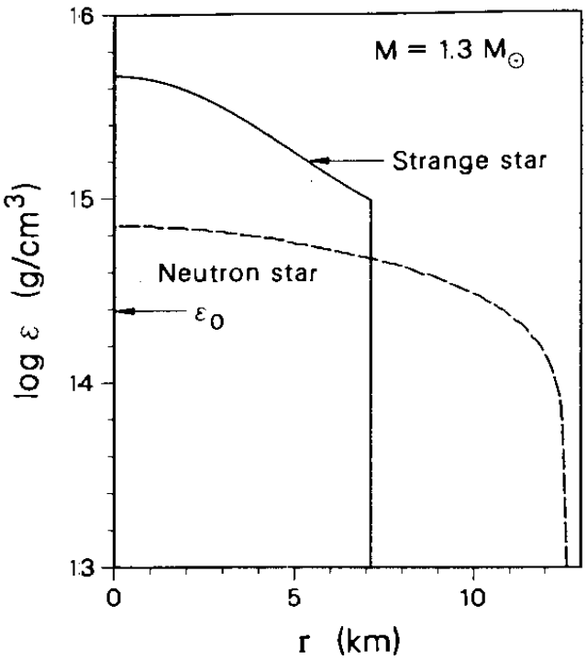

FIGURE 12.4. Mass–energy profile as a function of Schwarzschild coordinate r for a neutron star and a strange star ($B^{1/4} = 180$ MeV).

stars also terminate abruptly, but on a length scale of atomic spacing and at the much lower density of solid iron—about 7.85 g/cm^3 (see page 84). It is at this density that neutron star matter has zero pressure.)

Based on the bag model of confinement and the range placed on its parameters by the condition that strange quark matter is the ground state, several authors have asserted that strange stars cannot rotate rapidly [96, 337] or can do so only marginally [465]. This is an unfortunate confusion in logic in translating a statement that is true of a crude model to a statement about nature. We have emphasized elsewhere that whether or not strange stars can rotate very rapidly is entirely an experimental question, not a theoretical one [370]. For to determine on theoretical grounds whether the energy per nucleon in strange matter lies below that in Fe^{56} with $E/A = 930$ MeV, which would make it absolutely stable, or lies above the nucleon mass at 939 MeV, might require one percent accuracy, an accuracy certainly not possessed by the bag model, nor indeed by lattice QCD now or in the foreseeable future. Neither lattice QCD nor models of confinement can rule out the hypothesis that strange matter is stable, nor conversely can they be used to assert that it is the ground state. Nor can theory predict the equilibrium energy density of strange matter nor the velocity of sound, which in the bag model is $v^2 = (1/3)c^2$.

If the strange matter hypothesis is true, then some or all pulsars may be strange stars rather than neutron stars. Strange stars can be produced in at least two ways [454, 466]: (1) If the density in the core of the more massive neutron stars exceeds the transition density to quark matter (as seems likely from Chapter 9), the core will convert spontaneously to nonstrange quark matter. In turn, this matter will weak-decay to strange matter. Conversion of the entire star will then occur on a short timescale. (2) If a nugget of strange matter falls into a main sequence star, it will gravitate to the center and lie dormant until the star collapses. When the density exceeds the neutron drip density, the nugget will grow and then convert

the entire neutron star produced in the supernova. It is possible that the universe is sufficiently contaminated by strange nuggets (whose abundance is discussed in the next section) that the second process will always preempt the first [371, 467].

12.5 Simultaneous Existence of Strange and Neutron Stars

Neutron stars and strange stars are distinct and separate families of stars as illustrated in Fig. 3.6. In theory, both could exist. However, our universe may be too old for this to be possible. As discussed in Section 12.2.5, the Galaxy will be contaminated by strange nuggets from the collision of strange stars with another compact object, most likely a close binary. The nuggets are inert because of their positive electric charge except in a neutron-rich environment. Because by hypothesis, strange matter is the lowest energy state, neutrons will be absorbed by nuggets they come into contact with and add to the strange matter of the nugget. Even from collisions of strange stars within our own Galaxy, the flux of nuggets is likely to have contaminated every star so that the seed of conversion of a neutron star to a strange star is present even before its birth [371]. Moreover, Caldwell and Friedman estimate that the flux of nuggets from the nearby Virgo cluster of some 2000 galaxies is so large that the material of the clouds of rarefied gas that collapse to form stars, already contain strange nuggets even before a star is born. If these considerations are correct, then all neutron stars are in fact strange stars. As we have seen, both types of stars are of about the same mass. We have no radius measurements by which they might be distinguished. The main difficulty with the hypothesis that all neutron stars will have been converted to strange stars is that some pulsars are observed to glitch. It has been argued that this fact rules out the existence of strange stars because the glitch phenomenon requires a solid region within which stresses can be built [450]. However, a counter argument has been made [197] which we consider after we study strange stars with nuclear crusts in the following sections.

12.6 Strange Stars to Strange Dwarfs

12.6.1 Strange stars with nuclear crusts

A strange star has a sharp edge of thickness defined by the range of the strong interaction (cf. Fig. 8.2). Such "bare" strange stars were discussed in Chapter 8. However, strange stars can also carry a crust of nuclear material which is suspended from contact with the strange star by a strong electric dipole field. This was noted by Alcock, Farhi, and Olinto [379] who pointed out that the electrons (which neutralize the positive charge of strange quark matter and are bound to it

by the Coulomb attraction) extend several hundred fermis beyond the edge.[8] In consequence, just inside the surface, there is a positively charged layer (because strange matter by itself is slightly positively charged[9]). Together with the electrons that extend outside the sharp surface of the strange matter, a dipole layer of high voltage is created. The surface dipole layer supports ordinary matter (which it polarizes) out of contact with the core.

The gap between the core and its crust of heavy ions is estimated to be of the order of several hundred fermis [379]. Effects of finite temperature have been investigated in Ref. [198]. The maximum density of the nuclear "crust" is strictly limited by the neutron drip density ϵ_{drip} above which free neutrons would gravitate to the strange core and be converted to quark matter. It is also possible that the the limiting crust density is somewhat smaller [468]. Strange stars most likely do have crusts of various inner crust densities depending on their histories and ages. Interstellar space is not empty. Moreover, it is quite possible, as discussed in the preceding section, that strange stars are produced directly in supernova, in which case, the inevitable fallback of some material from the exploding star will add crustal material.

The above situation—an inner, high-density medium and an outer low-density one separated by a vacuum—is different than ordinarily encountered in stellar structure. However, because the gap between core and crust is negligible on the scale of the size of the star, the situation can be simulated by an effective equation of state [197].

The effective equation of state should consist of two parts: (1) The nuclear crust should be represented by a low-density equation of state of charge-neutral nuclear matter such as forms the crust of neutron stars (Section 5.3.8). The most significant aspect of this density domain is that it consists of a Coulomb lattice of heavy ions immersed in an electron gas. The heavy ions become ever more neutron rich as the neutron drip density is approached from below. The equation of state at subnuclear density down to very low density has been calculated by Baym, Pethick, and Sutherland (BPS) [80]. We use the BPS equation of state to describe the crust having a density at its inner edge at a value below or equal to the neutron drip,

$$\epsilon_{\text{crust}} \leq \epsilon_{\text{drip}} \approx 4 \times 10^{11}\ \text{g/cm}^3 . \tag{12.4}$$

(2) At pressures above that corresponding to ϵ_{crust}, the equation of state corresponds to strange quark matter. We use the simplest form of the bag model equation of state for strange matter because, as far as the relationship of energy density and pressure is concerned, it is accurate to within 4% of the more complicated form involving quark masses [379]. The simplest form is $P = (\epsilon - 4B)/3$.

---

[8]Because electrons are not subject to the strong interaction, their distribution can extend beyond the sharp edge of the quark distribution over a region of the order of the de Broglie wave length.

[9]Because of the strange quark mass, slightly less than 1/3 of the quarks in strange matter are strange.

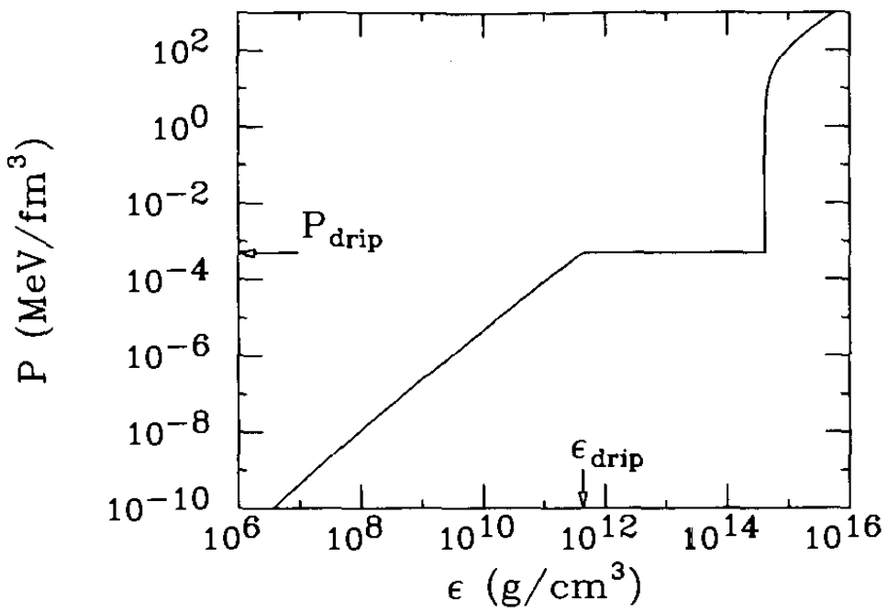

FIGURE 12.5. Equation of state of a strange star surrounded by a nuclear crust with inner density below neutron drip. The symbols P_{drip} and ϵ_{drip} refer to drip pressure and drip energy density. The quark matter equation of state is calculated for $B^{1/4}$=145 MeV. (From Ref. [197].)

The edge of stars occurs at $P = 0$, and, if a strange star is bare, the corresponding energy density is $\epsilon = 4B$. In the presence of a crust, the quark core will be slightly compressed by the weight of the crust, and the pressure at the edge of the core will be small but positive and equal to the pressure of the crustal material at the density ϵ_{crust}. Correspondingly, the energy density at the edge of the core will be slightly larger than $4B$. The equation of state is illustrated in Fig. 12.5 for the case that $P_{crust} = P_{drip}$. For other inner crust densities the equation of state is represented by

$$P(\epsilon) = \begin{cases} P_{BPS}(\epsilon), & \text{if } P < P_{crust}, \\ \frac{1}{3}(\epsilon - 4B), & \text{if } P \geq P_{crust}. \end{cases} \tag{12.5}$$

We adopt a value for the bag constant for which 3-flavor charge neutral strange matter is stable, $B^{1/4}$=145 MeV and 2-flavor quark matter is barely unstable. This value will serve to illustrate the general features of a nuclear crust on strange stars. For massless strange quarks, this bag constant corresponds to an equilibrium energy per baryon number of about 830 MeV. For strange quarks of 150 MeV mass, it corresponds to about 880 MeV per baryon number [381]. In other words, this choice represents strongly bound ($\geq$ 50 MeV/nucleon) strange matter that is absolutely stable with respect to ^{56}Fe by a large margin. Results for more weakly bound but stable strange quark matter can be found in Ref. [197].

Normally, there is one unique sequence of stars for a given equation of state, the mass increasing as the central density is increased—a single-parameter family. However, the density of the crust ϵ_{crust} (which is arbitrary save that it cannot exceed the drip density) constitutes a second parameter corresponding to the discontinuity in density at the surface of the strange core. The value of the crust density is

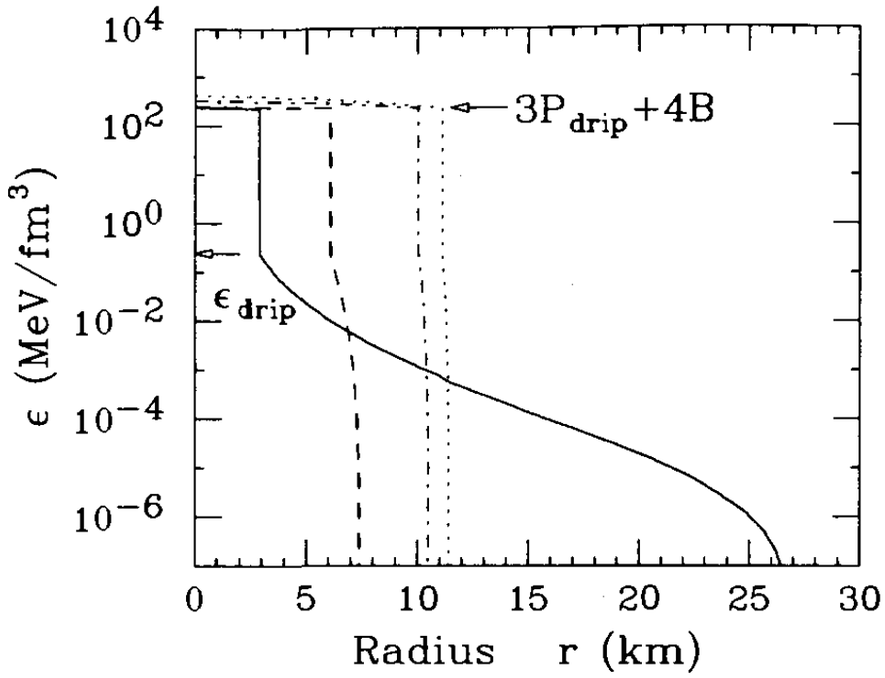

FIGURE 12.6. Strange stars with nuclear crusts at the drip density: energy density as a function of radial distance from the star's center for gravitational masses $M/M_\odot$=0.020 (solid line), 0.20 (dashed), 1.00 (dash-dotted), and 1.50 (dotted). The bag constant $B^{1/4}$ = 145 MeV. (From Ref. [197].)

arbitrary. In any particular case the crust depends on the particular circumstances under which the bare strange star acquired its crust.

Thus, strange stars with nuclear crusts form a two-parameter sequence corresponding to the central density and the inner crust density. In practice we fix the inner density of the crust and vary the central density to generate a corresponding sequence. For a particular equation of state of core and crust material, each pair of such parameters defines a unique stellar structure with a particular mass and radius.

Pressure in a star is a continuous and monotonically decreasing function of the Schwarzschild radial coordinate. However, there is a discontinuity in energy density between strange quark matter and hadronic matter at the pressure corresponding to the inner crust density. This is so because the density of quark matter is much higher than nuclear matter at a common pressure. The energy discontinuity is (Fig. 12.5)

$$\Delta\epsilon \equiv (3P_{\rm crust} + 4B) - \epsilon_{\rm crust} \ . \tag{12.6}$$

The energy density of the star will suffer this discontinuity (across the several hundred fermi gap described above) at the radius where the pressure equals $P_{\rm crust}$. The energy density and pressure profiles of several nonrotating sample stars are shown in Figs. 12.6 and 12.7 for gravitational masses in the range of $0.020 \leq M/M_\odot \leq 1.50$. The ends of this range correspond, respectively, to a light star close to the lower mass limit and one closer to the upper mass limit. The sharp fall in the energy profile marks the boundary between the quark core and the nuclear crust.

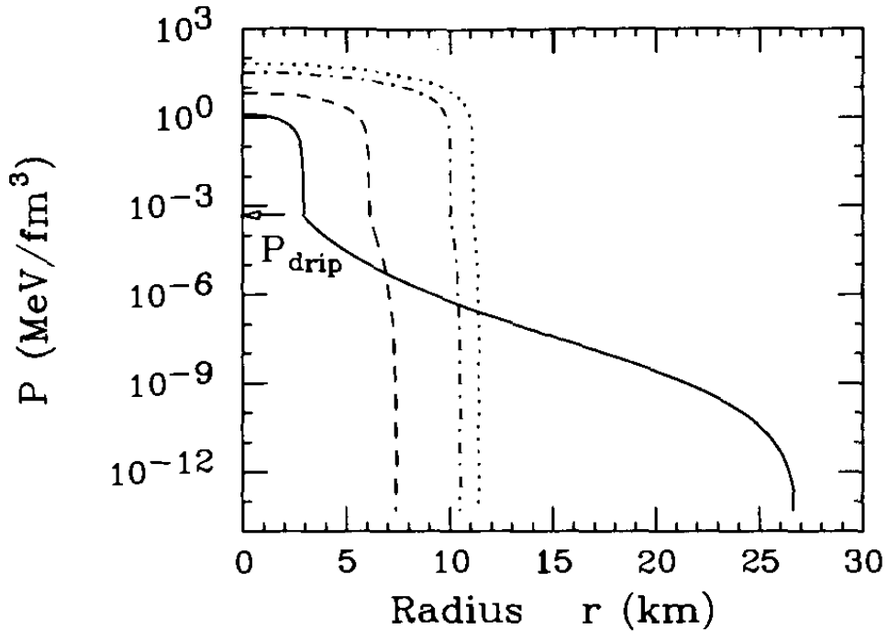

FIGURE 12.7. Pressure as a function of radial distance from the star's center for different gravitational masses (the labeling is the same as in Fig. 12.6). The bag constant $B^{1/4} = 145$ MeV. (From Ref. [197].)

If strange matter is the absolute ground state, stable objects of strange matter from microscopic nuggets to stars could exist. The nuclear crust, suspended out of contact with the core by the electric dipole layer, is attached to the star by the gravitational interaction. For a given inner density of the crust, the maximum of which is the drip density, the crust will be thinner the more massive the strange quark core.

The above behavior of the crust thickness can be understood as a consequence of the way the core radius scales with mass. For masses too small for gravity to play an important role, the relationship is $M = (4\pi/3)R^3\epsilon_0$ where $\epsilon_0 = 4B$ is the equilibrium density of strange matter in the bag model. This relationship is only somewhat modified near the most massive star in the sequence which gravity terminates. Because $R \propto M^{1/3}$, the (Newtonian) gravitational force acting on a unit mass at the surface of the core is $M/R^2 \propto M^{1/3}$. When the inner crust density is the neutron drip density, we find a minimum mass star of $\sim 0.015 M_\odot$, to be compared to $0.1 M_\odot$ for neutron stars [80]. Thus, the thickening of the crust illustrated in Fig. 12.6 for the $M/M_\odot = 0.02$ case (which is close to the lower mass limit for an inner crust density equal to the neutron drip density) illustrates profiles very close to the lower end point of stable strange stars with nuclear crusts of maximum density.

A comparison of these figures for different bag constants B can be facilitated by noting the scaling laws that apply to strange stars [93, 94]. For a central energy density that is some fixed multiple of B, the mass and radius of bare strange stars correspond to different assumptions about the bag constant scale as

$$M \propto 1/\sqrt{B}, \qquad R \propto 1/\sqrt{B}. \tag{12.7}$$

The maximum-mass strange star for a given B corresponds to a central density of $19.2B$.

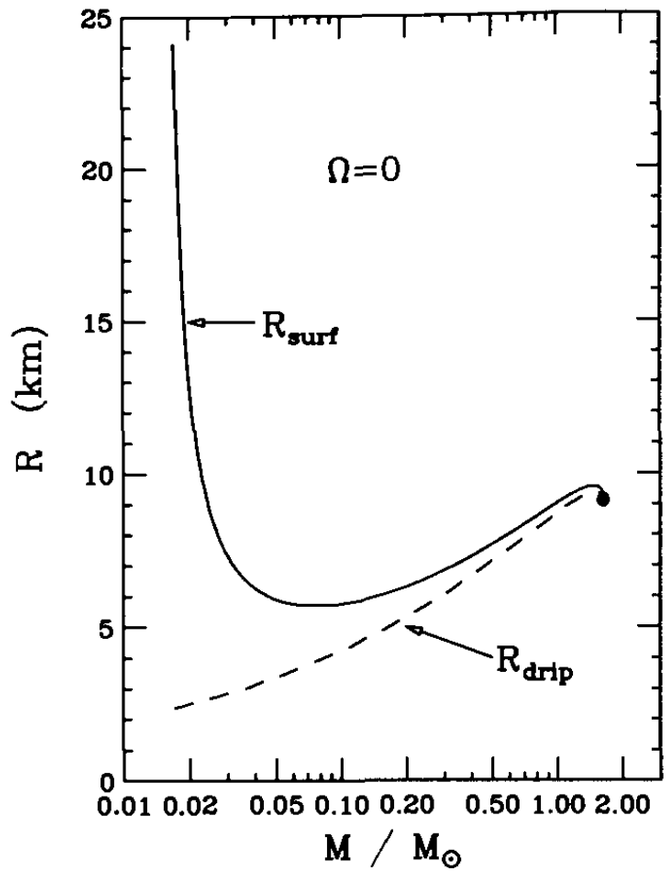

FIGURE 12.8. The radius of the strange core (dashed curve) and the radius of the star including nuclear crust (solid curve) as a function of stellar mass. (From Ref. [197].)

The mass–radius relationship for strange stars with a nuclear crust is shown in Fig. 12.8. Because the crust is bound by gravitational interaction, the relationship for *low-mass* stars is qualitatively similar to the one for neutron stars; the radius is largest for the lowest-mass stars. However, the gravitational attraction of more massive strange matter cores compresses the dilute nuclear material of the crust; the mass radius follows more closely that of strange stars. Indeed, the radius of the strange quark core is also shown, and it follows the inevitable behavior of objects that are self-bound, namely, the one mentioned above, $R \propto M^{1/3}$, which is only somewhat modified near the mass where gravity terminates the stable sequence. This behavior dominates the more massive of the strange stars with a crust because the crust becomes exceedingly thin (cf. Fig. 12.6).

12.6.2 Nuclear crust and pulsar glitches

The moment of inertia carried in the crust of a strange star is relevant to the question of whether strange stars are able to cause glitches in pulse timing as is observed in some pulsars. Figure 12.9 shows that the fraction of a strange star's moment of inertia that is carried in the crust varies between 10^{-3} for the lightest stars and $\sim 10^{-5}$ at the upper mass limit. This result differs by only a factor 2 to 3 depending on the bag constant. If the angular momentum of the pulsar is conserved in the quake, then the relative frequency change and moment of inertia change are equal,

$$\frac{\Delta\Omega}{\Omega} = \frac{|\Delta I|}{I_0} > \frac{|\Delta I|}{I} \equiv \frac{f I_{\rm crust}}{I} \sim (10^{-5} - 10^{-3}) f\,, \qquad (0 < f < 1) \quad (12.8)$$

where I_0 is the moment of inertia of that part of the star whose frequency is changed in the quake. It might be that of the crust only, or some fraction or all of the star, depending on how strongly the crust and core are coupled. The factor f in the above relation represents the fraction of the crustal moment of inertia that is altered in the quake, $|\Delta I| = f I_{\text{crust}}$. Because observed glitches have relative frequency changes $\Delta\Omega/\Omega$ of 10^{-9} to 10^{-6}, a change in the crustal moment of inertia by less than 1/10th would cause a giant glitch even in the least favorable case.

Of course that is not the whole story. There remains the questions of whether a sufficient build up of stress can occur and also of the recoupling of crust and core which involves the healing of the pulsar period. This is probably a very complicated process that does not simply involve the recoupling of two homogeneous substances.

The recoupling of crust and strange quark core is likely to have a long timescale, not unlike that expected for neutron stars (days to years). In addition, strange stars with crusts are likely to have a relatively short timescale coupling mechanism, namely, the abrasion of part of the inner surface of the crust by the core following a quake. Recall that the crust is suspended above the core by a few hundred fermis by the strong electric dipole layer on the core. If the relative change in the moment of inertia is attributed, for the sake of rough order of magnitude estimate, to a change in the radius of the crust, then the relation $\Delta I/I = 2\Delta R/R$ holds. For the above quoted range of relative frequency glitches, we have $\Delta R \sim (10^{-3} - 1)$ cm. So we expect a quake in the crust to cause the crust to momentarily come into physical contact with the core, a contact or bouncing that is unlikely to be symmetrical, and in any case that will transfer matter and therefore angular momentum to the core. However, this abrasion of parts of the inner surface of the crust will be a momentary perturbation. The abraded material will be dissolved into the quark core. Therefore, superimposed on the frequency change caused by the crust quake we suggest that there may be a smaller series of glitches associated with this transient mechanism.

The observation of pulsar glitches has been used as an argument against the strange matter hypothesis. The argument is twofold. One has to do with the assumption that strange quark stars have no internal structural differentiation that could give rise to pulsar glitches so that a *bare* strange star could not glitch. However, bare strange stars are not likely to exist, because the acquisition of a crust is likely to occur from birth in a supernova. Moreover, we simply do not know enough about quark matter to say for certain that quark matter is unable to support stresses.

The second argument is that even a strange star with a nuclear crust cannot glitch. This is based on assuming the near equality of I_{crust}/I and $\Delta\dot{\Omega}/\dot{\Omega}$ with the first ratio $\sim 10^{-5}$ by computation, and the second $\sim 10^{-3}$ to 10^{-2} by observation, yielding an apparent contradiction. However, using the same notation as in (12.8) we may write,

$$\frac{\Delta\dot{\Omega}}{\dot{\Omega}} \approx \frac{\Delta\dot{\Omega}/\dot{\Omega}}{\Delta\Omega/\Omega}\frac{|\Delta I|}{I_0} = \frac{\Delta\dot{\Omega}/\dot{\Omega}}{\Delta\Omega/\Omega}\frac{f I_{\text{crust}}}{I_0} > (10^{-1} \text{ to } 10) f\,. \tag{12.9}$$

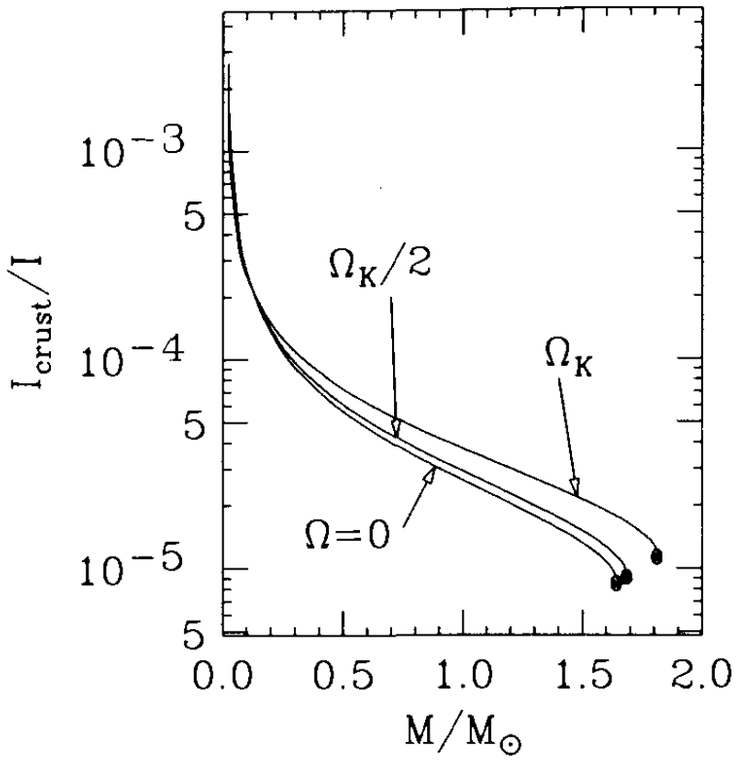

FIGURE 12.9. Fractional moment of inertia carried by the nuclear crust on a strange quark star rotating with various angular velocities. Assumed bag constant is $B^{1/4} = 160$ MeV. (Taken from Ref. [249].)

Let us use measured values of the ratio $(\Delta\Omega/\Omega)/(\Delta\dot{\Omega}/\dot{\Omega}) \sim 10^{-6}$ to 10^{-4} for the Crab and Vela pulsars, respectively. (See Ref. [202], tables on p. 118 and p. 193.) This yields a small f as before, $f < (10^{-4}$ to $10^{-1})$. So the observed range of the fractional change in $\dot{\Omega}$ *is* consistent with the crust having the small moment of inertia calculated and the quake involving only a small fraction, f, of that, just as in (12.8).

Nevertheless, without undertaking a study of whether the nuclear solid crust on strange stars could sustain a sufficient buildup of stress before cracking to account for such a sudden change in relative moment of inertia, or whether the healing time and intervals between glitches can be understood, we cannot say definitely that strange stars with a nuclear solid crust can account for any complete set of glitch observations for a particular pulsar. In any case, we should keep in mind that the problem of quakes or rotational timing glitches on compact stars, *whether* neutron stars or strange stars, does not appear to be simpler in nature than the prediction of earthquakes, a science with a notable dearth of successes!

12.6.3 Strange dwarfs with nuclear crusts

Strange stars—the counterparts of neutron stars—with central densities above nuclear saturation density, have been discussed extensively in Chapter 8 and in the literature [382]. Here we want to trace the connection between strange stars and strange dwarfs—stars falling in the mass and radius range of white dwarfs, but having a core of strange quark matter. We find a possible new class of very dense white dwarfs whose stability is established solely by a strange quark core [88, 199].

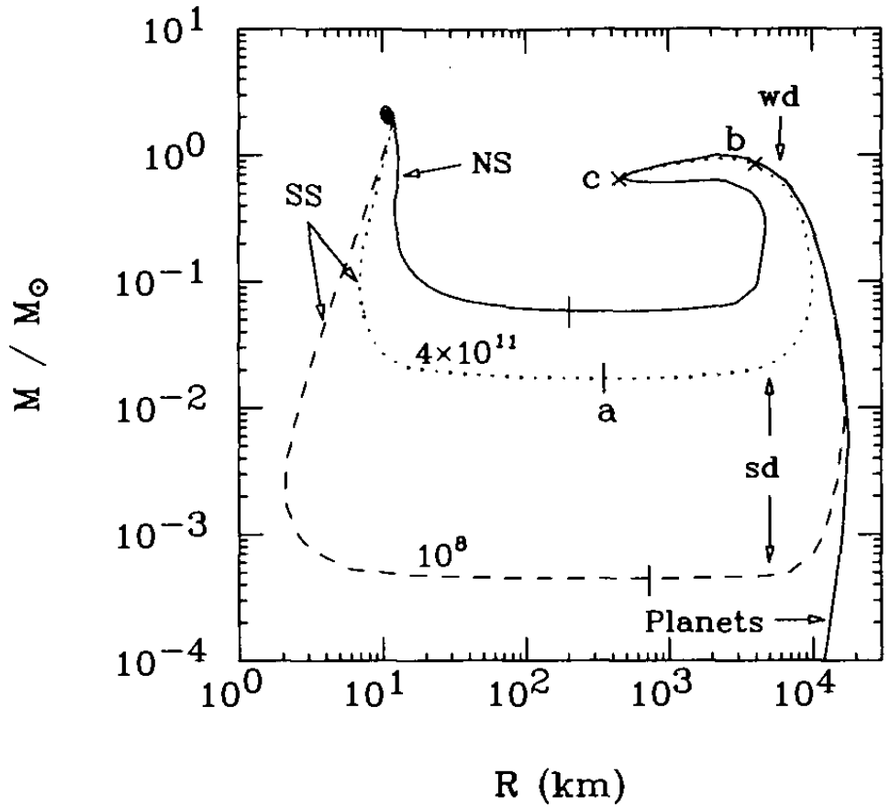

FIGURE 12.10. Neutron star (NS)–white dwarf (wd) sequence (solid line). Two strange star (SS)–strange dwarf (sd) sequences, for which the inner crust density of nuclear material has the indicated values (in gm/cm^3). The higher value is the drip density. Vertical bars mark minimum-mass stars. Crosses mark termination of the strange star sequences where the strange core shrinks to zero. At those points, strange dwarfs become identical to ordinary white dwarfs. (From Ref. [199])

The mass–radius relationship for a sequence extending from ordinary neutron stars to ordinary white dwarfs and then to planets is shown in Fig. 12.10. The stable neutron stars are the configurations extending from the maximum-mass neutron star (marked by a bullet) to the minimum-mass neutron star (marked by a vertical line). The stable white dwarf configurations extend from the maximum-mass dwarf (marked by "b") toward stars of larger radius.

By comparison, two out of a continuum of strange star sequences extending from strange stars to strange dwarfs are shown. In the one case the inner crust density is equal to the neutron drip density and, in the other, a much smaller density.

The minimum-mass star on any strange-star sequence (marked by a vertical line in Fig. 12.10) divides the sequence into two segments. One segment consists of *strange stars* whose more massive members are analogous in mass and size to neutron stars; the other consists of *strange dwarfs*. The strange stars illustrated consist primarily of a strange quark core surrounded by a thin nuclear crust of up to a few kilometers. The strange dwarfs consist of a small strange-matter core of very high density compared to an ordinary dwarf, and an envelope of nuclei arrayed in a Coulomb lattice region that is up to a few thousand kilometers thick.

Of course, the central density (and therefore the *radius* of the strange core) decreases along members of a sequence from the maximum mass strange star toward the dwarfs. In the limit that the radius of the strange core has shrunk to

zero, the star is identical to a white dwarf, and therefore the strange sequence terminates at a point on the white dwarf sequence.

The maximum central density of white dwarfs is $\epsilon_{wd} \approx 10^9$ gm/cm^3. White dwarfs with central densities up to this value that envelop a strange quark core are of no particular interest. They would not be distinguishable from any other white dwarf. They would lie on sequences whose inner crust density falls at or below the maximum density of ordinary white dwarfs such as the sequence labeled by the crust density of 10^8 g/cm^3 in Fig. 12.10.

However, aside from the trivial configurations mentioned above, there are also highly novel ones [199]. There are acoustically and hydrostatically stable strange dwarfs having crustal densities of nuclear material higher in density by orders of magnitude than is possible for the central densities of ordinary white dwarfs. These stable sequences can have nuclear material with densities as high as the neutron drip density—a few hundred times larger than would be found in the maximum-mass white dwarf and 4×10^4 times larger than in a typical $M = 0.6M_\odot$ white dwarf. The stable sequences include and lie below the one marked 4×10^{11} and above the one marked 10^8 in Fig. 12.10. These stellar sequences terminate on the *unstable* sequence between white dwarfs and neutron stars. Such stars owe their stability solely to the quark core. Their stability is proved in the next section and some of their characteristics in the following.

12.6.4 Stability

We discussed the normal modes of vibration of a neutron star in Section 3.18.2. Employing the solution of the Oppenheimer–Volkoff equations we have computed the frequencies of the vibrations for sequences of strange stars (exhibited in Fig. 12.10) having an inner crust density equal to the drip density [88, 199]. For the central density range relevant to the strange dwarfs, a convenient function of the vibrational frequencies is shown in Fig. 12.11. Point 'a' corresponds to the minimum-mass star and 'b' to the maximum-mass strange dwarf of the sequence with crust equal to the drip density. It will be noticed that, at the minimum mass (point 'a'), the squared frequency of the fundamental mode becomes zero, but does not change sign. So the strange star configurations to the left of 'a' and the strange dwarf configurations to the right are all stable. However, at 'b', the squared frequency of the fundamental mode does change sign. Configurations to the right of 'b' are stable and those to the left unstable.

A similar result holds for all other strange sequences with values of inner crust density lower than the drip density. The entire portion of the sequences of strange stars to strange dwarfs with crusts between the maximum-mass star of each class is stable. This is an interesting contrast with ordinary neutron stars and white dwarfs shown by the solid line of Fig. 12.10. In this case all stars in the sequence from the minimum mass neutron star to the maximum mass white dwarf are unstable. The stable part of the branch of white dwarfs are those that extend from the maximum mass toward the region labeled "planets"—namely, the dwarfs with larger radii

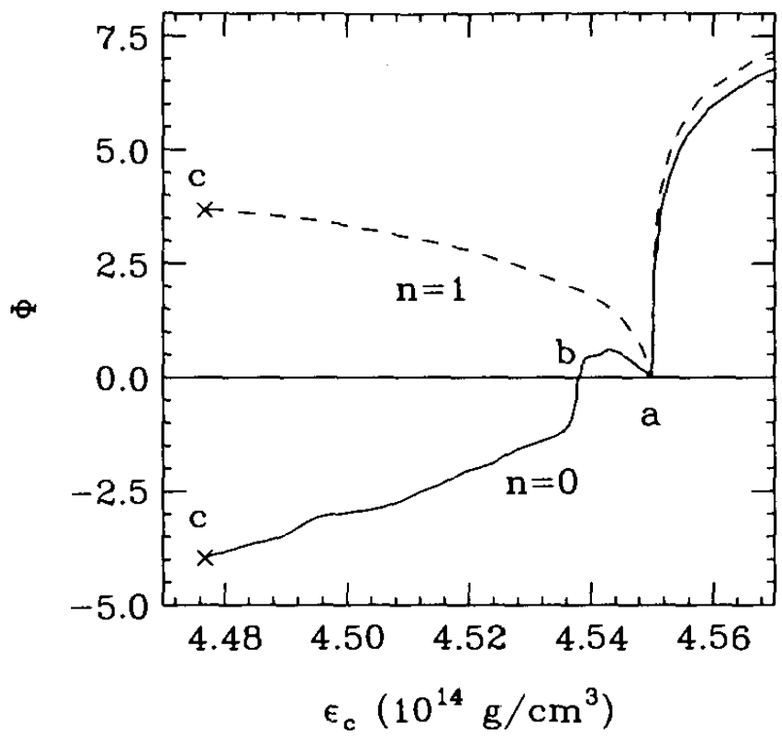

FIGURE 12.11. Pulsation frequencies for $n = 0, 1$ measured by $\Phi(x) \equiv \mathrm{sgn}(x)\,\log(1+|x|)$ where $x \equiv (\omega_n/\mathrm{s}^{-1})^2$ as a function of central star density in the vicinity of strange dwarfs having inner crust density equal to neutron drip. For $\Phi < 0$, the squared frequency is negative and the mode unstable. (From Ref. [199].)

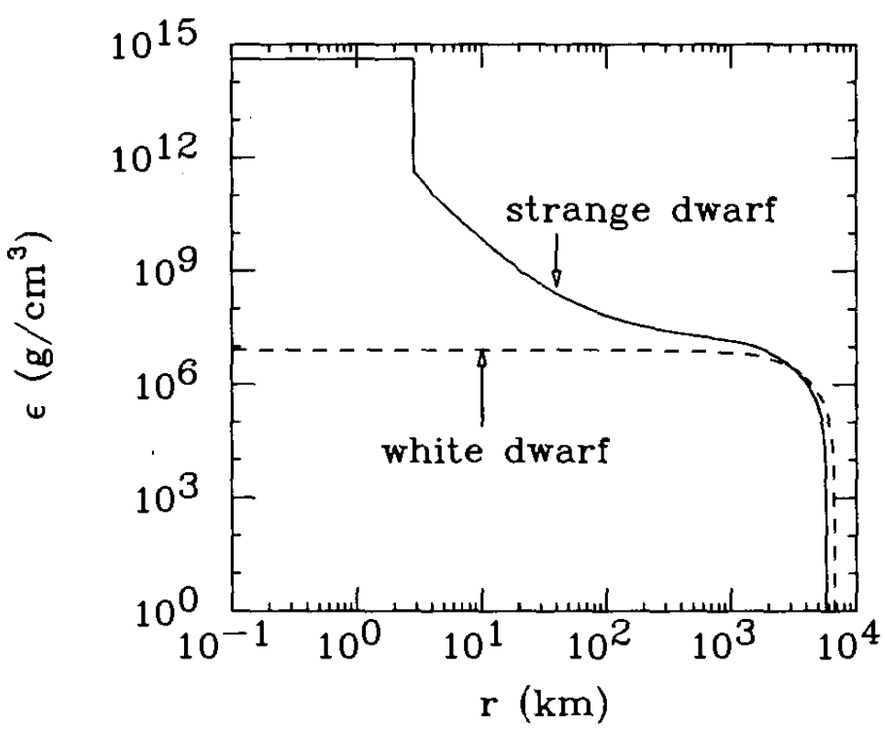

FIGURE 12.12. Mass–energy profile of a strange dwarf and a white dwarf of the same mass $0.6M_\odot$. The quark core of the strange dwarf is the structure within 3 km. Outside is nuclear material of inner density equal to the neutron drip density. (From Ref. [199].)

than that possessed by the one at the maximum mass. The unstable region spans about five orders in magnitude of central density.

12.6.5 Possible new class of dense white dwarfs

As just proved, stellar configurations with inner crust densities in the range from the neutron drip density down to the central density of the limiting-mass white dwarf,

$$4 \times 10^{11}\ \mathrm{g/cm^3} \approx \epsilon_{\mathrm{drip}} > \epsilon_{\mathrm{crust}} > \epsilon_{\mathrm{wd}} \approx 10^9\ \mathrm{g/cm^3}\,, \qquad (12.10)$$

are stabilized by the presence of the strange core. Without the strange quark matter core, these stars would have central densities that correspond to the unstable sequence of configurations that lie between the stable white dwarfs and neutron stars. We call these stars *strange dwarfs* and distinguish them from the trivial configurations consisting of a strange core and a white dwarf envelope $\epsilon_{\mathrm{crust}} < \epsilon_{\mathrm{wd}}$ which would be stable with or without the core [199].

The masses of the strange dwarfs range from values of about $10^{-4} M_\odot$ to about a solar mass—interesting candidates for gravitational microlensing searches. The lower limit can be compared to $\sim \frac{1}{10} M_\odot$ for a neutron star. They have strange cores of only several kilometers in radius and a baryon number in the range $1.5 \times 10^{54} < A < 2.5 \times 10^{55}$, compared to $A \sim 1.5 \times 10^{57}$ for a neutron star or white dwarf. The mass-energy profile of a strange dwarf is compared to a white dwarf profile in Fig. 12.12. In both cases they correspond to stable stars of a mass $0.6 M_\odot$ (typical of observed white dwarfs). In the case of the strange dwarf, the inner crust density is chosen to have its maximum possible value, the drip density. The inner density of nuclear material can be enormous—up to a few hundred times the maximum density possible in ordinary white dwarfs and about 4×10^4 times larger than the central density in the prevalent mass ($\sim 0.6 M_\odot$) of white dwarfs.

We will say a few words about ways in which the objects described here might be formed. There may be others which we have not imagined, and the history of astronomical discovery cautions us that the laws of nature are explored by the universe in many unanticipated ways. The capture of strange nuggets by main-sequence stars is probably an inevitable consequence if Witten's hypothesis is correct [469, 470]. The Galaxy would be filled with a flux of strange nuggets (Section 12.2.5) which would contaminate every object with which they come in contact—planets, neutron stars, white dwarfs, main-sequence stars, and so on. Main-sequence stars are ideal large-surface, long-integration-time detectors for the strange-matter flux because of their large size [469, 470]. In contrast to neutron stars and ordinary white dwarfs (whose material is characterized by a large structural constant so that the nuggets never reach their cores), nuggets accreted onto main-sequence stars can indeed gravitate to their centers, accumulate, and form a strange-matter core that grows with time until the star's demise as a main-sequence star. Those whose mass lies in the approximate mass range (~ 1 to $5 M_\odot$) would then give birth to a strange dwarf.

There are other possible modes of formation of dense strange dwarfs. As discussed in the literature, primordial bodies of mass between $\frac{1}{100}$ and $1\ M_\odot$ may be formed in the early universe and may survive to the present epoch [461]. Such objects will occasionally be captured by a main-sequence star and form a signifi-

cant core in a single and singular event. Finally, we mention that, in the very early evolution of the universe, lumps of hot, strange quark matter evaporated nucleons which are plausibly gravitationally bound to the lump. The evaporation continues until the quark matter has cooled sufficiently. Depending on the original baryon number of the quark lump, a strange star or a dwarf—both with nuclear crust, is formed.

12.7 Conclusion

The strange matter hypothesis is compatible with our knowledge of laboratory physics and with all that is known of the universe. It constitutes the most startling possibility conceived for the nature of dense matter. If it is true, all the visible matter of the universe is in a long-lived but metastable state—not the ground state of hadronic matter. The hypothesis has broad implications of great importance for cosmology, the early universe, its evolution, for compact stars, and for laboratory physics of high-energy nuclear collisions. Present searches of evidence for the truth of the hypotheses take place in several arenas. There are cosmic ray searches for strange nuggets having an anomalous charge-to-mass ratio [471, 472], there are laboratory searches for low-mass nuggets, possibly only metastable, that may be produced in the collisions of high-energy nuclei [473], and searches for sub-millisecond pulsars as signals of strange stars. (See D'Amico and L. Burderi in Ref. [205]).

Useful Astronomical Data

1. Distance: 1 ly (light year) = 9.4605×10^{12} km
2. Distance: 1 pc (parsec) = 3.2615 ly (light year) = 3.0856×10^{13} km
3. Solar mass: $M_\odot = 1.989 \times 10^{33}$ g = 1.477 km
4. Solar radius: $R_\odot = 6.9598 \times 10^5$ km
5. Solar luminosity: $L_\odot = 4 \times 10^{33}$ erg/s
6. Astronomical unit (au) = Sun–Earth distance = 1.4960×10^8 km
7. Siderial year: 1 yr = 3.1558×10^7 s
8. Milky Way galaxy mass: $4 - 10 \times 10^{11} M_\odot$
9. Milky Way galaxy disk radius (luminous matter): $\sim$ 15 kpc
10. Sun–galactic center distance: 10 kpc
11. Universe age: $> 1.8 \times 10^{10}$ yrs
12. Milky Way galaxy age (oldest disk stars): $\sim 10^{10}$ yrs
13. Earth age: 5×10^9 yrs
14. Time since extinction of dinosaurs: 7×10^7 yrs
15. Lifetime of 10 $M_\odot$ stars: 10^7 yrs

Some useful general references to astrophysical data and phenomena:

Encyclopedia of Astronomy and Astrophysics, R. A. Meyers, ed. Academic Press, San Diego, 1989.

The Astronomy and Astrophysics Encyclopedia, S. T. Maran, ed. Van Nostrand Reinhold, New York, 1992.

Astrophysical Data in two volumes, K. R. Lang, *Planets and Stars* and *Galaxies and the Universe*. Springer-Verlag, New York, 1991.

Books for Further Study

On Relativity:

B. K. Harrison, K. S. Thorne, M. Wakano and J. A. Wheeler, *Gravitation Theory and Gravitational Collapse* (University of Chicago Press, Chicago, 1965).

Ya. B. Zel'dovich and I. D. Novikov, *Relativisitc Astrophysics, Vol. 1, Stars and Relativity* (University of Chicago Press, Chicago, 1971).

S. Weinberg, *Gravitation and Cosmology* (John Wiley & Sons, New York, 1972).

C. W. Misner, K. S. Thorne and J. A. Wheeler, *Gravitation* (W. H. Freeman, San Francisco, 1973).

P. A. M. Dirac, *General Theory of Relativity* (John Wiley & Sons, New York, 1975).

M. Berry, *Principles of Cosmology and Gravitation* (Adam Hilgar, Bristol and Phiadelphia, 1989).

On Theory of Compact Stars:

S. L. Shapiro and S. A. Teukolsky, *Black Holes, White Dwarfs, and Neutron Stars* (John Wiley & Sons, New York, 1983).

On Observations on Compact Stars:

R. N. Manchester and J. H. Taylor, *Pulsars* (W. H. Freeman, San Francisco, 1977).

A. G. Lyne and F. Graham-Smith, *Pulsar Astronomy* (Cambridge University Press, Cambridge, 1990).

R. D. Blandford, A. Hewish, A. G. Lyne and L. Mestel, *Pulsars as Physics Laboratories* (Oxford University Press, Oxford, 1993).

References

[1] W. Baade and F. Zwicky, Phys. Rev. **45** (1934) 138.

[2] A. Einstein, Ann. Phys., **49** (1916) 769.

[3] A. Einstein, *The Meaning of Relativity*, 5th ed. (Methuen and Co., London, 1951). A lecture series at Princeton University, 1921, with several revisions in later editions.

[4] J. H. Taylor, A. Wolszczan, T. Damour and J. M. Weisberg, Nature **355** (1992) 132.

[5] C. M. Will, *Was Einstein Right?* (Oxford University Press, Oxford 1995).

[6] H. Minkowski, Ann. Phys. (Leipzig) **47** (1915) 927.

[7] J. D. Bjorken and S. D. Drell, *Relativistic Quantum Fields* (McGraw–Hill, New York, 1965).

[8] A. A. Michelson and E. W. Morley, Am. J. Sci. **34** (1887) 333.

[9] W. Voigt, Goett. Nachr. (1887) 41.

[10] W. J. Swiatecki, Phys. Scripta **28** (1983) 349.

[11] R. v. Eötvös, Math. Nat. Ber. Ungarn **8** (1890) 65.

[12] K. Nordvedt, Phys. Rev. **169** (1968) 1017; op. cit. **180** (1969) 1293; Phys. Rev. D **3** (1971) 1683.

[13] A. Einstein, unpublished manuscript in the Pierpont Morgan Library, New York (1920).

[14] R. V. Pound and G. A. Rebka, Phys. Rev. Lett. **4** (1960) 337.

[15] A. Schild, Texas Quarterly **3** (1960) 42.

[16] A. Schild, in *Evidence for Gravitational Theories*, ed. by C. Möller, (Academic Press, New York, 1962).

[17] A. Schild, in *Relativity Theory and Astrophysics* ed. by J. Ehlers (American Mathematical Society, Providence, R. I., 1967).

[18] J. Ishiwara, *Einstein Koēn-Roku* (Tokyo-Tosho, Tokyo, 1916). Record of Einstein's Kyoto lecture. The incident referred to is inferred by A. Pais to have occurred in November 1907.

[19] S. Weinberg, *Gravitation and Cosmology* (John Wiley & Sons, New York, 1972).

[20] M. Berry, *Principles of Cosmology and Gravitation* (Adam Hilgar, Bristol, 1989; 1st ed. 1976).
[21] A. Einstein and W. de Sitter, Proc. Nat. Acad. Sci. **18** (1932) 213.
[22] C. W. Misner, K. S. Thorne and J. A. Wheeler, *Gravitation* (Freeman & Co., San Francisco, 1973).
[23] J. R. Oppenheimer and H. Snyder, Phys. Rev. **56** (1939) 455.
[24] M. A. Abramowicz and A. R. Prasanna, Mon. Not. R. Astron. Soc. **245** (1990) 720.
[25] M. D. Kruskal, Phys. Rev. **119** (1960) 1743.
[26] G. Szerkeres, Publ. Mat. Debrecen. **7** (1960) 285.
[27] J. B. Hartle in *Relativity, Astrophysics and Cosmology*, ed. by W. Israel (D. Riedel, Dordrecht, Holland, 1973).
[28] B. K. Harrison, K. S. Thorne, M. Wakano and J. A. Wheeler, *Gravitation Theory and Gravitational Collapse*, (University of Chicago Press, 1965).
[29] T. D. Lee, Phys. Rev. D **35** (1987) 3637; R. Friedberg, T. D. Lee and Y. Pang, Phys. Rev. D **35** (1987) 3640; ibid. 3658; T. D. Lee and Y. Pang, Phys. Rev. D **35** (1987) 3678.
[30] N. K. Glendenning, T. Kodama and F. R. Klinkhamer, Phys. Rev. D **38** (1988) 3226.
[31] A. S. Eddington, Observatory **30** (1920) 353.
[32] E. M. Burbidge, G. R. Burbidge, W. A. Fowler and F. Hoyle, Rev. Mod. Phys. **29** (1957) 547.
[33] S. A. Colgate and R. W. White, Astrophys. J. **143** (1966) 626.
[34] S. Bludman, D. H. Feng, T. Gaisser and S. Pittel, eds. *The Physics of Supernovae*, Phys. Rep. **256** (1995) 1.
[35] A. Burrows and J. M. Lattimer, Astrophys. J. **307** (1986) 178.
[36] V. M. Kaspi, R. N. Manchester, S. Johnson, A. G. Lyne and N. D'Amico, Astron. J. **111** (1996) 2028.
[37] V. M. Kaspi, M. Bailes, R, N, Manchester, B. W. Stappers, J. S. Sandhu, J. Navarro and N. D'Amico, Astrophys. J. **485** (1997) 820.
[38] V. M. Kaspi, in *Neutron Stars and Pulsars*, ed. by N. Shibazaki, N. Kawai, S. Shibata, and T. Kifune (Universal Academy Press, Tokyo, 1998).
[39] V. M. Kaspi, Adv. Space Res. **21** (1998) 167.
[40] S. E. Thorsett and D. Chakrabarty, Astrophys. J. **512** (1999) 288.
[41] N. K. Glendenning, Phys. Lett. **114B** (1982) 392; Astrophys. J. **293** (1985) 470; Z. Phys. A **326** (1987) 57; Z. Phys. A **327** (1987) 295.
[42] W. Keil and H. T. Janka, Astron. Astrophys. **296** (1995) 145.
[43] N. K. Glendenning, Astrophys. J. **448** (1995) 797.
[44] M. Prakash, J. R. Cooke and J. M. Lattimer, Phys. Rev. D **52** (1995) 661.
[45] I. Bombaci, Astron. Astrophys. **305** (1996) 871.
[46] M. Prakash, I. Bombaci, M. Prakash, P. J. Ellis, J. M. Lattimer and R. Knorren, Phys. Rep., **280** (1997) 1.
[47] J. R. Ipser, Astrophys. J. **158** (1969) 17.
[48] D. N. Schramm and R. V. Wagoner, Ann. Rev. Nucl. Part. Sci. **27** (1979) 37.
[49] S. M. Austin, Prog. Part. Nucl. Phys. **7** (1981) 1.
[50] D. Arnett, *Supernovae and Nucleosynthesis* (Princeton University Press, 1996).
[51] W. D. Myers and W. J. Swiatecki, Nucl. Phys. **A601** (1996) 141.
[52] R. A. Hulse and J. H. Taylor, Astrophys. J. (Letters) **191** (1974) L 59; op. cit., **195** (1975) L 51; **201** (1975) L 55.
[53] J. H. Taylor and J. M. Weisberg, Astrophys. J. **345** (1989) 434.
[54] J. M. Weisberg and J. H. Taylor, Phys. Rev. Lett. **52** (1984) 1348.

[55] T. Kodama, Prog. Theor. Phys. **47** (1972) 444.
[56] Ya. B. Zel'dovich and I. D. Novikov, *Relativistic Astrophysics, Vol. I, Stars and Relativity* (University of Chicago Press, 1971).
[57] A. Einstein, Ann. Phys., **35** (1911) 898.
[58] A. S. Eddington, Observatory **58** (1935) 37.
[59] S. Chandrasekhar, from the Eddington Centenary Lectures, 1982, reprinted in *Truth and Beauty* (University of Chicago Press, 1987) Ch. 6.
[60] K. R. Lang, *Astrophysical Data, Planets and Stars* (Springer-Verlag, New York, 1992).
[61] E. E. Salpeter and H. M. Van Horn, Astrophys. J. **155** (1969) 183.
[62] S. L. Shapiro and S. A. Teukolsky, *Black Holes, White Dwarfs, and Neutron Stars* (John Wiley & Sons, New York, 1983).
[63] L. I. Schiff, *Quantum Mechanics* (McGraw Hill Book Co., 1949).
[64] I. S. Gradshteyn and I. M. Ryzhik, *Tables of Integrals, Series and Products* (Academic Press, New York, 1965).
[65] P. M. Morse and H. Feshbach, *Methods of Theoretical Physics*, (McGraw-Hill, New York, 1953).
[66] L. D. Landau and E. M. Lifshitz, *Statistical Physics* (Addison–Wesley, Reading, Mass., 1969) Chapter VIII.
[67] N. K. Glendenning, Phys. Lett. **114B** (1982) 392.
[68] N. K. Glendenning, Astrophys. J. **293** (1985) 470.
[69] R. H. Fowler, Mon. Not. R. Astron. Soc. **87** (1926) 114.
[70] S. Chandrasekhar, Astrophys. J. **74** (1931) 81.
[71] S. Chandrasekhar, Mon. Not. R. Astron. Soc. **95** (1935) 207.
[72] Rev. John Michell, Phil. Trans. R. Soc. (London) **74** (1784) 35–57.
[73] L. D. Landau, Phys. Z. Sowjetunion **1** (1932) 285.
[74] S. Chandrasekhar, Phys. Rev. Lett. **12** (1964) 114; op. cit. p. 437.
[75] E. Schatzman, Astron. Zhur. **33** (1956) 800.
[76] B. K. Harrison and J. A. Wheeler, cited in B. K. Harrison et al., *Gravitation Theory and Gravitational Collapse* (University of Chicago Press, 1965).
[77] S. Chandrasekhar and R. F. Tooper, Astrophys. J. **139** (1964) 1396.
[78] J. R. Oppenheimer and G. M. Volkoff, Phys. Rev. **55** (1939) 374.
[79] T. Hamada and E. E. Salpeter, Astrophys. J. **134** (1961) 683.
[80] G. Baym, C. Pethick and P. Sutherland, Astrophys. J. **170** (1971) 299.
[81] V. Weidemann, Annu. Rev. Astron. Astrophys. **28** (1990) 103.
[82] P. J. Siemens, Nucl. Phys. **A141** (1970) 225.
[83] G. Baym, H. A. Bethe, and C. J. Pethick, Nucl. Phys. **A175** (1971) 225.
[84] D. Koester, H. Shultz and V. Weidemann, Astron. Astrophys. **76** (1979) 262.
[85] L. L. Foldy, Phys. Rev. **83** (1951) 397.
[86] P. A. Seeger, Nucl. Phys. **25** (1961) 1.
[87] H. Nagara, Y. Nagata and T. Nakamura, Phys. Rev. A **36** (1987) 1859.
[88] N. K. Glendenning, Ch. Kettner, and F. Weber, Astrophys. J. **450** (1995) 253.
[89] H. A. Buchdahl, Phys. Rev. **116** (1959) 1027.
[90] R. C. Tolman, *Relativity, Thermodynamics and Cosmology* (Clarendon Press, Oxford, 1934).
[91] R. Geroch and L. Lindblom, Ann. Phys. **207** (1991) 394.
[92] H. Bondi, Proc. R. Soc. (London) **A282** (1964) 303.
[93] E. Witten, Phys. Rev. D **30** (1984) 272.
[94] C.-S. Wang and W. Wang, Commun. Theor. Phys. (China) **15** (1991) 347.

[95] J. L. Friedman, J. R. Ipser and L. Parker, Phys. Rev. Lett. **62** (1989) 3015.
[96] P. Haensel and J. L. Zdunik, Nature **340** (1989) 617.
[97] J. E. McClintock, in *Physics of the Accretion onto Compact Objects*, ed. by K. O. Mason et al., (Springer-Verlag, Berlin, 1986).
[98] A. P. Cowley, Annu. Rev. Astron. Astrophys. **30** (1992) 287.
[99] J. Casares, P. A. Charles and T. Naylor, Nature **355** (1992) 614.
[100] F. Zwicky, Phys. Rev. **55** (1939) 726.
[101] C. E. Rhoades and R. Ruffini, Phys. Rev. Lett. **32** (1974) 324.
[102] M. Nauenberg and G. Chapline, Astrophys. J. **179** (1973) 277.
[103] L. Pietronero and R. Ruffini, in *Physics and Astrophysics of Neutron Stars and Black Holes*, ed. by R. Giacconi and R. Ruffini (North-Holland, Amsterdam, 1978).
[104] J. B. Hartle, Phys. Rep. **46** (1978) 201.
[105] J. L. Friedman and J. R. Ipser, Astrophys. J. **314** (1987) 594.
[106] J. L. Friedman, J. R. Ipser and L. Parker, Astrophys. J. **304** (1986) 115.
[107] F. Weber and N. K. Glendenning, Astrophys. J. **390** (1992) 541.
[108] J. M. Bardeen, K. S. Thorne, and D. W. Meltzer, Astrophys. J. **145** (1966) 505.
[109] I. B. Khriplovich, Yad. Fiz. **10** (1969) 409; D. J. Gross and F. Wilczek, Phys. Rev. Lett. **30** (1973) 1343; H. D. Politzer, Phys. Rev. Lett. **30** (1973) 1346.
[110] N. K. Glendenning and C. Kettner, Astron. Astrophys. **353** (2000) L9-12.
[111] M. H. Johnson and E. Teller, Phys. Rev. **98** (1955) 783.
[112] H. P. Duerr, Phys. Rev. **103** (1956) 469;.
[113] J. D. Walecka, Ann. of Phys. **83** (1974) 491.
[114] M. G. Mayer and J. H. D. Jensen, *Elementary Theory of Nuclear Shell Structure* (John Wiley & Sons, New York, 1955).
[115] A. Bohr and B. R. Mottelson, *Nuclear Structure* (W. A. Benjamin, New York, 1969).
[116] M. A. Preston, *Physics of the Nucleus* (Addison-Wesley, Reading, 1962).
[117] A. deShalit and H. Feshbach, *Theoretical Nuclear Physics* (John Wiley & Sons, New York, 1974).
[118] P. Ring and P. Schuck, *The Nuclear Many-Body Problem* (Springer-Verlag, New York, 1980).
[119] S. E. Koonin, D. J. Dean and K. Langanke, Ann. Rev. Nucl. and Part. Sc., **47** (1997) 463.
[120] B. D. Serot and J. D. Walecka, in *Advances in Nuclear Physics*, ed. by J. W. Negele and E. Vogt (Plenum Press, New York, 1986).
[121] W. Koepf and P. Ring, Nucl. Phys. **A493** (1989) 61.
[122] J. König and P. Ring, Phys. Rev. Lett. **71** (1993) 3079.
[123] M.M. Sharma, G.A. Lalazissis, W. Hillebrandt, and P. Ring, Phys. Rev. Lett. **72** (1994) 1431.
[124] P. Ring, Progr. Part. Nucl. Phys. **37** (1996) 193.
[125] H. Toki, Y. Sugahara, D. Hirata, and B.V. Carlson Nucl. Phys. **A524** (1991) 633.
[126] V. Blum, J. A. Maruhn, P.-G. Reinhard, W. Greiner Phys. Lett. **B323** (1994) 262.
[127] N. K. Glendenning, Z. Phys. A **326** (1987) 57; ibid. **327** (1987) 295.
[128] Liu Zhi-cheng, Liang Shao-rong and Gao Shang-hui, Act. Astrophys. Sin. **5** (1986) 310.
[129] N. K. Glendenning, Nucl. Phys. **A493** (1989) 521.
[130] F. Weber and M. K. Weigel, Nucl. Phys. **A505** (1989) 779.
[131] J. Ellis, J. I. Kapusta and K. A. Olive, Nucl. Phys. **B348** (1991) 345.
[132] N. K. Glendenning and S. A. Moszkowski, Phys. Rev. Lett. **67** (1991) 2414.
[133] L. Lindblom, Astrophys. J. **398** (1992) 569.

[134] H. Goldstein, *Classical Mechanics* (Addison-Wesley, Cambridge, Mass., 1951).
[135] I. J. R. Aitchison, *An Informal Introduction to Gauge Field Theories*, (Cambridge University Press, Cambridge, 1982).
[136] C. Quigg, *Gauge Theories of the Strong, Weak, and Electromagnetic Interactions* (Benjamin Cummings, Menlo Park, Calif., 1983).
[137] E. Noether, Nachr. Kgl. Ges. Wiss. Gottingen, (1918) 235.
[138] P. A. M. Dirac, *The Principles of Quantum Mechanics* (Clarendon Press, Oxford, 1947).
[139] L. C. Gomes, J. D. Walecka and V. F. Weiskopf, Ann. Phys. (New York) **3** (1958) 241.
[140] R. B. Firestone, S. Y. F. Chu, and C. M. Baglin, 1998 Update to the 8th Edition of the Table of Isotopes CD-ROM (John Wiley & Sons, New York, 1998).
[141] P. Möller, W. D. Myers, W. J. Swiatecki and J. Treiner, Atomic Data and Nuclear Data Tables **39** (1988) 225.
[142] P. M. Möller and J. R. Nix, Nucl. Phys. **A361** (1981) 17.
[143] J. P. Blaizot, D. Gogny and B. Grammiticos, Nucl. Phys. **A265** (1976) 315; J. P. Blaizot, Phys. Rep. **64** (1980) 171.
[144] H. Krivine, J. Treiner and O. Bohigas, Nucl. Phys. **A336** (1980) 155.
[145] N. K. Glendenning, Phys. Rev. Lett. **57** (1986) 1120.
[146] N. K. Glendenning, Phys. Rev. C **37** (1988) 2733.
[147] M. M. Sharma, W. T. A. Borghols, S. Brandenburg, S. Crona, A. van der Woude and M. N. Harakeh, Phys. Rev. C **38** (1988) 2562.
[148] C. H. Johnson, D. J. Horen and C. Mahaux, Phys. Rev. C **36** (1987) 2252.
[149] C. Mahaux and R. Sartor, Nucl. Phys. **A475** (1987) 247.
[150] M. Jaminon and C. Mahaux, Phys. Rev. C **40** (1989) 354.
[151] H. A. Bethe and J. Goldstone, Proc. R. Soc. (London) **A238** (1957) 551.
[152] B. Banerjee, N. K. Glendenning and M. Gyulassy, Nucl. Phys. **A361** (1981) 326.
[153] N. K. Glendenning, B. Banerjee and M. Gyulassy, Ann. Phys. (New York) **149** (1983) 1.
[154] L. D. Landau and E. M. Lifshitz, *Fluid Mechanics* (Pergamon Press, Oxford, 1959, reprinted, 1982) Ch XV.
[155] R. Geroch and L. Lindblom, Ann. Phys. **207** (1991) 394.
[156] J. Boguta and A. R. Bodmer, Nucl. Phys. **A292** (1977) 413.
[157] Gao Shang-hui, Ge Zun-Zao, Y. C. Leung, Li Zong-Wei, and Liang Shao-Rong, Astrophys. J. **245** (1981) 1110.
[158] R. B. Wiringa, V. Fics and A. Fabriconi, Phys. Rev. C **38** (1988) 779.
[159] S. I. A. Garpman, N. K. Glendenning and Y. J. Karant, Nucl. Phys. **A322** (1979) 382.
[160] N. K. Glendenning, Phys. Lett. **114B** (1982) 392; Z. Phys. A **326** (1987) 57; ibid. **327** (1987) 295.
[161] N. K. Glendenning, Phys. Lett. **185B** (1987) 275; Nucl. Phys. **A469** (1987) 600.
[162] N. K. Glendenning, Nucl. Phys. **A512** (1990) 737.
[163] Ya. B. Zel'dovich, Soviet Physics—JETP **14** (1962) 1143.
[164] N. K. Glendenning, Phys. Lett. B **208** (1988) 335.
[165] S. A. Chin, Ann. Phys. (New York) **108** (1977) 301.
[166] B. D. Serot and J. D. Walecka, in *Advances in Nuclear Physics*, Vol. 16, ed. by J. W. Negele and E. Vogt, (Plenum Press, New York, 1986).
[167] R. C. Tolman, Phys. Rev. **55** (1939) 364.
[168] L. Woltjer, Astrophys. J. **140** (1964) 1309.
[169] F. Pacini, Nature **216** (1967) 567.

[170] A. Hewish, S. J. Bell, J. D. H. Pikington, P. F. Scott and R. A. Collins, Nature **217** (1968) 709.
[171] R. E. Rothchild, S. R. Kulkarni, R. E. Lingenfelter, Nature **368** (1994) 432; T Murakami, Y. Tanaka, S. R. Kulkarni, Y. Ogasaka, T. Sonabe Y. Ogawara, T Aoki and A. Yoshida, op. cit. 127.
[172] T. Gold, Nature **218** (1968) 731.
[173] V. Canuto in *Proceedings International School of Physics "Enrico Fermi"* Course **LXV** (North Holland, New York, 1978) 448.
[174] M. A. Ruderman, Nature **223** (1969) 597.
[175] M. A. Ruderman and P. G. Sutherland, Astrophys. J. **196** (1975) 51.
[176] E. Flowers and M. A. Ruderman, Astrophys. J. **215** (1977) 302.
[177] J. P. Ostriker and J. E. Gunn, Astrophys. J. **157** (1969) 1395.
[178] J. E. Gunn and J. P. Ostriker, Phys. Rev. Lett. **22** (1969) 728.
[179] J. E. Gunn and J. P. Ostriker, Astrophys. J. **160** (1970) 979.
[180] D. Pines and J. Shaham, Nature Phys. Sci. **235** (1972) 43.
[181] D. Pines and J. Shaham, Phys. Earth Planet. Inter. **6** (1972) 103.
[182] J. Shaham, Astrophys. J. **310** (1986) 780.
[183] M. A. Alpar, P. W. Anderson, D. Pines, and J. Shaham, Astrophys. J. Lett. **249** (1981) L29; op. cit. (1987) 2152.
[184] M. A. Alpar, A. F. Cheng, M. A. Ruderman and J. Shaham, Nature **300** (1982) 728.
[185] M. A. Alpar, H. F. Chau, K. S. Cheng and D. Pines, Astrophys. J. **459** (1996) 706.
[186] A. G. W. Cameron, Astrophys. J. **130** (1959) 884.
[187] V. A. Ambartsumyan and G. S. Saakyan, Astron. Zh. **37** (1963) 193 [Soviet Ast. – AJ,**4** (1960) 187].
[188] V. R. Pandharipande, Nucl. Phys. **A178** (1971) 123.
[189] H. A. Bethe and M. Johnson, Nucl. Phys. **A230** (1974) 1.
[190] S. A. Moszkowski, Phys. Rev. D **9** (1974) 1613.
[191] N. K. Glendenning, Z. Phys. A **327** (1987) 295.
[192] N. K. Glendenning, Z. Phys. **A 326** (1987) 57.
[193] N. K. Glendenning, F. Weber and S. A. Moszkowski, Phys. Rev. C. **45** (1992) 844.
[194] N. K. Glendenning, Nucl. Phys. B (Proc. Suppl.) **24B** (1991) 110.
[195] N. K. Glendenning, Phys. Rev. D **46** (1992) 1274.
[196] F. Weber, N. K. Glendenning and M. K. Weigel, Astrophys. J. **373** (1991) 579.
[197] N. K. Glendenning and F. Weber, Astrophys. J. **400** (1992) 647.
[198] Ch. Kettner, F. Weber, M. K. Weigel and N. K. Glendenning, Phys. Rev. D. **51** (1995) 1440.
[199] N. K. Glendenning, Ch. Kettner and F. Weber, Phys. Rev. Lett. **74** (1995) 3519.
[200] N. K. Glendenning, S. Pei and F. Weber, Phys. Rev. Lett. **79** (1997) 1603.
[201] N. K. Glendenning, *Pulsar Signal of Deconfinement*, Plenary talk at International Conference on Ultra-Relativistic Nucleus–Nucleus Collisions, Quark Matter 97, Japan; Nucl. Phys. **A638** (1998) 239c .
[202] R. N. Manchester and J. H. Taylor, *Pulsars* (W. H. Freeman, San Francisco, 1977).
[203] A. G. Lyne and F. Graham-Smith, *Pulsar Astronomy* (Cambridge University Press, Cambridge, 1990).
[204] A. Fruchter, M. Tavani and D. Backer, eds., *Millisecond Pulsars: A Decade of Surprises* (Astronomical Society of the Pacific Conference Series, San Francisco, 1995).

[205] Z. Arzoumanian, F. van der Hooft and E. P. J. van den Heuvel, eds., *Pulsar Timing, General Relativity and the Internal Structure of Neutron Stars* (Royal Netherlands Academy of Arts and Sciences, Amsterdam, 1996).
[206] S. Johnston, M. Walker and M. Bailes, eds., *Proceedings of the IAU Colloquium 160 – Pulsars: Problems and Progress* Sydney, Australia, January 8–12, 1996 (Astronomical Society of the Pacific Conference Series, 1996).
[207] R. Buccheri and J. van Paradijs and M. A. Alpar, eds., *Proceedings of the Many Faces of Neutron Stars*, Lipari, Sicily, Sept. 1996, (Kluwer, Dordrecht, 1998).
[208] D. H. Staelin and E. C. Reifenstein, Science **162** (1968) 1481.
[209] M. I. Large, A. F. Vaughan and B. Y. Mills, Nature **220** (1968) 340.
[210] J. H. Taylor, in *Pulsars as Physical Laboratories*, ed. by R. D. Blandford, A. Hewish, A. G. Lyne and L. Mestel (The Royal Society, Oxford University Press, 1993).
[211] A. Wolszczan, Nature **350** (1991) 688.
[212] D. C. Backer, S. Kulkarni, C. Heiles, M. M. Davis and W. M. Goss, Nature **300** (1982) 615.
[213] P. R. Bachus, J. H. Taylor and M. Damashek, Astrophys. J. Lett. **255** (1982) L63.
[214] V. Radharkrishnan and G. Srinivasan, Curr. Sci. **51** (1982) 1096.
[215] V. Boriakoff, R. Buccheri and F. Fauci, Nature **304** (1983) 417.
[216] R. Wijnands and M. van der Klis, Nature **394** (1998) 344.
[217] D. Chakrabarty and E. H. Morgan, Nature **394** (1998) 346.
[218] A. S. Fruchter, D. R. Stinebring and J. H. Taylor, Nature **333** (1988) 237.
[219] R. N. Manchester, A. G. Lyne, C. Robinson, N. D'Amico, M. Bailles and J. Lim, Nature **352** (1991) 219.
[220] A. Wolszczan and D. A. Frail, Nature **355** (1992) 145.
[221] A. Wolszczan, Science **264** (1994) 538.
[222] J. F. Bell, M. Bailes, R. N. Manchester, J. M. Weisberg and A. G. Lyne, Astrophys. J. Lett. **440** (1995) L81.
[223] J. M. Cordes, R. W. Romani, S. C. Lundgren, Nature **362** (1993) 133.
[224] L. A. Rawley, J. H. Taylor, and M. M. Davies, Astrophys. J. **326** (1988) 947.
[225] D. C. Backer and S. R. Kulkarni, Physics Today **43** (1990) 26.
[226] R. D. Blandford, A. Hewish, A. G. Lyne and L. Mestel, eds., *Pulsars as Physical Laboratories* (The Royal Society, Oxford University Press, 1993).
[227] M. A. Alpar, in *Proceedings of the Many Faces of Neutron Stars*, Lipari, Sicily, Sept. 1996, eds. M. A. Alpar, R. Buccheri and J. van Paradijs (Kluwer, Dordrecht, 1998).
[228] R. N. Manchester, in *The Structure and Evolution of Neutron Stars*, ed. by D. Pines, R. Tamagaki and S. Tsurata, (Addison-Wesley, Redwood City, Calif., 1992).
[229] J. McKenna and A. G. Lyne, Nature **343** (1990) 349.
[230] J. H. Taylor, R. N. Manchester and G. R. Huguenin, Astrophys. J. **195** (1975) 513.
[231] N. K. Glendenning, Astrophys. J. **359** (1990) 186.
[232] A. G. Lyne R. N. Manchester and J. H. Taylor, Mon. Not. R. Astron. Soc. **185** (1985) 409.
[233] A. G. Lyne, in *High Energy Phenomena Around Collapsed Stars*, ed. by F. Pacini (D. Riedel, Dordrecht, 1987).
[234] J. H. Taylor and D. R. Stinebring, Annu. Rev. Astron. Astrophys. **24** (1986) 285.
[235] S. R. Kulkarni, in *Pulsars as Physical Laboratories*, ed. by R. D. Blandford, A. Hewish, A. Lyne and L. Mestel (The Royal Society, Oxford University Press, 1993).
[236] D. Bhattacharya and E. P. J. van den Heuvel, Phys. Rep., **203** (1991) 1.
[237] L. Bildsten and T. Strohmayer, Physics Today **52** (1999) 40.
[238] A. G. Lyne and D. R. Lorimer, Nature **369** (1994) 127.

[239] D. A. Frail, W. M. Goss and J. B. Z. Whiteoak, Astrophys. J. **437** (1994) 781.
[240] D. A. Frail and S. R. Kulkarni, Nature **352** (1991) 785.
[241] P. Goldreich and W. H. Julian, Astrophys. J. **157** (1969) 869.
[242] V. Trimble, Astron. J. **73** (1968) 535.
[243] A. Hewish and S. E. Okoye, Nature **203** (1964) 171.
[244] F. Pacini, Nature **219** (1968) 145.
[245] J. M. Rankin, Astrophys. J. **274** (1983) 333; loc. cit. **301** (1986) 901.
[246] J. M. Rankin and J. A. Gil, Comments Astrophys. **14** (1989) 1.
[247] C. P. Lorenz, D. G. Ravenhall and C. J. Pethick, Phys. Rev. Lett. **70** (1993) 379.
[248] J. W. Negele and D. Vautherin, Nucl. Phys. **A178** (1973) 123.
[249] N. K. Glendenning, Phys. Rev. D **46** (1992) 4161.
[250] P. C. Joss and S. A. Rappaport, Ann. Rev. Astr. Astrophys. **22** (1984) 537.
[251] F. Nagase, Publ. Astron. Soc. Japan, **41** (1989) 1.
[252] M. H. Kerkwijk, J. van Paradijs and E.J. Zuiderwijk Astron. Astrophys. **303** (1995) 497.
[253] S. E. Thorsett, Z. Arzoumanian, M. M. McKinnon and J. H. Taylor, Astrophys. J. **405** (1993) L29.
[254] S. Bahcall, B. W. Lynn and S. B. Selipsky, Nucl. Phys. B **325** (1989) 606.
[255] F. X. Timmes, S. E. Woosley and T. A. Weaver, Astrophys. J. **457** (1998) 834.
[256] A. Akmal, V. R. Pandharipande and D. G. Ravenhall, Phys. Rev. C **58** (1998) 1804.
[257] E. J. Groth, Astrophys. J. Suppl. **29** (1975) 453.
[258] A. G. Lyne, R. S. Pritchard, and F. G. Smith, Mon. Not. R. Astron. Soc. **233** (1988) 667.
[259] A. G. Lyne, R. S. Pritchard, F. Graham-Smith and F. Camilo, Nature **381** (1996) 497.
[260] R. Manchester, J. Durdin, and L. Newton, Nature **331** (1985) 374.
[261] V. M. Kaspi, R. N. Manchester, B. Siegman, S. Johnston, and A. G. Lyne, Astrophys. J. **422** (1994) L83.
[262] R. N. Manchester and B. A. Peterson, Astrophys. J. **342** (1989) L23.
[263] H. Ögelman and G. Hasinger, Astrophys. J. **353** (1990) L21.
[264] F. Nagase, J. Deeter, W. Lewis, T. Dotani, F. Makino, and K. Mitsuda, Astrophys. J. **351** (1990) L13.
[265] Ch. Gouiffes, J. P. Finley, and H. Ögelman, Astrophys. J. **394** (1992) 581.
[266] N. K. Glendenning and F. Weber, Phys. Rev. D **50** (1994) 3836.
[267] B. D. Serot and J. D. Walecka, Phys. Lett. **87B** (1980).
[268] C. J. Horowitz and B. D. Serot, Nucl. Phys. **A368** (1981) 413.
[269] J. Boguta, Nucl. Phys. **A372** (1981) 386.
[270] P.-G. Reinhard, M. Rufa, J. Maruhn and W. Greiner and J. Friedrich, Z. Phys. **A323** (1986) 13.
[271] O. V. Maxwell, Astrophys. J. **316** (1987) 691.
[272] K. Nomoto and S. Tsuruta, Astrophys. J. **312** (1987) 711.
[273] M. Prakash, M. Prakash, J. M. Lattimer and C. J. Pethick, Astrophys. J. **390** (1992) L77.
[274] Ch. Schaab, F. Weber, M. K. Weigel and N. K. Glendenning, Nucl. Phys. **A605** (1996) 531.
[275] D. Page, in *The Many Faces of Neutron Stars* ed. by A. Alpar, R. Buccheri & J. van Paradijs (Kluwer, Dordtecht, 1998).
[276] C. Schaab, S. Balberg and J. Schaffner-Bielich, Astro. Phys. J. **504** (1998) L99.
[277] D. B. Kaplan and A. Nelson, Phys. Lett. **175 B** (1986) 57.
[278] W. H. Dickhoff, A. Faessler, H. Müther and S. S. Wu, Nucl. Phys. A **405** (1983) 534.

[279] J. Diaz Alonso and J. M. Ibanez Cabanell, Astrophys. J. **291** (1985) 308.
[280] J. Diaz Alonso, J. M. Ibanez and H. Shivak, Phys. Rev. C **39** (1989) 671.
[281] S. Sumiyoshi and H. Toki, Phys. Lett. B **276** (1992) 393.
[282] S. Balberg, I Lichtenstadt and G. B. Cook, Astrophys. J. (supl.) **121** (1999) 515.
[283] R. Hofstdter, ed. *Electron Scattering and Nuclear and Nucleon Structure* (W. A. Benjaomin, New York) 1963.
[284] M. R. Anastacio, L. S. Celenza, W. S. Pong and C. M. Shakin, Phys. Rep. **100** (1983).
[285] L. S. Celenza and C. M. Shakin, *Relativistic Nuclear Physics*, (World Scientific, Singapore, 1986).
[286] R. Brockmann and R. Machleidt, Phys. Lett. **149B** (1984) 283.
[287] R. Brockmann and R. Machleidt, Phys. Rev. C **42** (1990) 1965.
[288] B. ter Haar and R. Malfliet, Phys. Rev. Lett. **59** (1987) 1652.
[289] B. ter Haar and R. Malfliet, Phys. Rep. **149** (1987) 208.
[290] C. J. Horowitz and B. D. Serot, Nucl. Phys. **A464** (1987) 613.
[291] R. Machleidt and R. Brockmann, Phys. Lett. **B160** (1985) 364.
[292] R. Brockmann and R. Machleidt, Los Alamos e-print nucl-th/9612004 (1996); *Open Problems in Nuclear Matter*, ed. by M. Baldo (World Scientific, Singapore, in press).
[293] G. Q. Li, C. H. Lee and G. E. Brown, Phys. Rev. Lett. **79** (1997) 5214.
[294] O. V. Maxwell, Astrophys. J. **231** (19)79 201.
[295] G. Glen and P. Sutherland, Astrophys. J. **239** (1980) 671.
[296] D. Page and E. Baron, Astrophys. J. **354** (1990) L17.
[297] D. Page, in *Neutron Stars and Pulsars*, ed. by N. Shibazaki, N. Kawai, S. Shibata and T. Kifune (Universal Academy Press, Tokyo, 1998).
[298] N. K. Glendenning, *Spin-up of Solitary Pulsars: Signal of Phase Transition*, Proceedings of "Neutron Stars and Pulsars, Tokyo, 1997" (Universal Academy Press, Tokyo, 1998).
[299] D. Vautherin and P. Bonche, Nucl. Phys. **A372** (1981) 496.
[300] D. Q. Lamb, J. M. Lattimer, C. J. Pethick and D. G. Ravenhall, Nucl. Phys. **A360** (1981) 459.
[301] D. G. Ravenhall, C. J. Pethick and J. R. Wilson, Phys. Rev. Lett. **50** (1983) 2066; D. G. Ravenhall, C. J. Pethick and J. M. Lattimer, Nucl. Phys. **A407** (1983) 571, and references cited.
[302] R. D. Williams and S. E. Koonin, Nucl. Phys. **A435** (1985) 844.
[303] M. Van der Klis, in *Proceedings of the Many Faces of Neutron Stars*, Lipari, Sicily, Sept. 1996, ed. by M. A. Alpar, R. Buccheri and J. van Paradijs (Kluwer, Dordrecht, 1998).
[304] M. C. Miller, F. K. Lamb, and D. Psaltis, Astrophys. J. **508** (1998) 791.
[305] M. C. Miller, F. K. Lamb, and G. B. Cooke, Astrophys. J. **509** (1998) 793.
[306] W. Zhang, A. P. Smale, T. E. Strohmayer, and J. H. Swank, Astrophys. J. **500** (1998) L171.
[307] N. K. Glendenning, in *Relativistic Aspects of Nuclear Physics*, Rio de Janeiro, August 1989, ed. by T. Kodama K. Chung, S. Duarte and M. Nemes (World Scientific, Singapore, 1990).
[308] N. K. Glendenning, in *Proceedings of the Many Faces of Neutron Stars*, Lipari, Sicily, Sept. 1996, ed. by M. A. Alpar, R. Buccheri and J. van Paradijs (Kluwer, Dordrecht, 1998).
[309] J. I. Kapusta and K. A. Olive, Phys. Rev. Lett. **64** (1990) 13.
[310] R. Knorren, M. Prakash and P. J. Ellis, Phys. Rev. C **52** (1995) 3470.
[311] J. Schaffner and I. N. Mishustin, Phys. Rev. C **53** (1996) 1416.

[312] J. Boguta and S. Bohrmann, Phys. Lett. **102B** (1981) 93.
[313] G. E. Walker, Nucl. Phys. **A450** (1986) 287c.
[314] M. Rufa, H. Stocker, P.-G. Reinhardt, J. Maruhn and W. Greiner, J. Phys. **G13** (1987) L143.
[315] M. Rufa, J. Schaffner, J. Marhun, H. Stocker, W. Greiner and P.-G. Reinhard, Phys. Rev. C **42** (1990) 2469.
[316] D. J. Millener, C. B. Dover and A. Gal, Phys. Rev. C **38** (1988) 2700.
[317] N. M. Hugenholtz and L. Van Hove, Physica **24** (1958) 363.
[318] M. M. Sharma. W. Stocker, P. Gleissl, and M. Brack, Nucl. Phys. **A504** (1989) 337.
[319] C. B. Dover and A. Gal, Progr. Part. Nucl. Phys. **12** (1984) 171.
[320] N. K. Glendenning, D. Von-Eiff, M. Haft, H. Lenske, and M. K. Weigel, Phys. Rev. C **48** (1993) 889.
[321] J. Mares and B. K. Jennings, Phys. Rev. C **49** (1994) 2472.
[322] J. Mares, E. Friedman, A. Gal and B. K. Jennings, Nucl. Phys. A **594** (1995) 311.
[323] H. A. Bethe and G. E. Brown, Astrophys. J. Lett. 445 (1995) L129.
[324] J. M. Lattimer, C. J. Pethick, M. Prakash and P. Haensel, Phys. Rev. Lett. **66** (1991) 2701.
[325] E. Gudmundson, C. Pethick and R. Epstein, Astrophys. J. **272** (1983) 286.
[326] K. A. Van Riper, Astrophys. J. Suppl. **75** (1988) 449.
[327] N. K. Glendenning, in *Proceedings of the 1989 International Nuclear Physics Conference*, Sao Paulo, Brasil, Vol. 2, ed. by M. S. Hussein et al. (World Scientific, Singapore, 1990).
[328] P. J. Ellis, R. Knorren and M. Prakash, Phys. Lett. **B349** (1995) 11.
[329] N. K. Glendenning, P. Hecking and V. Ruck, Ann. Phys. (New York) **149** (1983) 22.
[330] J. B. Hartle, Astrophys. J. **150** (1967) 1005.
[331] J. B. Hartle and K. S. Thorne, Astrophys. J. **153** (1968) 807.
[332] B. Datta, Nature **308** (1984) 338; B. Datta and Kapoor, Nature **315** (1985) 557; B. Datta and Ray, Mon. Not. R. Astron. Soc. **204** (1983) 75P.
[333] F. Weber and N. K. Glendenning, Z. Phys. A **339** (1991) 211.
[334] F. Weber and N. K. Glendenning, Phys. Lett. B **265** (1991) 1.
[335] M. Salgado, S. Bonazzola, E. Gourgoulhon and P. Haensel, Astron. Astrophys. **291** (1994) 155.
[336] K. Sato and H. Suzuki, Prog. Theoret. Phys. (Tokyo) **81** (1989) 997.
[337] J. M. Lattimer, M. Prakash, D. Masak and A. Yahil, Astrophys. J. **355** (1990) 241.
[338] J. B. Hartle and D. Sharp, Astrophys. J. **147** (1967) 317.
[339] D. J. Hegyi, Astrophys. J. **217** (1977) 244.
[340] F. Weber, *Hadron Physics and Neutron Star Properties*, Habilitation Thesis, Ludwig-Maximilians University of Munich, 1992.
[341] H. Heiselberg and M. Hjorth-Jensen, Phys. Rev. Lett. **80** (1998) 5485.
[342] E. Chubarian, H. Grigorian, G. Poghosyan and D. Blaschke, Los Alamos e-print astro-ph/9903489 (1999), Astron. Astrophys. (in press).
[343] S. Bonazzola, E. Gourgoulhon and J. A. Marck, Phys. Rev. D **58** (1998) 104020.
[344] B. Friedman and V. R. Pandharipande, Nucl. Phys. **A361** (1981) 502.
[345] P. Poschenrieder and M. K. Weigel, Phys. Lett. **200B** (1988) 231; Phys. Rev. C **38** (1988) 471.
[346] R. Machleidt, K. Holinde, and Ch. Elster, Phys. Rep. **149** (1987) 1.
[347] K. Holinde, K. Erkelenz, and R. Alzetta, Nucl. Phys. **A194** (1972) 161; **A198** (1972) 598.

[348] L. S. Celenza and C. M. Shakin, *Relativistic Nuclear Structure Physics* World Scientific Lecture Notes in Physics, Vol. 2, (World Scientific, Singapore, 1986).
[349] F. Weber and N. K. Glendenning, *Hadronic Matter and Rotating Relativistic Neutron Stars*, in Proc. of the Nankai Summer School on Astrophysics and Neutrino Physics, Tianjin, China 1991, ed. by D. H. Feng, G. Z He and X. Q. Li (World Scientific, Singapore, 1993).
[350] S. Chandrasekhar, Phys. Rev. Lett. **24** (1970) 611.
[351] S. Chandrasekhar, Astrophys. J. **161** (1970) 561.
[352] J. L. Friedman and B. F. Schutz, Astrophys. J. **200** (1975) 204.
[353] J. L. Friedman and B. F. Schutz, Astrophys. J. **199** (1975) L157.
[354] J. L. Friedman and B. F. Schutz, Astrophys. J. **222** (1978) 281.
[355] L. Lindblom and S. L. Detweiler, Astrophys. J. **211** (1977) 565.
[356] E. Flowers and N. Itoh, Astrophys. J. **206** (1976) 218.
[357] C. Cutler and L. Lindblom, Astrophys. J. **314** (1987) 234.
[358] S. L. Detweiler, Astrophys. J. **197** (1975) 203.
[359] W. Thomson, Phil. Trans. R. Soc. (London) **153** (1863) 608.
[360] N. Comins, Mon. Not. R. Astron. Soc. **189** (1979) 233.
[361] N. Comins, Mon. Not. R. Astron. Soc. **189** (1979) 255.
[362] L. Lindblom, Astrophys, J. **303** (1986) 303.
[363] R. A. Managan, Astrophys. J. **309** (1986) 598.
[364] J. R. Ipser and L. Lindblom, Astrophys. J. **373** (1991) 213.
[365] C. Cutler, L. Lindblom and R. J. Splinter, Astrophys. J. **363** (1990) 603.
[366] S. Koranda, N. Stergioulas and J. L. Friedman, Astrophys. J. **488** (1997) 799.
[367] N. K. Glendenning, J. Phys. G **15** (1989) L255.
[368] A. R. Curtis, Proc. R. Soc. (London) A **200** (1950) 248.
[369] J. E. Dennis, Jr. and R. B. Schnabel, *Numerical Methods for Unconstrained Optimization and Non-Linear Equations* (Prentis-Hall, Englewood Cliffs, NJ, 1983).
[370] N. K. Glendenning, Phys. Rev. Lett. **63** (1989) 2629.
[371] N. K. Glendenning, Mod. Phys. Lett. A **5** (1990) 2197.
[372] S. A. Bludman and M. A. Ruderman, Phys. Rev. **170** (1968) 1176; Phys. Rev. D **1** (1970) 3243.
[373] M. C. Miller and F. K. Lamb, Astrophys. J. Lett. **499** (1998) L37-L40.
[374] M. C. Miller, F. K. Lamb, and D. Psaltis, *The Active X-ray Sky*, ed. by L. Scarsi, H. Bradt, P. Giommi, and F. Fiore, Nucl. Phys. B (Proc. Suppl.) **69** (1998) 123.
[375] B. W. Lynn, A. E. Nelson and N. Tetradis, Nucl. Phys. B **345** (1990) 186.
[376] J. L. Friedman, Phys. Rev. Lett. **51** (1983) 11.
[377] J. R. Ipser and L. Lindblom, Phys. Rev. Lett. **62** (1989) 2777.
[378] P. Haensel, J. L. Zdunik and R. Schaeffer, Astron. Astrophys. **160** (1986) 121.
[379] C. Alcock, E. Farhi and A. V. Olinto, Astrophys. J. **310** (1986) 261.
[380] A. R. Bodmer, Phys. Rev. D **4** (1971) 1601.
[381] E. Farhi and R. L. Jaffe, Phys. Rev. D **30** (1984) 2379.
[382] *Strange Quark Matter in Physics and Astrophysics*, ed. by J. Madsen and P. Haensel, Nuclear Physics B (Proc. Suppl.) **24B** (1991).
[383] S. Bahcall, B. W. Lynn and S.B. Selipsky, Nucl. Phys. B **331** (1990) 67.
[384] F. R. Klinkhamer and N. S. Manton, Phys. Rev. C **30** (1984) 2212.
[385] A. Chodos, R. L. Jaffe, K. Johnson, C. B. Thorne and V. F. Weisskopf, Phys. Rev. D **9** (1974) 3471.
[386] K. Schertler, C. Greiner, P. K. Sahu and M. H. Thoma, Nucl. Phys. A **637** (1998) 451.

[387] S. A. Chin, Phys. Lett. **78B** (1978) 552.
[388] J. I. Kapusta, Nucl. Phys. **B148** (1979) 461.
[389] O. K. Kalashnikov and V. V. Klimov, Phys. Lett. **88B** (1979) 328.
[390] N. K. Glendenning, in *1990 Summer School on the Structure of Hadrons and Hadronic Matter,* Dronton, The Netherlands, ed. by O. Scholten and J. H. Koch, (World Scientific, Singapore, 1991).
[391] C. W. Misner and H. S. Zapolsky, Phys. Rev. Lett. **12** (1964) 635.
[392] N. Itoh, Prog. Theor. Phys. (Tokyo) **44** (1970) 291.
[393] G. Baym and S. A. Chin, Phys. Lett. **62B** (1976) 241.
[394] G. Chapline and M. Nauenberg, Nature **264** (1976) 235; Phys. Rev. D **16** (1977) 456.
[395] B. D. Keister and L. S. Kisslinger, Phys. Lett. **64B** (1976) 117.
[396] W. B. Fechner and P. C. Joss, Nature **274** (1978) 347.
[397] B. Freedman and L. McLerran, Phys. Rev. D **17** (1978) 1109.
[398] H. A. Bethe, G. E. Brown and J. Cooperstein, Nucl. Phys. **A462** (1987) 791.
[399] B. D. Serot and H. Uechi, Ann. Phys. (New York) **179** (1987) 272.
[400] N. K. Glendenning, in *Proceedings of the 1989 International Nuclear Physics Conference*, Sao Paulo, Brasil, Vol. 2, p. 711, ed. by M. S. Hussein et al. (World Scientific, Singapore, 1990).
[401] J. Ellis, J. Kapusta and K. A. Olive, Nucl. Phys. **B348** (1991) 345.
[402] A. Rosenhauer, E. F. Staubo, L. P. Csernai, T. Overgard, and E. Ostgaard, Nucl. Phys. **540** (1992) 630.
[403] N. K. Glendenning, in *Structure of Vacuum and Elementary Matter*, ed. by E. Stein and H. Stocker, 1996 (World Scientific, 1997).
[404] H. Heiselberg, C. J. Pethick, and E. F. Staubo, Phys. Rev. Lett. **70** (1993) 1355.
[405] N. K. Glendenning and S. Pei, Phys. Rev. C **52** (1995) 2250.
[406] N. K. Glendenning and S. Pei, in the Eugene Wigner Memorial Issue of Heavy Ion Physics (Budapest) **1** (1995) 1.
[407] W. D. Myers, W. J. Swiatecki and C. S. Wang, Nucl. Phys. **A436** (1985) 185.
[408] M. B. Christiansen and N. K. Glendenning, Phys. Rev. C **56** (1997) 2858.
[409] V. R. Pandharipande and E. F. Staubo, in *Proc. 2'nd International Conf. of Physics and Astrophysics of Quark-Gluon Plasma,* Calcutta, 1993, ed. by B. Sinha, Y. P. Viyogi and S. Raha, (World Scientific, Singapore, 1994).
[410] N. K. Glendenning and J. Schaffner-Bielich, Phys. Rev. Lett. **81** (1998) 4564.
[411] N. K. Glendenning and J. Schaffner-Bielich, Phys. Rev. C **60** (1999) 25803.
[412] J. B. Hartle, R. F. Sawyer and D. J. Scalapino, Astrophys. J. **199** (1975) 471.
[413] W. Weise and G. E. Brown, Phys. Lett. **58B** (1975) 300.
[414] A. B. Migdal, A. I. Chernoustan and I. N. Mishustin, Phys. Lett. **83B** (1979) 158.
[415] A. B. Migdal, in *Mesons in Nuclei, Vol III* ed. by M. Rho and D. Wilkinson (North-Holland Publishing Co., Amsterdam, 1979) p. 941 see esp. p. 978.
[416] S.-O. Backman and W. Weise in *Mesons in Nuclei, Vol III*, ed. by M. Rho and D. Wilkinson (North-Holland Publishing Co., Amsterdam, 1979) p. 1095 see esp. p. 1116.
[417] G. E. Brown, K. Kubodera, M. Rho and V. Thorsson, Nucl. Phys. **A 291** (1992) 355.
[418] V. Thorsson, M. Prakash and J. M. Lattimer, Nucl. Phys. A **572** (1994) 693.
[419] F. Fujii, T. Maruyama, T. Muto and T. Tatsumi, Nucl. Phys. A **597** (1996) 645.
[420] N. K. Glendenning and J. Schaffner-Bielich, Phys. Rev. C **58** (1998) 1298.
[421] A. Faessler, A. J. Buchmann and M. I. Krivoruchenko, Phys. Lett. **B 391** (1997) 255.
[422] V. Koch, Phys. Lett. B **337** (1994) 7.
[423] T. Waas and W. Weise, Nucl. Phys. A **625** (1997) 287.

[424] E. Friedmann, A. Gal and C. J. Batty, Nucl. Phys. **A 579** (1994) 518.
[425] M. Lutz, Phys. Lett. **B 426** (1998) 12.
[426] J. Schaffner-Bielich, I. N. Mishustin and J. Bondorf, Nucl. Phys. **A 625** (1997) 325.
[427] Y. Sugahara and H. Toki, Nucl. Phys. A **579** (1994) 557.
[428] G. E. Brown, C.-H. Lee, M. Rho and V. Thorsson, Nucl. Phys. **A 567** (1994) 937.
[429] We thank Hirotsugu Fujii for providing us with the data tables to check the neutron population from Nucl. Phys. **A 597** (1996) 645.
[430] J. Schaffner, C. Greiner and H. Stocker, Phys. Rev. C **46** (1992) 322.
[431] D. G. Ravenhall, C. J. Pethick and J. R. Wilson, Phys. Rev. Lett. **50** (1983) 2066.
[432] M. Christiansen, private communication, Oct., 1998.
[433] M. B. Christiansen and N. K. Glendenning, Phys. Rev. C **56** (1997) 2858.
[434] D. Z. Freedman, Phys. Rev. D **9** (1974) 1389.
[435] S. A. Colgate and C. Fryer, *The Physics of Supernovae*, Phys. Rep. **256** (1995) 1.
[436] S. E. Woosley and T. A. Weaver, Ann. Rev. Astron. Astrophys. **24** (1986) 205.
[437] G. E. Brown and H. A. Bethe, Astrophys. J. **423** (1994) 659.
[438] I. Bombaci, M. Prakash, M. Prakash, P. J. Ellis, J. M. Lattimer and G. E. Brown, Nucl. Phys. **A583** (1995) 623.
[439] F. C. Michel, Nature **333** (1988) 644.
[440] A. Burrows, Astrophys. J. **335** (1988) 891.
[441] G. E. Brown and J. C. Weingartner, Astrophys. J. **436** (1994) 843.
[442] D. J. Helfand and R. H. Becker, Nature **307** (1994) 215.
[443] M. Prisznyak, B. Lukacs and P. Levai, *Are There Top Quarks in Superdense Hybrid Stars?*, Los Alamos e-print astro-ph/9412052 (1994).
[444] I. B. Khriplovich, Yad. Fiz. **10** (1969) 409; D. J. Gross and F. Wilczek, Phys. Rev. Lett. **30** (1973) 1343; H. D. Politzer, Phys. Rev. Lett. **30** (1973) 1346.
[445] C. Schaab, B. Hermann, F. Weber and M. K. Weigel, Astrophys. J. Lett. **480** (1997) L111.
[446] B. R. Mottelson and J. G. Valatin, Phys. Rev. Lett. **5** (1960) 511.
[447] A. Johnson, H. Ryde and S. A. Hjorth, Nucl. Phys. **A179** (1972) 753.
[448] F. S. Stephens and R. S. Simon, Nucl. Phys. **A183** (1972) 257.
[449] N. K. Glendenning, Nucl. Phys. B (Proc. Suppl.) **24B** (1991) 110; Phys. Rev. D **46** (1992) 1274.
[450] M. A. Alpar, Phys. Rev. Lett. **58** (1987) 2152.
[451] J. Madsen in *Strange Quark Matter in Physics and Astrophysics*, ed. by J. Madsen and P. Haensel, Nucl. Phys. B, Proc. Suppl. **24** (1991).
[452] J. Madsen, *Physics and Astrophysics of Strange Quark Matter*, Proceedings of the 2nd International Conference on Physics and Astrophysics of Quark-Gluon Plasma, January 19-23, 1993, Calcutta, India, ed. by B. Sinha, Y. P. Viyogi, and S. Raha, (World Scientific, Singapore, 1994).
[453] C. Alcock and E. Farhi, Phys. Rev. D **32** (1985) 1273.
[454] C. Alcock and A. V. Olinto, Ann. Rev. Nucl. Part. Sci. **38** (1988) 161.
[455] J. Madsen, Phys. Rev. D **47** (1993) 5156.
[456] J. Madsen, Phys. Rev. **50** (1994) 3328.
[457] E. Cappellaro and M. Turatto, Astron. Astrophys. **190** (1988) 10.
[458] J. P. A. Clark and D. M. Eardley, Astrophys. J. **215** (1977) 311.
[459] A. G. Lyne, B. Anderson, and M. Salter, Mon. Not. R. Astron. Soc. **201** (1982) 503.
[460] M. Brugger, K. Lutzenchirchen, S. Polikanov, G. Hermann, M. Overbeck, N. Trautmann, A. Breskein, R. Chechnik, Z. Fraenkel and U. Smilansky, Nature **337** (1989) 434.

[461] W. N. Cottingham, D. Kalafatis and R. Vinh Mau, Phys. Rev. Lett. **73** (1994) 1328.
[462] R. F. Sawyer, Phys. Lett. **233** (1989) 412.
[463] J. Madsen, Phys. Rev. D **46** (1992) 3290.
[464] J. Madsen, Phys. Rev. Lett. **16** (1998) 3311.
[465] J. A. Frieman and A. V. Olinto, Nature **341** (1989) 633.
[466] A. V. Olinto, Phys. Lett. **192B** (1987) 71.
[467] R. R. Caldwell and J. L. Friedman, Phys. Lett. B **264** (1991) 143.
[468] Y. F., Huang and T. Lu, Astron. Astrophys. **325** (1997) 189.
[469] J. Madsen, Phys. Rev. Lett. **61** (1988) 2909.
[470] J. Madsen, *Quark Nuggets, Dark Matter and Pulsar Glitches*, Proceedings of the XXIVth Rencontre de Moriond, Les Arcs, Savoie, France, March 5–12, 1989, ed. by J. Audouze and J. Tran Thanh Van, (Edition Frontiers, Paris, 1990).
[471] T. Saito, Y. Hatano, Y. Fukuda, and H. Oda, Phys. Rev. Lett. **65** (1990) 2094.
[472] T. Saito, *Search for Strange Quark Nuggets in Galactic Cosmic Rays*, Proceedings of the International Symposium on Strangeness and Quark, Crete, Greece, ed. by G. Vassiliadis, A. D. Panagiotou, S. Kumar, and J. Madsen, eds. (World Scientific, Singapore, 1995).
[473] C. Greiner, D. H. Rischke, H. Stocker and P. Koch, Phys. Rev. D **38** (1988) 2797.

Index

Accretion
  and pulsar spin-up, 215, 300, 305
  disk, 137, 205
  induced collapse, 130
Action principle in gravity, 55
Active galactic nuclei, 68, 137
Affine connection, 28–31, 35, 47, 48

Baade, W., 199
Baryon
  charge favored, 248
  current, 161
  density, 171
  mass of star, 53, 121, 334
  number of star, 120
  octet, 146
Bell, Jocelyn, 201
Beta equilibrium, 92, 232, 238, 267
Bianchi identities, 41
Big bang, 68, 393
Binding energy
  neutron star, 75, 121
  nucleus, 74
Black dwarf, 65
Black hole, 4, 44, 48, 53, 54, 68, 70, 73, 104, 107, 109, 137, 206, 254, 318, 334, 415
  density, 141
  formation of low-mass, 393, 395
  horizon, 48
  low-mass, 399
  massive, 396
Bohr radius, 114
Bondi, 125
BPS equation of state , 111
Braking index, 227, 407, 411

Canonical pulsar, 212
Causal limit, *see also* Causality, 108, 118
Causality, 108, 125, 129, 310
Chandrasekhar
  mass, 66, 223
  mass limit for white dwarf, 104, 106
Charge neutrality
  among baryons, 266, 331, 350, 354
  global, 340, 344
  local, 340, 342, 344, 345
  of stars, 82, 92, 232, 257, 266
Charge symmetry energy, *see* Nuclear or Isospin symmetry
Chemical equilibrium, 95, 233, 234
Chemical potential, 83, 95, 234, 245
  and conserved charges, 237